ICFM 2021

International Conference "Functional Materials" ICFM - 2021

BOOK OF ABSTRACTS

October 4 - 8, 2021

Crimea, Alushta

М-Гранат

ЭМТИОН

International Conference
"Functional Materials"

ICFM-2021

BOOK
OF
ABSTRACTS

October 4 – 8, 2021
Russia, Crimea, Alushta

International Conference "Functional Materials" ICFM-2021

Scientific Committee

V. Berzhansky (co-chairman),
V. Belotelov (co-chairman),
S. Nikitov (co-chairman)
N. Bebenin
I. Bychkov
A. Gorbatsevich
E. Ekomasov
Y. Fetisov
A. Fraerman
A. Kalashnikova
G. Kurlyandskaya
I. Lyubutin
S. Ovchinnikov
N. Perov
R. Pisarev
A. Pyatakov
K. Rozanov
A. Sadovnikov
V. Shavrov
A. Sigov
V. Shur
V. Ustinov
A. Zvezdin

Local Committee

S. Polulyakh (chairman)
S. Alieva
E. Barshak
N. Lugovskoy
T. Mikhailova
V. Popov
S. Tomilin
M. Yavorsky

Address of the Organizing Committee
ICFM'2021
V. I. Vernadsky Crimean Federal University,
Vernadsky Ave., 4, Simferopol, 95007 Russia
Phone: 8 978 7665730
E-mail: icfm@cfuv.ru
https://icfm-2021.ru/

Plenary reports

Chiral spintronics of helimagnets

Ustinov V.V. , Yasyulevich I.A.

Institute of Metal Physics, Ural Branch RAS, 620108, Ekaterinburg, Russia

The features of spin and charge transport in conductive helimagnets (HM), which are due to the action of an inhomogeneous exchange magnetic field on the spin of conduction electrons, are theoretically studied [1]. The interaction between the spin of moving particles and an inhomogeneous external magnetic field has been first recorded in the famous Stern-Gerlach experiment when investigating the quantum nature of spin.

In the present paper, we have demonstrated that two physical effects – the electrical magnetochiral effect (EMChE) and the kinetic magnetoelectric effect (KMEE) – can be explained through the interaction of the spins of itinerant electrons in chiral HM with spatially inhomogeneous effective magnetic field of exchange origin [2]. All parameters of the EMChE and KMEE are presented in terms of both the characteristic frequencies of spin relaxation of conduction electrons in a helimagnet and the frequencies of their Larmor precession in external and internal exchange fields.

It has been shown that the effective frequency of conduction electron spin relaxation in a HM contains three components: i) the rate of spin-lattice relaxation caused by spin-orbit scattering of conduction electrons by defects of the crystal lattice, ii) the rate of change in the average spin of electrons due to their "diffusion" escape from a region with a given direction of the average spin to a region with a different direction of spin density, and iii) the contribution of the Larmor precession of the spins of electrons moving in the helimagnet's exchange field that assigns the precession axis altering its direction in space. The peculiarities of the EMChE and KMEE that substantially depend on the ratio of the above-listed spin relaxation rates and the angular frequencies of electron precession are described.

The numerical estimates performed show that the mechanism of generating EMChE provides the effect magnitude sufficient to be experimentally detected in metallic helimagnets. The frequency regions of spin relaxation and spin precession are determined to observe a giant electrical magnetochiral effect (GEMChE) and resonant behavior of the chiral magnetoresistance. We have called the appropriate effect as "magnetochiral kinetic resonance" (MChKR). The physical nature of MChKR is elucidated. The latter arises due to the coincidence of the Larmor precession frequency of an electron in the effective field and the phase change frequency of the helicoidal exchange field acting on the electron moving along the helicoid's axis with a speed equal to that of the electron flow. We have demonstrated how the experimental studies of the KMEE can be used to directly determine the chirality of HM.

Suppose that the wave vector **q** of the magnetic helix of a monoaxial HM, the vector of the external magnetic field **B** and the vector of the electron current density **I** are oriented along the OZ-axis, the direction of which is defined by the unit vector $\mathbf{e}_z$. Apart from the vectors **B** and **I**, the unit vectors $\mathbf{b} = \mathbf{B}/B$ and $\mathbf{i} = \mathbf{I}/I$ should be introduced. Suppose that the local magnetization **M** depends only on the z-coordinate, and the OZ-axis rests on the screw axis of symmetry. When exposed to the magnetic field **B** directed along the axis of the helicoid, a simple spiral can transform into a conical one.

The direction of the helicoid's transverse magnetization vector is given by the unit vector $\mathbf{h}=\mathbf{h}(z)$. To characterize the direction of the "twisting" of the magnetic helicoid, we introduce the unit vector $\mathbf{h}'$ that sets out the direction of the $\partial/\partial z\,\mathbf{h}(z)$ derivative vector through the relation $\partial/\partial z\,\mathbf{h}(z)=q\mathbf{h}'$. The direction of the "twisting" of the magnetic helix is unambiguously determined by the vector $\mathbf{k}=[\mathbf{h}\times\mathbf{h}']$ called the HM chirality vector. Also, the vector $\mathbf{q}=q\mathbf{k}$ and the scalar characteristic of the helix, $K=(\mathbf{k}\cdot\mathbf{e}_z)$, should be entered. They bear the name of the wave vector of the magnetic helix and the chirality of the HM, respectively. A positive chirality value $K=+1$ corresponds to a right-handed helix, whereas a negative chirality $K=-1$ refers to a left-handed helix. The symmetry of conical magnetic helix (CMH) is defined by two unit vectors: the chirality vector **k** and the vector **b** that determines the direction of the axis of the magnetic cone. The common characteristic of CMH is the tensor dyadic product $\mathbf{k}\otimes\mathbf{b}$. Fig. 1 schematically shows four possible configurations of the **k** and **b** vectors together with a symbolic image of the cone of the corresponding magnetic spiral. Magnetiresistive properties of a helimagnet are completely determined by the value of $\varepsilon=^{3}\boldsymbol{e}\cdots[\mathbf{k}\otimes\mathbf{b}\otimes\mathbf{i}]$ that can take only two values: $\varepsilon=+1$ and $\varepsilon=-1$, depending on the mutual direction of the vectors **k**, **b**, and **i**. Fig. 2 shows all the possible magnetoresistive states of HM.

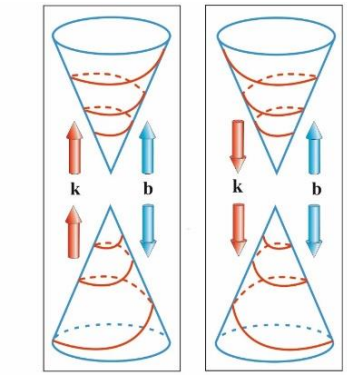

Fig.1. Schematic representation of possible configurations of a conical magnetic helix, defined by the **k** and **b** vectors and the $\mathbf{k}\otimes\mathbf{b}$ tensor. The left and right patterns reflect enantiomorphic states with symmetry of the group of right and left screws, respectively.

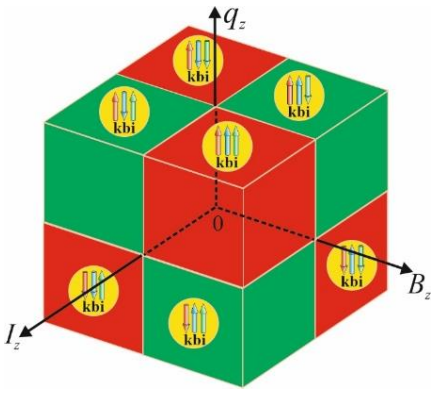

Fig.2. A state diagram for a helimagnet in the variables B_z, I_z, q_z. Regions for $\varepsilon=+1$ are shown in red, regions for $\varepsilon=-1$ are green. The colored arrows indicate the directions of the unit vectors **k**, **b**, and **i**.

The research was supported by RFBR (project No. 19-02-00057).

References

[1] V.V. Ustinov and I.A. Yasyulevich, Phys. Met. Metallogr. 121, 223 (2020).
[2] V.V. Ustinov and I.A. Yasyulevich, Phys. Rev. B 102, 134431 (2020).

Transverse magnetic routing of light emission and plasmon-to-exciton spin conversion in semiconductor-metal hybrid nanostructures

Akimov I.A.[1,2]

[1]*Experimentelle Physik 2, Technische Universität Dortmund, 44221 Dortmund, Germany*
[2]*Ioffe Institute, Russian Academy of Sciences, 194021 St. Petersburg, Russia*

Tailoring the optical and magnetic properties of semiconductor structures by bringing them together with plasmonic and ferromagnetic materials can be used to establish new functionalities in spintronic and photonic devices. The talk is focused on manifestation of novel magneto-optical phenomena in hybrid structures, which combine semiconductors quantum wells (QW) with excellent optical properties and metalic (plasmonic) nanostructures (gratings) with strong localization of electromagnetic field and tailored polarization properties.

First, a new class of emission phenomena where directionality is established perpendicular to the externally applied magnetic field for light sources located in the vicinity of a surface is presented. Here, we revealed transverse magnetic routing of light emission for excitons in a diluted-magnetic semiconductor QW [1]. When the distance between the excitons and the surface is large, the transverse spin of the emitted light is caused by the far-field interference effect and the routing is weak. The strongest directionality is achieved for a QW located several tens of nm apart from a metal-semiconductor interface. At such distance the QW is coupled to surface plasmon polaritons, that carry large transverse spin (spin flux) and are efficiently controlled by the magnetic field direction. In hybrid plasmonic semiconductor structures the directionality can reach up to 60%, which means that the ratio of light intensities for opposite emission angles is equal to 4.

Second, we demonstrate optical orientation of electron spins by linearly polarized light via plasmon-to-exciton spin conversion in the same type of hybrid plasmonic structures [2]. The metallic grating is exploited for the generation of plasmonic spin fluxes on ultimately short timescales. Using a pump-probe Kerr rotation experiment with 30 fs optical pulses we resolve in time the THz Larmor precession of photoexcited electron spins in external magnetic field, which is applied in-plane of the QW structure along the SPP propagation direction. It is demonstrated that the pump induced orientation of the photoexcited electron spins is locked to the propagation direction of the optically excited SPPs in hybrid nanostructure. Next, we show that using the polarization of the incident light as an additional degree of freedom, one can adjust not only the longitudinal, but also the transverse electron spin components normal to the light propagation at will.

References

[1] F. Spitzer, A.N. Poddubny, I.A. Akimov, et al., "Routing the emission of a near-surface light source by a magnetic field", Nature Physics **14**, 1043 (2018).

[2] I. A. Akimov, A. N. Poddubny, J. Vondran, et al., Plasmon-to-exciton spin conversion in semiconductor-metal hybrid nanostructures, Phys. Rev. B **103**, 085425 (2021).

Tunable spin-wave transport in magnonic microstructures

Sadovnikov A.V[1]., Beginin E.N.[1], Nikitov S.A.[1]

[1]Saratov State University, 410012, Saratov, Russian Federation
[2]Kotel'nikov Institute of Radioengineering and Electronics, RAS, 125009,Moscow, Russian Federation

In recent years much research has been directed towards the use of spin waves for signal processing at microwave and subterahertz frequencies due to the possibility to carry the information signal without the transmission of a charge current[1]. In the framework of the 2021 magnonics roadmap the straintronic is separated as the versatile tool to control the spin wave propagation [2]. The strain-mediated spin-wave channels can be used to route the magnonic information signal. The magnon straintronics could provide to fabricating magnonic platforms for energy-efficient signal processing [3]. Recent theoretical and experimental studies suggest that strain can be used to engineer energy-efficient complicated 2D and 3D piezoelectric heterostructures such as ferromagnetic/piezoelectric bi- and multilayers[4-7]. The strain-mediated control of spin-wave propagation was demonstrated via the experimental observations of the spin-wave coupling phenomena in different magnonic structures based on the adjacent magnonic crystals and adjacent magnetic yttrium iron garnet stripes in the form of magnonic spin-wave couplers. The model describing the spin-wave transport was proposed based on the self-consistent equations via the solution of the micromagnetic task in couple with the finite-element simulation of the static strain/stress in the ferromagnetic/piezoelectric structure. The obtained results open new perspectives for the future-generation electronics using integrated magnonic networks both in micro- and nanoscale [8].

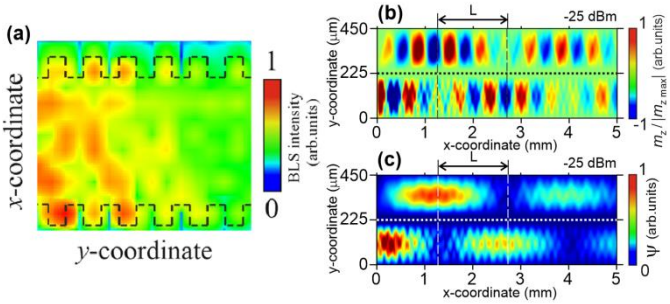

Fig.1. (a) BLS map of spin-wave propagation in magnonic crystal. (b) The distribution of z-component of dynamic magnetization under the influence of induced stress on the surface of YIG stripes. (c) Spin-wave intensity in lateral YIG stripes.

Here we report on strain mediated control of the spin-wave transport along the magnonic crystal with PZT layer. Magnonic crystal consists of yttrium iron garnet (YIG) "alligator-type" waveguide. We demonstrate the voltage-driven and laser-induced nonreciprocity of spin waves in the ferromagnetic-semiconductor and ferromagnetic-piezoelectric structure. The numerical model based on micromagnetic simulation was proposed. The multimode coupling regime was revealed by means of Brillouin light-scattering (BLS) spectroscopy and microwave spectroscopy techniques. The proposed structure can be used for frequency selective spin-wave

wave separation (demultiplexing) with the energy efficient tunability of microwave characteristics.

This work was supported by the Russian Science Foundation (Project #20-79-10191).

References

[1] Nikitov S A, et al, Phys. Usp. 63 (10) (2020);
[2] A. Barman, G. Gubbiotti, et al ," J. of Phys.: Condensed Matter (2021)
[3] Y. K. Fetisov and G. Srinivasan, Appl. Phys. Lett. 88, 143503 (2006).
[4] A.V. Sadovnikov, A. A. Grachev, et al, Physical Review Applied, 7, 014013 (2017)
[5] A. V. Sadovnikov, A. A. Grachev, et al, stripes, Phys. Rev. Lett. 120, 257203 (2018)
[6] A.V. Sadovnikov , A.A. Grachev, et al, IEEE Magn. Letters., 10, 5506405 (2019)
[7] A. V. Sadovnikov, S. A. Nikitov, et al Phys. Rev. B 99, 054424. 2019.

Exchange interaction under optical pumping and ultrahigh pressure in magnetic insulators

Gavrichkov V.A.[1], Polukeev S.I.[1], Ovchinnikov S.G.[1]

[1] *Kirensky Institute of Physics, Federal Research Center KSC SB RAS, 660036, Krasnoyarsk, Russia*

Magnetic order results from the interatomic exchange interaction of magnetic moments of ions that usually are in the grounds state. We discuss two situations when a contribution of the ionic excited states to the exchange interaction is important [1], the effect of resonant optical pumping of the d-d excitations and the effect of spin crossover under static high pressure. In both cases ionic spin in the initial and final states are different. Thus, the induced forbidden d-d excitations, for example, from the ground term of Fe^{+3} with S=5/2 into the excited term with S=3/2 may be considered as a dynamic spin crossover. The ultrafast magnetic dynamics under optical pumping have been studied by several groups, for example [2]. Recently we have shown that the d_d transitions from the $^6A_1$ ground state to the $^4T_2$ in $FeBO_3$ result in the exchange interaction sign inversion. While two Fe^{+3} ions with S=5/2 have the antiferromagnetic (AFM) interaction, the excited ion in $^4T_2$ state has the ferromagnetic interaction with its high spin 5/2 neighbour, and this conclusion agrees with the experimentally found origin of the ultrafast magnetic dynamics in $FeBO_3$ [3].

Under static high pressure the exchange interaction sign changes was also predicted. When the AFM high spin state in $FeBO_3$ transforms into the low spin S=1/2 state above the spin crossover pressure, the exchange interaction becomes the ferromagnetic one [4]. Recently, ultrafast pump-probe spectroscopy under high pressure in the diamond anvil cell conditions became available [5]. The time-resolved ARPES study of the $MoTe_2$ has revealed the dynamical modulation of the electronic correlations, particularly the decrease of the Hubbard U and Hund exchange coupling J resulting from the pump pulse [6]. It opens the possibility to realize the dynamical spin crossover under high pressure.

We are thankful to the RSF for a financial support under the project No. 18-12-00022 P.

References

[1] V.A. Gavrichkov, S.I. Polukeev and S.G. Ovchinnikov, Phys. Rev. B 101, 094409 (2020).

[2] A.M. Kalashnikova, A.V.Kimel, R.V.Pisarev, Physics-Uspekhi, 185, 1064 (2015).

[3] R.V. Mikhaylovskiy, T.J. Huisman, V.A. Gavrichkov, *et al.,* Physical Review Letters, 125, 157201 (2020).

[4] V.A. Gavrichkov, S.I. Polukeev and S.G. Ovchinnikov, JETP, 127, 713 (2018).

[5] Yanling Wu *et al*, Chin.Phys.Lett. 37, 4 047801 (2020).

[6] S. Beaulieu *et al*, arXiv:2003.04059 (2021).

Light-matter interactions in metal-dielectric nanocavities with tunable permittivity: fundamentals and applications

Nicolò Maccaferri[1,2]

[1]*Department of Physics and Materials Science, University of Luxembourg, 1511 Luxembourg, Luxembourg*
[2] *Department of Physics, Umeå University, 901 87, Umeå, Sweden*

Metal-dielectric multilayers composed by nm-thick films support a wide landscape of sub-diffraction optical modes, which can be excited via coupling with nanoscale diffraction gratings [1] or by local excitations, for instance by using high-energy electron beams [2]. In this framework, we experimentally demonstrate how disc-shaped multilayered metal-dielectric nanostructures can couple to far-field radiation and enable a full control of absorption and scattering of light at visible and near-infrared frequencies [3]. At the same time, we show that these nanostructures can enable a resonant magnetically induced modulation of the light polarization by exciting either electric or magnetic optical modes [4]. Moreover, the exploitation of the metal-dielectric interface-induced symmetry breaking has been explored as possible route to achieve enhanced nonlinear optical emission [5], largely independent from the exciting polarization and angle of incidence, unlocking promising applications of these structures as solvable nanostructures to generate visible light by using near-infrared (NIR) radiation. These multilayered metal-dielectric nanoparticles exhibit also a high (> 70%) absorption efficiency in the NIR region, and their light-to-heat conversion is demonstrated by a much larger temperature increase than that of metallic nanostructures with the same geometry and volume. As proof-of-concept, we introduce an approach for efficient in vitro hyperthermia of living cells with negligible cytotoxicity [6]. This type of architectures can also be used for a plenty of applications spanning from the detection of deep sub-wavelength deformation [7] and ultra-high-resolution imaging [8], to temperature sensing [9] and tailored ultrafast all-optical switching of light states with a relative modulation depth exceeding 100% [10].

References

[1] N. Maccaferri et al., APL Photonics 5(7), 076109 (2020).
[2] T. Isoniemi et al., Adv. Opt. Mater. 8(13), 2000277 (2020).
[3] N. Maccaferri et al., Nano Lett. 19(3), 1851–1859 (2019).
[4] J. Kuttruff et al., arXiv:2103.14180 (2021).
[5] N. Maccaferri et al., ACS Photonics 8(2), 512-520 (2021).
[6] Y. Zhao et al., arXiv:2005.13296 (2020).
[7] A. Carrara et al., Adv. Opt. Mater. 8(18), 2000609 (2020).
[8] V. Caligiuri et al., ACS Appl. Nano Mater. 3(12), 12218-12230 (2020).
[9] A. Gabbani et al., in preparation (2021)
[10] J. Kuttruff et al., Comm. Phys. 3, 114 (2020).

Resolving chicken-or-egg causality dilemma for magneto-structural phase transition in FeRh in high magnetic fields

A. V. Kimel
Radboud University, Institute for Molecules and Materials. Nijmegen, The Netherlands

The debates about the nature of the counter-intuitive heat induced ferromagnetism in FeRh have been going on already for 60 years resembling a dispute about chicken-or-egg causality dilemma[1-3]. While FeRh is antiferromagnetic at low temperatures, heating above 370 K turns the material into a ferromagnet with an expanded lattice. If it is a magnetic phase transition, which drives the lattice, or structural phase transition, which causes the changes of magnetic order, is a question, which is constantly raised ever again. Here we resolve this magnetism-or-lattice causality dilemma by accelerating the magnetic dynamics in high fields up to 25 T while observing both structural and magnetic changes in time domain with the help of optical and magneto-optical measurements, respectively [4]. We discover the regime of the ultimately fast emergence of ferromagnetism in step with the structural changes showing that magnetism-or-lattice causality dilemma is resolved by simultaneous evolution of the both actors.

References

[1] C.Kittel, Model of exchange-inversion magnetization. Physical Review, 120, 335(1960).
[2] P. Tu, A. J. Heeger, J. S. Kouvel, & J. B. Comly, Mechanism for the First-Order Magnetic Transition in the FeRh System J. Appl. Phys. 40, 1368 (1969).
[3] G. Ju et al. Ultrafast generation of ferromagnetic order via a laser-induced phase transformation in FeRh thin films. Phys. Rev. Let. 93, 197403 (2004).
[4] I. A. Dolgikh, T. G. H. Blank, G. Li, K. H. Prabhakara, R. Medapalli, S. K. K. Patel, E. E. Fullerton, E. I. Kunitsyna, O. V. Koplak, J. H. Mentink, A. K. Zvezdin, P. C. M. Christianen & A. V. Kimel, Ultrafast Emergence of Ferromagnetism in Antiferromagnetic FeRh in High Magnetic Fields (in preparation).

Control of interlayer exchange interaction in multilayer magnetic nanostructures: magnetoelectric and magnetocaloric effects

A.A.Fraerman

Institute for physics of microstructures RAS, GSP-105, Nizhny Novgorod, 603950, Russia

The problem of reducing energy losses is universal and fully concerns the use of magnetic materials. First, very large electric currents are required to control the magnetic state and dynamic properties of memory cells and magnetic nano-oscillators. This leads to heating of the working elements and low efficiency. the entire device. One of the possible ways to solve the problem is magnetization reversal under the influence of an electric field, i.e. use of the magnetoelectric effect. There are different approaches to implementing this feature. In particular, it is possible to electrically control the interlayer exchange interaction in magnetic tunnel contacts. Indeed, the energy of the exchange interaction of two ferromagnetic layers of the tunnel contact can be represented in the form $\varepsilon_{ex} = J(\boldsymbol{E})(\boldsymbol{M_1} \cdot \boldsymbol{M_2})$), where the interaction constant $J(\boldsymbol{E})$ depends on the voltage $\boldsymbol{E}$ applied to the magnetic contact. The report presents the results of our recent experiments with tunneling contacts CoFe / MgO / CoFe, which confirm the possibility of controlling the interlayer interaction under the action of an electric field [1].
Another area of work in the field of energy-saving magnetic materials is the problem of creating a magnetic refrigerator, the operation of which is based on the magnetocaloric effect. One of the problems of the "magnetic refrigerator" is the need to apply large magnetic fields ~ 1T. We have proposed a method for reducing these fields by using the spin valve effect in multilayer structures containing magnetic layers with different Curie temperatures. Then, the energy of the exchange interaction of two "strong" ferromagnetic layers through a spacer of a "weak" ferromagnet can be represented as $\varepsilon_{ex} = J(\mathrm{T})(\boldsymbol{M_1} \cdot \boldsymbol{M_2})$, where the interaction constant *J (T)* depends on the temperature of the sample *T*. The report presents the results of an experimental study of the magnetocaloric effect in multilayer structures CoFe / NiCu / NiFe and Fe / Gd / Fe, confirming the possibility of significant cooling in relatively low fields <0.1T [2-4].
This work was supported by the Russian Science Foundation # 21-12-00271

References

[1] I. Pashen'kin, M.Sapozhnikov, N. Gusev et al, JETP LETTERS, 111,690 (2020),
[2] M. A. Kuznetsov, I. Y. Pashenkin, N. I. Polushkin et al, J. Appl. Phys. 127, 183904 (2020)
[3] S. N. Vdovichev, N. I. Polushkin, I. D. Rodionov, et al, Phys. Rev. B 98, 014428 (2018)
[4] A.A.Fraerman, JETP LETTERS 113, 356-363 (2021)

On the magnetoelectricity in micromagnetism: the electric field-induced nucleation of 180^0-, 90^0-, and 0^0- domain walls

Pyatakov[1] A.P., Ren[2] W, Sundaresan[3] A.

1) M.V. Lomonosov Moscow State University, 119991, Moscow, Russia
2) Materials Genome Institute Physics Department, Shanghai University, Shanghai, China
3) Jawaharlal Nehru Centre for Advanced Scientific Research, Bangalore, India

More than a decade ago I.E. Dzyaloshinskii in his seminal paper [1] proposed the electric field nucleation of magnetic domain wall in single domain state. For topological reasons the conventional 180-degree domain wall cannot appear alone: the total angle of magnetization rotation in this type of the structure should be zero. Another factor is energy minimization so that the nucleation of magnetic topological defect should occur in the vicinity of the electrode. For these arguments the electric field-induced magnetic inhomogeneity should be either the bubble domain or the domain wall of special type, the zero degree one.

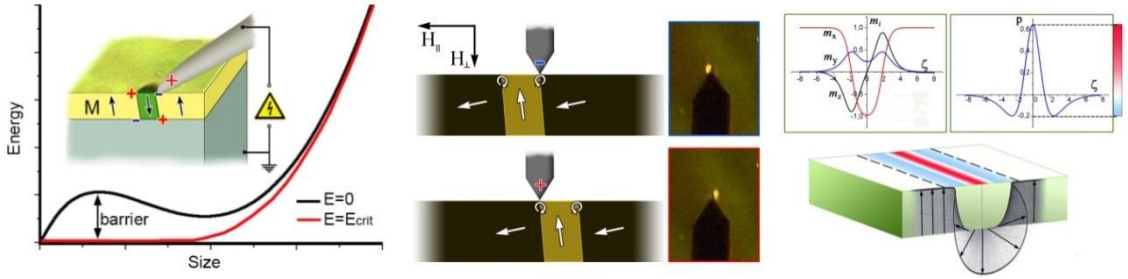

a) b) c)

Fig.1 The electric field nucleation of domains and domain walls: a) the composite experimental/schematic picture of 180^0-bubble domain generation by electric tip [2] b) the electric field-induced nucleation of 90^0 domain by atomic force microscope cantilever tip [3] c) the conceptual scheme of 0^0-domain nucleation by stripe electrode [4].

In this report we consider the experimental and theoretical works on electric field nucleation of various types of domain boundaries and their improper ferroelectricity [1-6].

The work is supported by joint RFBR grant #18-52-80028 Brics_T.

References

[1] I. Dzyaloshinskii, EPL **83**, 67001 (2008).
[2] D. P. Kulikova et al, Phys. Status Solidi - Rapid Res. Lett. **12**, 1800066 (2018).
[3] K. S. Antipin, et al, J. Appl. Phys. **129**, 24103 (2021).
[4] F. A. Maksutova, R. V. Solonetskiy, R. M. Vakhitov, and A. P. Pyatakov, EPL (Europhysics Lett). **129**, 27004 (2020).
[5] Y. Yang, H. Xiang, H. Zhao, A. Stroppa, J. Zhang, S. Cao, J. Íñiguez, L. Bellaiche, W. Ren, Physical Review B, 96 (2017)
[6] P. Yanda, S. Mishra, A. Sundaresan, Phys. Rev. Materials 5, 074406 (2021)

Magnon BEC aplication for quantum computing

Yu. M. Bunkov

M-Granat, Russian Quantum Center, 30, B. Bulvar, Skolkovo, 121205, Moscow, Russia

Our group "Quantum magnonics" is developing a new platform for quantum computing. This platform is based on a quantum property of magnons to form a Bose condensate at its high concentration. Magnons are quasiparticles in magnetically ordered materials that describe elementary excitations of the ground state. They possess spin equal to 1 and accordingly obey Bose statistics. In thermal equilibrium, the density of magnons is not significant and their properties are well described in the linear approximation. However, the concentration of magnons can be enhanced up to a very high number by pumping them under magnetic resonance conditions. The deviation of magnetization of Yttrium Iron Garnet (YIG) up to a 3^o leads to the formation of magnon Bose-Einstain condensation (mBEC) [1]. In the experiments carried out, we use out of plane magnetized epitaxial YIG film. Under these conditions, the magnons are repelled, the potential of which leads to the formation of the energy gap, and the stability of magnon supercurrent. Under these conditions, the properties of magnons are similar to their properties in the superfreight antiferromagnetic ^{3}He-B, where mBEC and magnon superuidity were discovered for the first time [2]. The first results of our experiments with mBEC in YIG film are very promising [3, 4, 5].

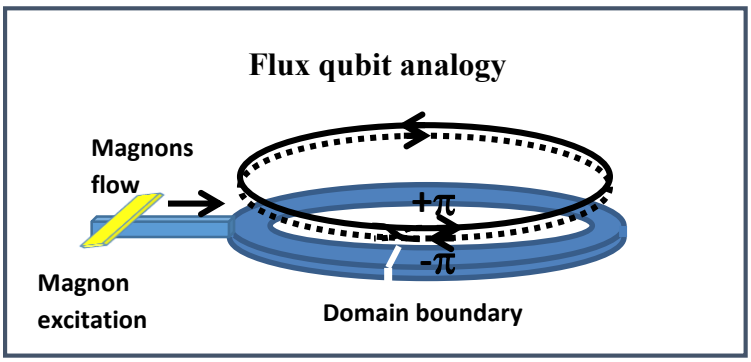

Fig. 1. Sketch of qubit based on the superposition of magnon supercurrents. On the left, the flow of excited magnons, which fills the YIG ring by mBEC. The domain wall forms π phase jump, which generate supercurrents. The states $J_+ + J_-$ and $J_+ - J_-$ forms a two quantum levels of qubit.

We consider three possible options for to form a qubit based on mBEK. First of all it is a qubit on the superposition of two circular magnon supercurrents (see Fig. 1). The stabilized domain boundary should change the phase of currents on π and, accordingly, form two quantum states with clockwise and counterclockwise circulation. These states should form two quantum states with a gap, similar to the case of a superconducting ring with Josephson junction. The second scheme is based on the interaction of two mBECs located in two YIG samples, which are connected by electromagnetic or acoustic interaction. The third scheme is based on composite magnon-photon qubit consisting of two or more samples with mBEC placed in high quality resonator. In this case, the interaction between mBECs can be controlled by changing

the local magnetic field on each sample or selectively exciting magnons in the each of sample. And finally, the qubit can be formed by two states in the same sample under double frequency parametric pumping. In this case, the difference between states is a phase that is shifted to π (see Fig. 2). Parametric pump can support both states. The energy barrier between states determines by pump amplitude. Quantum manipulations between states can be made by RFe pulses. Adiabatic approach can be made by changing the amplitude of parametric pumping.

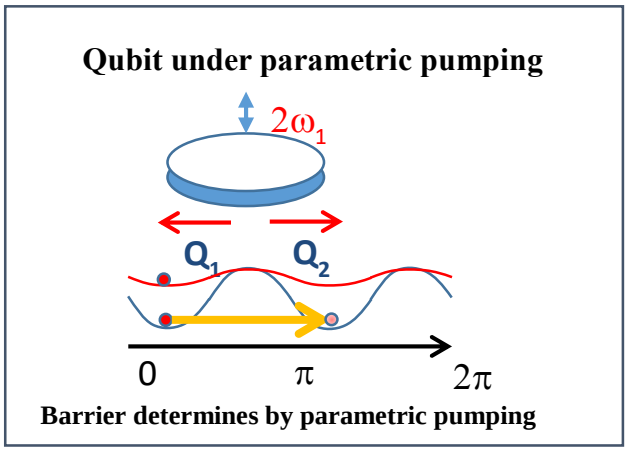

Fig. 2. Two states with phase differences π. The magnon density is stabilized by parametric pumping. The magnitude of the barrier determines by the pumping amplitude.

The methods of optical reading out of qubit states, its phase and amplitude is also preview and is currently in development.

Financial support by the Russian Science Foundation within the grant 19-12-00397 "Spin Superuids" is gratefully acknowledged.

References

[1] Yu. M. Bunkov, V. L. Safonov, J. Mag. Mag. Mat. 452, 30 (2018).
[2] Yu. M. Bunkov, G. E. Volovik, "Spin Superuidity and Magnon BEC" in Novel Superfluids, (eds. Bennemann & Ketterson), Oxford Univ. Press, Oxford, (2013).
[3] Yu. M. Bunkov, A. N. Kuzmichev, T. R. Sa_n, P. M. Vetoshko, V. I. Belotelov, M. S. Tagirov, Scientific Reports, 11, 7673 (2021).
[4] P. M. Vetoshko, G. A. Knyazev A. N. Kuzmichev, A. A. Holin, V. I. Belotelov, and Yu. M. Bunkov, JETP Lett., 112, 299 (2020).
[5] A. N. Kuzmichev, P. M. Vetoshko, G. A. Knyazev V. I. Belotelov, Yu. M. Bunkov, JETP Lett., 112, 710 (2020).

Frontiers of ultrafast magneto-acoustics

Vasily Temnov[1,2]

[1]*Institut des Molécules et Matériaux du Mans, UMR CNRS 6283, Le Mans Université, 72085 Le Mans, France*
[2]*LSI Ecole Polytechnique, CEA/DRF/IRAMIS, CNRS, Institut Polytechnique de Paris, F-91128 Palaiseau, France*

Here I review recent experimental and theoretical advances in ultrafast magneto-acoustics in magnetostrictive materials and nanostructures in the GHz-to-THz frequency range [1,2]. Ultrafast magneto-acoustics investigates the coupling between elementary excitations of magnetic order with lattice vibrations. The first example discusses magneto-elastic excitations of ferromagnetic resonance (FMR) with quasi-monochromatic GHz-frequency surface acoustic waves [3,4]. The underlying theory is reduced to an elementary equation of an externally driven parametric FMR-oscillator: the model that captures all essential experimental findings such as the resonant enhancement of FMR amplitude, the linear parametric sum- and difference frequency mixing and generation of fractional parametric frequencies. The second example discusses show how ~100 GHz frequency exchange magnons in ferromagnetic thin films are excited by ultrashort pulses of longitudinal acoustic phonons: the dominant role of the acoustic bandwidth in this process is revealed [5]. The outlook discusses some forward-looking simulations of resonantly enhanced interactions between acoustic and magnonic cavity modes in suspended ferromagnetic thin films and magneto-elastic coupling with THz-frequency inertial magnons [6], the new type of magnetic excitations predicted recently.

References

[1] V.V. Temnov, L.N. Kotov, I.V Bychkov, Journal of Physics D: Applied Physics, in *the 2022 Magneto-Optics Roadmap* (2022, forthcoming)

[2] V.V. Temnov, I. Razdolski, T. Pezeril, D. Makarov, D. Seletskiy, A. Melnikov, K.A. Nelson, J. Opt. 18, 093002 (2016)

[3] C.L. Chang, A.M. Lomonosov, J. Janušonis, V.S. Vlasov, V.V. Temnov, R.I. Tobey, Phys. Rev. B 95, 060409 (2017)

[4] V.S. Vlasov, A.M. Lomonosov, A.V. Golov, L.N. Kotov, V. Besse, A. Alekhin, D.A. Kuzmin, I.V. Bychkov, V.V. Temnov, Phys. Rev. B 101, 024425 (2020)

[5] V. Besse, A. Golov, V.S. Vlasov, A. Alekhin, L.N. Kotov, D.A. Kuzmin, I.V. Bychkov, V.V. Temnov, J. Magn. Magn. Mat. 502, 166320 (2020)

[6] A. Lomonosov, V.V. Temnov, J.-E. Wegrowe, Phys. Rev. B 104, 054425 (2021)

Bound states in continuum: Some intriguing results

Venu Gopal Achanta

National Physical Laboratory, Dr. K. S. Krishnan Marg, New Delhi 110012 INDIA
(On Lien from Tata Institute of Fundamental Research, Homi Bhabha Road, Mumbai 400005 INDIA)

The growth of semiconductor technology has revolutionized the human life in many ways with the development of electronic and opto-electronic applications. For future, nanophotonics is envisaged to play a crucial role where all-dielectric metamaterials with no metallic losses that effect the response of plasmonic structures are essential. For light-matter interaction, high quality factor (Q) structures are interesting. One of the semiconductor physics ideas that is well pursued in the recent times is the bound state in continuum (BIC) as the BIC resonance is shown to offer very high Q (in principle, infinity). While BIC resonance is an abstract concept with zero linewidth, quasi-BIC resonances in the vicinity of the BIC resonance could be of practical use. BIC resonance has interesting polarization properties. Other interesting concept from semiconductors is, superlattices which show the concept of Brillouin zone folding which can be used for engineering the band structure. In polar dielectric thin films, Berreman modes are excited at the longitudinal optical phonon mode useful in infrared nanophotonics.

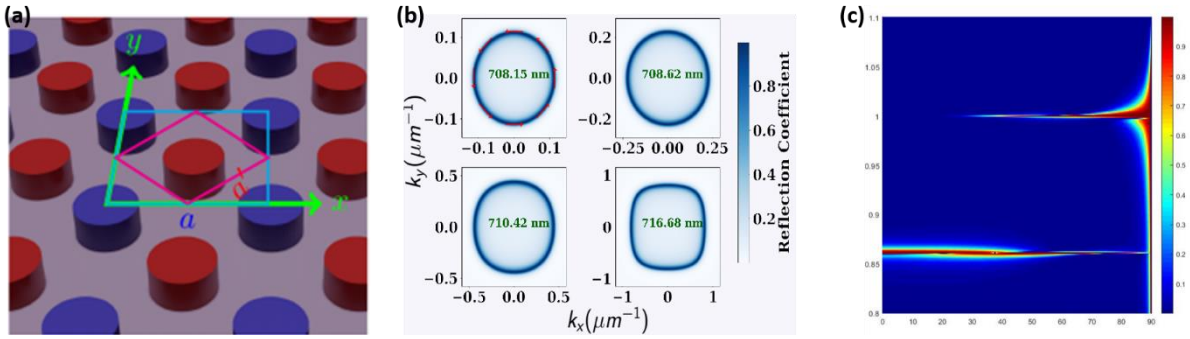

Fig. 1 (a) 2-d square lattice with dimension of alternating dielectric discs in a row changed. (b) RCWA calculated reflection coefficient showing circular symmetry for quais-BIC region and broken circular symmetry for leaky modes. (c) Numerical simulations showing the Berreman and epsilon near zero modes.

In this talk I will show examples of how zone folding due to phase change results in polarization independent BIC resonance in a square lattice (Fig.1(a)), interesting application of BIC mode in orbital angular momentum state generation (Fig. 1(b)) and the possibility of the evolution of leaky Berreman mode to BIC resonance in the presence of a thin metal film (Fig1(c)).

Acknowledgments : The results presented are 3 works done in partial collaboration with Pravin Vaity, Abhinav Kala, H. M. Gupta, Vladimir Tuz, Y. S. Kivshar, S. Dutta Gupta and G. Remesh.

Surface and Interface Nano-Engineering of Magnetic Thin Films for Controlled Magneto-Optical Effects

Yujun Song[1, 2*], Vladimir I. Belotelov[3,4] Peiyang Lou[1], Chang Zhang[1], Xiaomin Zhu[1]

[1] School of Mathematics and Physics, Research Center of Modern Physical Technology, Beijing Engineering Research Center of Detection and Application for Weak Magnetic Field, University of Science and Technology Beijing, Beijing 100083, China;
[2] Zhejiang Key Laboratory of Pulsed Power Technology Translational Medicine, Ruidi Biological Technology Company, Ltd., Hangzhou, Zhejiang 311121, China;
[3] Russian Quantum Center, Moscow 143025, Russia
[4] Lomonosov Moscow State University, Moscow 119991, Russia
[*]Email: songyj@ustb.edu.cn

Abstract

Magneto-optic effects (MOEs) are numbers of phenomena in which an electromagentic wave propagates through a gyrotropic or gyromagnetic medium that has been altered by the presence of a quasistatic magnetic field, where left- and right-rotating elliptical polarizations can propagate at different speeds, leading to a number of important physical phenomena. MOEs break time reversal symmetry locally as well as Lorentz reciprocity, which is one necessary condition to construct devices such as optical isolators,optical rotators and optical isomers. With the breakthrough of the physical mechanism of MOE (e.g., spin-orbit coupling, spin-lattice coupling) and the extended new application (e.g., weak detection, laser induced magnetization/demagnetization, spin qubit control), particularly the recently developed time-resolved magneto-optical Kerr effect detection based on ultra-fast laser pump-probing technique and the magneto-optical imaging technology, MOEs have been the efficient tools to study the intrinsic mechanism and the related multi-body coupling of light-matter (e.g., 2D/nanostructure materials) interaction. These studies also result into the development of novel optical technologies (e.g., THz emitter, high-order harmonics) and the discovery of ultrasensitive 2D/nanostructure materials for the spintronics and the quantum manipulation.

Here, we will summarize the above progress in the MOEs and then discuss the key issues in the development of hybrid materials in this field, or the surface and interface engineering of multi-layered thin films for enhanced MOE and the related spin-orbit coupling mechanism. Methods for the surface nanoengineering of thin films, such as template-assisted nanoprinting and UV-LIGA process in our group will be discussed. The interface engineering by changing the layer composition and thickness, and stacking sequences, such as using materials with strong surface plasmon resonance and/or spin-orbit coupling effect, will be discussed. It is found that surface and interface Nano-engineering can increase the MOE significantly and have the ability for the precise regulation of T-MOKE and L-MOKE. Figure 1 shows the result to enhance the MOKE rotation by adjusting the thickness of the high spin-orbit coupling Ta layer and the hole length of porous anodic alumina (AAO) templates. Our study also reveals that inversed MOKEs are observed in nanoporous heterogeneous films, showing pore size & spacing, layer composition (particularly for those with high spin-orbit coupling materials) and thickness dependence, which can be explained by spin-obit coupling, surface plasmon resonance and strong Fabry-Peru interference. In addition, induced wavelength or angle

dependent Fano-like resonance can be obtained with the sharp peak of T-MOKE, leading to the possibility to design ultrasensitive detectors based on the measurement of MOKE.

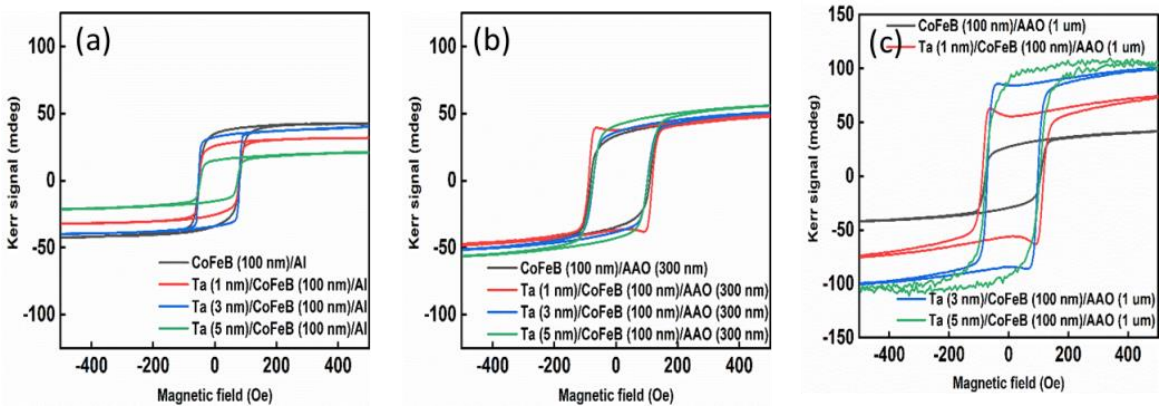

Fig. 1 Control of the MOKE rotation of Ta（x）/CoFeB/substrate thin films by the Ta layer thickness for different substrates: (a) Al plate; (b) AAO template with pore diameter of 100 nm and depth of 300 nm; (c) AAO template with pore diameter of 100 nm and depth of 1000 nm.

References

[1] G.A. Knyazev, P.O. Kapralov, N.A. Gusev,et al. ACS Photonics 5, 4951-4959 (2018).

[2] Z. Chen, L.W. Wang, Sci. Adv. 5(6)eaau8000 (2019)

[3] R. Shnaiderman, G. Wissmeyer, O. Ülgen, et al., Nature 2020, 585, 372–378.

[4] D. Huang, D. Lattery and X. Wang, ACS Applied Electronic Materials 3, 119-127 (2021).

[5] P.V. Shilina, D.O. Ignatyeva, P. O. Kapralov, et al. Nanoscale 13, 5791-5799 (2021).

[6] Song Y. (Ed.) Inorganic and Organic Thin Films, Chapter 1-5, 11-12 (Wiley-VCH, New York, 2021).

Plasmonic structures for neuroplasmonic applications

S. M. Hamidi

Magnetoplasmonic Lab, Laser and Plasma Research Institute, Shahid Beheshti University, Tehran, Iran
m_hamidi@sbu.ac.ir

Recently, a worldwide attempt for understanding the functions of brain and nervous system has been made based on new biocompatible structures and devices. Hence, various aspects of neuroscience have been investigated through different techniques such as neuroplasmonics to neural activity imaging and recording in *in vitro* or *in vivo* classifications. Due to the main physical phenomena as surface plasmon resonances (SPRs) in Neuroplasmonics, it's offers advantages comprising rapidity, high sensitivity, biological compatibility, label-free and real-time detection by benefiting from the sensing and thermal characteristics.

Neuroplasmonic can be divided to four main configurations as prism coupler, fluorescence microscopy and methods based on nanorods and plasmonic crystals. Each of them has some benefits or disadvantageous for specialized applications. Now we talk about these classifications and some applications of neuroplasmonic structures to detect and record neural activity in the worm, in tissues or in the cells. In these media, we use integrated plasmonic-ellipsometry platform to enhance signal to noise ratio and sensitivity without labeling and stimulation artifacts.

Section 1
Fundamental Physics of Functional Materials

Orbital effects in solids: recent progress

Streltsov S.V.[1]

[1]*Institute of Metal Physics, 620041, Ekaterinburg, Russia*

The properties of transition metal compounds are largely determined by nontrivial interplay of different degrees of freedom: charge, spin, lattice, but also orbital ones. Especially rich and interesting effects occur in systems with orbital degeneracy. They result in the famous Jahn--Teller effect leading to a plethora of consequences, in static and in dynamic properties, including nontrivial quantum effects. In the present talk we discuss the main phenomena in the physics of such systems, paying central attention to the novel manifestations of those. First we will shortly discuss the basic phenomena and their description and then concentrate on several specific directions in this field. One of them is the reduction of effective dimensionality in many systems with orbital degrees of freedom due to directional character of orbitals, with concomitant appearance of some instabilities leading in particular to the formation of dimers, trimers and similar clusters in a material. The properties of such cluster systems, largely determined by their orbital structure, are discussed in detail, and many specific examples of those in different materials are presented. Another big field which acquired special significance relatively recently is the role of relativistic spin--orbit interaction. The mutual influence of this interaction and the more traditional Jahn--Teller physics is treated in details in the second part of the review. In discussing all these questions special attention is paid to novel quantum effects in those.

We acknowledge support of Russian Science Foundation (project № 20-62-46047).

References

[1] D. I. Khomskii, S. V Streltsov, Chem. Rev. 121, 2992 (2021).

[2] S.V. Streltsov, D. I. Khomskii, Phys. Rev. X 10, 031043 (2020).

NMR spectroscopy of helical magnetic systems

Gippius A.A.[1,2], Tkachev A.V.[2], Zhurenko S.V.[2]

[1]*M.V. Lomonosov Moscow State University, 119991, Moscow, Russia*
[2]*P.N. Lebedev Physics Institute of RAS, 119991, Moscow, Russia*

In modern condensed matter physics, special attention is paid to the study of complex magnetic structures and, in particular, systems with helimagnetism. The helicoidal magnetic order can arise due to the competition of ferro- and antiferromagnetic interactions in frustrated systems or the Dzyaloshinsky-Moriya interaction. Helimagnetism, as a rule, is associated with a violation of the central symmetry due to the nonequivalence of the directions in the crystal relative to the propagation vector of the helicoid. Many classes of helimagnets are characterized by non-trivial properties (spontaneous electric polarization, magnetoelectric interaction, magnetoresistance), which also determines the possible use of helimagnets for the development of new functional materials for spintronics and magnetic memory.

In this talk, application of NMR spectroscopy to study various properties of helical magnetic systems is discussed. In the introduction, a brief overview of basic principles of solid state NMR and main characteristics of helical spin structures is presented. In the main part, our recent results on NMR study on FeP helimagnet [1] are discussed in detail. In particular, we observed the spin-reorientation transition of the FeP helical spin structure in the external magnetic field range of 4-7 T, which is accompanied by an effect of local field spatial redistribution at the P sites. We established the phenomenological model, which implies phase separation into field-dependent volume fractions with random and oriented responses. We have shown that there are two pairs of magnetically inequivalent phosphorus positions forming two planes of incommensurate helical local fields distribution with the angle of 47(2)º between them. We demonstrated that all observed ^{31}P spectra can be treated within a model of an isotropic helix of Fe magnetic moments in the (ab)-plane.

In conclusion, application of ^{31}P NMR spectroscopy to study the binary helimagnet FeP enabled us to obtain valuable novel information about the incommensurate helical spin structure and its evolution in external magnetic field, as well as to gain fine details of Fe-^{31}P hyperfine interactions.

This work was supported by RSCF grant № 21-72-00112.

References

[1] A.A. Gippius et al., Phys. Rev. B, 102, 214416 (2020).

Dark type discrete magnetic breathers and their stability in monoaxial chiral helimagnet

Ekomasov E.G.[1], Ovchinnikov A.S.[2], Bostrem I.G.[2], Sinitsyn V.E.[2], Fakhretdinov M.I.[1] , Kishine J.[3]

[1]Bashkir State University, 450076, Ufa, Russia
[2]Institute of Natural Sciences and Mathematics, Ural Federal University, 620026, Ekaterinburg, Russia
[3]The Open University of Japan, 261-8586, Chiba, Japan

The possibility of the existence of internal localized nonlinear excitations, namely, discrete "dark type" breathers, is shown for a one-dimensional chiral spin chain with an easy-plane anisotropy in the state of forced ferromagnetism. A spin chain of finite length L is described by the Hamiltonian:

$$H = -2J\sum_n S_n S_{n+1} + A\sum_n (S_n^z)^2 - H_0\sum_n S_n^2 + D\sum_n [S_n \times S_{n+1}]_z,$$

where S_n is the spin vector of the n site. The first term corresponds to the exchange interaction of spins along the z axis with the interaction constant $J > 0$, the second to the single-ion anisotropy of the quantity $A > 0$ of the "easy plane" type, the third term describes the Zeeman interaction with an external magnetic field H_0 directed along the axis chains z. The last term corresponds to the antisymmetric Dzyaloshinskii-Moriya exchange with the interaction vector D directed along the axis of the chain. We modify the numerical algorithm suggested in Ref. [1] to find the nonlinear solutions. Their analytical description in the continuum limit is developed, and their stability is proved by using the linear Floquet theory [2]. It is shown that "dark" breathers, in contrast to the previously considered "bright type" ones [3], which do not resonate with linear spin waves, can exist at a small values of the easy-plane magnetic anisotropy. This makes promising to detect experimentally these nonlinear excitations in real prototypes of chiral helimagnets.

The work is supported by the RFFI grant (project 20-02-00213).

References

[1] S. Rakhmanova and D.L. Mills, Phys. Rev. B 54, 9225 (1996).
[2] J.M. Khalack, Y. Zolotaryuk, and P.L. Christiansen, Chaos 13, 683 (2003).
[3] I.G Bostrem, Vl.E Sinitsyn, A.S. Ovchinnikov, E.G. Ekomasov, and J. Kishine, AIP Advances 11, 015208 (2021).

Magnetic phase diagram of Heusler alloys based on studies in pulsed magnetic fields up to 500 kOe and optical *in situ* studies up to 120 kOe

Kamantsev A.P., Koshkidko Yu.S., Dilmiyeva E.T., Koledov V.V., Shavrov V.G.

Kotelnikov IRE RAS, 125009, Moscow, Russia

Heusler alloys from the Ni_2MnGa family with additives of the 4th element, in particular Cu, have long attracted the attention of researchers [1] due to their improved functional properties: a higher magnetocaloric effect (MCE), a reduced width of thermal hysteresis, and lower temperatures of the martensitic phase transition (PT). In the Heusler alloy $Ni_{50}Mn_{18.5}Ga_{25}Cu_{6.5}$, the magnetostructural PT of the 1st order is observed in the temperature range of 300–313 K. The surface of the sample of this alloy was investigated by the optical method in situ in the fields of Bitter magnet up to 120 kOe; the method is described in detail in [2].The sample was initially in the austenite phase (H = 0 kOe), while magnetization of the sample leads to the nucleation of the martensite phase, and at H = 120 kOe, almost the entire surface of the sample is occupied by martensite twins (Fig. 1a). Subsequent demagnetization of the sample reduces the volume fraction of martensite in the alloy; however, martensite is predominantly observed on the metallographic surface; a magnetically induced first-order phase transition at T_0 = 312 K in magnetic fields up to 120 kOe is irreversible (Fig. 1a).

The maximal MCE value in this Heusler alloy obtained by the method described in [3] was ΔT = 20.5 K at T_0 = 309.2 K in pulsed field H = 500 kOe. Based on measurements of the magnetization in fields up to 70 kOe and of the MCE at 500 kOe the H-T phase diagram of the alloy was constructed. The tricritical point was found at T_{cr} = 333.8 K and H_{cr}= 302 kOe (Fig.1b), above which hysteresis-free behavior is realized as the 2nd order PT.

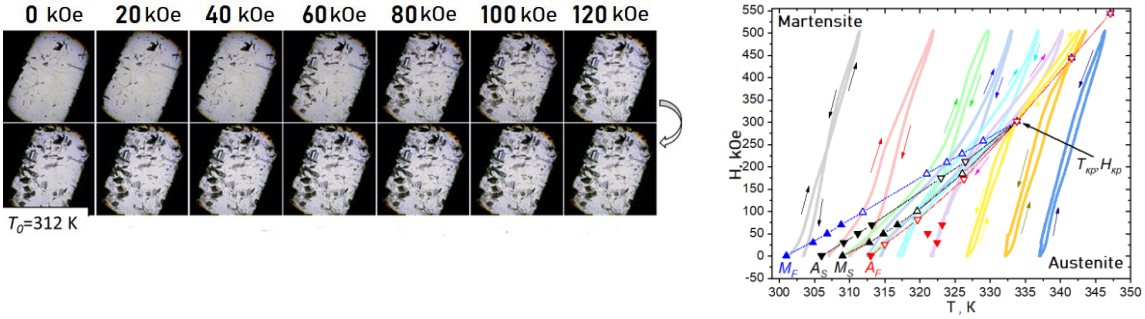

(a) (б)

Fig. 1. (a) Formation of the martensite phase in the Heusler alloy $Ni_2Mn_{0.74}Cu_{0.26}Ga$ under the action of a magnetic field up to 120 kOe under adiabatic conditions at an initial temperature of T_0 = 312 K.

(b) Magnetic phase H-T diagram of the Heusler alloy $Ni_2Mn_{0.74}Cu_{0.26}Ga$.

The work was carried out within the framework of the RFP resident grant № МК-355.2020.2.

References

[1] V. Sokolovskiy et al., Journal of Applied Physics. 114, № 18, 183913 (2013).

[2] E.T. Dilmieva et al., Bull. Russ. Acad. Sci.: Phys. 81, № 11, 1283-1288 (2017).

[3] A.P. Kamantsev et al., Physics of the Solid State. 62, № 1, 160-163 (2020).

Electronic properties of the half-metallic ferromagnet Co_2MnZ (Z= Al, Si, Ga, Ge) Heusler compounds

Semiannikova A.A.[1], Perevozchikova Yu.A.[1], Marchenkova E.B.[1], Marchenkov V.V.[1,2]

[1]*M.N. Mikheev Institute of Metal Physics, UB RAS, 620108, Ekaterinburg, Russia*
[2]*Ural Federal University, 620002, Ekaterinburg, Russia*

In half-metallic ferromagnets (HMFs) and spin gapless semiconductors (SGSs) based on Heusler compounds, close to 100% spin polarization of charge carriers can be realized. Consequently, these new materials are promising for use in spintronic devices [1]. At the Fermi level, HMF and SGS for electronic states with spin "down" have a wide (ΔE ~ 1 eV) gap, while for the opposite spin projection in the HMF there is no gap, and in SGS there is a zero energy gap [2, 3].

States close to HMF and / or SGS are observed in the Co_2YSi (Y = Ti, V, Cr, Mn, Fe, Co, Ni) Heusler compounds (see, for example, [4]). Apparently, such states can also appear in other Co-based Heusler compounds, in particular, in the Co_2MnZ system (Z = Al, Si, Ga, Ge) upon varying the Z-component, which should inevitably manifest itself in their electronic transport and magnetic properties. Thus, the purpose of this work is to study the structure, magnetic and electrical properties of the system of compounds Co_2MnZ (Z = Al, Si, Ga, Ge), to establish the regularities of their behavior and the possible relationship with the degree of spin polarization of current carriers.

As a result of the studies carried out, it was found that with a change in the Z-component, the residual resistivity ρ_0, the saturation magnetization M_s, change significantly, and there is a correlation between them as well and the spin polarization coefficients known from the literature. The normal and anomalous coefficients of the Hall effect, type and mobility of charge carriers were found. Based on the results obtained, it was suggested that the half-metallic ferromagnet Co_2MnSi compound can be used as an injector for spin-polarized electrons in spintronic devices.

The work was carried out within the framework of the state assignment of Ministry of Science and Higher Education of the Russian Federation (theme "Spin" No. AAAA-A18-118020290104-2), with partial support from the RFBR project No. 20-32-90065 and the Government of the Russian Federation (Decree No. 211, contract No. 02.A03.21.0006).

References

[1] N.A. Viglin, V.V. Ustinov, S.O. Demokritov, A.O. Shorikov, N.G. Bebenin, V.M. Tsvelikhovskaya, T.N. Pavlov, and E.I. Patrakov, Phys. Rev. B 96, 235303 (2017).

[2] M.I. Katsnelson, V.Y. Irkhin, L. Chioncel, A.I. Lichtenstein, and R.A. De Groot, Rev. Mod. Phys. 80, 315 (2008).

[3] X.L. Wang, Phys. Rev. Lett. 100, 156404 (2008).

[4] Yu.A. Perevozchikova, A.A. Semiannikova, A.N. Domozhirova, P.B. Terentyev, E.B. Marchenkova, E.I. Patrakov, M. Eisterer, P.S. Korenistov, and V.V. Marchenkov, Low Temp. Phys. 45, 789 (2019).

Looking inside a transition-metal cluster: Ba4NbTM3O12 (TM=Mn, Rh, Ir).

Komleva E.V.[1], Khomskii D.I.[2], Streltsov S.V.[1,3]

[1]*M.N. Mikheev Institute of Metal Physics UB RAS, 620137, Ekaterinburg, Russia*
[2]*II. Physikalisches Institut, Universität zu Köln, D-50937, Köln, Germany*
[3]*Ural Federal University, 620002 Ekaterinburg, Russia*

Having difficulties when describing single transition-metal (TM) ions in a crystal, one faces more serious problems with a structural cluster. Within such a cluster TM ions are tightly connected with each other that may cause new complicated phenomena and influence the choice of a model used to interpret them.

Investigation of the recently synthesized series of isostructural compounds $Ba_4NbTM_3O_{12}$ (TM=Mn, Rh, and Ir) with TM trimers in a face-sharing geometry [1,2] makes it possible to examine a tendency to the molecular orbitals (MO) formation in clusters going from 3*d* to 5*d* TM ions.

Our *ab initio* calculations of electronic and magnetic properties demonstrate gradual transition from the picture of localized electrons realized in Mn-*3d* (Figure 1a) to the MO picture for Rh-*4d* and especially for Ir-*5d* based compounds (Figure 1c and 1b) [3,4].

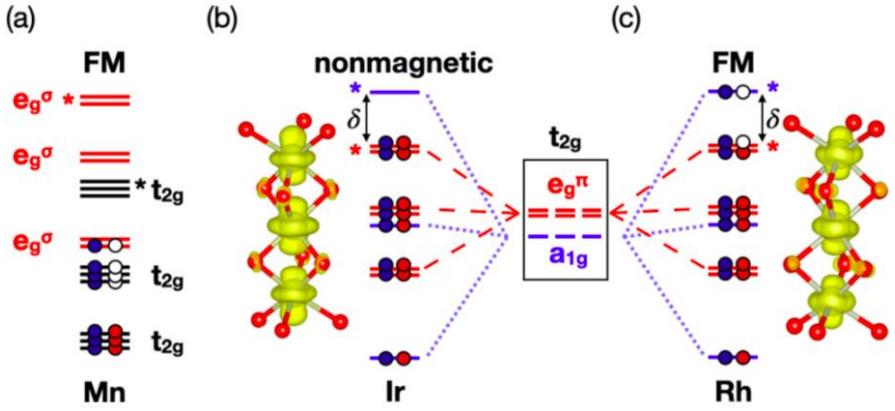

Figure 1: (a) Level diagram (with both t_{2g} and e^σ_g) for Mn trimer (localized electrons) and (b), (c) scheme of t_{2g} energy levels (no e^σ_g) for MO model and charge densities of the band above/at the Fermi level for (b) Ir and (c)

This research was supported by the Russian Foundation for Basic Researches (Grant No. RFBR 20-32-90073).

References

[1] L.T. Nguyen, T. Kong, and R. J. Cava, Mater. Res. Express **6**, 056108 (2019).

[2] L.T. Nguyen and R. J. Cava, Phys. Rev. Materials **3**, 014412 (2019).

[3] S.V. Streltsov and D. I. Khomskii, JETP Lett. **108**, 686 (2018).

[4] E.V. Komleva, D.I. Khomskii, and S.V. Streltsov, Phys. Rev. B **102**, 174448 (2020).

Iron Borate: Scientific Biography

M.B. Strugatsky

Iron borate single crystals are an extremely interesting object of numerous studies in the field of magnetism and solid state physics. Its "science intensity" is due to a rare combination of properties – magnetic, elastic, optical, resonance. It is a transparent magnet. Iron borate is a synthetic crystal grown for the first time 60 years ago. The authors are engaged in the synthesis and research of properties and effects in this material for a number of years. The report provides an overview of the study of iron borate and composite materials based on it. We consider, in particular, synthesis, surface magnetism, magnetoacoustics, magnetic resonance phenomena and much more. Modern high-tech applications of this unique crystal are also discussed.

Magnetic properties and combined hyperfine interactions in $FeBO_3$ single crystals near the Neel temperature

Lyubutin I.S.[1], Snegirev N.I.[1], Chuev M.A.[2], Starchikov S.S.[1],
Lyubutina M.V.[1], Yagupov S.V.[3] and Strugatsky M.B.[3]

[1]Shubnikov Institute of Crystallography of FSRC "Crystallography and Photonics" RAS, 119333 Moscow, Russia
[2]Valiev Institute of Physics and Technology of RAS, 117218 Moscow, Russia
[3]V.I. Vernadsky Crimean Federal University, Simferopol, Russia

The possibility of using synchrotron radiation as a high-intensity and focused Mössbauer source has already been realized at synchrotron stations in ESRF (France) and SPring-8 (Japan). It was proposed to use iron borate single crystals $FeBO_3$, which have optimal parameters for diffraction of nuclear resonance radiation, as ideal monochromators at the final stage of Mössbauer radiation tuning. However, the spectra of reflected radiation strongly depend on the hyperfine interactions in this crystal, while the required radiation parameters are achieved near the Néel point (T_N ~ 348 K) [1,2,3]. In this case, precise studies of the magnetic, electronic, and structural properties of an iron borate single crystal near the Néel point are of a great importance.

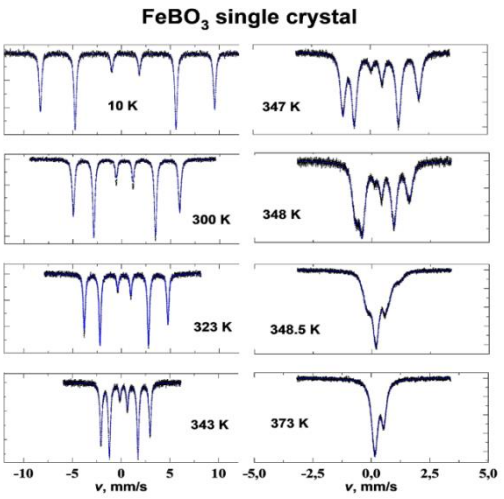

In our study, the Mössbauer spectra of $FeBO_3$ single crystals were investigated with high accuracy in the temperature range 4.2 – 400 K. The propagation vector of the Mössbauer gamma rays k_γ was directed along the *c* axis that is perpendicular to the basic plane (001) of the crystal in the hexagonal setup. The Mössbauer spectra were processed in the framework of combined magnetic and electric hyperfine interactions (Fig.1). In addition, at elevated temperatures, the thermally excited states of magnetic moments were taken into account [4]. We found that the magnetic moments of iron lie in the basal plane (001) of the crystal, and the threefold axis *c* and the main axis of the electric field gradient EFG (*Z*) are orthogonal to the direction of the magnetic moments. In addition, the values of the isomer shift, quadrupole constant, and magnetic hyperfine field were precisely examined in the $FeBO_3$ single crystal in a wide temperature range of 4.2 - 373 K. The results obtained can be very useful for tuning pure nuclear diffraction in synchrotron Mössbauer experiments.

Acknowledgment: This work was funded by RFBR, project number 19-29-12016\20-mk.

[1] G.V. Smirnov, A.I. Chumakov, V. Potapkin, et al., Phys. Rev. A., **84,** 053851. (2011).
[2] V. Potapkin, A. I. Chumakov, G. V. Smirnov et al., J. Synchrotron Radiat. **19,** 559 (2012).
[3] S.V. Yagupov, M. B. Strugatsky, et al. Crystal Growth & Design **18,** 7435 (2018).
[4] M.A. Chuev, JETP Lett. 103, 175 (2016).

Temperature- and field-induced magnetic transitions in the cobalt-containing borates

Kazak N.V.[1], Bel'skaya N.A.[1], Knyazev Yu.V.[1], Molokeev M.S.[1], Bezmaternykh L.N.[1], Velikanov D.A.[1], Yumashev V.V.[2], Gavrilkin S.Yu.[3], Ovchinnikov S.G.[1]

[1]*Kirensky Institute of Physics, FRC KSC SB RAS, 660036 Krasnoyarsk, Russia*
[2]*Institute of Chemistry and Chemical Technology, FRC KSC SB RAS, 660036 Krasnoyarsk, Russia*
[3]*Lebedev Physical Institute of RAS, 119991 Moscow, Russia*

Transition metal borates are of interest due to structural and electronic transitions, spin-state crossovers, charge ordering, and puzzle magnetic structure [1,2]. The cobalt compounds occupy a special place due to cobalt exhibits several possible oxidation states – $Co^{2+}(d^7)$, $Co^{3+}(d^6)$, and $Co^{4+}(d^5)$ as well as the ability of Co^{3+} ions to accommodate various spin states – low spin (S=0, LS), high spin (S=2, HS), and intermediate spin [3-5]. Here we present results of the comprehensive study of Co-containing borates adopting different structural types: kotoite ($Me_3B_2O_6$), pyroborate ($Me_2B_2O_5$), warwickite (Me_2BO_4), and ludwigite (Me_3BO_5). All compounds under consideration were synthesized by the flux technique. The crystal structure and the magnetic properties have been investigated by X-ray diffraction, magnetization, and specific heat experiments. The high-temperature X-ray diffraction and specific heat measurements on a Co_3BO_5 single crystal revealed the spin-state transition of the Co^{3+} ion.

The substitution effect of Co^{3+}→Fe^{3+}, Ga^{3+}, Ge^{4+}, and Nb^{5+} on the crystal structure and magnetic behavior was studied. The enhancement of exchange interactions leading to the stabilization of the ferrimagnetic state to higher temperatures and the appearance of an antiferromagnetic transition were found. All compounds exhibit strong magnetic anisotropy with the *b*-axis as the easy magnetization direction. The structural and magnetic affinity of borates is discussed.

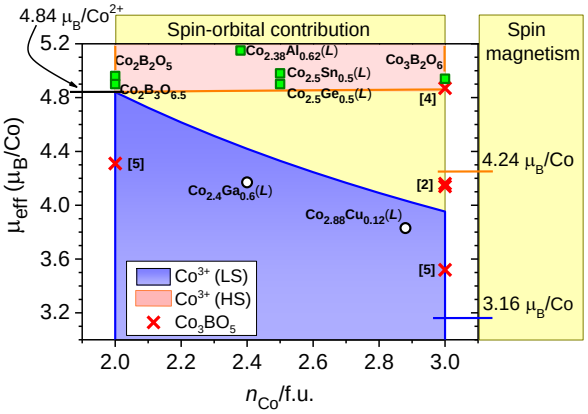

Fig. 1. Magnetic moment of Co-containing borates *vs* number of cobalt ions per formula unit. The symbol (*L*) denotes the ludwigite.

This work has been financed by the Russian Foundation for Basic Research (project no. 20-02-00559).

References

[1] P. Bordet and E. Suard, PRB 79, 144408 (2009).
[2] J. Bartolom´e, A. Arauzo, N.V. Kazak, *et al.* PRB 83, 144426 (2011).
[3] D.C. Freitas, C.P.C Medrano, D.R. Sanchez, *et al.* PRB 94, 174409 (2016).
[4] C.W. Galdino, D.C. Freitas, C.P.C. Medrano, *et al.* PRB 100, 165138 (2019).
[5] N.V. Kazak, M.S. Platunov, Yu.V. Knyazev, et al. PRB 103, 094445 (2021).

Structural stability and magnetic properties of Fe-Ni-Al and Co-Ni-Sn Heusler alloys

Buchelnikov V.D.[1], Sanosyan A.A.[1], Sokolovskiy V.V.[1], Miroshkina O.N.[1,2], Gruner M.E.[2]

[1]*Chelyabinsk State University, 454001, Chelyabinsk, Russia*
[2]*University of Duisburg-Essen, 47048, Duisburg, Germany*

Ferromagnetic shape memory alloys are promising candidates for application as actuators, sensors, magnetomechanical devices, harvesters, and magnetic cooling systems [1-3]. Such compounds can be classified as the high-performance intelligent materials with large deformation and fast response. The wide range of their potential applications is directly related to unique properties demonstrated in response to external influence [1-3].

Fe-Ni-Al and Co-Ni-Sn alloys are an interesting class of materials, as they are ductile, cheap, and easily synthesized. Moreover, while possessing a high Curie and martensitic transformation temperature. In this work, we report on systematic *ab initio* investigations of the structural and magnetic properties of $Fe_2Ni_{1+x}Al_{1-x}$ and $Co_2Ni_{1+x}Sn_{1-x}$ Heusler alloys. We calculated the ground state energy and magnetic properties of different crystal structures and degree of order. For the most favorable structures, we evaluated magnetocrystalline anisotropy and lattice free energy to assess the equilibrium properties for the compositions under study.

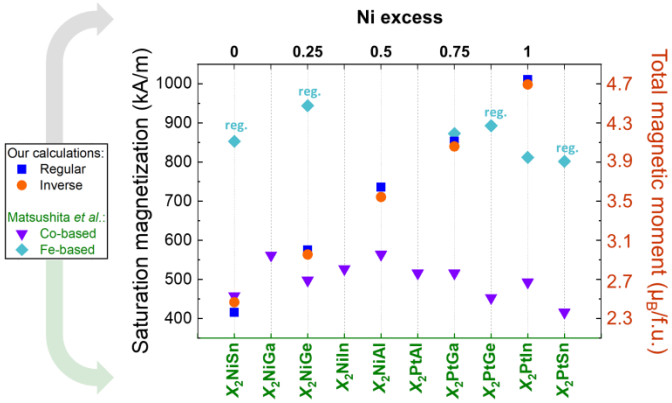

Fig. 1. Saturation magnetization and total magnetic moments for $Co_2Ni_{1+x}Sn_{1-x}$ (x = 0, 0.25, 0.5, 0.75, 1) in comparison with other Co- and Fe-based Heusler systems [3].

This work was supported by Russian Science Foundation No. 17-72-20022 and Russian Foundation for Basic Research No. 20-42-740003 and the German Research Foundation (DFG) – TRR 270, B06. Part of calculations were performed on MagnitUDE supercomputer (DFG INST 20876/209-1 and 20876/243-1 FUGG).

References

[1] A. Planes, et al., J. Phys.: Condens. Matter 21, 233201 (2009).
[2] P. Entel, et al., Mater. Sci. Forum 583, 21 (2008).
[3] Y.-I. Matsushita, et al., J. Phys. D: Appl. Phys. 50, 095002 (2017)

In situ TEM study of phase transformations in nonstoichiometric Geisler alloy $Ni_{46}Mn_{41}In_{13}$

Kuznetsov D.D.[1], Kuznetsova E.I.[2], Mashirov A.V.[1], Loshachenko A.S.[3], Danilov D.V.[3], Shandryuk G.A.[4], Kalashnikov V.S.[1], Shavrov V.G.[1], Koledov V.V.[1]

[1]*Kotelnikov Institute of Radio-engineering and Electronics, Russian Academy of Sciences, 125009, Moscow, Russia*
[2]*M.N. Miheev Institute of Metal Physics of Ural Branch of Russian Academy of Sciences, 620108, Ekaterinburg, Russia*
[3]*IRC Nanotechnology, Research Park, St. Petersburg State University, 199034, St. Petersburg, Russia*
[4]*A.V. Topchiev Institute of Petrochemical Synthesis, RAS, 119991, Moscow, Russia*

The report is dedicated to study of the metamagnetostructural transformation of the martensitic type in the $Ni_{46}Mn_{41}In_{13}$ alloy with magnetic shape memory and inverse magnetocaloric effect. The characteristic temperatures of the beginning and end of the forward and reverse martensitic transformation for bulk material were determined by differential scanning calorimetry (DSC) M_s = 253 K, M_f = 164 K, A_s = 203 K, A_f = 236 K. The characteristic features of the transformation and premartensitic states were studied by transmission electron microscopy. The estimation of the material thickness at which the martensitic transformation is blocked is carried out. The temperature dependence of the magnetization in fields of 1, 2, and 3 T. The presence of an SME demonstrates an anomaly on the $\sigma - \varepsilon$ curves in the temperature range of the beginning and end of the martensitic transformation. Curie temperature was determined by DSC and thermogravimetric analysis (TGA) T_c=325 K.

The dependence of the temperature of the onset of metamagnetostructural transformation of the martensitic type on the thickness of the sample in the form of a wedge-shaped foil is revealed. It was found that the martensite phase during the direct martensitic transformation, in thin foil regions with a thickness of less than 150 nm, begins to appear at Ms = 215 K (i.e., at temperatures lower than in the bulk material) after the first cooling-heating-cooling cycle, after the second cycle Ms = 210 K and after the third Ms = 208. A further decrease in temperature for each of the cycles leads to an increase in the proportion of martensite; however, the transformation is blocked at about 600 nm from the edge of the sample with a plate thickness of less than 50 nm, so the formation of a martensite structure is not observed here even at the temperature of liquid nitrogen (fig. 1).

The presence of (111) superstructure reflections indicate a well-ordered L21 phase in this system a=6,17 Å. The presence of (111) superstructure reflections indicate a well-ordered $L2_1$ phase in this system, fig. 2.

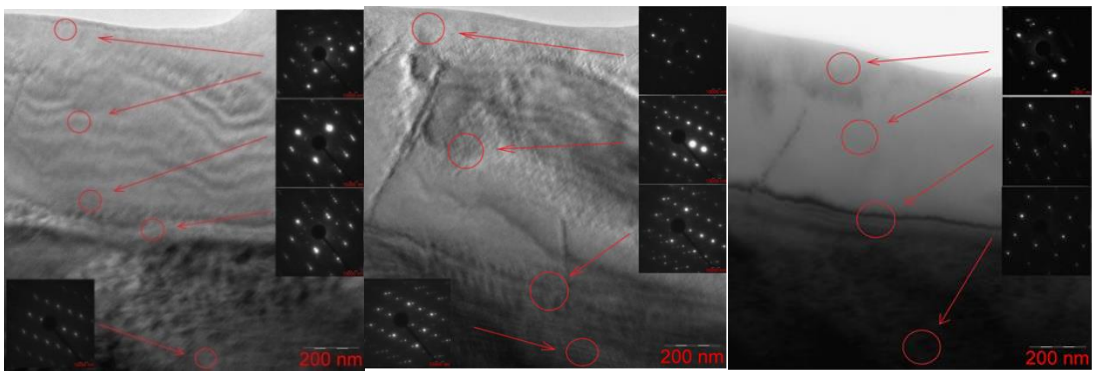

a b c

Fig. 1. Bright-field images and diffraction patterns of the selected regions of the $Ni_{46}Mn_{41}In_{13}$ alloy at temperatures of 215 K (a), 208 K (b), 100 K (c).

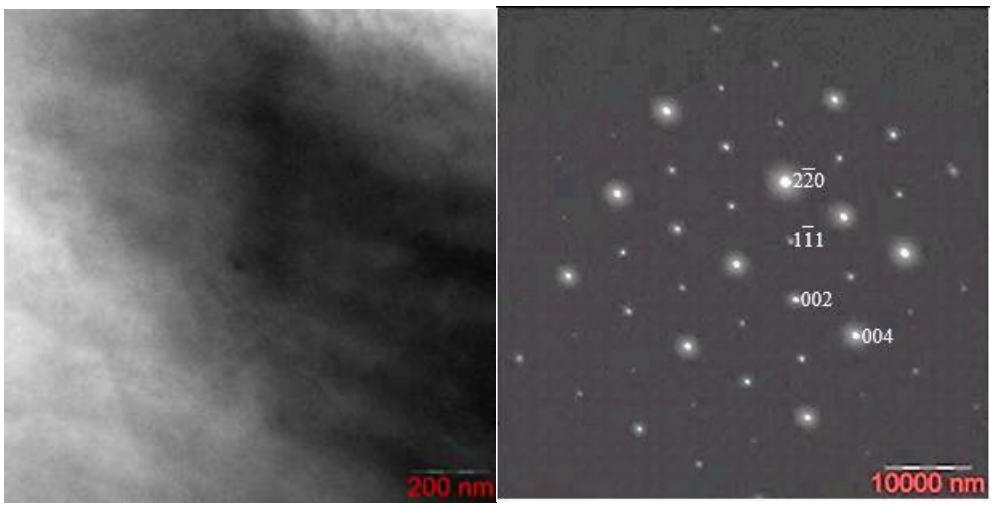

a b

Fig. 2 Microstructure of the austenitic phase of the Ni46Mn41In13 alloy: a - bright field image; b - electron diffraction pattern, zone axis [110] $_{L21}$.

The results obtained demonstrate that the phase transformation in the $Ni_{46}Mn_{41}In_{13}$ alloy occurs unevenly throughout the sample, as evidenced by the variety of the observed structures (black-and-white contrast, tweed, lamellar structure). Below Ms, the cubic L21 phase transforms into modulated martensitic variants with retained austenite. A further decrease in temperature leads to an increase in the proportion of the martensite phase; however, it was found that the martensitic transformation is completely suppressed at a plate thickness of less than 50 nm.

The temperatures of the forward and reverse martensitic transformation depend not only on the magnitude of the magnetic field, but also on the size and configuration of the sample. A decrease in the plate thickness and magnetic fields lead to a decrease in the temperature of direct martensitic transformation, expanding the region of existence of ferromagnetic austenite.

Electron microscopic studies and preparation of foils for TEM were carried out at the Interdisciplinary Resource Center for Nanotechnology, St. Petersburg State University, St. Petersburg.

Material based on superconduct YBaCuO used on magnetic levitation

Karpukhin D. A. [1,11], Terentyev Yu.A.[1,11], Shavrov V. G. [1,11], Koledov V. V. [1,11], Malinetsky G. G. [2], Sysoev M. A. [3], Brazhnik P. S. [4], Zimenkova T. S. [5], Kurenkov P. V. [6], Kamynin A.V. [7], Drozdov B. V. [8], Kovalev K. L. [9], Safonov A. A. [10], Poltavets V. N. [9], Shillo S. V. [3], Nizhelsky I. [3], Babachanakh IA.V. [11], Balabanov V. K. [11], Herman I. V. [11], Laryukhin V. S. [11], Petrov A. O. [1,11], Fongratovsky S. V. [1,11], Kamantsev A. P. [1,11], Dilmieva E. T. [1,11], Samvelov A.V. [12], Palchaev D. K. [13]

[1] Kotel'nikov institute of radio engineering and electronics of RAS, 125009, Moscow, Russia, [2] Keldysh Institute of Applied Mathematics, KIAM, 125047, Moscow, Russia, [3] Bauman Moscow State Technical University, 105005, Moscow, Russia, [4] Kurchatov Institute, 123182, Moscow, Russia, [5] Emperor Alexander I St. Petersburg State Transport University, 190031, St. Petersburg, Russia, [6] Federal state Autonomous educational institution of higher education " Russian University of transport", 127005, Moscow, Russia, [7] AO «Specmagnit», Moscow, Russia, [8] Institute of Information and Analytical-Technologies, Moscow, Russia, [9] Moscow Aviation Institute (MAI), 125993, Moscow, Russia, [10] AO «Neva Technology», St. Petersburg, Russia, [11] Sirius University of Science and Technology, 354340, Sochi, Russia, [12] AO OKB "ASTRON", Moscow, Russia, [13] Dagestan State University, 367000, Russia, Republic of Dagestan, Makhachkala

Abstract. The achievements of recent years in the field of physics and technology of magnetic functional magnetic materials, stimulate numerous pioneering applied research in various fields from energy to medicine. Of particular importance is the use of such new materials as superconductors, permanent magnets, and magnetocaloric materials to create a promising ultra-high-speed ground-based vacuum magnetolevitation transport (VMLT), which is expected to simultaneously dramatically increase the speed of movement and reduce specific energy consumption [1]. The aim of the work is an experimental study of the process of magnetic levitation of a cryostat with elements made of ceramics of a high-temperature superconductor Y-Ba-Cu-O on a model of a route made of lines of permanent magnets based on Nd-Fe-B.

Cryostat with HTSP MLT layout

The principle of operation of the magneto-levitation transport system is based on the use of the phenomenon of magnetic levitation of high-temperature superconductors of the second kind (Fig. 1.). A cryostat with a high-temperature superconductor (HTSC) of the YBaCuO composition is cooled over a track assembled from permanent magnets (Fig. 2). The HTSC transition temperature to the superconducting state is 93 K, which allows the cryostat to be cooled with liquid nitrogen.

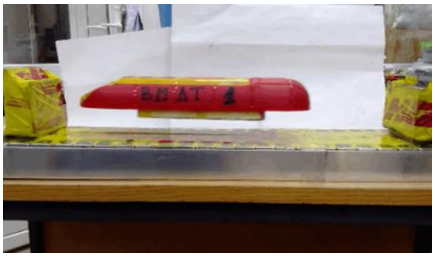

Fig. 1. The principle of magnetic levitation

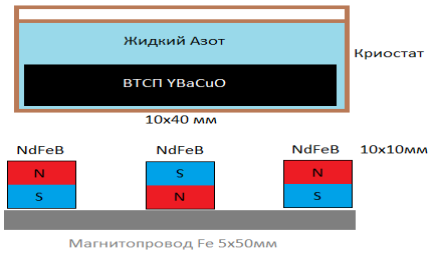

Fig. 2. Section of the MLT route

Высота захолаживания	Рабочий зазор	Установившаяся высота	Вертикальная нагрузка, кг
100	27	15	22,8
		8	44,7
		0,1	62
60	23	10	22,8
		3	44,7
		0,1	57
20	16	7	22,8
		3,5	44,7
		0,1	49
10	10	6	22,8
		1	44,7
		0,1	47

Высота захолаживания, мм.	Рабочий зазор, мм.	Максимальная боковая нагрузка Н.
100	27	3,4
60	23	5
20	16	8,5
10	10	15

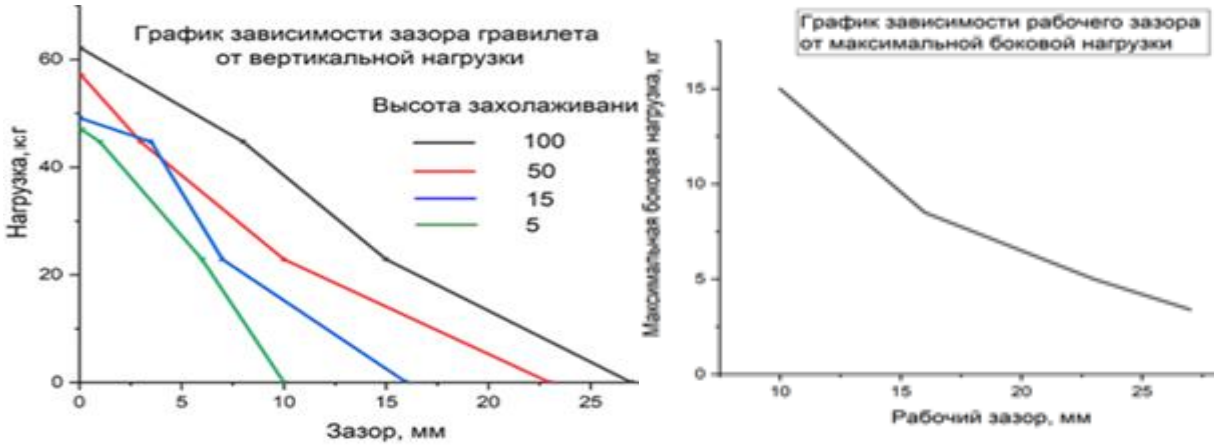

Fig. 3. Measurement of levitation force and lateral stability

The results obtained (Fig. 3.) on the used installation allowed to achieve a maximum load of 60 kg of vertical and 15 kg of lateral load, which opens the possibility of moving to the next level of scalability of the project: the length of the route is more than 10 meters, as well as the load capacity of 2000 N at speeds up to 20 km/h. Of great importance is the search for methods for the precise determination of drag forces and the separation of the contributions of aerodynamic friction forces and specific losses in sulfur conductors of the second kind. Of particular importance is the conduct of experiments on the separation of contributions from aerodynamic forces and other forces in a vacuum.

The research was carried out with the financial support of the RFBR, NTU "Sirius", JSC "Russian Railways" and the Educational Fund "Talent and Success" in the framework of the scientific project No. 20-37-51005".

References

[1] Terentyev, Y. A., Filimonov, V. V., Shavrov, V. G., Koledov, V. V., Fongratowski, S. V., Suslov, D. A., ... & Bogachev, T. V. (2019). Current Status and Prospects for the Development of the Integrated Transit Transport System (ITTS) of Russia on the Basis of Vacuum Magnetic Levitation Transport (VMLT). *Transportation Systems and Technology*, *5*(4), 25-62.

Machine learning methods for modeling multicomponent alloys

Chtchelkatchev N.M.[1], Ryltsev R.E.[1,2]

[1]*Vereshchagin Institute of High-Pressure Physics, 108840 Troitsk, Moscow, Russia*
[2]*Institute of Metallurgy, Amundsena str. 101, Ekaterinburg 620016, Russia*

Multicomponent alloys including high entropy and compositionally complex ones are in the focus of intensive researches because of their extraordinary physical properties and perspective for applications. Due to enormous number of possible compositions in such alloys, the methods for predicting their structure and properties are of great importance. One of the main theoretical tools on this way is ab initio simulations which allows addressing both atomic and electronic structure and calculating observable properties with experimental accuracy. However, performing ab initio simulations of highly-multicomponent alloys is an extremely difficult task.

The promising way to solve this problem is the use of machine learning (ML) for boosting computer simulations. The main idea is to fit properly the interatomic potential energy surface of a particle system using ab initio reference data. A properly designed machine learning interatomic potential (MLIP) can provide nearly ab initio accuracy with orders of magnitude less computational cost. Since pioneering works at the end of the 2000s [1,2], a number of approaches to fabricate MLIPs have been proposed so far and applied successfully for studying condensed matter systems of different nature. However, the application of these methods to study of multicomponent alloys has not yet been thoroughly validated. A lot of issues arise on this way: 1) How to generate properly the training dataset of ab initio configurations? 2) That is the best ML model to describe multicomponent systems? 3) Is that possible to develop MLIP which describes adequately a system with many (say, more than six) components? 4) Is it possible to extrapolate the domain of thermodynamic parameters available for simulations far beyond the training dataset?

Here we address these issues for a number of metallic multicomponent alloys including ternary Al-Cu-(Fe,Ni) alloys and high-entropy TiZrHfNbCoNiAl and TiZrHfNbVCrMoMnFeCoNiAl alloys. Using a training datasets of ab initio configurations corresponding to the liquid alloys, we develop MLIP (NNPs) as implemented in DeePMD code. For Al-Cu-(Fe,Ni) alloys, NNPs are trained on a few compositions covering a ternary composition triangle with a 15 at. % grid, allows describing both atomic structure and dynamics of the system in whole composition range and in a broad temperature range. The developed NNPs provide good accuracy for structural and dynamical properties in comparison to ab initio data. This is the first example of NNPs for alloys with so many components. The results obtained open up prospects for simulating structural and dynamical properties of multicomponent alloys with MLIPs. Support of Russian Science Foundation (#18-12-00438) is acknowledged.

References

[1] J. Behler and M. Parrinello, Phys. Rev. Lett. 98, 146401 (2007).

[2] A. P. Bartók, M. C. Payne, R. Kondor, et al, Phys. Rev. Lett. 104, 136403 (2010).

Impacts of exchange correlation effects on the ground state properties of Fe-Rh alloy

Sokolovskiy V.V., Pavlukhina O.O., Baigutlin D.R., Buchelnikov V.D.

Chelyabinsk State University, 454001, Chelyabinsk, Russia

For several decades, intensive theoretical studies have been carried out on the magnetic, structural, electronic, and thermodynamic properties of Fe-Rh alloys. One of the important issues is the estimation of the lattice (ΔS_{lat}), magnetic (ΔS_{mag}), and electronic (ΔS_{el}) contributions of entropies to the total change in entropy ΔS at the phase transition point. In Ref. [1], an emphasis was placed on the dominant role of ΔS_{el}, while in papers [2, 3] the essential role of the contribution ΔS_{mag} was discussed. On the contrary, in Ref. [4], an attention was drawn to the predominant contribution ΔS_{lat}. Nevertheless, despite numerous theoretical studies of Fe-Rh alloys, the issue of prediction of the metamagnetic transition temperature and the entropy contribution estimations by *ab initio* calculations taking into account both the well-known generalized gradient approximation (GGA) and the Debye model remains open. Since a number of factors prevent this. These factors include a large difference in energy between antiferromagnetic (AFM) and ferromagnetic (FM) phases [3, 4], a high Debye temperature for the FM phase compared to the AFM phase [5], and the presence of soft phonon modes in the AFM phase [4, 5]. In this regard, the solution of this issue by the example of Fe-Rh alloys seems to be interesting and relevant.

This work is devoted to the theoretical prediction of the metamagnetic transition temperature within the framework of the density functional theory formalism, taking into account the influence of exchange-correlation effects and the quasi-harmonic Debye model. The *ab initio* calculations were performed using the projector augmented wave method implemented in the VASP software package [6]. To describe the exchange-correlation effects, the GGA and meta-generalized gradient (meta-GGA) were selected within the framework of the Purdue-Burke-Ernzerhof (PBE) functional [7] and the new generation SCAN functional [8], which takes into account the gradient of the electron density and density of kinetic energy. Geometric optimization of the crystal lattice of cubic symmetry No. 225 is performed on a 16-atomic supercell (Fe_8Rh_8) taking into account the FM and checkerboard AFM ordering of Fe atoms. The calculation of free energies and lattice entropies of each phase was performed using the Debye model, neglecting the electronic and magnetic contributions. Debye temperatures for each phase are determined from the calculations of the elastic moduli.

Fig. 1 shows the dependences of the total energy on the lattice parameter of Fe-Rh, which obtained in the framework of electronic relaxation of the crystal structure within the GGA-PBE and SCAN functionals. Analysis of the results obtained shows the following. Both functionals predict AFM ordering as energetically favorable. However, SCAN gives a lower lattice constant for both types of magnetic ordering. It is noteworthy that taking into account additional electron correlations in the SCAN functional gives a significantly smaller energy difference ΔE (by about an order of magnitude) between the FM and AFM phases compared to the generally accepted PBE functional.

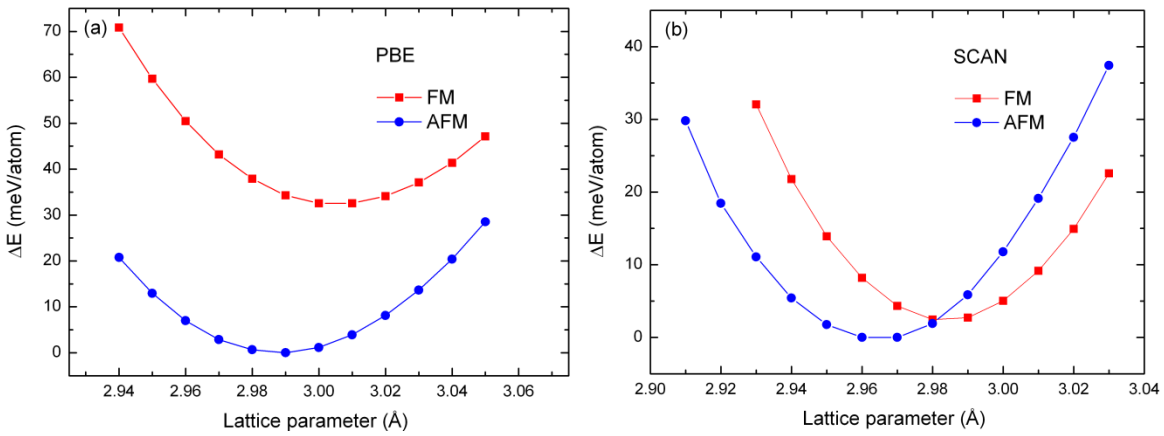

Fig. 1. Total energy difference as a function of the lattice parameter of Fe-Rh with FM and AFM order. The results are presented for (a) GGA-PBE and (b) SCAN functionals. The energies are plotted with respect to the AFM configuration.

Thus, in contrast to the GGA approximation, additional correlation effects within the meta-GGA approximation reduce sufficiently the energy difference between the FM and AFM phases and yield to a slightly higher Debye temperature for the AFM phase compared to the FM phase. Assuming the total energies and Debye temperatures obtained within SCAN, the phase transition temperature is predicted about 300 K, which is close to the experimental data. Besides, and the ΔS_{lat} at the transition point is evaluated which comparable with data reported in Ref. [5]. We believe that in the case of Fe-Rh alloys, the Debye model, together with calculations within the meta-GGA approximation, has an adequate predictive power along with the approach of calculating phonon spectra [5].

This work is supported by Russian Science Foundation No. 17-72-20022.

References

[1] P. Tu et al., J. Appl. Phys. 40, 1368 (1969).
[2] M. E. Gruner et al. Phys. Rev. B 67,064415 (2003).
[3] L.M. Sandratskii, P. Mavropoulos, Phys. Rev. B 83, 174408 (2011).
[4] M. Wolloch et al. Phys. Rev. B 94, 174435 (2016).
[5] R. Martinho Vieira et al. J. Alloys Compd. 857,157811 (2021).
[6] G. Kresse, J. Furthmüller, Comp. Mater. Sci. 6, 15 (1996).
[7] J. P. Perdew, K. Burke, and M. Ernzerhof, Phys. Rev. Lett. 77, 3865 (1996).
[8] J. Sun, A. Ruzsinszky, J.P. Perdew, Phys. Rev. Lett. 115,036402 (2015).

Exciton Phase in Strongly Correlated Systems with the Spin Crossover

Orlov Yu.S.[1,2], Nikolaev S.V.[1,2], Dudnikov V.A.[2], Ovchinnikov S.G.[1,2]

[1]Siberian Federal University, 660041, Krasnoyarsk, Russia
[2]Kirensky Institute of Physics, Federal Research Center KSC SB RAS, 660036 Krasnoyarsk, Russia

The formation and condensation of electron-hole pairs (excitons) in semimetals and semiconductors was predicted more than half a century ago. The weak coupling theory of the excitonic insulators has been developed analogously to the Bardeen-Cooper-Schrieffer (BCS) theory of superconductivity [1]. Later the ideas of excitonic condensation were discussed for strongly correlated materials within the Hubbard-type models. Within the multiband Hubbard-type model the interrelation of the excitonic condensation and the high spin (HS) - low spin (LS) crossover takes place [2].

The minimal model which contains the multiorbital physics and excitonic effects is the two-band Hubbard-type model both in the strong coupling and weak coupling regimes. In the strong coupling limit we have suggested [3] the similar approach as the Hubbard's original one that starts with the exact diagonalization of the local part of the Hamiltonian and construction the Hubbard X-operators. Within such approach the effective Hamiltonian has been obtained that was used to study the phase diagram and the HS-LS crossover under external pressure. A spin gap between the LS and the HS is an external parameter of our model that may be varied by pressure. The mean-field phase diagram in the plane spin gap - temperature (or pressure - temperature) contains the HS antiferromagnetic and paramagnetic, excitonic, and nonmagnetic LS phases. The excitonic phase appears in the spin crossover region and coexists with the HS AFM phase.

Two cases can be distinguished. In the first (weakly correlated) case, we have a two-band semiconductor or a semimetal (depending on the model parameters), in which an exciton condensate can form according to the BCS or Bose-Einstein condensation scenario. In the second case (strongly correlated), when the energy of the Coulomb interaction of electrons is larger than their kinetic energy and becomes comparable with the energy of the crystal field, the spin crossover and the formation of localized magnetic excitons become possible. In this study we showed using the two-band Hubbard-Kanamori model that there is a condensation of such excitons near the spin crossover, which, in turn, leads to the opening of a dielectric gap in the electronic spectrum and the occurrence of the antiferromagnetic ordering. The emergence of the magnetism induced by the condensation of excitons was found.

The authors thank the Russian Scientific Foundation for the financial support under the grant 18-12-00022.

References

[1] L.V. Keldysh and Y.V. Kopaev, Sov. Phys. Solid State 6, 2219 (1965).
[2] J. Kunes and P. Augustinsky, Phys. Rev. B 89, 115134 (2014).
[3] V.I. Kuz'min, Yu.S. Orlov, and et al., Phys. Rev. B 100, 144429 (2019).

Spin states of an anisotropic non-Heisenberg ferrimagnet

O.A.Kosmachev, A.V.Krivtsova, Ya.Yu.Matyunina, Yu.A.Fridman

V.I. Vernadsky Crimean Federal University, 295007, Simferopol, Russian Federation

Ferrimagnets are magnetic materials whose properties are in some sense intermediate between ferromagnets and antiferromagnets. Like antiferromagnets, ferrimagnets contain magnetic sublattices with antiparallel magnetizations. Ferrimagnets have always been considered as important materials of magnetic electronics, but new interesting properties are constantly being discovered in these materials. It is of interest to study the phase states of a non-Heisenberg ferrimagnet [1], in which one of the sublattices contains magnetic ions with spin 1 and the other with spin 1/2. In the sublattice with S = 1, we will take into account both bilinear and biquadratic exchange interactions. Moreover, this sublattice is anisotropic (easy-plane anisotropy). The Hamiltonian of such a system is determined by the expression

$$H = -\frac{1}{2}\sum_{n,n'}\left[J_2(n-n')(\mathbf{S}_n\mathbf{S}_{n'}) + K(n-n')(\mathbf{S}_n\mathbf{S}_{n'})^2 \right] - \frac{1}{2}\sum_{m,m'} J_1(m-m')(\boldsymbol{\sigma}_m\boldsymbol{\sigma}_{m'}) -$$

$$-\frac{1}{2}\sum_{n,m} A(n-m)(\boldsymbol{\sigma}_m\mathbf{S}_n) + \frac{\beta}{2}\sum_n \left(S_n^x\right)^2$$

where J_1 is the constant of the exchange interaction of the sublattice with spin 1/2; J_2, K - constants of bilinear and biquadratic exchange interactions of the sublattice with spin 1; β – single-ion agisotropy constant; A <0 is the constant of intersublattice interaction. The consideration will be carried out for the case of low temperatures ($T << T_N$, T_N – temperature Neel).

Analysis of the free energy density shows that at $J_2 > K, \beta$, the ferromagnetic (FiM) order is realized in the system. If the material parameters are such that $J_2 < \beta < K$, then the effect of quantum spin reduction takes place in the first sublattice, and the second sublattice plays the role of an effective "magnetizing" field. Let us call this state the quadrupole ferrimagnetic (QFiM). The magnetization vectors of the first and second sublattices are anticollinear, so in this state it is possible to compensate for the magnetic moments of the sublattices.

From the equality of the density of free energy in FiM - and QFiM-phases, we obtain the surface of the phase transition between these phases

$\left[y - 4(1-x) - z/3 \right]^2 + \frac{z}{3}\left[4(1-x) + z/3 \right] = 0$, where $y = |A|/K$, $x = J/K$, $z = \beta/K$

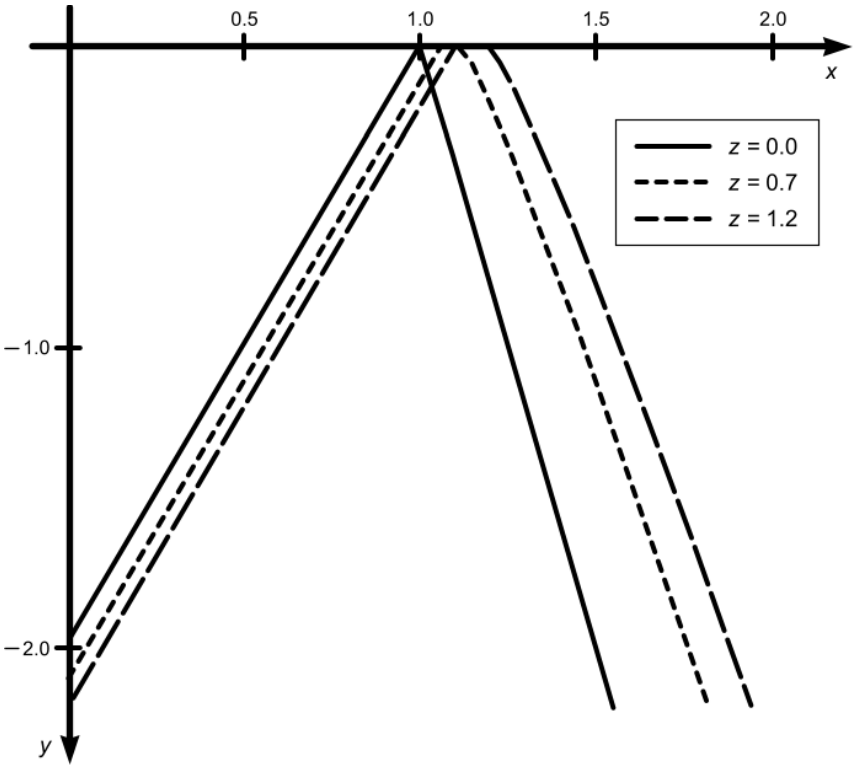

From the condition $\langle S^z \rangle = -\langle \sigma^z \rangle$, and taking into account that $\langle \sigma^z \rangle = 1/2$, we obtain an equation that determines the surface of the compensation of spins in the QFiM phase

$$y = 2x - 2 - z/6.$$

Thus, this equation describes the surface on which the total spin of the sublattices is zero.

The results obtained make it possible to construct a phase diagram of the system under study (see Fig.). To determine the type of the QFiM - FiM phase transition, we use the Landau thermodynamic theory of phase transitions, which shows that the QFiM-FiM phase transition is a first-order phase transition.

The research was funded by RFBR and Republic of Crimea, project number 20-42-910003 (O.A.Kosmachev, O.A., E.A, Yarygina, Ya.Yu.Matyunina)
The reported study was funded by RFBR according to the research project № 20-32-90027 (E.A,Yarygina)

References

[1] B.A.Ivanov, Fizika Nizkikh Temperatur, 2019, vol.45, no.9, pp.1095-1130

Electronic and magnetic properties of novel iron oxides Fe_4O_5 and Fe_5O_6 at high pressures

Zhandun V.S., Draganyuk O.N.

Kirensky Institute of Physics, Federal Research Center KSC SB RAS, 660036 Krasnoyarsk, Russia.

Iron oxides are attracting a lot of attention due to their complex structural properties and fundamental aspects from the point of view of natural sciences and industrial applications [1,2]. In the last decade, studies at high temperatures and high pressures have revealed the existence of new binary iron oxides with unusual stoichiometry, such as Fe_4O_5 [3] and Fe_5O_6 [4]. The discovery of new classes of systems with potentially complex electronic and magnetic properties motivated the study of their physical properties and potential for innovative applications [2]. While structural information and some properties of the new oxides at atmospheric pressure are available, information on their electronic and magnetic properties under extreme pressure-temperature conditions is very limited. Knowledge of these properties is important for both solid state physics and earth sciences.

We present here the *ab initio* investigation of the electronic and magnetic properties and the correlations between structural and electronic properties of novel iron oxides polymorphs Fe_4O_5 (Fig.1) and Fe_5O_6. The evolution of the electronic and magnetic structure under pressure is analyzed within GGA+U and SCAN methodology. The stability of the Fe_4O_5 and Fe_5O_6 compounds at different pressures are studied in terms of the enthalpy of formation.

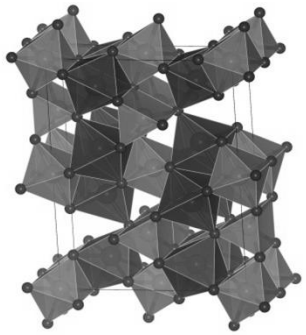

Fig. 1. Crystal structure of Fe_4O_5.

Acknolegments. This research is funded by the Russian Foundation for Basic Research (project no. 21-52-12033).

References

1. Delacotte, C., Bréard, Y., Caignaert, et al. Solid State Chem. 247, 13–19. (2017).
2. Ovsyannikov, S. V., Bykov, M., Bykova, et al. Nat. Commun. 9, 4142 (2018).
4. B. Lavina, P. Dera, E. Kim, et al. Proc.Natl.Acad.Sci. U.S.A. 108, 17281–5 (2011).
5. Lavina, B., Meng, Y. Sci. Adv. 1, e1400260–e1400260 (2015).

Structural, magnetic and electronic properties of Fe-Ge-Al from first principles

Zagrebin M.A.[1], Matyunina M.V.[1], Sokolovskiy V.V.[1], Buchelnikov V.D.[1]

[1]*Chelyabinsk State University, 454001, Chelyabinsk, Russia*

An assessment of the effect of a small addition of Al atoms in binary Fe-Ga alloys [1,2] showed that the tetragonal magnetostriction of ternary Fe-Ga-Al alloys decreases insignificantly, which is explained by a simultaneous increase of both the magnetoelastic constants and the tetragonal elastic moduli. These effects are due to changes in the electronic structure. The binary alloy Fe-Ge as Fe-Ga are also magnetostrictive material, but there is no data about Al atoms effect on the structural and magnetic properties. The present research aims to study replacing Ge atoms with Al atoms on the structural, magnetic, and electronic properties.

Using the density functional theory implemented in VASP program package [3,4], the two cubic structures A2 (group of symmetry *Im*-3*m*, #229) and $D0_3$ (group of symmetry *Fm*-3*m*, #225) were considered for $Fe_{100-x}(Ge_{x-y}Al_y)_x$ (x=9.375, 15.625, 21.875; y=3.125, 6.25). The exchange-correlation effects were taken into account by the generalized gradient approximation in the Perdew-Burke-Ernzerhof form [5] for the supercell approach (32 atoms in supercell). To create non-stoichiometric compositions and structural disorder in supercells, special quasirandom structures were used created using the ATAT package (Alloy Theoretic Automated Toolkit) [6].

At the first step, the geometry optimization of crystal structures was done by ionic relaxation (see Figure 1). It was found that the lattice constants have increased with increasing both Ge and Al atoms (x content).

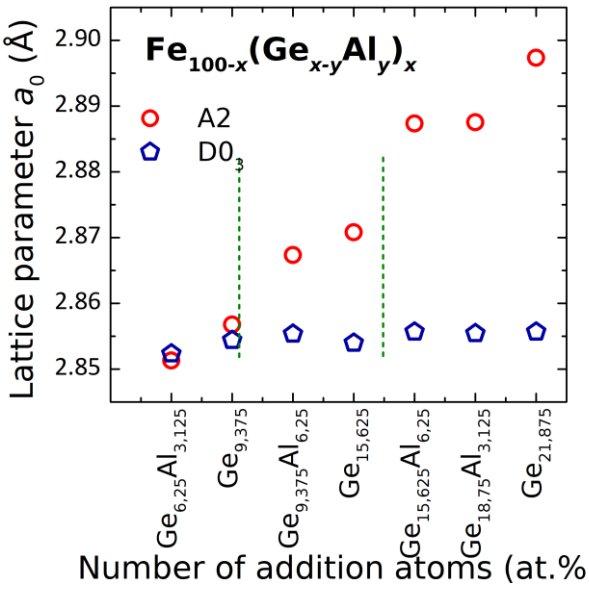

Fig. 1. The calculated values of the lattice parameters for structures A2 and $D0_3$ ($a_0/2$) of the $Fe_{100-x}(Ge_{x-y}Al_y)_x$ alloys. The lattice parameters for binary alloys are given from [7].

However, comparison ternary and binary Fe-Ge alloys [7] have shown replacing Ge atoms with Al atoms leads to a lower a_0 that the smaller atomic radius of Al could explain.

Figure 2 shows the calculated total densities of states for A2 and $D0_3$ phases of Fe-Ge-Al alloys. It was found that DOS profiles depend on both crystal structure and the number of Al and Ge addition.

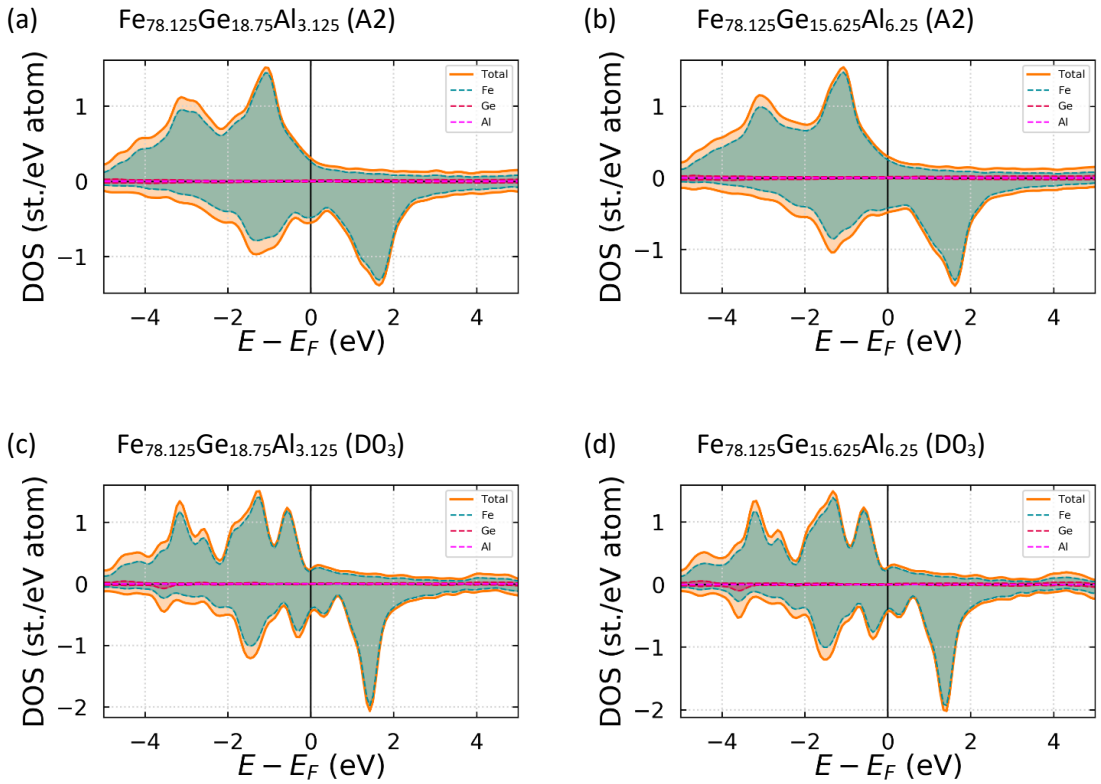

Fig. 2. The calculated total density of states depending on composition for A2 (a, b) and $D0_3$ (c, d) structures of $Fe_{100-x}(Ge_{x-y}Al_y)_x$ alloys

Acknowledgement. This work was supported by the Advanced science research foundation of the Chelyabinsk State University.

References

[1] J.B. Restorff, M. Wun-Fogle, K.B. Hathaway, A.E. Clark, T.A. Lograsso, G. Petculescu, J. Appl. Phys. 111, 023905 (2012).

[2] A.E. Clark, J.B. Restorff, M. Wun-Fogle, D. Wu, T.A. Lograsso, J. Appl. Phys. 103, 07B310 (2008).

[3] G. Kresse, D. Joubert, Phys. Rev. B. 59, 1758 (1999).

[4] G. Kresse, J. Furthműller, Phys. Rev. B. 54, 11169 (1996).

[5] J.P. Perdew, K. Burke, M. Enzerhof, Phys. Rev. Lett., 77, 3865 (1996).

[6] A.van de Walle, M. Asta, G. Ceder, Calphad, 26, 539 (2002).

[7] M.V. Matyunina, M.A. Zagrebin, V.V. Sokolovskiy, V.D. Buchelnikov, Physica B, 580, 411934 (2020).

Light-Induced Ultrafast Quantum Relaxation Dynamics of Magnetically Ordered Spin Crossover Systems under High Pressure

Orlov Yu.S.[1,2], Nikolaev S.V.[1,2], Ovchinnikov S.G.[1,2]

[1]*Kirensky Institute of Physics, Federal Research Center KSC SB RAS, Krasnoyarsk, 660036 Russia*
[2]*Siberian Federal University, Krasnoyarsk, 660041 Russia*

Within the multielectron model of magnetic insulator with two different spin terms at each cation and spin crossover under high pressure we have studied dynamics of a sudden excited non equilibrium spin state. We obtain the different relaxation of the magnetization, high spin/low spin occupation numbers, and the metal-oxygen bond length for different values of the external pressure. For each pressure-temperature values stationary state agrees to the mean field phase diagrams. We found the long living oscillations of magnetization for the high spin ground state at small pressure. Close to crossover pressure the smooth relaxation is accompanied with a set of sharp strongly non linear oscillations of magnetization and HS/LS occupation numbers that are accompanied by the Franck–Condon resonances.

Polarization eigenmodes in uncorrelated disordered magnetic media

Niyazov R.A.[1,2], Kozhaev M.A.[3], Belotelov V.I.[3,4]

[1]Department of Physics, St. Petersburg State University, 198504, St. Petersburg, Russia
[2]NRC ``Kurchatov Institute'', Petersburg Nuclear Physics Institute, 188300, Gatchina, Russia
[3]V.I. Vernadsky Crimean Federal University, 295007, Simferopol, Russia
[4]Moscow State University, Leninskiye Gory 1, 119991, Moscow, Russia

The study of light propagation in scattering media is essential for many disciplines ranging from chemistry and biology, including astronomy and physics [1]. Nowadays, the propagation of light in a disordered medium is actively studied both theoretically and experimentally. Much attention is paid to the polarization of light, the possibility of its control is being investigated. Since the magnetization of a medium significantly affects the polarization, an urgent task is to describe the propagation of light in a magnetoactive medium with the disorder.

Recently, the correlation matrix of the electric field has been calculated for magnetoactive media with the disorder [2]. It was shown that antisymmetric light correlations arise. It corresponds to the appearance of circular contributions to the polarization of light. However, the corrections coming from the magnetoactivity of the medium were taken into account only from one diffusive mode of polarization propagation.

In this work, we study the effect of magnetoactivity on all polarization modes. Theoretically, the propagation of light in a magnetoactive medium with the anisotropic disorder from the first principles is studied. Within the framework of multiple scattering theory, the energy density is calculated [3]. Its expansion by the polarizations eigenmodes allowed to estimate the characteristic lengths and the diffusion coefficients of every mode separately. Such decomposition will make it possible to obtain a clear physical picture of the propagation of light in media with scatterers and go beyond the diffusion approximation and take into account the higher corrections for the distance between the light source and the detector.

The work of R.N. was funded by RFBR, project number 19-32-60077. The work of M.K. and V.B. was funded by RFBR, project number 18-52-80038.

References

[1] B. J. Berne and R. Pecora, Dynamic light scattering: with applications to chemistry, biology, and physics (Courier Corporation, New York, 2000).

[2] M. A. Kozhaev, R. A. Niyazov, and V. I. Belotelov, Phys. Rev. A 95, 023819 (2017).

[3] K. Vynck, R. Pierrat, and R. Carminati, Phys. Rev. A 89, 013842 (2014).

Aharonov–Bohm Interferometry Based on Helical Edge States

Niyazov R.A.[1,2], Aristov D.N.[2,1], Kachorovskii V.Yu.[3]

[1]*St. Petersburg State University, 7/9 Universitetskaya nab., 199034, St. Petersburg, Russia*
[2]*NRC "Kurchatov Institute", Petersburg Nuclear Physics Institute, 188300, Gatchina, Russia*
[3]*A. F. Ioffe Physico-Technical Institute, 194021, St. Petersburg, Russia*

The Aharonov-Bohm (AB) interferometers made of quantum wires with single or few ballistic quantum channels are very attractive as prime devices to probe coherent quantum phenomena and because of possible applications as miniature and very sensitive sensors of a magnetic field. The ability to control interference by a magnetic field due to the AB effect [1] provides additional potential for experimental and theoretical analysis [2]. Rather stringent requirements limit the efficiency of practically used quantum electronic interferometers, for example, very low temperature for interferometers based on superconducting SQUIDs or the condition of very strong magnetic fields for interferometers based on the edge states of Quantum Hall Effect systems.

A promising opportunity for a technological breakthrough in this direction is associated with the discovery of topological insulators. In these materials, as in conventional insulators, the Fermi level lies in the band gap, so that there is no bulk conductivity. At the same time, conducting states exist on the surface of a topological insulator, and the conduction through these states is not suppressed by disorder scattering due to topological reasons [3]. Surface excitations exist due to strong spin-orbit interaction and have chiral symmetry: the direction of the momentum is rigidly related to the spin projection. These are the so-called helical edge states (HES), in which electrons with different spins propagate in opposite directions.

In two-dimensional topological insulators, interference of electron waves propagating at the edge state along the system's perimeter is possible. Thus, the transport through the edge states of the topological insulator is, in fact, the transport through the interferometer (see Fig. 1). We focus on the case of relatively high temperature when temperature much larger than the level spacing [4]. The tunneling conductance of the interferometer, G, is structureless in ballistic case but reveals sharp antiresonances, as a function of dimensionless flux, ϕ, in the presence of magnetic impurities. Although similar antiresonances are known to arise in the single-channel rings made of conventional materials, the helical AB interferometer shows essentially different behavior due to the specific properties of the HES. Most importantly, the effect is universal and robust to details of the setup, in particular, to relation between L_1 and L_2 and the position of the magnetic impurity. Another difference concerns the periodicity of the function $G(\phi)$, which obeys $G(\phi + 1/2) = G(\phi)$, while for interferometers made of conventional materials, this function is periodic with the period 1.

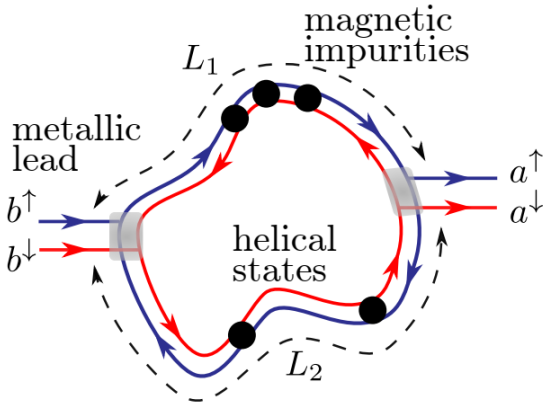

Fig. 1. Helical Aharonov-Bohm interferometer with the magnetic impurities.

Another property of the helical interferometer of crucial significance for quantum computations is the possibility to operate as a spin filter. Even for a non-magnetic lead, the incoming electron beam splits into two parts: right-moving electrons with spin up and left-moving electrons with spin down. If the transmission over one of the system's shoulders is blocked, say, by inserting the strong magnetic impurity into the upper shoulder, only the down shoulder remains active, and the spin polarization of outgoing electrons can achieve 100%. Remarkably, this mechanism is robust to dephasing and, therefore, works at high temperatures.

The quantum contribution to polarization shows AB oscillations with the magnetic flux piercing the area encompassed by HES and is therefore tunable by the external magnetic field. A very sharp dependence of the conductance and the spin polarization on ϕ is very promising for applications for tunable spin filtering and in the area of extremely sensitive detectors of magnetic fields.

Notably, the tunneling interferometer can be described in terms of an ensemble of flux-tunable qubits giving equal contributions to conductance and spin polarization. The number of active qubits participating in the charge and spin transport is given by the ratio of the temperature to the level spacing. Such an ensemble of qubits can effectively operate at high temperatures and can be used for quantum calculations [5]. This opens a wide avenue for high-temperature quantum computing.

Therefore, HES are candidates for efficient creation, control, and transfer of electron polarization. It is very promising from the point of view of the application in quantum spin-sensitive interferometry, especially in the modern and rapidly developing field of spintronics and the creation of quantum informatics devices using spin degrees of freedom as spin filters and quantum qubits.

RFBR, project number 19-32-60077, funded the work of R.N. The Russian Science Foundation funded the work of D.A. and V.K., Grant No. 20-12-00147.

References

[1] Y. Aharonov and D. Bohm, Phys. Rev. 115, 485 (1959).

[2] A. G. Aronov and Y. V. Sharvin, Rev. Mod. Phys. 59, 755 (1987).

[3] X.-L. Qi and S.-C. Zhang, Rev. Mod. Phys. 83, 1057 (2011).

[4] R. A. Niyazov, D. N. Aristov, and V. Y. Kachorovskii, JETP Lett. (2021).

[5] R. A. Niyazov, D. N. Aristov, and V. Y. Kachorovskii, npj Comput. Mater. 6, 174 (2020).

Influence of duration of electropulse treatment on structure and martensitic transformation of melt-spun TiNiCu alloys

Shelyakov A.V.[1], Sitnikov N.N.[1,2], Zaletova I.A.[1,2], Borodako K.A.[1] , Vysotina E.A.[1,2]

[1]National Research Nuclear University MEPhI (Moscow Engineering Physics Institute), Kashirskoe shosse 31, 115409 Moscow, Russian Federation
[2]Federal State Unitary Enterprise "Keldysh Research Center", Onezhskaya st. 8, 125438 Moscow, Russian Federation

Thin ribbons of quasi-binary TiNi–TiCu alloys with high copper content (more than 25 at.%), produced by melt spinning technique, are of great interest as shape memory materials to create micro-mechanical devices, in particular, microtweezers for gripping and holding of micro- and nanoscale objects for their further spatial manipulation and preparation [1]. These alloys have an amorphous state after quenching at a cooling rate of about 10^6 K/s. Upon further crystallization by isothermal heat treatment, they can form brittle Ti-Cu phases and therefore do not exhibit shape memory behavior. Recently it was shown that high-rate electropulse treatment (EPT) fundamentally changed the microstructure of the alloys [2]. In this work, we studied the influence of the EPT duration in the range from 1000 to 1 ms on the structure and martensitic transformation (MT) of TiNiCu alloy with 30 at.% copper content.

X-ray diffraction studies have shown that after the EPT with different duration the samples are completely in the martensitic state at room temperature. When the ribbons are heated to a temperature of 75°C, the peaks of the B19 martensite phase disappear, and only reflections of the B2 austenite phase are present due to the B19 ↔ B2 MT. A decrease in the EPT duration does not lead to a change in the phase composition of the ribbons, although the intensity of the peaks of the B19 phase for shorter crystallization times is somewhat lower.

Investigation of the cross-section of the ribbons in a scanning electron microscope revealed a columnar crystal structure near the ribbon surfaces, while in the ribbon volume there are single or grouped large grains (from 3 up to 12 microns). An increase in the EPT duration leads to significant decreasing both the average grain size and the height of the columnar crystals.

At the same time, results of differential scanning calorimetry (DSC) indicated that an increase in the EPT duration causes a decrease in the MT temperatures, while the MT enthalpy remains practically unchanged. In addition, the exposure time has a significant effect on the shape of the DSC curves, which is manifested in the bifurcation of the peaks of heat release and absorption during MT with a decrease in the exposure time less than 500 ms. Obviously, this is due to the bimodal structure of the alloys, which lead to superposition of peaks from each structure and bifurcation of the common peak.

The study is supported by Russian Science Foundation (project No. 19-12-00327).

References

[1] A. Shelyakov, N. Sitnikov, K. Borodako et al., J Micro-Bio Robot. 16, 43 (2020).
[2] A. Shelyakov, N. Sitnikov, I. Khabibullina et al., Mater. Lett. 248, 48 (2019).

Structural and thermal stability of B20-type monogermanides synthesized under high pressure

Magnitskaya M.V.[1], Chtchelkatchev N.M.[1], Kamaeva L.V.[2], Tsvyashchenko A.V.[1]

[1]*Vereshchagin Institute of High Pressure Physics, Russian Academy of Sciences, 108840, Troitsk, Moscow, Russia*
[2]*Institute of Physics and Technology of Udmurt Federal Research Center, Ural Branch of Russian Academy of Sciences, 426000, Izhevsk, Russia*

Transition metal monogermanides with a noncentrosymmetric B20-type crystal structure have long attracted the attention of researchers (see, e.g. [1]), since they represent a promising basis for the design of new thermoelectrics and spintronics-related materials. Here, the stability and phase transformations in the high-pressure-synthesized [2] B20 phases of FeGe, MnGe, and RhGe are studied theoretically using *ab initio* density functional calculations (using the VASP package [3]) and experimentally by means of differential scanning calorimetry (DSC).

An evolutionary search for the most energetically favorable polymorphic modifications was carried out using the VASP package [3] and the USPEX genetic algorithm [4]. Their stability regions on the pressure–temperature phase diagram were then determined in the quasi-harmonic approximation It follows from our calculations that, for a given input chemical composition, the existence of a structure stable at nonzero temperatures (and pressures) can be efficiently established by a zero-temperature evolutionary search, if this structure appears in the output short-list of low-energy states. We also evaluated finite-temperature properties of B20 phases under study (Fig. 1). The obtained temperature dependence of specific heat of MnGe is in good agreement with the available experimental data [2]. For the high-pressure phase B20-RhGe such measurements are still absent.

The calculated ground state of nonmagnetic MnGe is represented by a hypothetical tetragonal structure unusual for this class of compounds. For FeGe and MnGe in magnetic state, our evolutionary search yields the same set of preferred phases. In case of FeGe, this result is

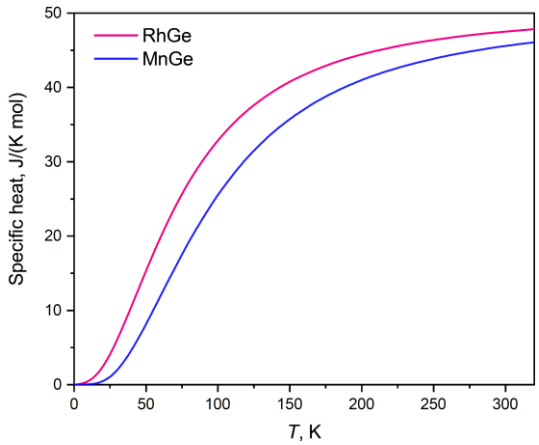

Fig. 1. Calculated specific heat of RhGe and MnGe.

consistent with the available information, while for MnGe, we find new equiatomic polymorphs, in addition to the known metastable high-pressure phase of B20 type [2].

Our measured DSC thermograms were used to determine the temperatures of phase transformations, which were compared with the known diagrams of equilibrium states. The experiments were carried out with heating in the temperature range from 310 to 1573 K and subsequent cooling at a rate of 10 K/min. X-ray diffraction analysis (XRD) of both the initial samples obtained at high pressures and samples after DSC measurements was carried out.

After DSC heating, the microstructure of the samples was also investigated. Fig. 2 shows optical micrographs of the FeGe sample. As is seen, the sample after heat treatment consists of three structural components: hexagonal η phase (light areas), tetragonal phase $FeGe_2$, and eutectic colonies formed as a result of the joint growth of these two phases. The microstructure of the initial sample before heat treatment shows that this structure is single-phase, despite the increased defectiveness of the metastable phase. The DSC thermograms of

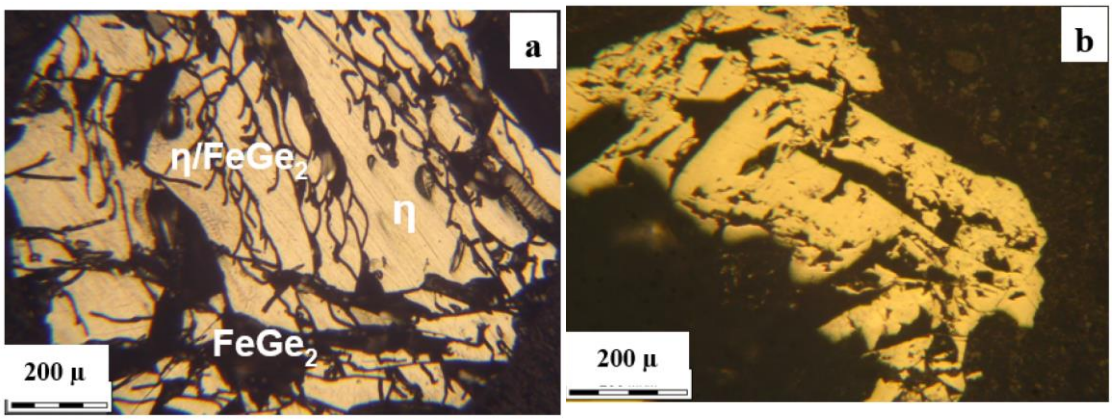

Fig. 2. Optical micrographs of the high-pressure-synthesized FeGe sample after (a) and before (b) DSC heating.

FeGe and MnGe are qualitatively similar, while B20-RhGe differs from FeGe and MnGe both in calculated structural hierarchy and in the shape of the DSC curve. The DSC experiments reveal that the studied metastable B20 phases are different in their properties from analogues obtained by other methods, for example, by mechanical allowing [5]. Their behavior on heating significantly depends on the preparation method and sample history.

This work was supported by the Russian Science Foundation under Grants RSF No.18-12-00438 and No.17-12-01050.

References

[1] N.M. Chtchelkatchev, M.V. Magnitskaya, V.A. Sidorov, L.N. Fomicheva, A.E. Petrova, and A.V. Tsvyashchenko, Pure Appl. Chem. 91, 941 (2019).

[2] A. Tsvyashchenko, V. Sidorov, L. Fomicheva, V. Krasnorussky, R. Sadykov, J. Thompson, K. Gofryk, F. Ronning, and V. Ivanov, Solid State Phenom. 190, 225 (2012).

[3] G. Kresse and J. Furthmüller, Phys. Rev. B 54, 11169 (1996).

[4] A.R. Oganov and C.W. Glass, J. Chem. Phys. 124, 244704 (2006).

Synthesis and magnetic properties of ferrite ceramics $Ba_{1-x}Sr_xFe_{12}O_{19}$.

Zhivulin V.E.[1], Boldin A.A. [1], Taskaev S.V.[1, 2], Vinnik D.A.[1]

[1]South Ural State University, 454080, Chelyabinsk, Russia
[2]Chelyabinsk State University, 454001, Chelyabinsk, Russia

Ferrites with a magnetoplumbite structure, such as barium hexaferrite ($BaFe_{12}O_{19}$) and strontium hexaferrite ($SrFe_{12}O_{19}$), have been known since the 60s of the 20th century and have been successfully used as a material for the manufacture of permanent magnets, devices for recording and storing information. Good magnetic properties of ferrites, combined with their low conductivity, make them a promising material for high frequency electronics applications.

Interest in hexagonal ferrites with a magnetoplumbite structure is increasing every year, which is confirmed by a large number of scientific works on this topic. Variations in the chemical composition of ferrite when some atoms are replaced by others in the crystal structure leads to a change in the physical properties of the material. Thus, we can regulate and customize the properties of the material for a specific task.

The presented work is devoted to the production of ferrite based on barium hexaferrite in which barium atoms are partially replaced by strontium atoms ($Ba_{1-x}Sr_xFe_{12}O_{19}$) and the study of the effect of substitution on the change in magnetic properties. Samples were synthesized using standard solid-phase technology [1]. Iron oxide (Fe_2O_3), barium and strontium carbonates ($BaCO_3$, $SrCO_3$) were used as the initial components for preparing the charge. The initial components were mixed in a stoichiometric ratio and ground for 40 minutes in an agate mortar.

After grinding, the resulting powders were pressed into pellets using a metal mold with a diameter of 20 mm. The pressing force was 3 tons/cm^2. The resulting pellets were sintered at a temperature of 1400 ° C for 5 hours. Thus, were prepared and studied 5 samples with degrees of substitution x(Sr) = 0, 0.2, 0.5, 0.7, 1.

According to the powder X-ray diffraction, all the prepared samples formed single phase with a magnetoplumbite structure. Elemental analysis data showed that the composition of the obtained samples is consistent with the initially specified.

Magnetic properties were measured using a Quantum Design PPMS VersaLab ™ vibration magnetometer in a magnetic field range of up to 3 T at room temperature.

It was found that the value of saturation magnetization does not depend on a degree of substitution of barium by strontium. Coercive force and residual magnetization behave in a non-monotonic way. The largest values of these parameters were found for the sample with the composition $Ba_{0.5}Sr_{0.5}Fe_{12}O_{19}$.

References

[2] D.A.Vinnik, A.Y. Starikov, V.E. Zhivulin, K.A. Astapovich, V.A.Turchenko, T.I. Zubar, S.V. Trukhanov, J Kohout., T. Kmječ, O. Yakovenko, L. Matzui, A.S.B. Sombra. Structure and magnetodielectric properties of titanium substituted barium hexaferrites. Ceramics International. V.47 (12), 17293-17306, 2021.

The reported study was funded by RFBR (project number 20-38-70057).

Magnetocaloric properties in polycrystalline Mn_5Si_3

Mashirov A.B.[1], Musabirov I.I.[2], Mitsiuk V.I.[3], Kamantsev A.P.[2], Shavrov V.G.[2]

[1]*Kotelnikov Institute of Radioengineering and Electronics, Russian Academy of Sciences, Moscow, Russia*
[2]*Institute for Metals Superplasticity Problems, Russian Academy of Sciences, Ufa, Russia*
[3]*Scientific-Practical Materials Research Centre of NAS of Belarus, Minsk, Belarus*

The interest of researchers in magnetics with phase transitions and with a magnetocaloric effect in the cryogenic temperature range is associated with the possibility of their application in cryocoolers [1]. The single-crystal Mn_5Si_3 sample demonstrates a strong inverse magnetocaloric effect upon the metamagnetic transition at T_{N1}= 65 K [2]. We have investigated the magnetic and magnetocaloric properties of a polycrystalline Mn_5Si_3 sample, which is easier to manufacture. A polycrystalline sample of the nominal composition Mn_5Si_3 was prepared by argon-arc melting with three remelts. The sample sealed in a vacuum quartz ampoule was annealed for 50 hours at a temperature of 1273 K, after which it was quenched in water at room temperature. Measurements of the isofield magnetization of the sample showed that a metamagnetic transition with temperature hysteresis is observed in the temperature range from 5 K to 70 K. With an increase in the magnetic field from 1 T to 10 T, the characteristic temperatures of this metamagnetic transition shift to low temperatures with a coefficient of 4.9 K/T (Fig. 1 left). A sample of the Mn_5Si_3 alloy at a temperature of 50 K demonstrates a sharp change in magnetization of about 20 emu/g in the range of the applied magnetic field from 5.5 T to 6.5 T (Fig. 1 right). In this region, an inverse magnetocaloric effect can be observed at cryogenic temperatures.

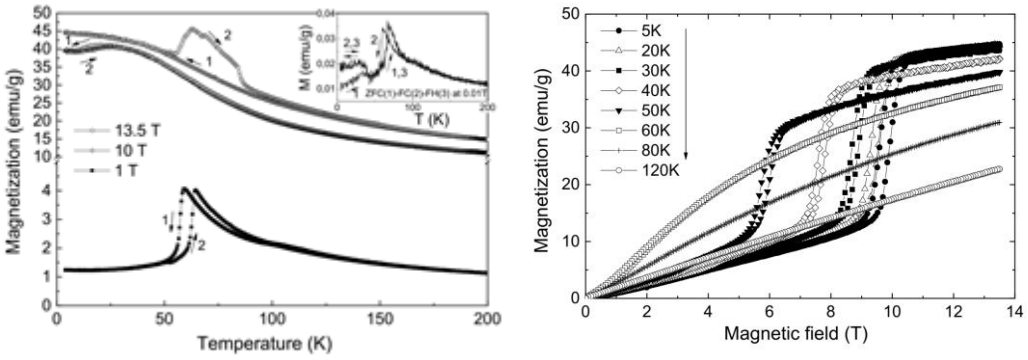

Fig. 1. Left graph: isofield magnetization of the Mn_5Si_3 sample versus temperature in magnetic fields. The inset shows the view isofield magnetization at magnetic field 0.01 T. Right graph:

The reported study was funded by RFBR and BRFBR, project number 20-58-00059 and T20R-204, respectively.

References

[1] I. Park and S. Jeong, Cryogenics 88, 106 (2007).
[2] R. F. Luccas et al., J. Magn. Magn. Mater. 489, 165451(2019).

Non-trivial features of magnetocaloric alloys of the system $MnCo_xNi_{1-x}Ge_{1.05}$

Valkov V.I.[1], Golovchan A.V.[1], Kovalev O.E.[1], Gribanov I.F.[1], Sivachenko A.P.[1], Mitsiuk V.I.[2], Mashirov A.V.[3]

[1]*Donetsk Institute for Physics and Engineering named after A.A.Galkin, 283114, Donetsk, DPR*
[2] *Scientific and Practical Materials Research Centre, National Academy of Sciences of Belarus, Minsk, 220072 Belarus*
[3] *Kotelnikov Institute of Radio Engineering and Electronics, Russian Academy of Sciences, Moscow, 125009 Russia*

The detection of the low-temperature inverse magnetocaloric effect (IMCE) in alloys of the $MnCo_xNi_{1-x}Ge_{1.05}$ system makes it possible to classify them as functional materials, in which the IMCE is determined by the magnetostructural transition from orthorhombic helimagnetic to hexagonal ferromagnetic HM(orth)↔FM(hex) (Fig.1). The explanation of the mechanism of realization of these transitions was carried out within the framework of the phenomenological theory of interacting parameters of magnetic and structural orders on the basis of the model of a displaced harmonic oscillator for the structural subsystem and the Heisenberg model for the spin subsystem with additional allowance for the internal periodic field orthogonal to the exchange field. Within this approach, it was found that the effect of an external magnetic field on the helimagnetic phase can lead to previously unknown irreversible (reversible) magnetostructural transitions HM(orth)→FM(orth)↔FM(hex) Fig.2.

This work was carried out with financial support from the Belarusian Republican Foundation for Fundamental Research and the Russian Foundation for Basic Research within the framework of scientific projects No. T20R-204 and No. 20-58-00059, respectively.

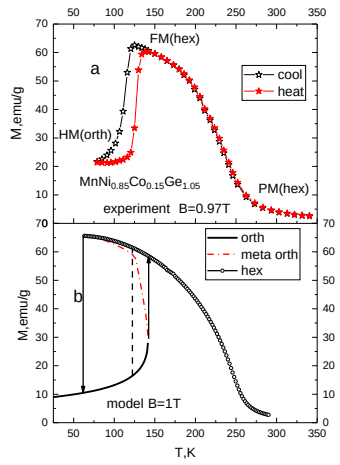

Fig. 1. Temperature dependences of magnetization in the region of magnetostructural HM(orth)↔FM(hex) and isostructural FM(hex)↔PM(hex) transitions.

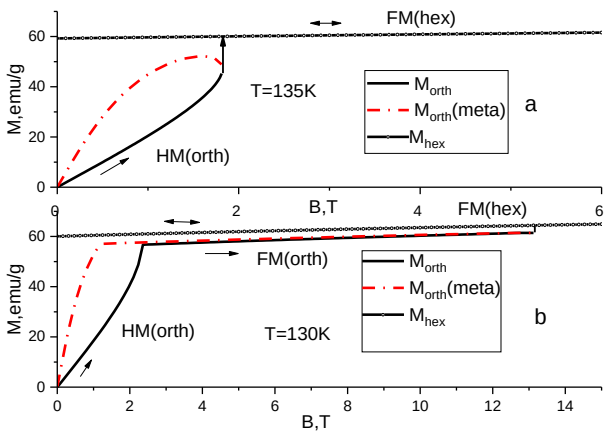

Fig.2 Isothermal field dependences of magnetization (model). a- irreversible (→) magnetostructural HM(orth)→FM(hex); b- reversible(↔) isostructural HM(orth)↔FM(orth), irreversible (→) magnetostructural transitions FM(orth)→FM(hex).

The critical currents of superconducting rhodium borides

Lachenkov S. A.[1], Vlasenko V. A.[2], Kasyanov V. S.[3], Gavrilkin S.Yu.[2], Kirillova V. M.[1], Dementyev V. A.[1], Sdobyrev V.V.[1]

[1] Federal State Budgetary Institution of Science A. A. Baykov Institute of Metallurgy and Materials Science of the Russian Academy of Sciences, 49 Leninsky Ave., Moscow, 119991, Russia.

[2] Federal State Budgetary Institution of Science P. N. Lebedev Physical Institute of the Russian Academy of Sciences, 53 Leninsky Ave., Moscow, 119991, Russia.

[3] Federal State Budgetary Educational Institution of Higher Education D. I. Mendeleev Russian University of Chemical Technology, 9 Miusskaya Square, Moscow, 125047, Russia

Ternary rhodium borides with the general chemical formula $RERh_4B_4$ (RE - rare earth metal atoms) differ in that their electro-physical properties are essentially determined by the rare earth metal atoms. Depending on RE, ternary rhodium borides can be superconductors, magnets, or simultaneously combine superconducting and magnetic properties [1, 2]. The objects of research in this work were two rhodium borides: YRh_4B_4 – "classical" superconductor (T_c ~10 K) and $HoRh_{3.8}Ru_{0.2}B_4$– a magnetic superconductor (T_c ~6 K). Both compounds were practically single-phase and mainly consisted of a $LuRu_4B_4$ phase. In the case of $HoRh_{3.8}Ru_{0.2}B_4$ to stabilize the required phase ($LuRu_4B_4$), rhodium was partially replaced with ruthenium.

Critical currents (J_c) are one of the most important characteristics of superconductors. J_c depends both on the critical temperature (T_c) of the superconducting material and on the presence of pinning centers, which are the places where the vortex filaments are fixed when an electric current flows [3]. Pinning centers can be formed on the basis of normal regions in a type II superconductor: point defects, grain boundaries, and inhomogeneities [3].

Not so long ago [4] , there was evidence that vortex filaments can be fixed in "additional" normal regions, the appearance of which is associated with the magnetic subsystem. From this point of view, it was important to study the field dependences of the critical currents of triple rhodium borides at different temperatures on the example of the traditional superconductor YRh_4B_4 and the magnetic superconductor $HoRh_{3.8}Ru_{0.2}B_4$ and analyze the influence of the magnetic subsystem on the nature of pinning in these compounds.

The critical current density of the samples was estimated in the approximation of the Bean model [5,6] for rigid superconductors-type II, based on the data obtained by measuring the magnetic moment (M(B)). To make measurements, samples of the required geometric shape were cut out of the melted ingots: cylinders with a diameter of 3 mm and a length of 4 mm. In the process of measuring M (B), two contributions to the magnetic moment are recorded: one is associated with the superconducting system, the other is due to the magnetic subsystem of the connection. Since the contribution to the loop width M (B) from the superconducting signal is much greater than from the hysteresis associated with magnetism, the critical currents can be calculated according to the Bean model for both a classical superconductor (YRh_4B_4) and a magnetic one ($HoRh_{3.8}Ru_{0.2}B_4$).

The dependences of the critical current density on the external magnetic field at different temperatures (below T_c) are shown in Fig. 1(a) and Fig.1 (b), respectively, for YRh_4B_4 and $HoRh_{3.8}Ru_{0.2}B_4$.

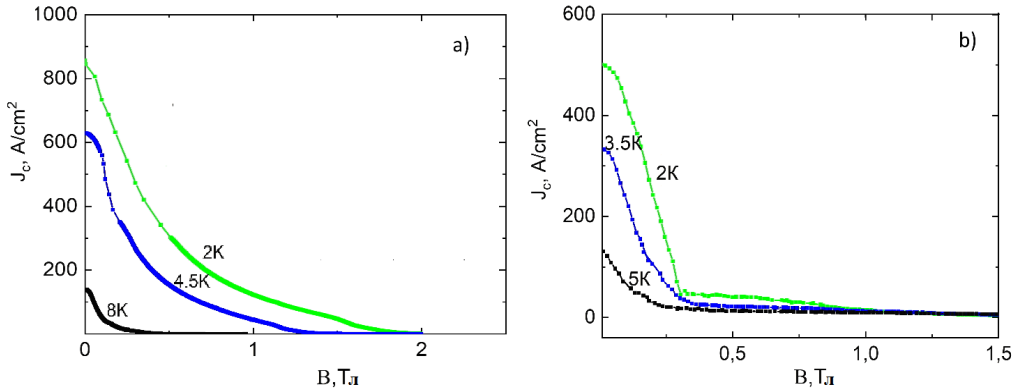

Figure 1 Critical current density from the external magnetic field: a) superconductor YRh_4B_4; b) superconductor $HoRh_{3.8}Ru_{0.2}B_4$

From the analysis of the data in Fig. 1, it follows that the largest J_c ~ 850 A/cm^2 (at T~2K) is shown by the nonmagnetic superconductor YRh_4B_4. This is due to the fact that the T_c of YRh_4B_4 is higher than the critical temperature of $HoRh_{3.8}Ru_{0.2}B_4$. Since YRh_4B_4 and $HoRh_{3.8}Ru_{0.2}B_4$ are superconductors of the second kind, J_c significantly depends on the value of the pinning force, which is a structurally sensitive parameter. Note that in the case of the superconductor $HoRh_{3.8}Ru_{0.2}B_4$ it is possible to form pinning centers on magnetic defects. In our case, the magnetic defects (additional pinning centers) can be the magnetic ions $HoRh_{3.8}Ru_{0.2}B_4$, localized in the lattice nodes. In order of magnitude, such microscopic formations correspond to a coherence length of ξ~10 Å in the limit of a "dirty superconductor" [3].

The dependences of the reduced pinning force ($F_p/F_{p\,(max)}$ on the value of the reduced magnetic field – $h_p=H/H_{(max)}$ showed that in the case of a non - magnetic superconductor- YRh_4B_4, the law of "similarity" holds, whereas in the case of a magnetic superconductor $HoRh_{3.8}Ru_{0.2}B_4$ at $h_p>0.2$, there is a significant deviation from the law of "similarity", which may be due to the magnetic subsystem of the superconductor, which gives new pinning centers on magnetic defects.

References

[1] Chevrel R., Sergent M., Prigent J. Solid State Chem. 1971. V. 3. № 4. P. 515.
[2] Burkhanov G. S., Lachenkov S. A., et al. Russian Metallurgy. 2012. No.5. P. 445
[3] Buckel V. Superconductivity. Moscow. Mir. 1975. p. 366.
[4] Jung S.-G., Kang J.-H., Park E. et al. Scientific Reports. 2015. V.5. P.16385.
[5] Bean C. P. Phys. Rev. Lett. 1962. V.8. P. 250.
[6] Bean C. P. Rev. Mod. Phys. 1964. V.36. P. 31.

Investigation of Fe49Rh51 alloy by wide-field Kerr microscopy

Taaev T.A.[1,2], Soldatov I.V.[3,4], Amirov A.A.[2,5], Aliev A.M.[2,5], Schäfer R.[4,6]

[1]Dagestan State University, 367000, Makhachkala, Russia
[2]H. Amirkhanov Institute of Physics of the DFRC of the RAS, 367015, Makhachkala, Russia
[3]Materials Science, TU Darmstadt, 64287, Darmstadt, Germany
[4]Leibniz Institute for Solid State and Materials Research (IFW) Dresden, Institute for Metallic Materials, D-01069 Dresden, Germany
[5]Laboratory of Novel Magnetic Materials, Institute of Physics, Mathematics and Information Technology, Immanuel Kant Baltic Federal University, 236016, Kaliningrad, Russia
[6]Institute for Materials Science, TU Dresden, 01062 Dresden, Germany

The wide-field Kerr microscopy has emerged to become a well-established, most versatile and flexible laboratory technique for the investigation of magnetic domains. The method is based on the magneto-optical Kerr effect [1,2] i.e., small alterations of the polarization plane of linearly polarized light upon reflection from a non-transparent magnetic specimen, which are then detected and used for magnetic domain image formation.

FeRh alloys (with the Rh content from 47 to 53%) serve as the most convenient model objects for studying the nature of magnetic phase transitions (PT) in materials showing giant magnetocaloric effect (MCE) [3,4]. The microstructures of FeRh are consisted of magnetic, bcc, α' (*B*2) and paramagnetic, fcc, γ (*A*1) phases [3].

Images of the magnetic domain structure were obtained by using a Kerr microscope. The branched polar magnetic domains of α' phase is clearly showed in the images. Analysis of the obtained image intensity of the surface of sample as a function of the temperature was allowed to see the start temperature of phase transition from the FM to the AFM state $T_1 \approx 322$ K and the finish temperature of the inverse AFM–FM transformation $T_2 \approx 317$K without magnetic field. In magnetic field of 500 mT the start of phase transition from the FM to the AFM state for $T_1 \approx 318$ K and the finish temperature of the inverse AFM–FM transformation $T_2 \approx 313$K.

This work was supported by funding under the joint program of the Ministry of Science and Higher Education of the Russian Federation and the German Academic Exchange Service DAAD "Mikhail Lomonosov/Immanuel Kant" (project passport № 2295-21).

References

[1] A. Hubert, R. Schäfer, Magnetic Domains: The Analysis of Magnetic Microstructures (Springer, New York, 1998) p. 696.

[2] I.V. Soldatov, R. Schäfer, Rev. Sci. Instrum. 88, 073701 (2017).

[3] A. Chirkova, F. Bittner, et al., Acta Mater. 131, 31 (2017).

[4] A.P. Kamantsev, A.A. Amirov, et al., Phisics of the Solid State 62, 160 (2020).

Multigap superconductivity and electron correlations in Mo_8Ga_{41} and $Mo_4Ga_{20}Sb$ as seen by NMR and NQR spectroscopy

Gunbin A.V.[1], Tkachev A.V.[1,3], Zhurenko S.V.[1,2], Gippius A.A.[1,2], Verchenko V.Yu.[3], Shevelkov A.V.[3]

[1]*P.N. Lebedev Physical Institute of the Russian Academy of Sciences, 119991, Moscow, Russia*
[2]*M.V.Lomonosov Moscow State University, Faculty of Physics, 119991, Moscow, Russia*
[3]*M.V.Lomonosov Moscow State University, Faculty of Chemistry, 119991, Moscow, Russia*

Intermetallic cluster superconductors Mo_8Ga_{41} and $Mo_4Ga_{20}Sb$ are studied by NMR and NQR spectroscopy. For Mo_8Ga_{41} superconductivity state appears below $T_c = 9.8\ K$ and for $Mo_4Ga_{20}Sb$ superconductivity transition is $T_c = 6.6\ K$ [1,2]. Both superconducting compounds show differences from the BCS gap theory and enhanced electron-phonon coupling.

NMR spectrum for the ^{69}Ga and ^{71}Ga nuclei central transition $(-½ \leftrightarrow ½)$ in Mo_8Ga_{41} was measured by sweeping of magnetic field at fixed frequency of *50 MHz* (Fig. 1). Knight shift was measured for ^{69}Ga isotope in Ga1 position with low EFG in range of frequencies *50* to *76 MHz*. Results of NMR measurement indicate the critical magnetic field of suppressing superconductivity in Mo_8Ga_{41} is $\mu_0 H_{c2}(4.2\ K) = 6.5\ T$ in good accordance with the specific heat data [1]. Knight shift does not go to zero with decreasing temperature as an evidence of the spin-orbital scattering [3].

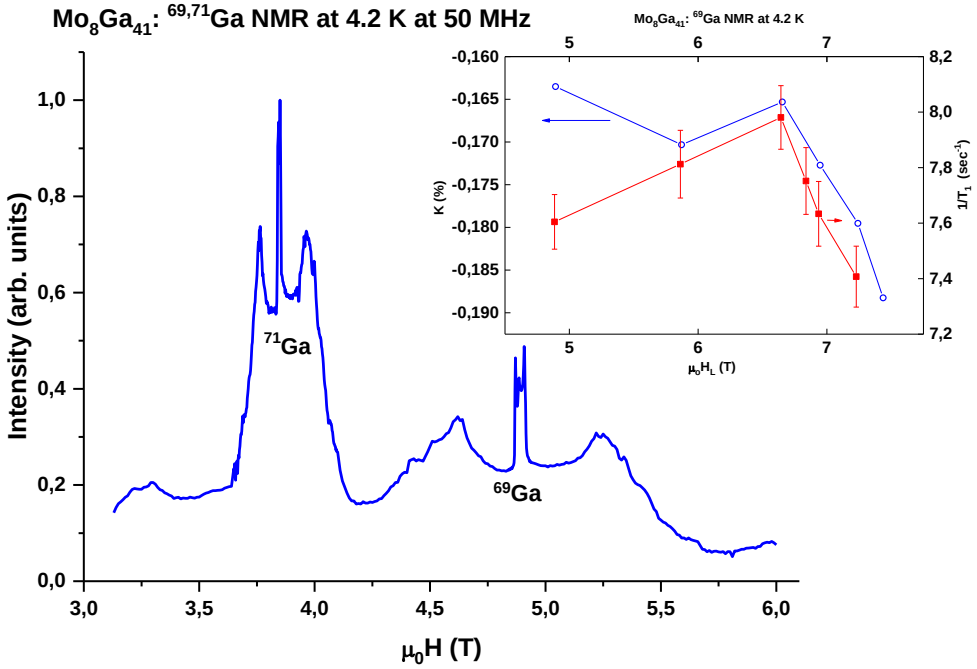

Fig. 1. Mo_8Ga_{41} field-sweep NMR spectrum at 50 MHz and 4.2 K. Inset: ^{69}Ga Knight shift (left) and spin-lattice relaxation rate (right) as a function of magnetic field.

^{69,71}Ga NQR measurements $Mo_4Ga_{20}Sb$ were carried out and the spectrum consisting of 4 pairs of gallium NQR lines corresponding to 4 nonequivalent Ga positions was observed. The width of ^{69}Ga NQR line in Ga1 position for temperature range above and beyond T_c = *6.6 K* shows sharp decrease around superconductive transition with rising temperature.

According to ^{69}Ga NQR spin-lattice relaxation measurements (Fig.2) at different temperatures $1/T_1T$ follows simple Korringa law in the normal state (T_1T = *0.38 s K*). Korringa ratio $S = \frac{4\pi k_B T_1 T K_s^2 \gamma_n^2}{\hbar \gamma_e^2} = 0.52 < 1$, which indicates antiferromagnetic electron correlations.

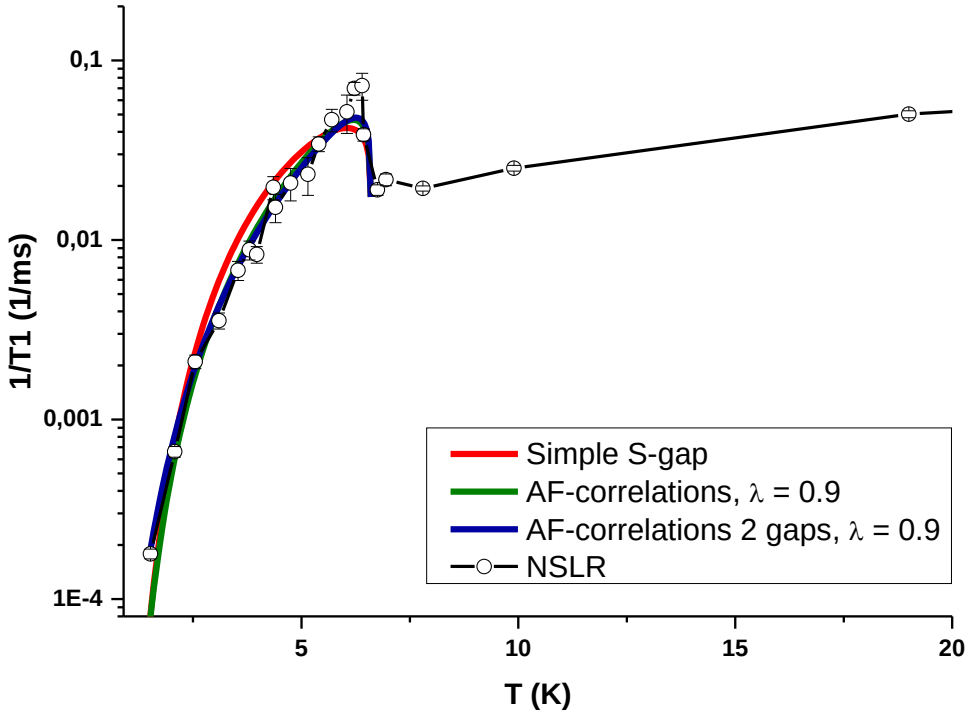

Fig. 2. $Mo_4Ga_{20}Sb$ spin-lattice relaxation rate with various model fitting curves

With decreasing temperature below T_c the Hebel-Slichter peak appears indicating full gap s-wave type superconductivity. However, experimental spin-lattice relaxation data below T_c reveals systematic deviation from the BCS behavior.

Simulation of relaxation data taking into account antiferromagnetic correlations [4] gives the value of two s-type gaps of *13* and *6 K*. The weighted average of *11.6 K* is consistent with the literature estimate of ~ *12.05 K* [2].

References

[1] V.Yu. Verchenko et al., Strong electron-phonon coupling in the intermetallic superconductor Mo_8Ga_{41}, Phys. Rev. B 93, 064501 (2016)

[2] V.Yu. Verchenko et al., Family of Mo_4Ga_{21}-Based Superconductors, Chemistry of Materials 2020 32 (15), 6730-6735 (2020)

[3] D.E. MacLaughlin, Magnetic Resonance in the Superconducting State, Solid State Physics, Volume 31 (1976)

[4] AJ Millis et al., Phenomenological model of nuclear relaxation in the normal state of $YBa_2Cu_3O_7$, Phys. Rev. B 42, 167 (1990)

Magnetic transitions in the $Co_{2.5}Ge_{0.5}BO_5$

N.A. Belskaya[1,2], N.V. Kazak[2], A.D. Vasilev[2], L.N. Bezmaternykh[2], D.A. Velikanov[2], S.Yu. Gavrilkin[3], S.G. Ovchinnikov[2]

[1]*Reshetnev Siberian State University of Science and Technology, 660037 Krasnoyarsk, Russia*
[2] *Kirensky Institute of Physics, FRC KSC SB RAS, 660036 Krasnoyarsk, Russia*
[3] *P.N. Lebedev Physical Institute of RAS, 119991 Moscow, Russia*

The transition metal oxyborates with a ludwigite structure are of interest due to their complex magnetic behavior. The magnetic properties, Mössbauer Effect, specific heat, and neutron diffraction measurements showed that iron ludwigite Fe_3BO_5 undergoes a cascade of the magnetic transformations PM-AFM-Ferri at critical temperatures T_{N1}=112 K and T_{N2}=70 K [1-3], as well as a charge ordering at T_{st}=283 K accompanying by the dimerization. At the same time, Co_3BO_5 demonstrates a single magnetic transition to the ferrimagnetic state at T_N = 43 K [4] without any structural and electronic transitions. The replacement of the Co^{3+} ions with Fe^{3+} results in the magnetic behavior becomes similar to that of the Fe_3BO_5. The role of the trivalent ion in the ludwigite's magnetic properties has been intensively studied through the synthesis and investigation of new magnetic materials, such as $Co_{1.5}Mn_{1.5}BO_5$ [5], $Co_{2.5}Ti_{0.5}BO_5$ [6], and $Co_{2.5}Sn_{0.5}BO_5$ [7].

The ludwigite's crystal structure is built of the oxygen octahedra and trigonal BO_3 groups. The divalent metal ions prefer to occupy the M1, M2, and M3 crystallographic sites, corresponding to the 2a, 2b, and 4g Wyckoff positions, respectively. The edge-sharing octahedra form the planes propagating along the *c*-axis, which are separated by borate groups and M4 (4h) site filled by the trivalent ions. At the moment, it is clear that the ludwigite's magnetic properties are closely related to the crystal structure and mainly depend on the type and concentration of the metal ion (both magnetic and nonmagnetic) localized at the M4 metal site.

Here, we report a new compound $Co_{2.5}Ge_{0.5}BO_5$, in which the substitution of Co^{3+}=1/2(Co^{2+}+Ge^{4+}) leads to the M4 site is filled by the divalent cobalt ions. The single crystals were obtained by the flux method. The single-crystal X-ray diffraction has revealed the orthorhombic crystal structure (sp. gr. *Pbam*). The unit cell parameters are *a*=9.3204(5) Å, *b*=12.1803(7) Å, *c*=3.0357(2) Å, and volume *V*=344.63(4) Å^3. The bond valence sums (BVS) calculations confirmed the expected charge distribution at the metal sites.

DC magnetization measurements were carried out on a regular shape single crystal (parallelepiped) along three crystallographic directions using the commercial MPMS equipment. Firstly, we observed a strong magnetic anisotropy inherent to the Co_3BO_5 with an easy magnetization *b*- axis. The presence of a large difference in the magnetic susceptibility for the field applied along *a*-, *b*-, and *c*-axes, which has been observed over the temperature range, up to 300 K, suggests the large single-ion anisotropy of Co^{2+} ions. Secondly, two anomalies on the ZFC and FC magnetization curves at T_{N1}=83 K and T_{N2}=34 K clearly indicate the onset of the antiferromagnetic and ferrimagnetic/metamagnetic transitions, respectively. The applied magnetic field has a drastic effect on the second transition shifting them towards higher temperatures (fig.1). At the range of T=150-300 K, an average magnetic susceptibility $\chi_{av}(T) = \frac{\chi_{dir\,a}+\chi_{dir\,b}+\chi_{dir\,c}}{3}$ obeys the modified Curie-Weiss law (insert to fig.1). A negative

Curie-Weiss temperature indicates the predominant antiferromagnetic interactions, which is in accordance with the ferrimagnetic order. The obtained magnetic moment μ_{eff} per Co^{2+} ion is well agreed with those for other ludwigites. At T=4.2 K, the M(H) curve presents a hysteresis loop (Fig. 1b). As the temperature increases, the curve is transformed, indicating a complex magnetization process for the several magnetic sublattices. The specific heat measurements performed in the range of 4.2-300 K revealed two anomalies associated with the magnetic transitions, confirming that the antiferromagnetic transition at T_{N1} is a thermodynamic phase transition. Unexpectedly, the second anomaly is clearly manifested when an external magnetic field is applied, indicating the metamagnetic origination of this transition. The magnetic properties of the new compound are discussed in comparison with other Co-containing ludwigites.

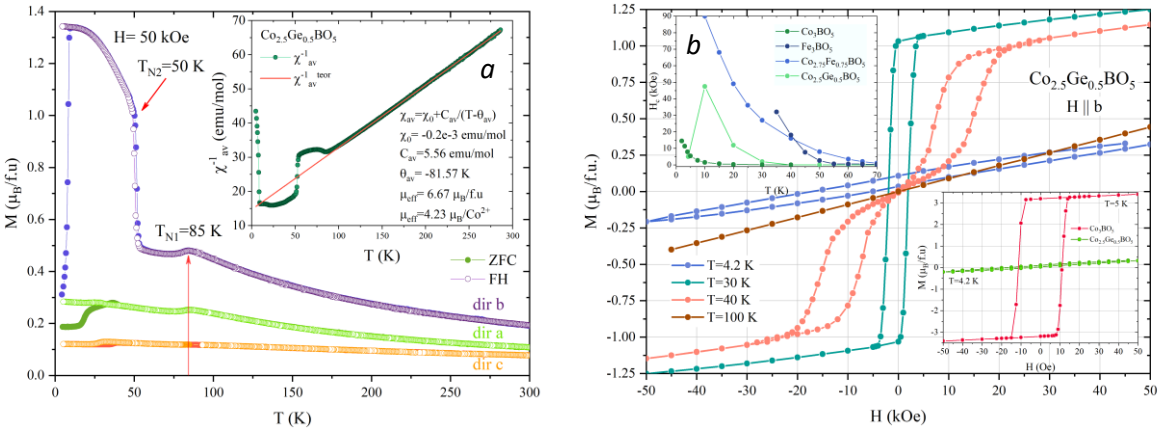

Fig 1. (a) Temperature dependences of the magnetization of the single crystal $Co_{2.5}Ge_{0.5}BO_5$ measured along *a*-, *b*-, and *c*- axes. The inset shows the inverse magnetic susceptibility vs. temperature. (b) The field dependences of the magnetization along *b*-axis. The upper inset is the coercive field $H_C(T)$. The bottom inset is M(H) curve of $Co_{2.5}Ge_{0.5}BO_5$ measured along easy magnetization direction compared with that of Co_3BO_5.

The reported study was funded by Russian Foundation for Basic Research (RFBR), project number 20-02-00559.

References

[1] J. Larrea J., D. R. Sánchez, Phys. Rev. B 70, 174452 (2004)
[2] P. Bordet and E. Suard, Phys. Rev. B 79, 144408 (2009)
[3] Yu.V. Knyazev, N.V. Kazak, JMMM 474, 493-500 (2019)
[4] D.C Freitas, M. A. Continentino, Phys. Rev. B 77, 184422 (2008)
[5] M. A. V. Heringer, D. L. Mariano, Phys. Rev. Materials 4, 064412(2020)
[6] D. C. Freitas, R. B. Guimarães, Phys. Rev. B 81, 024432 (2010)
[7] Cynthia P. Contreras Medrano, D. C. Freitas, Phys. Rev. B 91, 054402 (2015)

Magnetic birefringence of acoustic vortices in Iron Borate

Prilepsky D.Yu., Strugatsky M.B.

V.I. Vernadsky Crimean Federal University, 295007, Simferopol, Russia

In papers [1-3], the magnetic linear birefringence of a transversely polarized plane acoustic wave, which is an acoustic analogue of the well-known optical Cotton-Mouton effect, was discovered and experimentally and theoretically investigated. The observed birefringence of sound is caused by the interaction between the elastic and magnetic subsystems of the crystal, described by the magnetoelastic coupling, which due to the peculiarities of crystal and magnetic structure of iron borate is anomaly large in this crystal [4]. Acoustic waves induce magnetic oscillations, which, at frequencies much lower than the AFMR frequency, follow acoustic ones in a quasi-equilibrium manner. In the paper [5], magnetic oscillations in iron borate, caused by longitudinal sound excited by femtosecond laser pulses, were investigated.

In the present work, we theoretically investigate the magnetic birefringence of a transverse acoustic wave with a vortex structure propagating in iron borate. The fundamental possibility of the existence of such a process is shown, expressions for the magnetic and nonmagnetic acoustic modes are determined:

$$e_r = re^{-\alpha r^2}e^{im\psi}e^{i(\omega t - k_r z)},\ e_q = re^{-\alpha r^2}e^{im\psi}e^{i(\omega t - k_q z)},$$

$$k_r = \sqrt{\frac{\rho\omega^2}{C_{44}-\Delta C}},\ k_q = \sqrt{\frac{\rho\omega^2}{C_{44}}},\ \Delta C = \frac{4EB_{14}^2}{2M_0[H(D+2M_0H)+EH_{me1}]},$$

the boundaries of the area where the given solutions have a significant amplitude are established: $\lambda << r << (r_{max})^2/\lambda$ (r_{max} is the radius of the vortex area with the maximum amplitude). It is also shown that oscillations of the azimuthal angle of the magnetic moment repeat the shape of the magnetic acoustic mode: $\varphi = A_r k_r \Delta C \cdot e_r$.

References

[1] Yu.N. Mitsay, K.M. Skibinsky, M.B. Strugatsky, A.P. Korolyuk, V.V. Tarakanov, and V.I. Khizhnyi, JMMM, 219, 340-348 (2000).

[2] M.B. Strugatsky, and K.M. Skibinsky, JMMM, 309, 64–70 (2007).

[3] M.B. Strugatsky, K.M. Skibinsky, V.V. Tarakanov, and V.I. Khizhnyi, JMMM, 313, 84-88 (2008).

[4] Туров Е.А., Колчанов А.В., Меньшенин В.В. и др. Симметрия и физические свойства антиферромагнетиков (Физматлит, Москва, 2001).

[5] D. Afanasiev, I. Razdolski, K.M. Skibinsky, D. Bolotin, S.V. Yagupov, M.B. Strugatsky, A. Kirilyuk, Th. Rasing, and A.V. Kimel, Phys. Rev. Lett. 112, 147403 (2014)

Transformation of longitudinal sound in iron borate controlled by magnetic field

M. Strugatsky[1], K. Skibinsky[1], S. Yagupov[1], and V. Khizhnyi[2]

[1]Physical and Technical Institute of V.I, Vernadsky Crimean Federal University, 95007, Simferopol, Russia

[2]O. Usikov Institute for Radiophysics and Electronics NACU, 61085, Kharkiv, Ukraine

The strong magnetoelastic coupling, which is feature of easy-plane weak antiferromagnets, such as $FeBO_3$, hematite, etc., manifests itself in a significant mutual influence of the elastic and magnetic subsystems of the crystal. This makes it possible to control the parameters of elastic waves propagating through the crystals even with a small external magnetic field, which is attractive from the point of view of applications in spintronics, acousto-optics, and acousto-electronics. Until now, such effects at hypersonic frequencies (more than 10^8 Hz) in $FeBO_3$ have mainly been observed and studied for transverse acoustic modes [1]. In [2] it was observed magnetic oscillations induced by femtosecond laser pulses. It was found that laser pulses directly excite longitudinal sound, which generates the observed magnetic oscillations through magnetoelastic coupling.

This paper presents the results of experimental and theoretical studies of the discovered field dependences of the transmission coefficient of longitudinal hypersonic waves in iron borate. The first results demonstrating the longitudinal sound and the magnetic subsystem coupling are given in [3]. The experiments were carried out by the method of a standard acoustic resonance interferometer in the continuous generation mode. $FeBO_3$ samples specially synthesized by us were of basal plates form with an area about ~ 10 mm^2 and a thickness about ~ 100 μm [4]. Operating frequencies $f \approx 210$ MHz (close to Fabry-Perot acoustic resonance frequency). Experiments have shown that the curves of the field dependence of the transmission coefficient of longitudinal sound have an oscillating form. The experimental results are modeled on the basis of the developed theory. It is shown that the observed oscillations arise due to mixing of transverse acoustic modes with the longitudinal sound. The mixing mechanism is due to magnetoelastic coupling and is realized through the excitation of the magnetic subsystem.

The work was supported by the Russian Foundation for Fundamental Research (project No 19-29-12016).

References

[1]. Yu.N. Mitsay, K.M. Skibinsky, M.B. Strugatsky, A.P. Korolyuk, V.V. Tarakanov, and V.I. Khizhnyi, JMMM, **219**, 340 (2000).

[2]. D. Afanasiev, I. Razdolski, K. Skibinsky, D. Bolotin, S. Yagupov, M. Strugatsky, A. Kirilyuk, Th. Rasing, and A.V. Kimel, Phys. Rev. Lett., **112**, 147403 (2014).

[3]. V.I. Khizhnyi, T.M. Khizhnaya, V.V. Tarakanov, and A.P. Korolyuk, Telecom. and Radio Eng., **73**, 435 (2014).

[4]. S.V. Yagupov, M.B. Strugatsky, K.A. Seleznyova, Yu.A. Mogilenec, N.I. Snegirev, N.V. Marchenkov, A.G. Kulikov, Yan A. Eliovich, K.V. Frolov, Yu.L. Ogarkova and I.S. Lyubutin. Cryst. Growth Des., **18**, 7435, (2018).

Flux growth of $Fe_{0.94}Me_{0.06}BO_3$ (Me = Al, Ga, Sc) single crystals

Mogilenec Yu., Seleznyova K., Yagupov S., Seleznev K., Nauhatsky I., Maksimova E. and Strugatsky M.

Physics and Technology Institute, V.I. Vernadsky Crimean Federal University, Simferopol, Crimea

In recent years, the synthesis of diamagnetically diluted trigonal easy-plane weak ferromagnets based on iron borate $FeBO_3$ acquired paramount importance. This is due to the fact that such materials are in high demand for both fundamental science and practical applications. Indeed, on the one hand, such crystals allow one to study the nature of physical properties of magnetically ordered crystals, see, *e.g.* [1]. On the other hand, varying the content of diamagnetic impurity leads to creating materials with pre-determined properties. This fact is quite important for modern high-tech practical applications of single crystals based on iron borate [2]. Meanwhile, it is necessary to preserve the crystalline quality of undiluted $FeBO_3$, and even a small amount of impurity reduces structural perfection. Thus, the search for such diamagnetic ions that would minimize this reduction is necessary.

The present work aims to synthesize and obtain preliminary characteristics of $Fe_{1-x}Me_xBO_3$ (Me = Al, Ga, Sc) single crystals.

The synthesis was carried out in the Me_2O_3 - Fe_2O_3 - B_2O_3 - PbO - PbF_2 systems using the flux growth technique [3, 4]. The latter one has shown to be the most suitable for obtaining crystals of high perfection [5].

The impurity content was determined by X-ray fluorescence analysis. It was found that the content of impurity in crystals, $x_{crystal}$, differ from those in the initial charge, x_{charge}. Moreover, the value of $x_{crystal}$ has a certain distribution for crystals obtained in the course of one crystallization. As a result of a number of experimental crystallizations, the charge compositions were selected in such a way to obtain single crystals with the same impurity content including $x_{crystal}$ = 0.06, see Table 1. For each compound, the individual crystallization temperature mode was developed.

Table 1. x_{charge} and $x_{crystal}$ for $Fe_{1-x}Me_xBO_3$ single crystals

	$Fe_{1-x}Al_xBO_3$	$Fe_{1-x}Ga_xBO_3$		$Fe_{1-x}Sc_xBO_3$
x_{charge}	0.05	0.05	0.20	0.05
$x_{crystal}$	0.06 – 0.22	0.01 – 0.02	0.05 – 0.07	0.05 – 0.07

The synthesized $Fe_{1-x}Me_xBO_3$ single crystals had the shape of green hexagonal plates with dimensions up to 3 mm in the basal plane and 0.06 - 0.12 mm in thickness, as an example, Fig.1. shows single crystals $Fe_{1-x}Al_xBO_3$.

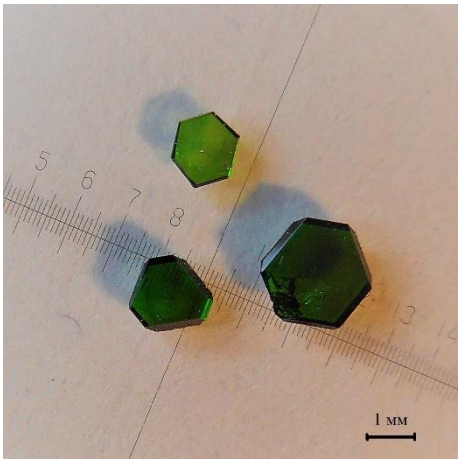

Fig. 1. The synthesized $Fe_{1-x}Al_xBO_3$ single crystals

X-ray diffraction analysis confirmed that the synthesized crystals have a trigonal structure, similar to $FeBO_3$. The crystal lattice parameters determined for $Fe_{0.94}Me_{0.06}BO_3$ single crystals are shown in Table 2. As one can see, the Al and Ga impurities less affect the crystal lattice parameters than Sc ions.

Table 2. Crystal lattice parameters of $Fe_{0.94}Me_{0.06}BO_3$ single crystals

	$FeBO_3$ [6]	$Fe_{0.94}Al_{0.06}BO_3$	$Fe_{0.94}Ga_{0.06}BO_3$	$Fe_{0.94}Sc_{0.06}BO_3$
a, Å	4.626(1)	4.6245(1)	4.6246(1)	4.6397(3)
c, Å	14.493(6)	14.4810(3)	14.4808(4)	14.5814(10)

The reported study was funded by RFBR, project number 19-32-90054 (crystal synthesis and X-ray studies) and 19-29-12016 (modernization of the crystallization setting).

References

[1] M.Strugatsky, K.Seleznyova, S.Yagupov, A.Drovosekov, J.Kliava, JMMM 442, 417 (2017)

[2] E.S.Smirnova, N.I.Snegirev, I.S.Lyubutin, S.S.Starchikov, V.V.Artemov, M.V.Lyubutina, S.V.Yagupov, M.B.Strugatsky, Yu.A.Mogilenec, K.A.Seleznyova, O.A.Alekseeva, Acta Cryst. B, 76, 1100 (2020).

[3] I.Bernal, C.W.Struck and J.G.White, Acta Cryst. 10, 849 (1963).

[4] S.Yagupov, M.Strugatsky, K.Seleznyova, E.Maksimova, I.Nauhatsky, V.Yagupov, E.Milyukova and J.Kliava, Applied Physics A 121(1), 179 (2015).

[5] S.Yagupov, M.Strugatsky, K.Seleznyova, Yu.Mogilenec, N.Snegirev, N.V.Marchenkov, A.G.Kulikov, YanA.Eliovich, K.V.Frolov, Yu.L.Ogarkova, I.S.Lyubutin, Crystal Growth & Design 18 (12), 7435 (2018).

[6] R.Diehl, Solid State Communications 17(6), 743 (1975)

Dipole-dipole contribution to magnetocrystalline anisotropy constants of iron-gallium borates

Seleznyova K.[1], Strugatsky M.[1], Mogilenec Yu. [1], Yagupov S. [1], Kliava J. [2]

[1] *Physics and Technology Institute, V.I. Vernadsky Crimean Federal University, 295007, Simferopol, Russia*
[2] *LOMA, UMR 5798 Université de Bordeaux-CNRS, 33405, Talence cedex, France*

Iron-gallium mixed borates, $Fe_xGa_{1-x}BO_3$, are isostructural to iron borate, $FeBO_3$, possessing rhombohedral calcite-type structure. Diamagnetically diluted $Fe_xGa_{1-x}BO_3$ single crystals show easy-plane weak ferromagnetism in the $0.34 \le x \le 1$ range [1].

The density of the energy of the magnetocrystalline anisotropy for these crystals can be expressed as [2]:

$$E_A = \frac{1}{2} a_{\text{eff}} \cos^2 J + d \sin^3 J \cos J \sin 3j + e \sin^6 J \cos 6j \ , \qquad (1)$$

where $a_{\text{eff}} = a + D^2/E$ is the *effective* uniaxial anisotropy constant, a, D and E being the uniaxial anisotropy, Dzyaloshinskii-Moriya and exchange constants, respectively; d and e are the basal anisotropy constants and J and j are the polar and azimuthal angles of the antiferromagnetic vector [2].

For $Fe_xGa_{1-x}BO_3$, a, d and e include contributions only of dipole-dipole and crystal field interactions [2]. Moreover, in the model of "point" dipoles the former contribution occurs only for uniaxial anisotropy and *not* for the basal one. In order to account for the experimental results, we have recently developed a new approach to calculating the dipole-dipole interaction energy in trigonal magnets by considering "extended", i.e., having a non-negligible size, dipoles [2]. For non-diluted iron borate, this approach has proved successful in interpreting the basal anisotropy in this crystal [2].

The actual work aims at evaluating the dipole-dipole contributions to the anisotropy constants of *diluted* iron-gallium borates. The *Ampérian current* model was used to describe an extended dipole. We have developed a computer code modelling $Fe_xGa_{1-x}BO_3$ crystal lattice and implementing the lattice sums including only iron-occupied sites.

As the main result, the dependences on x of the dipole-dipole contributions to a, d and e have been obtained for $Fe_xGa_{1-x}BO_3$ crystals at 0 K. With decreasing iron contents, the *absolute* values of a, d and e have been shown to decrease following a parabolic law.

This work was partially supported by the RFBR and the Ministry of Education, Science and Youth of the Republic of Crimea (Grant no. 18-42-910008 "p_a").

References

[1] K. Seleznyova, M. Strugatsky, S. Yagupov *et al.*, J. Appl. Phys. 125, 223905 (2015).

[2] M. Strugatsky, K. Seleznyova, S. Yagupov, *et al.*, JMMM 442, 417 (2017).

Influence of arsenic substitution for phosphorus on the helimagnetic structure of FeP

Zhurenko S.V.[1,2], Tkachev A.V.[1], Gunbin A.V.[1], Chernyavskii I.O.[3], Morozov I.V.[3], Moskvin A.S.[4], Gippius A.A.[1,2]

[1] *P.N. Lebedev Physics Institute, Moscow 119991, Russia*
[2]*Department of Physics, Lomonosov Moscow State University, 119991 Moscow, Russia*
[3]*Department of Chemistry, Lomonosov Moscow State University, 119991 Moscow, Russia*
[4]*Ural Federal University, 620083, Ekaterinburg, Russia*

The scientific interest into FeP, FeAs, CrAs and MnP are largely associated with intrinsic complexity of are unusual magnetic structure, details and generation mechanisms of which are still a matter of discussions. In our recent study, the magnetic structure of a polycrystalline and single crystal FeP was investigated in detail by means of NMR spectroscopy [1,2]. To study an influence of homovalent substitution at non-magnetic (phosphorus) site of the binary helimagnet FeP on its magnetic structure the single-phase polycrystalline sample $FeP_{1-x}As_x$ (x=0.33, 0.50) was synthesized.

Preliminary studies of the magnetic structure of $FeP_{0,5}As_{0,5}$ were carried out by Mössbauer spectroscopy, which found helimagnetic structure of $FeP_{0,5}As_{0,5}$ to be similar with that in the parent FeP compound. [3] However, because of the high quadrupole splitting of the Mössbauer spectra, it is not possible to reveal unambiguously the details of magnetic structure of this sample. Therefore, the most suitable method for studying the magnetic structure of this compound is NMR spectroscopy.

In this paper we present the field-sweep ^{31}P NMR spectra measurements at several fixed frequencies and zero-field NMR spectra at 4.2 K performed on the single-phase polycrystalline sample $FeP_{1-x}As_x$ with 33% and 50% substitution of As for P. In contrast to Mössbauer results, we observe dramatic symmetry reduction of magnetic structure in $FeP_{1-x}As_x$ (x=0.33, 0.50), resulting in essential narrowing ^{31}P NMR spectra. This narrowing points to phosphorous local fields decreasing compared to parent FeP.

Acknowledgments

This work was supported by grant 21-72-00112 from the Russian Science Foundation.

References

[1] A. A. Gippius, S. V. Zhurenko, N. Büttgen, M. Schädler, I. V. Morozov, and A. S. Moskvin. NMR analysis of the magnetic structure and hyperfine interactions in a FeP binary helimagnetic. Physics of the Solid State, 61(5):723–727 (2019).

[2] A. A. Gippius, A. V. Tkachev, S. V. Zhurenko, A. V. Mahajan, N. Büttgen, M. Schaedler, I. O. Chernyavskii, I. V. Morozov, S. Aswartham, B. Büchner, and A. S. Moskvin. NMR study of magnetic structure and hyperfine interactions in the binary helimagnet FeP. Physical Review B, 102:214416–214416 (2020).

[3] I. Presniakov, A. Sobolev, I. Chernyavskii, D. Pankratov, I. Morozov, and A. Shevelkov. Magnetic structure and anisotropic hyperfine interactions of the $FeP_{1-x}As_x$ system ($0 < x < 0.5$). In International Conference on the Applications of the Mossbauer Effect ICAME 2015 - Book of Abstracts, page 165. Hamburg, Germany (2015).

Thermal radiation from a magnetized semiconductor

Bychkov I.V.[1], Kuzmin D.A.[1], Shavrov V.G.[2],

[1]Chelyabinsk State University, 454001, Chelyabinsk, Russia
[2]Kotelnikov Institute of Radioengineering and Electronics of Russian Academy of Sciences, 125009, Moscow, Russia

Issues related to thermal radiation of solids were actively studied, in particular, in the middle of the last century [1-3] and at present [4, 5 and references therein]. Typically, thermal radiation has common characteristics: radiation is usually incoherent, broadband, unpolarized, and the radiation pattern is almost isotropic. It obeys a number of fundamental restrictions: the spectral density of thermal radiation is limited by Planck's law of thermal radiation. Heat radiators usually obey Kirchhoff's law, i.e. angular absorbance and emissivity should be equal to each other. All of this imposes serious restrictions on the ability to control thermal radiation. On the other hand, recently, new materials have attracted considerable attention of researchers: 2D materials and structures based on them, materials undergoing phase transitions, materials in which the interaction of subsystems is observed (for example, magneto-optical, magnetoacoustic effects, etc.). All this forces us to revise past results and apply them to new materials and structures.

We investigated the features of thermally stimulated radiation in an anisotropic medium using for example a semiconductor placed in a magnetic field. The electrodynamic characteristics of such a material can be described by an antisymmetric dielectric tensor with the following components: $\varepsilon_{xx} = \varepsilon_{yy} = 1 - \omega_P^2/(\omega^2 - \omega_H^2)$; $\varepsilon_{zz} = 1 - \omega_P^2/\omega^2$; $\varepsilon_{xy} = -\varepsilon_{yx} = -\omega_H \omega_P^2 / [\omega (\omega^2 - \omega_H^2)]$. Here ω_P and ω_H are plasma and cyclotron frequency, accordingly. For a given tensor, the magnetic field is directed along *z* axis. In such an environment, two types of waves can propagate. Therefore, the emissivity will consist of three terms [3] $\eta_\omega = \eta_{\omega,1} + \eta_{\omega,2} + \eta_{\omega,12}$, where $\eta_{\omega,i}$ is emissivity for waves of *i*-th type, $\eta_{\omega,12}$ is an interference term. As shown earlier [3], the last term does not play an essential role. For definiteness, we will choose vanadium dioxide VO_2, in which a metal-semiconductor phase transition occurs at temperatures close to room temperature. For the semiconductor phase, the characteristic parameters are as follows: $\omega_P \sim 10^{13}$ rad/s, $\omega_H \sim 10^8 H$ rad/s. The main issue in this work is to study the effect of an external magnetic field on the emissivity of an anisotropic medium. Consider, for definiteness, the radiation of the THz frequency range ($\omega = 5\ 10^{13}$ rad/s). The calculation results are shown in Fig. 1.

It can be noted that the difference in the emissivity for different types of waves is stronger in the direction along the magnetic field, across the magnetic field the emissivity of one of the waves does not depend on the magnitude of the field, while for the second wave it increases slightly. The total emissivity for the two types of waves grows with increasing magnetic field; however, at reasonable magnetic fields up to 1 T, this increase is insignificant. The polarization composition of radiation in a magnetic field will differ significantly from the polarization of radiation in the absence of a magnetic field. The results obtained awaken interest in the further study of these effects in multilayer nanostructures, when not only far-field radiation, but also near-field interactions will play an important role.

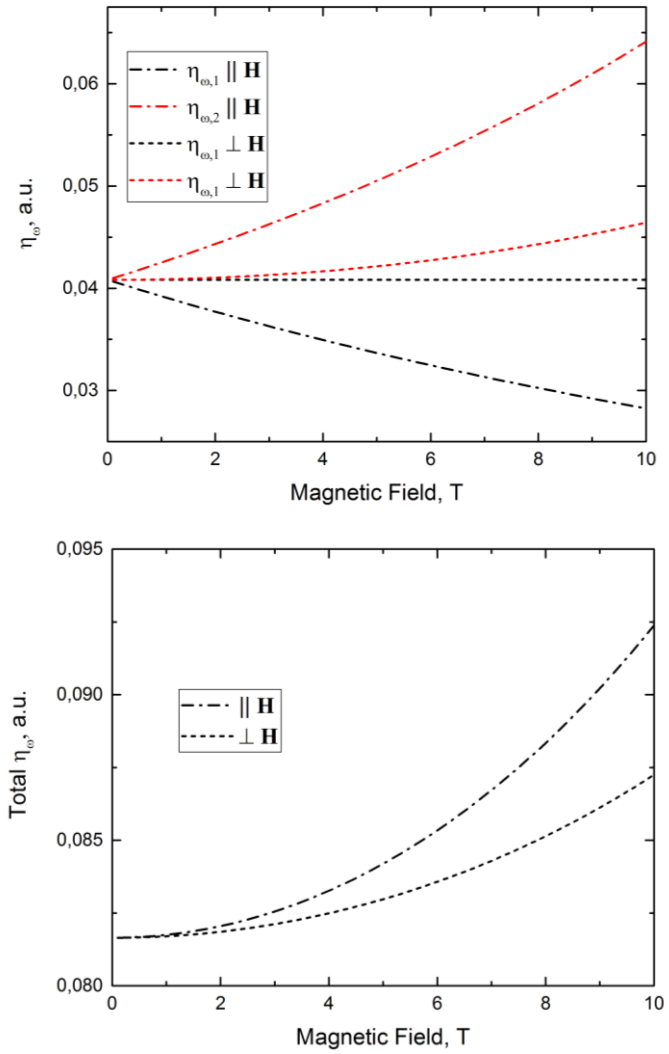

Fig.1. Emissivity of a semiconductor in a magnetic field.

This work was supported by the Russian Foundation for Basic Research (grants No. 20-37-70038, 19-07-00246, 20-47-740004), the Russian Science Foundation (grant No. 20-19-00745). Numerical calculations were performed with the support of the Ministry of Science and Higher Education of the Russian Federation within the framework of the state assignment project No. 075-00992-21-00.

References

[1] Rytov S.M., UFN 55, 299 (1955) (in Russian).

[2] Rytov S.M., UFN 63, 657 (1957) (in Russian).

[3] Bunkin F.V., Zh. Eksp. Teor. Fiz. 32(4), 811 (1957) (in Russian).

[4] E.A. Vinogradov, I.A. Dorofeev, Thermally stimulated electromagnetic fields of solids. M .: Fizmatlit. 2010 .—484 pp. (in Russian).

[5] Volokitin A.I., Persson B.N.J., Phys. Usp. 50 879 (2007).

Isotopically modified single crystal silicon as functional material: effect of isotopic composition on lattice constant

Sozontov E.A.

National Research Centre "Kurchatov Institute", 123182 Moscow, Russian Federation

The study of the effect of the isotopic composition on various properties of materials such as the lattice dynamics and the electronic band structure of crystalline solids has attracted increasing interest [1]. Practically all physical properties of crystals depend to some degree on their isotopic composition, sometimes yielding new, even exotic features. The thermal conductivity of isotopically enriched crystals, for example, can considerably exceed the values for the corresponding natural materials. By purifying silicon to >99.9% of ^{28}Si, the phonon mean free path increases, thereby significantly improving the thermal conductivity. The thermal conductivity is enhanced by approximately 70% at liquid nitrogen temperature and by a factor of 7.5 at 26.5 K. The maximum thermal conductivity of ^{28}Si at 26.5 K is 2.5 times higher than that of diamond [2].

A precise determination of the lattice constant of isotopically controlled Si is relevant, apart from basic interest, for its metrological and other applications. The influence of the isotopic composition on the lattice constant [3] is due to the combined effect of zero-point motion of the atoms and the anharmonicity of the potential. Thus, this is purely a quantum-mechanical effect. Compared to the influence of the isotopic mass on the vibrational properties of crystals, the effect is small. The x-ray standing wave (XSW) technique [4, 5, 6] can be used to determine the lattice constant difference with very high accuracy. Following our early work [7], we report here the application of the XSW method to the case of a highly enriched ^{30}Si film on a Si single crystal with natural isotopic composition. Employing XSW and photoemission we find the relative lattice constant difference ($\Delta a/a$) of -1.8×10^{-5} and -3.0×10^{-5} for Si at 300 and 30 K, respectively.

References

[1] M. Cardona, in *Advances in Solid State Physics*, edited by R. Helbig (Vieweg, Braunschweig/Wiesbaden, Germany), Vol. 34, pp. 35–50, (1994).

[2] A.V. Inyushkin, A.N. Taldenkov, A.M. Gibin, A.V. Gusev, and H.-J. Pohl, Phys. Stat. Sol. C 1, 2995 (2004).

[3] H. London, Z. Phys. Chem. 16, 302 (1958).

[4] B.W. Batterman, Phys. Rev. A 133, 759 (1964).

[5] M.V. Koval'chuk and V.G. Kohn, Sov. Phys. Usp. 29, 426 (1986).

[6] J. Zegenhagen, Surf. Sci. Rep. 18, 199 (1993).

[7] E. Sozontov, L.X. Cao, A. Kazimirov, V. Kohn, M. Konuma, M. Cardona, and J. Zegenhagen, Phys. Rev. Lett. 86, 5329 (2001).

Influence of the dislocation density on the dynamic yield stress under high strain rate deformation

Varyukhin V.N.[1], Malashenko V.V. [1, 3], Malashenko T.I.[2]

[1]*O.O. Galkin Donetsk Institute for Physics and Engineering, 283114, Donetsk*
[2] *Donetsk National Technical University, 283001 Donetsk*
[3] *Donetsk National University, 283001 Donetsk*

The mechanical properties of crystals are formed by the motion of dislocations and their interaction with other structural defects. The dependence of mechanical properties of functional materials on the dislocation density under quasi-static deformation is adequately described by the Taylor relationship where the yield stress of metals and alloys is proportional to the square root of the dislocation density. This relationship takes place in copper and steel under high strain rate deformation. However, Taylor relationship can be violated in the case of high strain rate deformation of aged binary alloys. High strain rate deformation has its own distinctive features [1, 2]. Dislocations make over-barrier sliding under such deformation. The dissipation mechanism under study consists in the transition of the kinetic energy of a dislocation to the energy of its transverse vibrations in the slip plane. The force of dynamic drag of a dislocation by structural defects depends not only on their concentration, but also on the spectrum of dislocation vibrations, primarily on the presence of a gap in it. Under high strain rate deformation, the dislocation density can reach values of $10^{15} - 10^{16}$ m^{-2}. In this case, the main contribution to the formation of the gap is made by interdislocation interaction. The theory of dynamic interaction of structural defects makes it possible to obtain an analytical expression for the yield stress [3, 4]

$$\tau = \frac{K}{\sqrt{\rho + b^{-2}\sqrt{n_d \chi^2}}} + \alpha\mu b\sqrt{\rho}$$

Here χ is the dimensionless misfit parameter of impurity atoms, n_d is the dimensionless concentration of these atoms, b is the modulus of dislocation Burgers vector, ρ is dislocation density, μ is a shear modulus, K is a coefficient depending on the concentration of Guinier-Preston zones. It is shown that dislocation density dependence becomes nonmonotonic and can have a maximum. The position of the maximum is determined by the dislocation density, at which the interdislocation interaction becomes dominant during the formation of a gap in the vibrational spectrum.

References

[1] D. Batani. EPL. 114, 6500 (2016).
[2] S. Kodambaka, V. Khare, W. Swich, K. Ohmori, I. Petrov, J. E. Greene. Nature. 429, 49 (2004).
[3] V.V. Malashenko, Phys. Sol. State. 62(10), 1886 (2020).
[4] V.V. Malashenko. Physica B: Phys. Cond. Mat. **404**, No 2, 3890 (2009).

Exchange interactions in $TbCu_2$

Golovchan A.V.[1],Nirkov N.Yu.[1], Andreychenko E.P.[1], Mitsiuk V.I.[2], Mashirov A.V.[3]

[1]Donetsk Institute for Physics and Engineering named after A.A.Galkin, 283114, Donetsk, DPR
[2] Scientific and Practical Materials Research Centre, National Academy of Sciences of Belarus, Minsk, 220072 Belarus
[3] Kotelnikov Institute of Radio Engineering and Electronics, Russian Academy of Sciences, Moscow, 125009 Russia

The $TbCu_2$ compound is interesting due to the existence at low temperatures of a long-period antiferromagnetic structure, giant magnetostriction, and the presence of direct and inverse magnetocaloric effects at low temperatures. In the presented work, an *ab initio* calculation of the electronic structure and an estimation of the parameters of interatomic exchange interactions were performed using the fully-relativistic SPRKKR package.

We found that the isotropic part of the Tb-Tb interatomic exchange interaction is relatively weak (3.3 meV) and rapidly decreases with increasing distance (Fig. 2). Fast oscillations of Jij indicates significant spatial anisotropy. The components of the antisymmetric part of the exchange interaction also rapidly decreases with interatomic distance. The strong spatial anisotropy of the vector Dij, in which the various components differ by more than an order of magnitude, turned out to be surprising.

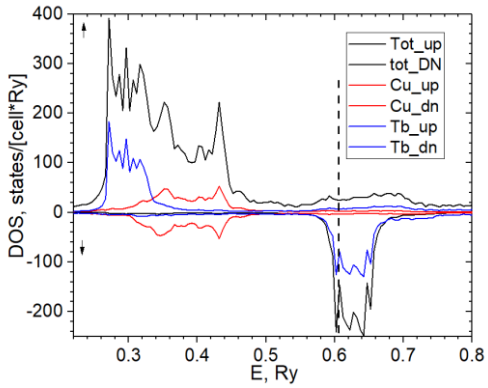

Fig. 1. Electronic structure of the ferromagnetic $TbCu_2$. The vertical line indicates Fermi level.

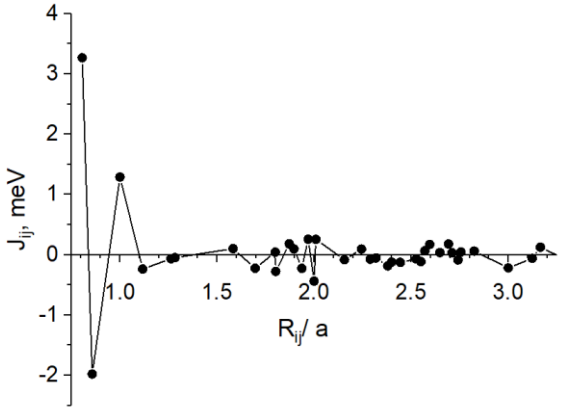

Fig.2. The isotropic exchange coupling parameters J_{ij} between Tb atoms.

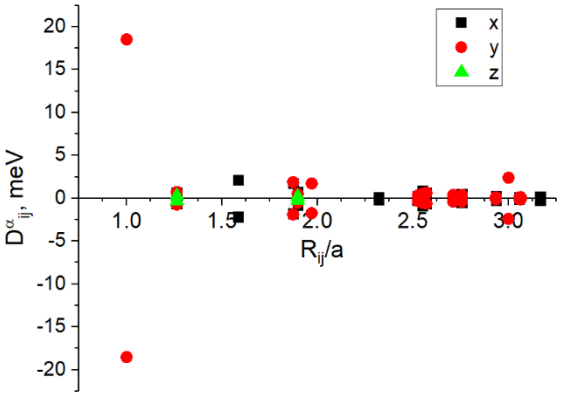

Fig.3. Components of Dzyaloshinskii-Moriya interaction vector between Tb atoms.

This work was carried out with financial support from the Belarusian Republican Foundation for Fundamental Research and the Russian Foundation for Basic Research within the framework of scientific projects No. T20R-204 and No. 20-58-00059, respectively.

Fermi surface nesting of Fe_3Ga_4 alloy

Sokolovskiy V.V.[1,4], Miroshkina O.N.[1,2,3], Zagrebin M.A.[1,4], Baigutlin D.R.[1,2], Buchelnikov V.D.[1,4]

[1]*Chelyabinsk State University, 454001 Chelyabinsk, Russia*
[2] *LUT-University, FI-53851 Lappeenranta, Finland*
[3] *University of Duisburg-Essen, 47057, Duisburg, Germany*
[4] *National Research South Ural State University, 454080 Chelyabinsk, Russia*

Multifunctional materials are of interest for fundamental condensed matter physics and decisive for the design of modern technologies. One of these materials is Fe_3Ga_4 which has a complex magnetic structure [1]. In this material, there is strong competition between the ferromagnetic (FM) and antiferromagnetic (AFM) states as shown in Fig. 1 (a). Due to this, several transitions between these states are observed when the temperature increases [2].

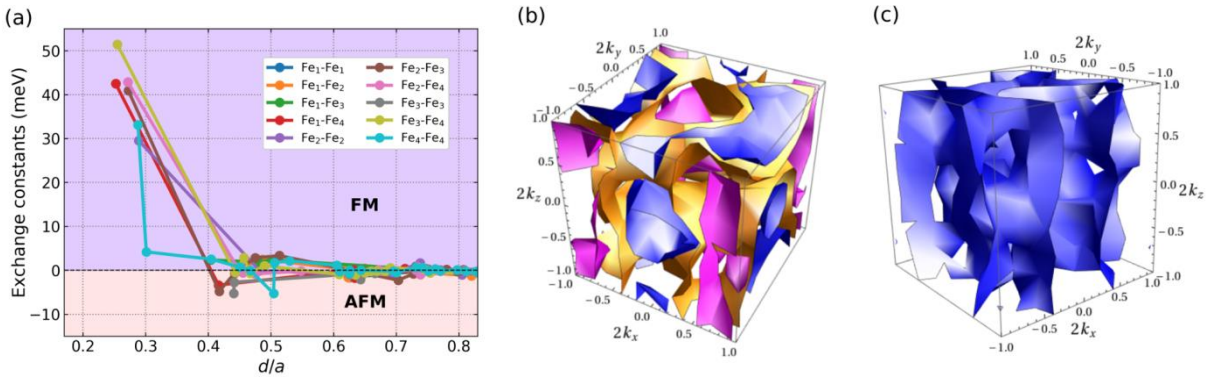

In addition to the AFM phase, the alloy also exhibits an incommensurate spin-density wave (ISDW) state [3]. The reason for the appearance may be in strong nesting in the spin-polarized Fermi surface. Figs 1(b, c) show the Fermi surfaces for both spin-up and spin-down electrons, which are the sets of parallel planes indicating strong nesting. Competitive behaviour between FM and ISDW states leads to susceptibility to external perturbation, allowing magnetic transitions to be controlled by temperature, external field, or pressure. Thus, Fe_3Ga_4 is a perspective material for new magnetic memory devices, such as components of spin valves with tunneling magnetoresistance.

This study was supported by the Ministry of Science and Higher Education of the Russian Federation within the framework of the Russian State Assignment under contract No. 075-002992-21-00.

References

[1] J.H. Mendez et al. Phys. Rev. B 91, 144409 (2015).
[2] H.Z. Wagini. Naturforsch. A 21, 528 (1966).
[3] Y. Wu, et al. Sci. Rep. 8(1), 1-8 (2018).

Quantum-chemical modeling of the efficiency of using polyarylenes in interface structures

Kalimullina L.R.[1], Lachinov A.N.[1,2], Baybulova G.Sh.[1]

[1]Bashkir State Pedagogical University n.a. M. Akmulla, 450000, Ufa, Russia
[2]Institute of Molecule and Crystal Physics – Subdivision of the Ufa Federal Research Centre of the Russian Academy of Sciences, 450075, Ufa, Russia

In this work, a quantum-chemical analysis of the efficiency of using polyarylenes in interface structures was carried out. Quantum-chemical calculations were carried out for molecular systems, which are model systems of polymers of the polyarylene class. In total, 27 representatives of this class of compounds were considered. For all molecules, quantum-chemical calculations were carried out using the density functional theory method B3LYP / 6-31 + G (d) and theoretically estimated such energy parameters as the total energies of molecules and their negative and positive ions in molecular and optimized ionic geometries; energies of occupied and vacant molecular orbitals; the values of the vertical and adiabatic electron affinity and ionization potential, as well as the dipole moment.

In this work, we propose an algorithm for processing the results of quantum chemical calculations based on the analysis of the energy characteristics of the monomer unit of the polymer, which makes it possible to reveal a certain relationship between the chemical structure of an organic compound and the electronic properties of the metal / polymer interface. The proposed algorithm made it possible to identify areas of maximum deviation of energy parameters and specific compounds that are of interest for the formation of hetero-structures.

This work was carried out with the support of the Mirror Laboratories project of the National Research University Higher School of Economics and the Bashkir State Pedagogical University n.a. M. Akmulla.

Spontaneous phase transitions in the bubble lattice of ferrite-garnet film

Siryuk Yu.A.[1], Bezus A.V.[1], Bondar E.D.[1], Kononenko V.V.[2]

[1] Donetsk National University, 283001, Donetsk, Ukraine
[2] Donetsk Institute for Physics and Engineering named after A.A. Galkin, 83114, Donetsk, Ukraine

The influence of temperature on a lattice of cylindrical magnetic domains (CMD) and on domain walls in magnetouniaxial film has been experimentally studied. The investigations were carried out on the film of $(TmBi)_3(FeGa)_5O_{12}$ composition (T_N=437K, T_C=120K, h=8.4μm), where is the T_N – Neel temperature, T_C– the magnetic compensation temperature, h– film thickness (Fig.1).

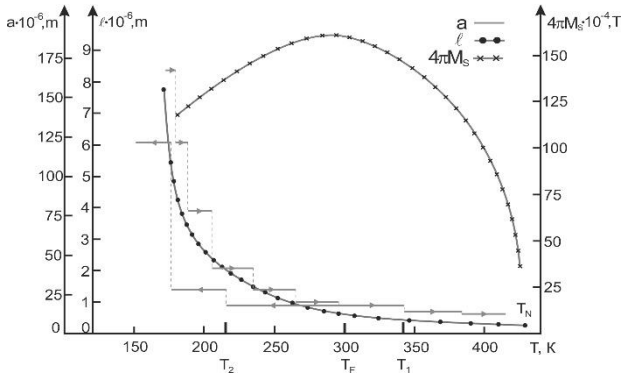

Fig.1. Temperature dependences of film parameters: saturation magnetization $4\pi M_s$, characteristic length *l* and the CMD lattice period.

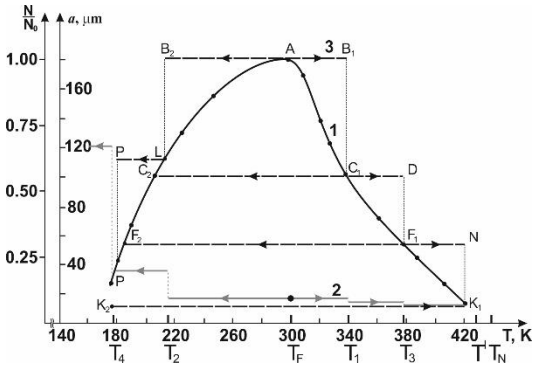

Fig.2. Temperature dependences of CMD lattices parameters: 1– N/N_0 VBL in DW of equilibrium lattice; 2– period of nonequilibrium lattice; 3– N/N_0 VBL in DW of nonequilibrium lattice.

The topicality of this study is that investigations performed in it can be used in constructing devices for recording and storing information on the spins of domain walls (DW). In these devices, simultaneous and/or parallel recording and storage of information on domains and on spins is possible, which can significantly expand the capabilities of such devices.

The lattice of CMD is formed by a monopolar pulsed magnetic field perpendicular to the film plane. Then the field is removed. The action of a pulsed magnet field creates vertical Bloch lines (VBL) in domain wall. Upon a change in the temperature, a first-order phase transitions occur on the DW, which induces a phase transitions in the lattice of CMD. The mechanisms of phase transitions in the domain wall upon heating and cooling of the film differ significantly. The number of VBLs in the domain wall decreases upon heating via annihilation, and upon cooling, due to unwinding. Temperature stability interval of CMD lattice depends on the structure of domain wall. Due to decrease in the number of VBLs in the domain boundary, the temperature stability interval of the CMD lattice increases. The CMD lattice with a simple Bloch wall is the most stable and persists in a wide temperature interval.

It was shown experimentally the quantization of domain walls upon a change temperature of film (Fig.2).

Experimental studies and *ab initio* calculations of $Tb_2Ti_2O_7$ and $(Er_{0.05}Y_{0.95})_2Sn_2O_7$ pyrochlore systems properties

Spiridonova A.V.[1], Romanova I.V.[1], Nedopekin O.V.[1]

[1]*Institute of Physics of Kazan (Volga Region) Federal University, 420111, Kazan, Russia*

Magnetism and magnetic materials are pervasive in everyday life from electric motors to hard disk data storage. From a fundamental perspective, magnetic materials and theoretical models of magnetic systems have, since the original works of Ising and Potts, offered physicists perhaps the best test bench to investigate the broad fundamental concepts, even at time universal ones, underlying collective phenomena in nature [1].

Nowadays geometrically frustrated magnetic systems are intensively studied theoretically rather as experimentally [2]. Pyrochlores of type $A_2B_2O_7$, where A = Er^{3+}, Dy^{3+}, Tb^{3+}, Ho^{3+}, Sm^{3+}, Yb^{3+}, Tm^{3+} stands for a rare-earth ion, show exotic magnetic behaviors such as dipolar spin ice and spin liquid phases, a first order transition in the spin dynamics and complex antiferromagnetic orders. The type of magnetic order depends on the balance between antiferromagnetic exchange, dipolar and crystal field energies.

The synthesis of rare-earth pyrochlores $Tb_2Ti_2O_7$ and $(Er_{0.05}Y_{0.95})_2Sn_2O_7$ was carried according to standard optical floating zone method. The pre-heating temperature was 600°C and the synthesis temperatures were about 1300–1400°C.

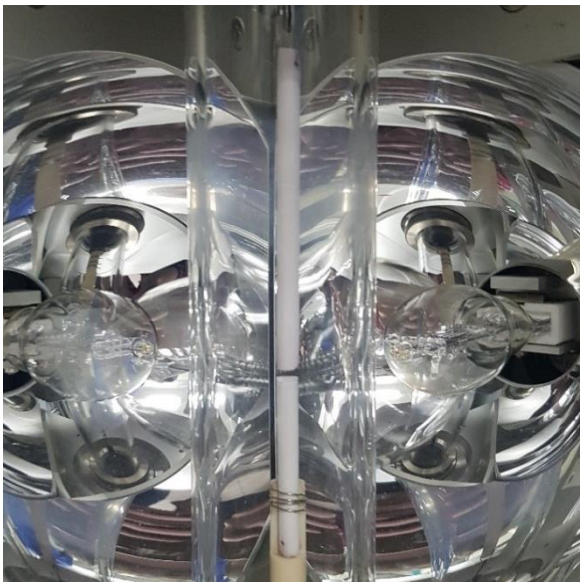

Fig. 1. Growing of $Tb_2Ti_2O_7$ single crystal by the optical floating zone technique

The samples were analysed by X-ray powder diffraction to confirm their phase purities. All XRD measurements in this study were done using a Bruker D8 ADVANCE diffractometer, Cu Kα radiation (λ = 1,5406 Å). Magnetic properties were determined by vibrating magnetometry using a Physical Properties Measurement System-9 by Quantum Design in the magnetic fields up to 90 kOe and the temperature range of 5 K to 300 K. EPR measurements were made using a laboratory EPR spectrometer.

The pyrochlores of type $A_2B_2O_7$ crystallize into a face centred cubic structure with the $Fd\bar{3}m$ space group (No. 227 in International Tables of Crystallography). Theoretical investigations on pyrochlores are mainly based on model Hamiltonians, involving Heisenberg exchange, dipole-dipole interactions and single ion anisotropy, which are parametrized by using experimental data. The lack of modern *ab initio* calculations on these materials prevents microscopic understanding of these magnetic model Hamiltonians. A phonon spectrum is most adequately reproduced from modern *ab initio* calculations of periodic structures, which allows the reproduction of all modes of a given structure.

The crystal structure and the phonon density and mode spectra *ab initio* calculations have been carried out by using GGA–PBE-sol functional by the density functional theory method [3]. The calculations were performed within VASP and Phonon modules of MedeA software. The IR-active, Raman-active and "silent" modes of single crystals were determined. The specific heat of $Tb_2Ti_2O_7$ were calculated.

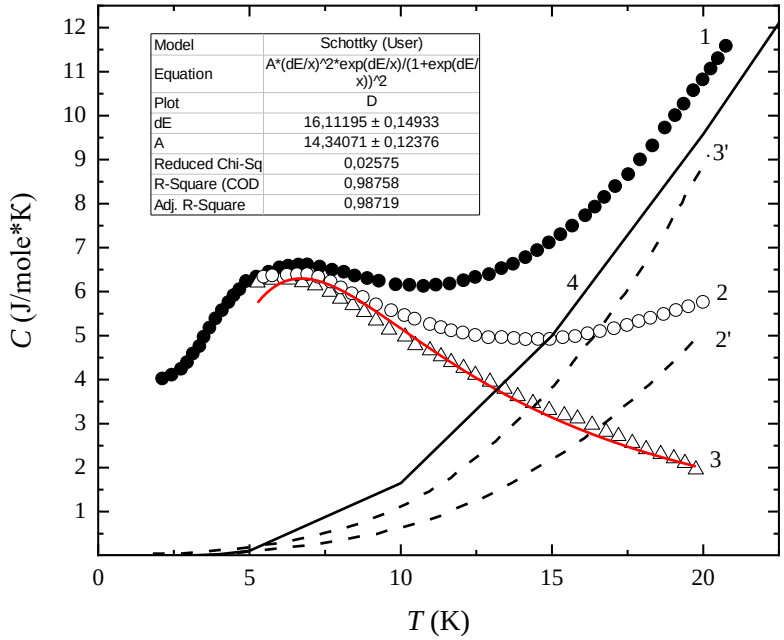

Fig. 2. $Tb_2Ti_2O_7$ specific heat dependences at the different initial conditions

All performed calculations are in a good agreement with experimental data and previous results [4]. The $(Er_{0.05}Y_{0.95})_2Sn_2O_7$ synthesis and measurements were carried for the first time. The *ab initio* calculations are extended to describe the whole range of rare-earth ions as A and concentrated on anisotropic magnetostriction of given pyrochlores.

References

[1] S. Petit et al., Phys. Rev. Let. 119, 187202 (2017).

[2] V.V. Klekovkina and B.Z. Malkin, Optics and Spectroscopy 116, 6 (2014).

[3] G. Kresse and J. Furthmuller, Phys. Rev. B 54, 11169 (1996).

[4] N. Deilynazar, E. Khorasani, M. Alaei and S. J. Hashemifar e-print arXiv:1502.01814v1 (2015).

Thermal transient mechanical loss in Ni-Mn-Ga alloys

Kaminskii V.V., Kalganov D.A.

ITMO University, 197101, Saint Petersburg, Russia

Investigation of materials with the magnetic shape memory effect in the Ni-Mn-Ga system is a challenging task from both a fundamental and an applied point of view. The urgency of this works is due to the prospect of creating micromechanical devices that are unique in their size and energy efficiency. Operation of these devices is based on the effect of magnetic domains reorientation under the influence of external fields.

Temperature dependence of internal friction curve in Ni-Mn-Ga alloys reflects the process of structural transformations from the initial cubic phase through a number of intermediate - modulated phases to the austenitic one [1,2].

In this work, we studied samples of the $Ni_{50.0}Mn_{28.4}Ga_{21.6}$ single crystal at different temperatures and heating rates and determined the thermal transient mechanical loss from the effective modulus (Fig.1) of elasticity using a composite piezoelectric oscillator [3].

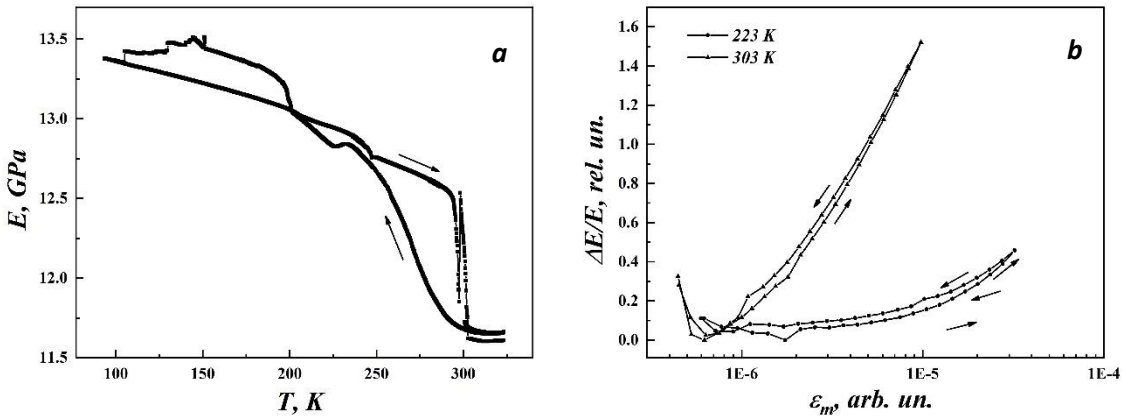

Fig. 1. Effective elastic modulus changes with heating – ***a*** and different temperatures – ***b***

The reported study was funded by RFBR, project number 20-32-90195

References

[1] A.N. Vasil'ev, V.V. Kokorin, Yu I. Savchenko and V.A. Chernenko, JETP. 98, 803 (1990).

[2] A. Sozinov, A.A. Likhachev, N. Lanska and K. Ullakko, Appl. Phys. Lett. 80, 746-1748 (2002).

[3] S. Kustov, A. Saren, A. Sozinov, V. Kaminskii and K. Ullakko, Scr. Mater. 178, 483-488 (2020).

Formation of the equilibrium lattices of stripe domain structure in the ferrite-garnet film

Siryuk Yu.A.[1], Bezus A.V.[1], Kapshukov R.A.[1], Kononenko V.V.[2]

[1] *Donetsk National University, 283001, Donetsk, Ukraine*
[2] *Donetsk Institute for Physics and Engineering named after A.A. Galkin, 83114, Donetsk, Ukraine*

The influence of temperature on a lattice of cylindrical magnetic domains (CMD) and on domain walls in magnetouniaxial film has been experimentally studied. The investigations were carried out on the film of $(TmBi)_3(FeGa)_5O_{12}$ composition (T_N=437K, T_C=120K, h=8.4μm), where is the T_N – Neel temperature, T_C– the magnetic compensation temperature, h– film thickness.

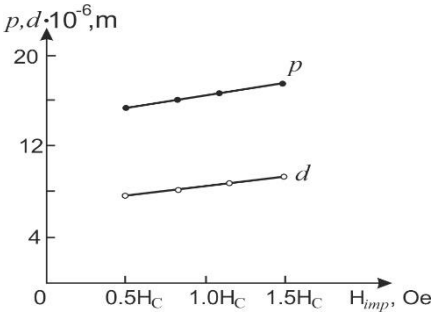

Fig.1. Dependences of lattice period *p* and domain width *d* on the strength of the pulsed magnetic field forming the DS at T= 300K.

The topicality of this study is that investigations performed in it can be used in constructing devices for transporting magnetically tagged microbiological particles. These devices can be used for sorting chemical particles according to their sizes at different temperatures.

An equilibrium lattice of stripe domain structure (DS) is formed by a monopolar pulsed magnetic field perpendicular to the film plane in zero bias field. The pulse frequency and duration are selected experimentally. Then the pulsed field is removed. It is found that the lattice period of a stripe DS depends on the pulsed field strength (Fig.1). We have obtained a number of equilibrium lattices of the stripe DS, which have been forms at T=300K by a pulsed magnetic field of strength $0.5H_c \leq H \leq 1.5H_c$, where

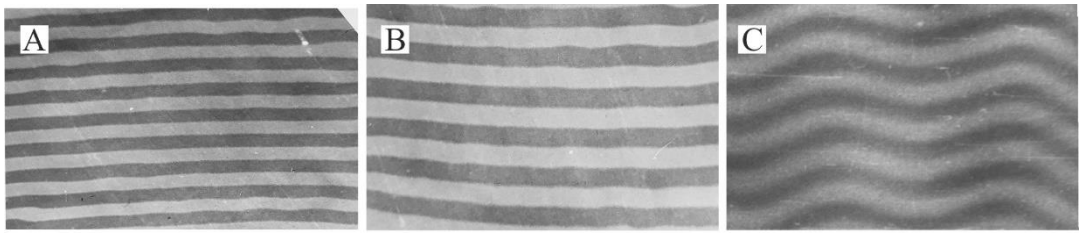

Fig.2. Types of domain structures of the film at T= 300K: (a) stripe DS lattice formed by pulsed field $H=0.5H_c$; (b) stripe DS lattice formed by field $H=1.5H_c$; (c) wavy DS after the removal of the pulsed field.

H_c is the CMD collapse field. The lattice formed by a field of strength $H= 1.5H_c$ has the largest period and is unstable (Fig.2). After the removal of the field, this lattice is transformed into an equilibrium wavy structure, i.e., a field-induced first-order phase transition occurs [1].

References

[1] Yu.A. Siryuk, A.V. Bezus, R.A. Kapshukov and V.V. Kononenko, in Proceedings of the First International Interdisciplinary Congress Phase Transitions and New Materials (Rostov-on-Don, p.371, 2020).

Atomic-force microscopy: Application to investigation of surface morphology of $R_2Fe_{14}B$ functional materials

Kaminskaya T.P.[1], Pelevin I.A.[2], Paukov M.A.[3,4], Tereshina I.S.[1,2]

[1] Faculty of Physics, M.V. Lomonosov Moscow State University, 119991, Moscow, Russia
[2] Catalysis Lab, National University of Science and Technology MISIS, 119991 Moscow, Russia
[3] Faculty of Mathematics and Physics, Charles University, Prague 12116, Czech Republic
[4] Department of Nuclear Fuel Cycle, Research Centre Řež, Hlavní 130, Husinec-Řež 25068,Czech Republic

Novel hard magnetic materials represent multicomponent alloys $R_2Fe_{14}B$-type, require special treatments aimed to form proper microstructure which provides high magnetic characteristics such as remanence and coercive force [1]. Investigation of microstructure of these alloys including volumetric and superficial features is separate complex scientific problem [2,3]. Present work is aimed to define all particularities of surface morphology study of $R_2Fe_{14}B$ (R = Nd, Gd, Er and Y) alloys using atomic-force microscopy technique.

The samples with corresponding compositions were obtained by means of rapid melt quenching method with various drum rotation speed, thus flake-shaped samples were formed. The rapid quenched samples had ultra-fine grain structure with nano-sized grains (70 nm average), so high resolution atomic-force microscopy is a suitable method of investigation of such samples and their surface morphology.

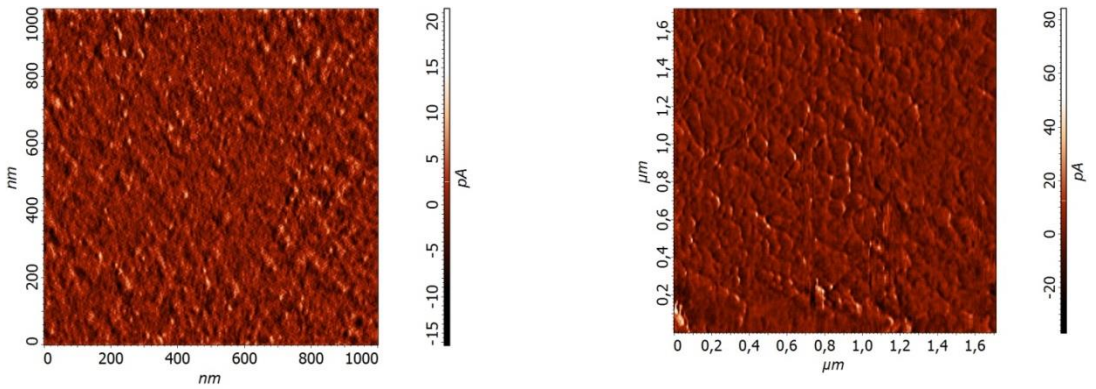

Fig. 1. Microstructure of $Y_2Fe_{14}B$ quenched with 20 m/s (left) and 30 m/s (right) drum rotation speed obtained using atomic-force microscopy.

The larger grains (structural elements observed on the surface by AFM are supposed to be grains) were found for $Nd_2Fe_{14}B$ alloy, whereas fine grains in $Gd_2Fe_{14}B$ are combined into agglomerations with average size of 120-300 nm. $Er_2Fe_{14}B$ rapid quenched alloy possesses the finest grain structure with 25-30 nm average size along with some amount of their agglomerations up to 100 nm size. $Y_2Fe_{14}B$ demonstrated medium characteristics. It should be noted that yttrium is a suitable non-magnetic analog of the rare-earth metals (REM) convenient for various structural investigations which further might be extrapolated on compounds with magnetic ions (R^{3+}).

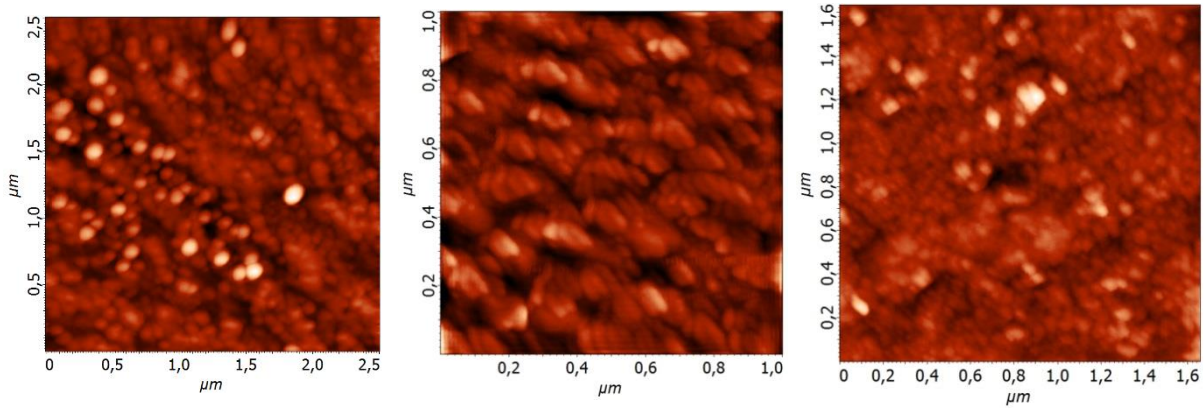

$Nd_2Fe_{14}B$ $Gd_2Fe_{14}B$ $Er_2Fe_{14}B$

Fig. 2. Atomic-force microscopy microstructures of $R_2Fe_{14}B$ (R = Nd, Gd, Er) quenched with 20 m/s drum rotation speed.

Among the information gathered for $R_2Fe_{14}B$ alloys there are the topography of the contact and free surface of ribbon samples, intergrain coupling, morphology of nanograins and clusters in the near-surface layers, the size of particles and their distribution. A comparative analysis of the results obtained has been carried out. The influence of the REM variety on the shape of the formed grains was found.

This work is performed with financial support of the grant of Russian Science Foundation (RSF), project # 21-79-10239.

References

[1] J.M.D. Coey, Engineering 6, 119-131 (2020).

[2] H. Sepehri-Amin, S. Hirosawa and K. Hono, Handbook of Magnetic Materials 27, 269-372 (2018).

[3] I.S. Tereshina, I.A. Pelevin, E.A. Tereshina, G.S. Burkhanov, K. Rogacki, M. Miller, N.V. Kudrevatykh, P.E. Markin, A.S. Volegov, R.M. Grechishkin, S.V. Dobatkin, L. Schultz, J. Alloys. Compd. 681, 555-560 (2016).

Thermal Behaviour of Hollandite-like Solid Solutions in the TiO_2-K_2O-MnO-Al_2O_3 System

Saunina S.I.[1], Tretyachenko E.V.[2], Maksimova L.A.[2], Vikulova M.A.[2],
Zakharyevich D.A.[1], Gorokhovsky A.V.[2], Iagafarov Sh.Sh.[1]

[1]*Chelyabinsk State University,shakir@csu.ru, Chelyabinsk, Russia*
[2]*Yuri Gagarin State Technical University of Saratov,vikulovama@yandex.ru, Saratov, Russia*

Currently, complex oxides based on titanium and alkali, alkaline-earth, transition and other metals with hollandite-like structures and the general chemical formula $AxTi_8O_{16}$ are attracting interest due to their electrical and magnetic properties [1]. Most methods for the synthesis of such structures involve the replacement of structure-forming titanium with one modifying metal. [2,3].

In this study, using a unique solution technology, hollandite-like solid solutions were obtained by modifying potassium polytitanate with compounds of two metals - manganese and aluminum. The evolution of the phase composition of potassium polytitanates (PPT) modified with manganese and aluminum salts at different molar ratios of metals (Mn:Al = 1:1; 2:1; 3:1) has been studied by X-ray diffraction and thermal analysis after heat treatments at 300, 550, 600, 750, and 900 °C.

According to the X-ray diffraction data, PPT - Mn/Al samples with a 1:1 and 3:1 ratio at temperatures of 550, 600, and 750 °C contain $KMnTi_3O_8$ phase with a hollandite-like structure and TiO_2 in the anatase modification. The amount of the anatase phase decreases with an increase in the heat treatment temperature, and at 900 °C only the $KMnTi_3O_8$ phase is detected in the samples. In the PPT - Mn/Al sample with a 2:1 ratio at 550 and 600 °C, the phases $KMnTi_3O_8$ and TiO_2 (anatase) are detected. However, the amount of anatase phase is negligible. After heat treatment at 750 and 900 °C, the sample becomes single-phase. Interlayer aluminum hinders the formation of the anatase phase by preventing the convergence of the octahedral layers.

On the DSC curve (Fig. 1) for the PPT - Mn/Al (1:1) sample, 2 endothermic effects are observed: 1 – removal of physically sorbed water from the surface and from the interlayer space at about 100 °C, 2 – reaction $Al(OH)_3 \rightarrow AlOOH$ at ~ 229 - 310 °C.

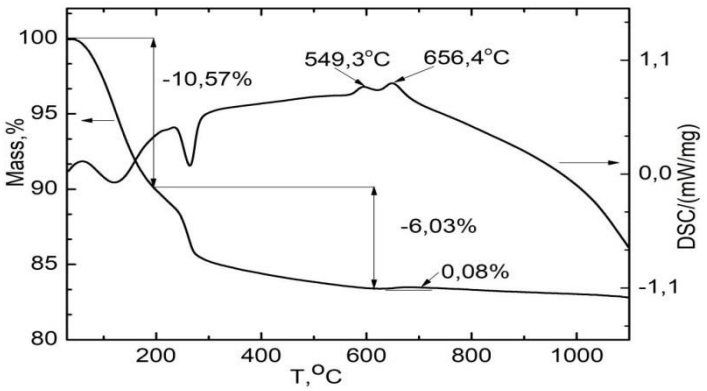

Fig.1. TG and DSC curves for PPT-Mn/Al (1:1)

In addition, two exothermic effects are observed on the same DSC curve. The first (T_{max} = 549.3 °C) is probably associated with processes involving interlayer Al^{3+} cations. The second (T_{max} = 656.4 °C), accompanied by an increase in the sample weight, is associated with the formation of hollandite-like structure (with a change in stoichiometry) involving manganese cations. Similar results were obtained for the PPT - Mn/Al (3:1) sample. For the PPT - Mn/Al (2:1) sample, the DSC curve contains only one exothermic effect with T_{max} = 596 °C, which is not accompanied by a change in the sample mass (Fig. 2).

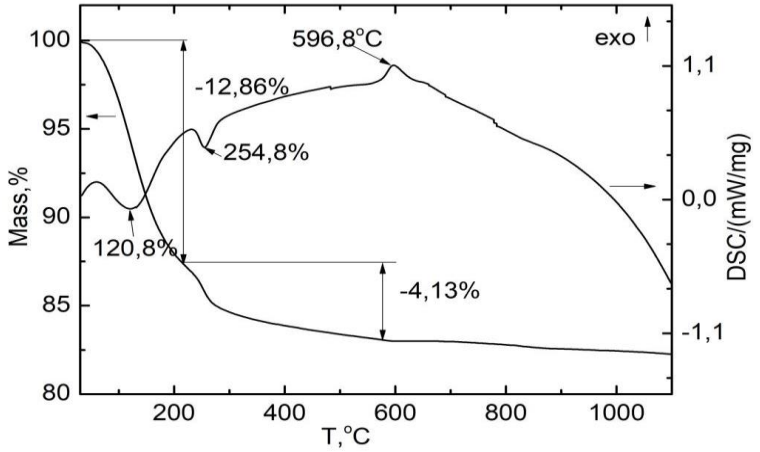

Fig.2. TG and DSC curves for PPT-Mn/Al (2:1)

Thus, aluminum cations as an additional modifying additive contribute to a decrease in the initial temperature of the formation of the tunnel structure of hollandite with the composition $KMnTi_3O_8$. X-ray phase analysis did not show a clear connection between exothermic effects and phase formation.

References

[1] Y. Muraoka, K. Noami, T. Wakita, et al., Physica Status solidi C. 8, 555 (2011).

[2] P. Moetakef, A. M. Larson, B. C. Hodges, et al., Journal of Solid State Chemistry. 220, 45 (2014).

[3] N. Kijima, M. Sakao, Y. Tanuma, et al., Solid State Ionics. 262, 14 (2014).

Influence of multi-axial isothermal forging on the stability of martensitic transformation in the Heusler alloy of the Ni-Mn-Ga system

Gaifullin R.Yu.[1, 2], Musabirov I.I.[2], Safarov I.M.[2], Galeyev R.M.[2]

[1]Bashkir State University, 32 Zaki Validi St., 450076, Ufa, Russia
[2]Institute for Metals Superplasticity Problems, Russian Academy of Sciences, 39 Khalturin St., 450001, Ufa, Russia

In Heusler alloys in the range of room temperatures, a martensitic transformation occurs, in the range of which such effects as the ferromagnetic shape memory effect and the magnetocaloric effect are observed. Due to these effects, alloys are classified as functional materials. A common disadvantage for monocrystalline and polycrystalline samples is reduced mechanical properties. With multiple cycles of direct and reverse martensitic transformation, the specimens are subject to destruction. To improve the mechanical properties of alloys, it is possible to use such methods of thermo-mechanical treatment (TMT) as severe plastic deformation by torsion, rolling, multi-axial isothermal forging (MIF), etc. The deformation of materials by torsion and rolling makes it possible to obtain thin samples (strips, disks) with required structure. In comparison with them, it is possible to obtain a volumetric billet by forging, which is an advantage over other TMT methods. The authors are intensively developing schemes and modes of thermo-mechanical treatment by methods of multi-axial isothermal forging and forging followed by extrusion and their influence on the functional properties of Heusler alloys of the Ni-Mn-Ga system [1-5]. The advantage of this processing method is the production of a bulk material with the required microstructure, different levels of microstresses and texture. At the last stages of deformation processing, with the so-called broaching, the formation of a sharp crystallographic texture is possible, which is an important aspect for obtaining the maximum possible value of the functional effect. After forging the alloy, a working element of the required shape and size can be cut from the already obtained workpiece.

This work presents the results of a study of the effect of thermo-mechanical treatment by the method of multi-axial isothermal forging of the Heusler alloy on the microstructure, physical and mechanical properties.

The alloy was forged on a Schenck Trebel RMC 100 complex loading machine. Staged upsetting of the sample by 35-40% was performed at a temperature of 973 K and a strain rate of 0.2 mm / min. The total true strain degree was $e \approx 3.9$.

The study of the mechanical properties and stability of the martensitic transformation of the alloy was carried out on a three-point bending device of our own design. It makes it possible to measure the dependence of the bending deformation of a specimen of a shape memory alloy on temperature and mechanical stresses in the specimen.

Precision analysis of the effect of deformation-heat treatment on the characteristic temperatures of martensitic transformation carried out using differential scanning calorimetry showed that as a result of deformation-heat treatment, there is a decrease in the characteristic points of martensitic transformation in the region of low temperatures by 28 K. The corresponding results are presented in Fig. 1.

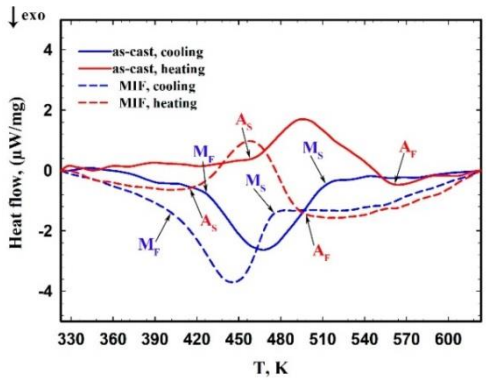

Fig. 1. Comparison of DSC curves of the alloy in the as-cast state and after forging.

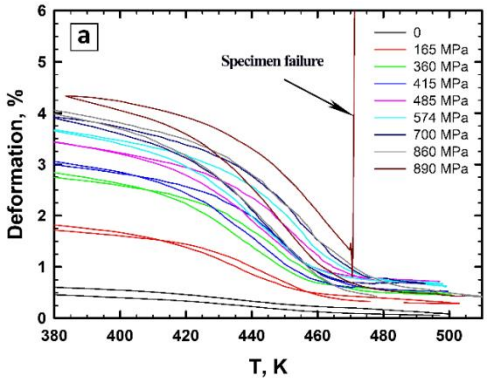

Fig. 2. Dependence ε (σ, t) for an alloy specimen in a forged state

The study of the dependence of the bending deformation of alloy specimens on temperature and the number of thermal cycles performed for the forged state of the alloy showed that the specimen demonstrates 3.1% reversible deformation at a stress of 860 MPa (σ_{cr}), and during cyclic tests showed 4.5-5% of reversible deformation at stress 550 MPa having passed more than 4000 thermal cycles without destruction (Fig. 2.). For alloys of this group, it should be noted that the applied stresses have practically no effect on the phase temperatures. In this case, the transformation interval Δt, which is calculated as the difference between the temperature of the end of the transformation from martensite to austenite Af and the temperature of the end of the transformation from austenite to martensite Mf, was approximately 50 K at low stresses (up to 360 MPa) and increased to 90 K at a voltage 860 MPa.

Thus, forging makes it possible to increase the performance properties of the material in comparison with the cast state of the alloy.

References

[1] I.I. Musabirov, I.M. Safarov, R.M. Galeyev, D.D. Afonichev, V.V. Koledov, A.I. Rudskoi, R.R. Mulyukov. Materials Physics and Mechanics. 33(1) (2017) 124-136. DOI: 10.18720/MPM.3312017_13

[2] Musabirov I.I., Safarov I.M., Galeyev R.M., Gaisin R.A., Koledov V.V., Mulyukov R.R., Physics of the Solid State. 60(6) (2018) 1061-1067. DOI: 10.1134/S1063783418060240

[3] Musabirov I.I., Safarov I.M., Galeyev R.M., Abdullina D.R., Koledov V.V., Mulyukov R.R. IOP Conf. Series: Materials Science and Engineering. 447 (2018) 012024. DOI: 10.1088/1757-899X/447/1/012024

[4] I.I. Musabirov, I.M. Safarov, R.M. Galeyev, D.R. Abdullina, R.Y. Gaifullin, D.D. Afonichev, V.V. Koledov, R.R. Mulyukov. Materials Physics and Mechanics. 40(2) (2018) 201-211. DOI: 10.18720/MPM.4022018_8

[5] I.I. Musabirov, R.M. Galeyev, I.M. Safarov. Journal of Magnetism and Magnetic Materials. 2020. V. 514. P. 167160

Phase states and spectra of isotropic non-heisenberg magnet with s = 2.

O.A.Kosmachev[1], Yu.A. Fridman[1], B.A.Ivanov[2]

[1]Vernadsky Crimean Federal University, Simferopol, Republic of Crimea, Russian Federation
2 National Research Technological University "MISiS", Moscow, Russian Federation

The phase states and spectra of elementary excitations of an isotropic magnet with S=2 are investigated taking into account all admissible spin invariants in the mean-field approximation and low temperatures.

The Hamiltonian describing such a model is:

$$H = -\frac{1}{2}\sum_{n\neq n'}\left\{J_{nn'}\left(\vec{S}_n\vec{S}_{n'}\right) + K_{nn'}\left(\vec{S}_n\vec{S}_{n'}\right)^2 + D_{nn'}\left(\vec{S}_n\vec{S}_{n'}\right)^3 + F_{nn'}\left(\vec{S}_n\vec{S}_{n'}\right)^4\right\}$$

The system under consideration assumes the possibility of splitting into two sublattices. It is known that at negative values of the exchange interaction constants, two-sublattice structures are realized: an anferromagnetic and orthogonally nematic phase for S=1 [1] and an anferromagnetic and antinematic phase for S=3/2 [2]. Naturally, in a magnet with S=2, in addition to the anferromagnetic phase, a wide variety of two-sublattice nematic phases of different symmetry can exist.

The analysis of the free energy density and the spectra of elementary excitations made it possible to determine all the permissible phase states of the system, as well as to determine the types of phase transitions between stable states. It should be noted that our results are in good agreement with the results of works [3]. It is shown that an orthogonally nematic phase is realized, in which the principal axes of the ellipsoid of quadrupole moments are orthogonal. The second two-sublattice nematic phase is realized only at a negative value of the exchange interaction F, and is characterized by corrugated ellipsoids rotated around the principal axis of the quadrupole moment tensor relative to each other by an angle $\pi/4$.

Phases characterized by higher multipole moments are investigated, since the average magnetization per site is zero, and the ellipsoid of the quadrupole moment tensor degenerates into a sphere: tetrahedral and antitetrahedral phases.

In addition, as a result of an analysis of the free energy, it was found that two-sublattice structures with nonequivalent sublattices can be realized in a magnet with S=2. These phases are characterized by a saturated value of the average spin of one of the sublattices and an unsaturation of the average spin of the second sublattice.

The research was funded by RFBR and Republic of Crimea, project number 20-42-910003 (O.A.Kosmachev)

References

[1] Yu.A. Fridman, O.A. Kosmachev, and Ph.N. Klevets, JMMM 325, 125 (2013).
[2] O.A. Kosmachev, Yu.A. Fridman, *at al*, JETF 147, 320 (2015).
[3] Ari M. Turner, Ryan Barnett, et al, Phys. Rev. lett. 98, 190404 (2007).

Phase states of spin-1 Ising-like magnetic with strong single-ion anisotropy

Yarygina E.A.[1], Klevets Ph.N.[1], Fridman Yu.A.[1]

[1]*V.I. Vernadsky Crimean Federal University, 295007, Simferopol, Russian Federation*

We study the phase states and dynamics of a two-sublattice Ising antiferromagnet with easy-plane single-ion anisotropy in an external magnetic field perpendicular to the easy-plane of the system. The model Hamiltonian has the following form:

$$\widehat{H} = \sum_{n_1,n_2} J_1(n_1 - n_2)\left(S^z_{n_1} S^z_{n_2}\right) + \sum_{m_1,m_2} J_2(m_1 - m_2)\left(S^z_{m_1} S^z_{m_2}\right) + \sum_{n,m} J_3(n-m)(S^z_n S^z_m) + \beta \sum_n (S^z_n)^2 + \beta \sum_m (S^z_m)^2 - H \sum_n S^z_n - H \sum_m S^z_m, \quad (1)$$

where J_1 and J_2 are the constants of in-sublattice exchange interaction of the ferromagnetic type, that is, both constants are negative; J_3 is the constant of inter-sublattices exchange interaction of the antiferromagnetic type, that is $J_3 > 0$; $\beta > 0$ is the constant of the easy-plane single-ion anisotropy; H is the external magnetic field.

It is shown that depending on the relationship between the material constant and the external field, one of the four phase states can realize in the system:

1. Ferromagnetic phase;
2. "Supersolid" magnetic phase or non-collinear antiferromagnetic phase in which each sublattice has non-zero magnetization, but they are tilted with respect to the OZ axis on different angles;
3. Mixed phase in which one of the sublattices is characterized with a vector order parameter, while another sublattice – with a quadrupole order parameter. At this, one sublattice has non-zero magnetization, while magnetic moment per site equals zero for another sublattice;
4. Quadrupolar phase in which both sublattices has zero magnetic moment per crystal site.

As we were interested in the case of strong single-ion anisotropy when the "supersolid" magnetic phase is possible, we have not considered the antiferromagnetic phase which can also realize in the model considered.

All phase transitions between the phases, listed above, are of the first kind. The phase diagram of the system for the case of strong single-ion anisotropy ($\beta_C > 4|J_1|$) is shown in Fig. 1 below.

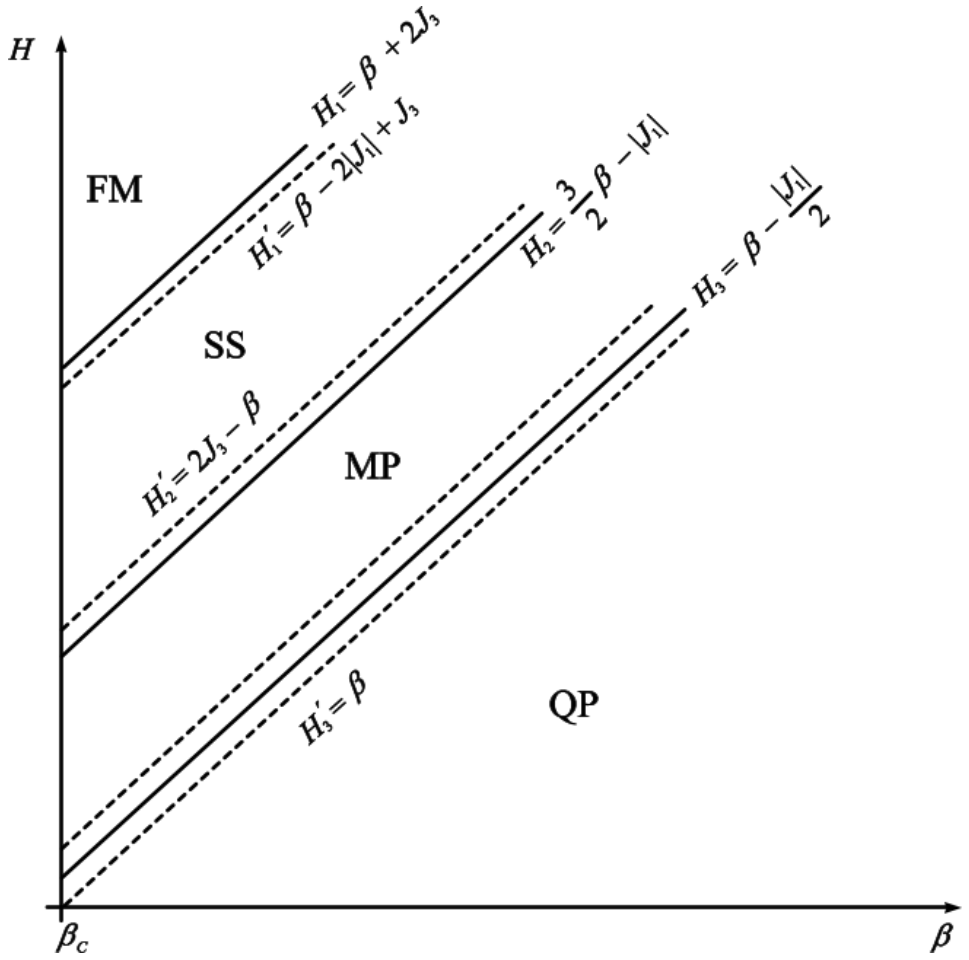

Fig.1. Phase Diagram of the system. Solid lines denote the phase transitions fields, dash lines – the fields of stability for the corresponding phases. FM denotes the ferromagnetic phase; SS – the "supersolid" magnetic phase; MP – the mixed phase; QP – the quadrupolar phase.

It should be noted that the SS phase becomes metastable when the constant of single-ion anisotropy is less that the β_C value, defined above.

Acknowledgements

The research was funded by RFBR and Republic of Crimea, project number 20-42-910003, and by RFBR, project number 20-32-90027.

Is it possible to control stress states in metals by conducting polymers.

Lachinov A.N.[1,2], Galiev A.F.[2], Karamov D.D.[2], Lachinov A.A.[2]

[1]Bashkirian State Pedagogical University, 450000, Ufa, Russia Federation
[2]Institute of Physics of Molecule and Crystals UFIC RAS, 450057, Ufa, Russia Federation

A fundamental feature of the stress states in metals is that they cause distortions of the equilibrium crystal lattice. Distortions can be of different dimensions, from zero-dimensional to three-dimensional. Hence, the shape and length of the stress states can be different. From the point of view of the band theory, it means that the Schrodinger equation in these areas will have different solutions. Therefore, the position of the high occupied level of the electrons will be different.

Currently, for obtaining useful electronic properties an interface approach to the design of multilayer hybrid structures is being actively developed. This approach is also very productive for the metal / polymer interface. In this case, the polymer is considered as a material with variable parameters due to variability of its chemical structure.

The report presents an alternative approach to this issue. In particular, the electronic properties of metals change in the metal / polymer interface. This change is created by deforming metals in various ways, from elastic to plastic deformation, including destruction of samples.

The electronic properties of the interface are very sensitive to minor changes in the equilibrium structure of the metal under small influences. It is shown on a large number of metal / polymer structures. It is established that elastic and plastic deformations lead to different changes in the energy structure of the contact. In one case, the potential barrier at the border increases. In the other case, it decreases. It depends on the reaction of the metal to the deforming effect. In one case, the effective work of the metal electron output decreases in the other case, it increases.

There is a synchronous rearrangement of the electronic properties of the polymer due to the large electron-phonon interaction in the polymer material. It causes a change of the charge carriers mobility and concentration of charge carriers. All this leads to a significant change in the conductivity of the structure under study.

The report presents the samples of practical application in the field of control of stress states in the metal constructions.

These works were supported by the project "Mirror laboratories" of the National Research University "High School of Economics" and the Bashkirian State Pedagogical University named after him M.Akmulla.

Theoretical prediction of the structure and electronic properties M_2AX phase (M=Fe, Cr, Mn; A=Al, Si; X=C)

Tomilin F.N.[1,2], Kozak V.V.[2], Ivanova D.A.[2], Fedorova N.A.[2], Shubin A.A.[2], Ovchinnikov S.G.[1]

[1]*Kirensky Institute of Physics SB RAS, FRC, 660036, Krasnoyarsk, Russia*
[2]*Siberian Federal University, 660041, Krasnoyarsk, Russia,*

The MAX phases are a unique material with the properties of metals and ceramics. Like ceramics, they have low density, high strength, good corrosion, and high-temperature oxidation resistance; like metals, they are high electrical/thermal conductivities, relatively soft, appreciable machinability, thermal shock resistance, and good damage and radiation tolerance. They are highly promising candidates for various applications, such as structural materials, corrosion protection, and nuclear fuel cladding coating materials These phases are also called nano-laminates because of their layered structures, which consist of hexagonal carbide blocks [$Mn+1X_n$] and planar *A* atomic sheets with a characteristic "*zigzag*" stacking along the *z*-axis in the sequence .../[$Mn+1X_n$]/A/[$Mn+1X_n$]/A/... The properties of MAX phases include high electrical and thermal conductivity, heat resistance, damage resistance, readily machinable, high modulus, and low density [1]. The atomic and electronic structure of Me_2XC (Me = *Fe*, *Cr*, *Mn*; X=*Al*, *Si*) was found using the DFT level of the theory by the CRYSTAL program [2]. Obviously, the obtained results depend on the functional used in the calculation, the choice of which can be carried out from a wide range of options. Among the widely known and traditionally used functionals for the DFT method, such as GGA (PBE), hybrid (PBE0-13, B3LYP), meta-GGA (M06L, M06, M062X, M06HF), and range separated (CAM-B3LYP) DFT functional. The analysis of the change in the optimized geometry parameters (CrFe)SiC in crystal cell and the atomic spins and charges of *Fe* and *Cr* were carried out depending on the used functional. According to calculations the PBE0-13, B3LYP, M06, and CAM-B3LYP functionals give a satisfactory result and are in good agreement with the literature data [3, 4]. To simulate the possible magnetic properties, structures with different spins were calculated. All MAX phases showed high spin on metal atoms. Then, carbon-terminated slab structures were obtained from these structures. Then various materials were placed on these slabs, such as graphene, *h*-BN, *g*-C_3N_4. These structures showed high stability, which shows the prospect of using such heterostructures in various applications in electronics.

Acknowledgement

This study was supported by the Government of the Russian Federation, the Mega-grant for the Creation of Competitive World-Class Laboratories, agreement no. 075-15-2019-1886.

References

[1] Shein I.R., Physica B: Condensed Matter. 2013. № 1(410). P. 42–48.
[2] Dovesi R. Wiley Interdiscip. Rev. Comput. Mol. Sci., 2018. V. 8, № 4. P. e1360
[3] Ghebouli M., Intermetallics. 2011. V. 19, № 12. p. 1936–1942.
[4] Liao T., J. Mater. Res. 2009. V. 24, № 2. p. 556–564.

Magnetic properties and size effect of iron borate $FeBO_3$

Snegirev N.I.[1], Lyubutin I.S.[1], Yagupov S.V.[2], Chuev M.A.[3], Chumakov N.K.[4], Svetogorov R.D.[4], Strugatsky M.B. [2]

[1] *FSRC "Crystallography and Photonics" RAS, Moscow, Russia*
[2] *V.I. Vernadsky Crimean Federal University, Simferopol, Russia*
[3] *Valiev Institute of Physics and Technology RAS, Moscow, Russia*
[4] *NRC "Kurchatov Institute", Moscow, Russia*

In this work properties of $FeBO_3$ nanoparticles were studied using X-ray diffraction analysis and magnetic measurements.

The experimental samples were prepared in the laboratory of crystal growth of the V.I. Vernadsky Crimean Federal University by grinding $FeBO_3$ single crystals in a vibratory ball mill for 20 hours [1,2]. According X-ray diffraction (using the Kurchatov synchrotron radiation source; see pattern on Fig. 1) there are no impurity phases in experimental sample, and the average crystallite size in the obtained nanoparticles was about 80 nm.

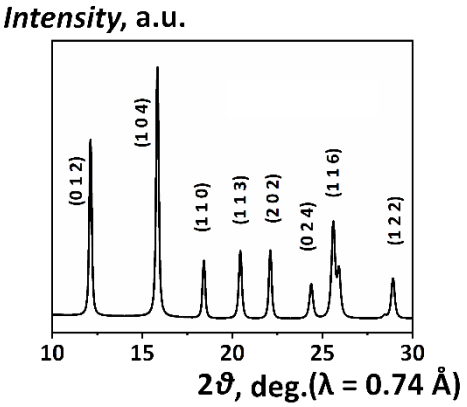

Fig. 1. X-ray diffraction pattern of $FeBO_3$ nanoparticles

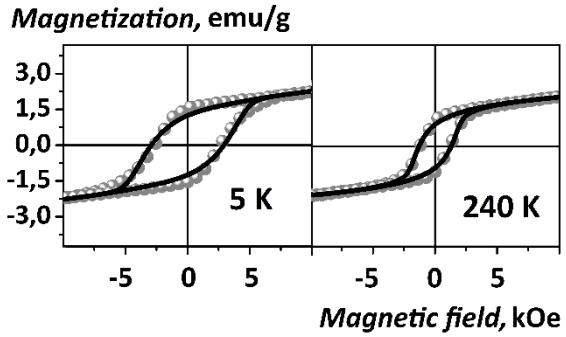

Fig. 2. Hysteresis loops of iron borate nanoparticles, at 5 K (left) and 240 K (right). The dots are experimental data and the line is a result of theoretical modeling

Fig. 2 shows the magnetization curves of $FeBO_3$ nanoparticles obtained at 5 K (left) and 240 K (right). The equipment of the Resource Center "Electrophysics" and of Kurchatov complex of NBIKS-technologies (LakeShore 7400 vibrating sample magnetometer) was used. The value of the critical field of magnetization reversal is 15.15 ± 0.06 kOe at 5 K and 98.68 ± 0.1 kOe at 240 K. Such a difference in the parameters of the magnetization compared with data for bulk $FeBO_3$ crystals is due to a significant increasing in the magnetic anisotropy energy in iron borate nanoparticles [3].

Acknowledgments: This study was funded by RFBR, project number 19-29-12016.

References

[1] S. Yagupov et al. Crystal Growth & Design 18, 7435 (2018).
[2] E. Smirnova et al. Acra Crystallogr. B 76, 1100 (2020).
[3] M. Chuev, J. Hesse, J. Physics: Condens. Matter 19, 506201 (2007).

Section 2
Ferro- and Antiferromagnetic Spintronics and Magnonics

Spin-Torque Diodes: From Fundamental Research to Applications

Petr N. Skirdkov, Alexander G. Buzdakov, and Konstantin A. Zvezdin

[1]*Prokhorov General Physics Institute of the Russian Academy of Sciences, Russia*
[2]*Moscow Institute of Physics and Technology, Russia*
[3] *New Spintronic Technologies, Russian Quantum Center, Russia*

Zvezdin.ka@phystech.edu

Among a rich variety of emerging spintronic devices, a spin-torque diode (STD) is among the most interesting ones, from both fundamental and applied point of view. The spin-diode effect occurs when microwave alternating electric current injected into magnetic tunneling junction (MTJ) is rectified due to the simultaneous actions of tunneling magnetoresistance and spin-transfer torque. While the sensitivity of STDs observed in the first works was rather modest (about 1.4 mV/mW), after only a few years the researchers managed to increase it up to 200 kV/W and to demonstrate the rectification at input power of nW level, which radically exceeds the capabilities of the mainstream technology of Schottky diodes. This impressive progress is based on a deep understanding of the complex STDs physics, and on the recent advances in MTJ fabrication technology.

In this talk we analyze the experimental pathway toward increasing of the sensitivity and extending the frequency range of STDs, as well as theoretical works aimed at explaining the complex nonlinear dynamics. Finally we review the wide variety of possible STDs applications.

This work was supported by Russian Science Foundation (grant # 19-12-00432)

References

[1] AG Buzdakov, PN Skirdkov, KA Zvezdin, Magnetostatically Induced Easy-Cone Magnetic State Tuning by Perpendicular Magnetic Anisotropy in an Unbiased Spin-Torque Diode, *Physical Review Applied* **15** (5), 054047 (2021)
[2] P.N.Skirdkov, K.A.Zvezdin, Spin-Torque Diodes: From Fundamental Research to Applications, *Annalen der Physik* **532** (6), 1900460 (2020)
[3] P.N. Skirdkov, A.F. Popkov, K.A. Zvezdin, Vortex spin-torque diode: The impact of DC bias, Applied Physics Letters 113 (24), 242403 (2019)
[4] A.A. Khudorozhkov, P.N. Skirdkov, K.A. Zvezdin, P.M. Vetoshko, A.F. Popkov, Spin-torque diode frequency tuning via soft exchange pinning of both magnetic layers, *Phys. Rev. B* **96**, 214410 (2017)

Spin injection switching on and switching off

Bebenin N.G.

M.N. Miheev Institute of Metal Physics of Ural Branch of Russian Academy of Sciences, 620137, Ekaterinburg, Russia

Spin injection from a ferromagnet to a semiconductor is investigated theoretically and experimentally for many years. The electric current and spin current are usually considered as being independent of time. A real device is however switched on and off, so it necessary to consider transients, that is, how magnetic moment injected from a ferromagnet propagates in non-magnetic material. For definiteness, this non-magnetic material is taken to be a semiconductor.

The ferromagnet is supposed to be located at $z<0$ and half-space $z>0$ is occupied by a the semiconductor. Electrons move along z-axis from the ferromagnet to the semiconductor and the drift velocity $V_z>0$. The magnetization **M** of electron gas is assumed to be along x-axis both in the ferromagnet and semiconductor, $M_x>0$. The equation for calculating the magnetization of electrons at $z>0$ can be written as

$$\tau_s \frac{\partial M_x}{\partial t} = L_D^2 \frac{\partial^2 M_x}{\partial z^2} - l_d \frac{\partial M_x}{\partial z} - M_x. \quad (1)$$

Here τ_s is spin relaxation time, $L_D = \sqrt{D\tau_s}$ is the diffusion length, and $l_d=V_z\tau_s$ is the drift length. When $\partial M_x/\partial t = 0$, the solution of (1) is $M_x = M_{x0}\exp(-z/L_D)$, because usually $L_D>>l_d$. We are interested in the dependence of M_x on time t and coordinate z inside the semiconductor after switching on and off.

Let the magnetization current be switched on at $t=0$. We suppose that the magnetization current through the interface does not depend on time, which means $\frac{\partial M_x(z=0,t)}{\partial z} = const$. Let us introduce variables $\zeta = z/L_D$, $\tau = t/\tau_s$, and define $u(\zeta, \tau)$ by relation $M_x = M_{x0}(e^{-\zeta} - u(\zeta, \tau))$. The equation for $u(\zeta, \tau)$ follows from (1); its solution can be written as

$$u(\zeta,\tau) = \frac{1}{2}\left[e^{-\zeta} Erfc\left(\sqrt{\tau} - \frac{\zeta}{2\sqrt{\tau}}\right) + e^{\zeta} Erfc\left(\sqrt{\tau} + \frac{\zeta}{2\sqrt{\tau}}\right)\right], \quad (2)$$

where $Erfc(x)$ is the error-function. We see that because of spin diffusion, the time dependence of the electrons magnetization does not follow the simple exponential law but is described by the complicated formula, which involves not only the spin relaxation time, but also the magnetization diffusion length and the distance from the interface.

Now let the magnetization current be switched off at $t=0$. The calculations are similar to that for switching on. It is easy to show that $M_x = M_{x0}u(\zeta,\tau)$ in this case. Again the decrease of electronic magnetization with time at a point inside semiconductor does not follow the exponential law due to spin diffusion.

The research was carried out within the state assignment of Ministry of Science and Higher Education of the Russian Federation (theme "Spin," No. AAAA-A18-118020290104-2), supported in part by RFBR (Grant No. 19-02-00038).

Detection of sub-THz frequency signals based on an antiferromagnet

Safin A.R.[1,2]

[1]*Kotel'nikov Institute of Radioengineering and Electronics RAS,Moscow, Russian Federation*
[2]*National Research University "MPEI", Moscow, Russian Federation*

Antiferromagnetic (AFM) materials have natural resonance frequencies in the sub-THz or THz frequency range. Thus, it is tempting to use antiferromagnets (AFM) as active layers in THz-frequency detectors. Recently [1], it has been shown theoretically that a dielectric AFM having bi-axial anisotropy, such as NiO, can be used for the resonance quadratic rectification of a linearly polarized AC spin current of THz frequency, and could have a sensitivity in the range of 100–1000 V/W.

Here we present both analytical and numerical data illustrating the performance of a possible electrically tunable resonance THz-frequency receiver based on an AFM crystal having the frequency of the antiferromagnetic resonance (AFMR) in the THz-frequency range [2]. The receiver is based (see Fig.1) on a layered structure consisting of a layer of a uniaxial AFM crystal and two layers of a heavy metal (HM). The conversion of the received AC signal into an output DC signal is done using the inverse spin Hall effect in the (AFM/HM) bilayer. An additional bias DC current in the bottom HM layer can be used for the tuning of the AFMR frequency of the system, and for a partial regeneration of the system losses. The AFMR frequency can be continuously tuned in a substantial frequency interval (of about 0.5 THz) by varying the magnitude of the DC electric current. It is shown that the AC sensitivity of the proposed AFM/HM-based detector is comparable to the sensitivity of the modern sub-millimeter-wave detectors based on the Schottky and Gunn diodes, and that the received DC signals are well above the level of the thermal noise for the AC signals having power of the order of several microwatts.

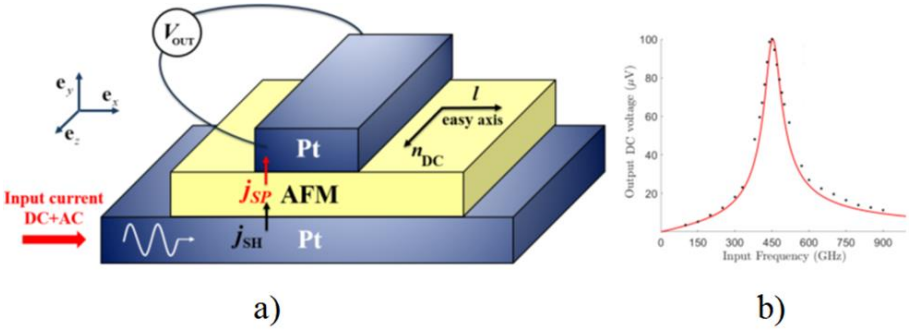

Fig. 1. (a) Schematic view of the THz-frequency resonance detector based on the AFM-Pt structure; (b) resonance curve of the output rectified DC voltage;

We acknowledge the support from the grant of Russian Foundation for Basic Research (Grant No. 19-29-03015, 18-29-27018, 18-57-76001).

References

[1] R. Khymyn et al., AIP Adv. 7, 055931 (2017).
[2] A. Safin et al., Appl. Phys. Lett. 117, 222411 (2020).

Magnonic control of the superconducting spiral spin valve

Pugach N.G.[1,2], Gusev N.A.[3,4], Safonchik M.O.[5], Belotelov V.I.[1,3,4]

[1]*Lomonosov Moscow State University, Leninskie Gory, 1 (2), 119991 Moscow, Russia*
[2]*HSE University, 101000 Moscow, Russia*
[3]*V.I. Vernadsky Crimean Federal University, Vernadsky Prospekt, 4, 295007, Simferopol, Russia*
[4]*Russian Quantum Center, Bolshoy Bulvar 30 b.1, 121205, Moscow, Russia*
[5]*A. F. Ioffe Physical-Technical Institute, RU-194021, St Petersburg, Russia*

We propose a superconducting spin-triplet valve, which consists of a superconductor and an itinerant magnetic material, with the magnet showing an intrinsic non-collinear order characterized by a wave vector that may be aligned in a few equivalent preferred directions under the control of a weak external magnetic field pulse. Re-orienting the spiral direction allows one to controllably modify long-range spin-triplet superconducting correlations, leading to spin-valve switching behavior. We developed a control method of such a bilayer superconducting spin valve (SSV) non-perturbing superconductivity and suitable for energy saving cryogenic electronics. This SSV consists of a superconducting layer and a helimagnetic layer of B20 family compounds, namely Nb and spiral antiferromagnetic MnSi. Thanks to unique properties of B20 family magnets – noncollinear (in general helicoidal) magnetic order and cubic crystal lattice, there are few ground state magnetic configurations with different directions of the magnetic spiral, divided by a potential barrier [1]. Superconductivity in such a bilayer is controlled by the spiral vector reorientation in the MnSi layer, which leads to a change in the critical temperature of the Nb superconducting layer [2] due to the proximity effect.

The switching is proposed to be carried out by a several hundred ps in duration magnetic field pulse of several kOe of magnitude. Such a pulse does not destroy the superconducting state of the Nb layer by itself but leads to the excitation of magnons in the MnSi layer, which triggers the process of reorientation of the magnetic spiral. Inverse switching returns the spiral to the initial state, opening the valve and turning on the superconducting state. The system can be switched there and back by a magnetic field of opposite signs along one direction in the layers plane, which allows easy control. Such SSV may be used as an element of superconducting memory for energy-efficient digital and quantum electronics [3].

The numerical experiments were financially supported by the Russian Ministry of Education and Science, Megagrant project N 075-15-2019-1934, the visualization of spin distributions was supported by the Mirror Laboratories collaboration project of the HSE University.

References

[1] Grigoriev, S. V., et al., Phys. Rev. B 76, 092407 (2007).

[2] Pugach, N. G., et al. Appl. Phys. Lett. 111, 162601 (2017).

[3] N. Gusev, D. Dzheparov, N. Pugach, and V. Belotelov Appl. Phys. Lett. 118, 232601, (2021).

Peculiarities of magnetoelastic waves focusing in thick YIG film

Bakharev S.M.[1,2], Borich M.A.[1,2]

[1]M.N. Miheev Institute of Metal Physics of Ural Branch of Russian Academy of Sciences, 620108, Ekaterinburg, Russia
[2]Ural Federal University named after the first President of Russia B.N.Yeltsin, 620002, Ekaterinburg, Russia

The present work is devoted to study of peculiarities of the focusing of magnetoelastic waves (MEW) near the magnetoelastic resonance in thick $Y_3Fe_5O_{12}$ (YIG) film. Due to the fact that the spectrum of MEW depends on the direction of the wave vector **q**, the group **V** and phase velocities are noncollinear. As a results, directions occur in the crystal along which waves predominantly propagate. The group velocities are condensed along these directions, the intensity of the wave increases, and the MEW focusing occurs [1,2]. It is shown that concave areas can appear on the surface of constant frequency in the regions of MEW focusing. Caustic, i. e. the phenomenon of a sharp increase in wave flow intensity [3], corresponds to the lines along which the transition from convexity to concavity occurs.

The purpose of this work is to calculate the directions of focusing and caustics of MEW. The approach for studying the properties of MEWs is based on the research of surfaces of constant frequency [1,2]. In this study, the MEW with long wavelength are considered, and the theory of magnon-phonon interaction in the framework of macroscopic approximation can be applied therefore [4]. Total energy of the system consists of elastic, magnetic, and magnetoelastic parts. The magnetic part of the energy contains magnetic dipole interaction than can be expressed through the demagnetization factors. The MEW spectrum consists of four eigenmodes, but one of them (*LmT*-mode) has the greatest spectrum anisotropy and is most interesting for the search for caustics therefore. This mode passes through two points of magnetoelastic resonance. The first of them relates to the interaction of longitudinal phonons (*L*) with magnetic mode (*m*), and the second one relates to the interaction of transverse phonons (*T*) with *m*-mode. It was found that two caustics occur in the range of magnetic fields $H_0 \approx 1909 - 2167$ Oe for waves with the frequency $\omega/2\pi = 159.44$MHz. The caustic directions are close to each other in the *q*-space, but the directions of the corresponding group velocities are well separated. Caustics can be found in a wide range of directions: $\pi/2 < \theta_{cV} < \pi$ for the first caustic, and $0\ \theta_{cV} < \pi/2$ for the second one, and the directions of the caustics are determined by the magnitude of the external magnetic field.

The research was carried out within the state assignment of FASO of Russia (theme "Function" AAAA-A19-119012990095-0).

References

[1] A.G. Every, Phys. Rev. B 34(4), 2852, (1986).

[2] S. M. Bakharev, M.A. Borich and S. P. Savchenko, JMMM 487, 165294 (2019).

[3] V.I. Arnold, Catastrophe Theory (Springer, Berlin, 1984).

[4] A.I. Akhiezer, V.G. Bar'yakhtar and S.V. Peletminskii, Spin waves (North-Holland Pub. Co., Amsterdam, 1968).

Investigation of the phase propagation of SMSW in a YIG film by the BLS method.

Gubanov.V.A.[1], Sadovnikov A.V.[1]

[1]*Laboratory «Magnetic Metamaterials», Saratov State University, 410012, Saratov, Russia*

The creation devices based on the principles of magnonics is of great interest for areas, included the development storage and information signals processing [1]. Using Brillouin spectroscopy of light scattering (BLS) technique, it is possible to detect the propagation of a spin wave (SW) - the precession of magnetization under the action of a microwave signal. In the classical BLS system we detected the intensity I_{BLS} of SW [2]. By adding an optical phase modulator to the BLS system, the phase of the propagating SW can be resolved [3].

In this work, we study the propagation of SW with a phase resolution in a yttrium iron garnet film [3] was fabricated by the laser scribing technique. Figure 1 shows a schematic representation of a structure consisting of YIG film with a thickness of t_{YIG} = 10 μm. Saturation magnetization of YIG is $4\pi M_0$ = 1750 G. YIG film formed on a gadolinium-gallium garnet (GGG) substrate with a thickness of t_{GGG} = 500 μm. A structure oriented in an external magnetic field M_0=1830 Oe to excite a surface magnetostatic spin wave (SMSW).

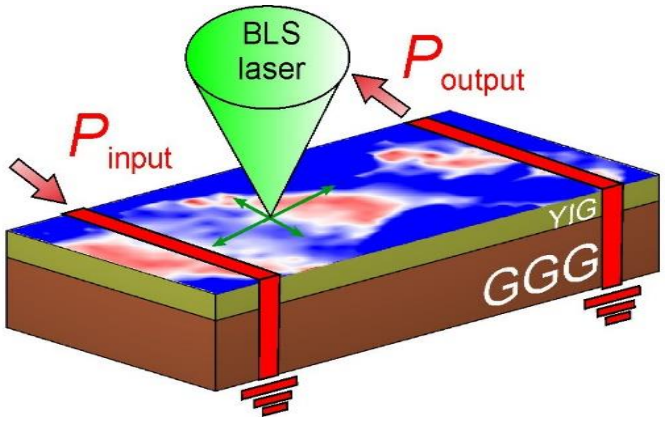

Scheme of the structure with a superimposed map of the SW phase distribution at a frequency of 6.88 GHz, obtained in the BLS experiment.

In this work, the BLS method will be used to study the formation the phase front of a spin wave in a YIG film. Using micromagnetic modeling, agreement with the experimental data will be shown. The intensity and phase of the SW will be compared and the optimal parameters for the propagation of SW in the YIG film are revealed.

This work was supported by the Russian Foundation for Basic Research (project No. 20-37-90020, project No.18-29-27026).

References

[1].Nikitov S A, Kalyabin D V, Lisenkov I V, et. Al Phys. Usp. 58 1002–1028 (2015)

[2].Zhu, Y. (Ed.). Modern Techniques for Characterizing Magnetic Materials. (2005).

[3].Serga, A. A., Schneider, T., Hillebrands, B., Demokritov, S. O., & Kostylev, M. P. Applied Physics Letters, 89(6), 063506. (2006).

Influence of the thin magnetic films anisotropy on detection of the magnetoelastic fields under magnetic field amplitude-modulated excitation

Pleshev D.A.[1,2], Asadullin F.F.[1], Vlasov V.S.[2], Kotov L.N.[2], Shcheglov V.I.[3]

[1]Saint-Petersburg state forest technical university named after S.M. Kirov, 194021, St-Petersburg, Russia
[2]Syktyvkar State University, 167001, Syktyvkar, Russia
[3]Institute of Radioengineering and Electronics of the Russian Academy of Sciences, 125009, Moscow, Russia

Microwave oscillations excitation under the effect of magnetostrictive transducers has application to hydroacoustics, flaw detection, ultrasonic technology, and processing of analog information in the microwave range [1, 2]. However, at present, the question of the reception and registration of such waves has been poorly studied, primarily in the separation of the microwave signal transmitted materials. The implementation of magnetoelastic oscillations in a magnetostrictive transducer in linear and nonlinear modes allows them to be used for recording the transmitted signal.

The paper is dealing with coupled oscillations of magnetization and elastic displacement in the normally magnetized ferrite plate that possesses magnetoelastic properties and crystallographic anisotropy. The coupled oscillations excited by the amplitude-modulated alternating magnetic field when the parametric excitation of spin waves was blocked [3, 4].

Time evolution of magnetic and elastic oscillations caused by the amplitude-modulated alternating field was analyzed in case of [001] and [111] crystallographic anisotropy type. Conditions of amplitude modulated signal detecting and various oscillations modes are considered in the paper.

The paper describes dependences of magnetoelastic oscillations on polarization and magnitudes of alternating magnetic fields, crystallographic anisotropy. The time dependences, parametric portraits and frequency response of the excited magnetic and elastic oscillations were made.

This work has been supported by the grants the Russian Science Foundation (project No. 21-72-20048)

References

[1] A. K. Biswas, S. Bandyopadhyay, J. Atulasimha. Energy-efficient magnetoelastic non-volatile memory. Applied Physics Letters. – 2014. – Vol.104, № 23. – P. 2403.

[1] Wei-Gang Yang and Holger Schmidt. Acoustic control of magnetism toward energy-efficient applications. Applied Physics Reviews 8, 021304 (2021)

[3] Suhl H. Theory of ferromagnetic resonance by high level of microwave power. J. Phys. Chem. Sol. 1957, vol. 1, № 4, P. 209

[4] D.A. Pleshev, F.F. Asadullin, S.M. Poleshchikov, L.N. Kotov, V.S. Vlasov, V.G.Shavrov, V.I.Shcheglov. Nonlinear Magnetoelastic Dynamics of the Ferrite Plate. Journal of Siberian Federal University. Mathematics & Physics 2017, 10(1), 36–39.

Temperature tuning of orthoferrite-based spin-Hall oscillator

Meshcheryakov A.A.[1,2], Safin A.R.[1,3], Kalyabin D.V.[1,2], Nikitov S.A.[1,2], Mednikov A.M.[2]

[1]*Kotel'nikov Institute of Radio-Engineering and Electronics of RAS, 125009, Moscow, Russia*
[2] *Moscow Institute of Physics and Technology, 141701, Moscow, Russia*
[3] *Moscow Power Engineering Institute, 111250, Moscow, Russia*

Currently, spin-transfer nanooscillators (STNO) based on multilayer structures are being actively investigated. Previously, such structure [1] and frequency tuning by magnetostriction [2] have already been theoretically studied. In this work, the model of a STNO with the possibility of frequency tuning by temperature changing is theoretically investigated [3]. The tuning of the oscillation frequency is possible due to the properties of the active element of the oscillator - holmium orthoferrite $HoFeO_3$. In $HoFeO_3$, in temperature interval 38 K-52 K several phase transitions are taking place. The physical structure of the consideration THz-oscillator is a two-layer nanostructure, in which the antiferromagnetic (AFM) layer ($HoFeO_3$) lies on the heavy metal layer (platinum). The oscillations are excited by the DC electric current flowing through the Pt layer. To describe the oscillations of the Neel vector $\mathbf{l} = (\mathbf{M}_1 - \mathbf{M}_2)/M_s$ (where $\mathbf{M}_{1,2}$ is AFM sublattice magnetizations, M_s is the magnetic saturation of the AFM sublattice), the "sigma-model" was used, which took into account the temperature dependence of the anisotropy of $HoFeO_3$. Figure 1 shows the dependence of the oscillation frequency on the density of the input DC current for damped oscillations regime and for self-oscillations regime. This dependence demonstrates a hysteretic behavior.

We acknowledge the support from the Russian Foundation for Basic Research (Grant No. 19-29-03015, 18-57-76001, 18-29-27018).

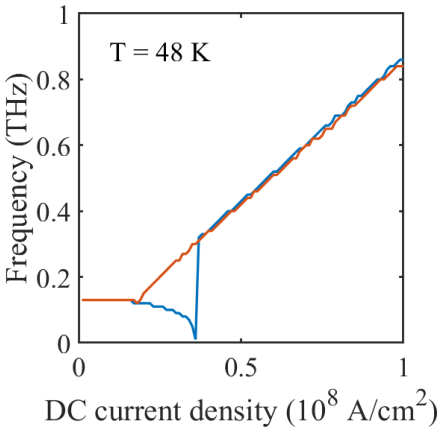

Fig. 1. Output oscillation frequency vs DC current density for the orthoferrite-based spin-Hall oscillator

References

[1] R. Khymin *et al*, Sci. Rep. 7, 43705 (2017).
[2] P.A. Popov *et al*, Phys. Rev. Applied 13, 044080 (2020).
[3] A.A. Meshcheryakov *et al*, J. Phys. D: Appl. Phys. 54, 195001 (2021).

Spin-wave beams formation in 3D magnonic arrays

Khutieva A.B.[1], Beginin E.N.[1], Sheshukova S.E.[1], Sadovnikov A.V.[1]

[1] *Laboratory "Magnetic Metamaterials" Saratov State University, Saratov*

Magnons, being the quanta of spin-wave excitations, can be used as the signal carriers at frequencies that are lying between a few GHz to hundreds of GHz [1]. Magnonic networks(MN) comprised of coupled YIG spin-wave stripes can be used to process information and at the same time providing the technologically relevant integration to the present CMOS architecture [2]. Recently, it was shown, that the three dimensional (3D) meander shaped magnonic crystal [3] can provide vertical spin-wave transport by using the vertical sections of magnonic waveguide. In the present work we use the dipolar stray fields of magnonic stripes to perform the vertical and lateral spin-wave transport and transfer of the signal between the magnonic stripes.

Figure 1 schematically shows the structure under consideration, consisting of 12 magnetic microwaveguides, which was fabricated from YIG film with thickness of d = 10 μm. YIG was epitaxially grown on a gallium-gadolinium garnet substrate. The distance between the magnetic microwaveguides is a = 20 μm and b = 15 μm. The length along the long side of the waveguides was l = 4 mm, the width of the waveguide was c = 200 μm. The excitation of spin waves was carried out using 1 μm-thick and 10 μm-wide microstrip antennas located on two central waveguides.

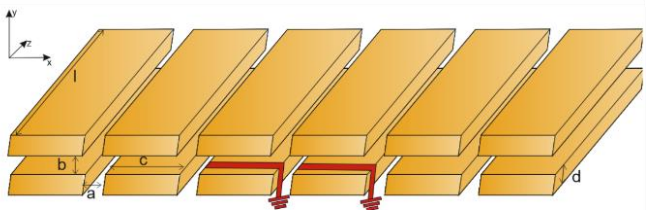

Fig. 1. Array of magnetic microwave guides

The features of the spin-wave propagation in 3D array of YIG films are revealed. The resuls of numerical simulation (MM and FEM) are in good accordance with experimental BLS data. The observed phenomena of tunable spin-wave beam formation in 3D magnonic structure can provide an in-depth insight into the physics of lateral and vertical spin-wave transport in array of micro- and nanoscale structures.

Work is supported by RFBR (No. 19-29-03034) and Grant of the President of RF (MK1870.2020.9)

References

[1] V. V. Kruglyak, J. Phys.D: Appl. Phys. 43, 264001 (2010).
[2] A.V. Sadovnikov, Phys. Rev. B 99, 054424 (2019).
[3] G. Gubbiotti, Phys. Rev. Applied. (2021).

Spin pumping experiment in heterostructures La0.7Sr0.3MnO3/SrIrO3 and La0.7Sr0.3MnO3/Pt

Atsarkin V.A.[1], Demidov V.V.[1], Ovsyannikov G.A.[1], Shaikhulov T.A.[1], Stankevich K.V.[1,2]

[1]Kotel'nikov Institute of Radio Engineering and Electronics of Russian Academy of Sciences, 125009, Moscow, Russia
[2]Lomonosov Moscow State University, 119992 Moscow, Russia

Spin pumping is based on the effect of a ferromagnetic resonance (FMR) in ferromagnet/normal metal (FM/NM) bilayers driven by microwave radiation. Localized d electrons precessing under FMR conditions transmit angular moment to s electrons of the NM through sd-exchange interaction. Then s electrons propagates into the bulk of NM due to diffusion motion resulting in the pure spin current [1]. The spin current flows without electric charge transfer that opens new possibilities in spintronic.

Our group actively study the magnetic properties and spin pumping effects in different heterostructures. Among them, the most promising heterostructures are bilayers in which manganite (La0.7Sr0.3MnO3) is used as a ferromagnetic layer. The platinum (Pt) or iridate (SrIrO3) is usually used as a nonmagnetic metal layer.

This talk is dedicated to our studies of the spin pumping effects in manganite/iridate and manganite/platinum bilayers. We will discuss the latest studies (see [2-7] and references therein) and present our new results on temperature dependences of the pure spin current, renormalization of the Gilbert damping constant and g-factor engendered by spin current flow.

References

[1] Y. Tserkovnyak, A. Brataas, G.E. Bauer and B.I. Halperin, Rev. Mod. Phys. 77, 1375 (2005).

[2] G.A. Ovsyannikov, T.A. Shaikhulov, K.L. Stankevich, Yu. Khaydukov and N.V. Andreev, Phys. Rev. B 102, 144401 (2020).

[3] V.A. Atsarkin, V.V. Demidov and T.A. Shaikhulov, J. Exp. Theor. Phys. 130, 228-234 (2020).

[4] V.A. Atsarkin, I.V. Borisenko, V.V. Demidov and T.A. Shaikhulov, J. Appl. Phys. 51, 245002 (2018).

[5] G.Y. Luo, et al., Sci. Rep. 7, 6612 (2017).

[6] S. Crossley, A.G. Swartz, K. Nishio, Y. Hikita and H. Y. Hwang, Phys. Rev. B 100, 115163 (2019).

[7] T. Nan, et al., Proc. Natl. Acad. Sci. U.S.A. 116, 16186 (2019).

RF-Circulator based on surface acoustic waves non-reciprocity induced by magnetoelastic interaction

Andreev A.V.[1], Safin A.R.[1,2], Nikitov S.A.[1,3]

[1]*Kotelnikov Institute of Radioengineering and Electronics of Russian Academy of Sciences, 125009, Moscow, Russian Federation*
[2]*Moscow Power Engineering Institute, 111250, Moscow, Russian Federation*
[3] *Moscow Institute of Physics and Technology, 141701, Dolgoprudny, Russian Federation*

Surface acoustic wave (SAW) devices is the one of the most useful type of devices in the current industry of telecommunications. These relatively small devices have good thermal stability parameters and wide bandwidth from hundreds of megahertz to several gigahertz. Classic design of SAW device consist of several main parts: interdigital transducer(IDT), which excite the acoustic waves by electric current, piezoelectric substrate there waves, are propagate and damping material, which covered piezoelectric waveguide borders for eliminate parasitic waves reflections. In depends of type the device piezoelectric waveguide surface may contain different additional structures: grooves, reflectors, couplers etc.

Usually AW in piezoelectric crystals are reciprocal that means AW propagating in opposite direction has similar properties. However, non-reciprocity is strong mechanism allows to create different special devices like vents, insulators, circulator etc. Different methods to made AW non-reciprocal in crystals are exist [1,2]. One of the most reliable methods for that is the magnetoelasticity, which allow to change SAW properties by coverage part of piezoelectric waveguide magnetic thin film [3] or magnetic heteroscturcture [4]. Surface acoustic wave giant non-reciprocity effect is actively studied [4-6]. The SAW circulator based

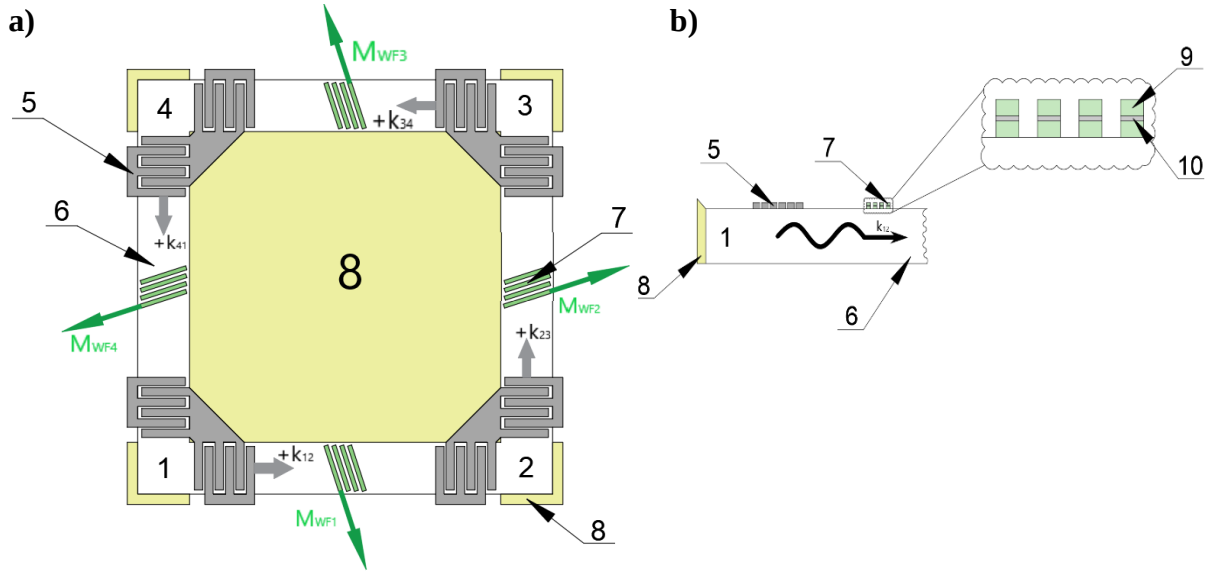

Fig. 2. Scheme of SAW circulator with SAFM heterostructures located on waveguides. **(a)** circulator scheme; 1,2,3,4 – ports numbers, respectively; 5 – paired IDT; 6 – piezoelectric structure (waveguide); 7 – SAFM heterostructure; 8 – layer of damped material; 9 ferromagnet layer in SAFM heterostructure; 10 – spacer.

on SAW phase non-reciprocity was theoretically proposed in [7]. It was shown that circulator based on the ring resonator is suitable for GHz SAW frequencies [8].

We propose another design for GHz SAW circulator, schematically shown in Fig. 1. Proposed design consist of piezoelectric single crystal substrate made from lithium niobate ($LiNbO_3$) on Y-cut, which is the classic materials for SAW devices, paired IDTs turned on 90 degrees, trilayered heterostructure with antiferromagnetic properties, so-called synthetic antiferromagnet (SAFM) and area of damping material to exclude parasitic reflections of SAW.

A special feature of this structure is the paired IDT, which generates acoustic waves with the same properties in two directions at once and the array of SAFM stripes located in the middle of waveguides. The SAW generated by such IDT have the same propagation velocity and properties due to the Y-cut 90-degree symmetry of lithium niobate.

We have shown that in this structure, it is possible for surface acoustic waves to be non-reciprocal in a wide frequency band without the application of an external bias magnetic field.

We acknowledge the support from the grant of Russian Foundation for Basic Research (grant No. 19-29-D3015, 18-29-27018, 18-57-76001)

References

[1] Zm. Gu, J. Hu, and B. Liang, et al. Sci Rep 6, 19824 (2016).

[2] R. Fleury D. Sounas, et al. Science (New York, N.Y.). 343. 516-519. 1246957 (2014).

[3] R. Sasaki, Y. Nii, et al. Phys. Rev. B. 95. 020407 (2016).

[4] R. Verba, I. Lisenkov, et al. Phys. Rev. Applied. 9. 064014. (2018).

[5] R. Verba, V. Tiberkevich and A. Slavin, 12. 054061 (2019).

[6] P. Shah, D. Bas, Sci. Adv. 6. eabc5648. (2020).

[7] R. Verba, E. Bankowski Adv. Elec. Mat. 2100263. (2021).

[8] Boucher P., Rauwerdink S. Applied Physics Letters. 105. 161904 (2014)

Spin wave control in magnon dielectric microcavities by ultrashort laser pulses

Khramova A.E. [1,2], Kobecki M. [3], Akimov I.A. [3,6], Savochkin I.V. [1,2], Kozhaev M.A. [1,4], Shaposhnikov A.N. [5], Berzhansky V.N. [5], Zvezdin A.K. [1,4,7], Bayer M. [3,6], Belotelov V.I. [1,2]

[1] *Russian Quantum Center, 45, Skolkovskoye shosse, Moscow, 121353, Russia*
[2] *Faculty of Physics, Lomonosov Moscow State University, Leninskie Gory, Moscow 119991, Russia*
[3] *TU Dortmund, Experimentelle Physik 2, D-44221 Dortmund, Germany*
[4] *Prokhorov General Physics Institute RAS, 38 Vavilov Street, Moscow 119991, Russia*
[5] *Vernadsky Crimean Federal University, 4 Vernadskogo Prospekt, Simferopol, 295007, Russia*
[6] *Ioffe Institute, Russian Academy of Sciences, 194021 St. Petersburg, Russia*
[7] *NTI Center for Quantum Communications, National University of Science and Technology MISiS, Leninsky Prospekt 4, Moscow, 119049, Russia*

The practical application of spin waves is rapidly developing as an alternative to existing methods of transmitting digital information, as well as for use in quantum communication. Spin waves in magnetic microcavities are at the heart of modern magnonics [1].

In this work, we study magnetostatic spin waves in iron-garnet microdiscs of different diameters, excited by a sequence of ultrashort laser pulses. Optical excitation of spin waves occurred at a frequency comparable to the natural frequency of magnetization precession, which provided a cumulative effect leading to quasi-stationary magnon oscillations in microdisks, which allows us to observe interference effects and excite various magnon modes. The interference of backward volume magnetostatic spin waves in disks with a diameter of 300 μm was found (Fig. 1.). With a decrease in the diameter of the disks, modes of various types (BMVSW and MSSW) were excited due to the greater localization of electromagnetic energy in small disks. It was demonstrated that the amplitudes of some of the first magnetostatic modes with a frequency close to the pump beam frequency are doubled in comparison with other modes (Fig. 2) [2,3].

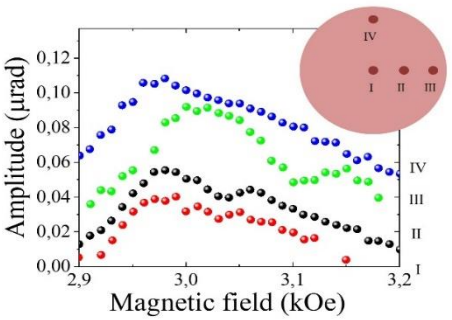

Fig. 1. Dependence of the spin waves amplitude on the applied magnetic field at four different positions of the pump and probe beams

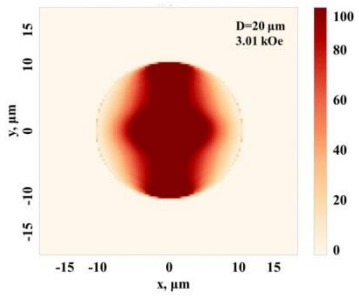

(a)

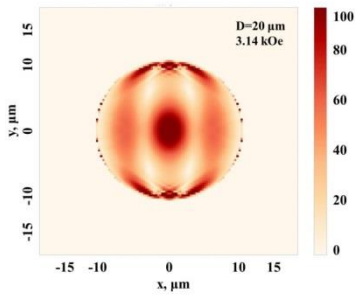

(b)

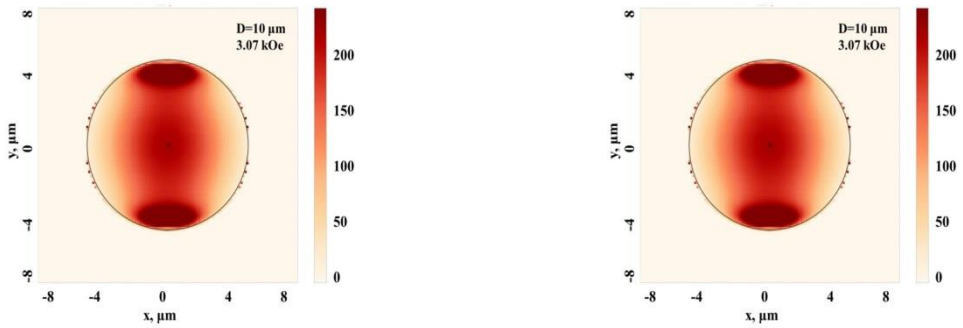

(c) (d)

Fig. 1. Spatial distribution of the spin wave amplitude for the 20 μm disk at H = 3.01 kOe (a) (the lower field resonance peak), and at H = 3.14 kOe (b) (the higher field resonance peak), for the 10 μm disk at H = 3.07 Oe (c) (the lower field resonance peak), and at H = 3.12 Oe (d) (the higher field resonance peak).

References

[1] Gündoğan, M., Ledingham, P. M., Kutluer, K., Mazzera, M., & De Riedmatten, H, Phys. Rev. A ,230501 (2015).

[2] Edwards E.R., Buchmeie M., Demidov V. E., Demokritov S. O , Journal of App. Phys. 113, (2013)

[3] Chernov A.I., Kozhaev M.A. , A. K. Zvezdin, , Belotelov, V. I., Opt. Lett. 42 (2017)

Magnetotransport properties of spin valves based on chiral helimagnets Dy and Ho

Zavornitsyn R.S. , Naumova L.I. , Milyaev M.A. , Makarova M.V. ,
Krinitsina T.P. , Proglyado V.V. , Maksimova I.K. , Ustinov V.V.

Institute of Metal Physics, Ural Branch RAS, 620108, Ekaterinburg, Russia

New magnetic nanostructures of the "spin valve" type have been synthesized, the main functional elements of which are made from natural metallic helimagnets Dy and Ho (see Fig.1). The possibility of controlling magnetotransport characteristics of chiral helimagnets (HM) by the action of an external magnetic field, which causes the rotation of the magnetic spiral of the chiral nanolayer due to the presence of an uncompensated magnetic moment, has been experimentally shown.

Spin valves comprising a synthetic antiferromagnet and a CoFe/HM/CoFe structure in the pinned layer, HM being Dy or Ho, were prepared by magnetron sputtering.

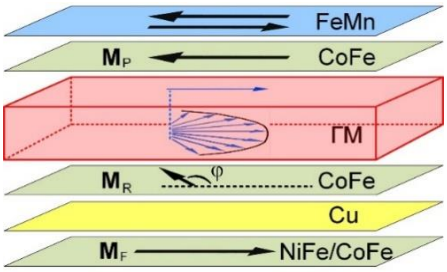

Fig.1. Schematic of a chiral spin valve. The arrows show the magnetic moments of a fragment of the helimagnet Dy (Ho) layer, an antiferromagnetic FeMn layer, and ferromagnetic CoFe layers: pinned $\mathbf{M}_P$, referent $\mathbf{M}_R$, and free $\mathbf{M}_F$.

It is shown that the Dy layer is characterized by crystallites, the [0002] direction of which is perpendicular to the film plane. Variations of magnetotransport properties of the spin valve, which are due to the formation of antiferromagnetic order in the dysprosium layer, are observed. Peculiarities of noncollinear magnetic order of the Dy layer were found to depend on the direction of magnetic moments of adjacent layers and magnetic field strength when passing through the Néel temperature.

A holmium layer in the spin valves is polycrystalline with weak axial texture. The structural coherence length along the hexagonal c-axis is approximately 2/5 of the total thickness of the holmium layer. Field dependences of the spin valves magnetoresistance were measured at different temperatures. Correlation was revealed between magnetic state in holmium layer and the shape of magnetoresistive curve. Deviation of magnetic moments of the reference layer and the adjacent part of holmium from the applied magnetic field was investigated. The field induced mobility of the magnetic helicoid in holmium layers was revealed.

The research was supported by RFBR (project No. 19-02-00057).

References

[1] R.S. Zavornitsyn, L. I. Naumova, M. A. Milyaev, M. V. Makarova, T. P. Krinitsina, V.V. Proglyado, and V.V. Ustinov, Phys. Met. Metallogr. 121, 624 (2020).
[2] R.S. Zavornitsyn, L.I. Naumova, M.A. Milyaev, M.V. Makarova, V.V. Proglyado, I.K. Maksimova, and V.V. Ustinov. Current Applied Physics 20, 1328 (2020).

Spin-polarized conductance of point contacts with non-collinear magnetization of electrodes

Useinov N. Kh.

Institute of Physics, Kazan Federal University, 420004, Kazan, Russia

The work represents a theoretical generalization and modeling of spin-polarized conductivity (conductance) in magnetic nanoscale heterostructures based on the extended model of magnetic point contact (PC) [1]. The theory describes diffuse, quasi-ballistic, ballistic and quantum conduction modes and creates a convenient formalism for modeling and researching spintronic devices. The PC model assumes that the middle layer between ferromagnetic electrodes (with non-collinear magnetization) can be replaced by different materials: dielectric, ferroelectric, magnetic domain wall, semiconductor or compounds of metals.

According to the theoretical model, the spin-polarized conductivity of the PC, taking into account the quantum boundary conditions, can be found from the general expression for the spin component of the electric current [1]:

$$I_s(V,\Theta) = G_0 \frac{k_{F,s}^2 a^2 V}{2} \int_0^{\infty} \left[T_{\text{bal},s}(V,\Theta) + \Omega_{\text{heter},s}(k) + \Omega_{\text{grad},s}(k) \right] \frac{J_1^2(ka)}{k} dk ,$$

$$T_{\text{bal},s}(V,\Theta) = \int_0^{\vartheta_{\text{cr}}} \sin(\vartheta_s)\cos(\vartheta_s) D_s(\vartheta_s, V, \Theta)\, d\vartheta_s$$

where s is the spin index, G_0 is the conductance quantum, $k_{F,s}$ is the minimum of the Fermi wave vectors of the spin subbands of the electrodes, a is the radius of the point contact, V is applied voltage, $J_1(ka)$ is the Bessel function. The $T_{\text{bal},s}$, $\Omega_{\text{heter},s}$ and $\Omega_{\text{grad},s}$ are functions of integrals depending on the transmission coefficient $D_s(\vartheta_s, V, \Theta)$ of electrons, mean free paths l_s, Fermi wave vectors $k_{F,s}$. In integral the upper limit ϑ_{cr} is the angle determined by the conservation law for the longitudinal components of the Fermi wave vectors; ϑ_s is the angle of incidence of an electron on the interface between the media from the normal to the PC plane; Θ is the angle between the mutual orientations of the domains of the PC magnetic electrodes. The functions $T_{\text{bal},s}$, $\Omega_{\text{heter},s}$ and $\Omega_{\text{grad},s}$ are responsible for ballistic (tunneling), quasi-ballistic and diffusion modes of conduction of PC and heterogeneity of chemical potentials on the interfaces, see their exact expressions in [1]. The $D_s(\vartheta_s, V, \Theta)$ can be found by the transfer matrix method as a function of the width L, the energy height U_B of the barrier, and other parameters of the PC, see [2].

References

[1] A. Useinov, H. Lin, N. Useinov, L. Tagirov, JMMM 508, 116729 (2020)

[2] N. Kh. Useinov, *et al.*, Phys. Solid State 62, 1706–1712 (2020)

Dynamics of an exceptional point in a system of two coupled magnetic waveguides

Temnaya O.S.[1], Kalyabin D.V.[1,2], Nikitov S.A.[1,2,3]

[1]*Kotel'nikov Institute of Radio-Engineering and Electronics of RAS, 125009, Moscow, Russia*
[2]*Moscow Institute of Physics and Technology, 141701, Dolgoprudny, Russia*
[3]*Laboratory "Metamaterials", Saratov State University, 410012, Saratov, Russia*

Magnonic systems have attracted great attention over the last years because of their applicability for creation of functional electronics elements, such as mode selectors and directional couplers[1,2]. Two normal modes could exist in the spin wave (SW) spectrum of a system consists of magnonic waveguides with strong coupling between them. In the case when we have balanced gain and loss[3], a point called "exceptional point" appears in the SW spectrum where two normal modes transfers to eigenfrequencies of individual ones. Up to now, the most studied magnonic systems are multilayered structures which consists of ferromagnetic layers separated by a thin nonmagnetic material[1], however, lateral structures are more attractive[4,5].

In this work, we demonstrate dynamics of an exceptional point induced by wavenumber change in a system of coupled magnonic waveguides (Fig. 1). We show that one can effectively change positions of exceptional points by varying the wavenumbers and values of effective damping within waveguides.

We acknowledge the support from the grant of Russian Foundation for Basic Research (Grant No. 19-29-03015, 18-29-27018, 18-57-76001).

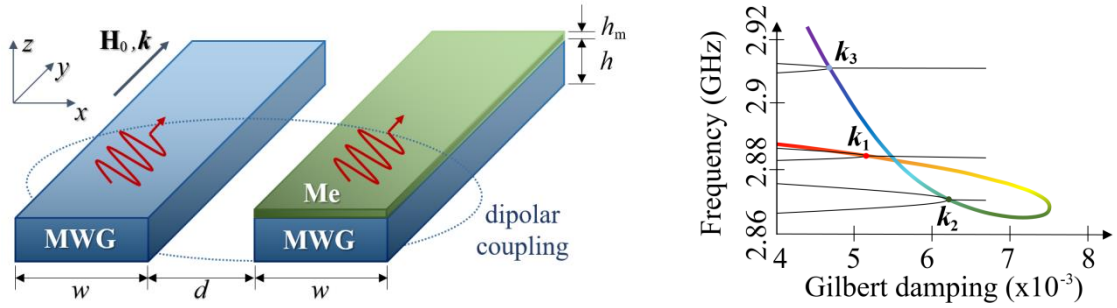

Fig. 1. The investigated magnonic system, where backward volume waves are excited (left); exceptional point dependence on wave number, $\boldsymbol{k}_1$ = 1 rad/μm, $\boldsymbol{k}_2$ = 10 rad/μm, $\boldsymbol{k}_3$ = 30 rad/μm (right).

References

[1] Q. Wang, et al. Sci. Adv. 19, 4(1) (2018).
[2] Q. Wang, et al. Nat. El. 3, 765–774 (2020).
[3] R. Verba, V. Tyberkevich, and A. Slavin. Phys. Rev. B 98, 104408 (2018).
[4] A. Sadovnikov, et al. JETP Let. 107, 25-29 (2018).
[5] X. Wang, G. Guo, and J. Berakdar. Phys. Rev. Appl. 15, 034050 (2021).

Elastic Dipole Mechanism of the Collapse of Fano Resonances

Sukhorukova O.S.[1], Tarasenko A.S.[1], Tarasenko S.V.[1], and Shavrov V.G.[2]

[1] *Donetsk Institute of Physics and Engineering, , Donetsk, 283048 Ukraine*
[2] *Kotelnikov Institute of Radio Engineering and Electronics, Russian Academy of Sciences, Moscow, 125009 Russia*

One of the main directions in the modern physics of composite elastic media is the search for acoustic analogs of resonant polariton effects characteristic of the dynamics of electromagnetic metamaterials. Great attention is recently paid to the study of the polariton mechanism of the formation of the Fano resonance and the related dynamic effects (e.g., the collapse of Fano resonances, "dark" modes, superresonance, and superradiance). These studies contribute to the development of the modern physics of elastic metamaterials, and intense studies on the hybridization of spintronics and straintronics are focused on the possibilities of using magnetic heterostructures (in particular, layered) as a new elemental base for the fabrication of efficiently controlled metamaterials. In particular, the search for magnetoacoustic analogs of the mentioned dynamic polariton effects is of significant interest. For example, the possibility of the existence of the magnetoelastic variant of the Fano resonance at an oblique incidence of a plane bulk elastic shear wave on a tangentially magnetized ferromagnetic layer acoustically hard coupled to an unlimited isotropic elastic nonmagnetic insulator (acoustic analog of the Voigt geometry) was theoretically considered in recent works. However, in this works authors used a theoretical model that did not involve the contribution of propagating magnetostatic and exchange spin waves to the magnetoelastic dynamics of the magnetic layer.

In view of the above presentation, we study in this work the magnon contribution to the elastodipole mechanism of the formation of the Fano resonance and the related dynamic effects, including the collapse of the Fano resonance, the formation of bound states in the continuum, and superradiance for the case of the tunneling of the plane bulk elastic SH- wave through acoustically continuous heterostructures involving superconducting, as well as magnetic and nonmagnetic dielectric, layers.

It has been shown that the effect of the elastic dipole interaction on the transmission of elastic shear phonons through magnetic insulator–superconductor sandwich structures involving ferromagnetic or antiferromagnetic layers allows the implementation of magnetoacoustic analogs of polariton effects well known in the physics of semiconductor heterostructures, including the formation and collapse of the acoustic Fano resonance, bound states in the continuum of transverse phonons, "dark" and "light" modes, and acoustic superradiance. These effects for asymmetric layered magnetic heterostructures can be non-reciprocal with respect to the inversion of the direction of the longitudinal wave vector (the angle of incidence of the shear plane wave incident from outside). It is also noteworthy that the linewidth of the outgoing SH magnetoelastic wave associated with radiative damping near the mentioned bound states in the continuum within the considered non-dissipative model can be arbitrarily small according to the Friedrich -Wintgen theory.

Focusing and Caustic of Magnetoelastic Waves in Monocrystalline Ga_xFe_{100-x}

M.A. Borich[1,2], S.M. Bakharev[1,2], S.P. Savchenko[1]

[1]*Institute of Metal Physics, 620108, Ekaterinburg, Russia*
[2]*Ural Federal University, 620002, Ekaterinburg, Russia*

Spin waves propagating in systems with strong magnetoelstic interaction have peculiarities that seem to be perspective for spintronics applications. There are no clear magnetic or elastic modes in such systems, but only coupled magnetoelastic waves (MEW). The direction of the group velocity of MEW may differ significantly from the direction of the the wave vector, and the focusing of MEW occurs. Moreover, in the specific directions, the MEW intensity increases sharply. This phenomena is called caustic, and the MEW caustic can definitely be used in spintronic devices.

Galphenol alloys Ga_xFe_{100-x} represent a class of materials in which the MEW caustic can be observed, for the following reasons: high magnetization, high anisotropic in the elastic subsystem, and strong magnetostriction effects due to the strong magnetoelastic interaction [1]. The Ga concentration x may be varied over a wide region ($0<x<30$). The change in x produces the change in all parameters: the magnetization decreases from 1700 G/cm^3 at x=0 to 950 G/cm^3 at x=30, the exchange coupling constant A also decreases with x by about 30%, the elastic constants c_{11}, c_{44}, c_{12} depends on x nonmonotonically, and the magnetoelastic interaction constants b_1, b_2 even change sign: $b_2>0$ for $x<13.2$, and $b_2<0$ for $x>13.2$ [2,3].

The MEW spectrum in galfenol demonstrates interesting features. When the quasilongitudinal phonon mode (L) becomes close to the quasimagnetic mode (m), the modes interact each other, and mL resonance occurs. The polarization vector of L mode obtains a magnetic part, while m mode gets elastic components. The same situation is realized when quasimagnetic mode is close to the fast (T_1) and slow (T_2) quasitransverse phonon modes. Thus, we deal with three magnetoelastic resonances: mL, mT_1 and mT_2. In the vicinity of the resonances, the MEW acquire the specific properties: the waves with different directions of wave vectors (in a certain solid angle) have practically the same direction of the group velocity, and the intensity of the wave flow increases sharply. These directions (caustics) do not coincide with characteristic crystalline direction [001], [100], [101], [111], and depend on the parameters of the system. In this report, the dependencies of caustic directions on (1) magnitude of external field, (2) wave frequency, and (3) concentration x are investigated. It is shown that the caustic picture is significantly different for different x, but for each value of x the caustic directions can be effectively controlled by the external field.

The research was carried out within the state assignment of FASO of Russia (theme "Function" AAAA-A19-119012990095-0).

References

[1] Y. Zhang and R. Wu, IEEE Transaction on Magnetics, 47, 4044 (2011).
[2] A.E. Clark, and K.B. Hathaway, et. al., Journal of Applied Physics, 93, 8621 (2003).
[3] R. A. Kellogg, Development and modeling of iron-gallium alloys, dissertation (2003).

Magnetoelastic Waves Anisotropy in Galfenol Crystal

Bakharev S.M.[1,2], Borich M.A.[1,2], Savchenko S.P.[1]

[1]Institute of Metal Physics, 620137, Ekaterinburg, Russia
[2]Ural Federal University, 620002 , Ekaterinburg, Russia

The report is devoted to the theoretical investigation of the propagational peculiarities of magnetoelastic waves in a bulk galfenol ($Fe_{1-x}Ga_x$) sample in the vicinity of magnetoelastic resonance. The chosen material has several features; one of them is the strong dependence of material properties on gallium concentration. E.g. increasing in Ga concentration from 13.2% to 20% causes noticeable modification of such properties as density, saturation magnetization, elastic and magnetoelastic moduli [1]; another feature is that galfenol alloys are materials with strong elastic anisotropy and strong magnetoelastic interaction.

The magnetoelastic waves in a cubic lattice have been theoretically studied for a long time [2], but the investigations usually explored the waves propagating in principal directions only ([100], [001], [101], [111]). In the present work, the external magnetic field is assumed to be applied along the [001] crystal axis of a bulk galfenol sample, and the directions of the wave vectors are chosen to be arbitrary. The typical wavelengths in experiments with galfenol are about 1 μm, and the typical frequencies are about 10 GHz. A phenomenological model of the dynamics of magnetic and elastic subsystems can be employed therefore. The spectrum of the magnetoelstic waves consists of four modes, and three magnetoelastic resonances occur: mL-resonance, when the quasi-magnon frequency becomes close to quasi-elastic quasi-longitudinal one, mT_1 and mT_2-resonances, when quasi-magnon mode becomes close to fast and slow quasi-transverse quasi-phonon modes, respectively. The waves demonstrate highly anisotropic behavior in the vicinity of resonances. They propagate nonuniformly and focus along the specific directions. In the present report, it is shown that the focusing directions do not coincide with the principal directions, and they can be effectively controlled by the wave frequency and the magnitude of external magnetic field.

The results of presented research are as follows. The frequency regions of mL, mT_1 and mT_2 resonances are determined. For instance, if gallium concentration is equal to x=13.2% and the value of external magnetic field is about 10 kOe, then the resonance frequency region is about (28-35) GHz. If the wave frequency is located in this region, then the resonance conditions are satisfied only for specific regions of the directions. Thus, magnetoelastic resonances become "oriented", namely, in some directions the magnetic and elastic modes interact stronger than in others.

The research was carried out within the state assignment of FASO of Russia (theme "Function" AAAA-A19-119012990095-0), and by IMP UB RAS project No. м 1-21.

References

1. A. E. Clark *et.al.* Extraordinary magnetoelasticity and lattice softening in bcc Fe-Ga alloys, J. Appl. Phys., 93, 8621 (2003).
2. A.I. Akhiezer, V.G. Bar'yakhtar, S.V. Peletminskii, Spin waves (North-Holland Pub. Co., Amsterdam, 1968).

Study of mixing formulae application for description of the microwave properties of periodic structures

Bobrovskii S.Yu.[1], Petrov D.A.[1], Rozanov K.N.[1]

[1]*Institute for Theoretical and Applied Electromagnetics RAS, 125412, Moscow, Russia*

At the present time, metamaterials based on periodic structures are widely used in the microwave technology. Such structures can be applied both as a radio-absorbing material and as a part of so-called frequency-selective surfaces [1]. Fibers, microwires, spirals, hooks, etc. could be implemented as a unit element of a periodic structure. [2]. In the present work, a metamaterial in a dielectric matrix with inclusions in the form of conducting squares of small thickness is studied. The aim of this work is to find a suitable mixing formula to describe the microwave properties of the system.

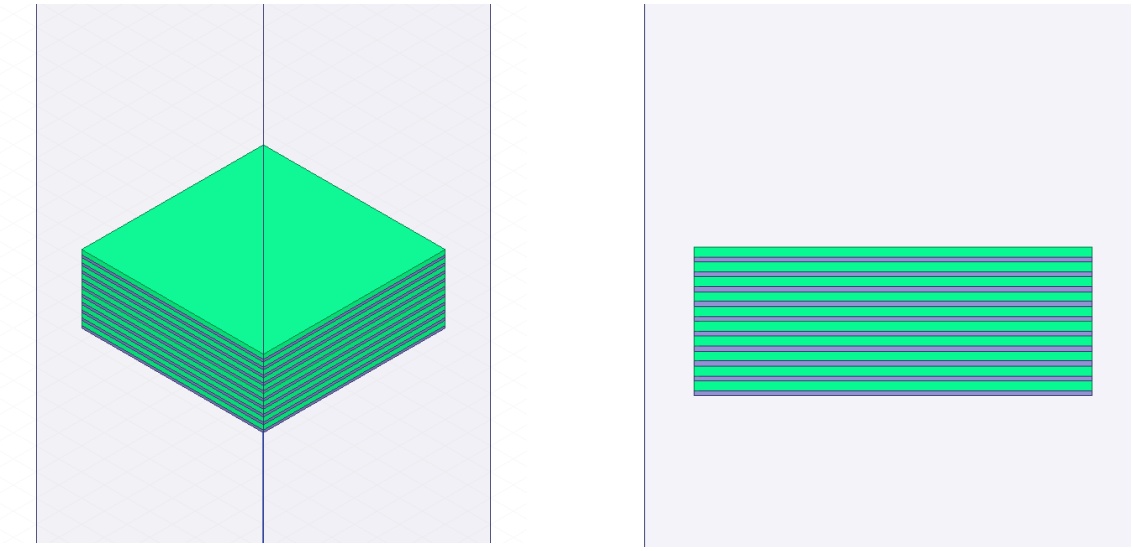

Fig.1. Appearance of a computational model with 10 layers of conductive inclusions

The problem is solved using the numerical simulation of the transmission and reflection coefficients with periodic boundary conditions by the finite element method. The computational model (Fig.1) is a semi-infinite layer of conductive inclusions of square form and small thickness, placed in a dielectric matrix, with the possibility of changing the distance between the inclusions. Both single layer and multilayer structures with the number of layers up to 10 are calculated. The distance between the layers is fixed or changed simultaneously with the distance between the elements in the plane.

To approximate the obtained dependences of the static susceptibility, the Odelevsky formula [3] is used:

$$\chi = \frac{p}{(1 - p/p_c)N},$$

where χ is an effective susceptibility of the system, p is a volume concentration of conductive inclusions, p_c is a percolation threshold and N is a depolarization factor, also known as form factor of the inclusions. It is easy to see, that when p_c=1, Odelevsky formula transforms into Maxwell Garnett formula.

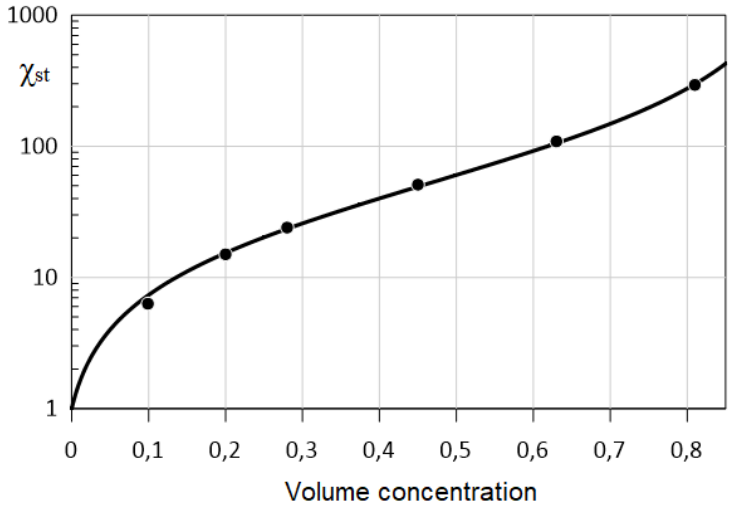

Fig. 2. The calculated dependence of the static susceptibility of the periodic structure on the volume concenctration of inclusions, obtained by numerical simulation. The curve is an approximation by the Odelevsky formula

Figure 2 shows the calculated dependence of the static susceptibility (χ_{st}) on the volume concentration of the system with ten layers of conductive inclusions. It is shown, that the microwave properties of the investigated periodic structure are correctly described by the Odelevsky mixing formula. The effective depolarization coefficient of inclusions is calculated and it is demonstrated that the value of the depolarization coefficient of a multilayer structure is close to a single-layer one. It is also shown, that the applicability of the selected mixing formula does not depend on the number of layers in the system under study.

This study was financially supported by the Russian Science Foundation (RSF) under project No. 21-19-00138 (https://rscf.ru/en/project/21-19-00138/).

References

[1] V.I. Ponomarenko, I.M. Lagunov, JTF 90, 6, 1009 (2020)
[2] A.N. Lagarkov et al, High Temperature 48, 983 (2010)
[3] S.N. Starostenko et al, J. Comm. Technol. Electron, 65, 12, 1407 (2020)

Thin superconducting film in proximity with a ferromagnetic insulator

Seleznyov D.V.[1], Yagovtsev V.O[1,2]., Pugach N.G.[1,3]

[1] *National Research University Higher School of Economics, Moscow 101000, Russia 1V.I.*
[2]*Vernadsky Crimean Federal University, Vernadsky Prospekt, 4, Simferopol 295007, Russia*
[3] *Skobeltsyn Institute of Nuclear Physics, Lomonosov Moscow State University, Leninskie Gory, 1 (2), GSP-2 Moscow 119991, Russia*

Combining superconducting (S) films with a strongly spin-polarized ferromagnet (F) gives opportunities for creation new superconducting spintronic devices based on generation of spin-triplet Cooper pairs because of the inverse proximity effect. Such a bilayer can be described in terms of quasiclassical theory, which is based on calculation of propagator $\hat{g}$, known as Green function. The Green function is a 4x4 matrix in spin-space, whose normal and anomalous components depends on the energy of the quasiparticle ϵ and a distance z from the SF inteface. The propagator $\hat{g}$ can be found in the dirty limit as a solution of Usadel equations

$$iD\partial_z(\hat{g}\partial_z\hat{g}) = \left[(\epsilon + i\eta)\widehat{\tau_3} + \hat{\Delta},\ \hat{g}\right]$$

here *D* is the electrons diffusion coefficient, $\epsilon + i\eta$ is the energy variable with a small imaginary term, $\widehat{\tau_3}$ - the third Pauli matrix, $\hat{\Delta}$ - the matrix order parameter.

The boundary-value problem should be added by the boundary conditions appropriate for the case of strong spin polarization of the ferromagnet [1]. The boundary conditions depend on spin-mixing angle, which determine the phase difference for electrons with spin-up and spin-down, reflected from the SF interface.

The singlet and the triplet components of the anomalous Green function were found analytically from linear approximation of Usadel equations for such boundary conditions in our works [2-3]. In this work, we numerically solved this boundary value problem, using Riccati parametrization [4] of the propagator to satisfy the normalization condition $\hat{g}^2 = 1$:

$$\hat{g} = \begin{pmatrix} N & 0 \\ 0 & \tilde{N} \end{pmatrix}\begin{pmatrix} 1+\gamma\tilde{\gamma} & 2\gamma \\ 2\tilde{\gamma} & 1+\tilde{\gamma}\gamma \end{pmatrix}$$

where $\gamma(z,\epsilon)$, $\tilde{\gamma}(z,\epsilon)$ – Riccati parameters, $N = (1-\gamma\tilde{\gamma})^{-1}$, $\tilde{N} = (1-\tilde{\gamma}\gamma)^{-1}$ – normalization matrices. From the anomalous Green functions, we determined the order parameter in a superconducting film using the self-consistency equation:

$$\Delta(z) = \frac{1}{2}N_0\lambda\int_0^{\Delta_0 cosh(1/N_0\lambda)} d\epsilon[f_s(z,\epsilon) - f_s(z,-\epsilon)]tanh(\epsilon/2T)$$

where f_s – singlet anomalous Green function, N_0 – density of states at the Fermi level, λ – BCS coupling constant, Δ_0 is the order parameter in the bulk S material.

The numerical calculation of the Green's functions coincides with the previously obtained analytical solution in the temperature range close to the critical temperature T_c. We studied the influence of a ferromagnetic insulator on the order parameter (Fig.1) as a function of the spin mixing angle. The superconducting order parameter decreases with increasing spin mixing angle near the S-F interface. The density of states (DOS) is also investigated in the S/F bilayer.

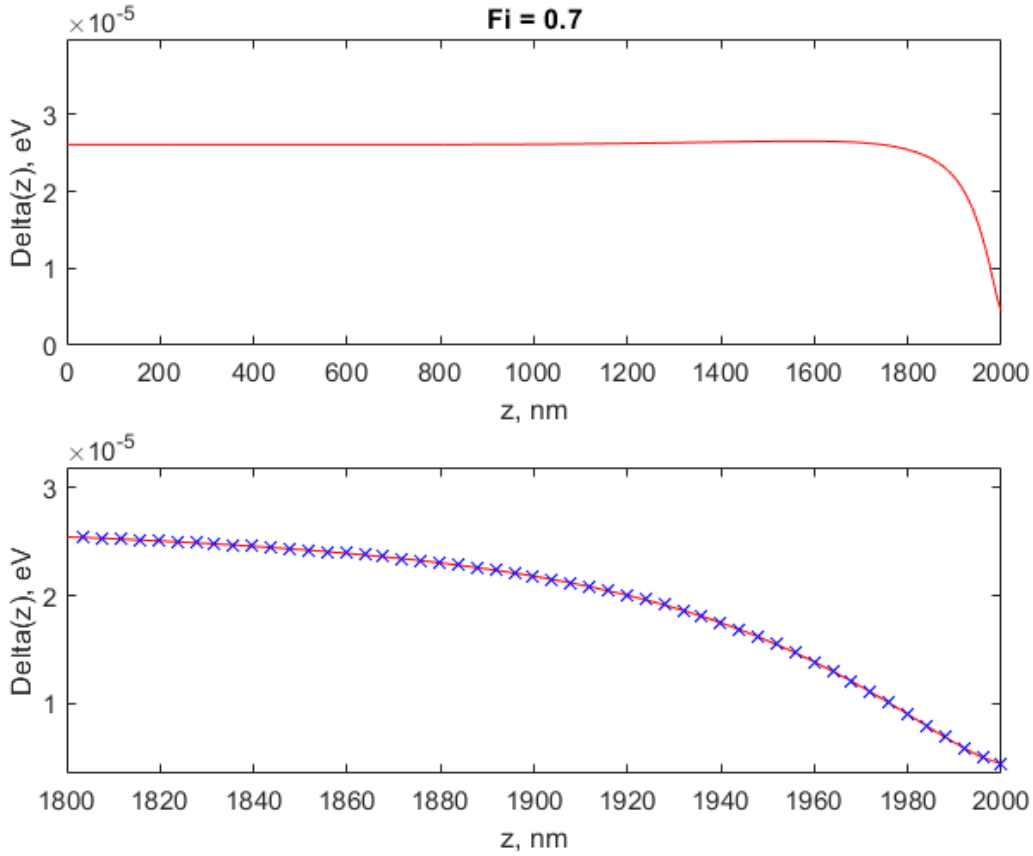

Fig.1 The suppression of the order parameter $\Delta(z)$ in the vicinity of the SF interface.

The DOS calculations were financially supported by the Russian Ministry of Education and Science, Megagrant project N 075-15-2019-1934, the estimation of the order parameter suppression was supported by the RFBR project N 19-02-00316.

References

[1] J.A. Ouassou, A. Paul, M.Blamire, M.Eschrig, and J.Linder, Sci. Rep. 7(2016).

[2] V.O. Yagovtsev and N.G. Pugach and M.Eschrig, Supercond. Sci. Technol. 34, 025003 (2021).

[3] V.O. Yagovtsev and N.G. Pugach, Phys. Metals Metallogr 277 (2020).

[4] S.H. Jacobsen, J.A. Ouassou and J. Linder, Phys. Rev. B 92, 024510 (2015)

Polarization control of THz emission in spintronic multilayer structure [$TbCo_2$/FeCo]x3

Ovcharenko S.V. [1], Khusyainov D.I.[1], Gaponov M.S. [1], Klimov A.A. [1]

[1]*MIREA - Russian Technological University, 119454, Moscow, Russia*
[2]*Prokhorov General Physics Institute of RAS, 119991, Moscow, Russia*

In THz emitters based on the ferromagnet (FM) / nonmagnetic (NM) nanoscale heterostructure, the generation of radiation is based on spintronic effects. Such emitters have an ultra-wide generation spectrum of THz radiation (up to 30 THz) and allow to control the parameters of THz radiation directly in the emitter [1,2].

In our work, a spintronic emitter based on the [TbCo2 / FeCo] x3 multilayer structure was investigated by the method of time-resolved THz spectroscopy. This structure is characterized by an easy-axis magnetic anisotropy induced during fabrication and, as a consequence, by the presence of a spin-reorientation transition (SRT) [3]. The paper proposes a method for controlling the polarization based on magnetic field-induced SRT with magnetization along the hard axis [4]. The SRT provides magnetization rotation when magnetic field is changed by its value only, giving rise to polarization rotation of the THz pulse. This makes the multilayers with SRT very different from the magnetic / nonmagnetic structures. In the latter, the polarization rotation can be achieved by rotation magnetic field around them, that is much less technologically justified. Figure 1 shows the dependence of the THz wave polarization rotation angle on the magnitude of the constant magnetic field for its fixed direction.

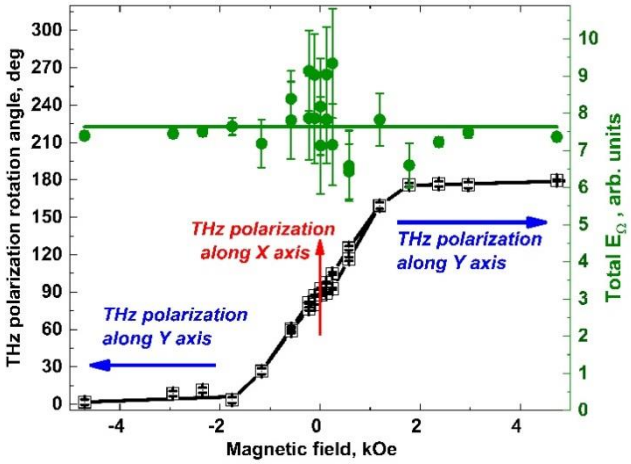

Fig. 1. - The dependence of the polarization angle and the magnitude of the THz field at different values of the magnetic field. Left scale: Magnetic field dependence of the THz polarization angle obtained from the fits of angular diagrams by magnetizing the sample along the hard axis. Right scale: total THz field dependence. Lines are guides for eye.

It is important that the rotation of the polarization plane occurs without loss of the THz radiation intensity. Figure 2 shows a scheme for generating THz radiation in a multilayer structure. The most likely emission mechanism is photoinduced ISHE. An argument in favor of this mechanism is the observation of ISHE in this structure earlier using direct injection of spin current from a YIG film at ferromagnetic resonance [6].

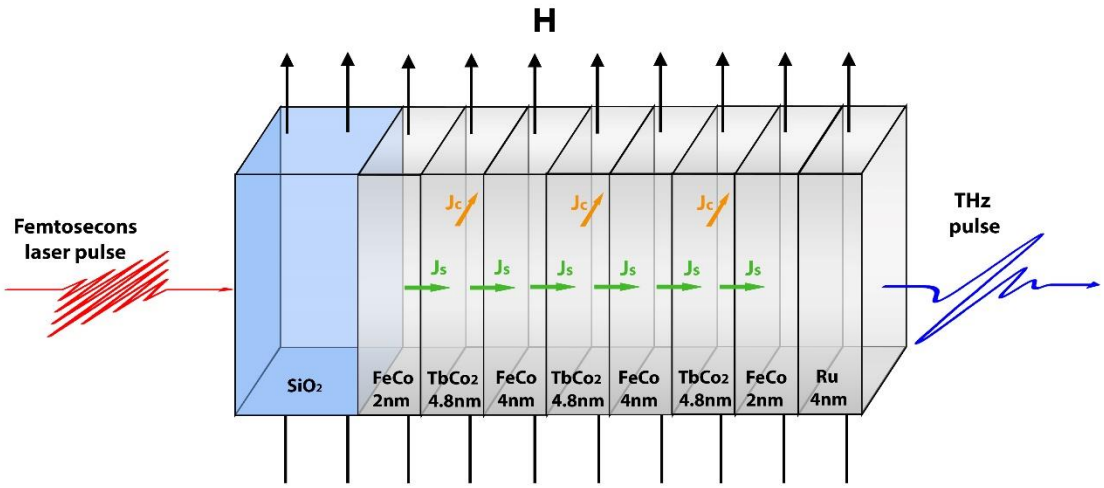

Fig.2. Illustration of the sample structure and directions of valuable vectors. H is magnetic field strength, J_S is the spin-current, J_C is the charge current.

The work of Russian side is supported by Russian Science Foundation (Grant 20-12-00276). The authors are grateful to Tiercelin N. and Pernod Ph. (Univ. Lille, CNRS, Centrale Lille, Univ. Polytechnique Hauts-de-France, UMR 8520-IEMN, 59000, Lille, France) for sample preparation.

References

[1] Kampfrath T. et al., Nat. Nanotechnol., 8, 4, 256–260 (2013).

[2] J. Walowski and M. Münzenberg, J. Appl. Phys. 120(14), 140901 (2016).

[3] Millev, Y. T., Oepen, H. P., & Kirschner, J., Physical Review B, 57(10), 5837, (1998).

[4] Khusyainov, D., Ovcharenko, S., Gaponov, M., Buryakov, A., Klimov, A., Tiercelin, N., ... & Preobrazhensky, V., Scientific reports, 11(1), 1-8, (2021).

[5] Shaikhulov, T. A., Ovsyannikov, G. A., Constantinian, K. Y., Klimov, A. A., Demidov, V. V., Stankevich, K. L., ... & Nikitov, S. A.. Ferromagnetism in the ferromagnetic yttrium iron garnet film/ferromagnetic intermetallic compound heterostructure. Physics of the Solid State, 62(9), 1653-1658, (2020).

Investigation of second-order magnetization precession modes in a two-layer ferromagnetic structure

Abramovski I.E.[1], Vlasov V.S.[1], Pleshev D.A.[1,2], Kotov L.N.[1], Shcheglov V.I.[3]

[1]*Department of Radiophysics, Pitirim Sorokin Syktyvkar State University, 167001 Syktyvkar, Russia*
[2]*Saint-Petersburg state forest technical university named after S.M. Kirov, 194021, St-Petersburg, Russia*
[3]*Institute of Radioengineering and Electronics of the Russian Academy of Sciences, 125009, Moscow, Russia*

In last decades there are many works on computer modeling of nonlinear magnetic dynamics in nanostructures. This interest is caused by creation of fundamentally new computing technical devices [1]. The work devoted to the modeling of the second order magnetization precession modes in a normally magnetized two-layer ferromagnetic structure with cubic anisotropy. Let's consider perpendicular magnetized two-layer film. The material of the film similar to YIG. The alternating magnetic field lies in the plane of the film and has circular polarization. The Landau-Lifshitz equation is used to describe the magnetic dynamics of the film. The field of cubic anisotropy, the demagnetizing fields and the interaction field were taken into account [2]. The paper considers types of layer anisotropy: [100], [110], [111] [2]. Landau-Lifshitz equation was solved numerically by the 4-5 orders Runge-Kutta method in the Scilab. A specific equilibrium position precession mode for anisotropy type [111] has been detected, which was strongly dependent on the size and direction of the field of interlayer interaction. It was shown that in the absence of the second layer, the precession of the position breaks into a low-amplitude circular precession. When the field of interlayer interaction becomes comparable to the anisotropy field the precession portraits appear new condensations (which are not so pronounced, but are noticeable), which, depending on the value of interlayer interaction J, can coincide with the condensations of anisotropy. Starting with the value of J = 300 erg/cm^3, the ring of the second order precession begins to expand markedly. With the further growth of J, the influence of the anisotropy field decreases, the thickening becomes less pronounced until the large ring is completely evenly filled with small rings. Starting at the value of J = 800 erg/cm^3, the thickenings cease to be visible, and the large ring looks evenly filled with small rings.

This work has been supported by the grants: Russian Science Foundation (project No. 21-72-20048); RFBR and Komi Republic (project No. 20-42-110004).

References

[1] C. Abert, European Physical Journal B 92, 120 (2019).
[2] V. S. Vlasov et al., J. Commun. Technol. Electron. 58, 857 (2013).

Section 3
Plasmonics and Nanophotonics

Anomalous magneto-optical effects in high index contrast magneto-optical Mie resonators

Lei Bi

School of Microelectronics and Solid State Electronics, University of Electronic Science and Engineering of China,
Chengdu, Sichuan, 610054 China

High index contrast dielectric Mie resonators featuring unique modal profiles, strong light-matter interaction at the nanoscale has led to the discovery of a variety of novel photonic phenomena recently. In this work, we report the observation of anomalous magneto-optical effects in Si/Ce:YIG/YIG/SiO2 high index contrast Mie resonators. Giant s-polarized transverse magneto-optical Kerr effect (TMOKE) up to 6.5% and longitudinal magneto-optical Kerr effect (LMOKE) in transmission mode (LMOKE-T) of ~0.1° under near normal incidence (q=3°) are observed experimentally, which are either non-existent or orders of magnitude weaker in planar magneto-optical thin films. These novel magneto-optical effects originated from the circular displacement current in high index contrast Mie resonators. Our work indicates an uncharted territory of light polarization control based on the complex modal profiles in all-dielectric magneto-optical Mie resonators and metasurfaces, which opens the door for versatile control of light propagation by magnetization for a variety of applications in vectoral magnetic field sensing, biosensing, non-reciprocal photonic devices, magneto-optical imaging and optomagnetic memories.

Magnetoplasmonic waveguides based on metal/opal composite

Kolmychek I.A.[1], Romashkina A.M.[1], Mamonov E.A.[1], Novikov V.B.[1], Gusev N.S.[2], Sapozhnikov M.V.[2,3], Golubev V.G.[4], Murzina T.V.[1]

[1]*Lomonosov Moscow State university, Physics department, 119991 Moscow, Russia*
[2]*Institute for Physics of Microstructures, RAS, Nizhny Novgorod, GSP-105, Russia*
[3]*N.I. Lobachevsky State University of Nizhny Novgorod, Nizhny Novgorod, 603950, Russia*
[4] *Ioffe Institute, St. Petersburg, 194021, Russia*

The field of plasmonics is being actively developing as a lot of novel experimental realizations of subwavelength periodic structures become possible when using modern technological methods [1]. At the same time, well known systems such as opal films can serve as well as a powerful platform for the fabrication of resonant plasmonic structures. It was shown that when a metal layer covers an opaline structure, its optical properties is governed by the diffraction of a light beam on both the periodically structured metal film and on the 3D lattice of opal photonic crystal (PhC). If the metal is ferromagnetic, then the magnetooptical response of the composite can reveal interesting features. In this work we demonstrate resonant optical and magnetooptical response of thin high quality opal films covered by (i) a thin ferromagnetic Co layer, and (ii) Co+Ag thin layer.

Opal films containing up to 15 layers of SiO_2 colloidal spheres of 270-630 nm in diameter were synthesized by liquid phase colloid epitaxy, so that the closely-packed hexagonal structure with the (111) plane parallel to the films' surface was formed [2]. Afterwards, a cobalt film with the effective thickness of approximately 10% of the spheres' diameter was deposited by magnetron sputtering; in some cases a 10 nm thick Ag layer was deposited above cobalt film. At such thicknesses, metal film is inhomogeneous in thickness, has a pronounced profile with a periodic array of nanoholes.

Wavelength-angular spectra of the transmitted radiation reveal a number of peculiarities associated with the surface plasmon-polariton (SPP) excitations and/or opal photonic band gap, their dispersion being dependent on the size of the SiO_2 spheres. Furthermore, a strong enhancement of the magneto-optical effects in attained close to the resonant SPP excitation. We show that the presence of Ag layer increases the quality factor of the SPP resonances, as well as of the magneto-optical contrast in the Voigt geometry, which approaches the value of 1%. The obtained results are perspective for the development of the new lithography-free platform of transparent magnetoplasmonics.

Acknowledgements. Financial support from Russian Science Foundation (RSCF) (19-72-20103) is acknowledged.

References

[1] Borovkova O.V., Hashim H., Ignatyeva D.O. et al., Phys. Rev. B 102, 081405 (2020).

[2] Shishkin I.I. et al. Phys. Rev. B 89, 3, 035124 (2014).

Magneto-optics of all-dielectric nanostructures with guided modes

Ignatyeva D.O.[1,2,3], Voronov A.A.[2,3], Karki D.[4], Kozhaev M.A.[1,2], Levy M.[4], Belotelov V.I.[1,2,3],

[1]*Vernadsky Crimean State University, 295007, Simferopol, Russia*
[2] *Russian Quantum Center, 121205, Moscow, Russia*
[3]*Lomonosov State University, 119992, Moscow, Russia*
[4]*Michigan Technological University, 49931, Houghton, USA*

Magneto-optics of nanostructured materials significantly differ from that of the smooth films and crystals. Excitation of various types of optical modes change the spin-photon interaction leading to the significant enhancement of the known magneto-optical effects and appearance of the new effects that in the smooth films were absent. We consider bismuth-substituted iron-garnet films nanopatterned with 1D or 2D periodicity that can support guided modes of TM or TE types. Such modes reveal themselves as the narrow resonances in the optical spectra with Q-factor higher than 100. We show that excitation of such kind of modes is responsible for the new mechanisms of the magneto-optical interaction.

The dispersion of the TM-type modes is sensitive to the transverse external magnetic field applied to the structure. It causes the nonreciprocal shift of the guided mode resonance position under the action of the external magnetic field applied in $+H_y$ and $-H_y$ directions. Therefore, the transmittance and reflectance spectra are also changed resulting in the modulation of the light intensity – so called transverse magneto-optical Kerr effect. As the mechanism of this effect is different from that of a smooth film, all-dielectric nanostructure exhibits simultaneous high transparency, low absorption and up to 2% TMOKE [1].

Although TE-type waves in smooth materials are not sensitive to the transverse magnetic field, the 2D nanostructures can change the situation. A complex picture of the excitation, dispersion and polarization characteristics of the guided modes excited in the 2D periodic nanostructures gives rise to the transverse magneto-photonic intensity effect [2]. In contrast to the TMOKE, it can be observed both in p and s polarizations of the incident light and reach about 0.5% for both of them.

Another important feature of the nanostructures with the guided modes is the possibility of the subwavelength light localization inside the iron-garnet material. The low optical absorption makes the non-thermal excitation of the spin waves in such structures efficient while the subwavelength light localization allows for the tunable excitation of the perpendicular standing spin waves or high orders [3].

We acknowledge the financial support from Russian Ministry of Education and Science (Megagrant Project 075-15-2019-1934).

References

[1] A.A. Voronov et al., Optics Express 28(12), 17988 (2020).
[2] D.O. Ignatyeva et al., Nature Communications 11(1), 1 (2020).
[3] A.I. Chernov at al., Nano Letters, 20 (7), 5259 (2020).

Three-periodic one-dimensional magnetic photonic crystals

Dadoenkova N.N.[1,2], Dadoenkova Yu.S.[3], Panyaev I.S.[2], Sannikov D.G.[2]

[1]*Donetsk Institute for Physics and Engineering, 283114, Donetsk, DPR*
[2]*Ulyanovsk State University, 432027, Ulyanovsk, Russia*
[3]*Lab-STICC (UMR 6285), CNRS, ENIB, 29238, Brest Cedex 3, France*

In this communication, we present the results of theoretical and numerical investigation of optical and magneto-optical properties of one-dimensional (1D) three-periodic magnetic photonic crystals (MPCs). This research is a development of our previous study of dielectric three-periodic photonic crystals [1-3]. For the constituting materials of the structure we choose the magnetic yttrium-iron garnet $Y_3Fe_5O_{12}$ (YIG) and bismuth-doped YIG (Bi:YIG) and nonmagnetic dielectric oxides SiO_2 and TiO_2. The 1D three-periodic MPCs are formed by two alternating unit cells which are the finite fragments of photonic crystals PC1 and PC2, respectively. Depending on the chosen combination of the constituting materials, one or both unit cells can contain magnetic layers. We focus on the case of nonmagnetic PC1 and magnetic PC2 unit cells. We choose PC1 to be composed of SiO_2 and TiO_2 layers of thicknesses d_1 and d_2, respectively, with the period $D_1 = d_1 + d_2$ and the structure formula $(SiO_2/TiO_2)^N$. We assume PC2 to be of structure $(YIG/Bi:YIG)^M$ with thicknesses of YIG and Bi:YIG layers denoted d_3 and d_4, respectively, which is characterized by the sub-period $D_2 = d_3 + d_4$. The resulting 1D three-periodic MPC has the structure $[(SiO_2/TiO_2)^N/(YIG/Bi:YIG)^M]^K$ (see Fig. 1) and it is characterized by the super-period $D_3=ND_1+MD_2$, where N and M are sub-period numbers and K is a super-period number.

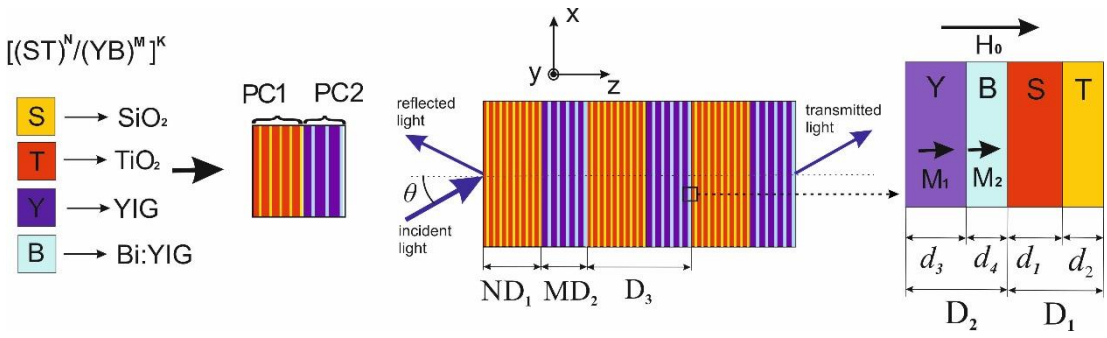

Fig. 1. Schematic of the 1D three-periodic magnetic crystal $[(SiO_2/TiO_2)^N/(YIG/Bi:YIG)^M]^K$.

A plane electromagnetic wave of wavelength λ is incident in the vacuum on the left-hand-side of the MPC's surface in xz-plane under the incidence angle θ. We considered the case of polar magneto-optical configuration (see Fig. 1) when both YIG and Bi:YIG layers are magnetized along the z-axis, *i.e.* perpendicularly to the interfaces of the films. We restrict our consideration of the incident electromagnetic waves within the wavelength range λ = (1 - 5) μm, where all the chosen materials are transparent, and YIG and Bi:YIG materials possess magneto-optical properties. The layers thicknesses are chosen to satisfy the Bragg condition $n_i(\lambda_0)\, d_i = \lambda_0/4$ (here n_i is the refractive index, i is the number of the layer) at λ_0 = 1.55 μm for all the layers, as well as for different values λ_{01} and λ_{02} for the nonmagnetic and magnetic layers, respectively.

We calculated the transmittivity and reflectivity spectra of the electromagnetic waves for the considered three-periodic MPC using the method of the transfer matrix (4×4) [4]. We examined the modifications of both TE- and TM-modes spectra within the first photonic bandgap and its vicinity with the change of the sub-period- and super-period numbers *N*, *M*, and *K*, incidence angle θ and the layers thicknesses d_i. The bandgap spectra are polarization-dependent and exhibit a set of complex intra-band modes. The number and positions of the intra-band modes are correlated with the sub- and super-period numbers and strongly depend on the layers thicknesses (or on the choice of λ_{01} and λ_{02}). The change of θ allows to govern the positions of both bandgap edges and intra-band modes, as well as to open or to close the bandgaps. Modifying d_i, one can reach a significant shift of the intra-band modes towards the bandgap edges, as well it is possible to increase the intra-band modes number and to obtain satellite bandgaps.

We showed a significant increase of the Faraday and Kerr rotations at the frequencies of intra-band modes with the increase of the magnetic periods *M* where the transmittivity values are close to unity. This fact demonstrates one of the advantages of multiperiodic MPCs compared to single-periodic photonic crystals, where the maximal polarization plane rotation occurs at lower transmittivities. The change of the incidence angle also allows to reach Faraday rotation of about some tens degrees.

This research is supported by: RFBR, Russia, project number 19-42-730008 (I.S.P., D.G.S., N.N.D., and Y.S.D.). Y.S.D. acknowledges support from École Nationale d'Ingénieurs de Brest under the project CF-SPEACS, Conseil Régional de Bretagne under the project SPEACS, and the Collège de France (Programme PAUSE).

References

[1] I.S. Panyaev, L.R. Yafarova, D.G. Sannikov, N.N. Dadoenkova, Yu.S. Dadoenkova, I.L. Lyubchanskii, One-dimensional multiperiodic photonic structures: A new route in photonics (four-component media), J. Appl. Phys. 126 103102 (2019).

[2] I.S. Panyaev**,** D.G. Sannikov, Yu.S. Dadoenkova, N.N. Dadoenkova, One-dimensional three- periodic photonic crystals for the design of the photonic devices operating in the infrared regime, Applied Optics, Vol. 60, No. 6, 1943 (2021).

[3] I.S. Panyaev**,** D.G. Sannikov, N.N. Dadoenkova, Yu.S. Dadoenkova, Energy flux optimization in 1D multiperiodic four-component photonic crystals, Opt. Comm. 489, 126875 (2021).

[4] D.W. Berreman, J. Opt. Soc. Am. 62, 502 (1972).

Plasmonics of magnetic and topological graphene-based nanostructures

Kuzmin D.A.[1], Bychkov I.V.[1], Shavrov V.G.[2], Temnov V.V.[3]

[1]Chelyabinsk State University, 454001, Chelyabinsk, Russia
[2]Kotelnikov Institute of Radioengineering and Electronics of Russian Academy of Sciences, 125009, Moscow, Russia
[3]Institut des Molécules et Matériaux du Mans, CNRS UMR 6283, Université du Maine, 72085 Le Mans Cedex, France

Graphene is a unique material to study fundamental limits of plasmonics. Apart from the ultimate single-layer thickness, its carrier concentration can be tuned by chemical doping or applying an electric field. In this manner the electrodynamic properties of graphene can be varied from highly conductive to dielectric. Graphene supports strongly confined, propagating surface plasmon-polaritons (SPPs) in a broad spectral range from terahertz to midinfrared frequencies. It also possesses a strong magneto-optical response and thus provides complimentary architectures to conventional magneto-plasmonics based on magneto-optically active metals or dielectrics. In this work we present main results of our long time complex theoretical investigations of electrodynamic properties of graphene-based nanostructures.

Electrodynamic properties of the graphene–magnetic semiconductor–graphene sandwich-structure have been investigated theoretically with taking into account the dissipation processes [1]. Influence of graphene layers on electromagnetic waves propagation in graphene–semi-infinte magnetic semiconductor and graphene–magnetic semiconductor–graphene sandwich-structure has been analyzed. Frequency and field dependences of the reflectance, transmittance and absorbtance of electromagnetic waves by such structure have been calculated. The size effects associated with the thickness of the structure have been analyzed. The possibility of efficient control of electrodynamic properties of graphene–magnetic semiconductor–graphene sandwich-structure by an external magnetic field has been shown. Change in speckle-pattern of linearly polarized light passed through graphene-covered optical fiber placed in external magnetic field has been investigated, the possibility of magnetic speckle-pattern rotation suppression and inverse speckle-pattern rotation effect has been shown [2]. Magnetic field switching of plasmon-polaritons propagating into a planar gyrotropic waveguide covered by two graphene layers at a deeply subwavelength scale has been predicted, it has been shown that applying an external magnetic field may lead to energy redistribution between two waveguide surfaces [3]. Magnetic field induced by guiding plasmonic modes in graphene-coated nanowire via an inverse Faraday effect has been calculated [4]. Conditions of transverse electric plasmonic mode existence in graphene-based cylindrical waveguide has been obtained and analized [5]. Giant Faraday rotation of high-order plasmonic modes in graphene-based nanowires has been predicted. Upon the reversal of the external magnetic field pointing along the nanowire axis some high-order plasmonic modes may be rotated by up to ∼100° on the length scale of about 500 nm at mid-infrared frequencies. Tuning the carrier concentration in graphene by chemical doping or gate voltage allows for controlling SPP-properties and notably the rotation angle of high-order azimuthal modes [6]. We investigated topological nanostructures covered with graphene-based meta-surfaces, which consist of a periodic pattern of subwavelength stripes of graphene winding around the (meta-) tube or

(meta-)torus. We establish the relation between the topological and plasmonic properties in these structures, as justified by simple theoretical expressions. Our results demonstrate how to use strong asymmetric and chiral plasmonic responses to tailor the electrodynamic properties in topological meta-structures. Cavity resonances formed by elliptical and hyperbolic plasmons in meta-structures are sensitive to the one-way propagation regime in a finite length (Fabry–Perot-like) meta-tube and display the giant mode splitting in a (Mach–Zehnder-like) meta-torus. [7, 8]. Surface plasmon-polaritons in gain-loss metasurfaces have been investigated. A fundamentally new concept of realization of hyperbolic plasmonic metasurfaces by anisotropic gain–loss competition is proposed, and the possibility of highly directional propagation and amplification of surface plasmon polaritons is predicted. A simple realistic configuration of such a metasurface represents the periodic array of lossy metallic slabs embedded in the gain matrix. [9].

We believe that these results extend beyond the graphene plasmonics as they are qualitatively valid for arbitrary nanostructures formed by artificial 2D meta-surfaces supporting the propagating SPP modes.

This work was supported by the Russian Foundation for Basic Research (grants No. 20-37-70038, 19-07-00246, 20-47-740004), the Russian Science Foundation (grant No. 20-19-00745). Numerical calculations were performed with the support of the Ministry of Science and Higher Education of the Russian Federation within the framework of the state assignment project No. 075-00992-21-00.

References

[1] Kuzmin D.A., Bychkov I.V., Shavrov V.G., Photonics and Nanostructures - Fundamentals and Applications 12, 473 (2014)

[2] Kuzmin D.A., Bychkov I.V., Shavrov V.G., Optics Letters 40, 890 (2015)

[3] Kuzmin D.A., Bychkov I.V., Shavrov V.G., Optics Letters 40, 255 (2015)

[4] Kuzmin D.A., Bychkov I.V., Shavrov V.G., Temnov V.V., Lee H.-I., Mok J., Optics Letters 41, 396 (2016)

[5] Kuzmin D.A., Bychkov I.V., Shavrov V.G., Kotov L.N., Scientific Reports 6, 26915 (2016)

[6] Kuzmin D.A., Bychkov I.V., Shavrov V.G., Temnov V.V., Nano Letters 16, 4391 (2016)

[7] Kuzmin D.A., Bychkov I.V., Shavrov V.G., Temnov V.V., ACS Photonics 4, 1633 (2017)

[8] Kuzmin D.A., Bychkov I.V., Shavrov V.G., Temnov V.V., Nanophotonics 7, 597 (2018)

[9] Kuzmin D.A., Bychkov I.V., Shavrov V.G., Temnov V.V., Optics Letters 46, 420 (2021)

Linear and nonlinear surface plasmon polaritons

Dzedolik I.V.

*V. I. Vernadsky Crimean Federal University, **295007**, Simferopol, Russian Federation*

Electromagnetic field of optical frequency, falling on the interface between dielectric and conductive (metallic) media, causes oscillations of both free and bound charges in the media. As a result of charge oscillations secondary electromagnetic waves are re-emitted. They hybridize with polarization waves of bound and free charges and under the corresponding boundary conditions these waves propagate along the interface [1]. These evanescent waves are surface plasmon polaritons. They are attached to the interface and are not radiated in the absence of inhomogeneities of the interface. Linear or nonlinear waves of surface plasmon polaritons are formed depending on the power of the exciting electromagnetic signal.

Metals have a negative real part of the permittivity at optical frequencies which are lower than the plasma frequency in this metal [1]. Such photons create electron interband transitions in the metal by the optical thermal effect, which leads to a nonlinearity of the metal permittivity [2]. The third-order nonlinear dielectric susceptibility for gold in the frequency range from 350 nm to 750 nm has a complex frequency dependence. The real and imaginary parts of the third-order nonlinear dielectric susceptibility change the sign from negative to positive, and they tend to zero with increasing of electromagnetic signal wavelength. When electromagnetic field frequency is higher than the plasma frequency, the metal permittivity becomes positive; with increasing frequency the permittivity tends to unity in the limit. At optical frequencies the dielectric media (such as fused silica) have a positive real part of the susceptibility of both the first and third order, and they imaginary part is practically equal zero. But the value of the third-order nonlinear permittivity of fused silica is less on 7 orders of magnitude than the nonlinear susceptibility of gold in the visible range [2].

As a result of the nonlinear response of the dielectric and conducting media at a sufficient intensity of the optical signal, nonlinear (cnoidal) plasmon-polariton waves and solitary waves (solitons) appear at the interface [3]. The complex frequency dependence of the nonlinear permittivity of metal leads to instability of the plasmon soliton at optical frequencies in the visible range. But at telecommunication signal wavelengths (more than 750 nm), the nonlinear response of noble metals is equal zero, and in dielectrics such as fused silica, the third-order nonlinear response maintains a soliton signal at the interface. The envelope of the plasmon-polariton pulse at the fused silica-gold interface is shown in Fig. 1. Here the third-order nonlinearity only of gold is taking into account. The variable tau is the "running time", and tau equal zero corresponds to the top of the surface plasmon-polariton pulse excited by an ultrashort light pulse.

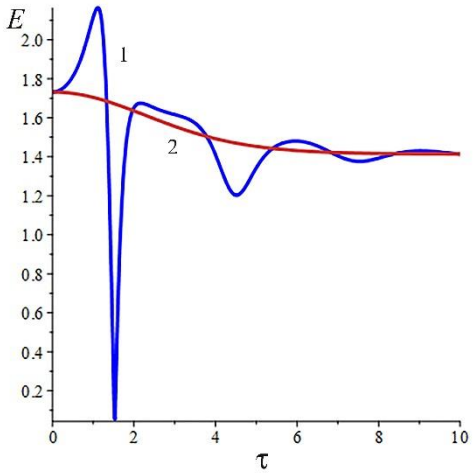

Fig. 1. Envelope of the electric field of surface plasmon-polariton pulse: curve 1 - wavelength $\lambda = 500$ nm; curve 2 - wavelength $\lambda = 633$ nm in air. Arbitrary units.

The properties of nonlinear plasmon-polariton waves depend on the parameters of the exciting electromagnetic signals, on the geometry and parameters of the media in which the plasmon-polaritons are excited. The parameters of plasmon-polariton waves in plasmon waveguides, which have composite structures as dielectric-metal-dielectric or metal-dielectric-metal, are determined by the parameters of the waveguide and the power of electromagnetic signal that excites plasmon-polaritons [4].

The studying of linear and nonlinear processes during the propagation and interaction of the surface plasmon-polaritons in waveguide structures of various configurations and the design of plasmonic nanodevices operating at optical frequencies on their basis is one of the most promising directions in the field of modern plasmonics.

The work is supported by the Russian Science Foundation grant No. 19-72-20154.

References

[1] S.A. Maier, Plasmonics: Fundamental and Applications (New York: Springer, 2007).
[2] A. Marini, M. Conforti, G. Della Valle, H.W. Lee, Tr.X. Tran, W. Chang, M.A. Schmidt, S. Longhi, P. St. J. Russell, F. Biancalana, New J. Phys., **15**, 013033 (2013).
[3] I.V. Dzedolik, Solitons and nonlinear waves of phonon-polaritons and plasmon-polaritons (New York: Nova Science Publishers, 2016).
[4] I.V. Dzedolik, A.Yu. Leksin, J. Opt., **22**(7), 075001 (2020).

Surface plasmon polaritons in a hybrid layered structure based on graphene and phase change material

Kharitonova O.G.[1], Bychkov I.V.[1], Shavrov V.G.[2], Kuzmin D.A.[1]

[1] *Chelyabinsk State University, Chelyabinsk 454001, Russian Federation*
[2]*Kotelnikov Institute of Radioengineering and Electronics of Russian Academy of Sciences, 125009, Moscow, Russia*

In this work, we theoretically investigate surface plasmon polaritons (SPPs) in a hybrid layered structure based on graphene and material with phase transition (VO_2).

Plasmons possess appealing properties for photonic technologies and promises a new generation of highly miniaturized photonic devices [1]. Graphene is one of the materials, that supports highly restricted propagating SPPs in a wide spectral range. Graphene is a unique plasmonic material [2-4]. Its optical properties can be controlled by external parameters such as electrostatic bias, magnetic field or chemical doping. Thus, it is possible to vary the electrodynamic properties of graphene can be varied from highly conductive to dielectric. In recent years, the interaction of graphene-based layered structures with the electromagnetic field of has been actively studied.

Phase change materials are paving the way towards improved functionality of metamaterials. Vanadium dioxide (VO_2) with the phase transition near-room-temperature (340 K) is an appealing candidate as an active component in metamaterials because its phase transition temperature (340 K) can be easily accessed. Also high-quality thin films are available [5].

Our hybrid layered structure consists of three layers: a graphene, a graphene layer, a dielectric layer of thickness *d* and vanadium dioxide VO_2 (Fig. 1).

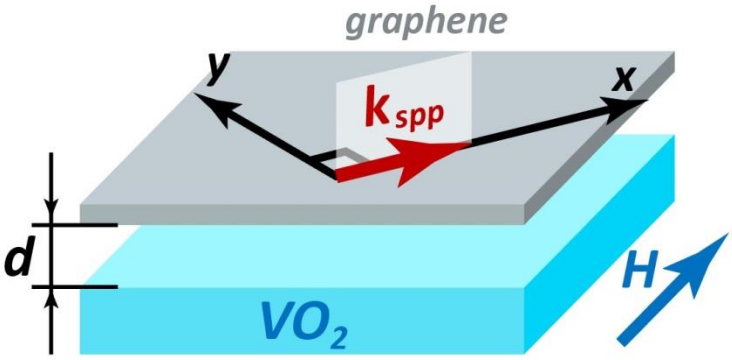

Fig. 1. A hybrid layered structure based on graphene and phase change material (VO_2)

To find SPP in this structure, we solved the dispersion equation, which was got from Maxwell's equations with applying of the boundary conditions at each of the interfaces. In the calculations, it was assumed that VO_2 is in the conducting phase, the thickness of the dielectric gap is d = 50 nm, and the dielectric constant of the gap is ε_d = 2. Results of calculation are shown on Fig 2.

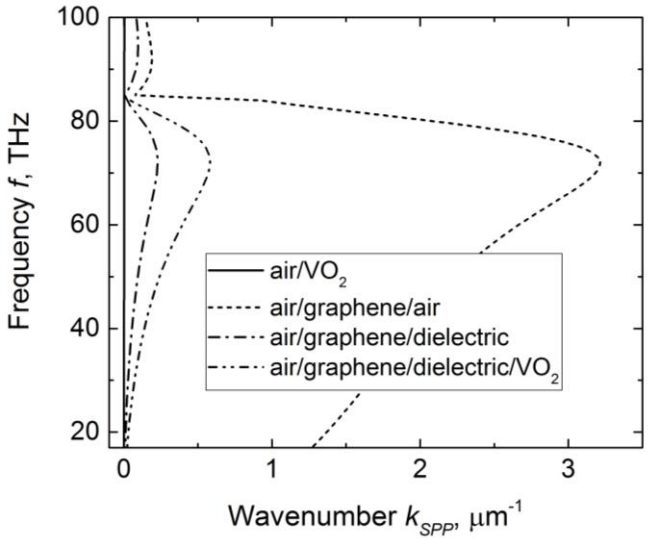

Fig. 2. Dispersion characteristics of SPPs propagating along air/VO_2, air/graphene/air, air/graphene/dielectric and air/graphene/dielectric/VO_2 nanostructures.

It can be noted that no significant localization of electromagnetic energy occurs at the air/VO_2 interface in the considered frequency range. The graphene layer maintains well-localized SPPs at frequencies near 70 THz. The combination of graphene and VO_2 into one structure leads to a significant increase in the localization of light near the graphene layer.

This work was supported by the Russian Foundation for Basic Research (grants No. 20-37-70038, 19-07-00246, 20-47-740004), the Russian Science Foundation (grant No. 20-19-00745). Numerical calculations were performed with the support of the Ministry of Science and Higher Education of the Russian Federation within the framework of the state assignment project No. 075-00992-21-00.

References

[1] A. Polman, Plasmonics Applied, Science 322, 868-869 (2008)
[2] F.J.G. de Abajo, Graphene plasmonics: challenges and opportunities, ACS Photonics 1, 135 (2014)
[3] P-Y Chen, Ch. Argyropoulos, M. Farhat and J. S. Gomez-Diaz, Flatland plasmonics and nanophotonics based on graphene and beyond, Nanophotonics 6(6), 1239–1262 (2017)
[4] D. A. Kuzmin, I. V. Bychkov, V. G. Shavrov and V. V. Temnov, Plasmonics of magnetic and topological graphene-based nanostructures, Nanophotonics 7(3), 597-611 (2018)
[5] C. V. S. Kumar, F. Maury and N. Bahlawane. Vanadium Oxide as a Key Constituent in Reconfigurable Metamaterials, Metamaterials and Metasurfaces. 151 (2018)

Excitation of surface plasmon polaritons in the vanadium dioxide-silicon dioxide-hyperbolic metasurface structure.

Usik M.O.[1], Kuzmin D.A.[1], Bychkov I.V.[1], Shavrov V.G.[2]

[1]Chelyabinsk State University, 454001, Chelyabinsk, Russia
[2]Kotelnikov Institute of Radioengineering and Electronics of Russian Academy of Sciences, 125009, Moscow, Russia

In this paper, we studied the excitation of surface plasmon polaritons in the vanadium dioxide-silicon dioxide-hyperbolic metasurface structure. Since the influence of phase transitions on the excitation pattern of surface plasmons is of particular interest, vanadium dioxide was taken as one of the layers, since its phase transition from the dielectric state to the metallic state occurs at temperatures close to room [1].

A lattice of graphene strips was taken as a hyperbolic metasurface [2]. Such a surface is capable of supporting the propagation of both TM and TE-polarized plasmons.

When taking into account the phase transition of vanadium dioxide, we took the already known data on the behavior of vanadium dioxide and performed a linear approximation, using the Drude theory [3], which allowed us to obtain a model that is quite simple to describe. As can be seen from Figure 1 the phase transition is not instantaneous and the behavior of vanadium dioxide depending on the temperature can be divided into four stages: 1) up to 337 K; 2) from 337 K to 346 K; 3) from 346 K to 352 K; 4) from 352 K.

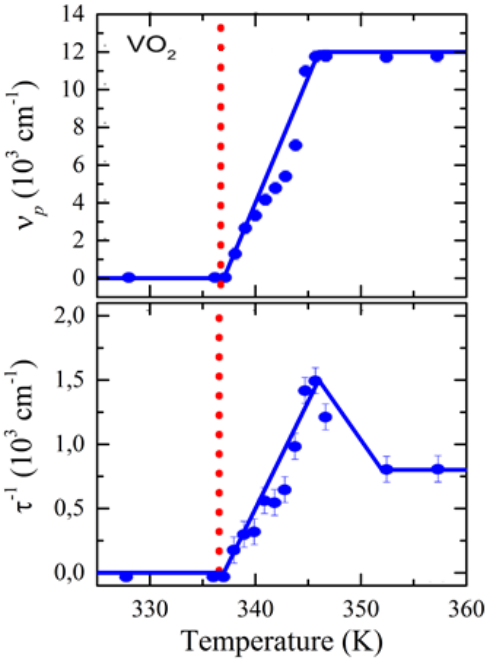

Fig. 1. The behavior of vanadium dioxide during the phase transition.

When studying the excitation of surface plasmon-polaritons, the method of total internal reflection in the Otto geometry was used. When the angle of incidence is greater than the angle of total internal reflection, using Maxwell's equations and the corresponding boundary conditions, it is possible to calculate the reflection coefficient, by which it is possible to judge how much of the energy of the incident radiation has gone into the excitation of surface plasmons [4].

By setting the parameters at which the surface plasmons are excited in the absence of a layer of vanadium dioxide, we calculated the reflection coefficient of the system as a function of frequency for different temperatures.

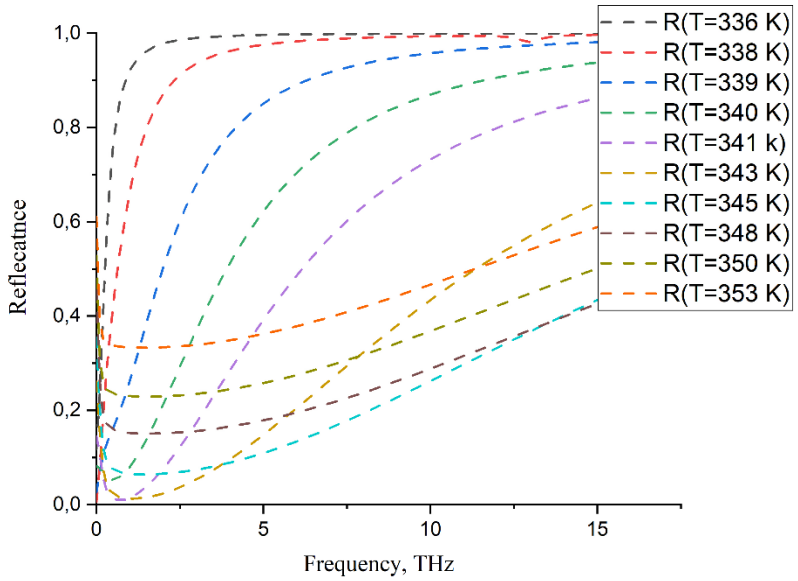

Fig. 2. The reflection coefficient of the structure at different temperatures.

We believe that our research can help to study the behavior of surface plasmons in systems with variable parameters, and also opens up new possibilities for controlling electromagnetic radiation at the nanoscale.

This work was supported by the Russian Foundation for Basic Research (grants No. 20-37-70038, 19-07-00246, 20-47-740004), the Russian Science Foundation (grant No. 20-19-00745). Numerical calculations were performed with the support of the Ministry of Science and Higher Education of the Russian Federation within the framework of the state assignment project No. 075-00992-21-00.

References

[1] Tobias Peterseim, Martin Dressel, Marc Dietrich and Angelika Polity, Optical properties of VO_2 films at the phase transition: Influence of substrate and electronic correlations, Journal of Applied Physics 120, 075102 (2016).

[2] J. Sebastian Gomez-Diaz, Mykhailo Tymchenko, and Andrea Alù, Hyperbolic Plasmons and Topological Transitions Over Uniaxial Metasurfaces, Physical Review Letters, PRL 114, 2015

[3] Masato Tazawa, Ping Jin, and Sakae Tanemura, Optical constants of $V_{1-x}W_xO_2$ films, APPLIED OPTICS, 1 April 1998, Vol. 37, No. 10

[4] Maksim O. Usik, Igor V. Bychkov, Vladimir G. Shavrov, and Dmitry A. Kuzmin, Surface plasmon-polaritons in deformed graphene excited by attenuated total internal reflection, Open Material Science, 2019, 5:7–11.

MOD-made bismuth-substituted yttrium iron garnet and oxides for 1D magnetophotonic crystals

Efremova S.L.[1,2], Salatov A.V.[1,3], Kulikova D.P.[1,2], Kasyanov A.A.[1], Bykov I.V.[1,4], Afanasiev K.N.[1,4], Tananaev P.N.[1], Baryshev A.V.[1]

[1]Dukhov Automatics Research Institute (VNIIA), 127055, Moscow, Russia
[2]Lomonosov Moscow State University, 119991, Moscow, Russia
[3]D. Mendeleev University of Chemical Technology of Russia, 125047, Moscow, Russia
[4]Institute for Theoretical and Applied Electromagnetics of RAS, 125412, Moscow, Russia

Photonic crystals (PCs)–the dielectric structures with spatial modulation of refractive index–are widely used in fundamental and applied research since the light propagation in it can be modified by tuning the physical and optical properties of layers consisting PC. PC's remarkable extensions are magnetophotonic crystals (MPCs) [1]. Studies on MPCs are motivated by fundamental and practical interest to enhancing magneto-optical (MO) responses of existing MO materials and possibilities of controlling the flow of light by external magnetic fields [2].

The main aim of our work was to fabricate high-quality 1D MPC with the microcavity structure–MO material was sandwiched between two Bragg mirrors (BM). The MO material in our study was bismuth-substituted yttrium iron garnet (Bi:YIG) manufactured by metal-organic decomposition (MOD) method. For this fabrication approach thermal annealing at 750 °C in air is essential for garnet crystallization. The surface of obtained Bi:YIG samples had granular structure with typical roughness RMS = 3 nm. The XRD pattern of the fabricated proves successful crystallization. Dielectric constants of the fabricated Bi:YIG are in a good agreement with referenced data from [3] and [4].

There is an unavoidable limitation since the first Bragg mirror is annealed simultaneously with the Bi:YIG on it. Therefore, annealing-induced modification of BM affects the structural and optical properties of the final resonator. This is why it is important to note the main features of oxides happening upon their annealing for the fabrication of high-quality MPC.

The BM samples under our study were multilayers $(ZrO_2/SiO_2)^7$, $(HfO_2/SiO_2)^8$ and $(Ta_2O_5/SiO_2)^7$ deposited on quartz substrates by electron beam sputtering. The surface of the $(Ta_2O_5/SiO_2)^7$ sample became grainy because of Ta_2O_5 crystallization, $(HfO_2/SiO_2)^8$ cracked producing areas with dimensions on micron scale. As for $(ZrO_2/SiO_2)^7$ samples, their surface structure and transmissivity didn't undergo significant changes after the annealing.

For all the fabricated BM, annealing of them at 750 °C was accompanied by a spectral shift of their stopband to the shorter wavelength range. Since the photonic stopband wavelength λ_0 is proportional to refractive indices n and thicknesses d of oxide layers, $\Delta\lambda$ can be interpreted as the change in the mentioned parameters upon annealing. To confirm this and to take it into account during MPC fabrication process, an analysis of modification of thicknesses and dielectric constants of single layers ZrO_2 and SiO_2 was carried out.

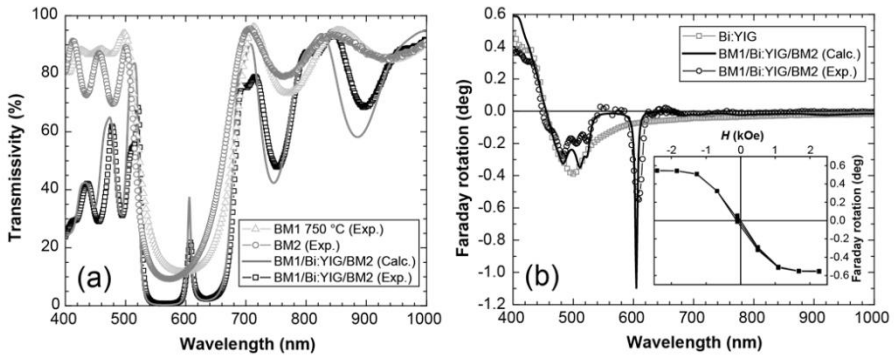

(a) Transmission spectra of BM 1 annealed at 750 °C for 45 minutes, as-deposited BM 2 and fabricated MPC ($(ZrO_2/SiO_2)^7$/Bi:YIG/$(ZrO_2/SiO_2)^7$); the calculated spectrum is given by a solid line. (b) Angle of Faraday rotation of the single Bi:YIG film (squares) and MPC; measured and calculated dependencies for MPC are shown as circles and a solid line, respectively. Inset illustrates a hysteresis curve of Faraday rotation for MPC.

After summarizing of the obtained data, we chose ZrO_2/SiO_2 pair for BM and fabricated 1D MPC with the following structure: $(ZrO_2/SiO_2)^7$/Bi:YIG/$(SiO_2/ZrO_2)^7$. It is worth noting that the second BM deposited on the crystallized Bi:YIG layer should have the same optical properties as the first annealed BM. Transmission spectra of the first and second BM $(ZrO_2/SiO_2)^7$ and the resulting MPC are shown in plot (a). Magneto-optical spectra of fabricated Bi:YIG film and the 1D MPC are demonstrated in plot (b). One can see that the Faraday rotation increased by an order of magnitude at a wavelength of the Fabry-Perot resonance.

References

[1] M. Inoue, M. Levy, A.V. Baryshev, Magnetophotonics: from theory to applications (Springer, 2013).

[2] S. Kharratian, H. Urey, and M.C. Onbaşlı, Sci. Rep. 9, 644 (2019).

[3] S.H. Wemple, S.L. Blank, J.A. Seman, and W.A. Biolsi, Phys. Rev. B 9, 2134 (1974).

[4] S. Wittekoek, T. J. A. Poprna, J. M. Robertson, and P.F. Bongers, Phys. Rev. B 12, 2777–2788 (1975).

Structural, optical and magneto-optical properties of binary $NiFeO_x$/Pt nanofilm for hydrogen detection

Kulikova D.P., Efremova S.L. [1,2], Afanasyev K.N.[1,3], Bykov I.V.[1,3], Baryshev A.V.[1]

[1]*Dukhov Automatics Research Institute (VNIIA), 127055, Moscow, Russia*
[2]*Faculty of Physics, Moscow State University, 119991, Moscow, Russia*
[3]*Institute for Theoretical and Applied Electromagnetics RAS, 125412, Moscow, Russia*

Magneto-optical materials are of interest due to possibility for monitoring changes in the polarization state and intensity via transformation in magnetic properties upon their interaction with hydrogen [1]. In our recent work [2], we demonstrated that oxidized permalloy ($NiFeO_x$) nanofilms showed a significant growth of the Faraday rotation angle (and the figure of merit, FOM) in the near-infrared range since they were compositions of various magnetic oxides (see the figure). The nanofilms were covered by a thin Pt layer and the $NiFeO_x$/Pt bilayer was tested as the magneto-optical sensing element. It was found that the magnitude of the Faraday rotation changed significantly in the presence of H_2. Another finding was a transformation in the spectrum of the Faraday rotation of $NiFeO_x$ nanofilms due to the Pt layer.

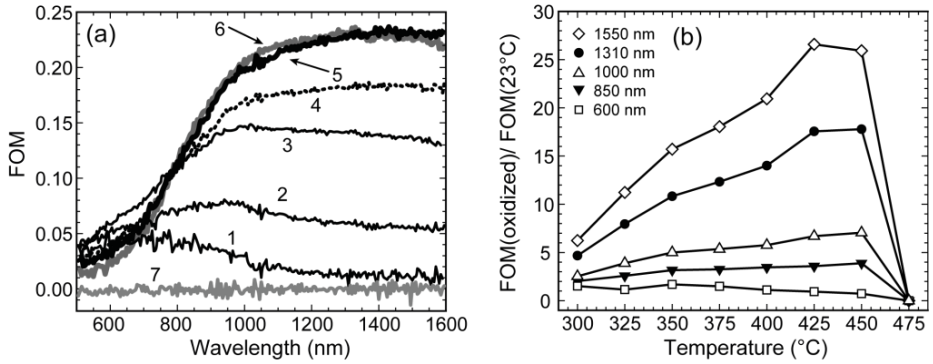

(a) Changes in FOM = $\theta_F\sqrt{T}$ for the nanofilms: initial permalloy nanofilm (curve 1) and oxidized ones during annealing for one hour at the series of temperatures (curves 2-7 correspond to 300, 350, 400, 425, 450 and 475°C, respectively). (b) Normalized FOM for selected wavelengths versus the oxidation temperature.

Magneto-optical sensing elements and, in particular, $NiFeO_x$ are promising materials for the further development of optical and magneto-optical hydrogen gas sensors. The nonreciprocal magneto-optical effects make it possible to accumulate the polarization rotation in the multipass regime. In perspective, this feature can provide much more high selectivity to a target gas and more robust sensing platform.

References

[1] P.-C. Chang, Y.-Y. Chang, W.-H. Wang et al., *Commun. Chem.* 2:89 (2019).
[2] D.P. Kulikova et al., Opt. Mater. 107, 110067 (2020).

Magneto-Optical Response Enhancement by Surface Plasmon-Polariton Resonance in GGG/IGEF/Au Structure

Basiladze G.D., Tomilin S.V., Berzhansky V.N.

Institute of Physics and Technology, V.I. Vernadsky Crimean Federal University, Vernadsky avenue, 4, Simferopol, 295007, Russia

Magneto-plasmonic structures based on dielectric magnetic films are of interest with the possibility of their use as magnetically controlled light modulators and sensors [1, 2]. An increase in the efficiency of such devices is achieved by enhancing the plasmonic and magneto-optical (MO) properties of the main functional materials [3].

This report presents the results of experiments to study the influence of surface plasmon-polariton resonance (SPPR) on the enhancement of the MO response in a magneto-plasmonic structure. This structure was created based on an 11 μm thick iron-garnet epitaxial film (IGEF) on a 500 μm thick $Gd_3Ga_5O_{12}$ (GGG) single crystal substrate with a (111) surface orientation. The IGEF surface was coated with a plasmonic gold (Au) film with a thickness of 38 nm. The general structure of the sample can be represented by the formula GGG(500 μm)/IGEF(11 μm)/Au(38 nm).

The IGEF was obtained by liquid-phase epitaxy and has the composition $(Bi,Lu)_3(Fe,Ga)_5O_{12}$. IGEF has an "easy-plane" magnetic anisotropy with a saturation field in the plane along the hard magnetization axis (HMA) – 12 Oe, along the easy magnetization axis (EMA) – 1.5 Oe, and in the direction normal to the film plane – 1500 Oe. The specific Faraday rotation was 1 deg/μm at λ = 640 nm. Plasmonic Au coating was synthesized by thermal deposition of gold (95.83 %) in vacuum ($P \leq 6 \times 10^{-4}$ Pa).

The excitation of the SPPR was carried out using a prismatic input according to the Kretschman scheme. The structure was located on the hypotenuse face of an isosceles triangular prism ($n_{prism} \approx 1.51$ at λ = 640 nm) using an immersion liquid for optical contact ($n_{im} \approx 1.47$ at λ = 640 nm). The IGEF is oriented so that the HMA is perpendicular to the plane of the light incidence, and the EMA is parallel to the projection of the light wave vector $\boldsymbol{k}$ onto the IGEF plane. In the IGEF plane along the HMA, a constant external magnetic field with strength ≥ 25 Oe was acted to remove the remanent magnetization of IGEF in the EMA direction. The Faraday effect was measured when the IGEF was magnetized by an external magnetic field, which was applied in the IGEF plane along the EMA ‖ $\boldsymbol{k}$.

Fig. 1 show the angular dependences of the intensity of reflected p-polarized beams I_{RP} with wavelength 640 nm and 1550 nm. The exciting radiation was a linearly polarized laser beam (ø ≈ 2 mm), which was focused on the structure by a lens ($D = 5$ m^{-1}).

As can see in fig. 1 the absorption of light with λ = 640 nm occurs in a rather wide angular range (approximately 45 – 65 deg), while the periodic oscillations of the intensity are observed, which associated with the interference of rays reflected from the lower and upper boundaries of the IGEF layer (excitation of waveguide modes). The period of these oscillations can change with a change in the wavelength of light or thickness of the IGEF, which can be seen in Fig. 1 by the example of the resonance curve measured for λ = 1550 nm.

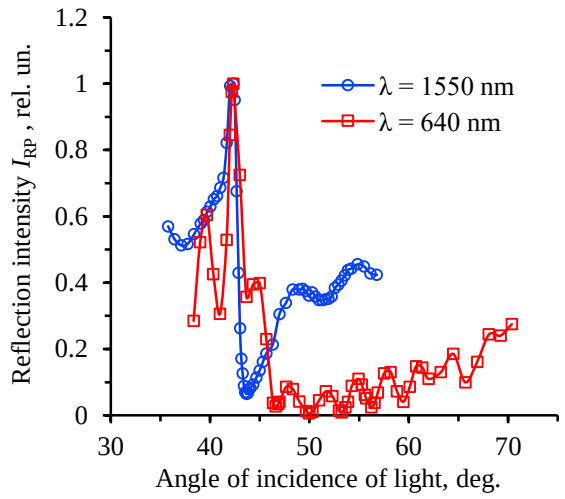

Fig. 1. Angular dependences of reflection of p-polarized beams with λ = 640 nm and λ = 1550 nm

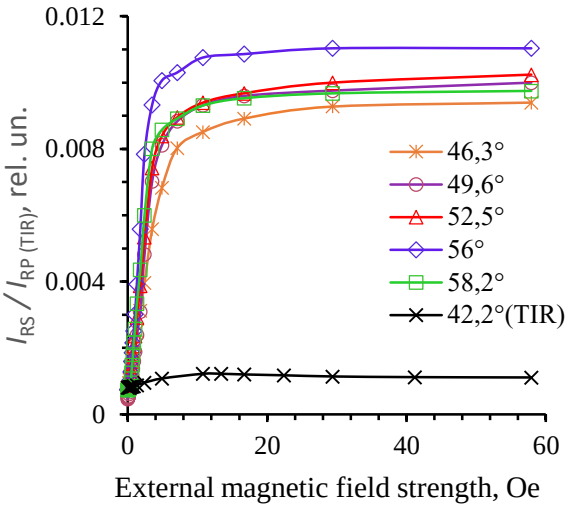

Fig. 2. Magnetic field dependences of MO response at different angles of light incidence (λ=640 nm)

Figure 2 shows the field dependence of the intensity of the s-polarized component of the reflected light I_{RS} normalized to the intensity of the p-polarized component reflected at the total internal reflection (TIR) angle $I_{RP\ (TIR)}$ (wavelength λ = 640 nm, the angle of beam incidence is indicated in the legend, external magnetic field is applied along the EMA). Fig. 2 shows that an increase in the external field leads to an increase in I_{RS} up to 10 Oe. At a field strength of more than 10 Oe, the IGEF film is magnetized to saturation and the I_{RS} signal takes on a constant value. It is clearly seen that the MO response at the angles of SPPR excitation is 10 times higher than that at the TIR angle, where is no plasmon resonance.

So, it has been shown that the magnitude of the MO response in the magneto-plasmonic structure GGG(500 μm)/IGEF(11 μm)/Au(38 nm) increases by an order of magnitude upon the condition of excitation of SPPR. This effect is found in a wide range of angles of the exciting radiation incidence, which makes it possible to simplify the alignment of the structure at the resonance angle and allows to use it in systems with non-collimated beams of exciting light, for example, beams which are formed at the exit from an optical fiber.

The work was carried out with the financial support of the Russian Science Foundation grant No. 19-72-20154.

References

[1] K. J. Chau, S. E. Irvine, A. Y. Elezzabi, IEEE J. Quant. Electron, 40 (5), 571 (2004).

[2] Basiladze G.D., Dolgov A.I., Shaposhnikov A.N., Berzhansky V.N. Waveguide phase-sensitive plasmonic sensor based on ferrite-garnet film // XVIII International Conference «Electromechanics, Electrotechnology, Electromaterials and Components» Proceedings of ICEEE-2020, 21-25 September 2020. – M.: Znak, 2020. – P. 297-302.

[3] Z.-C. Wu, E. T. Arakawa, T. Inagaki, and T. Thundat, Phys. Rev. B, 49 (11), 7782 (1993).

Excitation of different modes in magneto-photonic crystal with plasmonic subsystem

Tomilina O.A., Berzhansky V.N., Tomilin S.V.

Physics and technology institute, V.I. Vernadsky Crimean Federal University, Vernadsky avenue, 4, Simferopol, Russia

Photonic and magneto-photonic crystals (MPC) are very perspective materials in modern sectors of science and technology, such as photonics, optics, sensorics, spintronics, magnonics, quantum technologies, etc. One of the ways to modified the properties of magneto-photonic crystals is to integrate a plasmonic subsystem into (onto) the crystal [1].

The investigated magneto-photonic(plasmonic) crystal (Fig. 1,a inset) is consisting of a Bragg mirror (4 pairs of TiO_2/SiO_2 layers), a magneto-optical layer of bismuth substituted iron-garnet $Bi_{1.0}Y_{0.5}Gd_{1.5}Fe_{4.2}Al_{0.8}O_{12}$, a buffer SiO_2 layer with a gradient of thickness, and plasmonic subsystem. Plasmonic subsystem is the layer of self-assembled gold nanoparticles (Fig. 1,b inset). Fig. 1,a,b is demonstrate the spectra of transmittance and the spectra of Faraday rotation for MPC in different areas of thickness gradient of SiO_2 buffer layer.

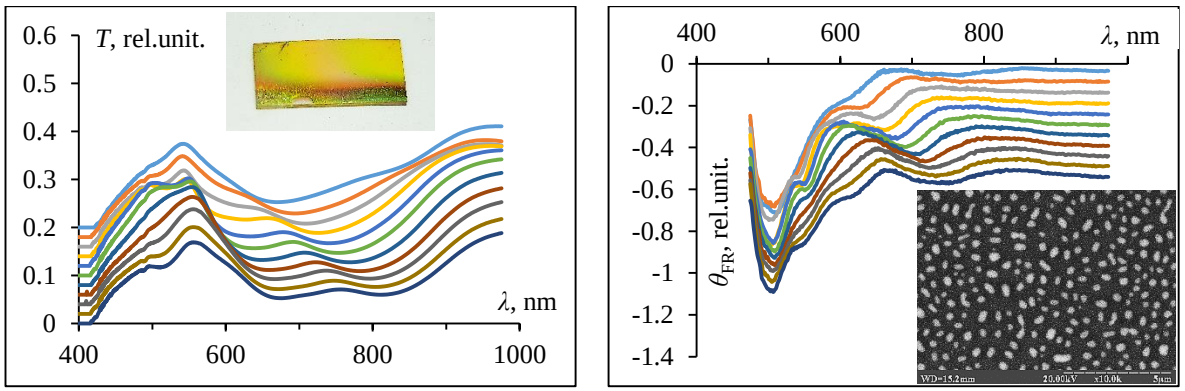

a b

Fig. 1. The magneto-optical properties of MPC with plasmonic subsystem in different areas of thickness gradient of SiO_2 buffer layer: a – the transmittance spectra (inset photo of the sample), b – the spectra of Faraday rotation (inset SEM-image of plasmonic subsystem).

As can see in Fig. 1,a in photonic band gap the peak of plasmonic resonance is presents and his position is determined by thickness h_{SiO2} of SiO_2 buffer layer (the top curve is conform to h_{SiO2} = 100 nm, the bottom curve is conform to h_{SiO2} = 300 nm). As can see in Fig. 1,b the plasmonic subsystem leads to enhancement of Faraday rotation on the wavelength of plasmonic resonance.

The work was carried out with the financial support of the Russian Science Foundation grant No. 19-72-20154.

References

[1] T.V. Mikhailova, A.N. Shaposhnikov, S.V. Tomilin, D.V. Alentiev, J. of Phys. Conf. Ser., 1410, 012163 (2019).

High sensitive THz detector based on monolayer of WSe2 with plasmonic amplification

Zaynullin F.A.[1], Gorbatova A.V.[1], Lavrov S.D.[1]

[1]*MIREA - Russian Technological University, Moscow, Russia*

Study of interaction of THz radiation with graphene-like materials based on transition metal dichalcogenides attracts a large number of scientific teams. This is primarily due to the potential use of these materials in flexible optoelectronic devices in the visible and terahertz range[1,2]. However, there is a problem associated with the small absorption of laser radiation in the monolayer. One way to solve this problem is to use a plasmonic structure[3]. In this work we analyze the parameters of terahertz field detection by an antenna based on a monolayer film of tungsten diselenide with a plasmonic structure. The detection of terahertz radiation by the experimental antenna was investigated by time-resolved terahertz spectroscopy. The monolayer tungsten diselenide substrate was obtained by chemical vapor deposition. The electrodes and the plasmonic structure were deposited by electron beam lithography.

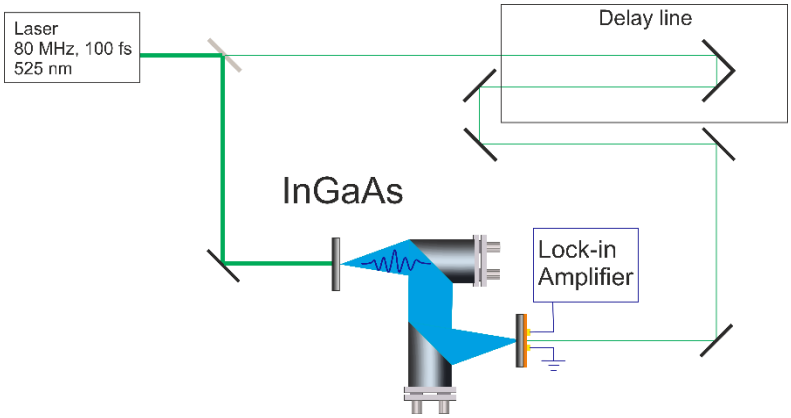

Figure 3. Scheme of experiment setup.

Femtosecond laser with pulse duration of 100 fs, pulse repetition rate of 82 MHz, 1050 nm wavelength, and frequency doubler at the output was used as a source of femtosecond laser radiation. Temporal waveform and spectrum of THz pulse were received, the bandwidth of the studied antenna was estimated. The characteristics of the manufactured THz detectors (signal-to-noise ratio, sensitivity) were obtained. The effect of plasmonic arrays in the gap between the electrodes on detected THz signal was shown.

This work was supported by the Ministry of Education and Science of the Russian Federation (state task No. FSFZ-0706-2020-0022) and. Russian science foundation No 19-72-10165

References

[1] T. Basu, A. Banerjee, S. Vajandar, Ter. Biom. and Heal. Tech., P. 75-87(2020)
[2] L.Viti, A. Politano, M.S. Vitiello. APL Mater. AIP. Vol. 5, № 3. P. 35602(2017)
[3] Y. Salamin et al., Nat. Commun. Nature Research, 2019. Vol. 10, № 1.

Broadband enhancement of TMOKE in nanostructured bismuth-substituted iron-garnet films with hybrid localized and lattice modes

Ignatyeva D.O.[1,2,3], Zimnyakova P.E.[1], Karki D.[4], Voronov A.A.[1,3], Shaposhnikov A.N.[2], Berzhansky V.N.[2], Levy M.[4], Belotelov V.I.[1,2,3]

[1]*Faculty of Physics, M.V. Lomonosov Moscow State University, 119992, Moscow, Russia*
[2]*V.I. Vernadsky Crimean Federal University, 295007, Simferopol, Russia*
[3]*Russian Quantum Center, 121205, Moscow, Russia*
[4]*Physics Department, Michigan Technological University, 49931, Houghton, USA*

The transverse magneto-optical Kerr effect reveals itself as the modulation of the transmitted or reflected light intensity in magnetized materials. It is essential for probing of the in-plane magnetization component, however its magnitude is below 10^{-4} for the smooth iron-garnet films. Recent studies showed that TMOKE can be enhanced by the guided mode excitation [1-3], however the enhancement takes place in a very narrow wavelength and angular range.

We propose a novel type of the two-dimensional arrays of cylinders made of bismuth-substituted iron-garnet that support both localized (Fabri-Perrot-like) and lattice (guided-like) modes. In such a structure, TMOKE is enhanced in the a wide range and exceeds 2% for the angles from 5 to 25 degrees (Fig.1). The angular width of the TMOKE resonance is 50 nm.

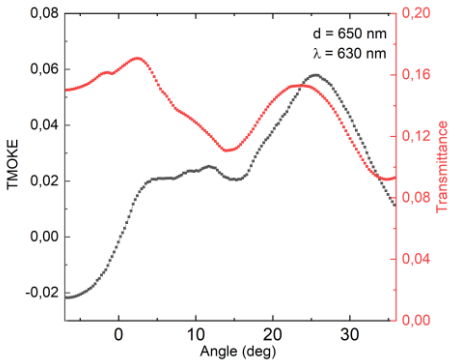

Fig. 1. Angular dependance of the TMOKE for the wavelength λ = 840 nm in structure with the diameter of cylinders 650 nm

The broadband enhancement of the TMOKE makes the proposed structures interesting for applications with ultrashort and tightly-focused laser pulses.

The research was supported by RSF (project No. 21-72-10020).

References

[1] A.A. Voronov et al., Optics Express 28(12), 17988 (2020).

[2] E. Gamet, E., Varghese, B., Verrier, I., and Royer, F. Journal of Physics D: Applied Physics, 50(49), 495105 (2017).

[3] Maksymov, I. S., Optics Express, 22(7), 8720-8725 (2014).

Reflection electron loss spectroscopy and electronic structure silicon dioxide

Parshin A.S.

Reshetnev Siberian State University of Science and Technology, 660037, Krasnoyarsk, Russia

Silicon dioxide (SiO_2) is widely used in the formation of plasmonic photovoltaic structures [1-3]. These structures have potential applications in biodiagnostics, sensing, bioimaging, solar cells and other devices, the operation of which is based on the phenomenon of localized surface plasmon resonance.

The SiO_2 layer of 93 nm thick was formed by thermal oxidation of Si(100) substrate. The reflection electron energy loss spectra (REELS) were obtained in the integral form using a SPECS spectrometer at incident electron energies E_0 of 300, 600, 1200, 1900, and 3000 eV in the electron energy loss range from 0 to 150 eV with a step of 0.1 eV. From the experimental REELS with the software package QUASES™ XS REELS [4] were calculated inelastic electron scattering cross section spectra which are products of inelastic mean free path λ and inelastic scattering cross-section $K(E_0, T)$, were T – energy loss.

To quantitatively estimate the contributions of different origins to the inelastic electron scattering cross section spectra and to reliably determine their energies, we approximated the spectra for SiO_2 by the three-parametric Lorentz-like Tougaard functions [5]:

$$\lambda K = \frac{BT}{(C - T^2)^2 + DT^2}$$

B, *C*, *D* are fitting parameters. The method of the inelastic electron scattering cross section spectra decomposition into the elementary peaks made it possible estimate the contributions of individual loss processes to the resultant spectrum silicon dioxide. The results obtained agree with the literature data on the electronic structure of silicon dioxide

References

[1] A. A. Semenova, A. P. Semenov, E. A. Goodilin, and I. A. Semenova, Bull. Rus. Acad. Sci. Phys. 83, 1415 (2019).
[2] H. Sun, M. Yu, G. Wang, X. Sun, and J. Lian, J. Phys. Chem. C 116, 9000 (2012).
[3] Y. Battie, A. Naciri, and M. Vergnat, J. Appl. Phys. 122, 213101 (2017).
[4] S. Tougaard, http://www.quases.com.
[5] S. Tougaard, Surf. Interface Anal. 25, 137 (1997).

Sensitivity enhancement of two-dimensional WSe_2-based photodetectors by ordered Ag plasmonic nanostructures

Guskov A.A.[1], Avdizhiyan A.Yu.[1], Lavrov S.D.[1], Galiev R.R.[2], Gorbatova A.V.[1]

[1]Department of Nanoelectronics, MIREA - Russian Technological University, 119454, Moscow, Russia
[2]V.G. Mokerov Institute of Ultra High Frequency Semiconductor Electronics of RAS, 117105, Moscow, Russia.

Two-dimensional (2D) semiconductors have recently been widely used as active elements in optoelectronic devices due to their special photoelectric properties [1]. However, the efficiency of such devices is limited by the small absorption of two-dimensional semiconductor films, which leads to a decrease in photosensitivity [2]. The most effective way to increase absorption in 2D materials is to increase the electric field by excitation of local plasmons [3-7]. However, most of the modern works demonstrate disordered plasmonic structures, in which the distribution of elements has a random character. This leads to broadening of the plasmon resonance spectra peaks and decreasing of their intensity [8,9]. In this work we report a multiple increase in photosensitivity of photodetectors based on two-dimensional semiconductor WSe2 due to ordered silver plasmonic structures.

References

[1] J. Kang, W. Cao, X. Xie, D. Sarkar, W. Liu, and K. Banerjee, Micro- and Nanotechnology Sensors, Systems, and Applications VI (2014).

[2] A.M. Gilbertson, Y. Francescato, T. Roschuk, V. Shautsova, Y. Chen, T.P.H. Sidiropoulos, M. Hong, V. Giannini, S.A. Maier, L.F. Cohen, and R.F. Oulton, Nano Lett. A 15, 3458 (2015).

[3] A. V. Gorbatova, D.I. Khusyainov, A.E. Yachmenev, R.A. Khabibullin, D.S. Ponomarev, A.M. Buryakov, and E.D. Mishina, Tech. Phys. Lett. A 46, 1111 (2020).

[4] L. Yu, D. Liu, X.-Z. Qi, X. Xiong, L.-T. Feng, M. Li, G.-P. Guo, G.-C. Guo, and X.-F. Ren, Chinese Phys. B A 27, 047302 (2018).

[5] A.D. Johnson, F. Cheng, Y. Tsai, and C.-K. Shih, Nano Lett. A 17, 4317 (2017).

[6] J. Guo, S. Li, Z. He, Y. Li, Z. Lei, Y. Liu, W. Huang, T. Gong, Q. Ai, L. Mao, Y. He, Y. Ke, S. Zhou, and B. Yu, Appl. Surf. Sci. A 483, 1037 (2019).

[7] Y. Li, J.G. DiStefano, A.A. Murthy, J.D. Cain, E.D. Hanson, Q. Li, F.C. Castro, X. Chen, and V.P. Dravid, ACS Nano A 11, 10321 (2017).

[8] V.G. Kravets, A. V. Kabashin, W.L. Barnes, and A.N. Grigorenko, Chem. Rev. A 118, 5912 (2018).

[9] Y. Nishijima, L. Rosa, and S. Juodkazis, Opt. Express A 20, 11466 (2012).

Effects of strain and structure defects on polaritonic excitations dispersion in non-ideal lattices of coupled microcavities containing quantum dots

Yu. Paladyan, S. Fedorov and V. Rumyantsev

Donetsk Institute for Physics and Engineering named after A.A. Galkin,
Donetsk 83114, Ukraine

Designing and utilization of novel materials for manufacturing of the sources of coherent irradiation is currently a vast interdisciplinary area, which spans various theoretical and fundamental aspects of laser physics, condensed matter physics, nanotechnology, chemistry as well information science [1]. Physical realization of corresponding devices requires the ability to manipulate the group velocity of propagation of electromagnetic pulses, which is accomplished by the use of the so-called polaritonic crystals [2]. The latter represent a particular type of photonic crystals featured by a strong coupling between quantum excitations in a medium (excitons) and optical fields.

We considered 1D polaritonic crystal as a topologically ordered systems – array of coupled microcavities containing quantum dots. It is of substantial interest to investigate electromagnetic excitations in a non-ideal one-dimensional microcavity lattice subjected to a uniform elastic stress described by the dielectric tensor $\hat{\varepsilon}$.

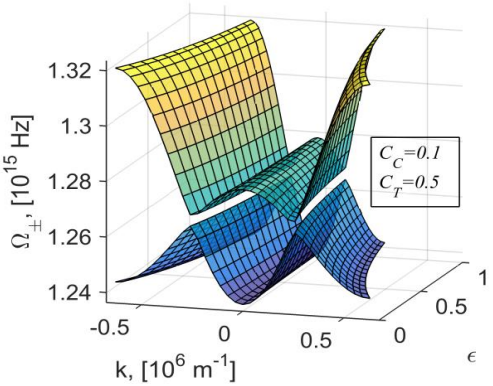

Fig. 1. Dispersion of polaritonic excitations in a one-sublattice quantum-dot-containing chain of unevenly spaced microcavities plotted

The presence of deformation and of structural defects may lead to an increase of the effective mass of corresponding excitations and therefore to a decrease of their group velocity. The results of numerical calculation performed on the basis of the constructed model contribute to modeling of the new class of functional materials – photonic crystalline system constituted of couple microcavities.

References

[1] P. Lodahl, S. Mahmoodian and S. Stobbe, Rev. Mod. Phys. 87, 347 (2015).

[2] V.V. Rumyantsev, S.A. Fedorov, K.V. Gumennyk, D.A. Gurov, A.V. Kavokin, Superlattices and Microstructures. 120, 642. (2018).

Iron-garnet films on various substrates for magnetoplasmonic structures

Mikhailova T.V.[1], Osmanov S.V.[1], Skorokhodov E.V.[2], Gusev S.A.[2], Lyashko S.D.[1], Karavainikov A.V.[1], Kudryashov A.L.[1], Nedviga A.S.[1], Milyukova E.T.[1], Semuk E.Yu.[1], Boyko V.O.[1], Linnik V.V[1], Berzhansky V.N.[1] and Shaposhnikov A.N.[1]

[1]V. I. Vernadsky Crimean Federal University, 295007, Simferopol, Russia
[2]Institute for Physics of Microstructures of the Russian Academy of Sciences (IPM RAS), 603087, Nizhny Novgorod, Russia

Investigations of various materials and nanostructures with a significant magneto-optical (MO) response is relevant in order to create new devices and systems for transmission and processing of information [1]. The effects observed in such materials and nanostructures (Faraday, Kerr and Cotton-Mouton Effects) make it possible to control lightwave by constant and alternating magnetic fields. The films of Bi-substituted iron garnets (Bi:IG) occupy a special place among MO materials. This work presents the results of investigations of structural parameters and MO properties of Bi:IG films, which are subsequently used to form one-dimensional and two-dimensional magnetoplasmonic structures.

The films of various compositions with nanoscale thickness were synthesized by vacuum sputtering and thermal annealing at air on substrates of monocrystalline gadolinium gallium garnet (GGG) with smooth or nanostructured surface and fused silica. Structuring of substrates for synthesis of samples was carried out using the equipment of Common Research Center «Physics and technology of micro- and nanostructures» of the IPM RAS.

The authors acknowledge support by Russian Science Foundation (project no. 19-72-20154) for research on crystallization dynamics of Bi:IG on GGG substrates with smooth and structured surface and the Ministry of Science and Higher Education of the Russian Federation (Megagrant project N 075-15-2019-1934) for optimization of magnetic parameters of films.

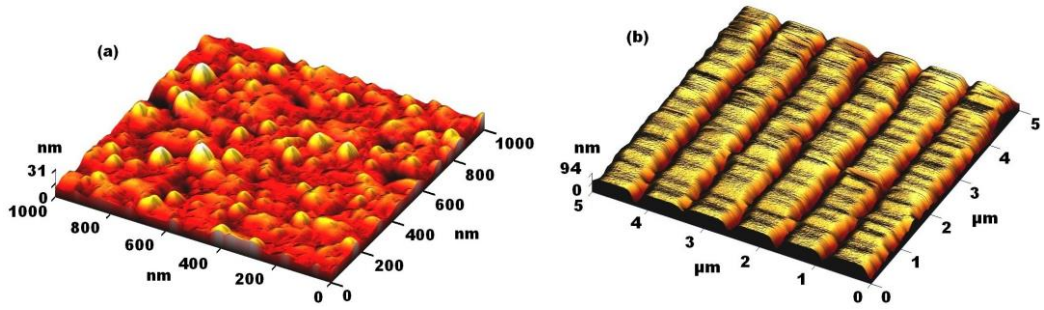

Fig. 1. Atomic force microscopy images of surfaces of Bi:IG film with average grains size of 75.5 nm and structured GGG substrate

References

[1] D.O. Ignatyeva, D. Karki, A.A. Voronov, M.A. Kozhaev, D.M. Krichevsky, A.I. Chernov, M. Levy, V.I. Belotelov, Nature communications 11, 1 (2020).

Composite (SiO_2-Au) films for magnetophotonics

Mikhailova T.V., Lyashko S.D., Osmanov S.V., Karavainikov A.V.,
Kudryashov A.L., Nedviga A.S., and Shaposhnikov A.N.

V. I. Vernadsky Crimean Federal University, 295007, Simferopol, Russia

Structuring opens up the possibility of localizing and amplifying the electromagnetic field of a light wave inside the magnetic components of 1D, 2D and 3D nanostructures (NS), thereby creating resonance features in optical and magneto-optical (MO) spectra. The use of metal and composite metal-dielectric components allows the transformation of properties due to excitation of propagating surface plasmon-polaritons and localized plasmons. It should be noted that the properties of NS based on composites with Au nanoparticles having a size less than 50 nm are not previously considered. At the moment, there are only theoretical works in which it is shown that two types of localized states are possible in structures based on composite (SiO_2-Ag) – Tamm states (Tamm plasmon-polaritons, TPP) and resonant defect modes [1].

The investigation presents the optical and structural properties of composite films (SiO_2-Au), model optical and MO spectra of NS with composite (SiO_2-Au) and magnetic iron garnet layers. The possibility of implementing configurations has been experimentally demonstrated. Figure 1 shows optical spectra and topology of composite films (a and b, respectively) and model spectra of Faraday Effect of a one of the configurations (c).

The authors acknowledge support by Russian Science Foundation (project no. 19-72-20154).

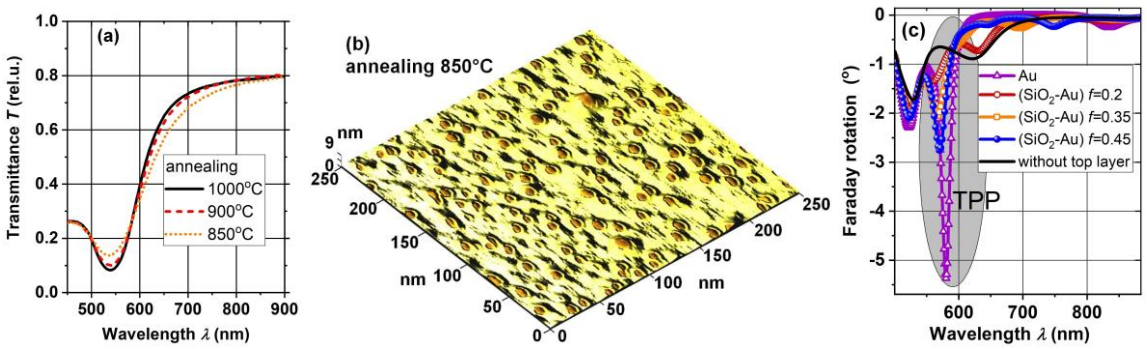

Fig. 1. Optical spectra (a) and topology (b) of (SiO_2-Au) films annealed at different temperature and simulated spectra of Faraday Effect (c) of configuration
$(TiO_2 / SiO_2)^4$ / YIG / Bi:YIG with top layers of Au, (SiO_2-Au) composite with different fractions of Au nanoparticles or without top layer

References

[1] R.G. Bikbaev, S.Y. Vetrov, I.V. Timofeev, Photonics 5, 22 (2018).

Garnet materials for nanophotonics: nanomechanical and Raman analysis

Mikhailova T.V.[1], Vysokikh Yu.E.[2], Krasnoborodko S.Yu.[2], Berzhansky V.N.[1], Shaposhnikov A.N.[1], Bulatov M.F.[2], Churikov D.V.[2]

[1]V. I. Vernadsky Crimean Federal University, 295007, Simferopol, Russia
[2]Scientific and Technological Centre of Unique Instrumentation of the RAS, Moscow, 117342, Russia

Iron garnet films is one of perspective material for magneto-plasmonic applications. It has high magneto-optical activity and might be modified by different process parameters to satisfy a particular requirement. It is important to understand how different process parameters will impact on surface and structure quality. Force-distance curves obtained by atomic-force microscopy tool might be used not only for topography imaging but also for structure characterization by evaluating such parameters as local stiffness, adhesion. Raman spectroscopy is a powerful method for structure investigation. This work presents results of structural characterization of iron garnet films by force-distance curves and Raman study.

The different compositions films deposited on various substrates (gadolinium gallium garnet and fused quartz) with nanoscale thickness were synthesized by vacuum sputtering and thermal annealing at air. Force-distance curves obtained from each sample are used to calculate topography, stiffness and adhesion maps. It is possible by analyzing tilt, forward and reverse steps length, sticking and other curves parameters. Raman spectra helps us understand internal structure symmetry and its changing caused by different process parameters.

The authors from V.I. Vernadsky Crimean Federal University TVM, ANSh, VNB acknowledge support by the Russian Ministry of Education and Science (Megagrant project N 075-15-2019-1934) for the synthesis of film samples. The authors from Scientific and Technological Centre of Unique Instrumentation of the RAS YuEV, SYuK, MFB, DVCh acknowledge support by the Ministry of Science and Higher Education of the Russian Federation under the State contract No. 0069-2019-0009 for the films measurements. This work was performed using the equipment of the Shared Research Facilities of the STC UI RAS.

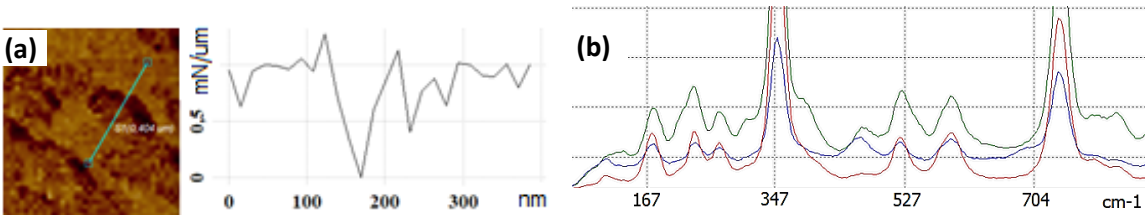

Fig. 1. Stiffness map of the bi-layer Bi-substituted iron garnet film (a), Raman spectra of GGG substrate – red, $Bi_{2.8}Y_{0.2}Fe_5O_{12}$ layer on GGG – blue, $Bi_{1.0}Lu_{0.5}Gd_{1.5}Fe_{4.2}Al_{0.8}O_{12}$ layer on GGG – green (b)

References

[1] Magnetophotonics (eds. Inoue M., Levy M., Baryshev A.; Springer, Berlin, Heidelberg, 2013).

Modulation of light by acoustically perturbed layered nanostructures

Knyazev G.A.[1,2], Sopko I.M.[1], Belotelov V.I.[1], Kapralov P.O.[2]

[1]*Lomonosov Moscow State University, 119992 Moscow, Russia*
[2] *Russian Quantum Center, 121205 Skolkovo, Russia*

Plasmon modes observed in the simplest structures such as dielectric-metal-dielectric or dielectric-dielectric-metal are characterized by a large width, which leads to a low efficiency of acousto-optic interaction [1,2]. At the same time, waveguide modes provide very narrow resonances, but the structure turns out to be rather complicated to fabricate. The use of photonic crystal layers makes it possible to find a compromise - to create a structure with long-range plasmons. In this structure, it is possible to obtain plasmon modes with a sufficiently high Q factor [3], providing a high level of the acousto-optical effect and at the same time making the structure simple for carrying out experimental studies. Moreover, the use of photonic crystal layers makes it possible to select the position of the resonant mode for a given wavelength.

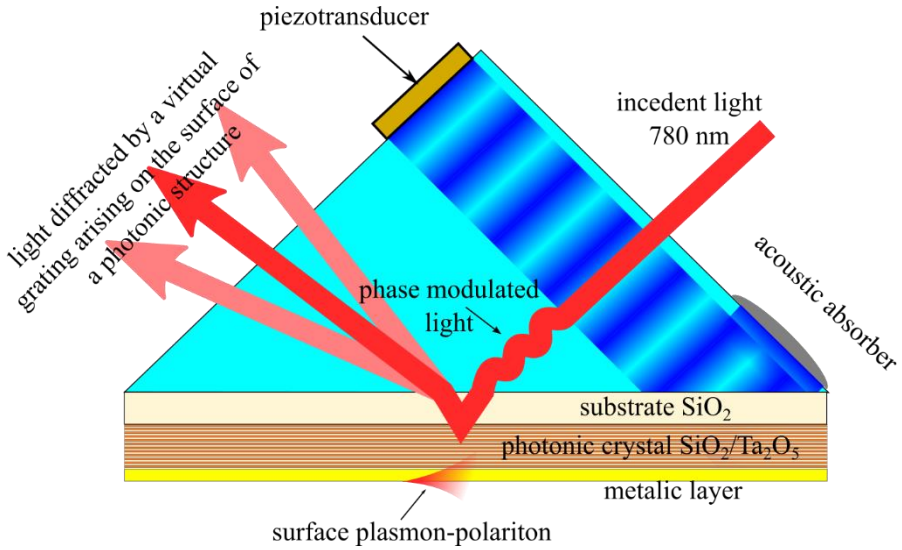

Fig. 1. Scheme of the experiment

The parameters of the photonic crystal were optimized for the realization of a long-range plasmon. The fabricated photonic crystal is deposited on a fused silica substrate by magnetron sputtering and contains 14 layers of tantalum pentoxide Ta_2O_5 with a thickness of 119 nm, alternating with layers of quartz SiO_2 with a thickness of 164 nm, and ending with an additional layer of Ta_2O_5 with a thickness of 108 nm. A thin film of cobalt 11 nm was deposited on a photonic crystal, on which gold was deposited 18 nm.

The experimentally measured angular reflection spectra for a number of wavelengths confirm the excitation of the long-range plasmon-polariton mode in both samples and agree well with the results of numerical simulations [4]. The plasmon resonance width was 0.1 °, and thus the resonance Q-factor was 400 at a wavelength of 780.1 nm. o measure the acoustic characteristics of the fabricated sample, an experiment was carried out (see Fig. 1), in which a uniform rocking of the front of a highly collimated beam, close in parameters to a plane wave, was carried out. photodetector aperture. As a result of the experiment, the modulation of the

intensity of the light reflected from the photonic structure was recorded. The measured characteristics of the modulation depth depending on the angle of incidence of light on the structure are shown in Fig. 2. The red line corresponds to the reflection coefficient of the photonic crystal structure. The maximum modulation value was 0.07 in the linear mode and 0.06 in the quadratic mode. The equivalent ultrasound power required to observe modulation at a frequency of 1 MHz was 0.6 W (the required power increases with decreasing frequency).

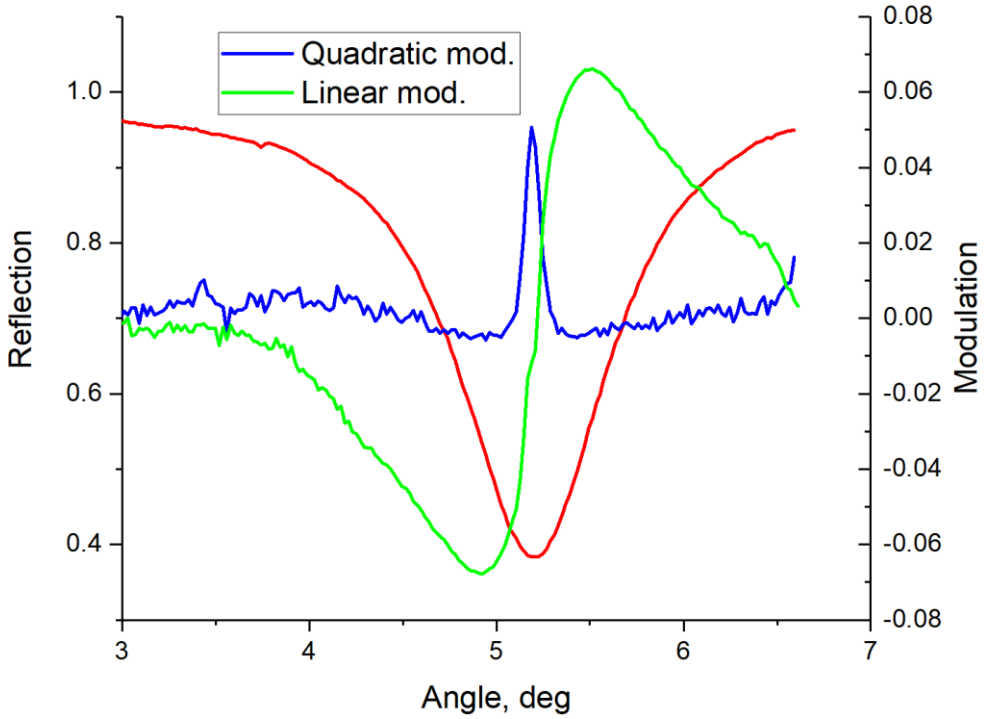

Fig. 2. Dependence of modulation coefficient on the angle of incidence

An increase in the frequency of ultrasound will lead to inhomogeneous modulation of the light field in space, which subsequently turns into diffraction.

References

[1] I.M. Sopko, D.O. Ignatyeva, G.A. Knyazev and V.I. Belotelov Phys. Rev. Appl. 13 3 (2020).

[2] I.M. Sopko and G.A. Knyazev, Appl. Opt. 57, C42 (2018).

[3] G.A. Knyazev, P. O. Kapralov, N. A. Gusev, A. N. Kalish, P. M. Vetoshko, S. A. Dagesyan, A. N. Shaposhnikov, A. R. Prokopov, V. N. Berzhansky, A. K. Zvezdin, and V. I. Belotelov, ACS Photonics 5, 4951(2018).

[4] D.O. Ignatyeva, P.O. Kapralov, G.A. Knyazev, S.K. Sekatskii, G.Dietler, M.Nur-E-Alam, M.Vasiliev, K.Alameh, and V. I. Belotelov, JETP Lett. 104, 679 (2016).

Section 4
Ultrafast Magnetism and Spin Dynamics

Spin dynamics in ferrimagnets near the angular momentum compensation point

Zvezdin A.K.[1], Gareeva Z.V.[2]

[1]*A1Prokhorov General Physics Institute, Russian Academy of Sciences, 119991, Moscow, Russia*
[2]*Institute of Molecule and Crystal Physics, Subdivision of the Ufa Federal Research Centre of the Russian Academy of Sciences, 450075, Ufa, Russia*

Ultrafast spin dynamics in antiferromagnets (AFMs) and ferrimagnets (FiMs) near compensation temperature are receiving much attention owing to the potential applications for spin electron devices [1]. Currently researches focus their efforts on the study of extremely fast domain walls (DWs) dynamics in AFMs whose velocities can attain V~20 km/s and in FiMs close to the compensation temperature with velocities up to V~5 km/s. The most favorable compounds to study the phenomena are transition metal rare earth FiMs (CoGd, GdFeCo, TbFeCo) whose magnetic sublattices have two compensation temperatures: the magnetization compensation temperature T_M and the angular momentum compensation temperature T_A.

In our work, we explore the DW dynamics excited by the spin – polarized current and driving magnetic field near the angular momentum compensation temperature of FiMs and focus the featured dynamic properties: DW speed, mobility, precession in the stationary and non – stationary regimes. The enhancement of the DW velocity in the vicinity of angular momentum compensation point at different values of driving magnetic field is shown in Fig. 1, here we use the parameters of GdFeCo.

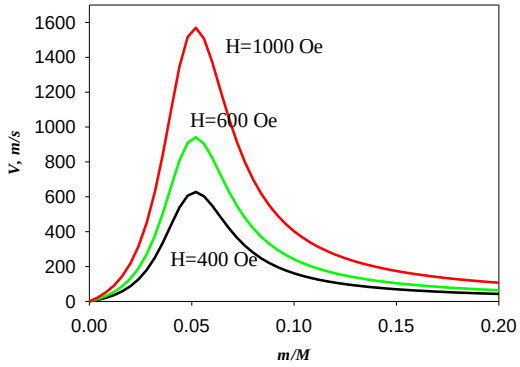

Fig.1. The dependence of the DW velocity of the non – steady motion on the net magnetization

We perform the analysis of steady motion and post Walker dynamics including analysis of specific features of Walker field, ultimate DW velocity, the precession in the non – stationary post – Walker regime. Our findings showed anomalous behaviour of DW dynamic properties near the angular momentum compensation point in ferrimagnets.

References

[1] K.-J Kim, S.K. Kim, Y. Hirata, S.H. Oh, T. Tono, D.H. Kim, T.Okuno,…, T.Ono, Nature Materials 16, 1187 (2017)

Spin wave resonances excited by inverse Faraday effect in magnetophotonic microcavity

Kozhaev M.A.[1,2], Krichevsky D.M.[1,2,3], Sylgacheva D.A.[1,4], Ozerov V.A.[1,2,3], Belkova A.V.[1,4], Evstigneeva S.A.[1,5], Pakhomov A.S.[3], Chernov A.I.[1,2,3], Polulyakh S.N.[2], Semuk E.Yu.[2], Berzhansky V.N.[2], Belotelov V.I.[1,2,4]

[1]Russian Quantum Center, 143025, Skolkovo, Moscow Region, Russia
[2]V.I. Vernadsky Crimean Federal University, 295007, Simferopol, Russia
[3]Moscow Institute of Physics and Technology (National Research University), 141700, Dolgoprudny, Russia
[4]Faculty of Physics, Lomonosov Moscow State University, 119991, Moscow, Russia
[5]National University of Science and Technology, MISiS, 119991, Moscow, Russia

Nowadays spin waves are of prime interest in context of data processing and spintronic applications [1-3]. This is due to the fact that spin waves can be used to transfer information with low heat-related losses, and the frequency of spin-based devices can be potentially reach THz range. Spin wave logic devices are currently being actively developed [3].

One of the prominent ways to excite and control spin waves is by inverse magnetooptical effects. Thus, inverse Faraday effect is when circularly polarized light pulse produces effective magnetic field at the moment of passing through magnetic media owing to stimulated Raman scattering. The possibility to use inverse Faraday effect to excite spin waves was first demonstrated in 2005 [4] and since then the optical nonthermal control of spin waves has been studied in detail.

In general case, there are several types of magnetostatic spin waves depending on magnetic field direction might be excited: backward volume magnetostatic spin wave (order n=0, 1, 2, …), magnetostatic surface spin wave, and forward volume magnetostatic spin wave (order n=0, 1, 2, …). However, optical research is mainly devoted to the excitation of 0^{th} order modes. This is due to the fact that special pump and probe pulses field distribution for efficient excitation and detection of n≠0 modes are necessary.

Recently it was demonstrated that magnetophotonic crystal allows to control distribution of inverse Faraday effective field in a very successful way [5]. It not only makes it possible to amplify the field in the region of the microcavity layer, but also to make it inhomogeneous. Nevertheless, the optical excitation of n≠0 modes in magnetophotonic structures has not been considered previously.

Here we demonstrate all-optical excitation and detection of n≠0 backward volume magnetostatic spin waves by inverse Faraday effect (Fig. 1). It is shown that magnetophotonic structures allow to excite them almost as efficiently as n=0 mode. Moreover, the number n of excited spin wave can be controlled by the pump pulse wavelength.

The magnetophotonic crystal has the following structure: GGG substrate (500 μm) / $Bi_{0.9}Lu_{2.1}Fe_5O_{12}$ (280 nm) / four pairs of SiO2 (110 nm) +TiO2 (70 nm) layers.

The research was financially supported by the Russian Ministry of Education and Science, Megagrant (project No. 075-15-2019-1934) and partly by Russian Foundation for Basic Research (project number 18-52-80038).

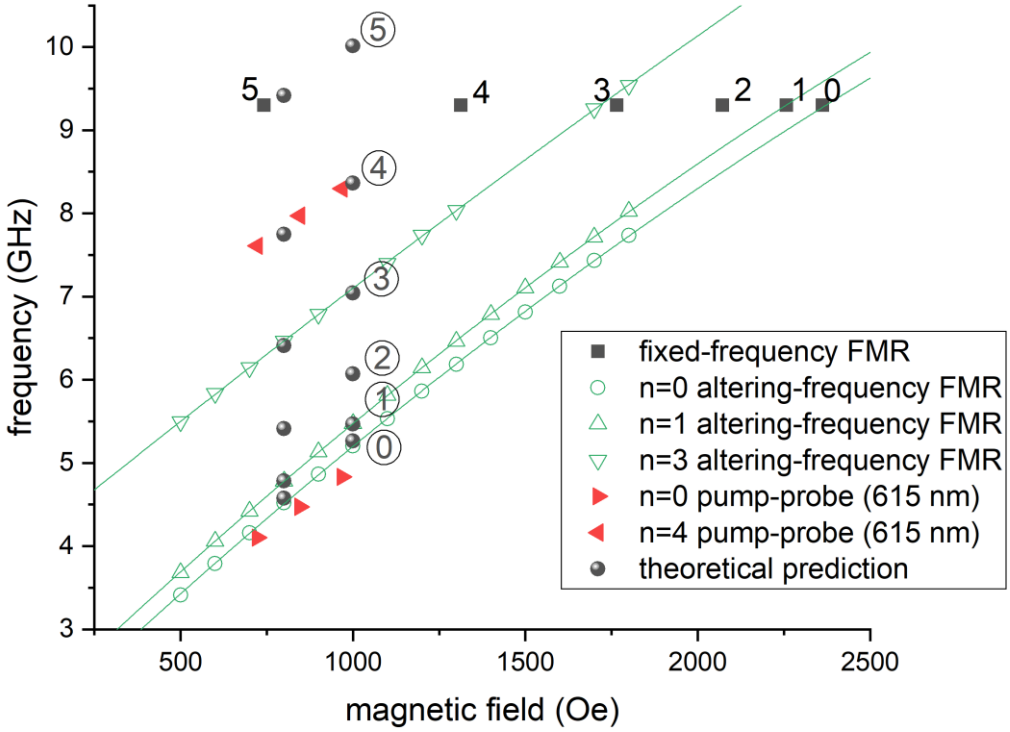

Fig. 1. Magnetization dynamics excited by: FMR measurements with fixed (black squares) and altering (green circles and triangles) frequency setup, pump-probe setup (at 615 nm, red triangles), and its theoretical predictions. Numbers correspond to the mode number.

References

[1] A.V. Chumak, A.A. Serga, and B. Hillebrands. Nature communications 5(1), 1-8 (2014).

[2] E.Y. Tsymbal and I. Žutić, eds. Spintronics Handbook: Spin Transport and Magnetism: Volume Two: Semiconductor Spintronics (CRC press, 2019).

[3] A.V. Chumak, e-print arXiv:1901.08934 (2019).

[4] A.V. Kimel, et al., Nature 435(7042), 655-657 (2005).

[5] M.A. Kozhaev, et al., Scientific reports 8(1), 1-7 (2018).

Spectrum evolution of magnetostatic waves optically excited by ultrafast magnetic anisotropy change

Khokhlov N.E.[1], Filatov Ia.A.[1], Gerevenkov P.I.[1], Wang M.[2], Rushforth A.W.[2], Kalashnikova A.M.[1]

[1] *Ioffe Institute, 194021, St. Petersburg, Russia*
[2] *The University of Nottingham, NG7 2RD, Nottingham, United Kingdom*

Femtosecond laser pulses became a powerful tool for driving ultrafast magnetization dynamics with a number of significant advantages over conventional techniques [1]. Consistent evolution of modern magnetism brought femtomagnetism [1] in touch with magnonics [2], as the optical excitation of spin waves (SWs) was demonstrated recently [3]. On the other hand, active optical control of SWs propagation is up-to-date task in magnonics [4]. But the rates of the control are far from ultrafast regime yet. Therefore, exploiting femtosecond laser pulses in reconfigurable magnonics is modern challenge for fundamental magnetism with potential impact on future data processing applications.

In the report we present the study of femtosecond laser pulses' influence on propagation of magnetostatic surface waves (MSSW) in ferromagnetic films with pronounced in-plane magnetic anisotropy. We show experimentally that the feature provides the opportunity to excite MSSW via ultrafast thermal magnetocrystalline anisotropy changes [5]. Next, we examine feasibility of MSSW control with fs-laser pulses not only during excitation but upon propagation as well. Particularly, we demonstrate the narrowing of the spectrum of the laser-excited MSSW wave packet as it propagates away from the excitation area [6,7]. Moreover, we control whether the low- or high-frequency part of the spin waves spectrum is suppressed upon propagation by changing the orientation of external magnetic field with respect to the anisotropy axes. The theoretical description of the effect is given in terms of the spatial gradient of magnetization and anisotropy parameters of the film induced by the laser pulse. The concept of MSSW control by fs laser pulses is extended further by analysing properties of the MSSW optically excited near a Néel domain wall in the thin film [7]. Micromagnetic modelling reveals the appearance of controllable resonance peaks in the MSSW spectrum and shows that the combination of femtosecond optical excitation with magnetic nonuniformity of the film, e.g. a domain wall, serves as a tuneable source of MSSW wavepackets.

The work is supported by RFBR (project 20-32-70149).

References

[1] A.M. Kalashnikova, A.V. Kimel and R.V. Pisarev, Phys. Usp. 58, 969-980 (2015).
[2] S.A. Nikitov, et al. Phys.-Usp. 63, 945 (2020).
[3] T. Satoh, et al. Nat. Photonics 6, 662-666 (2012).
[4] M. Vogel, et al. Nat. Physics 11, 487–491 (2015).
[5] N.E. Khokhlov, et al. Phys. Rev. Applied 12, 044044 (2019).
[6] Ia.A. Filatov, et al., J. Phys. Conf. Ser. 1697, 012193 (2020).
[7] N.E. Khokhlov, et al. JMMM, 534, 168018 (2021).

Ultrafast laser-induced demagnetization in thin ferromagnetic galfenol films

Kuntu D.V.[1], Shelukhin L.A.[1], Rushforth A.W.[2], Kalashnikova A.M.[1]

[1]*Ioffe Institute, 194021, Saint-Petersburg, Russia*
[2]*School of Physics and Astronomy, University of Nottingham, NG7 2RD, Nottingham, UK*

Manipulating the magnetization of a material is so far one of the most promising ways to improve existing and to develop new information storage and processing techniques. Magnetic state of the media can be altered at a subpicosecond timescale and nanometer spatial scale by light [1]. The possibility of magnetization switching by a single-shot laser pulse was experimentally demonstrated in 2007 in a ferrimagnetic alloy GdFeCo [2]. Following experimental and theoretical studies have shown that a process of ultrafast (less than 1 ps) demagnetization underlies the magnetization reversal in this material [3, 4]. Ultrafast laser-induced demagnetization was discovered in 1996 in thin films of ferromagnetic nickel [5]. However, rigorous theoretical interpretation of the process remains challenging and several competing physical models have been suggested [6, 7]. This motivated ongoing investigations of the ultrafast laser-induced demagnetization under various conditions and in various media.

We report on the experimental study of the process of the ultrafast laser-induced demagnetization in thin films of ferromagnetic metal galfenol $Fe_{0.81}Ga_{0.19}$ (FeGa) on GaAs substrate. A series of samples with FeGa layer thicknesses from 4 to 100 nm and multilayer structures FeGa(7nm)/Cu(5nm)/GaAs and FeGa(7nm)/Cu(5nm)/FeGa(4nm)/GaAs have been used in the work. All samples had been grown on a GaAs (001) substrate by magnetron sputtering. The experiment was performed using femtosecond time-resolved optical pump-probe technique (Fig. 1). Magnetization dynamics was excited by a 170-fs laser pump pulse with a wavelength of 1030 nm and fluences ranging from 2 to 36 mJ/cm^2. Longitudinal magneto-optical Kerr effect for a reflected probe pulse (170 fs, 515 nm, 0.4 mJ/cm^2) was measured as a function of the time delay between the pump and probe pulses in order to detect laser-induced changes of the magnetization.

The following features of the ultrafast demagnetization process have been revealed. The dynamics of the demagnetization after the excitation by a laser pulse is seen as a fast decrease of the magnetization at a timescale of less than 1 ps, followed by a slower partial magnetization recovery process lasting for several picoseconds. The Fig. 1 shows demagnetization curves for the 100-nm-thick FeGa film grown on a GaAs substrate. As can be seen from the figure, the magnetization decreases in less than 1 ps by a value reaching approximately 8 % for pump pulse fluence of 14 mJ/cm^2. Relaxation to initial value takes place at a significantly larger timescale. The demagnetization magnitude increases linearly with the pump pulse fluence, which is typical of transition metals. A similar demagnetization pattern has been observed in all FeGa films of smaller thicknesses and multilayer structures, except the 4-nm-thick FeGa film. The latter exhibited a two-step magnetization decrease, while the maximum demagnetization value was reached at time delays of approximately 10 ps. Furthermore, demagnetization magnitudes in the 4-nm-thick film for similar pump fluences were significantly larger than in the other FeGa films and multilayer structures.

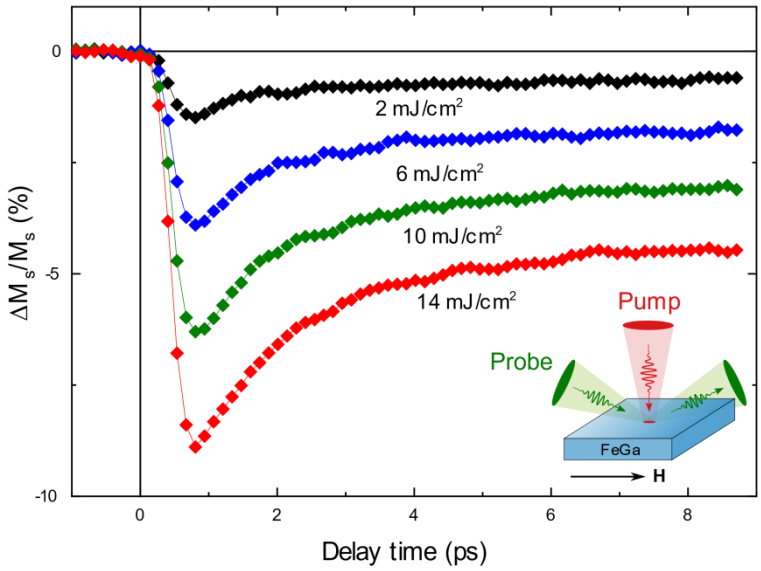

Fig 4. Laser-induced relative change ($\Delta M_s/M_s$) of the saturation magnetization (M_s) of the FeGa 100-nm-thick film as a function of the delay time between the pump and probe laser pulses measured for various pump pulse fluences. Inset: schematic representation of the pump-probe experimental technique. External magnetic field (H) is applied in the plane of the sample. All measurements were conducted at room temperature.

Complex and mutually linked dynamics of electron, lattice and spin subsystems of a material under optical excitation has been shown to underlie the phenomena of ultrafast demagnetization [1, 6]. We have conducted numerical modelling of the ultrafast demagnetization in FeGa films of thicknesses from 4 to 100 nm in terms of the microscopic three-temperature model (M3TM) [6]. Both qualitative consistency with experimental data and similar order of magnitude of the demagnetization have been obtained for all film thicknesses using the same material parameters, except for the 4-nm-thick film. The two-step demagnetization in the 4-nm-thick film could be reproduced in the calculations only under the assumption that microscopic material properties were changed. We anticipate the observed effect may indicate that in thin films modified spin-orbit interaction at the FeGa/GaAs interface starts to affect the ultrafast demagnetization. The demagnetization dynamics in thin FeGa films may also be influenced by a superdiffusive spin transport, which is not included in the model.

The work was partially supported by RFBR (grant No. 19-52-12065) and RSF (grant No. 20-12-00309).

References

[1] A. Kirilyuk, A.V. Kimel, and T. Rasing, Rev. Mod. Phys. 82, 2731 (2010).
[2] C.D. Stanciu *et al.*, Phys. Rev. Lett. 99, 047601 (2007).
[3] T.A. Ostler *et al.*, Nature Commun. 3, 666 (2012).
[4] K. Vahaplar *et al.*, Phys. Rev. Lett. 103, 117201 (2009).
[5] E. Beaurepaire *et al.*, Phys. Rev. Lett. 76, 4250 (1996).
[6] B. Koopmans *et al.*, Nature Mater. 9, 259 (2010).
[7] M. Battiato, K. Carva, and P.M. Oppeneer, Phys. Rev. Lett. 105, 027203 (2010).

Photoinduced spin dynamics in a uniaxial intermetallic heterostructure $TbCo_2$/FeCo

Gaponov M.S.[1], Ovcharenko S.V.[1]

[1] *MIREA - Russian Technological University, 119454,Moscow, Russia,*

The need to study ultrafast processes in magnetism is due to the prospects for creating ultrafast magnetic recording and ultrafast spintronic devices [1–3]. At present, the deformation control of magnetic states in magnetoelectric heterostructures is considered as a breakthrough in promising applications of nanoelectronics [4-7].

Intermetallic heterostructures of rare earth and transition metals have physical properties that are promising for various applications. These structures combine giant magnetostriction, controlled magnetic anisotropy, magneto-optical activity, and allow spin reorientation transitions (SRT) induced by a magnetic field at room temperature. In this work, we studied the spin dynamics induced by ultrafast optical excitation in the $TbCo_2$ / FeCo heterostructure. The time dependence of the rotation of the polarization of light excited by an optical pump pulse with a duration of 35 fs has been measured in the entire range of SRT generated by an external constant magnetic field. A hysteresis dependence of the polarization rotation on the magnetizing field is found, which is characteristic of spin dynamics near the SRT.

To understand the experimental results and obtain quantitative information, a numerical model was developed based on the Landau-Lifshitz-Hilbert (LLG) equation.
Within the framework of the hypothesis of photoinduced violation of magnetic anisotropy, we include in the free energy of the film the anisotropy energy with the time-dependent parameter $H_A(t)$ and the energy of interaction of the magnetic moment with external and demagnetizing fields, determined by H_x, H_y and $2\pi M^2$, respectively:

$$F = -\frac{1}{2}MH_A(t)\sin^2\theta\cos^2\theta - H_xM\sin\theta\cos\varphi - H_yM\sin\theta\sin\varphi + 2\pi M^2\cos^2\theta \quad (1)$$

From the analysis of the experimental results, two relaxation parameters were introduced, η1 and η2:

$$H_A(t) = H_{A0}(1 - x_1e^{-\eta_1 t} - x_2e^{-\eta_2 t}) \quad (2)$$

These parameters show thermalization of the electronic system due to the electron-phonon interaction and thermal relaxation in the phonon system.

The proposed mechanism of interaction between the optical pulse and the spin system, which consists in thermal destruction of the anisotropy field, fully explains the observed experimental results. Comparison of experimental data with calculations also revealed the values of the spin relaxation parameter and thermal relaxation characteristics of anisotropy. The latter can be used as a guideline, in particular, when creating promising heterostructures for MELRAM.

Acknowledgements

This work was supported Russian Science Foundation (Grant 20-12-00276). The authors are grateful to N. Tiercelin and P. Pernod (Univ. Lille, CNRS, Centrale Lille, Univ. Polytechnique Hauts-de-France, UMR 8520 -IEMN, 59000, Lille, France) for sample preparation.

References

[1] Sander D., Valenzuela S.O., Makarov D., Marrows C.H., Fullerton E.E., Fischer P., McCord J., Vavassori P., Mangin S., Pirro P., Hillebrands B., Kent A.D., Jungwirth T., Gutfleisch O., Kim C.G., Berger A. The 2017 Magnetism Roadmap. J. Phys. D. Appl. Phys. 2017; 50(36): 363001 (2017).

[2] Beaurepaire E., Merle J.-C., Daunois A., Bigot J.-Y. Ultrafast spin dynamics in ferromagnetic nickel. Phys. Rev. Lett; 76(22):4250-4253 (1996).

[3] Kirilyuk A., Kimel A.V., Rasing T. Ultrafast optical manipulation of magnetic order. Rev. Mod. Phys. 82(3): 2731-2784 (2010).

[4] Staruch, M. et al. Reversible strain control of magnetic anisotropy in magnetoelectric heterostructures at room temperature. Sci. Rep. 6, 37429 (2016).

[5] Roy, K. Separating read and write units in multiferroic devices. Sci. Rep. 5, 10822 (2015).

[6] Bukharaev, A. A., Zvezdin, A. K., Pyatakov, A. P. & Fetisov, Y. K. Straintronics: a new trend in micro- and nanoelectronics and materials science. Phys. Uspekhi 62, 1175 (2018).

[7] Tiercelin, N. et al. Strain mediated magnetoelectric memory, Chap. 8. In Nanomagnetic and Spintronic Devices for Energy Efficient Computing (eds. Bandyopadhyay, S. & Atulasimha, J.) (Wiley, Hoboken, 2016), 221–257. ISBN 978-1-118-86926-0.

Domain wall motion across magnetic and spin compensation points in ferrimagnets

Logunov M.V.[1], Safonov S.S.[1], Fedorov A.S.[1,2], Fedorova A.A.[1,2], Moiseev N.V.[3], Safin A.R.[1,4], Nikitov S.A.[1,2], and Kirilyuk A.[1,5]

[1]*Kotel'nikov Institute of Radio-Engineering and Electronics of RAS, 125009, Moscow, Russia*
[2]*Moscow Institute of Physics and Technology, 141701, Dolgoprudny, Moscow Region, Russia*
[3]*National Research Mordovia State University, 430005, Saransk, Russia*
[4]*Moscow Power Engineering Institute, 111250, Moscow, Russia*
[5]*FELIX Laboratory, Radboud University, 6525 ED, Nijmegen, Netherlands*

Recent years have seen an increase of interest in the dynamics of ferrimagnetic materials, in particular in the motion of domain walls [1-4]. Ferrimagnetic materials represent unique systems where the ease of manipulating the spins with applied magnetic fields is combined with exchange-driven acceleration of the internal spin dynamics. Of particular interest is the temperature range around the magnetic and spin compensation points, finely balancing both magnetic moment and angular momentum of the system, and leading to a very particular character of magnetic switching by the domain wall motion.

Here we present our studies of the temperature-dependent domain wall dynamics in the temperature range covering both angular momentum and magnetization compensation points in garnet film, and reaching up to the Curie temperature. This is made possible by the very low coercive field of the material (the sample used in our experiments is a single-crystal thin film of magnetic garnet), not exceeding 5 mT even in the close vicinity of magnetization compensation temperature. A very unusual behavior of the domain-wall dynamics is observed, such as extraordinarily high mobility of the domain walls at very low fields. Drastic changes of both domain-wall velocity and mobility by more than 2 orders of magnitude are observed across a relatively small temperature range, related to the delicate balance of magnetization and spins of iron and rare-earth sublattices [5]. Therefore, such fine tuning of the corresponding momenta could be the key for developing ultrafast ferrimagnetic spintronic devices.

The work was supported by the Russian Foundation for Basic Research (Projects No. 18-52-16006, 18-29-27020) and the Government of the Russian Federation (Project No. 075-15-2019-1874).

References

[1] K.-J. Kim, S.K. Kim, Y. Hirata et al., Nature Mater. 16, 1187 (2017).

[2] B.A. Ivanov, Low Temp. Phys. 45, 935 (2019).

[3] J. Finley and L. Liu, Appl. Phys. Lett. 116, 110501 (2020).

[4] E. Haltz, J. Sampaio, S. Krishnia et al., Sci. Rep. 10, 16292 (2020).

[5] M.V. Logunov, S.S. Safonov, A.S. Fedorov et al., Phys. Rev. Appl. 15, 064024 (2021).

Nonlinear magnezation dynamics in bistable ferromagnetic nanoparticles via oscillating magnetic/magnetolastic fields

Vlasov. V.S.[1], Golov A.V.[1], Gurov O.E.[1], Kotov L.N.[1], Shcheglov V.I.[2], Lomonosov A.M.[3], Temnov V.V.[4, 5]

[1]*Department of Radiophysics, Pitirim Sorokin Syktyvkar State University, 167001 Syktyvkar, Russia*
[2]*Institute of Radioengineering and Electronics of the Russian Academy of Sciences, 125009, Moscow, Russia*
[3]*Prokhorov General Physics Institute of the Russian Academy of Sciences, 119991 Moscow, Russia*
[4]*Institut des Molécules et Matériaux du Mans, UMR CNRS 6283, Le Mans Université, 72085 Le Mans, France*
[5]*LSI, Ecole Polytechnique, CEA/DRF/IRAMIS, CNRS, Institut Polytechnique de Paris, F-91128, Palaiseau, France*

The strong magnon-phonon coupling in ferromagnetic films and particles has led to emergence of new phenomena including the spin Seebeck effect, spin pumping, magnon-phonon conversion and magnetization switching [1]. Recently, strong magnon-phonon coupling was experimentally observed in magnetic nanoparticles [2]. Earlier we considered the magnetization switching in elliptical magnetostrictive nanomagnets induced by ultrashort surface acoustic waves (SAWs) pulses [3]. The switching threshold between two metastable single-domain magnetization states depends on the amplitude and duration of SAW pulses, the magnetoelastic coupling efficiency, and the height of the potential barrier between these states. We enable tuning the height of the potential energy barrier between the two meta-stable states of the particle with well-defined magnetization directions by applying a DC magnetic field [3]. It has been shown recently that similar magnetic systems driven by monochromatic excitations display bifurcations and chaos [4]. In this work we investigate the nonlinear magnetization dynamics in single elliptical nanomagnets via a weak monochromatic magnetic/magnetoelastic fields in the kHz-GHz frequency range.

We model the nonlinear magnetic dynamics in the vicinity of the switching threshold by numerical solution of Landau-Lifschitz-Gilbert equation, including thermal noise [3]. The impact on the amplitudes of DC and alternating magnetic fields on magnetic switching and chaotic regimes of magnetization dynamics oscillation will be discussed in the present paper.

This work has been supported by the grants: Russian Science Foundation (project No. 21-72-20048); RFBR and Komi Republic (project No. 20-42-110004).

References

[1] W.G.Yang, H.Schmidt, Appl. Phys. Rev. 8, 021304(2021).
[2] C. Berk et al.,Nat. Commun. 10, 2652(2019).
[3] V.S. Vlasov et al., Phys. Rev. B 101, 024425 (2020).
[4] A. M. Ferona, R. E. Camley, Phys. Rev. B 95, 104421(2017).

Laser-Induced Magnetization Precession in Individual Magnetoelastic Domains of a Multiferroic CoFeB/$BaTiO_3$ Structure

Shelukhin L.A.[1], Pertsev N. A.[1], Scherbakov A.V.[1,2], Kazenwadel D.L.[3], Kirilenko D.A.[1], Hämäläinen S.J.[4], van Dijken S.[4], Kalashnikova A.M.[1]

[1]Ioffe Institute, 194021, St. Petersburg, Russia
[2]Experimental Physics II, Technical University Dortmund, D-44227 Dortmund, Germany
[3]University of Konstanz, D-78457, Konstanz, Germany
[4]NanoSpin, Department of Applied Physics, Aalto University School of Science, P.O. Box 15100, Aalto FI-00076, Finland

Multiferroics attract a lot of attention due to possibility to control their magnetization with electric field and electric polarization with magnetic field [1]. However, number of single-phase materials demonstrating such properties is very limited and many of them possess multiferroic properties significantly below room temperature. Thereby, artificial multiferroic structures based on the ferromagnetic and ferroelectric layers with strain-mediated coupling between them are the prospective alternative to obtain indirect magnetoelectric interaction of sufficient strength.

Femtosecond (fs) laser pulses are a powerful tool to control magnetization [2], while the optical control of electron polarization is still an open question. In this work we studied experimentally a possibility to affect an indirect magnetoelectric coupling by fs laser pulses in a composite amorphous ferromagnetic/ferroelectric structure CoFeB(50nm)/$BaTiO_3$ (see Fig. 1. (a)). In CoFeB/$BaTiO_3$ the inverse magnetostriction along the transfer of mechanical stress from ferroelectric to ferromagnetic layer results in the imprinting of domain structure from $BaTiO_3$ to CoFeB [3]. In such domains in CoFeB magnetoelastic interactions are the only source of magnetic anisotropy. Thus, laser-induced changes of magnetic anisotropy in the CoFeB layer provide control of the magnetoelastic coupling in the structure.

In experiments the CoFeB layer was excited by 170 fs laser pulses focused down to 5 μm. Magnetization dynamics was measured by detecting time-resolved polar magneto-optical Kerr rotation for the probe pulses focused to the same spot. Thus, the laser-induced magnetization dynamics could be excited and detected in individual domains of CoFeB. It was demonstrated that fs laser pulses launch magnetization precession in individual pinned ferromagnetic domains. Analysis of the precession frequency and initial phase dependences on the external magnetic field showed that underlying mechanism of laser-induced ultrafast magnetization dynamics is thermal laser-induced change of magnetic anisotropy [4]. In order to examine the validity of the suggested mechanism, we performed calculations of precession frequency and amplitude based on Smit-Suhl approach [5] taking into account ultrafast laser-induced change of magnetoelastic coupling parameter and demagnetization. The calculations of the precession frequency are in agreement with the experiment. However, there was a discrepancy between calculated and measured amplitude of the precession when the external field applied along the anisotropy hard axis. Numerical simulation based on Landau Lifshitz Gilbert equation solution revealed that such a discrepancy is a mark of the laser-induced magnetization switching in the stroboscopic pump-probe measurements.

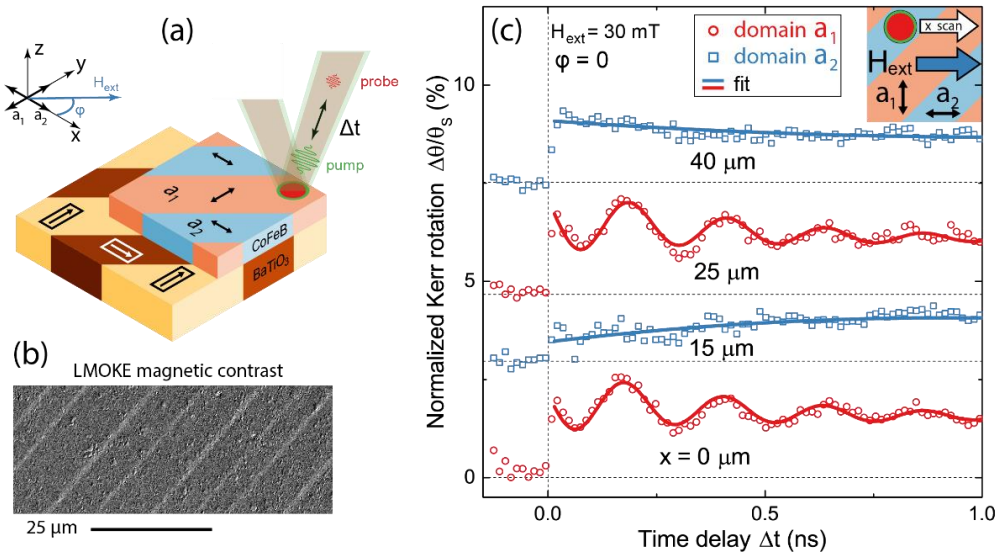

Fig. 1. (a) Schematic illustration of the $CoFeB/BaTiO_3$ structure and the pump-probe experiment. The arrows in rectangles and the double-headed arrows indicate the spontaneous polarization in the ferroelastic domains of the $BaTiO_3$ and the strain-induced magnetic anisotropy axes of the a_1 and a_2 domains in the CoFeB layer, respectively. (b) Magnetooptical image of a sample obtained using longitudinal Kerr microscopy. (c) Laser-induced Kerr rotation of the probe pulse polarization plane as a function of time delay Δt measured for different positions of pump and probe spots (see inset) on the sample surface in H_{ext} = 30 mT directed along the easy axis of a_2 domain. At x = 15 μm and 25 μm no precession is observed, which corresponds to the a_2 domains. Open dots are experimental points, lines are fit exponentially decaying sine-function.

To conclude, our results show a possibility to reduce significantly the magnetoelastic coupling in CoFeB layer in $CoFeB/BaTiO_3$ multiferroic on an ultrafast time scale by laser pulse excitation. This paves a way to alter the indirect magnetoelectric coupling in this structure. Further, we demonstrated excitation of the magnetization precession and switching in individual domains in composite multiferroic structure ferromagnetic/ferroelectric by fs laser pulses, which broadens potential applications of $CoFeB/BaTiO_3$ and related structures in magnonics.

The work is partly supported by the RSF grant (Grant No. 20-12-00309)

References

[1] J. Hu, L. Chen, and C. Nan, C., Adv. Mater. 28, 15 (2016).
[2] A. Kirilyuk, A. V. Kimel, and Th. Rasing, Rev. Mod. Phys. 82, 2731 (2010).
[3] T. H. E. Lahtinen, J. O. Tuomi, and S. van Dijken, Adv.Mater. 23, 3187 (2013).
[4] L. A. Shelukhin, V. V. Pavlov, P. A. Usachev, P. Yu. Shamray, R. V. Pisarev, and A. M. Kalashnikova, Phys. Rev. B 97, 014422 (2018).
[5] H. Suhl, Phys. Rev. 97, 555 (1955).

Interference of spin waves excited by a train of fs-laser pulses in YIG

Kolosvetov A.A.[1,2], Kozhaev M.A.[1], Belotelov, V.I. [1,3,4], Chernov A.I.[1,2]

[1]*Russian Quantum Center, Skolkovo, 143025 Moscow, Russia;*
[2]*Center for Photonics and 2D Materials, Moscow Institute of Physics and Technology (National Research University), 9 Institutskiy per., Dolgoprudny, 141700, Russia*
[3]*Vernadsky Crimean Federal University, Simferopol, 295007, Russia*
[4]*Faculty of Physics, Lomonosov Moscow State University, Moscow, 119991, Russia*

Spin waves are promising as Ohmic heating-free information carriers with possible applications in quantum information processing [1]. In particular, an all-magnon switch based on spin-wave interference can be implemented [3].

The work is devoted to the study of the spin waves interference excited in a thin film of yttrium iron garnet (YIG) by trains of femtosecond laser pulses. We reveal the possibility to manipulate the overall intensity of the spin waves by manipulating the spatial arrangement of the local spin wave sources. Utilizing the YIG as a platform for spin waves interaction provides the lowest known spin-wave damping among other materials, while femtosecond optical excitation of the YIG samples allows us to obtain a system with tunable spin-wave wavelength [4] and wavenumber distribution [5]. We studied experimentally and numerically a case when the 1.1 um-thick YIG sample is pumped by 200-fs laser pulses at a repetition frequency of 80 MHz. The value of the longitudinal external field was set 89 mT. Within the framework of the pump-probe technique, the oscillations of the Faraday rotation of the probe beam polarization demonstrate the precession of the sample magnetization. To analyze interference, we constructed a model of our system in the micromagnetic simulation framework (Mumax3) [6]. The pump beams that excite the waves can be differently oriented in space on the surface of the film.

Results obtained using the simulation corroborate the possibility to use spin wave interference to manipulate their propagation pattern. The modelling allowed to reveal the interference of the surface and volume modes of spin waves for different configurations of the external electromagnetic field. The obtained results pave the way for the new approach for manipulation of spin waves.

References

[1] A. V. Chumak, A. A. Serga, and B. Hillebrands, “Magnon transistor for all-magnon data processing,” Nature Communications 5 (2014)

[2] M. Balynsky, A. Kozhevnikov, Y. Khivintsev, T. Bhowmick, D. Gutierrez, H. Chiang, et al., “Magnonic interferometric switch for multi-valued logic circuits,” Journal of Applied Physics 121, 024504 (2017).

[3] Savochkin, I.V., Jäckl, M., Belotelov, V.I., et al. Generation of spin waves by a train of fs-laser pulses: a novel approach for tuning magnon wavelength. Sci Rep 7, 5668 (2017).

[4] Satoh, T., Terui, Y., Moriya, R. et al. Directional control of spin-wave emission by spatially shaped light. Nature Photon 6, 662–666 (2012).

[5] The design and verification of MuMax3 AIP Advances 4, 107133 (2014);

Acknowledgement

The work was supported by RSF project No. 21-12-00316.

Faraday rotation dependence of a highly focused Laguerre-Gaussian beam on the focusing position relative to the magnetic film

A.Yu. Fedorov[2,3], M.A. Yavorsky[1], M.A. Kozhaev[1,2], D.V. Vikulin[1], E.V. Barshak[1], V.N. Berzhansky[1], P.O. Kapralov[2], and V.I. Belotelov[1,2,4].

[1]*V.I. Vernadsky Crimean Federal University, Simferopol, 295007, Russia*
[2]*Russian Quantum Center, Skolkovo, Moscow Region 143025, Russia*
[3]*Moscow Institute of Physics and Technology, Dolgoprudnyi, Moscow Region 141700, Russia.*
[4]*Lomonosov Moscow State University, Moscow 119991, Russia*

Optical vortex beams (OVBs) are widely used in various fields of physics due to their phase structure [1]. Such beams can carry an additional orbital angular momentum (OAM) [2] $l\hbar$ per quantum, $l = \pm 1, \pm 2, \ldots, -$ topological charge, in comparison with plane waves, which carry only spin angular momentum (SAM). Recent experimental studies have shown that the interaction of a terahertz OVBs with magnetized media leads to dichroism, that differ from that for a wave with only SAM [3, 4]. This finding proves that involving OVBs in the standard Faraday configuration can invoke principally novel magneto-optic phenomena.

Thus, in this work, we make the first steps to study the influence of the presence of an orbital angular momentum in a beam on the main effects of magneto-optics. Namely, we investigate the Faraday rotation dependence of a highly focused Laguerre-Gaussian beam on the focusing position relative to the magnetic film (Fig. 1). In the experiment, we generate optical vortices with a topological charge of $l = 0, \pm 1$, which are focused on a iron-garnet film with a thickness of 6.2. For each position of the sample relative to the waist, we measure the Faraday rotation. The corresponding figure 2. shows the Faraday rotation in relation to the considered topological charge of the vortex.

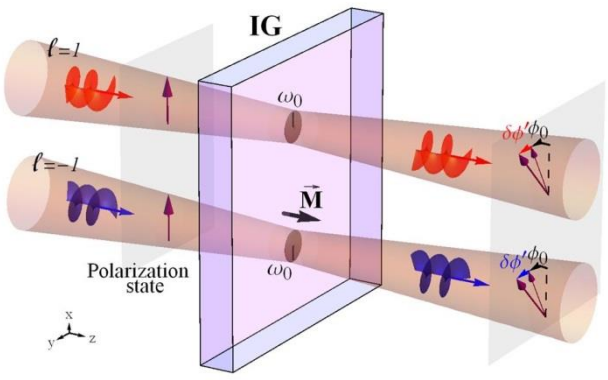

Fig.1 Transmission of a focused OVB through a magnetic film with subsequent rotation of the polarization plane.

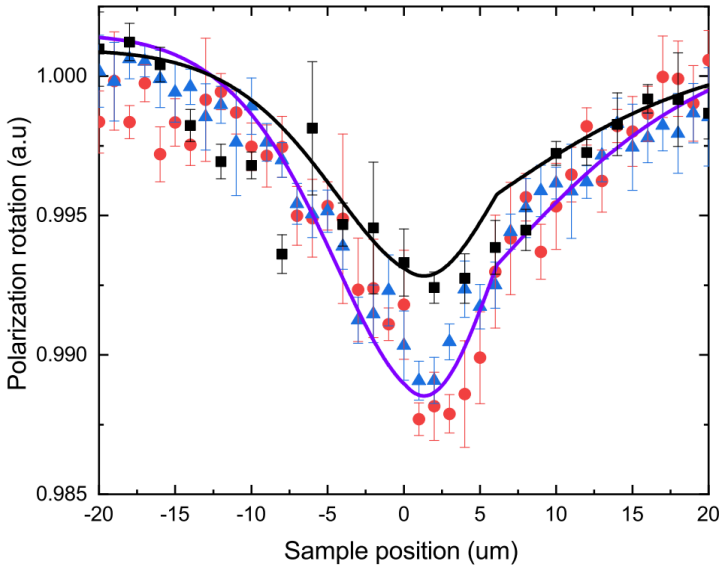

Fig.2 Polarization of the OVBs for different topological charges $\mathbf{l = 0}$ (black dots), $\mathbf{1}$ (red dots), and $\mathbf{-1}$ (blue dots), depending on the position of the sample relative to the waist ($\mathbf{z = 0}$).

From the data obtained, it can be seen that there is a nonmonotonic dependence of the rotation of the plane of polarization of a linearly polarized optical vortex passing through a iron-garnet film in a perpendicular magnetic field (Faraday effect), both on the topological charge and on the position of the sample relative to the waist (z = 0). At the location of the waist, the rotation has a minimum: at $z = 0$ for $l = 0$ this value is 0.7%, and for $l = +1, -1$ by about 1.4% less than the Faraday effect of an unfocused beam. Consequently, the presence of orbital angular momentum in the beam increases the deviation of the Faraday angle from Faraday angle of the plane wave.

The research was financially supported by the Russian Ministry of Education and Science, Megagrant (project No. 075-15-2019-1934) and by the RSF (project No. 21-12-00316).

References

[1] Y. Shen, X. Wang, X. Zhenwei, C. Min, X. Fu, Q. Liu, M. Gong, and X. Yuan, Light.Sci.Appl. 8, (2019).

[2] A. Bekshaev, K. Y. Bliokh, and M. Soskin, Journal of Optics 13, 053001 (2011).

[3] A. A. Sirenko, P. Marsik, C. Bernhard, T. N. Stanislavchuk, V. Kiryukhin, and S.-W. Cheong, Phys. Rev. Lett. 122, 237401 (2019).

[4] V. S. Liberman and B. Y. Zel'dovich, Phys. Rev. A 46, 5199 (1992).

Photoinduced dynamics of magnetization in $TbCo_2$/FeCo multilayer structures

Bezvikonnyy N.V.[1] ,Gaponov M.S.[1], Ovcharenko S.V. [1]

[1]*MIREA - Russian Technological University, 119454, Moscow, Russia*

The paper considers the dynamics of the magnetization of $TbCo_2$ / FeCo heterostructures. According to recent research those stress-mediated magnetoelectric heterostructures represent a very promising approach for the realization of ultra-low energy Random Access Memories [1]. Here the results of an experiment on measuring the time-resolved photoinduced magnetooptical Kerr effect in series of different $TbCo_2$ / FeCo structures, approximated by the phenomenological dependence.

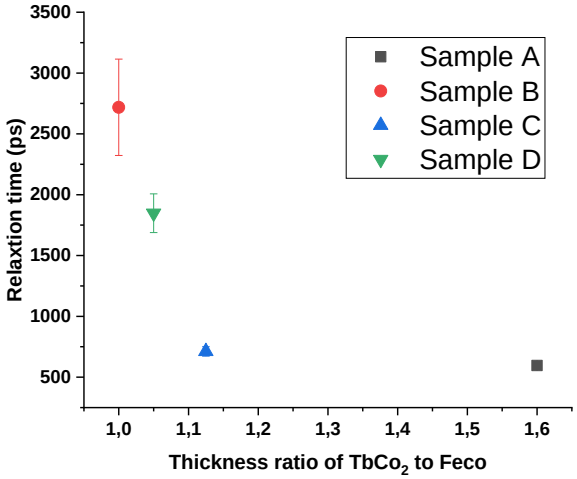

Fig. 1. Dependence of relaxation time on thickness of $TbCo_2$ layers.

Damping constants of relaxation processes are calculated. It is found that the damping constant, associated with the restoration of the uniaxial magnetic anisotropy after its destruction by a pump pulse[2], and precession frequency depends on the magnitude of the external magnetic field. The dependence of the temporal characteristics of the dynamics of magnetization on the composition of the structures is estimated.

The work of Russian side is supported by Russian Science Foundation (Grant 20-12-00276). The authors are grateful to Tiercelin N. and Pernod Ph. (Univ. Lille, CNRS, Centrale Lille, Univ. Polytechnique Hauts-de-France, UMR 8520-IEMN, 59000, Lille, France) for sample preparation.

References

[1] V. Preobrazhensky et al., J. Magn. Magn. Mater., v. 459, p. 66–70, (2018).

[2] Y. Dusch et al, , J. Appl. Phys., v. 113, 17C719, (2013).

Selective and tunable excitation of standing spin waves by optical guided modes

Krichevsky D.M.[1,2,3], Ignatyeva D.O.[1,3,4], Ozerov V.A.[1,2,3] and Belotelov V.I.[1,3,4]

[1] *V.I. Vernadsky Crimean Federal University, 295007 Simferopol, Crimea*
[2] *Moscow Institute of Physics and Technology (MIPT), 141700 Dolgoprudny, Russia*
[3] *Russian Quantum Center, 121353 Moscow, Russia*
[4] *Physics Department, Lomonosov Moscow State University, 119991 Moscow, Russia*

Spin wave control in magnetic materials is a fundamental basis of the most current energy efficient devices, such as magnetic memory, Boolean and quantum logical elements [1]. In the last few decades, femtosecond lasers opened up opportunities for ultrafast control of spin waves in a diverse magnetic material [2]. Special attention is paid to nonthermal approaches, for instance, inverse magnetooptical effects, such as inverse Faraday, inverse transverse magnetooptical Kerr, or inverse Voigt effects. In the systems supporting optical modes propagation these effects significantly modify spin wave dynamics that brings new horizons to all-optical spin control in magnetic materials [3,4].

Here we report on selective and tunable excitation of standing spin waves excited by optical guided modes inside thin Bi substituted iron garnet film (BIG). The theoretically studied structure consists of GaP prims, SiO_2 cladding layer (350 nm), BIG core (400 nm) and SiO_2 substrate. The structure supports excitation TM guided modes inside the core layer in range of 500-1500 nm of electromagnetic spectra (Fig. 1a). TM guided modes being elliptically polarized are characterized by E_x, H_y, E_z components which result in inverse transverse magnetooptical Kerr effect effective (ITMOKE) field formation (H_y^{eff}) (Fig. 1b).

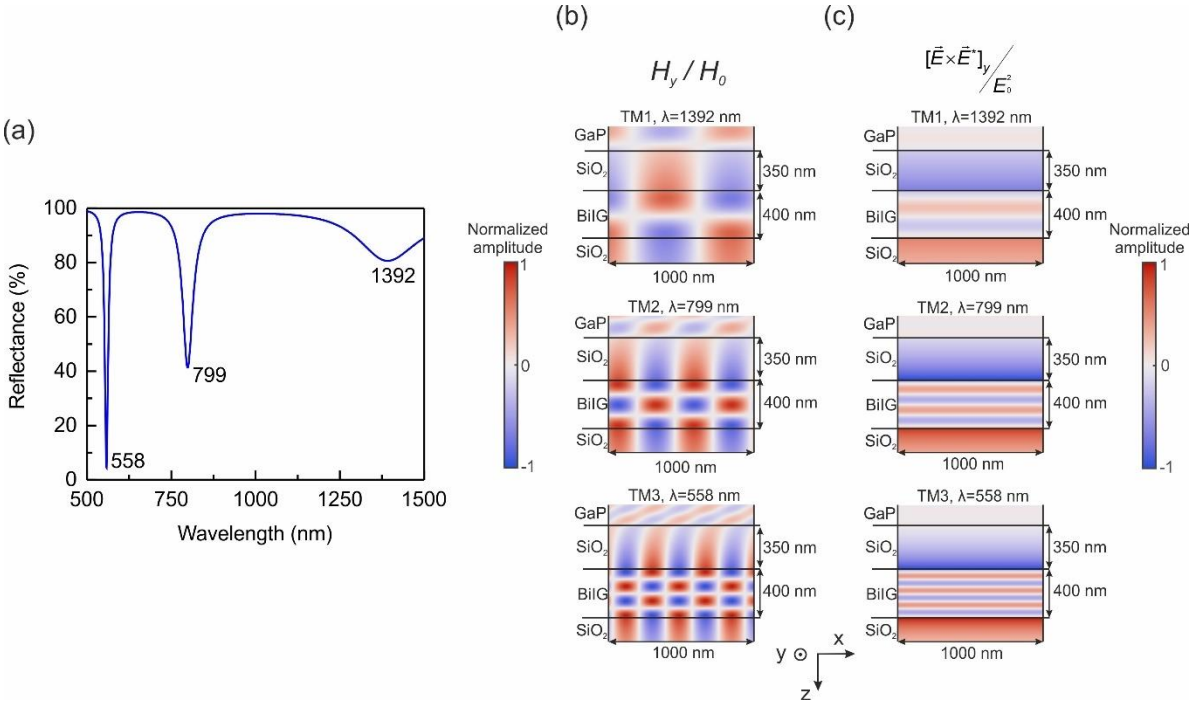

Fig. 1. Reflection spectrum of the structure (a), normalized H_y and H_y^{eff} distributions of the exited modes (b)

Spin wave dynamic launched by optical pump pulse was studied and analyzed using Landau-Lifshitz-Gilbert equation. TM guided mode excite a series of standing spin wave mode

inside BIG layer. The highest spin wave excitation efficiency can be achieved when H_y^{eff} field profile coincides spin wave profile (fig. 2a-c). Consequently, excitation of a certain TM mode result in selective standing spin wave mode which is illustrated in Fig. 2d-f.

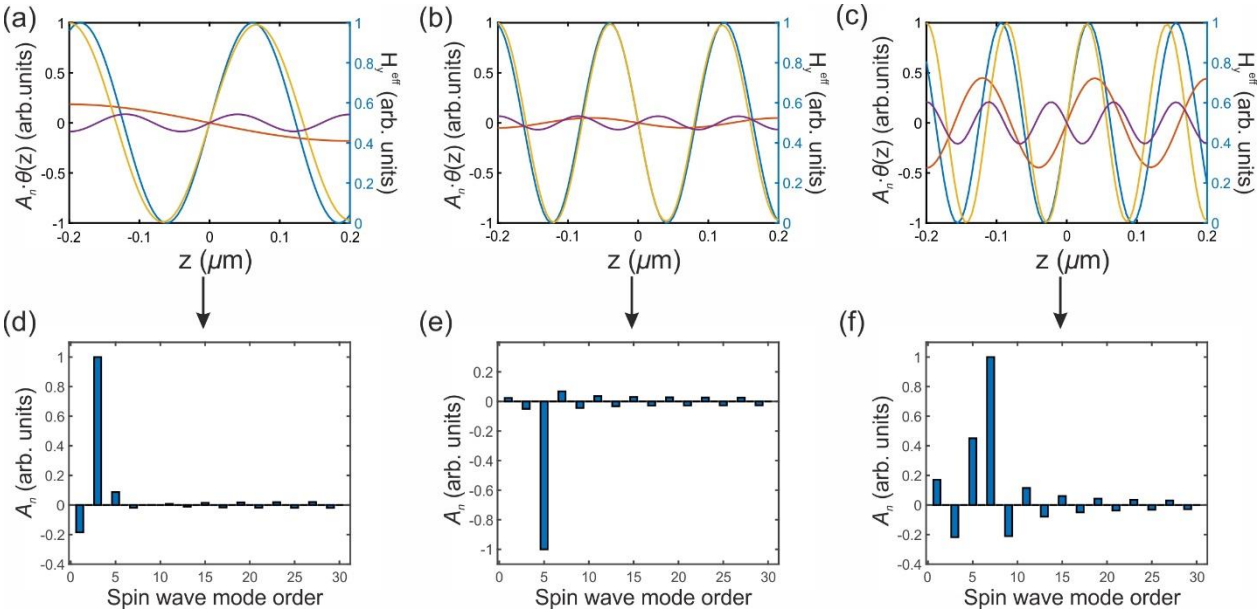

Fig. 2 (a)–(c) Calculated effective magnetic field (blue) and spin-wave profiles in the cross section of the waveguide. (d)–(f) Bar plots of standing spin waves amplitudes A_n (normalized on the major spin-wave maxima) for the corresponding effective magnetic field profiles of (a)–(c).

References

[1] A. V. Chumak et. al. Nature Physics, 11(6), p. 453, (2015)
[2] A. Kirilyuk et. al. Reviews of Modern Physics, 82(3), p. 2731, (2010).
[3] A. I. Chernov et. al. Nano Letters, 20(7), p. 5259, (2020).
[4] A. L. Chekhov et. al. Nano letters, 18(5), p. 2970, (2018).

Static and dynamic spin and orbital angular moments in ferromagnet

Osmanov R.S.[1], Butrim V.I.[1], Ivanov B.A.[2]

[1]V.I. Vernadsky Crimean Federal University, Simferopol 95007, Russia
[2]National University of Science and Technology "MISiS",Moscow,119049, Russia

Well know, that spin - orbit interaction for ions with non-frozen orbital moments, leads "exchange" amplification characteristic magnetic [1,2]. This get the magnetic resonance frequencies in the range of terahertz . A generic example is cobalt oxide CoO, having the frequencies 4 – 10 THz [2]. Generally, the orbital magnetic moment of the ion $\mathbf{l}$ is frozen and does not affect the high-frequency properties of magnetic materials. We consider model of anisotropic ferromagnetic with unfrozen orbital angular momentum, the Hamiltonian of which has the form

$$\hat{H} = \sum_{\mathbf{n}} \left[\lambda \hat{\mathbf{S}}_{\mathbf{n}} \hat{\mathbf{l}}_{\mathbf{n}} - C \hat{l}^2_{\mathbf{n},z} + B \hat{l}^2_{\mathbf{n},y} - K \hat{S}^2_{\mathbf{n},z} - \mu_{\mathrm{B}} \mathbf{H}_0 \left(\gamma_S \hat{\mathbf{S}}_{\mathbf{n}} + \gamma_L \hat{\mathbf{l}}_{\mathbf{n}} \right) \right]. \qquad (1)$$

Here $\hat{\mathbf{S}}_{\mathbf{n}}$ and $\hat{\mathbf{l}}_{\mathbf{n}}$ - operators of spin and orbital angular momentum in the node $\mathbf{n}$, λ - constant of spin-orbital interaction, C, B and K - the anisotropy constant, μ_{B} - Boron magneton, γ_S, γ_L - gyromagnetic ratio for spin and orbital momentum, $\mathbf{H}_0 = H_0 \mathbf{e}_z$ - magnetic field. For $l = 1$ the dynamics of the orbital angular momentum should be described with taking into account the full set of quantum states of the operator $\mathbf{l}$, both dipole $<\mathbf{l}>$ and quadrupole $<l_i l_j + l_j l_i>$ averages. The spin dynamics can be described in a framework of the Landau-Lifshitz equation. At $(C+B)(K+\lambda\gamma_S/2\gamma_L) > \lambda^2$ in the ground state the vectors $\mathbf{S}$ and $\mathbf{l}$ collinear to the z-axis and the length of the vector of the orbital angular momentum and quadrupole averages are

$$\left|\langle \mathbf{l} \rangle\right| = \frac{2S\cos\alpha_0 \left(\gamma_L H_0 - \lambda S\right)}{\sqrt{B^2 + 4\left(\gamma_L H_0 - \lambda S\right)^2}}, \quad \left\langle l^2_{x,y} \right\rangle_0 = \frac{1}{2}\left(1 \pm \sqrt{1 - \langle \mathbf{l} \rangle^2}\right), \quad \cos\alpha_0 = \frac{<\mathbf{l}>\mathbf{H_0}}{|<\mathbf{l}>|H_0}. \qquad (2)$$

The full set of the normal modes includes different types of oscillations. First, it is longitudinal mode with frequency $\omega_{\square} = \sqrt{B^2 + 4\left(\lambda S - \gamma_L H_0\right)^2}/\hbar$. This mode is associated with the oscillations of the length of the vector $\mathbf{l}$ and are not coupled with the spin oscillations. Other two modesare coupled oscillations of the transverse components of the dipolar degrees of freedom for spin and orbital moments. The frequencies of these coupled spin - orbital modes are lower than $\omega_{\square}$.

References

[1] V.I.Butrim, Low Temp. Phys. **40**, 508 (2014).
[2] T. Satoh, R. Iida, T. Higuchi, Y. Fujii, A. Koreeda, H. Ueda, T. Shimura, K. Kuroda, V. I. Butrim & B. A. Ivanov, Nat. Comm. **8**, 638 (2017).

Ultrafast magneto-elastic switching in ferromagnetic nanoparticles via picosecond pulses of surface acoustic waves.

Gurov. O.E.[1], Golov A.V, Vlasov V.S.[1], Kotov L.N.[1], Temnov V.V.[2, 3]

[1]Department of Radiophysics, Pitirim SorokinSyktyvkar State University, 167001 Syktyvkar, Russia
[2]Institut des Molécules et Matériaux du Mans, UMR CNRS 6283, Le Mans Université, 72085 Le Mans, France
[3]LSI, Ecole Polytechnique, CEA/DRF/IRAMIS, CNRS, Institut Polytechnique de Paris, F-91128, Palaiseau, France

The interaction of surface acoustic waves (SAWs) with magnetization in ferromagnetic thin films and nanoparticles has attracted significant interest motivated by development of information processing devices [1–2]. Here we focus on ultrafast magnetization switching in nickel nanoparticles, which can be achieved by readily available ultrashort SAW transients with strain magnitudes not exceeding 0.1%. The geometry of the problem is described in [2] and the modeling of magnetization switching was made by numerical solving of Landau-Lifschitz-Gilbert equation for different sizes of elliptical magnetostrictive nanomagnets. We tune the energy gap between two metastable states of magnetization in the nanoparticle by weak external magnetic field. Under certain conditions a picosecond SAW pulse triggers the magnetization switching between these states. The switching phenomena are quantified by the phase diagram (Fig. 1), which displays not only the switching zones for different pairs of acoustic amplitude η (vertical axis) and duration τ (horizontal axis), but also shows the switching time (color-coded).

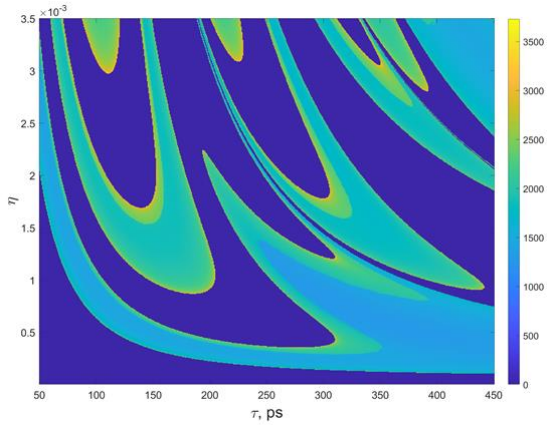

Fig.1. The magneto-elastic switching diagram of a single nickel nanoparticle of size 100×1600×20 nm^3 on glass substrate. Switching times (in ps) are color-coded.

This work has been supported by the grants: Russian Science Foundation (project No. 21-72-20048); RFBR and Komi Republic (project No. 20-42-110004).

References

[1] C. Chang et al., Phys. Rev. B 95, 060409 (2017).
[2] V.S. Vlasov et al., Phys. Rev. B 101, 024425 (2020).

Selective excitation of magnetization precession in magnetophotonic crystals

Sylgacheva D.A.[1,2], Kozhaev M.A.[1], Kalish A.N.[1,3], Belotelov V.I.[1,2,3]

[1]Russian Quantum Center, 121205, Moscow, Russia
[2]Vernadsky Crimean Federal University, 295001, Simferopol, Russia
[3]M.V.Lomonosov Moscow State University, 119991, Moscow, Russia

The inverse Faraday effect creates spatially distributed effective magnetic field $\mathbf{H_{eff}}$ by focused laser pulses in magnetic material [1]. It causes a different deviation of the magnetization from the external magnetic field in different parts of the structure.

In this work, we study the behavior of the effective magnetic field by the rigorous coupled-wave analysis [2] in the magnetophotonic crystal, which composition [GGG / $\{Bi_3Fe_5O_{12}/Sm_3Ga_5O_{12}\}$ / $Bi_3Fe_5O_{12}{}^2$ / $\{Sm_3Ga_5O_{12}/Bi_3Fe_5O_{12}\}^5$]. Photonic crystals with nonmagnetic Bragg mirrors have been studied earlier [3]. Results of numerical simulation show that a ratio of magnetization excitation efficiency in microcavity to one in Bragg mirrors varies in the range from 4:1 to 1:3 with a wavelength (Fig. 1).

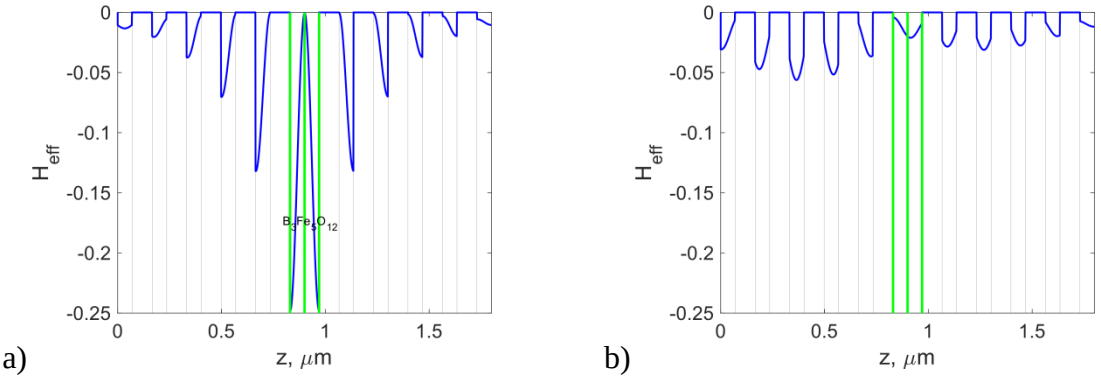

Fig. 1. Calculated distribution of the effective magnetic field in the studied magnetophotonic crystal (a, b). a- wavelength 745nm, b-880nm.

Excitation selectivity of the magnetophotonic crystal different parts looks promising for many novel applications in the field of magnonic logic. Magnonic technologies are developing very actively these days, and precise optical control of spin dynamics is vital for implementing optical-to-microwave transducers, interfacing of the superconducting magnons, etc.

The work was supported by the Russian Science Foundation (grant No.19-72-10139).

References

[1] A.V. Kimel, A. Kirilyuk, P.A. Usachev, R.V. Pisarev, A.M. Balbashov, and Th. Rasing, Nature 435, 655–657 (2005).

[2] V.I. Belotelov and A.K. Zvezdin, J. Opt. Soc. Am. B 22, 286-292 (2005).

[3] M.A. Kozhaev, A.I. Chernov, D.A. Sylgacheva, A.N. Shaposhnikov, A.R. Prokopov, V.N. Berzhansky, A.K. Zvezdin, and V.I. Belotelov, Sci. Rep. 8, 11435 (2018).

Temperature dependence of Gilbert damping constant in permalloy/topological insulator heterostructures

Pakhomov A.S.[1,2], Skirdkov P.N.[1,2,3], Chernov A.I.[1,2] and Zvezdin K.A.[1,2,3],

[1]*Moscow Institute of Physics and Technology, 141700, Dolgoprudnyy, Russia*
[2]*Russian Quantum Center, 143025, Moscow, Russia*
[3]*Prokhorov General Physics Institute of the Russian Academy of Sciences, 119991, Moscow, Russia*

Huge spin-orbit coupling makes topological insulators (TI) very attractive for topological spintronics. In our work we present FMR experiment with heterostructure TI/Ferromagnetic layer. As ferromagnetic layer we used Py (Ni80Fe20) with 20 nm thickness. Topological insulator was Bi2Se3, due to its record values of spin Hall angle. Thickness of TI layer was 5 nm. In this work S21 parameter was measured as a function of external magnetic field. Then results were approximated with sum of symmetric and asymmetric Lorentzians. Then Gilbert-damping parameter was calculated.

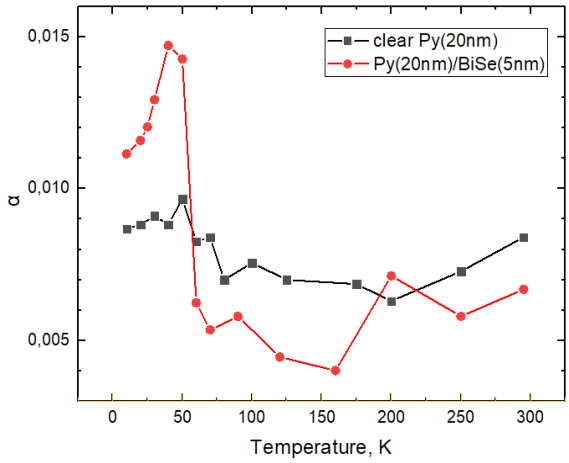

Fig. 1. Temperature dependence of Gilbert damping constant for Py (black line) and Py/TI heterostructure (red line).

We obtained that Gilbert-damping in TI/FM structure is 0.0066 ± 0.0005 and 0.014 ± 0.001 for 295K and 50K, respectively. In pure Py films with 20 nm thickness Gilbert-damping parameter was much lower. Same result was obtained in work [1] but only in pure permalloy samples with thickness 3 nm and mechanism of this phenomenon is in surface and bulk damping. For permalloy sample with same thickness Gilbert parameter was approximately 0.006 in all temperature range. Our hypothesis is that this phenomenon may relay on spin-orbit coupling, or may be spin-orbit coupling can amplify surface and bulk damping.

This work was supported by RSF grant 17-12-01333.

References

[1] Yuelei Zhao et al., Scientific Reports 6 (2016).

Free-carrier generation dynamics induced by ultrashort intense terahertz pulses in silicon

Kudryavtsev A.V.[1], Mishina E.D.[1]

[1]*MIREA - Russian Technological University, Vernadsky Ave. 78, 119454, Moscow, Russia*

We report the results of experimental studies and numerical simulation of the electron-hole pairs formation dynamics in silicon during the action of a two-period terahertz pulse with a maximum electric field strength of up to 23 MV/cm. The formation of an inhomogeneous distribution of the carrier concentration over the depth of the silicon sample is shown, which persists for several microseconds. This inhomogeneity is formed due to a sharp increase in the rate of filling the conduction band with free carriers in the subsurface input slab of the silicon wafer, which occurs at a field strength above 15 MV/cm.

When exposed to a THz pulse, additional free carriers are generated due to the impact ionization mechanism [1, 2], which leads to absorption of the probe pulse by free carriers and a decrease in the transmission of the silicon wafer. Calculations show that the concentration of free carriers along the direction of propagation of the THz radiation pulse at an electric field strength of 22.4 MV/cm reaches ~ 10^{19} cm^{-3} in the input surface slab, and ~ 10^{17} cm^{-3} at the exit of the sample. The calculated time dependences of the probe pulse transmittance correlate well with the experimental data for silicon wafers with different thicknesses.

To calculate the time dependence of the conduction electrons concentration, we used modified Boltzmann equations for the impact ionization dynamics. We also used a modified Keldysh formula for impact ionization model [3], which takes into account the contribution of higher conduction bands.

Studies of the free charge carriers dynamics in semiconductors in a strong electric field of electromagnetic radiation of far infrared and terahertz spectral ranges radiation are of significant interest for controlling the properties of a material. The possibility of a rapid change in the concentration of free carriers in the bulk of a silicon wafer (depending on the electric field strength of a THz pulse) makes it possible in the future to use the results obtained to create new high-speed optoelectronic devices.

References

[1] N. Sano, T. Aoki, M. Tomizawa, and A. Yoshii, Phys. Rev. B 41, 12122 (1990).

[2] A. V. Ovchinnikov, O. V. Chefonov, E. D. Mishina, and M. B. Agranat, Sci. Rep. 9, (2019).

[3] R.Redmer, J.R. Madureira, and N.Fitzer, Journal of Applied Physics 87, 781 (2000).

Section 5
Nanostructured Materials and Composites

Nanowires of various types: production, structure, magnetic properties, applications

Zagorskiy D.[1], Doludenko I.[1], Cherkasov D.[2], Zhigalina O.[1], Khaibullin R.[3]

[1] *Shubnikov Institute of Crystallography of RAS, 119333, Moscow, Russia*
[2] *Moscow Institute of Physics and Technology, 121205, Dolgoprudny, Russia*
[3]*Zavoisky Physico-Technical Institute, Kazan Scientific Center of RAS, 420029,Kazan, Russia*

Nanomaterials of various types are of great interest both from the point of view of theory and in terms of possible practical applications. One of the most interesting types of nanomaterials is one-dimensional structures, the so-called "nanowires" (NWs, - nanorods, nanoneedles). Such structures can be obtained by the method of matrix synthesis: by filling with the required material the cylindrical through pores in a previously prepared matrix (for example, in a track membrane). In this work, the preparation of both homogeneous structures (NWs from alloys) and heterogeneous structures (layered NWs) is considered. The type of obtained NW depends on the electrolyte content and the deposition regimes.

The synthesis of NWs from alloys was carried out in potentiostatic or galvanostatic modes, with obtaining a control graphs I(t) or U(t) respectively. The synthesis of layered NWs was carried out in two ways - the so-called "one-bath" or "two-bath". In the first case, one electrolyte was used containing the required ions. The alternation of deposition of different metals was achieved by alternating deposition potential. In the second case, the alternation of different layers was achieved by using different electrolytes ("baths").

The study of the structure of the nanoparticles obtained was carried out by microscopy methods - SEM (with elemental analysis) and TEM, as well as by the X-ray method. The narrow layers were determined by TEM in layered NWs and interfaces between these layers were investigated. It has been shown that the composition of NWs made of iron-cobalt alloy practically corresponds to the composition of the growth electrolyte. At the same time, in iron-nickel NWs, the iron content significantly exceeded its content in the electrolyte. The structure of iron-containing NWs in most cases is determined by the structure of iron (bcc). Only in the case of high concentrations of the second element, cobalt or nickel (more than 70-85%), the hcp or fcc structure (respectively) is observed.

Magnetometry showed that for NWs arrays with a large diameter (200 nm and more), the observed properties are close to those of bulk materials: cobalt NWs were comparatively magnetically hard (Coercive Force about 700-1000 Oe), while nickel NWs were magnetically soft (CF about 100 Oe). At the same time, a decrease in the diameter in nickel NWs led to a sharp increase in the coercive force. For layered nanowires, the easy magnetization axis coincided with the NW` axis if the layers were thicker than the wire diameter. With a decrease in the layer thickness, the easy axis became perpendicular to the NW axis.

The possibilities of application of NW arrays was reviewed: as emitters (the spike effect in conical nanoparticles), as blanks for obtaining magnetic particles of definite sizes (by separating layers into fragments) for use in biology (drug delivery) and as generators of Terahertz frequency particles (when spin-polarized current pass through the transitions between different magnetic layers in the NW).

Acknowledgments. This work was supported by State Task of FSRC "Crystall. and Photonic"

Fabrication and characterization of FeNi-based thin film periodic microstructures for high frequency applications

Svalov A.V.[1], Buznikov N.A.[2], Melnikov G.Yu.[1], S.M. Bhagat[3], Kurlyandskaya G.V.[1,4]

[1]*Institute of Natural Sciences and Mathematics, Ural Federal University, Ekaterinburg 620002, Russian Federation*
[2]*Scientific and Research Institute of Natural Gases and Gas Technologies – Gazprom VNIIGAZ, 142717, Razvilka, Vidnoye, Moscow Region, Russian Federation*
[3]*Physics Department, University of Maryland, College Park, USA*
[4]*Universidad del País Vasco UPV/EHU, Leioa, 48940, Spain*

Thin films and multilayered structures were the subject of the research and applications in the last decades [1-2]. Magnetic thin film elements of different electronic devices are most compatible with semiconductor technologies. Special efforts were made in the development of multilayered nanostructures with high magnetic permeability [3-4]. Magnetoimpedance effect (MI) attracted special attention and different types of thin film elements were developed [5]. Recently promising approaches were reported and tested for multilayered FeNi films: the employment of magnetic spacers for multilayered structures [6], asymmetric MI multilayers [7], profiled structures [8]. In the last case multilayer consists of a conductive central lead and two ferromagnetic layers located below and above. The upper layer is a periodic structure (N elements and N + 1-zones, in which elements are not deposited). It was shown theoretically that for such structure a decrease in the deviation angle of the effective magnetic anisotropy axis from the transverse direction leads to an increase of the transverse permeability and, correspondingly, enhances the skin effect and MI [8].

In this work, we had designed and fabricated thin 100 nm FeNi films and FeNi periodic structures. They were deposited by sputtering technique onto glass substrates using Cu meshes in the external magnetic field of 250 Oe applied during deposition along the direction parallel to one of the size of the squire element (EMA). Different sizes of the square unit of the mesh were used for preparation of different periodic structures. Their structure, static magnetic properties and ferromagnetic resonance were comparatively analyzed. The thickness of 100 nm was selected as typical thickness for FeNi layers for MI sensors. Fig. 1 shows examples of obtained periodic structures, describes their geometrical parameters and shows results of the in-plane measurements of the magnetic hysteresis loops using magneto-optical Kerr effect. One can see that FeNi film without patterning had uniaxial in-plane magnetic anisotropy and different types of magnetization processes for EMA and hard magnetization direction (HMA). Even so, low field magnetization processes of periodic structures differ from the magnetization processes corresponding to thin film. It can be related to the dipole-dipole interactions between the elements and size effects. However, the parameters of the ferromagnetic resonance (FMR) curves measured by cavity perturbation technique for the frequencies close to 9 GHz (value of ferromagnetic resonance fields for in-plane and out-of-plane configuration, the FMR peak width, effective magnetization values) were close to each other, indicating similar feature of dynamic magnetic permeability and therefore applicability for high frequency application.

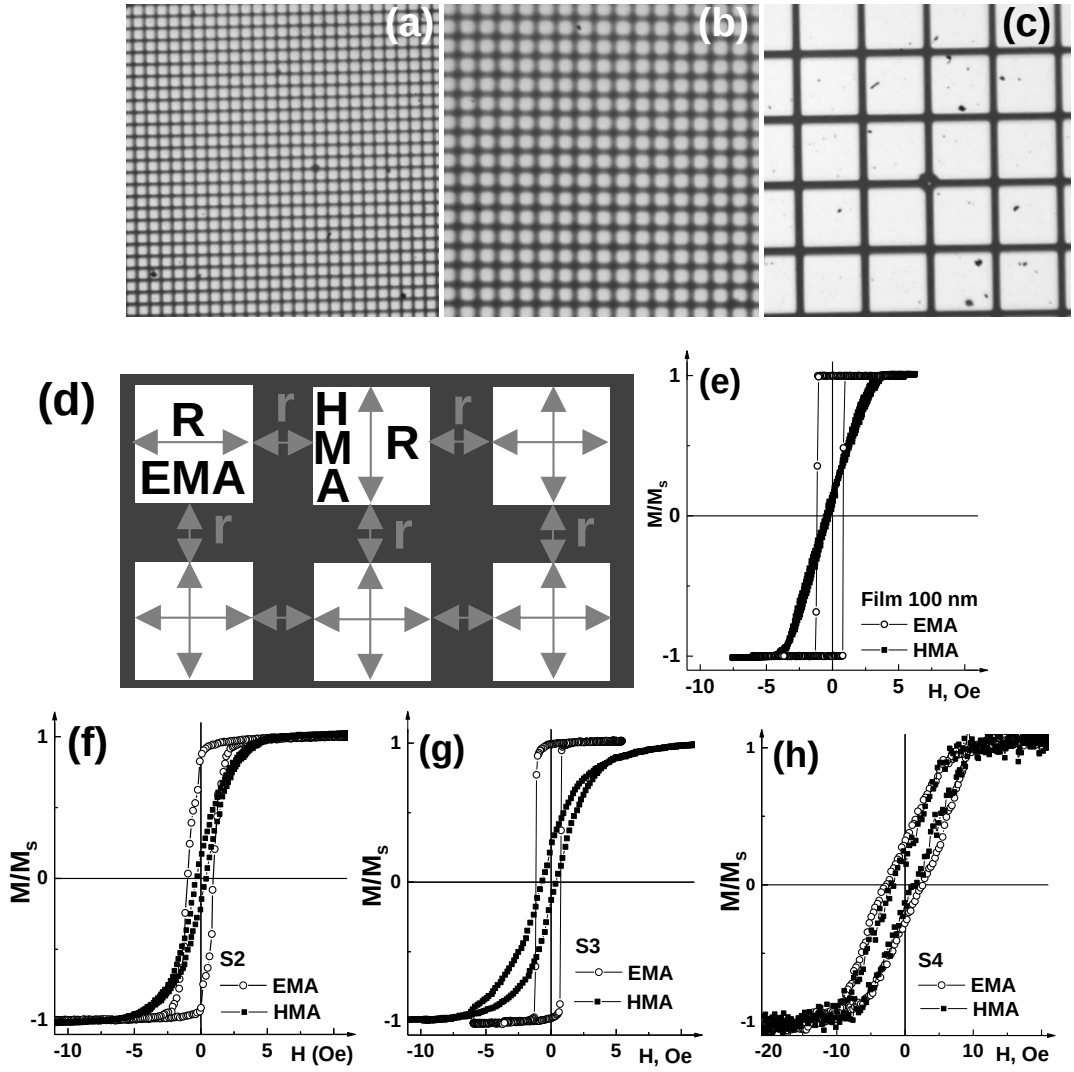

Fig. 1. Examples of periodic FeNi film structures (thickness of 100 nm), optical microscopy: S2 element size R of 50 μm × 50 μm and distance between elements r of 20 μm (a); S3 element size R of 70 μm × 70 μm and r of 30 μm (b); S4 element size R of 300 μm × 300 μm and r of 20 μm 30 μm (c). General description of the periodic structure: EMA - easy magnetization axis; HMA – hard magnetization axis (d). Hysteresis loops: S1 is a thin FeNi film (e); S2 (f); S3 (g) and S4 (h) measured in EMA and HMA.

This work was supported by the Ministry of Science and Higher Education of the Russian Federation (project No. FEUZ -2020-0051).

References

[1] G.A. Prinz, J. Magn. Magn. Mater., 200, 57 (1999).
[2] H.A. Ferreira, D.L. Graham, P.P. Freitas et al., J. Appl. Phys. 93, 7281 (2002).
[3] S.F. Cheng, P. Lubitz, et.al., J. Magn. Magn. Mater 2004, 282, 109 (2004).
[4] A.S. Antonov, S.N. Gadetskii, et al., Phys. Met. Metallogr. 83, 612 (1997).
[5] N.A. Buznikov, A.P. Safronov, et. al., Biosens. Bioelectron. 117, 366 (2018).
[6] A.V. Svalov, E. Fernandez, et al., Appl. Phys. Lett. 100, 162410 (2012).
[7] N.A. Buznikov, G.V. Kurlyandskaya, Sensors 19, 176 (2019).
[8] N.A. Buznikov, G.V. Kurlyandskaya, Fiz. Metall. Metalloved. 8, 1 (2021).

Valley polarization effects in TMDC and iron garnet heterostructures

Kravtsov V.[1], Ivanova T.[1], Abramov A.N.[1], Shilina P.V.[2], Kapralov P.O.[3], Krizhanovskii D.N. [1,4], Berzhansky V.N.[5], Belotelov V.I. [3,5,6], Shelykh I.A.[7,1], Chernov A.I.[2,3,5], Iorsh I.V.[1]

[1]Department of Physics and Engineering, ITMO University, Saint Petersburg 197101, Russia
[2]Center for Photonics and 2D Materials, Moscow Institute of Physics and Technology, National Research University, Dolgoprudny 141700, Russia
[3]Russian Quantum Center, Skolkovo Innovation City, Moscow 121353, Russia
[4]Department of Physics and Astronomy, University of Sheffield, Sheffield S3 7RH, UK
[5]Vernadsky Crimean Federal University, Simferopol 295007, Russia
[6]Faculty of Physics, Lomonosov Moscow State University, Moscow 119991, Russia
[7]Science Institute, University of Iceland, Dunhagi-3, IS-107 Reykjavik, Iceland

Transition metal dichalcogenides (TMDs) in their monolayer form are attractive candidates for integration into future on-chip opto-electronic devices as atomically thin and air-stable materials that support strongly bound excitons [1]. One of the promising approaches to control the TMD excitonic valley properties is via interfacing the layer with magnetic materials [2]. It allows, for example, lifting the energy degeneracy at the K and K' points through proximity effects and eliminating the need for large external magnetic fields. The aforementioned energy degeneracy can be required for potential information storage applications. This has generated much interest in experimental studies of TMD systems that are in proximity with various bulk, thin films, or layered van der Waals ferromagnetic and antiferromagnetic crystals.

Iron garnets, in particular yttrium iron garnet (YIG), have attracted much attention as promising magnetic substrates for TMD-based heterostructures. These heterostructures provide an opportunity to study valley physics of charged excitons in TMDs, as it was discussed in recent reports of trion valley polarization in MoS_2/YIG [3] and WS_2/YIG samples.

In this work we study circularly polarized photoluminescence of trions (a quasiparticle which consists of three in total electrons and holes) in $MoSe_2$ monolayers interfaced with thin films of bismuth iron garnet (BIG) deposited on gadolinium gallium garnet (GGG) substrates. Due to the out-of-plane magnetization in the BIG film, these systems exhibit contrast in the co-polarized photoluminescence of trions under right and left circularly polarized excitation. Importantly, the extracted magnitude of the effective magnetic field appears to be almost an order of magnitude larger than the saturation magnetization of BIG, which we measure independently. This indicates the emergence of proximity effects at the $MoSe_2$/BIG interface and suggests that interfacing TMDs with thin magnetic films could give access to large effective magnetic fields and associated magnetic phenomena even in the absence of strong external fields [4].

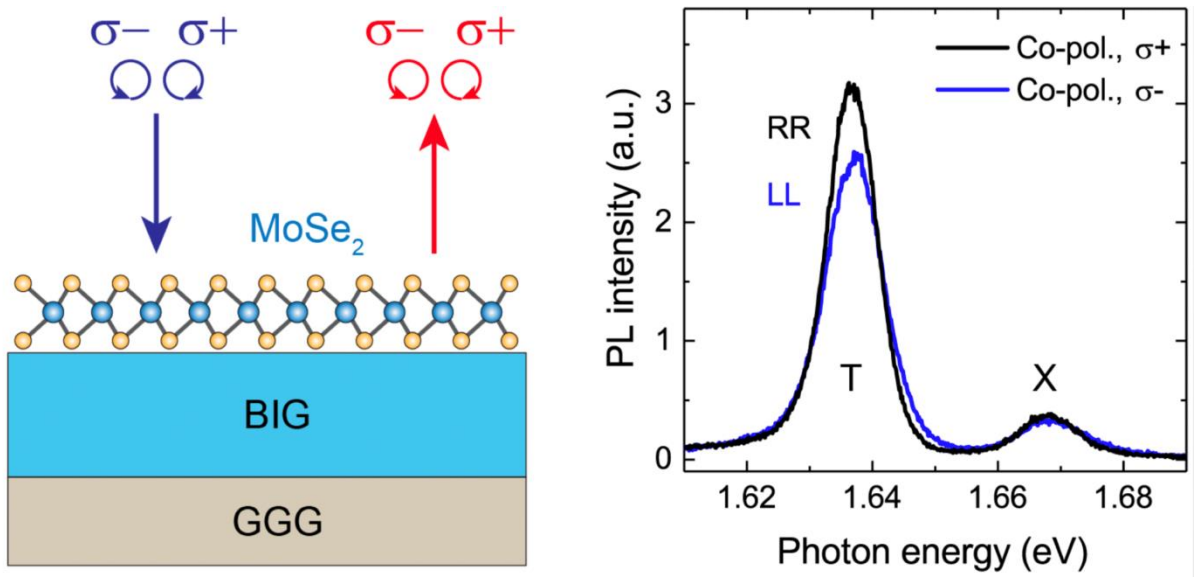

Fig. 1. Left is the principle scheme of the sample, consisting of monolayer $MoSe_2$ transferred onto thin film of bismuth iron garnet (BIG) on gadolinium gallium garnet (GGG) substrate, and types of different excitation/detection with circular polarization. Right – is the typical photoluminescence spectra from the $MoSe_2$ monolayer positioned on the magnetic film. T marks the area of the trion peak, X is the area of the neutral exciton.

Moreover, we observe an inverted trion valley polarization response, which depends crucially on temperature and excitation energy, being most pronounced at low temperatures and pump energy close to the B exciton. The ability to controllably invert the valley polarization of trions in TMDs without applying high external magnetic fields opens new routes for the development of valleytronic devices.

Our results provide basic understanding of the mechanisms of trion polarization in such systems for the development of future devices based on the combination of electronic and valley degrees of freedom for information storage and processing.

Acknowledgements

The authors acknowledge funding from the Ministry of Education and Science of the Russian Federation through Megagrant No. 14.Y26.31.0015. Optical measurements were funded by the Russian Science Foundation, project No. 19-72-00146. Magnetic properties investigation was supported by RSF project No. 21-12-00316. V.K. acknowledges support by the Government of the Russian Federation through the ITMO Fellowship and Professorship Program.

References

[1] K.F. Mak, J. Shan, Nat. Photonics 10, 216–226 (2016).
[2] Q. Zhang, S.A. Yang, W. Mi, Y. Cheng *et al.*, Adv. Mater. 28, 959–966 (2016).
[3] B. Peng *et al.*, ACS Nano 11, 12257–12265 (2017).
[4] V. Kravtsov, A.I. Chernov, I.V. Iorsh *et al.*, e-print, arxiv 2105.04327 (2021).

A theoretical study of magnetoimpedance effect in multilayered film in the presence of ferrogel

Buznikov N.A.[1], Kurlyandskaya G.V.[2,3]

[1]*Scientific and Research Institute of Natural Gases and Gas Technologies – Gazprom VNIIGAZ, 142717, Razvilka, Vidnoye, Moscow Region, Russian Federation*
[2]*Institute of Natural Sciences and Mathematics, Ural Federal University, 620002, Ekaterinburg, Russian Federation*
[3]*Universidad del País Vasco UPV/EHU, 48940, Leioa, Spain*

The magnetoimpedance (MI) effect consists in significant change in the impedance of a ferromagnetic conductor in an external magnetic field. High sensitivity of the MI is promising for different applications including biosensing [1–3]. The use of MI sensitive elements for measurement of the concentration dependence of the magnetic nanoparticles embedded in ferrogel was demonstrated recently [4,5]. At the same time, the understanding of the origin and limits of biosensor sensitivity for detection of magnetic nanoparticles requires further experimental and theoretical studies. In this work, we develop a model to describe the MI response of multilayered film in the presence of ferrogel.

The studied film structure consists of central copper layer and two external multilayers. The external multilayers contain permalloy sub-layers separated by non-magnetic spacers. The spacers are added in order to avoid the "transcritical state" transition and to increase the total thickness of the multilayer [6]. Both the symmetric and multilayered films are studied. The non-symmetric multilayers can be obtained by the deposition of top and bottom ferromagnetic parts of a multilayer with different thickness [7]. The layer of ferrogel is placed on the top surface of the multilayer. Since the multilayer length and width are much higher than its thickness, the distribution of the electromagnetic fields within the multilayer–ferrogel structure can be found in the one-dimensional approximation by means of a solution of Maxwell equations taking into account the continuity conditions [8].

The presence of ferrogel changes the field distribution within multilayered film and correspondingly affects the MI response. The ferrogel layer has a double effect on the MI response. The first contribution to the MI effect comes from high permittivity of the ferrogel, which results in an increase of the MI in the multilayer with ferrogel. The second contribution of the ferrogel layer is attributed to stray fields of magnetic nanoparticles. To describe the influence of stray fields on the MI response, it is assumed that ferrogel layer induces a spatially homogeneous effective stray field H_p in the multilayered film. The value of H_p is assumed to be proportional to the concentration of magnetic nanoparticles, since the saturation magnetization of the ferrogel increases linearly with the concentration of nanoparticles [4,5]. The effective stray field changes the magnetization distribution and affected the transverse permeability in the permalloy sub-layers. The transverse permeability is found from a solution of the Landau–Lifshitz equation.

The following multilayer parameters are used in calculations: the thickness of the central copper layer is 500 nm, the external multilayers contain five permalloy sub-layers with the thickness of 100 nm separated by titanium spacers with the thickness of 3 nm. The ferrogel

layer thickness is 1 mm and its permittivity is 80. General view of the gel without magnetic nanoparticles and ferrogel is shown in Fig. 1(a).

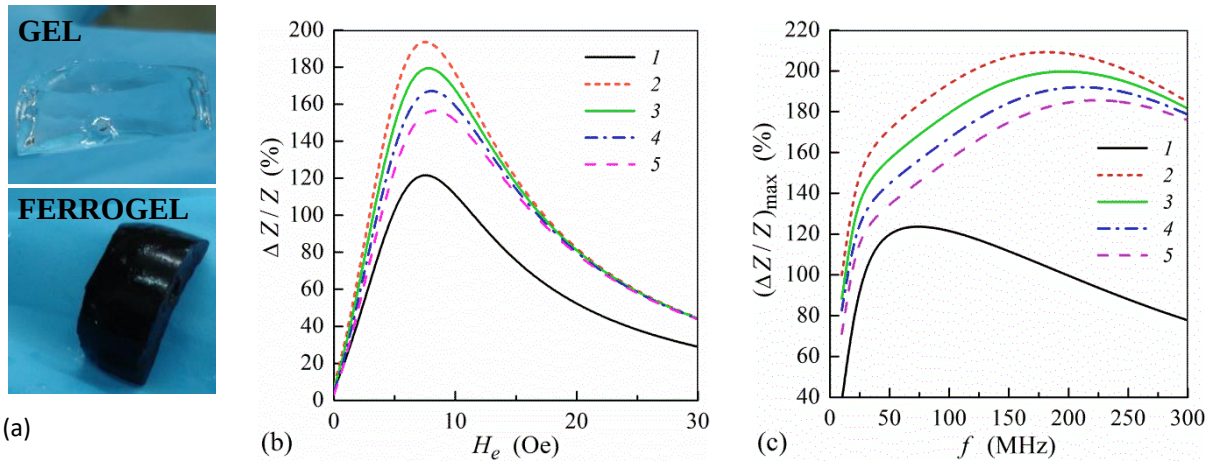

Fig. 1. General view of polyacrylamide gel and ferrogel filled with Fe_2O_3 nanoparticles (a), calculated MI ratio as a function of the external field at $f = 100$ MHz (b) and frequency dependence of the maximum MI ratio (c). Curves 1, multilayer without gel; curves 2, $H_p = 0$; curves 3, $H_p = 0.25$ Oe; curves 4, $H_p = 0.5$ Oe; curves 5, $H_p = 0.75$ Oe.

To describe a relative variation of the impedance we use the MI ratio $\Delta Z/Z = [Z(He) - Z(H_0)]/Z(H_0)$, where H_e is the external magnetic field and $H_0 = 100$ Oe. Fig. 1 (b) shows the field dependence of the MI ratio calculated at the frequency $f = 100$ MHz for the multilayer without ferrogel and multilayer with ferrogel for different values of the effective stray field H_p. The frequency dependence of the maximum MI ratio $(\Delta Z/Z)_{max}$ for the same multilayer is shown in Fig. 1 (c). In the presence of the gel without magnetic nanoparticles ($H_p = 0$), the MI ratio increases due to high permittivity of the gel. The effective stray field increases with the concentration of nanoparticles due to a growth of the ferrogel saturation magnetization. The stray field decreases the transverse permeability in the permalloy sub-layer, and, as a result, the MI ratio decreases with an increase of the stray field H_p. The calculated dependences are in a qualitative agreement with experimental results [4,5].

References

[1] G.V. Kurlyandskaya, M.L. Sánchez et al. Appl. Phys. Lett. 82, 3053 (2003).
[2] F.S. Blanc-Béguin, S. Nabily et al. J. Magn. Magn. Mater. 321, 192 (2009).
[3] T. Wang, Y. Zhou, et al. Biosens. Bioelectron. 90, 418 (2017).
[4] G.V. Kurlyandskaya, E. Fernandez et al. Appl. Phys. Lett. 106, 193702 (2015).
[5] N.A. Buznikov, A.P. Safronov et al. Biosens. Bioelectron. 117, 366 (2018).
[6] G.V. Kurlyandskaya, L. Elbaile et al. J. Phys.: Condens. Matter 16, 6561 (2004).
[7] G.V. Kurlyandskaya, A.A. Chlenova et al. J. Magn. Magn. Mater. 383, 220 (2015).
[8] N.A. Buznikov and G.V. Kurlyandskaya, Sensors 19, 176 (2019).

Multimagnetic core/shell microwires with asymmetric nano-shell

V. Kolesnikova[1], I. Baraban[1], M. Vazquez[2], M. Gorshenkov[3], V. Rodionova[1,3]

[1]*Immanuel Kant Baltic Federal University, 236004, Kaliningrad, Russia*
[2] *Institute of Materials Science of Madrid, CSIC. 28049 Madrid. Spain*
[3] *National University of Science and Technology "MISIS", Moscow 119049, Russia*

The family microwires (amorphous, nanocrystalline, bi- and multiphase) are used for logic, coding and sensing devices [1-3], for μ-magnets applications [4] and actuators [5,6]. A novel family of core/shell bimagnetic microwires is here introduced consisting of a cylindrical magnetic core covered by a concentric but asymmetric external shell. The two magnetic phases are isolated by an intermediate glassy microtube and are designed to show differential soft/soft or soft/hard magnetic behavior.

In this work either soft FeNi or harder Co polycrystalline shell was asymmetrically sputtered onto a precursor glass-coated rapidly solidified soft magnetostrictive Fe-based and Co-based microwire. The magnetic and mechanical properties have been investigated in terms of the asymmetric nano-shell influence on the banding and magnetic response. An initial characterization was performed by XRD and HRTEM to determine the structural features and identify the crystalline phases. Bulk magnetic properties of each magnetic phase were analyzed by vibrating sample magnetometry (VSM) and the hysteretic contributions of the shell were compared to local surface hysteresis loops determined by magneto-optical Kerr effect. The azimuthal angular dependence of MOKE surface loops allows us to confirm the asymmetry of the shell. To understand the origin of the magnetic interaction between the different magnetic phases FORC-analysis was applied. FORC-curves and magnetic properties were measured via VSM. Differences between magnetic properties of the magnetic phases as well as clearly observed interactions were shown in the Switching Field Distribution (SFD) plots and in the FORC – diagrams. The magnetostrictive action of a DC magnetic field proves to compensate the spontaneous bending observed in such microwires. The asymmetric shell confers outstanding technical magnetic properties to these bimagnetic microwires very suitable for sensing and particularly microactuator applications

References

[1] Sulla I. et al., J. Elect. Eng. 66.7 (2015): 161-163.
[2] Gudoshnikov S., et al. Physica status solidi (a) 211.5 (2014): 980-985.
[3] Morón C., et al. Sensors 15.11 (2015): 28340-28366.
[4] Hoshino K., et al. Lab on a Chip 11.20 (2011): 3449-3457.
[5] Torrejón J., et al. Sensor Letters 7.3 (2009): 236-239.
[6] Serrano I. G., et al. Journal of Applied Physics 115, 033903 (2014).

Bismuth-substituted Yttrium Iron Garnet locally crystallized by laser at controlled gas atmosphere

Shelaev A.V.[1], Sgibnev E.M [1], Salatov A.V.[1,2], Tananaev P.N.[1], Yankovskii G.M.[1], Baryshev A.V.[1]

[1]*Dukhov Research Institute of Automatics (VNIIA), 127055, Moscow, Russia*
[2]*Mendeleev University of Chemical Technology of Russia, 125047, Moscow, Russia*

Bismuth-substituted Yttrium Iron Garnet (Bi:YIG) is one of the most prominent materials for spintronics and photonics [1, 2]. The ability of microfabrication crystallized Bi:YIG thin film expands possible applications of this material. We report on local crystallization of metal-oxide film under a laser irradiation. Crystallization was performed by a 525 nm laser with pulse duration of 200 fs, repetition rate of 80 MHz and pulse energy 14nJ. Laser beam was focused to a spot size of about 100 μm and crystallization was performed when writing by the spot at a speed of 100 μm/s.

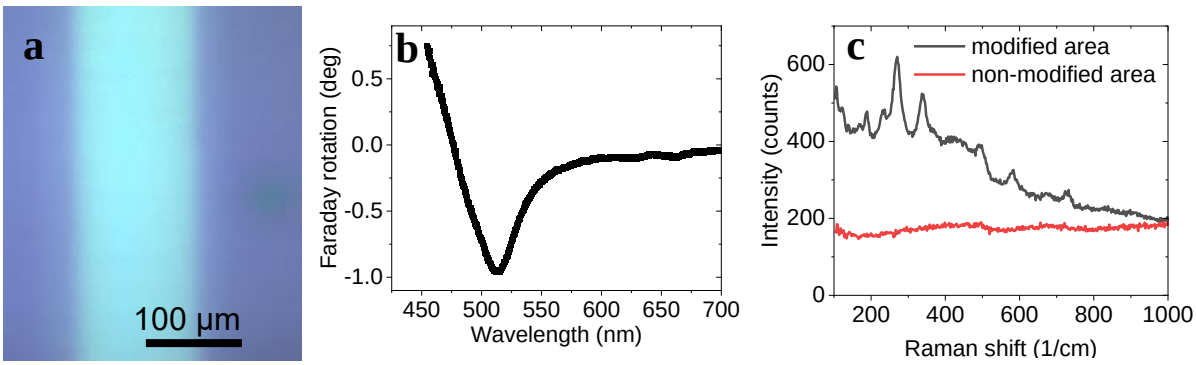

Optical image of crystallized garnet area (a), Faraday rotation (b) and Raman shift (c) spectra. Crystallization was done in air at room conditions.

Bi:YIG was obtained as a result of local laser annealing of an initial metal-oxide film due to its thermal decomposition followed by crystallization. In the viewing microscope it is clearly seen the bright line on the dark substrate (see image a). Local changes in magneto-optical properties, transmission, Raman spectroscopy and topography were studied. Faraday rotation from center of modified area was about -1 degree at 510 nm (plot b). In the Raman spectra taken from non-modified area, there were no Raman peaks. It indicates the absence of crystal structure in the initial oxide film. In the Raman spectra from the center of modified area, there were intensive peaks which represent crystal structure of Bi:YIG (plot c).

To investigate influence of the atmosphere on crystallization regimes and magneto-optical properties of Bi:YIG, the experiment was performed when irradiating initial metal-oxide film placed into a gas cell that was supplied with different gases (N_2, O_2, air and Ar).

References

[1] Yang, Y., Liu, T., Bi, L., & Deng, L. J. Alloys Compd., 860, 158235 (2021).

[2] M. Inoue, M. Levy, A.V. Baryshev, Magnetophotonics: from theory to applications (Springer, 2013).

Cryogenic transmission electron microscopy in material science.

Vasiliev A.L. [1], [2]

[1]*National Research Center "Kurchatov Institute", Moscow 123182, Russia*
[2]*A.Shubnikov Institute of Crystallography of FSRC "Crystallography and Photonics" Russian Academy of Sciences, Moscow 119333, Russia*

During last years, the electron microscopy (EM) instrumentation and techniques have changed drastically. Spherical aberration correctors (Cs-correctors) of electromagnetic lenses, electron gun monochromators, new high-performance electron-optical systems make it possible to focus the beam on the sample with the probe diameter less than 1 Å, and the ultra-pure vacuum allows obtaining nanodiffraction patterns from particles of sub-nanometer size. The Cs corrected condenser systems permit to obtain electron-beam images with a high resolution in Z-contrast mode with a sub angstrom resolution allowing to detect point defects like atomic vacancies or substitutions. Another amazing direction of transmission EM (TEM) is the cryogenic TEM (Cryo-TEM). Of course, in the first order this method was applied to the study of proteins, viruses and macromolecules. Three founders of this method, namely J. Dubochet, J. Frank and R. Henderson were awarded the Nobel Prise in Chemistry in 2017. The number of investigations in this area exceed by now 16K releases. There are two methods in life science Cryo-TEM: single particles analysis and tomography. The second methods can be successively applied to the study of material science specimens. The 3D reconstruction of different microstructures, which cannot be studied by conventional 3D TEM, was performed using Cryo-TEM. That could be electron beam sensitive or liquid contain materials, even hydrosols. One remarkable example is the study of detonation nanodiamonds (DND) hydrosols [1]. Remarkable hysteresis of viscosity founded in the samples have been explained in the frame of percolation theory based on the network formation due to faceted DND particles interactions (see Fig.1).

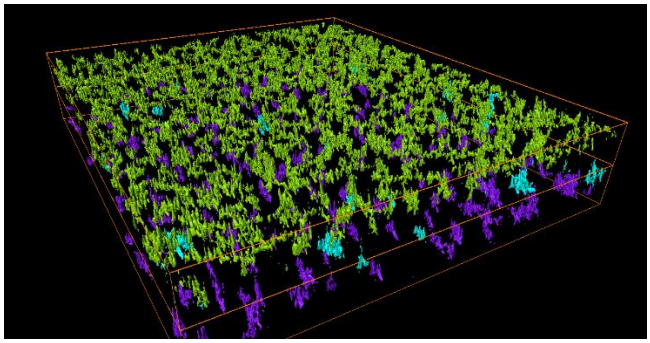

Fig.1. Cryo-electron tomography 3D model for 1 wt% nanodiamonds hydrosol with positive ζ-potential.

Other examples like gold nanoparticles in water solution and palygorskite particles contain water will be present.

References

[1] N.M. Kuznetsov, S.I. Belousov, A.V.Bakirov, et al. Carbon 161, 486 (2020).

THz radiation spectra of nanowires of magnetic metals

Fomin L.[1], Krishtop V.[1,2], Zagorskiy D.[3],Doludenko I.[3],Chigarev S.[4],Vilkov E.[4],Zhukova E.[2,5]

[1]Inst. of Microelectronics Technology and High Pure Materials, Chernogolovka, Russia
[2]Moscow Institute of Physics and Technology, Dolgoprydny, Russia
[3]Shubnikov Institute of Crystallography of RAS, 119333,Moscow, Russia
[4]Fryazino Branch of Institute of Radioelectronic Engineers of RAS , Fryazino, Russia
[5]Institute of General Physics of RAS. Moscow, Russia

Metal nanowires (NWs) obtained by the matrix synthesis method are of particular interest. The advantage of the method is its variability, the ability to obtain various types of NWs in the pores of the matrix. The first works were devoted to the deposition of NWs from one metal, then multicomponent NWs were obtained - homogeneous (so-called alloys) and heterogeneous (so-called layered). One more application of structures based on NW was proposed: for the generation of terahertz radiation. In theoretical works [1, 2], the possibility of spin-injection radiation (in the freq. range 3–40 THz) in structures with transitions between magnetic metals, when currents of 10^5–10^7 A / cm^2 flow through them, were predicted.

Spin injection by current through a nanojunction between two ferromagnetic metals can lead to a significant nonequilibrium accumulation of spin in the region of the immediate vicinity of the contact. In particular, an inverted population of the spin subbands of a ferromagnet can arise, into which hot electrons that are not spin equilibrium are injected. In this case, radiative spin-flip transitions of conduction electrons will take place, which can be stimulated indirectly through the s-d exchange interaction with the electromagnetic wave. The frequency of radiation is determined by the energy of the effective exchange splitting of the spin subbands and lies in the terahertz (THz) range.

In this work, we studied arrays of heterogeneous NWs from two ferromagnetic materials - Ni / Co, FeNi / Co and Ni / Fe. The emission and absorption spectra of the samples were studied on a Golay cell and a Bruker "Vertex80v" IR Fourier spectrometer in the THz range depending on the current density in the NWs. The nonthermal nature of the radiation is shown. In the range 55 150 THz, the transmittance of -polyethylene (the matrix in which the NWs array is located) is about 90%, which makes it possible to use it as a medium for operation in this range. The dips at frequencies around 90 and 104 THz are due to absorption by polymer bonds. The transmittance of the membrane with NWs is reduced (for example, up to 20% for Ni / Co wires).

Additional peaks appear at 56 and 60 THz for Ni / Co NW, 73 and 113 THz for FeNi / Co NWs, and 57, 70, and 114 THz for Ni / Fe NWs. Thus, NWs arrays increase the absorption of the membrane in the entire investigated frequency range, and this absorption depends on the NWs material. Further study of emission and absorption spectra is aimed at creating sources and detectors of THz radiation.

References

[1] A. Kadigrobov, R. Shechter, M. Johnson. Phys. Low Temp.,V.31, N3-4, P.463
[2] Yu.Guliaev, P. Zilberman, Chigarev S.et al. ZhETP Letters, V.1. P.16.

Property control of h-BN nanosheets via tailoring of its orientation and composition

Merenkov I.S.[1,2], Varrla E.[3]

[1]*Skolkovo institute of science and technology, 121205, Moscow, Russia*
[2]*Nikolaev institute of inorganic chemistry, 630090, Novosibirsk, Russia*
[3]*SRM Institute of Science and Technology, 603203, Kattankulathur, India*

Two-dimensional nanostructures and single-layered materials are the forefronts of materials science. In particular, h-BN nanosheets are well-known for outstanding thermal conductivity and electronic properties, in addition to excellent mechanical strength, chemical inertness, and distinctive deep UV luminescence. These and many other properties make pristine and functionalized h-BN nanosheets highly-promising for diverse applications in biomedical, electronic, composite, environmental and sustainable energy-related fields. Many of these applications rely on the structural and morphological properties determined by the dimensionality, content and orientation of the structures.

However, the presently available options to control dimensionality, content and orientation of h-BN nanostructures are more less explored and utilized as compared to similar carbon nanostructures, even though h-BN is an isostructural analog of carbon. Indeed, a very large number of publications report on graphene sheets with different orientations including vertical oriented structures (nanowalls). This morphological flexibility combined with graphitic structure and chemical modification possibility make them ideal for applications in electrochemical capacitors, electron emitting, environmental and bio-sensing devices. In contrast, only a limited number of articles on the synthesis and no reports on composition modification of vertically oriented h-BN nanosheets (h-BN nanowalls (BNNWs)) have been published so far.

Here, we will report how using of organoboron compounds, such as amine-boranes, and low-temperature thermally non-equilibrium plasma in chemical vapor deposition (CVD) process can result to form the oriented and ordered h-BN structures with controlled carbon doping. Simple variation of the process temperature makes it possible to produce different morphological types of h-BN nanowalls. We performed a study of structural features, cytotoxicity, thermal stability and luminescence of these morphological types. The h-BN lattice of nanowalls can contain the graphene domains, which amount was successfully controlled by content of the initial gas mixture. In addition, we will present study of thermal stability of h-BN nanowalls in oxidative (air) and inert (argon) atmospheres. Annealing in oxygen-containing atmosphere resulted to formation oxygen-doped h-BN nanowalls that demonstrated enhanced luminescent properties in the blue-green region. Significant cytotoxicity of morphologically different h-BN nanowalls against E. coli was demonstrated for the first time.

The reported study was funded by the RFBR and DST according to research project 19-53-45012.

Crystallization of bismuth-substituted yttrium iron garnet under low power femtosecond laser irradiation

Sgibnev E.M.[1], Shelaev A.V.[1], Kulikova D.P.[1,2], Salatov A.V.[1,3], Tananaev P.N.[1], Yankovskii G.M.[1], Baryshev A.V.[1]

[1]*Dukhov Research Institute of Automatics (VNIIA), 127055, Moscow, Russia*
[2]*Lomonosov Moscow State University, 119991, Moscow, Russia*
[3]*MendeleevUniversity of Chemical Technology of Russia, 125047, Moscow, Russia*

Bismuth-substituted yttrium iron garnet (Bi:YIG) is one of the most extensively studied and widely used material for magneto-optical devices development [1]. Conventional methods of Bi:YIG synthesis include liquid phase epitaxy, pulsed laser deposition, sputtering, and metal-organic decomposition (MOD). The latter is characterized by simplicity, flexibility, low cost, and scalability of the process. The MOD technique is based on spin-coating of a metal-organic solution, drying the solution, annealing at temperature around 400°C for oxidation of organics, and crystallization of Bi:YIG from the oxide film obtained at the previous step at temperature 600-800°C [2]. This high-temperature annealing is a limiting factor for fabrication of high-efficient 1D magnetophotonic crystals as it may result in occurring of cracks, crystallization, and changing optical properties of Bragg mirror layers.

The 200 nm oxide film was fabricated by the MOD method as reported earlier [3]. For Bi:YIG crystallization a laser beam was focused with a micro-objective (10×, NA=0.25) on the sample placed on an XY motorized stage, scanning speed was 100 μm/s. The center wavelength, pulse duration, and repetition rate were 525 nm, 200 fs, and 80 MHz, respectively. For further study seven 2×2 mm squares were annealed by the femtosecond laser with pulse energy in the range of 9-24 nJ. The irradiated film was characterized by optical and Raman spectroscopies, optical and atomic-force microscopies, and ellipsometry. Ellipsometric parameter ψ measured with an applied external magnetic field was used to calculate Faraday rotation.

Faraday rotation spectra of the structures recorded with different pulse energy are shown in Fig. 1a. The unmodified oxide film and irradiated with the pulse energy 9 nJ showed no magneto-optical properties. Structures irradiated with the higher pulse energy possessed Faraday rotation spectra typical for Bi:YIG films with the minimum in the green spectral range. Faraday rotation amplitude was found to continuously grow with the pulse energy up to 21 nJ reaching -1.3 degrees (Fig. 1b). Further increase in the pulse energy up to 24 nJ resulted in lowering Faraday rotation. It should be noted that Bi:YIG obtained by thermal annealing in a furnace possessed Faraday rotation -2.5 degrees at 515 nm that almost in two times higher compared to the laser-annealed film. This stems from the inhomogeneous annealing obtained after the laser-induced crystallization (Fig. 2). Originally reddish-brown film turned to green, yellow, orange, and even black depending on the pulse energy. Black color in optical images was related to growth of Fe_2O_3 phase as revealed by Raman spectroscopy. Iron oxide(III) formation was also the reason for decrease in Faraday rotation observed after the laser irradiation with the pulse energy equaled to 24 nJ.

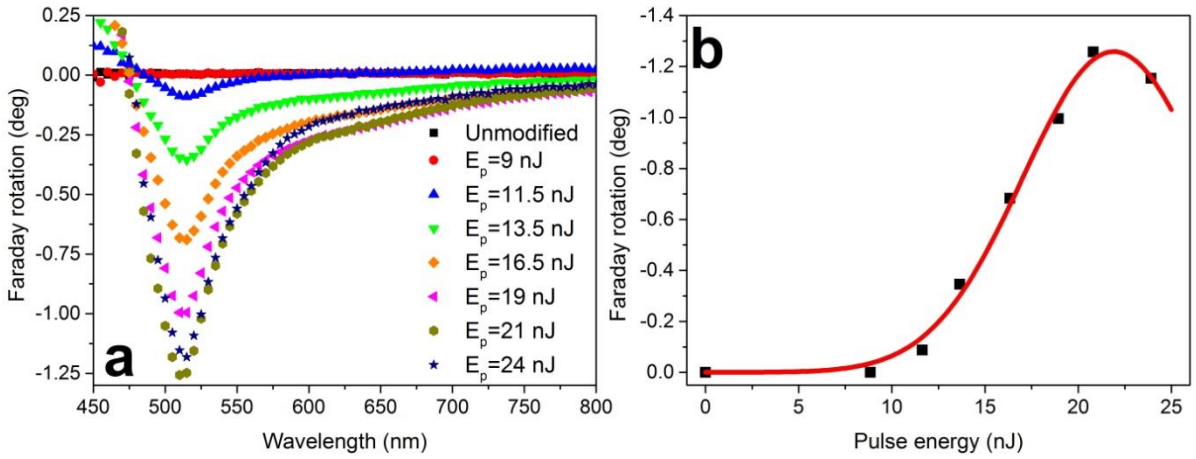

Fig. 1. Faraday rotation spectra of the unmodified oxide film and irradiated by femtosecond laser pulses with different energy (a), dependence of Faraday rotation at 515 nm on the pulse energy (b).

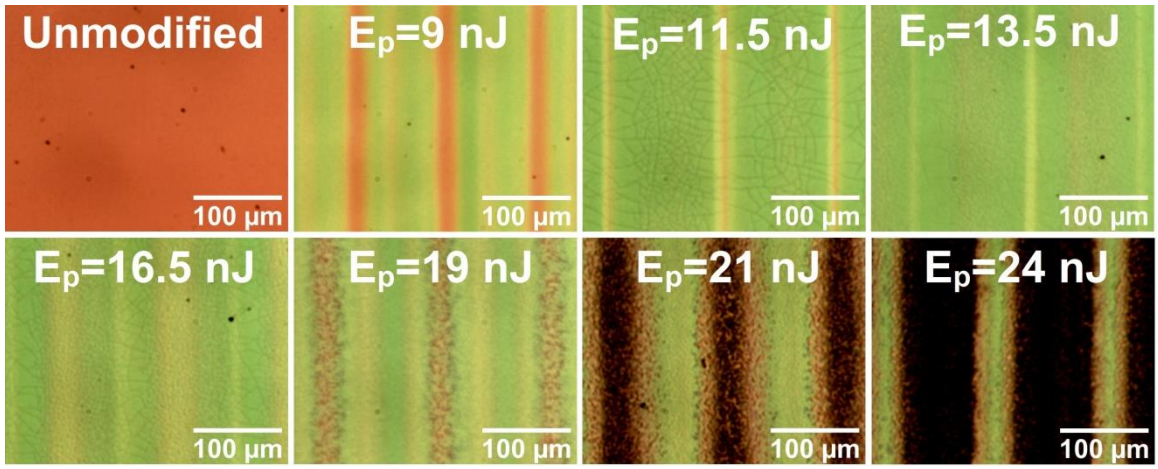

Fig. 2. Optical images of the non-irradiated oxide film and irradiated by femtosecond laser pulses with different energy.

The possibility of Bi:YIG crystallization from oxide film prepared by the MOD technique was demonstrated and studied. Faraday rotation spectra typical for Bi:YIG films were observed after the laser irradiation with the pulse energy in the range 12-24 nJ. Growth of hematite crystal phase took place under laser pulses with the energy above 20 nJ. Further optimization of the laser-induced crystallization is required to improve magneto-optical properties of Bi:YIG thin films. Laser-induced crystallization of Bi:YIG is the promising technique for fabrication of high-efficient 1D and 2D magnetophotonic crystals and waveguide magneto-optical devices.

References

[1] A.A. Voronov, D.O. Ignatyeva, N.A. Gusev, P.M. Vetoshko, N.V. Lugovskoy, Y. Song, V.N. Berzhansky, and V.I. Belotelov, in Inorganic and Organic Thin Films: Fundamentals, Fabrication, and Applications (Wiley-VCH, Weinheim, 2021).

[2] T. Ishibashi, T. Kosaka, M. Naganuma, and T. Nomura, J. Phys. Conf. Ser. 200, 112002 (2010).

[3] S.L Efremova, A.V. Salatov, D.P. Kulikova, A.A. Kasyanov, I.V. Bykov, K.N Afanasiev, P.N. Tananaev, and A.V. Baryshev, submitted to J. Phys. D Appl. Phys.

UHF negative magnetoresistance of composite metal-dielectric films CoFeB/SiO2

Kotov L.N.[1], Lasek M.P.[1], Vlasov V.S.[1], Kalinin Yu.V.[2], Sitnikov A.V.[2]

[1]*Pitirim Sorokin Syktyvkar State University, 167001, Syktyvkar, Russia*
[2]*Voronezh State Technical University, 394006, Voronezh, Russia*

This paper reports a UHF negative magnetoresistance (M) in composite metal-dielectric films was observed. M was defined as $(|Z_H|-|Z_0|)/|Z_0|$ where $|Z_H|$ and $|Z_0|$ are absolute values of impedances of the films in static magnetic and without magnetic fields respectively. The films were constituted by ferromagnetic nanoparticles of CoFeB alloy in an insulating amorphous SiO2 matrix have been studied. Negative UHF magnetoresistance was observed in the longitudinal configuration that is, when the current is parallel to the magnetic field and the magnetic field is in plane of the films. The investigated films were received by the ion beam sputtering method in the argon atmosphere with pressure 0.04 Pa [1]. Atomic compositions of the films were determined by a scanning electron microscope Tescan Mira 3. The atomic compositions of the films were $(Co_{0.44}Fe_{0.36}B_{0.20})_x(SiO_2)_y$ where x was from 0.42 to 0.85 and y=(1-x)/3. Magnetic force microscopy images of the composite films were obtained by atomic force microscope Integra Prima. Spectrum analyzer (INSTEK GSP-7830), sweep-frequency generator, coplanar line and electromagnet were used to study the UHF magnetoresistance spectra. The frequency range was from 0.2 GHz to 3 GHz. The range of magnetic field was from 0 to 7 kOe. The films were put in the rupture of the centre conductor of the coplanar line. The coplanar line was connected with sweep-frequency generator and spectrum analyzer. All measurements were obtained at room temperature.

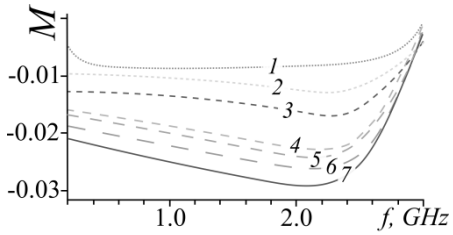

Fig. 1. Magnetoresistance spectrum of $(Co_{0.44}Fe_{0.36}B_{0.02})_{0.67}(SiO_2)_{0.11}$ film where number of line corresponds to magnetic field in kOe

The negative magnetoresistance was observed in the composite films for x from 0.67 to 0.85. Maximum value of the negative magnetoresistance was equal to 6% and observed for x=0.84, H=7 kOe and f=1.2 GHz. Frequency range of the magnetoresistance was dependences of *x*. An increase of the x led to a decrease of the frequency range with the maximum value of the negative magnetoresistance.

The study was supported by a grant from the Russian Science Foundation (project No. 21-72-20048).

References

[1] Antonets I.V., Kotov L.N., Kalinin Yu.E., Sitnikov A.V., Shavrov V.G., Sheglov V.I., Technical Physics Letters, 40 (7), 584-586 (2014).

Self-oscillations in a freely suspended amorphous tape of Ti2NiCu alloy under the influence of an electric current

Morozov E.V., Koledov V.V., Shavrov V.G.

Kotelnikov Institute of Radioengineering and Electronics (IRE) of Russian Academy of Sciences, Moscow, Russia

In recent years, the creation and study of new functional materials has been of great interest. Many works are devoted to miniature and high-speed actuators based on alloys with a thermoelastic martensitic transition and shape memory effect (SME); could be the basis of a new solid-state cooling technology.

Analysis of the world literature shows that studies of amorphous alloys and amorphous-crystalline composites attract a lot of attention [1-3]. In [1], the amorphization of metals leads to an increase in their strength. In [3], it is said about the improvement of corrosion resistance during the amorphization of metals.

The authors of the work noticed an unexpected effect of the appearance of self-oscillations in a freely suspended strip of Ti_2NiCu amorphous alloy under the influence of a direct electric current (Fig.1). At a load of up to 1.2 MPa and at a current of 0.7 A to 1 A, the effect of the appearance of oscillations in an amorphous tape 40 μm thick, 1.5 mm wide and over 25 sm long is observed. At higher current values, the tape begins to anneal and pass into the crystalline austenitic phase of the Ti2NiCu alloy. At current values less than 0.7 A, no oscillations were observed.

(a) (b)

Fig.1. Photos during the experiment. a) no oscillations, b) oscillations are present

When the DC current reaches a critical value, at which oscillations appear, oscillations of the first type first appear. With some anticipation, the swinging belt begins to tremble and vibrations of the second type arise. With a further increase in the current strength, the tape continues to support both types of oscillations, with a decrease in the current strength, the oscillations disappear.

This work was supported by Grant of the Russian Science Foundation 17-19-01748

References

[1] Inoue A, Acta mater. 48, 1, 279 (2000).

[2] Lu Z. et al. J. Iron Steel Res. Int. 23, 1, 37 (2016).

[3] Dai H. et al. Appl. Sci. 8, 6, 956 (2018).

Magnetic circular dichroism and Faraday effect of Bi-containing nanometer-thick garnet films

Fedorov A.S.[1,2], Fedorova A.A.[1,2], Safonov S.S.[1], Kotov V.A.[1], Nikitov S.A.[1,2], Stognii A.I.[3], Logunov M.V.[1]

[1]*Kotel'nikov Institute of Radio-Engineering and Electronics of RAS, 125009, Moscow, Russia*
[2]*Moscow Institute of Physics and Technology, 141701, Dolgoprudny, Moscow Region, Russia*
[3]*Scientific and Practical Center for Materials Science of NAS, 220072, Minsk, Belarus*

The magneto-optical effects are used in numerous applications [1]. Their practical inertia-free nature also makes it possible to use them to study ultrafast processes in magnetic materials in the nano-, pico-, and femtosecond ranges of durations [2-4]. Iron garnet films with the addition of bismuth have record values of the Faraday effect, which allows them to be used as the basis of applied devices and used as a model dielectric medium for the study of fast-flowing processes. In this work, we study the magnetic circular dichroism (MCD) and the Faraday effect (FE) of iron garnet films depending on the film thickness. To do this, areas with different thicknesses (270, 175, 75, ~1 nm) were formed in polycrystalline Bi-YIG film by ion-beam sputtering with an oxygen ion beam [5]. It is found that the film has a high uniformity of parameters in thickness (Fig.1). It is shown that for the study of ultrathin films, it is preferable to register the MCD, and then, using the Kramers-Kronig relations, it is possible to effectively restore the FE spectra for ultrathin films.

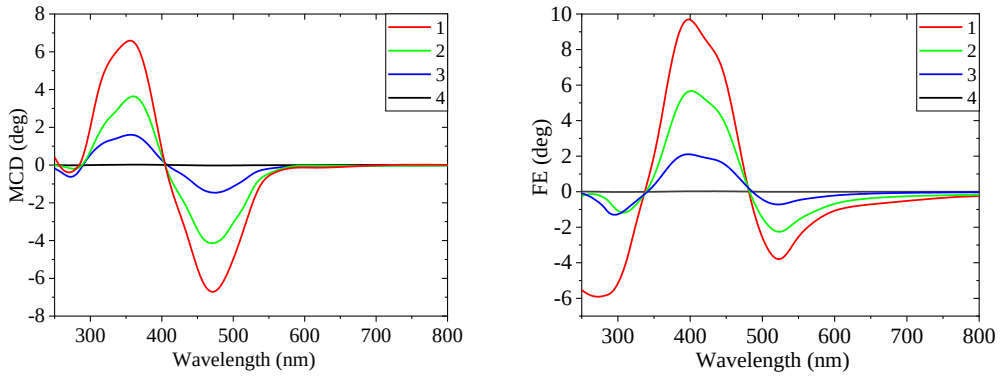

Fig. 1. MCD and FE spectra for film areas with different thicknesses.

The work was supported by the Russian Foundation for Basic Research, projects No.18-52-16006 and 18-29-27020.

References

[1] A.K. Zvezdin and V.A. Kotov, Modern Magnetooptics and Magnetooptical Materials (IOP Publishing, Bristol, Philadelphia, 1997).

[2] M.V. Gerasimov, M.V. Logunov, A.V.Spirin et al., Phys. Rev. B 94, 014434 (2016).

[3] A. Stupakiewicz, K. Szerenos, D. Afanasiev et al., Nature 542, 71, (2017).

[4] S. A. Nikitov, A. R. Safin, D. V. Kalyabin et al., Phys. Usp. 190, 945 (2020).

[5] M.V. Logunov, S.A. Nikitov, A.I. Stognii et al., Bull. RAS: Physics, 83, 866 (2019).

Local atomic structure and magnetic properties of amorphous iron-based alloys deformed by high-pressure torsion at different temperatures

Sundeev R.V.[1], Shalimova A.V.[2], Glezer A.M.[2], Veligzhanin A.A.[3], Perov N.S.[4], Alekhina Yu.A.[4]

[1] "MIREA - Russian Technological University", 119454, Moscow, Russia
[2] I.P. Bardin Science Institute for Ferrous Metallurgy, 105005, Russia
3 National Research Centre "Kurchatov Institute", 123182, Moscow, Russia
[4] Department of Physics, Lomonosov Moscow State University, 119991, Moscow, Russia

The study of soft magnetic amorphous alloys is one of the important directions in condensed matter physics. As a rule, amorphous soft magnetic alloys (ASMA) based on ferromagnetic components have higher magnetic characteristics than crystalline analogs and are harder at room temperatures. Some properties of ASMA, e.g., high magnetic permeability, low magnetic anisotropy (lower than that of crystalline alloys by two orders of magnitude), and high electrical resistivity, which substantially reduces Foucault current losses, are directly related to their disordered structure and cannot be achieved in crystalline alloys. However, like all amorphous alloys obtained by melt quenching (MQ), ASMA are metastable; therefore, the unique properties of such materials noticeably change under external actions. Since recently, the attention of researchers has been attracted by the effect of the change in the magnetic properties of amorphous alloys under external actions, which mainly retain the amorphous structure of the alloys. The question of how the magnetic properties of ASMA can change under extreme conditions of high-pressure torsion (HPT) at different temperatures and degrees of deformation is of great interest. To solve this problem, we thoroughly experimentally studied the evolution of the local atomic structure of amorphous ferromagnetic materials upon HPT.

In this work, we studied the Fe-based $Fe_{50}Ni_{33}B_{17}$, $Fe_{54}Ni_{29}B_{17}$, $Fe_{58}Ni_{25}B_{17}$ and $Fe_{75}Si_8B_{17}$ ASMA with the same B content. The ribbons of the alloys were obtained by melt spinning in an argon atmosphere at a melt quenching rate of 10^5-10^6 K/s. The resulting ribbons of the amorphous alloys were 8-10 mm wide and 20-30 microns thick.

The structure of the amorphous alloys was identified by X-ray diffraction (XRD) and transmission electron microscopy (TEM) methods. All alloys in the amorphous state were deformed by the HPT method to a degree of deformation corresponding to n = 1 (where n is the number of full revolutions of the movable anvil) at room temperature (293K) and boiling point of liquid nitrogen (77K). Differential scanning calorimetry with a Setaram DSC 111 setup at a heating rate of 20 K/min was used to study the alloys after MQ and HPT at different temperatures. Magnetic properties were determined at room temperature with a Lake Shore model 7407 vibrating magnetometer in fields of up to 1.7 T. The EXAFS (Extended X-Ray Absorption Fine Structure) spectra above the *K*-edges of the absorption of Ni and Fe were measured at the Structural Materials Science end station at the Siberia-2 facility of the Kurchatov synchrotron radiation source in transmission mode at room temperature.

The initially amorphous alloys remain amorphous after HPT at 77K according to the XRD and TEM data. The analysis of the EXAFS spectra showed that, upon HPT, both the chemical environment of the selected Fe atom and the average interatomic distance of the Fe-Fe, Fe-Si, and Fe-Ni pairs change. The $Fe_{58}Ni_{25}B_{17}$ and $Fe_{75}Si_8B_{17}$ alloys revealed a change in

the nature of the composite short-range order for Fe atoms with a simultaneous decrease in the average interatomic distance for the Fe-Fe atom pairs. In the $Fe_{50}Ni_{33}B_{17}$ and $Fe_{54}Ni_{29}B_{17}$ alloys, no changes in the interatomic distances were observed for different pairs of atoms. Only a change in the chemical composition of the Fe atom environment, in which some of the Fe atoms are replaced by Ni atoms, is found in the alloys. A similar change in the local atomic structure in both cases leads to a decrease in the saturation magnetization in the Fe-based amorphous alloys studied after HPT at 77K (Fig. 1).

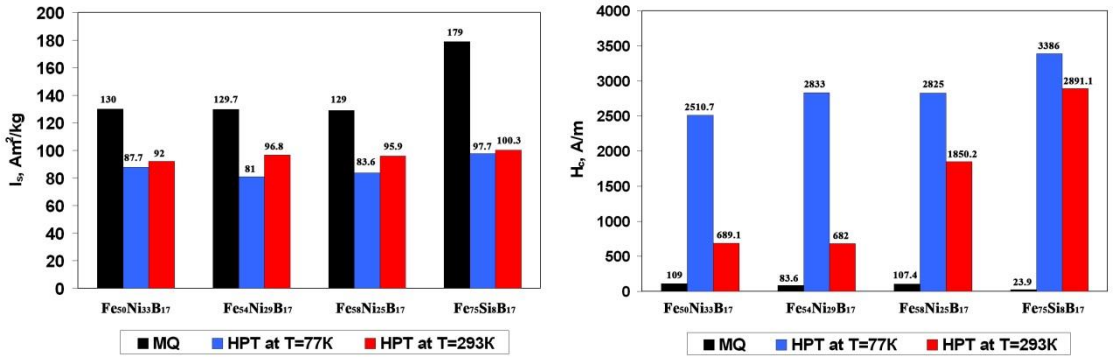

a) b)

Fig. 1. Magnetic properties of the $Fe_{58}Ni_{25}B_{17}$, $Fe_{54}Ni_{29}B_{17}$, $Fe_{50}Ni_{33}B_{17}$, and $Fe_{75}Si_8B_{17}$ alloys after MQ and HPT (n = 1) at 293 and 77K: (a) I_s in a field of 1.7 T, (b) H_c.

The sharp increase in the coercive force after HPT at 77K is explained by the absence of relaxation channels for elastic stresses due to the suppression of thermal activation processes. It is shown that HPT at 77K leads to the formation of the amorphous state that is more resistant to crystallization than that realized after MQ (Table 1).

Table 1. Results of calorimetric analysis of the Fe-based amorphous alloys:

Alloys	T_{cr}, K	ΔH_{MQ}, J/g	$\Delta H_{HPT-293}$ J/g	ΔH_{HPT-77} J/g	$\Delta H_{HPT-293}$ - ΔH_{MQ} J/g	ΔH_{HPT-77} - ΔH_{MQ} J/g	V_{cr} 293K
$Fe_{50}Ni_{33}B_{17}$	674	72	54	83	- 18	+11	0.25
$Fe_{54}Ni_{29}B_{17}$	689	80	67	90	- 13	+10	0.17
$Fe_{58}Ni_{25}B_{17}$	692	84	70	96	- 14	+12	0.17
$Fe_{75}Si_8B_{17}$	785	111	99	116	-12	+5	0.1

T_{cr} is the crystallization temperature of the alloy after MQ and HPT; ΔH_{MQ} is the crystallization thermal effect of the alloys after MQ; $\Delta H_{HPT-293}$ and ΔH_{HPT-77} are the crystallization thermal effects of the alloys after HPT at 293 and 77K, respectively.

This work was supported by the Russian Foundation for Basic Research (projects № 19-72-20066) and the grant of President of the Russian Federation (No. МК-43.2020.2).

Effect of isothermal and electric-pulse processing on the structure and properties of rapid-quenched $Ti_{50}Ni_{25}Cu_{25}$ ribbons with a surface crystal layer

Sitnikov N.N.[1,2], Shelyakov A.V.[2], Zaletova I.A.[1, 2]

[1]State Scientific Center «Keldysh Research Center», 125438, Moscow, Russia
[2]National Research Nuclear University MEPhI (Moscow Engineering Physics Institute), Kashirskoe sh. 31, 115409 Moscow, Russia

In the present work, laminated amorphous-crystalline $Ti_{50}Ni_{25}Cu_{25}$ alloy ribbons with different crystal layer thicknesses were obtained by rapid-quenched technique on a rotating disk (planar casting method) at cooling rates of about 10^5 K/s. The amorphous-crystalline ribbons were subjected to heat treatment in a calorimeter, isothermal treatment (IT) in a furnace (for 300 s) and electric-pulse processing (EPP) with a processing time of 5 s to 1 ms. The obtained samples were thoroughly studied using metallography, scanning electron microscopy (SEM), x-ray diffraction analysis and differential scanning calorimetry (DSC).

Studies have confirmed that in the obtained samples, the layer of the structure with a non-contact (free) surface of the ribbon with respect to the quenching disk is crystalline. At room temperature, x-ray diffraction pattern from a non-contact surface together with the B19 martensitic phase present a residual B2 austenitic phase. The residual B2 phase did not turn into B19 phase during cooling due to mechanical stresses in the surface crystal layer. It is noted that the most intense reflexes of the B19 phase are observed in the area of 58-65 degrees 2θ, and not in the area near 42 degrees, which is usually typical for this alloy. This arrangement of the main peaks indicates the texture of the surface crystal layer. In the crystal layer, B2-B19 phase transitions occur during thermal cycling in the range of martensitic transformation (MT).

The study of the effect of IT of amorphous-crystalline samples of ribbons in a muffle furnace was conducted at a temperature of 500 C with an exposure of 300 seconds in the "free" state and in a mandrel to preserve a straight shape. After crystallization in the free state, the samples are characterized by a curved shape. When the crystallized samples are heated to a temperature of 100 C, they do not exhibit shape memory effect (TWSME). Only a single SME is present in the samples, i.e. the samples restore the shape of the ring when heated after their preliminary deformation. After cooling, the samples retain the curved shape of the ring. Samples crystallized in a mandrel to preserve a straight shape are characterized by a straight shape after cooling and extraction from the mandrel. When the samples are heated to a temperature of 100 C, they bend slightly (much less than the bend when implementing TWSME in the initial rapid-quenched state) relative to the original straight shape, and when cooled to room temperature, they take a straight shape. Thus, there is a "weakened" (residual) TWSME. It is noted that in the samples crystallized in the mandrel, the value of the residual TWSME is greater than in the samples of ribbons with large thicknesses of the crystal layer in the initial state. To study the microstructure of the resulting samples, their transverse sections were made, as well as X-ray diffraction studies were carried out.

IT of amorphous-crystalline ribbons in mandrels that fix the ribbon in a certain position showed that this method allows the formation of a structure in the ribbons with internal stresses that lead to the manifestation of TWSME during thermal cycling in the MT range. The most

noticeable TWSME are in samples of amorphous-crystalline ribbons with a crystal layer thickness of more than 5 microns.

To carry out the crystallization of the amorphous state of rapid-quenched amorphous-crystalline ribbons made of Ti50Ni25Cu25 alloy without high-temperature exposure to preserve the characteristics of the initial crystal layer, an experimental setup was designed and upgraded, which allows heat treatment of thin rapid-quenched amorphous and amorphous-crystalline thin ribbons by passing a single or several pulses of electric current through the sample EPP. Studies have shown that in EPP with a duration of less than 1000 ms, the microstructure of the ribbons in cross-section has a non-uniform distribution of crystals over the thickness of the ribbon: a structure of columnar crystals is formed near the ribbon surfaces,and single or grouped large crystals are present in the volume of the ribbon. In the near-surface areas of the ribbons, crystals with a columnar structure are formed, and large crystals are formed in the middle part. Columnar crystals from the surface go into the inner part of the ribbon to the crystals formed in the volume of the ribbon, and an inhomogeneous boundary is formed. The proportion of columnar crystals increases with decreasing exposure time, and there are areas where columnar crystals touch in the central part of the ribbon, while a smooth interface is formed between them. At EPP with a duration of 10 ms or less, the transverse size of the crystals begins to decrease – columnar crystals are thinned, and large crystals are broken into smaller ones. During electro-pulse heat treatment in the loaded state, the proportion of columnar crystals touching in the middle part increases.

It is noted that columnar crystals on the non-contact side are formed from the initial crystal layer and repeat its crystallographic orientation. The crystallographic reflexes from the non-contact surface of the ribbon have a non-standard arrangement of the main reflexes of the B19 structure in the region of 58-65 degrees, and the peaks with a lower intensity are located in the region of 28-32 degrees. The crystallographic reflexes on the contact side of the ribbon after electro-pulse heat treatment are similar to those obtained after isothermal treatment. There are reflexes of phase B 19, located in the region of 38-46 degrees (main), and less obvious reflexes in the region of 58-65 degrees. Studies of DSCs have shown that the presence of different types of crystals in the distribution structure is consistent with the calorimetric effects and their stages during martensitic transformations.

In all the crystallized samples, a pronounced single SME is observed, but in the case of amorphous-crystalline ribbons with the application of a load in the obtained crystal samples, TWSME is observed with a different character than it was in the initial state: in the low-temperature state (martensitic), the ribbon is bent towards the initial amorphous layer (initial state); when heated above the temperature of the beginning of the austenitic transformation, the ribbon begins to straighten and then bends in the other direction (towards the initial crystal layer); upon subsequent cooling below the end temperature of the martensitic transformation, the ribbon takes its initial shape.

The study was carried out at the expense of a grant from the Russian Science Foundation (Project No. 19-12-00327).

The controlled synthesis of multilayer nanotubes performed by chemical vapor deposition.

Sokologorskiy.Y.Y.[1], Panov V.A.[1], Shamsuvaleev R.I.[1],
Lavrov.S.D.[1], Nikolaeva S.S.[2]

[1]*MIREA - Russian Technological University, 119454, Moscow, Russia.*
[2]*North Caucasus Federal University, 355017, Stavropol, Russia.*

Multilayer nanotubes are the perspective material for creating electronic devices. E.g., Field-effect transistors and diodes extensively used in solar cells. Carbon nanotubes (CNTs) can be conductors and semiconductors; therefore, they are the good basis for creating 2D-Thin Film Transistors [1]. Semiconductor features make possible the usage of Carbon Nanotubes as the solar cells diodes [2].

CVD-method allows the growing of nanotubes in the form of a relief layer. This structure is typical for the growth of nanotubes from a sol-gel catalyst. When the gel is heated, the bond between chlorine (Cl) and ammonia (NH4OH) is destroyed, and clusters of nickel (Ni) and nickel oxide (NiO) remain on the surface. Once in the chamber, ethanol (C2H5OH) is oxidized in the residual atmosphere to carbon monoxide (CO), then, getting on the catalyst, carbon monoxide (CO), by decomposition, is converted into carbon (C). A catalyst fraction (in which carbon dissolves) floats in a drop of its own adsorbate. As the temperature in the chamber decreases, the carbon (C) dissolved in the fraction begins to transform into the adsorbate, which subsequently desorbs into drops. A drop moving along the surface of the substrate leaves a trail in the form of a carbon nanotube.

The size of nanotubes depending on pressure and temperature does not change. Using CVD-method the temperature during the process of nanotubes growth will be 550 K (T = 550 K) and the pressure of 20 kPa (P = 20 kPa). This happens taking into account errors, due to the impossibility of creating an ideally equilibrium system. We can see changes in the surface relief of the nanotube layer, as well as in the number of nanotubes at different concentrations of reagents in the catalyst (fig.1). This is due to the number of sorption sites in the catalyst.

We have considered the following concentrations: 19 ml of ammonia (NH4OH) and 500 mg of nickel fractions (Nl) – a, 30 ml of ammonia (NH4OH) and 500 mg of nickel fractions (Nl) – b, 60 ml of ammonia (NH4OH) and 500 mg of nickel fractions (Nl) – c. The results are shown in Figure 1. The nanotubes were obtained using CVDomna machine.

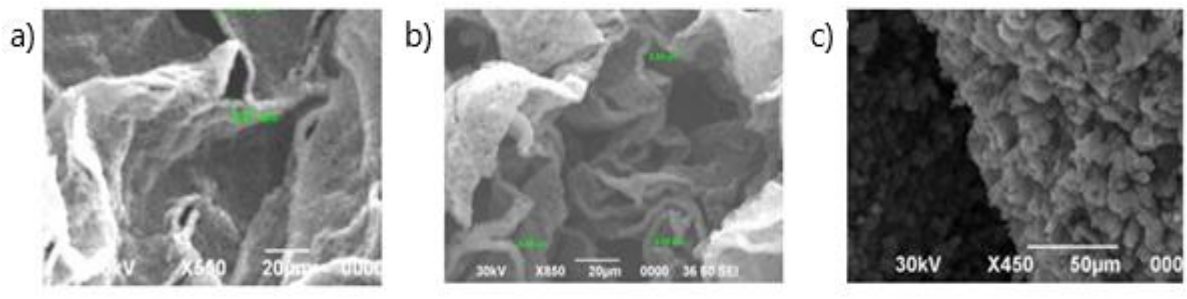

Figure 1. SEM-image of carbon nanotubes structures.

Based on the SEM-images, we can draw the following conclusions:

- It is possible to control the geometric parameters of the catalytic sites by varying the composition of the catalyst;
- The size of nanotube flocks decreases as the size of catalytic centers;
- The conductive features of the layer change due to the change in the geometric shapes of the nanotubes.

After applying the electrodes by magnetron sputtering method, we measured the current-voltage characteristics and resistance of areas with different relief. As the result, the type of electronic structure is determined.

This work was supported by the Ministry of Education and Science of the Russian Federation (state task No. FSFZ-0706-2020-0022).

References

[1] Katherine R. Jinkins. et al. //Substrate-Wide Confined Shear Alignment of Carbon Nanotubes for Thin Film Transistors (2018).

[2] Prathamesh A. Dhakras. et al. //Ideal p–n Diodes from Single-Walled Carbon Nanotubes for Use in Solar Cells: Beating the Detailed Balance Limit of Efficiency (2019).

Magnetoresistive composite materials based on organic matrixes

Kabirov Yu.V.[1], Sidorenko E.N.[1], Belokobylsky M.V.[1],
Klochnev A. M.[1], Prutsakova N.V.[2], Chernyaev V.V.[1]

[1]Department of Physics, Southern Federal University, Bolshaya Sadovaya street, 105/42, 344090, Rostov-on-Don, Russia
[2]Don State Technical University, Gagarin square 1, 344010, Rostov-on-Don, Russia

The creation of new composite materials with more than one response to external influences is of interest, both from a physical and practical point of view. It is known that composite materials may exhibit properties that are not inherent in the individual components that make up the composite [1, 2]. In our work, composite materials of polyethylene (or Na-carboxymethylcellulose)-graphite-manganite composition have been synthesized and investigated. For the synthesis of materials, low density polyethylene (LDPE), natural large crystal graphite (C) and manganite $La_{0.7}Sr_{0.3}MnO_3$ (LSMO) are used. Composites are characterized by X-ray diffraction and electron microscopy. Depending on the ratio of components, composites exhibit positive or negative magnetoresistivity. Materials of the composition 15%LDPE/55%C/30%LSMO have a positive magnetoresistive response 7.5% in a constant magnetic field 15 kOe due to the diamagnetism of graphite. The microstructure of one of the samples is shown in Fig. 1.

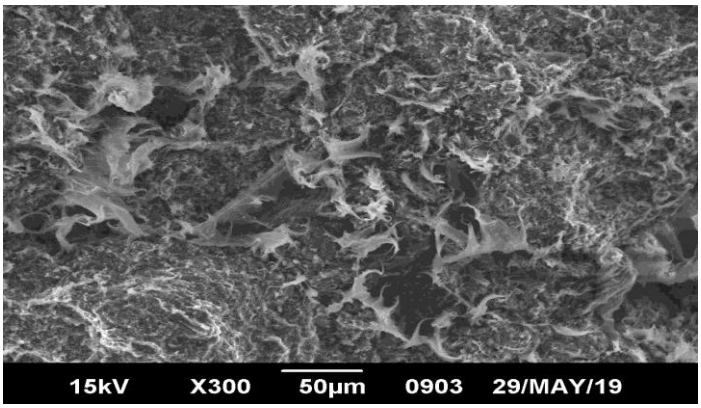

Fig. 1. Microstructure of a 15% LDPE/55% C/30%LSMO cleaved sample.

The microstructure contains amorphous polyethylene agglomerates and graphite particles, with an average size of about 5 microns. Composite materials 15%CMC/70%C/15%LSMO have even higher positive magnetoresistivity values of the order 10%.

References

[1] M. H. G. Wichmann, S. T. Buschhorn, J. Gehrmann, and K. Schulte // Phys. Rev. B 80, 245437-1-245437-8 (2009).

[2] Yu.V. Kabirov, A.S. Bogatin, Sidorenko E.N., M.V. Belokobylsky, A.S. Mikheykin, A.O. Letovaltsev, A.L. Bulanova, N.V. Prutsakova. Lett. on Mater., 9(2), 223-227 (2019).

Martensitic transformation at the nanoscale: experiment and computer simulations

P.V. Lega[1], A.I. Kartsev[2,3]

[1] *Kotelnikov Institute of Radioengineering and Electronics of Russian Academy of Sciences, 125009, Moscow, Russia*
[2] *Computing Center FEB RAS, Khabarovsk, 680063, Russia.*
[3] *Bauman Moscow State Technical University, Moscow, 105005, Russia*
E-mail: lega_peter@list.ru

The TiNi nano-plates deploying martensitic transition at critical temperature T_c was studied. We demonstrated that $T_c(h)$ has a strongly descending character as a function of plate thickness h [1]. Whereat the critical thickness h_c exist at which the transition is completely suppressed. Combining *ab-initio* and molecular dynamics (MD) simulations it was shown that austenite is more stable than martensite at nanometer-scaled plates. While the complete suppression of the phase transition occurs for a 10 nm thick plate which is in good agreement with an experimentally observed h_c value.

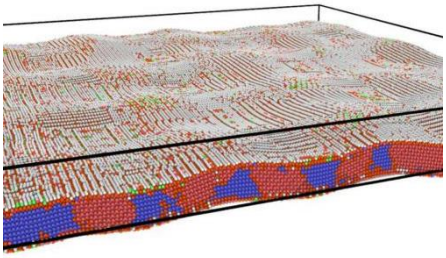

Fig. 1. Formation of the TiNi austenite phase simulated using the MD method within the LAMMPS package. The blue color denotes austenite (B2), the red color - martensite phase (B19).

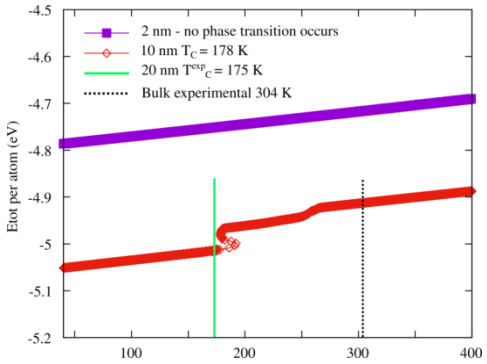

Fig. 2. Temperature dependence versus total Energy per atoms for 10 nm and 2 nm thickness of the TiNi plate using molecular dynamics simulation.

We performed an investigation on the crystal structures in the local areas of the wedge-shaped plates of the TiNi and Ti_2NiCu alloys in the thickness range of 10–100 nm in the temperature range of 100–400 K. We also observed that the area of the austenite phase expands with a decrease in temperature. While the transition temperature decreases with decreasing plate thickness and having a hysteretic character. The aforementioned behaviour is found to be in good agreement with density functional theory and molecular dynamics simulations (Fig. 1 and Fig. 2). This approach based on a nano-size control paves a new way of the shape memory effect modulation and fine-tuning work parameters of nanodevices.

Acknowledgement

The study was supported under the State task of Kotelnikov IRE RAS

References

[1] P.V. Lega, Phys. Rev. B 101, 214111 (2020).

Functional properties of multilayer structures based on aluminum nitride

Solnyshkin A.V.[1], Sergeeva O.N.[1], Shustova O.A.[1], Fenogenova V.V.[1],
Pronin I.P.[2], Sharofidinov Sh.Sh.[2]

[1]*Tver State University, 170100, Tver, Russia*
[2] *Ioffe Institute, 194021, St. Petersburg, Russia*

The properties of nitrides of metals of the third group, for example, AlN and GaN, make them unique and promising for the creation of electronic, optoelectronic and acoustoelectronic devices based on them. The presence of a simultaneously spontaneously polarized state makes it possible to use it as functional materials for pyroelectric applications.

This paper presents the results of studies of the dielectric and polar properties of multilayer structures based on aluminum nitride. The formation of alternating layers of aluminum and gallium nitride can lead to special piezoelectric and pyroelectric properties due to the formation of heterojunctions with a system of space charges. Figure 1 shows the SEM image of an AlN/AlGaN multilayer structure grown by chloride-hydride epitaxy on a Sic/Si template [1] followed by separation from the substrate and its energy-dispersion analysis.

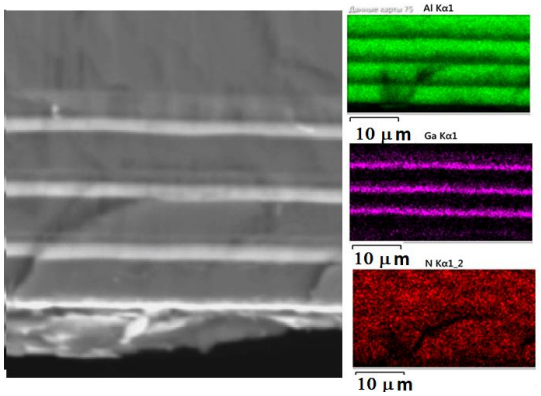

Fig. 1 SEM - image and energy dispersive analysis of a multilayer AlN / AlGaN structure

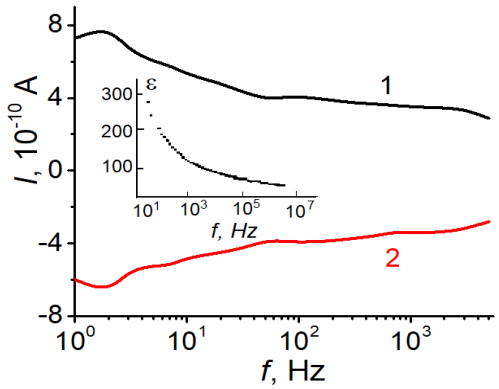

Fig. 2. Frequency dependences of the pyrocurrent and dielectric constant (inset) of the AlN / AlGaN multilayer structure

Dielectric properties were investigated using an E7-30 immittance meter in the frequency range 10 Hz - 3 MHz. Pyroelectric responses were investigated by a dynamic method using rectangular modulation of the heat flux. In fig. 2 shows the dispersion dependences of the pyroelectric current and, in the inset, the dielectric constant for the AlN / AlGaN structure.

If the strongly pronounced dispersion of the permittivity indicates the contribution of the interface boundaries of aluminum and galium nitride layers to the dielectric response, while the frequency dependences of the pyrocurrents (on heating (curve 1) and cooling (curve 2), Fig.2) indicates a sufficiently uniform distribution of polarization over the thickness of the structure, which makes structures based on aluminum nitride promising functional materials for pyrodetectors.

References

[1] S. A. Kukushkin and A. V. Osipov, J. Phys. D: Appl.Phys. **47**, 313001 (2014).

Atomic diffusion analysis of Al-Ti composite by atomistic simulation

Polyakova P.V.[1], Baimova J.A.[1]

[1]*Institute for metals superplasticity problems of the RAS, 450001, Ufa, Russia*

In-situ composites have attracted considerable scientific research interest recent years. It is a class of composites with the structure obtained in the course of any processing, when the precipitation of new phases occurs spontaneously. Earlier it was shown that the production of such composites can be observed at high-pressure torsion (HPT), since severe plastic deformation can facilitate diffusion [1-4].

Atomistic simulation is an effective tool for studying different processes on atomistic level. In the present work, atomistic simulation is applied to study atomic diffusion behavior at the bonding interface in the Al-Ti sample during compression combined with shear strain. Mechanical strength of the obtained composite is studied under uniaxial tension normal to the bonding interface.

The atomic structure of a bimetallic AlTi interface is presented in Fig. 1. A bilayer model of Ti (HCP lattice, green atoms) and Al (FCC lattice, blue atoms) is assembled from two unrelaxed perfect crystals with lattice parameters of a_{Mg} = 3.203 Å, c_{Mg} = 5,2 Å and a_{Al} = 4.05 Å. Crystal size is $L_x = L_y = L_z \approx 100$ Å. The interlayer distance between two crystals calculated as $(a_{\mathrm{Ti}} + a_{\mathrm{Al}})/2$ = 3.3 Å. The periodic boundary conditions are applied along *x*, *y* and *z* directions. The structure is initially relaxed at 300 K to find structural configuration with minimum potential energy.

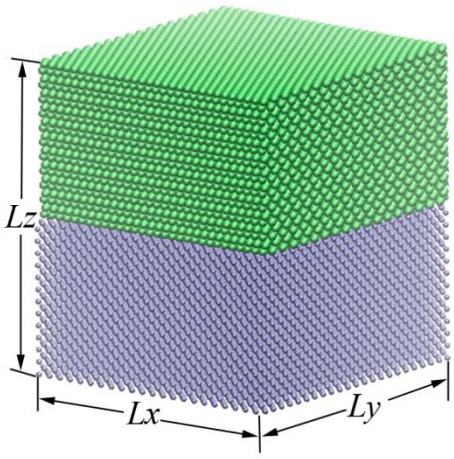

Fig. 1. Simulation cell. Al atoms are shown by blue, Ti atoms are shown by green.

The simulations are carried out by molecular dynamics using the LAMMPS free simulation package. Embedded atom method (EAM) interatomic potential for Ti and Al is used [5]. For temperature control, the Nose-Hoover thermostat is applied.

To study the process of fabrication of Ti-Al composite and phase transformation in the system, pressure along *z*-axis ε_{zz} combined with shear strain ε_{xy}. Strain rates are $\dot{\varepsilon}_{zz}$ = 0,00005 ps^{-1} and $\dot{\varepsilon}_{xy}$ = 0,005 ps^{-1}.

Present simulation made it possible to trace on the atomistic level the mixing of Ti atoms with Al atoms from two initially separated crystals as a result of shear deformation. The proposed model is a simplification of the scenario previously observed experimentally. Al atoms diffuse more easily into the Ti matrix than Ti atoms diffuse into the Al matrix.

Uniaxial tensile loading normal to the interlayer boundary of the two metals, shows that rupture occurs precisely in the Al part of the sample for Al-Ti. This means that interlayer mixing of atoms results in appearance of interface stronger than Al part.

References

[1] V.N. Danilenko, G.F. Korznikova, A.P. Zhilyaev, S.N. Sergeev, G.R. Khalikova, R.Kh. Khisamov, K.S. Nazarov, L.U. Kiekkuzhina, R.R. Mulyukov. IOP Conf. Ser.: Mat. Sci. and Eng. 447. 012021 (2018).

[2] G.F. Korznikova, R.R. Mulyukov, A.M. Zhilyaev, V.N. Danilenko, R.Kh. Khisamov, K.S. Nazarov, S.N. Sergeyev, G.R. Khalikova, R.R. Kabirov. AIP Conf. Pro. 2053. 030028 (2018).

[3] V.N. Danilenko, S.N. Sergeev, J.A. Baimova, G.F. Korznikova, K.S. Nazarov, R.Kh. Khisamov, A.M. Glezer, R.R. Mulyukov. Mat. Let. 236. 5155 (2019).

[4] R.R. Mulyukov, A.A. Nazarov, R.M. Imayev Let. on Mat. 510516 (2018).

[5] Farkas D., Mod. Sim. Mat. Sci. Eng. 2. 975984 (1994).

[6] P.V. Polyakova, J.A. Baimova. IOP Conf. Ser.: Mat. Sci. and Eng. 1008. 012052 (2020).

Magnetic properties, domain structure and magnetoimpedance effect in multilayered elements based on permalloy

Pasynkova A.A.[1,2], Svalov A.V.[1], Kurlyandskaya G.V.[1,3]

[1]*Ural Federal University, 620002, Ekaterinburg, Russia*
[2]*M.N. Mikheev Institute of Metal Physics of the UB RAS, 620108, Ekaterinburg, Russia*
[3]*Universidad del País Vasco UPV-EHU, 48940, Leioa, Spain*

Magnetic field sensors with thin-film detecting element are widely requested in technological and biomedical applications [1-3]. They insure effective detection of very small magnetic fields with present goal to approach the range of biomedical signals analyzed in magneto- cardio or encephalography. One of the effects promising for such a sensitive detection is magnetoimpedance (MI) [4-5]. In recent years, the multilayered structures with FeNi magnetic layers separated by spacers showing high MI effect were the subject of special attention [6-7]. However, careful analysis of magnetostatic parameters, magnetic domain structure and MI for the samples with different arrangement and thicknesses of magnetic layers and spacers prepared in the same conditions is still requested. In this work multilayered FeNi-based rectangular sensitive elements with high MI effect were considered for their comparative analysis of the magnetostatic properties, domain structure, and magnetoimpedance characteristics.

Thin films were obtained by magnetron sputtering technique as elongated stripes (10 mm × 0.5 mm). The transverse in-plane magnetic anisotropy was formed during deposition by application of the external magnetic field onto Corning glass substrates. Structure and magnetic properties were studied by X-ray diffraction technique and transmission electron microscopy. A vibrating sample magnetometer (VSM), a magneto-optical Kerr (MOKE) microscope, and a magnetoimpedance analyzer were used for investigation of static and dynamic magnetic properties. Usually MI is focused on the frequencies for which the maximum MI effect is observed. Here, as the analysis of magnetic domains is involved we use quite low frequency of the driving current of about 18 MHz. The analysis is not straight forward as in this frequency range the domain wall movements are suppressed but we consider it is still useful. Surface magnetic domains were visualized by MOKE technique for different external fields up to saturation. MI elements were $[Ti(6\ nm)/FeNi(100\ nm)]_5/Ti(6\ nm)/Cu(500\ nm)/Ti(6\ nm)/[FeNi(100\ nm)/Ti(6\ nm)]_x$ ($x = 0 – 5$) type structures.

Structural analysis confirmed that obtained materials are multilayered structures with the average size of the grains of magnetic layers of the order of 20 nm and the size of the grains in the central Cu layer of the order of 50 nm.

According to MOKE analysis, uniaxial transverse effective magnetic anisotropy was formed in all multilayered elements. Figure 1(a) show M(H) loop of $[Ti/FeNi]_5/Ti$ sample as an example. The shape of the MOKE hysteresis loop indicates that the magnetization reversal for in-plane magnetization along the hard magnetization axis (long side of the rectangular element) occurred by rotation of the magnetization. Figure 1(b) shows examples of the external magnetic field dependences of MI responses of selected elements at relatively low frequency.

The main result of a comparative analysis can be expected in advance: higher MI properties were observed when the magnetization reversal process corresponded to the rotation

of the magnetization vector. Comparative analysis of magnetic domains and MI revealed interesting features, which can be understood taking into account the difference of magnetostatic energy contributions in the MI elements with different degree of the asymmetry.

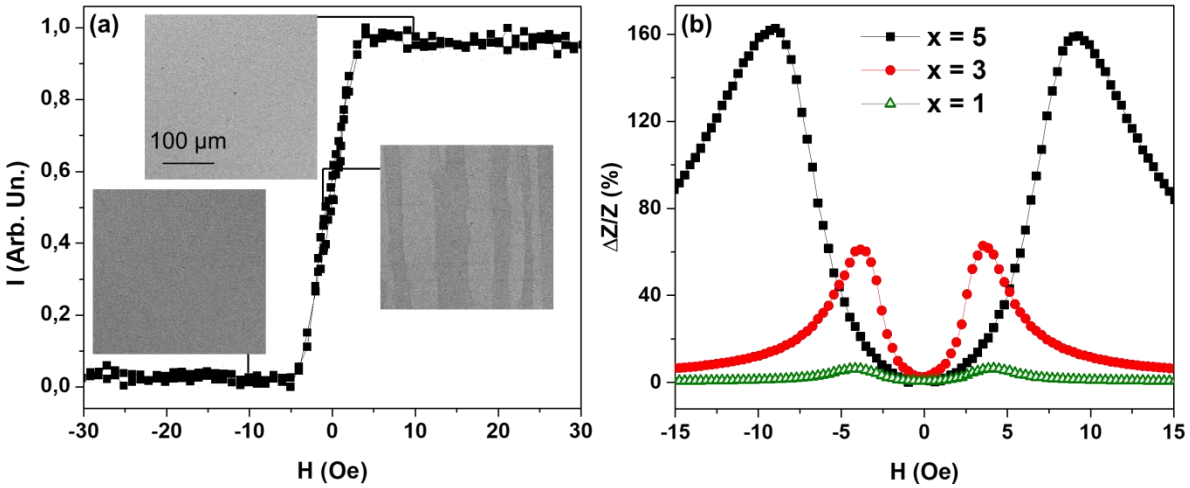

Fig. 1. (a) Hysteresis loop and magnetic domains obtained using an MOKE microscope for element [Ti(6 nm)/FeNi(100 nm)]$_5$/Ti(6 nm). The external magnetic field and an element long side is oriented horizontally in the plane of the page, easy magnetization axis (EMA) is oriented vertically. All images are the same size. (b) Examples of the field dependence of the MI of [Ti(6 nm)/FeNi(100 nm)]$_5$/Ti(6 nm)/Cu(500 nm)/Ti(6 nm)/[FeNi(100 nm)/Ti(6 nm)]$_x$ (for x = 1, 3 and 5) type structures, measurements done at relatively low frequency of the driving current of 22 MHz. MI was calculated as $\Delta Z/Z = 100\ \% \times ((Z(H)-Z(H_{max}))/Z(H_{max}))$, where H_{max} = 100 Oe.

This study was supported by the Ministry of Science and Higher Education of the Russian Federation (project No. FEUZ-2020-0051).

References

[1] D.R. Baselt, G.U. Lee, M. Natesan, S.W. Metzger, P.E. Sheehan and R.A. Colton, Biosens. Bioelectron. 13, 731 (1998).

[2] G.V. Kurlyandskaya, J. Magn. Magn. Mater. 321, 659 (2009).

[3] T.P. Krinitsina, T.A. Chernyshova, V.V. Proglyado, and V.V. Ustinov, Phys. Met. Metallogr. 120, 429 (2019).

[4] A.S. Antonov, S.N. Gadetskii, A.L. D'yachkov, V.P. Paramonov, A.N. Lagar'kov, A.B. Granovskii, N.S. Perov, A.F. Prokoshin, N.A. Usov, Phys. Met. Mettalogr. 83, 612 (1997).

[5] T. Morikawa, Y. Nishibe, H. Yamadera, Y. Nonomura, M. Takeuchi, Y. Taga, IEEE Trans. Magn. 33, 4367 (1997).

[6] A.A. Chlenova, A.V. Svalov, G.V. Kurlyandskaya, S.O. Volchkov, J. Magn. Magn. Mater. 415, 87 (2016).

[7] N.A. Buznikov, A.V. Svalov, G.V. Kurlyandskaya, Phys. Met. Metallogr. 122, 223 (2021).

Photoresistors based on polyindole thin films

Mullagaliev I.N.[1], Andriianova A.N.[1], Salikhov R.B.[1]

[1]*Basjkir State University, 450076, Ufa, Russia*

Organic optoelectronics is a rapidly developing field of research, which is aimed at creating a new generation of light, flexible and transparent electronic devices, such as organic phototransistors and organic light-emitting devices (lasers, LEDs) [1-2]. The production of optoelectronic thin films is of key importance, since they are needed in optics and optoelectronics (protective, antireflection and other coatings for lenses, fiber optic cables, optoelectronic devices). Polyindoles (PIn) are being intensively studied [3]. PIn and its derivatives are of interest for applications in organic electronic devices.

In this work, samples of photoresistor devices are made. The glass substrate with an ITO conductive layer was cleaned and dried in an oven. A polyindole film was deposited from a solution on top of the ITO by spin-coating. At different speeds of rotation, the thickness of the films was: 700, 500, and 400 nm. The resulting films were heated in an oven to evaporate the remaining solvent. The top contact in the form of an aluminum film was deposited on top of the polyindole by thermal spraying in vacuum on a VUP-5 installation. The contact has the shape of an open square ring with a wall width of 1 mm and a side of 5 mm. The thickness of the aluminum contact is 500 nm. The morphology of the films was studied using a scanning probe microscope and the Gwydion program.

According to the research results, it was found that the photoconductivity of the samples increases by almost 2 orders of magnitude in comparison with the dark conductivity. The dependence of the photoconductivity on the thickness of the films is found. In addition, during centrifugation, the rotation speed affects the homogeneity, structural ordering and thickness of the films, as a result, the resistance of the samples and the mobility of charge carriers, and hence the photoconductivity, change. With a decrease in the radiation power density from 3500 mW / cm^2 to 350 mW / cm^2, the photoconductivity decreases by a factor of 4-5.

References

[1] A. R. Tuktarov, R. B. Salikhov, A. A. Khuzin, N. R. Popod'ko, I. N. Safargalin, I. N. Mullagaliev and U. M. Dzhemilev, RSC Advances V 9, 7505-7508 (2019).

[2] T.R. Salikhov, Y.M. Yumaguzin, and R.B. Salikhov, 2015 International Siberian Conference on Control and Communications (SIBCON), IEEE Proceedings, 7147207 (2015).

[3] A.G. Mustafin, L.R. Latypova, A.N. Andriianova, S.M. Salikhov, A.F. Sattarova, I.N. Mullagaliev, R.B. Salikhov, and I.B. Abdrakhmanov, Macromolecules V 53(18), 8050–8059 (2020).

Thin-film phototransistors based on fullerene and photochrome derivatives

Salikhov R.B., Mullagaliev I.N., Salikhov T.R.

Bashkir State University, 450076, Ufa, Russia

Thanks to organic electronics, a wide range of devices (displays, microcircuits, sensors, etc.) may appear in the near future, which will be ultra-thin, lightweight, flexible and transparent [1]. It is important to obtain new effective photochromic systems that are promising for micro- and nanoelectronics [2-3].

In this work, samples of phototransistors are manufactured and investigated. Glass with a conductive ITO layer, which plays the role of a gate, was used as a substrate. A polyaniline film 500 nm thick was deposited on top by thermal sputtering in a vacuum from a Knudsen cell. Polyaniline was in a non-conducting state and acted as a gate dielectric. Were investigated three types of transistors: the first type of transistor structures, separate layers of photochromic organic compounds and C60 with a thickness of each film 200 nm. The second type of structures is a film of physically mixed powders of photochrome and C60. The third type is an active layer made of fullerene and photochrome derivatives. On top of the active layers by thermal sputtering in vacuum on a VUP-5 device (vacuum universal post), two aluminum electrodes, a drain and a source with a thickness of 500 nm, were deposited. The film thickness was monitored using an SPM. The created devices were characterized by a channel width of 10 mm and a channel length of 50 μm.

A study of the current-voltage characteristics of the manufactured transistors showed that, in the absence of irradiation, the currents in the phototransistors are of the order of or less than 1 nA. Under the influence of ultraviolet light (350 nm) of the gap region of the transistors, the drain-source current increases by three orders of magnitude for both devices. Mixed active layers have high currents of current-voltage characteristics. And the most stable work is with hybrid layers. Dependencies are non-linear. There are no saturation areas on the output characteristics. All measurements were carried out under normal conditions - atmospheric air, which is an advantage of the investigated transistor structures in comparison with others.

References

[1] Y.N. Biglova, R.B. Salikhov, T.R. Salikhov, I.N. Safargalin, A.G. Mustafin, I.B. Abdrakhmanov, Physics of the Solid State, V 59, № 6, 1253-1259 (2017).

[2] A.R. Tuktarov, R.B. Salikhov, A.A. Khuzin, N. R. Popod'ko, I. N. Safargalin, I.N. Mullagaliev, U.M. Dzhemilev, RSC Advances V 9(13), 7505–7508 (2019).

[3] A.R. Tuktarov, R.B. Salikhov, A.A. Khuzin, I.N. Safargalin, I.N. Mullagaliev, O.V. Venidiktova, T.M. Valova, V.A. Barachevsky, U.M. Dzhemilev, Mendeleev Communications V 29(2), 160–162 (2019).

Co/Cu Nanowires and the effect of Co layer thickness on Magnetic Properties

Gilimyanova A.R.[1,2], Doludenko I.M.[2], Zagorskiy D.L.[2], Menushenkov V.P.[1], Bizyaev D.A.[3], Khaibullin R.I.[3]

[1]NUST "MISiS", Institute of New Materials and Nanotechnologies, Department of Physical Materials Science, 119049, Moscow, Russia
[2]Federal Scientific Research Center "Crystallography and Photonics" RAS, 119333, Moscow, Russia
[3]Zavoisky Physical-Technical Institute, FRC Kazan Scientific Center, Russian Academy of Sciences, 420029, Kazan, Russia

Nowadays many types of nanoobjects attract great attention and find wide applications. One of the types of materials are nanowires (NWs), which can be obtained by matrix synthesis. Interest in NWs is associated with their magnetic properties. These properties depend both on the material (elemental composition) and on the method of their manufacture.

In this work, we have obtained arrays of nanowires with a diameter of 100 nm, composed of the Co/Cu layers. The thickness of the Co layers in the first three samples of the nanopowder arrays varied (25, 50, 300 nm) at a constant Cu thickness (300 nm). The fourth sample had a Co layer thicker than the Cu layer: the Co / Cu layers were 350/25 nm, respectively. A sample was also grown with an array of Co / Co nanowires with the thickness of each layer of 100 nm. The features of the electrodeposition of such structures in a galvanic cell were studied. For further research (for example, electron microscopic), the array of metal NWs was either removed from the matrix (by etching the latter), or remained in it, forming a kind of "metal-polymer composite" (for magnetic and X-ray studies).

Electron microscopic studies of the obtained NW arrays made it possible to confirm the calculated layer thicknesses and its elemental composition. The phase composition was determined by the X-ray method (diffractometry). Measurements of the magnetic characteristics (on a vibromagnetometer) made it possible to estimate the main parameters of the obtained arrays of NW - coercive force and remanent magnetization. Thus, it has been shown that when the thickness of the magnetically hard material in the nanowire changes, the coercive force changes depending on the direction of the external magnetic field (along the nanowire growth axis and across). Based on the obtained results, we can talk about the possibility of creating such metal-polymer nanocomposites that will have controlled anisotropy of magnetic properties.

The influence of catalyst size on carbon nanotubes synthesis

Konshyn A.A., Tomilin S.V., Osokin K.S., Berzhansky V.N.

Physics and technology institute, V.I. Vernadsky Crimean Federal University, Vernadsky avenue, 4, Simferopol, Russia

Carbon nanotubes (CNT) is one of most popular nanomaterial. CNT has unique physical properties, such as mechanical strength, electrical and thermal conductivity, surface absorption, etc. In this case the actual problem of carbon nanoindustry is the controlled synthesis of CNT with specified parameters.

In our research we have been investigate the influence of size of Ni nanocatalyst on the features of CNT synthesis process. Ni catalyst was synthesized by thermal deposition in vacuum on glass-ceramic substrate with followed vacuum annealing at 450°C during 3 hours. For create the nanocatalysts with different size the method of "thin screen" was used [1]. This method allows to synthesize the Ni film with gradient of effective thickness, which after annealing granulated into self-assembled nanoparticles with different size.

Synthes of CNT was carried out by CVD-method (catalytic pyrolysis of ethanol). The surface morphology of CNT in different areas of Ni catalyst gradient is demonstrated in Fig. 1 (Scanning electronic microscopy, SEM).

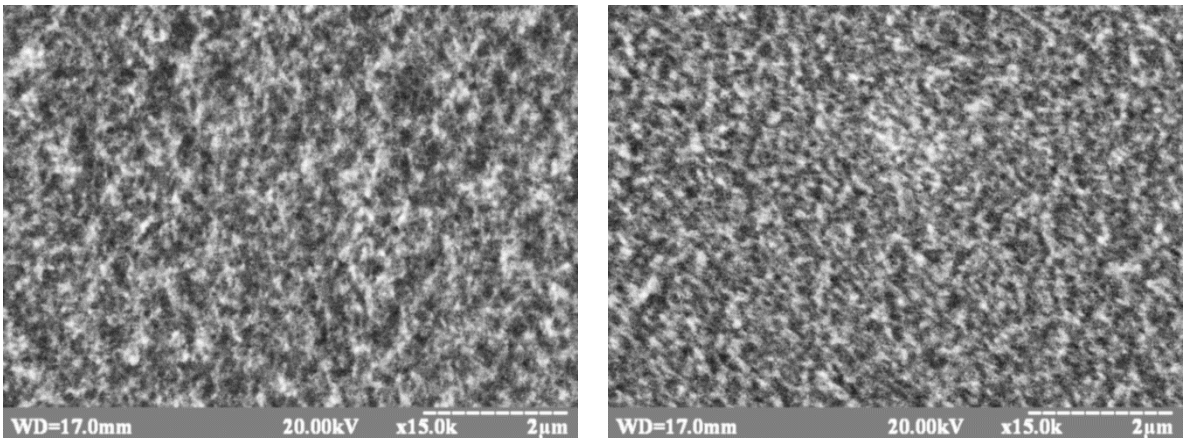

a b

Fig. 1. SEM images of surface morphology of synthesized CNT in different areas of Ni catalyst gradient: a) thickness of Ni is 10 nm, b) thickness of Ni is 2 nm.

As can see, the size of Ni catalyst is influence on the properties of synthesized CNT. The change of catalyst size leads to change of CNT size.

The work was carried out with the financial support of the Russian Science Foundation grant No. 19-72-20154.

References

[1] S.V. Tomilin, V.N. Berzhansky, A.S. Yanovsky, and O.A. Tomilina, Journal of Surface Investigation: X-ray, Synchrotron and Neutron Techniques, 10 (4), 868 (2016).

Modification of iron-garnet films properties by the method of ionic etching

Syrov A.A., Tomilin S.V., Semuk E.Yu., Berzhansky V.N.

Physics and technology institute, V.I. Vernadsky Crimean Federal University, Vernadsky avenue, 4, Simferopol, Russia

Manufacturing of smoothed profile of film edge is the main factor for excluding the edge magnetic domains. It is very important for manufacturing ultrahigh-sensitive sensors of magnetic fields in magnetocardiography, magnetoencephalography, low-field tomography, etc.

Layered etching is the perspective method, which allows to determine the structure of epitaxial iron-garnet films, to create the needle structure of surface relief with very high space permission, and to clean the surface from unwanted impurity. The results of investigation can be interesting for design of optoelectronic devices, which can used in data translation, or data save and processing [1]. Ionic etching allows to carry out modification of iron-garnet films by layered delete or creation a smooth profile of film edge.

In Fig. 1,a the changes of peak height of main FMR signal during layered etching of epitaxial iron-garnet $(BiLu)_3Fe_5O_{12}$ film are presents. At the films manufacturing on their surface the bismuth substituted layer is forming. This layer does not make a contribution into main FMR signal, but create an additional signal. At the etching of such layer the intensity of main signal does not change. After delete of surface layer, the gradual etching of main layer is beginning, and the intensity of main signal is decrease monotonously. In Fig.1,b the smoothed profile of film edge after ionic etching with mask. At the film thickness of 160 nm the width of profile is 10 μm.

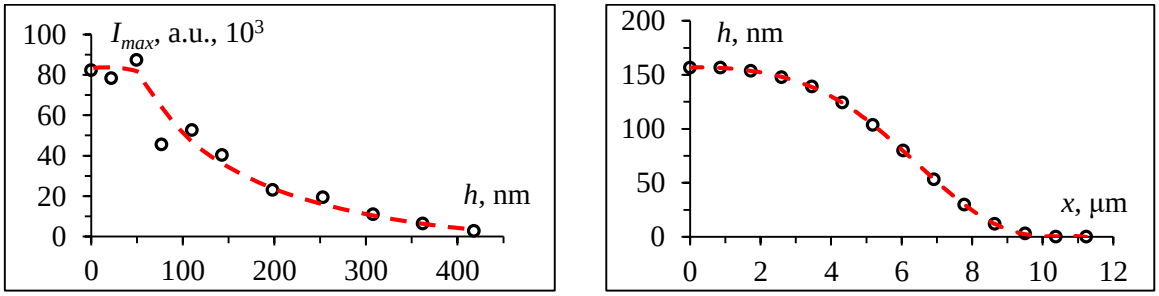

Fig. 1. An example of changes of iron-garnet films properties: a – the change of FMR signal during layered ionic etching of film surface, b – the form of film edge with smoothed profile after ionic etching with mask.

This work was financially supported by the Russian Ministry of Education and Science, Megagrant project N 075-15-2019-1934

References

[1] D.M. Krichevsky, D.O. Ignatyeva, V.A. Ozerov, and V.I. Belotelov. Phys. Rev. App. 15, 034085 (2021).

The distribution of film thickness during magnetron deposition

Tomilin S.V., Berzhansky V.N., Tomilina O.A.

Physics and technology institute, V.I. Vernadsky Crimean Federal University, Vernadsky avenue, 4, Simferopol, Russia

Magnetron sputtering in vacuum is the very popular method for films manufacturing. This method allows to deposit coatings from different materials including multi-component materials. The magnetron coatings have a high adhesivity, high structural homogeneity and stechiometry [1]. The magnetrons with circle sputtering area are used most often. In this case the most important parameter of coating is the thickness distribution. For carried out films with homogeneous thickness the rotate holders are used, but for some research problems the using of rotation is not possible.

In our research we have been investigate the distribution of film thickness when the substrate is located in different distance from sputtered target during magnetron deposition. In Fig. 1,a the model of magnetron circle sputtering area is demonstrated. The radius of sputtering area is 5 sm. The distribution of sputtering intensity into circle is described by Gaussian.

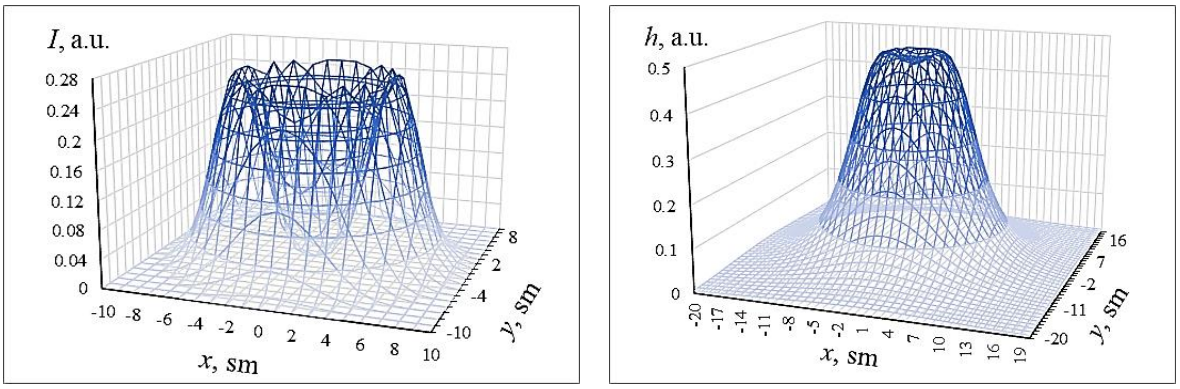

a b

Fig. 1. The model of magnetron sputtering: a) the distribution of sputtering intensity into magnetron circle sputtering area, b) the distribution of film thickness when the substrate is located in distance of 4 cm from target

In Fig. 1,b the distribution of film thickness during magnetron deposition is demonstrated. In this case the distance from target to substrate is 4 sm. As can see the film thickness has a minimum in the center of investigated area. The radius of area with maximum thickness is near 3.5 sm, less then radius of sputtering area.

The work was carried out with the financial support of the Russian Science Foundation grant No. 19-72-20154.

References

[1] T.V. Mikhailova, A.N. Shaposhnikov, S.V. Tomilin, D.V. Alentiev, J. of Phys. Conf. Ser., 1410, 012163 (2019).

Reveal of a new source of magnonic relaxation rate in the interface between epitaxial iron garnet ferrite film and GGG substrate.

A.N. Kuzmichev[1], Y.M. Bunkov[1], P.M. Vetoshko[1,2,3], V.I. Belotelov[1,3], V.N. Berzhansky[3], A.N. Shaposhnikov[3], A.A. Fedorenko[3]

[1]*Russian Quantum Center, 121353, Moscow, Russia*
[2]*Institute of Radioengineering and Electronics, Russian Academy of Sciences, 103907, Moscow, Russia*
[3]*Vernadsky Crimean Federal University, 295007, Simferopol, Russia*

The possibility of obtaining a condensed state of magnons paves the way for the creation of highly coherent qubits [1]. However, a strong increase in relaxation rate at temperatures below 100 K was detected [2]. It is assumed that the main mechanism of this low-temperature relaxation is the presence of impurities of rare earth elements [3, 4]. Another mechanism for accelerating relaxation may be the appearance of ion defects Fe^{2+} and Fe^{4+} in a crystal lattice. They could appear in presence of the $^{2+}$ and $^{4+}$ valence impurities in the melt [5, 6] like Pb^{2+} and Pt^{4+}. Aside from that the paramagnetic influence of the gadolinium-gallium garnet (GGG) substrate at low temperature causes an additional magnetic damping [7, 8]. We found the formation of an additional interlayer between the Gallium Gadolinium Garnet substrate and the epitaxial film of Yttrium-Iron Garnet. This interlayer is characterized by a large magnetic moment at low temperatures (Fig 1), which leads to an anomalous dependence of susceptibility and magnetic resonance frequency shift at cooling, which is much larger than expected due to the anisotropy of magnetization, paramagnetic substrate ions and magnetostriction.

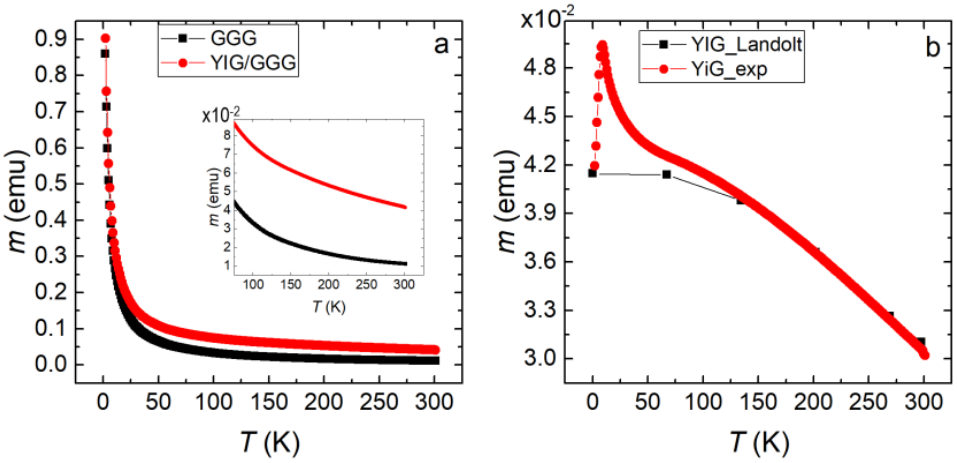

Figure 1: (a) Temperature dependence of the total magnetic moment of the film grown from MoO_3-Li_2MoO_4 melt on a GGG substrate (black) and for the pure GGG wafer (red) from 4 to 300 K. In insert the same dependences from 100 to 300 K. (b) Difference between magnetic moment of the our YIG film sample and a bulk YIG crystal. Obtained magnetic moment related to the YIG film (red). Please, notice that ordinate axis is multiplied by factor 10^{-2}. Data obtained from Landolt-Bornstein for the YIG of the same volume (black).

This interlayer plays a significant role in magnetic relaxation processes in the temperature range below 50 K. In this work, we compared three samples with difference interface layer width grown from different melts. Usually, single-crystal YIG films are grown on substrates made of

Gallium Gadolinium garnet. We have established that in this case, a compound with Gd^{3+} ions is formed in the transition layer, which has a considerable magnetic moment. The presence of this interlayer leads to a change in the effective magnetic field and furthermore to an acceleration of magnon dissipation. Unlike other relaxation mechanisms described in the article, this one cannot be compensated for. The only way for further improvement, apparently, lies in the use of substrates without strong paramagnetic ions. We suggest to use a $Y_3Ga_3Sc_2O_{12}$ substrate. This material is now actively used for the manufacture of laser crystals. A significant decrease in relaxation processes is expected with this substrate below 50 K. That is very important for creating thin-film structures based on YIG films capable of operating with a small dissipation parameter at low temperatures. Such systems can be useful for creating functional elements of magnonic, spintronic and quantum computing devices.

References

[1] Y. M. Bunkov, Journal of Experimental and Theoretical Physics 131, 18-28 (2020).
[2] C. L. Jermain, et al., Physical Review B 95, 174411 (2017).
[3] G. Dionne, J. Phys. IV France 7, 174411 (1997)
[4] G. F. Dionne, G. L. Fitch, Journal of Applied Physics 87, 4963 (2000).
[5] E. Spencer, R. Lecraw, J. R.C. Linarks, Physical Review 123, 1937-1938 (1961).
[6] C. Vittoria, P. Lubitz, P. Hansen, W. Tolksdorf, Journal of Applied Physics 57, 3699 (1985).
[7] M. G. Balinskii, V. V. Danilov, A. Y. Nechiporuk, V. M. Talalaevskii, Radiophysics and Quantum Electronics 29, 954-958 (1986).
[8] V. Danilov, D. Lyfar, Y. Lyubon'ko, A. Nechiporuk, S. Ryabchenko, Russian Physics Journal 32, 276-280 (1989)

Ab initio study of phase stability of Ni-Co-Mn-Ga Heusler alloys

Erager K.R., Sokolovskiy V.V., Buchelnikov V.D.

Chelyabinsk State University, eragerk@rambler.ru, Chelyabinsk, Russia

Currently, the promising potential of Heusler alloys is due to the presence of number of different functional properties, such as shape memory effect, magnetoresistance, magnetocaloric effect, etc. However, recent experimental studies [1-3] have shown that Mn - excess compounds are found to be unstable and decompose into dual phase components consisting of $L2_1$ cubic Ni_2MnX phase and $L1_0$ tetragonal NiMn phase depending on the heat treatment.

In this work, $Ni_{2-x}Co_xMn_{1+y}Ga_{1-y}$ Heusler alloys are considered. First-principles segregation studies are performed using the VASP (Vienna ab initio simulation package) [4]. A complete optimization of the geometry of more favorable atomic positions is carried out using the ATAT software package and the SQS method [5]. The calculations are performed for a 64-atom supercell in the GGA-PBE approximation [6] for various types of crystal structures in the cubic and tetragonal phases. As decay, components considered stable 19 base compounds according to Materials project data.

Fig. 1 shows the calculated values of the formation energy of $Ni_{31}Co_1Mn_{16}Ga_{16}$. A negative value of the mixing energy (E_{mix}) indicates that a compound can be stable under equilibrium conditions. It is seen that ~37.5 % reactions reveal the stability $Ni_{31}Co_1Mn_{16}Ga_{16}$ against the segregation into a set of stable compounds. This finding allows to suggest that this composition can be metastable.

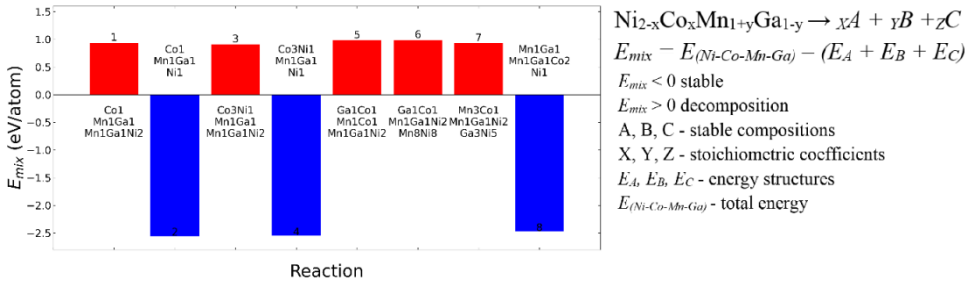

Fig. 1. Formation energy and decomposition reaction for the composition $Ni_{31}Co_1Mn_{16}Ga_{16}$

This work was supported by the Ministry of Science and Higher Education of the Russian Federation within the framework of the Russian State Assignment under contract No. 075-00992-21-00.

References

[1] W. M. Yuhasz et al., J. Appl. Phys. 105, 07A921 (2009).
[2] W. M. Yuhasz et al., J. Alloys Compd. 492, 681 (2010).
[3] T. Krenke et al., J. Appl. Phys. 120, 243904 (2016).
[4] G. Kresse and J. Furthmüller, Phys. Rev. B 54, 11169 (1996).
[5] A. van de Walle, Calphad Journal. 42, 13 (2013).
[6] J. P. Perdew, K. Burke, and M. Ernzerhof, Phys. Rev. Lett. 77, 3865 (1996).

Granulometry Of Nanocomposite Films Using Modern IT Techniques

Ustyugov V.A., Makarov P.A., Vlasov V.S., Kotov L.N., Turkov V.K.

Syktyvkar State University named after Pitirim Sorokin, Syktyvkar, Russia, 167001, Oktyabrsky 55, Syktyvkar, Russia

A wide range of composite materials representing two- or three-dimensional structures is being studied [1-3]. The range of elementary units composing these structures is also rich: quantum dots, nanowires, rings, more complex particles with a core-shell structure, films, etc. Particles may be interacting or non-interacting. Note that the modeling of composite structures usually considers regular structures of homogeneous elements.

Obviously, combining particles of different types in a two-dimensional matrix, or, for example, in a gel, may allow to significantly expand the range of obtained magnetic characteristics, and in some cases to obtain qualitatively new properties (for example, to obtain a heterogeneous medium with several resonance frequencies when using ellipsoidal-shaped magnetic particles and rings).

Machine learning and generative design methods, developed using the methods of modern IT science, make it possible to solve such problems in a reasonable computational time.

Filtering and clustering algorithms, a type of machine learning task, can improve the accuracy of image analysis. Machine learning algorithms can also help with the accumulation of material for analysis. In mathematical statistics, "bootstrap" techniques are used to create pseudo-samples to test empirical distributions. If we use convolutional neural networks to analyze images of films with specified parameters in order to identify patterns, and then generative neural networks to produce new images that take into account these laws, it becomes possible to accumulate a base for research without spraying real films, which will greatly simplify the research process.

This study was supported by the Russian Science Foundation, project 21-72-20048.

References

[1] S. Bedanta, A. Barman, W. Kleemann et al. Magnetic Nanoparticles: A Subject for Both Fundamental Research and Applications // Journal of Nanomaterials. — 2013. — Vol. 2013 — Article ID 952540. — P.22.

[2] Kotov L. N., Turkov V. K., Vlasov V. S. et al. Relaxation of magnetization in thin composite (Co45Fe45Zr10)X(Al2O3)100−X films // Materials Science and Engineering. — 2006. — Vol. 442. — No 1. — P. 352.

[3] Kotov L. N., Vlasov V. S., Turkov V. K. et al. Influence of Annealing on Magnetic, Relaxation and Structural Properties of Composite and Multilayer Films // JNN. — 2012. — Vol. 12. — No 2. — P. 1696.

Study of the effect of optical radiation on the photoconductivity of the interface between two polymer dielectrics

Yusupov A.R.[1], Panova N.A.[1], Lachinov A.N.[1,2]

[1]Bashkir State Pedagogical University n.a. M. Akmulla, 450000, Ufa, Russia
[2]Institute of Molecule and Crystal Physics – Subdivision of the Ufa Federal Research Centre of the Russian Academy of Sciences, 450075, Ufa, Russia

A highly conductive region formed on the boundary between two dielectrics polymer films[1] has unique properties, whose investigation revealed promising new effects for future use. In particular, it was shown in [2] that irradiation of the polymer / polymer interface leads to an increase in the current. In this work, the main goal is to study the effect of the wavelength of optical radiation and the method of manufacturing thin polymer films on the photoconductive properties of the interface.

Polydiphenylenephthalide (PDP) polymer was used as the main material. The samples were prepared by spin coating methodin an electric field with different strengths (from 0 to 8 V / m). Studies of the PDP / PDP interface showed that an increase in current is observed at all used wavelengths of 405 nm, 520 nm, and 636 nm. More clearly the contribution of each wavelength is shown in luxury - voltage characteristic in Fig. 1.

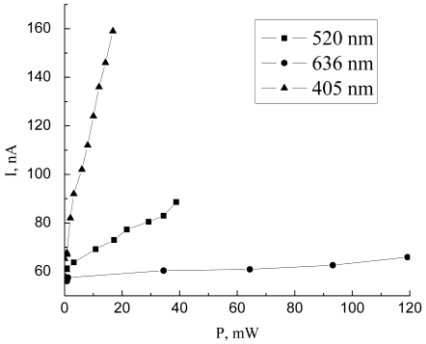

Fig. 1. Lux-ampere characteristic (LAC) of the investigated structures.

As can be seen, irradiation with a laser with a wavelength of 405 nm makes the greatest contribution to the increase in the photocurrent. The curves on the LAC are significantly different. In particular, the LAC obtained at 405 nm has two pronounced regions, in contrast to the LAC obtained at 520 nm and 636 nm.

An analysis of the experimental structures fabricated in an electric field showed a significant difference from the samples fabricated under normal conditions. This result will be presented in detail in the report.

This work was carried out with the support of the Mirror Laboratories project of the National Research University Higher School of Economics and the Bashkir State Pedagogical University n.a. M. Akmulla.

References

[1] Gadiev R.M. JETP Letters. 2010. T. 90. № 11. C. 726-730.

[2] Yusupov A.R., Physics of the Solid State. 2020. T. 62. № 7. C. 1251-1255.

Studying magnetic properties of PVDF-TrFE-based nanocomposites

Gritsenko Ch.A.[1], Omelyanchik A.S.[1], Kolesnikova V.G.[1] and Rodionova V.V.[1]

[1]*Research and Education Center "Smart Materials and Biomedical Applications", Immanuel Kant Baltic Federal University,236041 Kaliningrad, Russia*

We prepared nanocomposites based on two types of polymers: poly (vinylidene fluoride) (PVDF) and its copolymers with trifluoroethylene (PVDF-TrFE). The nanocomposites were combinations of $CoFe_2O_4$ (CFO), $Zn_{0.25}Co_{0.75}Fe_2O_4$, and $BaTiO_3$ nanoparticles embedded into the piezoelectric polymer matrix. The samples were prepared by the solvent evaporation method assisted by the Doctor Blade technique [1]. An external magnetic field was applied to order magnetic nanoparticles in the polymer matrix. Structural properties of the nanoparticles were studied by X-ray diffraction. High crystallinity of the particles was revealed. Size distribution was estimated with transmission electron microscopy.

Macroscopic magnetic properties of composites samples were studied with vibrating magnetometry (VSM). Saturation magnetization of composite samples was reduced concerning CFO powder due to the presence of diamagnetic polymer content. Coercive field of the PVDF-based composites was almost equal to the same value of CFO powder ~1.3 kOe. PVDF-TrFE-based composites demonstrated a slightly higher coercive field of ~1.5 kOe. Angular dependence of hysteresis loops recorded for oriented CFO/PVDF-TrFE sample in two different orientations of the magnetic field and sample axis (along chains of CFO nanoparticles clusters). In the first case, when the orientation of the sample was always in-plane the hysteresis loops did not depend on the orientation of the field. In the second case, when the direction of the field changed from in-plane to out of plane orientation, a small difference was observed in both random and oriented samples but this was mainly due to the geometrical change of measuring configuration (mutual position of a sample and pick-up coils of VSM). Notably, the formation of those ordered chains does not induce any magnetic anisotropy of composite samples. This fact can be explained by the dominant role of intra-aggregate interparticle magnetic interactions on macroscopic magnetic reversal processes. In other words, the arrangement of the clusters' chains in the magnetic field orients aggregates of several particles but inside those aggregates, the easy axes of magnetic anisotropy of individual NPs are still distributed randomly [2].

References

[1] Ribeiro, C.; Costa, C.M.; Correia, D.M.; Nunes-Pereira, J.; Oliveira, J.; Martins, P.; Gonçalves, R.; Cardoso, V.F.; LancerosMéndez, S. Electroactive poly(vinylidene fluoride)-based structures for advanced applications. Nat. Protoc. 2018, 13, 681–704, doi:10.1038/nprot.2017.157.

[2] Vaganov, M.V.; Borin, D.Y.; Odenbach, S.; Raikher, Y.L. Training effect in magnetoactive elastomers due to undermagnetization of magnetically hard filler. Phys. B Condens. Matter. 2020, 578, 411866, doi:10.1016/j.physb.2019.411866.

Scanning probe microscopy as a multifunctional tool to study polymer-based composites

Sobolev K.[1], Antipova V.[1], Amirov A.1, Rodionova V.[1]

[1] *Immanuel Kant Baltic Federal University, 236004, Nevskogo 14, Kaliningrad, Russia*

Polymer-based magnetoelectric composite materials have attracted a lot of attention due to their high potential in various types of applications as magnetic field sensors, energy harvesting, and biomedical devices [1]. One new strategy to increase the value of the desired effects in the composites is to prepare materials with the differently distributed magnetic and / or piezoelectric particles inside the polymer matrix [2]. This strategy may help to increase the magnetoelectric effect of such composites and to make them applicable as bioactive surfaces for neural crest stem cell cultures [3,4].

Scanning probe microscopy, which includes atomic-force, magnetic-force, piezoelectric-force, etc. microscopy turned out to be a multifunctional tool to study the properties of the composite materials. The main advantage is that the desired properties can be examined not only separately but also in conjunction which is undoubtedly helpful for the multiferroics where each of the components (magnetic, electric or elastic) can be strongly dependent on the other one and vice versa. Another valuable advantage is the possibility to plot the mapping of the studied properties across the sample surface. If one can see the different regions, for example, with and without nano- and microparticles, it is possible to differentiate which region gives the impact to the magnetic or piezoelectric response of the whole sample [5].

In this work we studied the sample of the piezoelectric elastic composite, consisting of the PVDF-TrFE polymer matrix with $Zn_{0.25}Co_{0.75}Fe_2O_4$ magnetic nanoparticles, distributed in it. On the first step we studied the mechanical properties on this composite using NTEGRA scanning probe microscope (НТ-МДТ, Russia) in the hybrid scanning mode. In this mode the probe retracts from the surface in each single point of the scan and then reaches the surface again, while the software mathematically fits the obtained force versus distance to the surface curves, extracting the values of the Young modulus, mechanical stiffness and adhesion force in the same time with the roughness. Due to this method we visualized the distribution of the magnetic nanoparticles across the surface and studied the way it affects the mechanical properties of the sample. The obtained mapping was in the good agreement with the previously achieved X-ray computer tomography 3D-scans. Afterwards we investigated the magnetic properties of the polymer using magnetic-force microscopy. We obtained the pictures of the magnetic dipoles, corresponding to the zinc-cobalt-ferrite nanoparticles, distributed inside the diamagnetic matrix and observed their motion when the external magnetic field was applied. The obtained results let us conclude on the mechanisms of the interaction between the particles and the matrix and gave us the important insights about the formation of the properties in the studied class of composites.

References

[1] Ze Q., et. al., Adv. Mater. 32, 1–8 (2020)

[2] Martins P., et. al., Polymers 9, 62 (2017)

[3] Murzin D., et. al., Sensors 20, 1569 (2020)

[4] Roy K., et. al., ACS Appl. Nano Mater. 2, 2013–2025 (2019)

[5] Omelyanchik A., et. al., Nanomaterials 11(5), 1154 (2021)

Ion beam engineering of magnetic nanostructures

Gusev S.A[1], Sapozhnikov M.V[1]., Tatarskiy D.A[1], Yu. V. Petrov[2]

[1]*Institute for Physics of Microstructures of the Russian Academy of Sciences, Nizhniy Novgorod, 603950, GSP-105, Russia*
[2]*Saint-Petrersburg State University, Universitetskay nab. 7/9, Saint-Petersburg, Russia*

Noncollinear spin textures is one of the most interesting and intensively studied objects of the magnetism during last decade due to their unusual topological and transport properties and their potential applications for data storage and information carriers in low-power nanoelectronics. Chiral magnetic quasi-particles, skyrmions, are considered the most promising stable twisted spin textures that can be used to create devices of this type. Understanding the mechanism of formation of these quasi-particles, their energetic stability, and how to control their size and the density, is crucial in order to manipulate their behavior.

Multilayer metal films consisting of alternating layers of ferromagnet (FM) and heavy metals (HM) are one of the most promising systems in which it is possible to stabilize the existence and control the parameters of skyrmions. The magnetic properties of such films can be tuned by appropriate selection of different layer materials, thickness and number of layers, and their crystal structure. In addition, using focused beams of ionizing radiation (X-ray, ion and electron), it is possible to produce a local change in the magnetic characteristics of metal structures, which helps to form localized inhomogeneous spin configurations at nanometer scales of a given type, shape, size and location [1-3]. In this work, we demonstrate that focused ion beams can be used to form magnetic bubbles with different topological charges (including skyrmions) up to 100 nm in size at zero field and room temperature in the Co/Pt multilayer with perpendicular anisotropy.

The magnetic multilayers with structure of Ta(3)/Pt(3)/$[Co(0.5)/Pt(1)]^5$/Pt(2) (where index 5 denotes the number of layers, numbers in brackets are thicknesses in nm) were grown by DC magnetron sputtering on 50-nm-thick Si_3N_4 membrane windows for direct TEM observation and simultaneously on SiO_2 substrate with standard 50 μm or 150 μm wide Hall crosses for transport property measurements, magnetic force microscopy (MFM) and MOKE experiments. Orion helium ion microscope equipped with a Nanomaker pattern generator was used to irradiate rectangular lattices of the spots in the Hall cross and to irradiate the same pattern in the case of Co/Pt structures on the Si_3N_4 membrane. Irradiation was performed with He^+ ion energy of 30 keV. Helium ion beam was focused to the diameter of about 1 nm. The exposed spots have a circular or elliptical shape with a size ranging from 50 nm to 600 nm, they were periodically arranged in a square lattice or hexagonal lattice. Irradiation of each spot was performed using point-by-point serpentine scanning with a step between irradiated points of 3 nm. The irradiation fluence was varied from 5×10^{14} to 10^{16} cm^{-2}. Such structures demonstrate the formation of dense lattices of magnetic bubbles (MB) of different types in the process of magnetization reversal [3]. Preliminary micromagnetic calculations showed that the topology of arising MB depends on the distribution of the He + ion fluence over the area of the illumination spot. If the fluence of He^+ is concentrically distributed (leading to concentrically modulated value of the anisotropy) the forming MB have the topology of a magnetic skyrmion [4].

We used MFM to visualize magnetic states, existing at zero field. These measurements cannot resolve a topological structure of appearing magnetic bubbles but it allows us to verify uniformity of the obtained domain lattices, to estimate the density of the bubble domains, and to distinguish magnetic vortices from magnetic bubbles. The topology of magnetization distribution in the appearing magnetic bubbles is examined by Lorentz transmission electron microscopy (LTEM) measurements (Fig.1). Initially, the Cs-corrected transmission electron microscope TITAN 80-300 (FEI) operating at 300 kV was used, recently we adapted the LIBRA 200MC microscope for such experiments. These LTEM experimental observations show that, depending on the size of the irradiated areas, the distribution and magnitude of the fluence, skyrmions of the Neel, Bloch, or hybrid type or trivial magnetic vortices, can be formed.

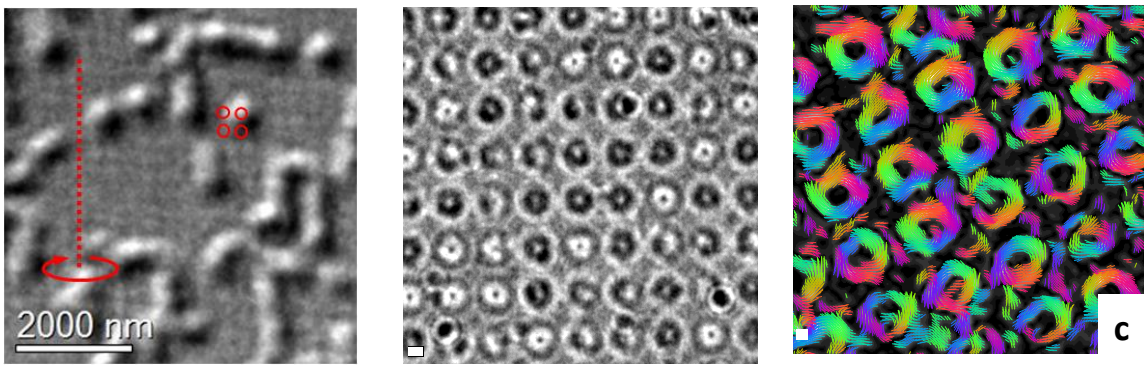

Fig. 1. LTEM images of a lattice of magnetic bubbles in a demagnetized state. The observed contrast corresponds to the distribution of magnetization for Neel (**a**) and Bloch (**b**) skyrmions; (**c**) reconstructed magnetization distributions from LTEM micrographs with differential phase contrast It is observed from the skyrmion with both right and left helicity

For the first time, direct observation of the topological Hall effect in artificial lattices of magnetic skyrmions was carried out using simultaneous measurements of the Hall effect and the magneto-optical Kerr effect in nanostructured Co/Pt multilayers [4]. The measured topological Hall effect is proportional to the skyrmion density in the system.

This work was supported by the Russian Science Foundation (Grant No. 21-12-00271). The facilities of Center "Physics and technology of micro- and nanostructures" at IPM RAS were used for the TEM analysis of the samples. Helium ion irradiation was performed using equipment of Interdisciplinary Resource Center for Nanotechnology of Research Park of SPbSU.

References

[1] Y. Guang et al. Nature Comm., 11:949, (2020)
[2] Y. Guang et al. Adv. Mater2003003, (2020).
[3] M.V. Sapozhnikov et al. Appl. Phys. Lett. 109, 042406 (2016)
[4] M. V. Sapozhnikov et al. Phys. Rev. B 103, 054429 (2021)

Magneto-optical studies of nanostructured InAs:Fe layers

Gan'shina E.A.[1], Golik L.L.[2], Kun'kova Z.E.[2], Pripechenkov I.M.[1], Rukovishnikov A.I.[2], Markin Yu.V.[2]

[1]*Department of Physics, Lomonosov Moscow State University, 119991, Moscow, Russia*
[2]*Kotel'nikov Institute of Radioengineering and Electronics, RAS, Fryazino Branch, 141190, Fryazino, Russia*

Diluted ferromagnetic semiconductors (DFSs) are considered as the base materials of next generation semiconductor devices. Recently, significant progress has been made in obtaining DFS (III,Fe)V (III = Ga, In; V = Sb, As) and structures based on them [1 for example]. Thin DFS (III,Fe)V layers with Fe content up to 30%, in which the Curie temperature (T_C) exceeds room one (T_{room}) and both *p*- and *n*-type of conductivity are realized, have been obtained using low-temperature molecular beam epitaxy (LT-MBE). DFS layers (In,Fe)As were also fabricated by ion implantation followed by pulsed laser melting (II+PLM). In these layers, nonzero magnetization was recorded at T_{room} and anisotropic spinodal decomposition determining the magnetic and magnetotransport properties was revealed [2].

In the present work, we studied electronic and magnetic structures of InAs:Fe layers prepared by II+PLM technique at various energies of the recrystallizing laser pulse. The samples were obtained at the Ion Beam Center of Helmholtz–Zentrum Dresden–Rossendorf. Information on the technology details, methods and results of the characterization of similar samples is contained in [2]. We measured the spectral, temperature, magnetic field and orientation dependences of the magneto-optical transversal Kerr effect (TKE), as well as ellipsometry spectra. It has been found that the laser pulse energy strongly influences the TKE spectra shape, signals magnitude and TKE dependences on temperature and magnetic field. All samples contain the insignificant Fe inclusions amount, the Fe content being negligibly small in sample N1 prepared at the minimum pulse energy (W = 0.1 J/cm^{-2}). The TKE spectroscopy data shows that this sample is magnetically inhomogeneous. It consist of weakly doped paramagnetic host and local ferromagnetic (In,Fe)As nanoregions, whose $T_C \approx 200$ K. The nonzero magnetization of such samples detected at T_{room} in [2] is possibly due to the Fe inclusions. The TKE spectra of other samples (N2 - 4, W = 0.2 - 04 J/cm^{-2}) are the superposition of contributions from the Fe and (In,Fe)As inclusions. The Fe contribution are predominant that indicates an enhancement of the Fe diffusion to the layer surface with increasing the pulse energy. The TKE signal value depends on the magnetic field orientation relative to the layer crystallographic axes. The optical constants dependence on the incidence plane orientation relative to the layers axes also takes place. The observed anisotropy is apparently caused the anisotropic spinodal decomposition in the layers under study.

References

[1] Tu N.T., Hai P.N., et al, Appl. Phys. Express 12, 103004 (2019).
[2] Yuan Ye, Hübner R., et al, Phys. Rev. Mat. 2, 114601-1 (2018).

Analysis and FDTD modelling of electromagnetic waves propagation in magnetic inhomogeneous composite films

Makarov P.A., Ustyugov V.A., Vlasov V.S., Kotov L.N

Pitirim Sorokin Syktyvkar State University, 167001, Oktyabrsky 55, Syktyvkar, Russia

The model of a inhomogeneous and especially randomly inhomogeneous medium has been in great demand for many years both in fundamental science and in applied research and engineering applications. There are specific problems of radiophysics and acoustics, in which this model plays an important role. In this regard, there is important to development of methods that make it possible to analys, visually and simply represent the process of signal propagation in specific inhomogeneous systems. Currently, there are many similar techniques, but the most widespread are grid methods. They are based on the procedure for discretizing space-time and the transition from differential equations for continuous functions to finite-difference equations for functions of discrete variables. The fundamental work in this direction was [1], in which the method of finite differences in the time domain (FDTD) was first described. This work did not receive a wide response in the scientific community but recently the FDTD method is experiencing a "rebirth". There is an extensive literature on the use and development of the FDTD method in the field of electrodynamics of randomly inhomogeneous media [2-5].

In this work an algorithm for the modelling of the propagation of electromagnetic waves in magnetic inhomogeneous and randomly inhomogeneous media by the FDTD method has been developed. That algorithm is suitable for analyzing the main time characteristics, as well as identifying the features of the propagation of various types of electromagnetic signals in layered randomly inhomogeneous magnetic media. The simulation of the various types electromagnetic signals (single impulses, series of pulses, continuous signals) propagation in stationary randomly inhomogeneous media is carried out. The propagation of electromagnetic signals in smoothly inhomogeneous and randomly inhomogeneous media is regarded. Moreover, random scatterers against the background of an inhomogeneous medium with different profiles of inhomogeneity are considered. The simulation of the signal propagation in stationary randomly inhomogeneous magnetic media with a low level of phase contrast of two types – with a "diffuse" distribution of inhomogeneities and their "close packing" is performed. Revealed influence concentration of inhomogeneities and the type of their distribution on the characteristics of the transmitted and reflected signals.

This study was supported by the Russian Science Foundation, project 21-72-20048.

References

[1] K. Yee, IEEE Trans. AP 14, 302 (1966).
[2] C.D. Moss et al., IEEE Trans. GRS 40, 178 (2002).
[3] S.H. Tseng et al., Optics Letters 29, 1393 (2004).
[4] Y. Miyazaki, K. Kouno, IEEJ Trans. FM 129, 693 (2009).
[5] T. Tan, A. Taflove, V. Backman, IEEE Trans. AP 61, 818 (2013).

Superexchange in 2D perovskite HTSC with stripe nanostructure

Gavrichkov V.A.

Kirensky Institute of Physics, 660036, Krasnoyarsk, Russia

The subtle experimental studies using scanning tunneling conductivity and multiscale scanning nano x-ray diffration over a wide range of temperature and doping unambiguously indicate that there is a clear connection between the multiscale stripe texture and the quantum coherence of quasiparticles in perovskite high-Tc 2D superconductors which resists to the decoherence effects of high temperature.

The key idea is to approach [1] this problem by identifying stripes by the type of nuclear configuration, the so-called. "tilting" effects (tilt of oxygen octahedra as a whole). The fact is that different stripes differ not only in the concentration of carriers, but in the type of nuclear configuration - this is the stripe's "visit card"[2].

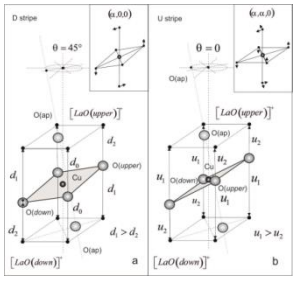

Fig. 1 Tilting of CuO_6 octahedra in U(b) and D(a) stripes between rock salt layers LaO.

We have classified the observed configurations into a ninth-order symmetric Abelian group consisting of two types (so-called U and D) of stripes rotated at right angles relative to each other. The special role of rock salt layers in 2D perovskite materials is confirmed by the absence of superconductivity in ideal AFM CuO layers on graphene. The number of nuclear configurations of the observed stripes, for example, in $La_{(2-x)}Sr_xCuO_4$, is reduced to just one form (group generator), and their spatial distribution in a regular lattice is represented by possible planar graphs with chromatic number $\chi \le 4$ in the well-known four-color theorem.

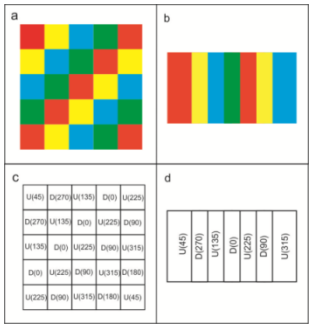

Fig.2 The regular stripe structures: linear (*b*,*d*) and checkerboard (*a*,*c*). R color – $U(\theta = 45°)$ stripe, Y - $D(\theta = 270°)$, B - $U(\theta = 135°)$, G – $D(\theta = 0°)$ in stripe group $G(\varphi)$.

However, in contrast to the chaotic structure, for regular stripe structures: linear and checkerboard (see Fig.2), the stripe group is a symmetry group, since for them, the property of invariance with respect to the precession of the c-axis of the inclined octahedron to any angle θ multiple of $45°$ takes place. The "fast" (- tunneling) dynamics of nuclear configurations of stripes restores the structure of an ideal CuO_2 layer, but with nonlocal ion positions (see Fig.3).

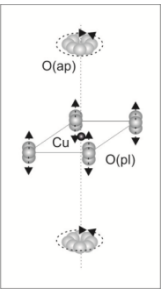

Fig.3 Dynamic picture for CuO_6 octahedra tunneling across $U(\theta)$ and $D(\theta)$ stripe positions. Tilting angle $\varphi = const$.

Let us assume that the Jahn-Teller instability $(A_{1g} + B_{1g}) \otimes (a_{1g} + b_{1g})$ takes place only in the hole sector N_+ (see Fig. 4), where active tilting modes $a_{1g} + b_{1g}$ mix the Zhang Rice singlet A_{1g} with

the B_{1g} state. The linear and chess structures remain invariant with respect to the precession of the local c axis of CuO_6 octahedron, except for the transverse and diagonal uniform shifts, respectively (see Fig.2). Here, the situation with nuclear density is reminiscent of the refusal in the crystal field theory from the point representation of negatively charged ions in favor of symmetric ligands.

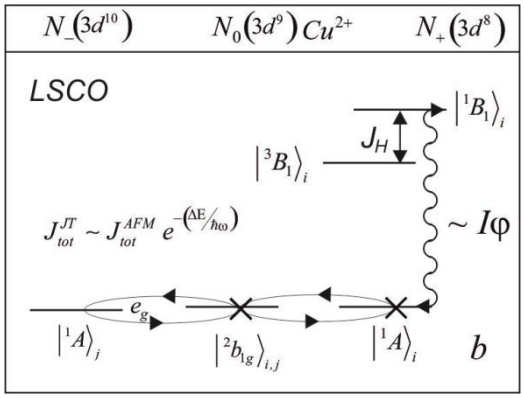

Fig.4 Jahn-Teller interaction $\sim I\varphi\cdot\left[\delta(\theta-45°)+\delta(\theta-135°)\right]$ in N_+ sector of configuration space for D stripes with $(A_{1g}+B_{1g})\otimes(a_{1g}+b_{1g})$ instability.

In this case, all off-diagonal matrix elements from electronic operators, including the exchange constant J_{ij}, contain Ham's exponential multiplier $\exp\{-\Delta E/\hbar\omega\}$ [3], where ΔE is the difference in adiabatic potentials in the sectors N_- and N_0 of the configuration space (see Fig.4). The super-exchange interaction in doped 2D HTSC cuprates undergoes an additional reduction due to nonlocality effects in comparison with undoped materials, where the position of the ions is fixed.

The reported study was supported by the grant RFFI 19-02-00034 and the Russian Foundation for Basic Research, Government of Krasnoyarsk Territory, and Krasnoyarsk Regional Fund of Science according to the research project "Studies of superexchange and electron-phonon interactions in correlated systems as a basis for searching for promising functional materials No. 20-42-240016.

References

[1] Vladimir A. Gavrichkov, Yury Shan'ko, Natalia G. Zamkova, and Antonio Bianconi, J. Phys. Chem. Lett., 10, 1840-1844, 2019.

[2] A. Bianconi, N. L. Saini, A. Lanzara, M. Missori, and T. Rossetti, Phys. Rev. Lett., 76, 3412 (1996).

[3] Frank S. Ham, Phys. Rev., 138, A 1727 (1965).

Development of a technique for studying thin films by scanning electron microscopy

Utkin A.A., Kotov L.N, Urban V.V.[1]

[1]*Syktyvkar State University, 167001, Syktyvkar, Russia*

Scanning electron microscope (SEM) studies of metal-dielectric films. The chemical compositions of the elements and the linear dimensions of metal-dielectric composite films (CoFeZr-Al2O3), (CoFeB-SiO2), (CoTaNb-Zr2O3) were studied. To measure the thickness of films on a thin Mylar substrate, the method of "scraping" the film from the substrate was developed and tested.

Interest in the study of metal-dielectric composite films is associated with the fact that they are nanostructured materials. The sizes of individual magnetic metallic or dielectric regions for most compositions of composite films are from 10 to 300 nm, their small size contributes to the formation of a complex of unique physical properties [1, 2]. The purpose of this work is to develop methods for studying the chemical composition and linear dimensions of thin metal-dielectric films. For this, it is necessary to carry out a statistical study of a large amount of data obtained as a result of experimental measurements on a scanning electron microscope MIRA3.

The film was divided and cut into sections of 2x2 mm2 along the long side of the sheet; in total, from 100 to 150 pieces were obtained (depending on the initial size of the sheet of a particular sample). 10 X-ray spectra were taken from each area. From the data obtained, using the Irwin and Romanovsky criteria, gross errors and outliers were excluded, and for the remaining ones, the mathematical expectation and standard deviation were calculated. Then the experiment was repeated, but only 3 spectra were recorded from one area, the values of which were averaged and the error was found as the root-mean-square deviation.

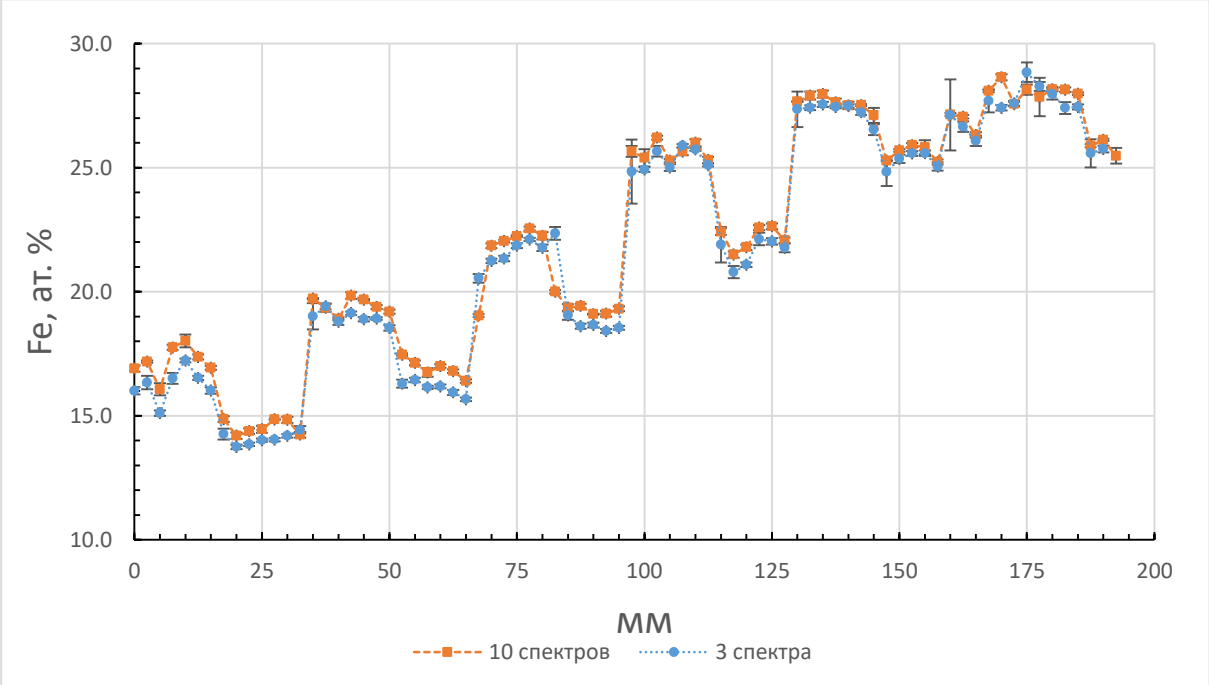

Fig 1. Percentage of Fe atoms in the sample. Abscissa - coordinates in millimeters along the length of the original sample.

To measure the thicknesses obtained in the previous experiment, small areas of films on a sitall substrate were sprayed with a thin layer of carbon to obtain a stable and clear electronic image of the surface. Using the tools built into the microscope software, the thickness of the sprayed layer of the metal-dielectric composite film was measured.

Due to the high flexibility and plasticity of the thin lavsan substrate, the method used above did not work: the film was curled, not allowing it to be fixed in the required area for taking a picture. Then another method was proposed: a piece of a sample on a mylar substrate was fixed above the surface of an SEM stage, glued with double-sided carbon tape. Further, using a thin and sharp blade from the end of the piece, microscopic particles are scraped off directly from the layer of the metal-dielectric film. Due to the brittleness of the surface of the metal-dielectric film layer and the strength of the polymer structure of the lavsan substrate, only microscopic fragments of the film get and stick to the carbon tape. Excess that has not adhered to the stage is blown away by a jet of compressed air. It is also worth noting that this method does not require preliminary preparation of samples, in the form of deposition of a thin conductive layer, which greatly simplifies and speeds up research.

As can be seen from the comparison of the results, when studying the chemical composition, the results obtained when taking 10 and 3 spectra coincide within the error limits, which means there is no need to make unnecessary measurements, and to limit ourselves to only three spectra per area, which significantly speeds up work, simplifies data analysis and reduces the likelihood of errors in their processing. Similar conclusions can be drawn for measurements of thicknesses up to 50 nm in thin films. The method of "scraping" the film from the substrate is convenient for measuring the thicknesses of thin structures and will be used in further studies.

The study was supported by a grant from the Russian Science Foundation (project No. 21-72-20048).

References

[1]. Kotov L.N. Spectra of the magnetic permeability and the magnetic structure of the composite films / L.N. Kotov, M.P. Lasek, D.V. Bogachuk, Yu.E. Kalinin, A.V. Sitnikov // VI Euro-Asian Symposium “Trends in MAGnetism” (EASTMAG-2016): book of abstracts. – Krasnoyarsk, Kirensky Institute of Physics, Russian Academy of Sciences, Siberian Branch. – 2016. – P. 256.

[2]. Kotov L.N. The size and shape of particles and magnetic properties of composite films / L.N. Kotov, M.P. Lasek, M.U. Dianov, D.V. Bogachuk, E.A. Golubev, Yu.E. Kalinin, A.V. Sitnikov // IV International Conference on Competitive Materials and Technology Processes: book of abstracts. – Miskolc-Lillafüred, Hungary – 2016. – P. 75.

Magnetoresistance of $(Co_{40}Fe_{40}B_{20})_{34}(SiO_2)_{66}$/ZnO multilayer films

Zhilova O.V., Makagonov V.A., Pankov S.Yu., Babkina I.V., Kashirin M.A.

Voronezh State Technical University, 394024, Voronezh, Russia

Zinc oxide is used in many areas of technology. Zinc oxide thin films ZnO have unique electrophysical and piezoelectric properties. ZnO can be used to create various microelectronic devices (thin-film solar modules; thin-film field-effect transistors; gas sensors, etc.) [1]. One of the possible technical applications of zinc oxide as layers in metal-dielectric/oxide composites.

To obtain a multilayer system $(Co_{40}Fe_{40}B_{20})_{34}(SiO_2)_{66}$/ZnO, by method of ion-beam sputtering was used [2]. Two targets were alternately sputtered onto the rotating substrate: the first target of the $(Co_{40}Fe_{40}B_{20})_{34}(SiO_2)_{66}$ composite, and the second, the ZnO semiconductor. As a result, a multilayer system with 112 bilayers $[(Co_{40}Fe_{40}B_{20})_{34}(SiO_2)_{66}/ZnO]_{112}$ was formed, the thickness of which varied from 0.16 to 0.35 μm.

The structure of the multilayer system was studied by X-ray diffraction and transmission microscopy. Analysis of the data obtained showed that the film is X-ray amorphous with a periodic multilayer structure, which is retained up to 723 K [3].

The figure shows the dependence of the electrical properties of the ferromagnetic interlayers of the composite $(Co_{40}Fe_{40}B_{20})_{34}(SiO_2)_{66}$ on the applied external magnetic field. The samples under study have a magnetoresistance of ~ 2.5% at room temperature in a field of 9 kOe (curve 2). With a decrease in the measurement temperature, the value of the magnetoresistive effect increases to ~ 9% (curve 4). These values of the magnetoresistance are higher than in the pure composite $(Co_{40}Fe_{40}B_{20})_{34}(SiO_2)_{66}$ (~ 1.5 and 6%, curves 1 and 3, respectively).

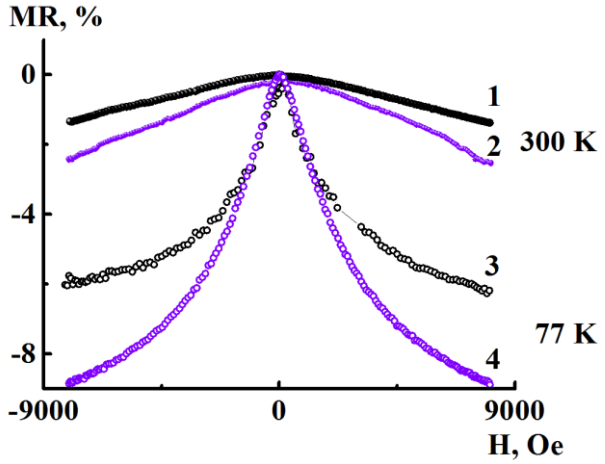

Figure. Field dependences of the magnetoresistance of the multilayer structure $[(Co_{40}Fe_{40}B_{20})_{34}(SiO_2)_{66}/ZnO]_{112}$ (curves 2, 4) and the composite $(Co_{40}Fe_{40}B_{20})_{34}(SiO_2)_{66}$ (curves 1, 3) at T = 300 K and T = 77 K, respectively

This work was supported by the Ministry of Education and Science within the framework of state assignment No. FZGM-2020-0007.

References

[1] V.A. Coleman and C. Jagadish, Zinc oxide bulk, thin films and nanostructures: processing, properties and applications (Elsevier science bv, Amsterdam, 2006).

[2] S.A. Gridnev et al., Nonlinear phenomena in nano-and microheterogeneous systems (Monograph Moscow, Russia, 2012).

[3] O.V. Zhilova et al., IOP Conf. Ser.: Mater. Sci. Eng. 1035 012013 (2021).

The method for efficient extraction of fullerenes and enrichment of EMF in an extractor

Elesina V.I.[1,2], Churilov G.N.[1,2], Vnukova N.G.[1,2]

[1]*Kirensky Institute of Physics, FRC KSC SB RAS, 660036, Krasnoyarsk, Russia*
[2]*Siberian Federal University, 660062, Krasnoyarsk, Russia*

The study of fullerenes and endohedral metallofullerenes (EMF) is of interest for modern science, since these molecules have high reactivity, which makes it possible to form materials with fundamentally new properties. EMF and their derivatives, for example, $Gd@C_{82}$, $Y@C_{82}$, ($Gd@C_{82}O_x(OH)_y$), already have areas of potential application [1,2].

To study the properties of new materials, significant amounts of EMF are required, which are difficult to isolate due to the tendency to form clusters with fullerenes of various types, as well as particles of fullerene-containing soot (soot). Analysis of the literature has shown the relevance of the study and introduction of new devices and methods for the isolation of fullerenes, since the existing ones do not always show their effectiveness. The number of works aimed at studying the processes of isolation of higher fullerenes (HF) and EMF is limited (mainly studies are devoted to the extraction of fullerenes C_{60} and C_{70}).

The aim of the work was to develop a method that allows you to quickly obtain HF and EMF in macro quantities.

The technique is as follows:

1. Synthesis of soot by the electric arc method (in graphite rods Ø=6 mm, L=100 mm, TC 3497-001-51046676-2008, an axial hole Ø=3 mm, L=85 mm is drilled and filled with a mixture of graphite and metal oxide powders (for example, Y_2O_3 or Gd_2O_3) in a mass ratio of 1:1. The yield of fullerenes in soot with Y is about 5 wt%, in soot with Gd - 3wt%.

1. Isolation of fullerenes on the Extractor developed by us [3], which simultaneously implements a mechano-activation effect on the components of the treated suspension (from soot with solvent) and filtration. The release of fullerenes occurs from a thin layer of soot. The work on approbation of the technique was carried out with different solvents: carbon disulfide, o-xylene, and pyridine.

2. Enrichment of a fullerene extract with EMF contained in it according to the method using the Lewis acid - $TiCl_4$ [4], implemented in an automatic mode using the Extractor [3].

All obtained fullerene extracts were filtered, the extractant was distilled off on a rotary evaporator. Then, they were separated by HPLC on an Agilent 1200 Series chromatograph with a Cosmosil Buckyprep-M column (10 mm × 250 mm). Toluene was used as an eluent; the flow rate was 1.6 ml/min. The relative content of each component in the mixture was calculated by normalizing the area of each peak relative to the total area of the entire spectrum on the HPLC chromatogram. For this, a specially developed software algorithm was used, which numerically integrates the spectrum using the trapezoidal method, using a linear approximation to take into account the background.

All the obtained extracts with EMF were also analyzed by the method of atomic emission spectroscopy, according to the method developed by us [5], the amount of the formed EMF was calculated.

The results showed that the amount of C_n fullerenes ($70<n\leq84$) isolated on the Extractor by carbon disulfide ≈ 6%, pyridine ≈ 1.8%, o-xylene ≈ 4.35%. In the isolation of fullerenes C_m

(m>84) and EMF c Y using carbon disulfide, it was possible to isolate the largest amount of fullerenes - 6.19%, using o-xylene - 2%, pyridine - 4.06%. The strongest extractant in the isolation of higher fullerenes and EMF in the Extractor was carbon disulfide, the weakest was o-xylene. The duration of the isolation of fullerenes with the use of mechano-activation action was 15 minutes.

Using the enrichment technique by $TiCl_4$, we carried out additional purification of the fullerene mixture synthesized with the addition of Gd_2O_3, and obtained a sample enriched in $Gd@C_{82}$, Fig. 1.

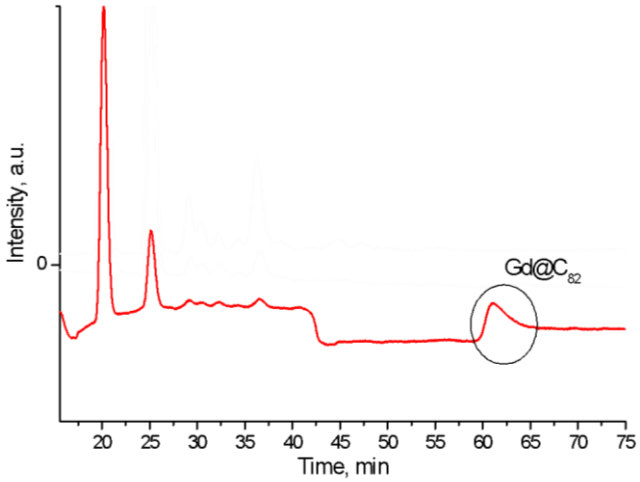

Fig. 1. Chromatogram of the sample after processing by $TiCl_4$ in automatic operation using the Extractor [3]. The following areas of peaks of various fullerenes types (%) were established: C_{60} - 59.33; C_{70} - 20.67; C_{84} -1.93 and $Gd@C_{82}$ - 18.07

The enrichment technique proposed by us eliminates the need for separate, rather time-consuming filtration and washing procedures in a separating funnel with distilled water, significantly reducing the duration of the process. The enrichment procedure lasted 5 minutes.

The reported study was funded by RFBR according to the research project № 18-29-19003.

References

[1] Z. Chen, R. Mao and Y. Liu, Current Drug Metabolism 13(8), 1035 (2012).

[2] A.A. Popov, S. Yang and L. Dunsch, Chemical Reviews 113(8), 5989 (2013).

[3] G.N. Churilov and V.I. Elesina, Patent № RU 2744434, 20.01.2021 (in Russian).

[4] K. Akiyama, T. Hamano, Y. Nakanishi, E. Takeuchi, S. Noda, Z. Wang, S. Kubuki and H. Shinohara, JACS 134, 9762 (2012).

[5] G.N. Churilov, A.A. Popov, U.E. Guliaeva, N.A. Samoylova, N.G. Vnukova, A.L. Kolonenko, V.G. Isakova, A.I. Dudnik and V.S. Koravanets, Nanosystems: Phys. Chem. Math. 7(1), 140 (2016).

Storage of metal nanoparticles in the pores of crumpled graphene

Safina L.R.[1], Krylova K.A.[2,3], Murzaev R.T.[2], Baimova J.A.[2,3]

[1]Ufa State Petroleum Technological University, 1 Kosmonavtov St., 450062, Ufa, Russia
[2]Institute for Metals Superplasticity Problems, Russian Academy of Sciences, 39 Khalturin St., 450001, Ufa, Russia
[3]Bashkir State University, 32 Zaki Validi St., 450076, Ufa, Russia

Extensive studies have been carried out over the past few decades to investigate the crumpling behaviour of thin sheets like graphene both by theoretical and experimental methods [1-2]. It was shown that crumpled structures can have excellent compression and aggregation-resistant properties [3]. One of the new and important applications using crumpled graphene is natural containers for other elements. In this work, the molecular dynamics simulation is used to study the possibility of accumulation of nickel nanoparticles of different sizes in the pores of the crumpled graphene at different temperatures. The dynamics of structures is investigated at an exposure time of 20 ps. The simulation is carried out using the LAMMPS package with the adapted AIREBO empirical intermolecular interaction potential for carbon-carbon interaction. The Morse potential is used to describe the interaction between Ni-Ni and Ni-C atoms. It reproduces well the behavior and properties of carbon materials and metal nanoparticles and is widely used in modeling of various compounds [4]. To study the interaction of Ni-C atoms, we used the potential parameters obtained by the *ab-initio* method, presented in [5], and to describe the interaction of Ni-Ni atoms, the parameters proposed in [6].

To study the possibility of storing metal nanoparticles in the pores of crumpled graphene, a single element of crumpled graphene is considered - a rolled flake. A graphene flake (GF) is created from a small CNT (11, 11) 1.3 nm long, and two rows of atoms are removed along the nanotube axis. The flake is filled with nickel nanoparticles of different sizes, consisting of 21 and 66 atoms.

In fig. 1, the potential energy is shown as a function of exposure time for the Ni_{21} (a) and Ni_{66} (b) nanoclusters after exposure at 300 K (blue line) and 1000 K (red line). Corresponding snapshots of the structure of a crumpled graphene flake filled with a nanocluster at different times of exposure are also shown. It is found that the total potential energy of the system is saturated to a practically constant value at the end of the equilibration process, indicating the system has reached equilibrium and a stable state. All the changes in the energy curves correspond to some structural changes. The longest time of stabilization at 300 K is found for Ni_{21} (5 ps). Graphene flake with Ni_{66} reach equilibrium after holding during 3.2 ps. Bigger the diameter of the nanocluster, less the equilibration time. This can be explained by the mutual arrangement of the nancluster and GF. For a small nanocluster, distance between nanocluster and flake walls is two times higher than for the biggest one which means that time required to attach the nanocluster by the graphene flake is longer. At higher temperature (1000 K), again, a strong correlation between equilibration time and size of the nanocluster is found. For GF with Ni_{21} nanocluster, the transformation is fast since the temperature is close to the melting point and the nanocluster can be easily destroyed. Temperature fluctuations facilitate the crumpling process and the appearance of new bonds between the edges of GF. For structure with Ni_{66}, the temperature slightly affects the time of equilibration. However, temperature decreases the total potential energy of the system.

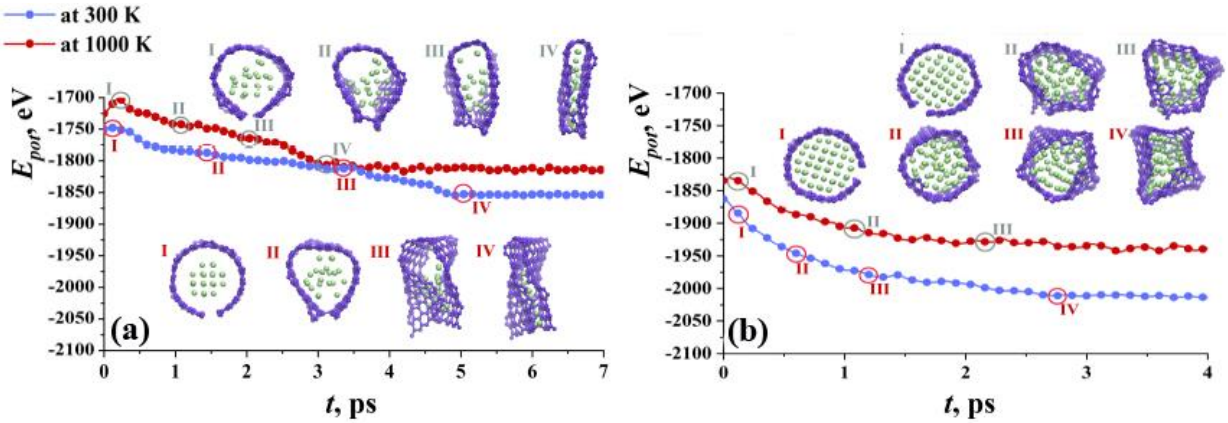

Fig. 1. Potential energy as the function of exposure time for Ni21 (a) and Ni66 (b). Corresponding snapshots of the structure of crumpled graphene flake filled with nanocluster.

during exposure at 300 K (bottom line of snapshots) and 1000 K (upper line of snapshots). Carbon atoms are shown by violet and nickel atoms - by green.

At the beginning of the crumpling process at both 300 K and 1000 K, GF starts to change its round shape, and the fcc crystalline order of Ni nanocluster is destroyed. Metal atoms are attracted by the graphene surface and tend to occupy equilibrium positions above the center of the carbon hexagon. The edges of GF can attach to each other with the formation of new covalent bonds. During exposure, graphene flake transforms to a capsule containing nickel nanocluster. Nanocluster Ni_{66} almost completely fills the graphene flake, in comparison with Ni_{21}, therefore, the deformation of such a structure is more difficult. Note that GF always tends to wrap the metal cluster.

In this work, nanoclusters consisting of 21 and 66 nickel atoms inside the pores of crumpled graphene are considered. It is found, that the graphene flake can easily cover nanocluster, but the dynamics of the interaction strongly dependent on the nanocluster size. Small nanoclusters can be easily bent by rigid graphene flake, while the biggest conserve their shape. Such structure, composed of Ni nanoclusters and graphene flakes, can be further used to obtain composite material with improved mechanical properties.

References

[1] Meyer J.C., Geim A.K., Katsnelson M.I., et al, Nature, 446, 60-63 (2007).
[2] Tallinen T., Åström J.A., Timonen J., Nature Materials, 8, 25-29 (2008).
[3] Baimova Y.A., et al, Phys. Solid State, 56, 2010-2016 (2014).
[4] Safina L.R., Baimova J.A., et al, Letters on Materials, 10, 3, 351-360. (2020).
[5] Katin K. P., et al, Micro Nano Lett., 13, 160-164. (2018).
[6] Girifalco L.A., Weizer V.G., Phys. Rev., 114, 687-690 (1959).

Effect of thickness on the electrical and optical properties of NbO_x thin films

Pankov S.Yu., Zhilova O.V., Kashirin M.A., Makagonov V.A., Chetverikova A.P.

Voronezh State Technical University, 394024, Voronezh, Russia

Thin films of niobium oxides have significant physical properties such as high refractive index, low absorption and high transmittance in the UV - visible - near IR regions. They are widely used in modern electronic devices: solid state electrolytic capacitors, photochromic devices, memristors, optical waveguides, antireflection coatings, gas sensors, etc. [1]. The physical properties of niobium oxides strongly depend on the preparation conditions [2]. Therefore, in this work, we considered the effect of thickness on the electrical and optical properties of amorphous NbO_x thin films.

Samples from 60 to 130 nm of thickness were obtained by ion-beam deposition on glass and sitall substrates in an argon atmosphere. XRD analysis showed that the films are amorphous. The electrical resistance was measured by a two-probe method through ultrasonic-soldered indium contacts.

Figure 1a showed that amorphous NbO_x films have a high electrical resistivity (ρ), about $10^2 – 10^3$ Ohm·cm, which is lower than the values of the electrical resistivity of amorphous Nb_2O_5 films ($10^{11} – 10^{13}$ Ohm·cm [3]) and is comparable with the ρ value in thin films of nonstoichiometric NbO_x ($2.5 > x > 2.489$) ($10^{-6} – 10^3$ Ohm·cm [2]) or NbO_2 (10^4 Ohm·cm). As the thickness increases, ρ decreases unevenly from 10^3 to 10^2 Ohm cm.

Behavior of the *ρ(h)* dependence can be explained by two reasons: the manifestation of the classical size effect and the change in the phase composition of the film from higher to low resistance with thickness increasing.

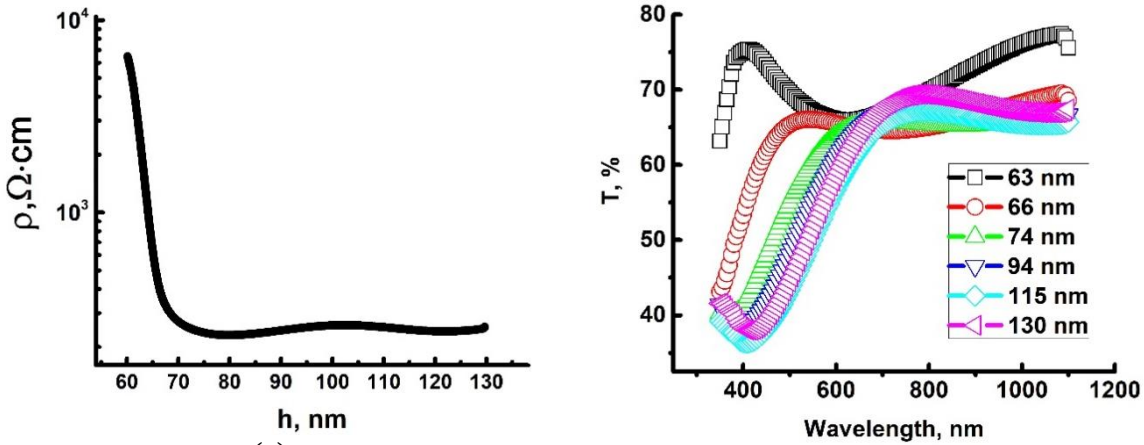

(a) (b)

Figure 1. (a) *ρ(h)* dependence and *(b)* Optical spectra of the NbO_x thin films

To determine the effect of the thickness of the niobium oxide film on its optical properties, the optical transmission spectra of light were measured in the wavelength range from 400 to 1100 nm. The resulting films have a maximum transparency of about 65-70% in the wavelength range 600 – 1200 nm (fig 1.b). To determine the optical band gap Eg_{opt} from the spectral dependence of the absorption coefficient:

$$\alpha = -\, lg(T)/h_{film}, \quad (1)$$

where T - transmittance,

h_{film} - film thickness.

By linear extrapolation of the dependence of $(\alpha hv)^2$ on the photon energy hv to the value $\alpha = 0$ in the region of the fundamental absorption edge, the optical band gap Eg_{opt} was determined. It was found that Eg_{opt} decreases with increasing h from 3.0 eV for films with a thickness of 63 nm to 1.64 eV for 130 nm. In this case, according to the literature, the band gap for amorphous Nb_2O_5 films is ~ 3.4 eV [4], for NbO_2 ~ 1.1 eV [2].

It can be concluded that an increase in the film thickness leads to a redistribution of the phase composition from the high-resistance Nb_2O_5 phase to the low-resistance NbO_2 phase, which affects the electrical and optical properties.

This work was supported by the Ministry of Education and Science within the framework of state assignment No. FZGM-2020-0007.

References

[1] A.A. Atta, M.M. El-Nahass, A.M. Hassanien, et. al., Materials Today Communications 13, 112-118 (2017).

[2] C. Nico, T. Monteiro, M.P.F. Graça, Prog. Mater Sci 80, 1–37 (2016).

[3] A. Imtiaz, et. al., Inorganic and Nano-Metal Chemistry 50, 22–27 (2019).

[4] E.T. Salim, et. al., Materials research express 6, 126459 (2019).

Studies of the phase composition in a nanostructured alloy 36H

Yusupova N.R.[1], Krylova K.A.[2], Mylukov R.R.[2]

[1] Ufa State Petroleum Technjlogical Uneversity, 1 Kosmonavtov St., Ufa 450062, Russia
[2] Institute for Metals Superplasticity Problem, Russian Academy of Sciences, 39 Khalturin St., Ufa, 450001, Russia

Recently, great interest of researchers has been attracted by nanostructured (NS) and ultrafine-grained (UFG) materials, which significantly differ in properties from coarse-grained (more than 10 μm) analogs. Due to the unique physical and mechanical properties, such as high strength and impact strength, increased plasticity, special electrical, magnetic and other properties, NS materials are promising for use in various industries and techniques. [1].

Alloys of the Fe-Ni system have found wide application in modern technology and instrument making. One of the most famous Fe-Ni alloys is the Invar alloy of the composition 36N GOST 10994-74 (with a Ni content of 36%), which has a low coefficient of linear expansion. A significant drawback of this alloy, which limits its use, is its low strength and hardness [2,3]. An effective method for increasing the strength properties of alloys is deformational nanostructuring by torsion under high pressure.

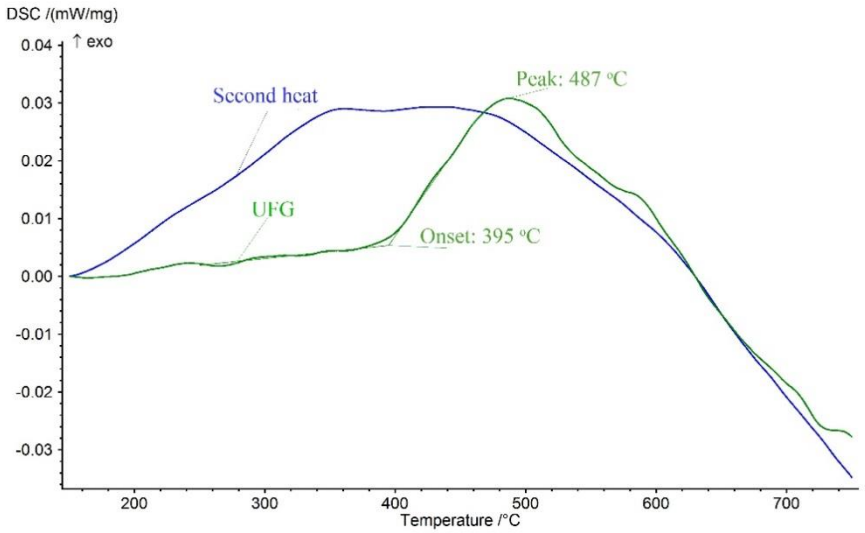

Fig. 1. DSC curves of Invar alloy 36N after deformation nanostructuring (green curve) and upon reheating (blue curve))

Deformation nanostructuring was carried out by torsion under quasi-hydrostatic pressure on Bridgman-type anvils. After deformation, the structure of the 36H alloy consisted of fragments with an average size of about 100 nm. The thermal analysis of the obtained 36H samples is shown in Fig. 1, which shows that heating above 395℃ leads to the appearance of an exothermic peak on the curves obtained in the differential scanning calorimetry mode, indicating a phase transformation in the nanostructured alloy. Note that the large-crystal alloy 36H is a single-phase FCC alloy. However, the formation of a nonequilibrium highly defective structure after nanostructuring leads to an increase in the diffusion capacity in the alloy, as a result of which a phase transformation is observed. A similar effect was observed in [3] for a nanostructured Fe - 36% Ni alloy. When the same sample is reheated, the exothermic peak is

not observed on the DSC curves, which indicates the formation of an equilibrium structure in the alloy after the first heating.

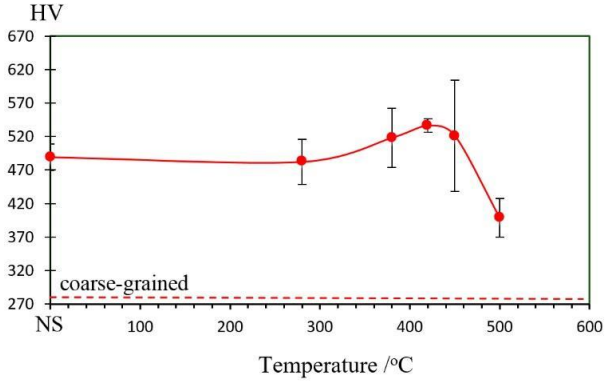

Fig. 2. Graph of the dependence of microhardness (HV) on the annealing temperature of Invar alloy 36H after deformation nanostructuring (NS) and annealing at different temperatures. The dashed line shows the microhardness of the 36H alloy in the coarse-crystalline state.

After analyzing the DSC curves, the 36H nanostructured samples were subjected to sixty-minute vacuum annealing at 280, 380, 420, 450, and 500 ° C. In each of the obtained structural states, the microhardness was measured, as shown in Fig.2. Nanostructuring leads to an increase in microhardness by about 2 times compared to the large-crystal state. The increase in microhardness in the temperature range from 380 to 450 ° C is associated with dispersion hardening due to the separation of the nanoscale BCC phase after nanostructuring followed by annealing [3].

As a result of the study, it was found that the formation of NS leads to an increase in the strength characteristics of the 36H alloy (microhardness increases by about 2 times compared to the large-crystal state). The presence of an exothermic peak on the DSC curves and a maximum after annealing of the 36H nanostructured alloy at 420 ° C indicate the release of the BCC phase in the invar alloy. This is due to a significant increase in the diffusion capacity in the alloy due to the strong nonequilibrium of the grain boundaries and a large concentration of defects after deformation nanostructuring [4].

References

[1] GOST 10994-74. Precision alloys. Stamps

[2] A. Vinogradov, S. Hashimoto, V.I. Kopylov. Materials Science and Engineering: A. 2003. 355 (1–2). P.277-285.

[3] K. A. Krylova, I. Kh. Bitkulov, R. R. Mulyukov. IOP Conf. Series: Materials Science and Engineering. 2018. 447. 012015.

[4] A. A. Nazarov, R. R. Mulyukov. Nanostructured Materials. Handbook of Nanoscience, Engineering, and Technology (CRC Press, USA). 2002. Chapter 22. p 22-1.

Plasma-chemical doping of hexagonal boron nitride nanowalls and related properties

Voroshnina A.A.[1], Merenkov I.S.[1,2]

[1]Nikolaev institute of inorganic chemistry, 630090, Novosibirsk, Russia
[2]Skolkovo institute of science and technology, 121205, Moscow, Russia

The possibility of controlling the properties of nanomaterials is one of the most promising areas of nanomaterials science since tunable properties allow creating devices with desired characteristics. The modification of the morphology or composition of the material is a commonly used approach to controlling the properties of nanostructures.

Vertically oriented nanosheets (nanowalls) are one of the morphological modifications of hexagonal boron nitride (h-BN), which demonstrates antibacterial properties, intense cathodoluminescence, and the possibility of adjusting the contact angle [1]. All of these properties are related to the presence of sharp edges open to interaction and a large surface area. Surficial doping is an effective method of composition modification to control the properties of nanostructures such as graphene and h-BN. Existing studies demonstrate that it is possible to tune the emission [2] and electrochemical [3] properties via h-BN oxidation. But doping of hexagonal boron nitride nanosheets is challenging so far because this material has high chemical and thermal stability. In addition, a combination of morphological and compositional modifications can also be promising. Thus, the purpose of this work is to develop an approach for the surficial oxidation of vertically oriented h-BN nanosheets and to study their properties.

The h-BN nanowalls obtained by the PECVD method were used as initial samples [2]. The synthesis was performed from a mixture of $(C_2H_5)_3N{\cdot}BH_3$ and NH_3 at 400ºC and plasma power of 25 W. Low-temperature oxidation of the samples was performed in a synthetic air atmosphere (79 vol.% N_2 + 21 vol.% O_2). The series of experiments with changing one of the parameters: synthetic air pressure, treatment temperature, exposure time and plasma power were performed.

As a result, we established the dependences of changes in the surface composition and morphology of nanowalls on the synthesis conditions. Based on the obtained data, it was suggested that the process of plasma chemical oxidation of nanowalls is limited by the kinetics of the reaction. The plasma power is found to be a key parameter influencing the rate and depth of the process. The optical and electrophysical properties of oxygen-doped BNNWs were studied, in particular, a light-sensitive increase in conductivity was found. The samples after plasma treatment have superhydrophobic properties, which makes them promise for further study in the field of medical coatings.

The reported study was funded by the RFBR and DST according to research project 19-53-45012

References

[1] H. Achour, Diam. Relat. Mater., 77, 110–115 (2017).
[2] I. S. Merenkov, Nano Res., 12, 91–99 (2019).
[3] J. W. Feng, J. Mol. Model., 20, 4 (2014).

Ultrafast Carrier Dynamics in $MoS_2/SiO_2/Si$

Lebedeva E.D., Pimenov N.Yu., Brekhov K.A., Lavrov S.D.

MIREA - Russian Technological University, 119454, Moscow, Russia

2D transition metals dichalcogenides (TMD) are semiconductors with a direct band gap of 1–2 eV. TMDs are also characterized by effective photoluminescence and high mobility of carriers. That why 2D TMDs are good basis to create flexible, highly efficient devices, such as gas sensors, solar cells, terahertz antennas, and LEDs [1]. Also, it should be noted that 2D TMDs may be used as high-performance optical saturable absorbers which are needed to create Q-switching and mode-locking fiber lasers resonators [2]. This is possible due to the ultrafast relaxation of the electron subsystem in the TMD.

The short relaxation times of the electron subsystem are the main advantage for optical bleaching speed and for the time characteristics of pulsed Q-switched lasers.

When studying the sample, we need to take into account that the 2D TMDs and SiO2 are partially transparent in the visible range of optical radiation and the Si is a semiconductor. This means that a significant part of the pump energy, passing through the 2D TMDs, transfers energy to the substrate, exciting it. Thus, the substrate influences significantly the detection of the excitation and relaxation processes of electrons and holes in 2D flakes of TMDs. Also, substrate affects the estimation of the characteristic times of these processes, which leads to optoelectronic devices speed calculation errors.

This work presents the MoS_2 monolayer on a SiO_2/Si substrate electronic subsystem relaxation studying results. Maps of MoS_2 flake on a SiO_2/Si substrate photoinduced reflection coefficient changing distribution were made. The relaxation mechanisms in Si and $MoS_2/SiO_2/Si$ at different times after excitation were investigated. The substrate contribution to the electronic subsystem relaxation times is determinated, and the relaxation times of the TMD are estimated.

This work was supported by the Ministry of Science and Higher Education of the Russian Federation (state task No. FSFZ-0706-2020-0022).

References

[1] Omkaram I. et al. //Two-Dimensional Materials for Photodetector. – 2018

[2] Chen B. et al. //Optics express. – 2015. – Т. 23. – №. 20. – С. 26723-26737

Microwave reflecting and absorbing properties of thin metal films during the percolation transition

Fitaev I.S.[1], Mazinov A.S.[1]

[1]*V.I. Vernadsky Crimean Federal University, Simferopol, Russia*

Abstract: The paper presents the results of numerical and experimental studies of the effect of the percolation transition in thin aluminum films on the reflecting, transmitting and absorbing properties in the microwave range.

The paper considers the growth mechanism of a thin aluminum film with a thickness range from 1 to 20 nm [1]. The island-structured of the conductor layer was confirmed at the initial stages of growth. Experimentally revealed a burst [2] of the reflective and absorbing capacity of the formed thin film at the merging of individual islands, which is confirmed by a numerical model. The numerical calculation of the transmittance, reflectance and absorbtance was carried out in CST Studio. A unit cell with a nanometer hemispherical formation was simulated, the base size of which varied from 1 nm to a cell size of 25 nm, at a constant structure height. The simulation result is shown in Figure 1.

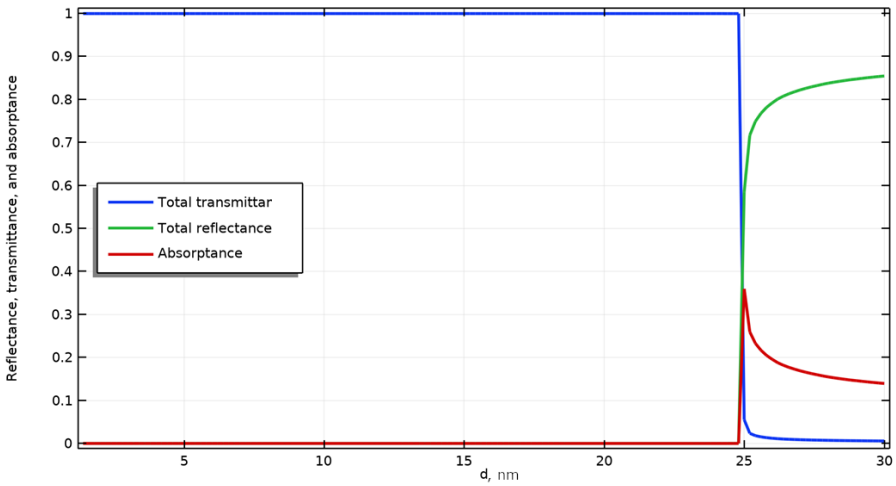

Fig 1. Dependence of transmission, reflection, and absorption on the diameter of the structure base in the simulated cell

References

[1] V.V. Starostenko, A.S.Mazinov, I.S. Fitaev, E.P. Taran, V.B. Orlenson, Forming surface dynamics of conductive aluminum films deposited on amorphous substrates. Applied Physics, (4), P. 60–65(2019)

[2] V.V. Starostenko, V.B. Orlenson, A.S. Mazinov, I.S. Fitaev, A Study of Microwave Radiation Absorption in Ultrathin Conducting Films. 65(8), P. 1296–1300 (2020)

Research of heterojunctions based on the system of fullerene and Zinc complex

Mazinov A.S., Tyutyunik A.S., Gurchenko V.S.

V. I. Vernadsky Crimean Federal University 4 Vernadskogo Ave., Simferopol, Republic of Crimea, 295007, Russia

Abstracts

Organic molecules and coordination compounds based on them have attracted great interest in recent decades due to their potential application in the creation of optical and optoelectronic devices [1, 2]. Among the various classes of luminescent materials, coordination compounds based on zinc (II) complexes with organic ligands are of particular interest due to their availability, low cost, low toxicity, and interesting photochemical characteristics [3]. It is on the basis of the considered prerequisites that an attempt to create a thin-film heterostructure based on C_{60} fullerene and a zinc complex based on Schiff is quite interesting.

Zinc complexes were obtained by the following procedure. To a solution of 4-formyl-3-methyl-1-phenylpyrazol-5-one (808 mg, 4 mmol) in 50 ml of methanol was added the corresponding diamine (2 mmol) and stirred under reflux for 1 hour. Thereafter, solid $Zn(AcO)_2 \cdot 2H_2O$ (438 mg, 2 mmol) and a solution of Et3N (400 mg, 4 mmol) in 10 ml of methanol were added to the solution (Fig. 1a). Stirring was maintained at 50°C overnight. During this time, a precipitate formed. The precipitate was collected by filtration, washed with cold methanol and ether, and dried under vacuum (Fig. 1b).

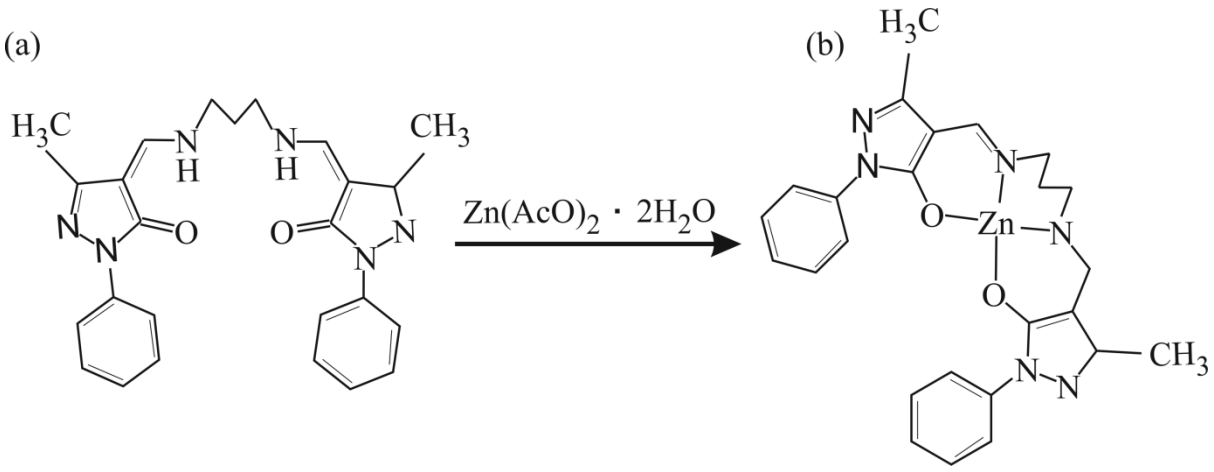

Fig. 1. a – Ligand used in this paper; b – synthesized zinc complex.

The formation of film structures based on powder fullerene C_{60} and 4-methylphenylhydrazone N-isoamylisatin was carried out by pouring from a solution [4]. Non-aromatic compounds were used as solvents: dichloromethane for fullerene and chloroform for isatin. The fixed concentration of the solid phase of the starting material in the solution was 0.5 mg / ml. To assess the homogeneity of the film surface and reveal new formations, the initial substances in solution were applied to dielectric substrates with geometric dimensions of 18×18 mm. The analysis of the relief of the films was carried out by means of transmission and reflection microscopy based on a LOMO Mii-4M microinterferometer with additional illumination with a semiconductor laser and an extended optical path on a camera with a ½ FF 10MP matrix. To obtain thin films of fullerene and zinc complex, solutions were prepared from

initial powders. Carbon tetrachloride (CCl_4) was used as a solvent for fullerene, and chloroform was used for the zinc complex. Fullerene films are characterized by a relatively heterogeneous surface, with thicknesses of 300-500 nm [5] (Fig. 2a). The thickness of the films of the coordination compound was 280-330 nm (Fig. 2b).

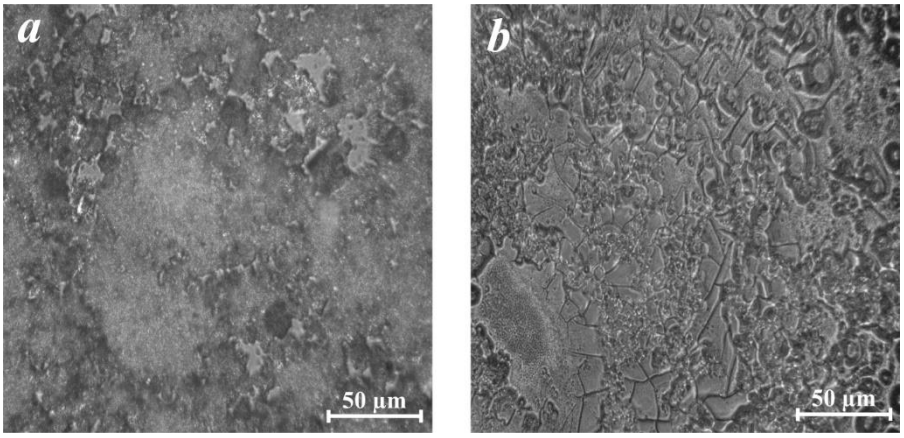

Fig. 2. Microphotographs of fullerene (a), zinc complex (b) films.

To measure the volume resistivity, an aluminum substrate (Al) 120 nm thick and indium tin oxide (ITO) were used as a contact group. To form a heterojunction, fullerene C_{60} was deposited on an aluminum substrate, and a zinc complex was deposited on a glass substrate with a conducting layer of indium-tin oxide. An analysis of the current-voltage characteristics (CVC) showed that the creation of a heterostructure based on a coordination compound and C_{60} fullerene made it possible to obtain a semiconductor structure with a potential barrier. The I - V characteristic is similar to the diode characteristic. In the range of voltages from -1 to 1 V, the current values in the forward direction are 50 µA, in the reverse direction - 250 nA.

References

[1] D. Amgar, S. Aharon and L. Etgar, Adv. Funct. Mater. 26, 8576–93 (2016).

[2] S.V. Eliseeva and J-C.G. Bunzli, Chem. Soc. Rev. 39, 189–227 (2010).

[3] S.S. Pasha, H.R. Yadav, A.R. Choudhuryb and I.R. Laskar, J. Mater. Chem. C. 5, 9651–8 (2017).

[4] V.V. Starostenko, A.S. Mazinov, A.S. Tyutyunik, I.Sh. Fitaev, V.S. Gurchenko, St. Petersburg Polytechnical State University Journal. Physics and Mathematics. 1(13), 106-117 (2020).

[5] A.N. Gusev, A.S. Mazinov, A.I. Shevchenko, A.S. Tyutyunik, V.S. Gurchenko and E.V. Braga, Prikl. Fiz. 6, 48 (2019).

Magnetoelectric transformer with variable thickness of the magnetic layer

Chashin D.V., Fetisov L.Y., and Fetisov Y.K.

MIREA –Russian Technological University, Pr. Vernadskogo 78, 119454 Moscow, Russia

A magnetoelectric (ME) transformer parameters could be tuned by magnetic field unlike piezoelectric traditional transformers [1]. Such a transformer is fabricated on a basis of a ferromagnetic (FM)–piezoelectric (PE) heterostructure comprising two equally thick laminated layers of an amorphous FM alloy and a piezoceramic lead zirconate-titanate layer sandwiched between them. It is well known that magnetoelectric parameters of the structure strongly depends on its' composition, number of layers etc. This work describes the effect of the thickness of the FM layer on the characteristics of the ME transformer.

The PE layer was made of piezoceramics $Pb(Zr,Ti)O_3$ (PZT-47, manufactured by the JSC Research Institute "Elpa", Russia). The FM layers with a thickness a_m = 23 μm were made of amorphous magnetic alloy (FeBSiC) ribbons 2605SA1 (Metglas Co, USA). The thickness of the FM layers of the structure was changed by gluing 1, 2, or 3 layers on each side of the PE layer together. All layers of the structure were connected under pressure using a cyanoacrylate adhesive. The total number of individual Metglas layer was 2, 4 and 6, respectively.

Measured on the open circuit condition transformation ratio *K* dependence on magnetic field is shown in Fig. 1. It is seen that maximal value of *K* is observed in a structure with 3 FM layers as well as maximal tuning ratio of magnetic fields.

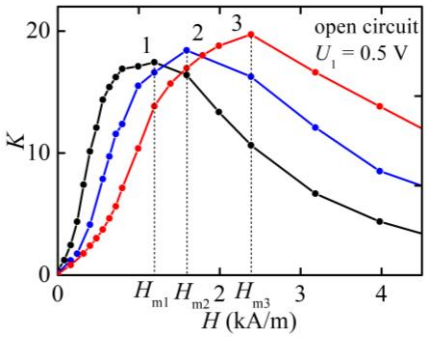

Fig. 1. Magnetic field dependences of transformation ratio *K* on magnetic field at resonance conditions for structures with different total thicknesses of the FM layer a_m, μm: 1 – 46 μm, 2 – 92 μm, 3 – 138 μm.

The voltage transformation ratio of the magnetoelectric transformer could be tuned from 0 to 19.7 in *H* = 2.4 kA/m at the largest total thickness of ferromagnetic layers of 138 μm. The power transfer efficiency η reached 45% at the matched resistive load of about 20 Kω.

This work was supported by the Russian Science Foundation [grant 19-79-10128].

References

[1] D. Saveliev, L.Fetisov, D. Chashin, Y. Fetisov, and M. Shamonin, Materials, 13, 8, 3981(2020).

The effect of heat treatment on structure and soft magnetic properties of $Fe_{70.8}Co_{10}B_{10}Si_{1.5}P_7Cu_{0.7}$ nanophase composite

Vasiliev S.V.[1,2], Svyrydova K.A.[1,2], Kostyrya S.A.[1], Moiseeva T.N.[1], Glazunova V.A.[1], Konstantinova T.E.[1], Tkatch V.I.[1]

[1]A.A. Galkin Donetsk Institute for Physics & Engineering, 283114, Donetsk, Ukraine [2]Donbas National Academy of Civil Engineering and Architecture, 286123, Makeyevka, Ukraine

The development of soft magnetic materials with high saturation magnetic induction B_s combined with good soft magnetic properties is still in demand for high performance and miniaturization of magnetic parts and devices such as transformers, inductors, magnetic recording heads and others. Among a large variety of soft magnetics, the new alloys with nanocomposite structure based on the Fe–Cu–Si–B–P system (NANOMET) have attracted great attention due to their low saturation magnetostriction and high saturation induction above 1.8 T [1]. However, the magnetic properties of NANOMET alloys strongly depend on not only on chemical composition but also on structure of nanophase composites which formed by heat treatment of glassy precursors [3071]. The aim of this study is to establish relation between the annealing regimes of $Fe_{70.8}Co_{10}B_{10}Si_{1.5}P_7Cu_{0.7}$ glass its structural parameters and soft magnetic properties.

Rapidly solidified alloy ribbons of about 25 μm thick and 10 mm width were prepared by melt spinning in air onto a Cu-Cr wheel of 620 mm in diameter at tangential velocity of ~40 m/s. Structural characterization of the samples was performed by using X-ray diffraction (DRON-3M automated diffractometer) and transmission electron microscopy (JEM-200A). Crystallization kinetics was monitored using differential scanning calorimetry (NETZSCH DSC 404) and electrical resistance measurements (a four-probe method). Magnetic properties were measured with a MS-02 B-H analyzer at 400 Hz under a field up to 2 kA/m.

Amorphous structure of the as-prepared ribbons was confirmed by XRD (scan 1 in Fig. 1) and TEM data. The DSC thermogram showed that crystallization of amorphous phase took place via two separated stages. Analysis of the XRD patterns of the heat treated samples showed that nanophase composite consisted of nanoscale crystals of bcc α-Fe and residual glassy matrix formed at the first stage (scan 2 in Fig. 1), while the lines of unidentified iron boride and phosphide observed in the XRD pattern of fully crystallized sample (scan 3 in Fig. 1).

The studies of the effect heating up temperature at 10 K/min on the structural parameters of nanophase composite showed that both the sizes of α-Fe nanocrystals and its volume fraction crystallized monotonically increased up to 0.53 and 52 nm, respectively, at the end of nanocrystallization. The increase of the heating rate to 40 K/min resulted in the decrease of the nanocrystal sized to 32 nm but the volume fraction remained unchanged.

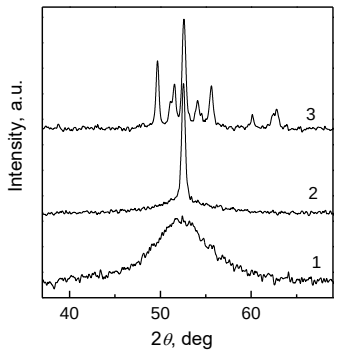

Fig. 1. X-ray diffraction patterns of the as-quenched (1), partially (2) and fully crystallized melt-spun ribbons

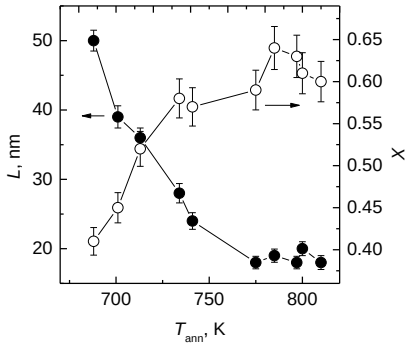

Fig. 2. Changes of average sizes of α-Fe nanocrystals (●) and their volume fraction (○) vs. temperatures of annealing up to end nanocrystallization

Accounting the above results and the literature data showing that the essential improvement of the soft magnetic properties is reached in nanophase composites with nanocrystal sizes ≤ 20 nm [3] a series of isothermal annealings was performed in a salt bath. The estimated heating rates of ribbon samples in these experiments were about 200 K/s. The experiments have shown that growth of α-Fe nanocrystals is very fast at all annealing temperatures and does not follow the well-established classical Zener equation [4]. As can be seen from the data in Fig. 2 the increase of annealing temperature results in the increase of the volume fraction crystallized (up to 0.6–0.65) and to decrease of α-Fe nanocrystals (to 17–19 nm). The volume density of α-Fe nanocrystals is in the range $(1–2)\times10^{23}$ m^{-3} which is typical for nanophase composites with the high soft magnetic properties [3]. The XRD data were confirmed by the TEM studies which showed the presence of near spherical particles with bcc structure dispersed in the glassy matrix.

In order to estimate the coil made of the as-prepared ribbon was heat treated by immersing into a salt bath at 755 K for 4 min. The size of nanocrystals formed at this annealing conditions was 18 ± 1 nm and the volume fraction crystallized was estimated to be 0.57. The heat treatment resulted in the decrease of the coercive force from 21 to 6 A/m and to increase of the initial permeability from 4000 to 11000.

The possible mechanisms of the nanocomposite structure formation in $Fe_{70.8}Co_{10}B_{10}Si_{1.5}P_7Cu_{0.7}$ glass as well as the ways of subsequent improvement of its soft magnetic properties are discussed.

References

[1] M. Ohta and Y. Yoshizawa, J. Phys. D: Appl. Phys. 44, 064004 (2011).
[2] A. Makino, IEEE Trans. Magn. 48, 1331 (2012).
[3] P. Sharma, X. Zhang, Y. Zhang, A. Makino, Scr. Mater. 95, 3 (2015).
[4] C. Zener, J. Appl. Phys. 20, 950 (1949).

The role of oxygen in the formation of a continual metal shell strongly bonded to the carbon surface

Churilov G.N.[1,2], Glushenko G.A.[1,2], Tomashevich Ye.V.[3], Nikolaev N.S.[1], Vnukova N.G.[1,2]

[1]*Kirensky Institute of Physics, FRC KSC SB RAS, 660036, Krasnoyarsk, Russia*
[2]*Siberian Federal University, 660062, Krasnoyarsk, Russia*
[3]*Institute of Chemistry and Chemical Technology, FRC KSC SB RAS, 660036, Krasnoyarsk, Russia*

We have synthesized and studied nanodispersed particles with the (Mg@C)@Pd structure, which can be used to solve problems in hydrogen energy, both as hydrogen accumulators and for its purification. It turned out that after ten cycles of hydrogenation / dehydrogenation, the particles are destroyed, Fig.1 [1]. X-ray phase studies have shown that the β-phase is absent, i.e. the reason for the destruction of the palladium shell is not associated with the loss of plasticity of palladium [2]. We assumed that when exposed to oxygen and temperature, the palladium-carbon composite in the nanodispersed state behaves differently from the monolithic one.

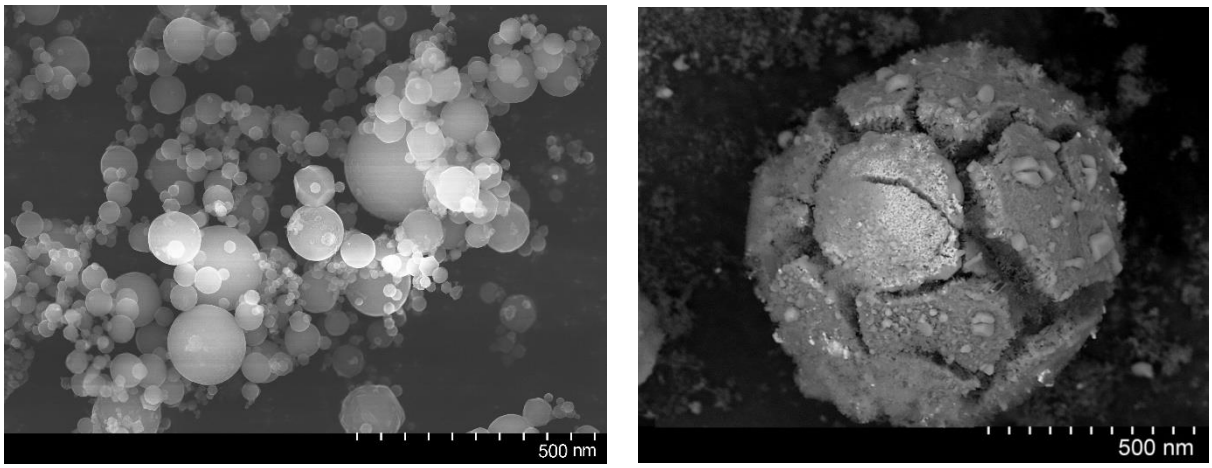

Fig. 1. SEM image: left – before hydrogenation, on right – after 10 cycles of hydrogenation/dehydrogenation [1]

In this work, we present the results of a study of the process of thermal oxidation of carbon condensate (CC) containing palladium in a nanodispersed state in an oxygen flow. CC was obtained by sputtering carbon rods with an axial hole containing metallic palladium in an HF arc discharge using the technology described in [3]. The studies were carried out by the following methods: XPS, electron microscopy, thermogravimetry, XRF, Raman scattering. As it turned out, even in the samples annealed in argon at a temperature of 1200 °C, in addition to metallic palladium and carbon in Sp2 hybridization, their presence is observed in the oxidized state, Fig. 2, Fig. 3.

The mathematical expansion of the Pd3d, C1s, and O1s lines shows the presence of Pd, C, and O peaks with concentrations of 20.55, 28.83, and 50.62 at%, respectively.

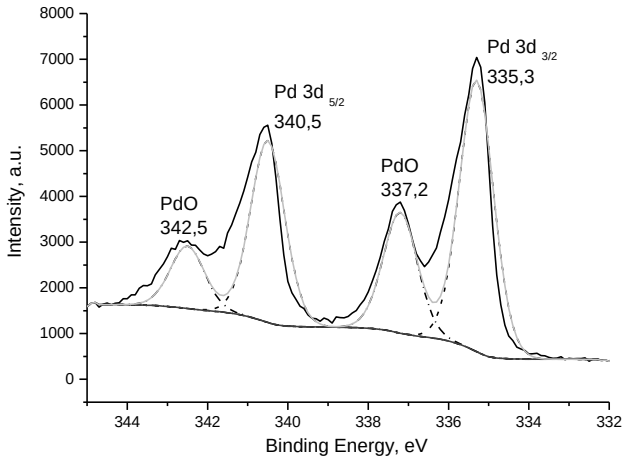

Fig. 2. XPS: Pd3d line

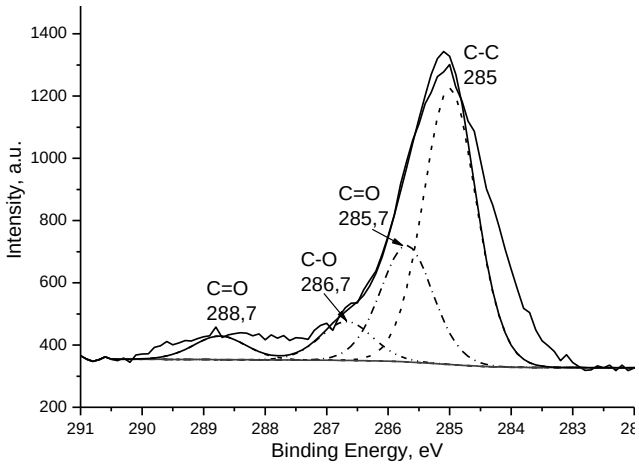

Fig. 3. XPS: C1s line

In addition, the sample annealed under the same conditions, but located in a gradient temperature field (the lower part of the crucible is 1000 °C, the upper part is 800 °C), clearly divided into 2 samples: the lower sample is black powder 0.11, 88.56, 11.33 Pd3d, C1s, O1s at.%, Respectively, and the upper one is light gray, in the form of tangled hairs 17.35, 35.74, 46.91 Pd3d, C1s, O1s at.% , respectively.

Thus, a composite of carbon, palladium, and oxygen behaves ambiguously when exposed to temperature and undergoes structural and stoichiometric changes.

References

[1] G.N. Churilov, N.S. Nikolaev, G.A. Glushenko, V.I. Elesina, V.G. Isakova and Ye.V. Tomashevich, International Journal of Hydrogen Energy (2021). https://doi.org/10.1016/j.ijhydene.2021.03.042

[2] G.S. Burkhanov, N.B. Gorin, N.B. Kolchugina and N.R. Roshan, Russian Chemical Journal L(4), 36 (2006) (in Russian).

[3] G. Churilov, A. Popov, N. Vnukova, A. Dudnik, N. Samoylova and G. Glushenko, Fullerenes, Nanotubes and Carbon Nanostructures 24(11), 675 (2016).

Synthesis and proton conductivity of hybrid materials based modified by polyantimonic acid

Yaroshenko F.A., Lupitskaya Yu.A., Filonenko E.M.

Chelyabinsk State University, 454001, Chelyabinsk, Russia

Ion-exchange membranes are commonly used in purification and electrochemical synthesis processes and in low-temperature fuel cells [1–3]. The use of these membranes makes it possible to design highly efficient compact energy sources of varying power. To provide efficient operation, the membranes should exhibit a number of physicochemical properties, the most important of which are high proton conductivity, temperature stability, and low hydrogen permeability [1, 3]. The properties of MF-4SK membranes are close to optimum. However, these membranes have some disadvantages, such as an abrupt decrease in proton conductivity at low air humidity and with an increase in temperature above 100°C.

The properties of MF-4SK membranes can be improved owing to the introduction of nanoparticles of inorganic materials into the polymer matrix. These materials include heteropoly acids and their acid salts and SiO_2, ZrO_2, and CeO_2 metal oxides. We believe that a promising dopant is polyantimonic acid (PAA), which is known to be an excellent proton conductor containing oxonium ions and water molecules localized in the compound structure and on the particle surface.

The aim of this study was to develop a method for the preparation of hybrid materials by modifying the MF-4SK membrane with PAA and determine the effect of humidity and temperature on the proton conductivity.

Synthesis of the samples was carried out by in situ method by treating the final MF-4SK membrane with a precursor which was prepared by oxidizing $SbCl_3$ with nitric acid, followed by storing the membrane in distilled water. To create the same conditions, all the samples were conditioned. The proton conductivity was measured on a symmetrical cell in the frequency range of 10 Hz-2 MHz using an Elins Z-1500J impedance analyzer.

In work proton-conducting materials based on the membrane MF-4SK and antimony acid were obtained. Their dielectric properties and conductivity at various temperatures and relative air humidity were studied. The introduction of particles of polyantimony acid significantly increases the values of proton conductivity of membranes at low humidity from 3.2×10^{-5} to 2.5×10^{-4} Sm/sm. An investigation of the proton conductivity at various temperature showed that the activation energy decreases from 16.8 to 12.9 kJ/mol with doping of the MF-4CK membrane by antimony acid.

References

[1] E.Yu. Safronova and A.B. Yaroslavtsev, Pet. Chem. 56, 281 (2016).

[2] S.S. Ivanchev and S.V. Myakin, Russ. Chem. Rev. 79, 101 (2010).

[3] H. Strathmann, A. Grabowski, and G. Eigenberger, Ind. Eng. Chem. Res. 52, 10364 (2013).

Thin-film phototransistors based on fullerene and photochrome derivatives

Salikhov R.B., Mullagaliev I.N., Salikhov T.R.

Bashkir State University, 450076, Ufa, Russia

Thanks to organic electronics, a wide range of devices (displays, microcircuits, sensors, etc.) may appear in the near future, which will be ultra-thin, lightweight, flexible and transparent [1]. It is important to obtain new effective photochromic systems that are promising for micro- and nanoelectronics [2-3].

In this work, samples of phototransistors are manufactured and investigated. Glass with a conductive ITO layer, which plays the role of a gate, was used as a substrate. A polyaniline film 500 nm thick was deposited on top by thermal sputtering in a vacuum from a Knudsen cell. Polyaniline was in a non-conducting state and acted as a gate dielectric. Were investigated three types of transistors: the first type of transistor structures, separate layers of photochromic organic compounds and C60 with a thickness of each film 200 nm. The second type of structures is a film of physically mixed powders of photochrome and C60. The third type is an active layer made of fullerene and photochrome derivatives. On top of the active layers by thermal sputtering in vacuum on a VUP-5 device (vacuum universal post), two aluminum electrodes, a drain and a source with a thickness of 500 nm, were deposited. The film thickness was monitored using an SPM. The created devices were characterized by a channel width of 10 mm and a channel length of 50 μm.

A study of the current-voltage characteristics of the manufactured transistors showed that, in the absence of irradiation, the currents in the phototransistors are of the order of or less than 1 nA. Under the influence of ultraviolet light (350 nm) of the gap region of the transistors, the drain-source current increases by three orders of magnitude for both devices. Mixed active layers have high currents of current-voltage characteristics. And the most stable work is with hybrid layers. Dependencies are non-linear. There are no saturation areas on the output characteristics. All measurements were carried out under normal conditions - atmospheric air, which is an advantage of the investigated transistor structures in comparison with others.

References

[1] Y.N. Biglova, R.B. Salikhov, T.R. Salikhov, I.N. Safargalin, A.G. Mustafin, I.B. Abdrakhmanov, Physics of the Solid State, V 59, № 6, 1253-1259 (2017).

[2] A.R. Tuktarov, R.B. Salikhov, A.A. Khuzin, N. R. Popod'ko, I. N. Safargalin, I.N. Mullagaliev, U.M. Dzhemilev, RSC Advances V 9(13), 7505–7508 (2019).

[3] A.R. Tuktarov, R.B. Salikhov, A.A. Khuzin, I.N. Safargalin, I.N. Mullagaliev, O.V. Venidiktova, T.M. Valova, V.A. Barachevsky, U.M. Dzhemilev, Mendeleev Communications V 29(2), 160–162 (2019).

Section 6
Multiferroics

Magnetoelectric effect in perovskite – based multiferroics $RCrO_3$

Zvezdin A.K.[1], Gareeva Z.V. [2], Chen X.M.[3]

[1]*A1Prokhorov General Physics Institute, Russian Academy of Sciences, 119991, Moscow, Russia*
[2]*Institute of Molecule and Crystal Physics, Subdivision of the Ufa Federal Research Centre of the Russian Academy of Sciences, 450075, Ufa, Russia*
[3]*Laboratory of Dielectric Materials, School of Materials Science and Engineering, Zhejiang University, 310027, Hangzhou, China*

Currently, active research is aimed at perovskite – based oxides, including rare earth orthochromites, which exhibit magnetoelectric properties owed to intrinsic magnetic interactions in external electric and magnetic fields. Due to a variety of structural instabilities and couplings in these materials, understanding the underlying magnetoelectric mechanisms is a challenge.

Here, we explore magnetoelectric properties of the rare earth orthochromites in the framework of symmetry analysis. Our calculations show the presence in $RCrO_3$ of electric dipole moments localized in the vicinity of Cr^{3+} ions. The electric dipole moments, appearing due to the displacements of oxygen ions from their highly symmetric positions in the parent perovskite phase, are arranged in an antiferroelectric mode (Fig.1).

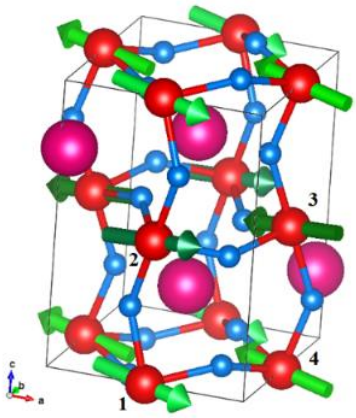

Fig.1. Electric dipole moments (green arrows) arrangement in $RCrO_3$ unit cell.

We have demonstrated the presence of electric dipole moments in the unit cell of $RCrO_3$, localized in the vicinity of Cr^{3+} ions. The inversion symmetry breaks due to the displacements of oxygen ions from their highly symmetric positions in the parent perovskite phase, the electric dipoles become arranged in an antiferroelectric mode. We have introduced the basic distortive order parameters in consistence with the symmetry of $RCrO_3$: the polar order parameters ($\boldsymbol{D}$, $\boldsymbol{Q}_2$, $\boldsymbol{Q}_3$, $\boldsymbol{P}$) and the axial order parameter Ω and classified them according to the irreducible representations of the $RCrO_3$ symmetry group (D_{2h}^{16}).

$$\begin{aligned} \boldsymbol{P} &= \boldsymbol{d}_1 + \boldsymbol{d}_2 + \boldsymbol{d}_3 + \boldsymbol{d}_4 \\ \boldsymbol{Q}_2 &= \boldsymbol{d}_1 - \boldsymbol{d}_2 - \boldsymbol{d}_3 + \boldsymbol{d}_4 \\ \boldsymbol{Q}_3 &= \boldsymbol{d}_1 - \boldsymbol{d}_2 + \boldsymbol{d}_3 - \boldsymbol{d}_4 \\ \boldsymbol{D} &= \boldsymbol{d}_1 + \boldsymbol{d}_2 - \boldsymbol{d}_3 - \boldsymbol{d}_4 \end{aligned} \qquad (1)$$

where $\boldsymbol{d}_i = 3e\boldsymbol{r}_i$ is the dipole moments calculated in a frame of point charge model

$$\boldsymbol{r}_q = \frac{\left(+\frac{3}{8}e\right)\cdot\sum_{i=1}^{8}\boldsymbol{r}_R + \left(-\frac{2}{2}e\right)\cdot\sum_{i=1}^{6}\boldsymbol{r}_O}{\left|8\cdot\left(+\frac{3}{8}e\right)+6\cdot\left(-\frac{2}{2}e\right)\right|} \qquad \boldsymbol{r} = (x, y, z) \qquad (2)$$

where e is the elementary charge, $\boldsymbol{r_R}$ are the radius vectors of the rare earth ions, $\boldsymbol{r_O}$ are the radius vectors of the oxygen ions measured from Cr^{3+} ion. So, each of the dipoles has its own orientation, and the ferroelectric ordering established in $RCrO_3$ is characterized by 4 ferroelectric sublattices with electric dipoles $\boldsymbol{d}_i$. The electric dipoles appear due to the outcome of oxygen ions from their high symmetry positions, in the first approximation, the displacements of the R^{3+} ions from their high symmetrical positions give no impact into the electric dipole moments. To find the basic ferroelectric vectors transforming on the irreducible representations (IR) of the *Pnma* space symmetry group, we consider the possible linear combinations between electric dipole moments given by eq. (1).

We have determined the symmetry - allowed couplings between distortive, ferroelectric and magnetic orderings and found possible exchange- coupled magnetic and ferroelectric structures. The presented analysis makes it possible to explain experimentally observed polarization reversal and the concomitant reorientation of spins in a series of $RCrO_3$ compounds [1] and to predict the possible scenarios of phase transitions in RCrO3.

The work was supported by the Russian Foundation for Basic Research (grant No. 19-52-80024).

References

[1] B. Rajeswaran, D. I. Khomskii, A. K. Zvezdin, C. N. R. Rao, and A. Sundaresan, Phys. Rev. B 86, 214409 (2012)

Transformation of micromagnetic structures arising in uniaxial films with the flexomanitoelectric effect in a magnetic field

Vakhitov R. M.[1] , Guryanova V. R. [2], Nizyamova A. R. [1], Solonetsky R. V. [1], Fomin V. V. [1]

[1]Bashkir State University, 450076, Ufa, Russia
[2]Ufa Law Institute of the Ministry of Internal Affairs, 450091, Ufa, Russia

At present, studies of various magnetoelectric effects in magnetic materials are becoming very relevant, which is associated with the discovery of new physical properties in them, which can be used in energy-saving devices in spintronics [1]. In particular, the phenomenon of domain wall (DW) displacement in iron garnet films under the action of an inhomogeneous electric field, discovered in [2], also belongs to such effects. To explain the observed effect, two possible mechanisms were proposed: a flexomagnetoelectric mechanism due to the presence of inhomogeneous magnetoelectric interaction in the samples under study [3] and a mechanism associated with a change in the material magnetic anisotropy constants [1]. Both mechanisms qualitatively fully explain the pattern of DW behavior in an inhomogeneous electric field. To identify the dominant mechanism, other aspects of this phenomenon were experimentally studied, in particular, it was shown that the structure and some characteristics of the DW in an inhomogeneous electric field are significantly influenced by an external magnetic field and, in particular, its planar component perpendicular to the plane of rotation of spins in the DW. [1]. The presence of the latter can lead to an increase in the magnetoelectric effect on the DW. In this work, we consider, within the framework of the flexomagnetoelectric mechanism, the effect of an external magnetic field **H** on the structure and properties of magnetic inhomogeneities induced by an inhomogeneous electric field **ε** in magnetically uniaxial films. As shown in [4], in such magnets in an inhomogeneous electric field at $H = 0$, three types of micromagnetic structures can occur: 180 degree DWs with a noncircular trajectory of the magnetization vector **M**, 0 degree DWs with a quasi-Bloch structure, and 0 degree DWs of the Neel type. The appearance is due to the inhomogeneous nature of the electric field, the value of its integral polarization is zero.

It is shown that in a nonzero magnetic field the topology of these inhomogeneities will change, but the nature of these transformations will depend both on their structure and on the orientation of the magnetic field. It is revealed that for each type of micromagnetic structures there is always such a direction of the magnetic field at which the integral value of the polarization of the inhomogeneity under consideration increases, which means an increase in the flexomagnetoelectric effect. In particular, in a transverse magnetic field (**H** is perpendicular to the plane of the DW), with its increase, the integral value of the polarization of the 180° DW also increases. In addition, by changing the direction of the magnetic field to the opposite, the character of the interaction of the DW with the source of the electric field can be changed to the opposite, for example, from attraction to repulsion and conversely.

It follows from the calculations that the nucleation of a DW with a quasi-Bloch structure in a uniaxial film occurs only when the field ε reaches a certain critical value $\varepsilon = \varepsilon_c$. When a magnetic field **H**||Oz is applied (Oz coincides with the easy axis of uniaxial anisotropy), the value of the critical field ε_N can be controlled, and, in particular, it is possible to achieve that the DW is nucleated at $\varepsilon \approx 0$.

In the case of a DW of the Néel type, under the action of a magnetic field with **H**||Ox on it, its magnetic moments, turning towards Ox, leave the plane yOz. Due to the exchange interaction, a dependence of the polar angle θ(y) of the vector **M** appears, which ultimately leads to the appearance of a nonzero integral polarization N(ε). As a result, a flexomagnetoelectric effect, sufficient for its observation under experimental conditions, also arises in a DW of the Néel type.

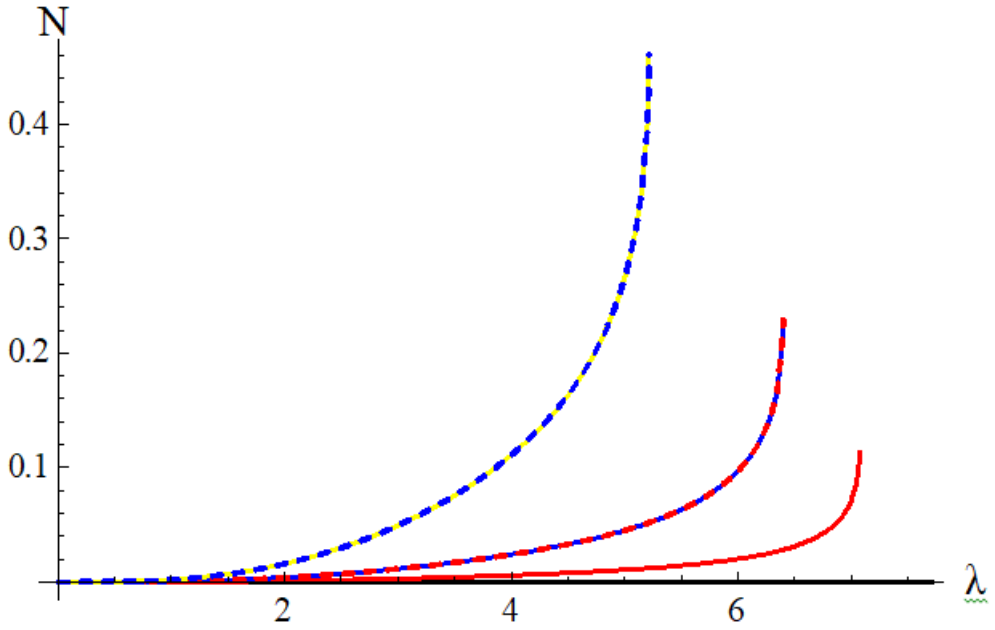

Fig. 1. Graphs of the dependences of the integral polarization (N) 0° DW of the Néel type on the parameter λ in the magnetic field **H||**Ox. The black line corresponds to h = -1, h = 0.1 h = 0, red – h = 0.2, blue – h = 0.4, yellow – h = 0.8, red dashed–h = -0.4, blue dashed–h = -0.8. Here λ= ε/ ε_0, h=H/H_u, where ε_0 – is the characteristic value of the electric field [3], H_u – is the field of uniaxial anisotropy [4].

References

[1] A. P. Pyatakov, etc., UFN, 185 (2015), 1077-1088.
[2] A. S. Logginov etc., JETP Letters, 86 (2007), 124-127.
[3] R. M. Vakhitov, etc., FTT 61 (2019), 1120-1127.
[4] R. M. Vakhitov, R. V. Solonetsky, A. A. Akhmetova, FMM,121 (2020), 462-468.

Nd-Fe exchange interaction in Nd ferroborate with multiferroic properties under optical pumping

Gavrichkov V.A., Malakhovskii A.V., Ovchinnikov S.G.

Kirensky Institute of Physics, 660036, Krasnoyarsk, Russia

We considered the effect of optical pumping at the frequency of f-f transitions on the d-f superexchange in the AFM ferroborate of rare-earth elements $Nd_{0.5}Gd_{0.5}Fe_3(BO_3)_4$ between Nd^{3+} ions in the excited states $4G_{5/2} + 2G_{7/2}$ and Fe^{3+} to the $^6A_1$ ground state. In this ferroborate, the d-f superexchange is directly related to the strong magnetoelectric coupling observed in the ground state of the material. In a magnetic field, with the establishment of a simple collinear AFM ordering between the basic hexagonal planes, the magnitude of the electric polarization reaches a maximum.

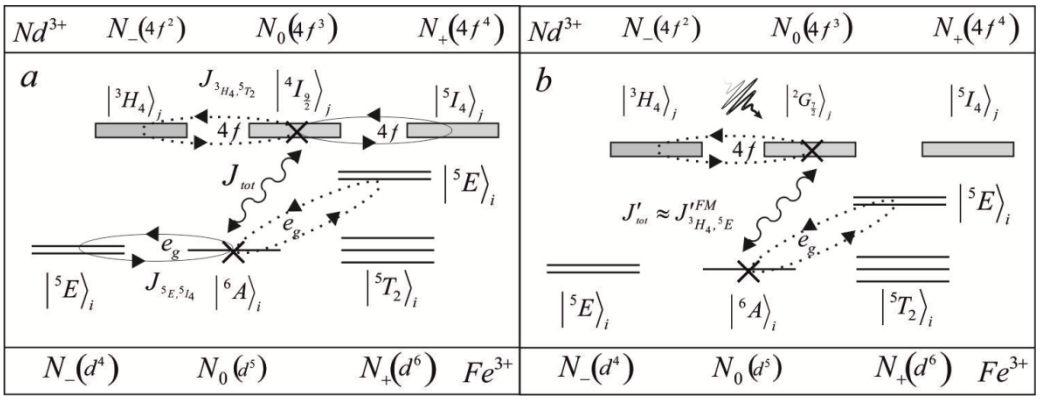

It is shown that under optical pumping at the f-f frequency of the $4I_{9/2} \rightarrow (4G_{5/2} + 2G_{7/2})$ transitions in the Nd^{3+} ion, the character of the d-f interaction changes to FM (see Figure) [1]. The phenomenon can be explained by the occupation of optical excited "pure spin" states of Nd^{3+} with spin 1/2, as well as their mixing with optical excited states with spin 3/2 due to the spin-orbit interaction. In connection with the high $T_C \sim 300$ K observed in rare-earth oxides with transition elements, the specific features of the d-f superexchange, which are absent in the d-d interaction, are considered.

The reported study was supported by the grant RFFI 19-02-00034 and the Russian Foundation for Basic Research, Government of Krasnoyarsk Territory, and Krasnoyarsk Regional Fund of Science according to the research project "Studies of superexchange and

electron-phonon interactions in correlated systems as a basis for searching for promising functional materials No. 20-42-240016.

References

[1] V.A.Gavrichkov, A.V.Malakhovskii, S.G.Ovchinnikov, submitted to Phys. Rev. B, (2021).

Tailoring of stable induced domains near a charged domain wall in lithium niobate by probe microscopy

Kislyuk A.M.[1], Kubasov I.V.[1], Ilina T.S.[1], Turutin A.V.[1], Kiselev D.A.[1], Temirov A.A.[1], Malinkovich M.D.[1], Parkhomenko Yu.N.[1]

[1]National University of Science and Technology MISiS, 119049, Moscow, Russia

The influence of a charged domain wall on the formation of the induced domain structures in congruent x-cut lithium niobate crystals ($LiNbO_3$) was studied. By diffusion annealing in air ambient near Curie temperature, as well as infrared annealing in oxygen-free ambient bi- and multidomain ferroelectric structures containing charged domain walls "head-to-head" and "tail-to-tail" were formed. By Kelvin probe mode of atomic force microscopy (AFM) surface potential near the charged domain walls was investigated. We studied surface needle-shaped induced microdomains which were formed in a vicinity of the domain boundary and far from it by applying of voltage to the cantilever being in a contact with the surface of the sample. Dependence of morphology of the induced domain structure on the crystal's electric conductivity was demonstrated. Screening effect of charged "head-to-head" domain wall on a shape and size of the domain, that was induced near the boundary was shown. We described partition of the single needle-shaped domains formed by AFM cantilever to several microdomains having a shape of several beams based in a common nucleation point. We found an influence of the charged domain wall on the topography of the samples, which consisted in the appearance of a long groove corresponding to the domain boundary after the reducing annealing.

The study was supported by the Russian Science Foundation, project No. 21-19-00872

Gradient Magnetoelectric Current Sensor

Turutin A.V.[1,2], Kuts V.V.[1], Kubasov I.V.[1], Kislyuk A.M.[1], Leontiev V.S.[3], Malinkovich M.D.[1], Parkhomenko Yu.N.[1]

[1] National University of Science and Technology MISiS, 119049 Moscow, Russia
[2] Department of Physics and I3N, University of Aveiro, 3810-193 Aveiro, Portugal
[3] Novgorod State University, 173003, Veliky Novgorod, Russia

Investigation presents a theoretical and experimental study of a magnetoelectric (ME) current sensor based on a gradient structure. The use of gradient structures in ME composites makes it possible to create a self-bias structure, which leads to miniaturization and a decrease power consumption of the device. Current sensors based on a gradient structure of bidomain LiNbO3 (LN) / Ni / Metglas operate on a linear section of the dependence of the ME coefficient on the magnetic field and do not require an external constant bias field.

The gradient structure was obtained by electrochemical deposition of nickel on the surface of lithium niobate with a Ti layer. To obtain a self-bias effect, the gradient structure was annealed in a constant uniform magnetic field (H = 1.2 kOe) at a temperature above the Curie point of nickel Tc = 358 °C. The samples before and after annealing were examined by magnetic force microscopy (MFM). The measurement results are shown in Figure 1a, b.

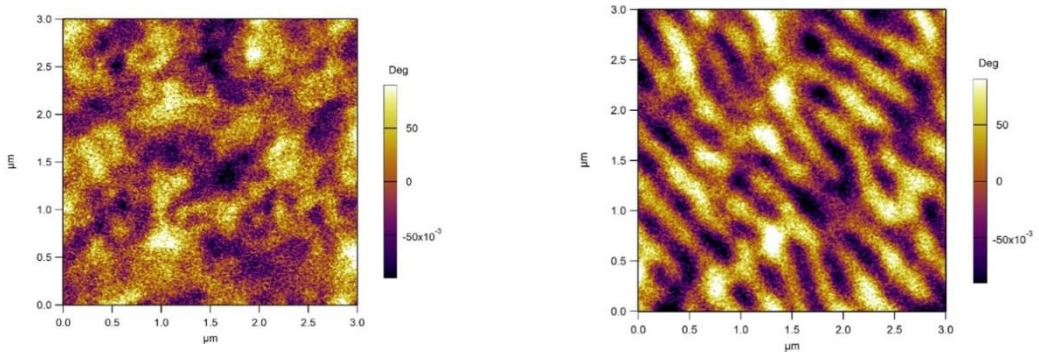

(a) (b)

Fig. 1. MFM scans of the Ni layer before (a) and after (b) annealing.

After annealing in the nikel film the domain structure is ordered in the direction of the applied magnetic field. Also, a remanent magnetization of the nickel film appears, which is capable of acting on the more magnetically soft material of metglas, thereby magnetizing it in a certain direction.

The main characteristics of the non-contact ME current sensor: the range of the detected current is from 0 to 10 A, the sensitivity is 0.9 V/A, the linearity of the sensor reaches an accuracy of 99.8%. Also, the advantages of current sensors based on bidomain lithium niobate are the high sensitivity of the device due to the use of electromechanical resonance of the ME structure and the absence of lead in the device.

Suppression of acoustic and thermal noises in magnetoelectric sensors based on bidomain lithium niobate

Turutin A.V.[1,2], João V.V.[2], Kubasov I.V.[1], Kislyuk A.M.[1], Malinkovich M.D.[1], Parkhomenko Yu.N.[1], Kobeleva S.P.[1], Sobolev N.A.[2]

[1]National University of Science and Technology MISiS, 119049, Moscow, Russia
[2]Department of Physics and I3N, University of Aveiro, 3810-193 Aveiro, Portugal

The study reports the creation of a highly sensitive, low-frequency magnetic field sensor based on a composite multiferroic consisting of a bidomain lithium niobate / metglas laminate shaped in form of a tuning fork. An efficient suppression of acoustic and thermal noises in the measurements of AC magnetic fields has been achieved. As a piezoelectric component we used a y+128°-cut lithium niobate single crystal. A metglas foil (serving as a magnetostrictive component) was asymmetrically bonded to each tine of the tuning fork. The sensor demonstrated 6.7 times increase of the sensitivity to magnetic fields as compared to a single-plate magnetoelectric (ME) sensor: the magnetic field detection limit was enhanced from 20 pT to 3 pT at a frequency of ca. 318 Hz, without any additional shielding from external noises. The advantages of the ME sensors based on bidomain lithium niobate over those based on PZT or PMN-PT are a much higher thermal and chemical stability, non-hysteretic piezoelectric effect, large resistance to creep and ageing effects, lead-free origin, and simple and cheap fabrication process. Ultimately, the tuning-fork ME sensors based on bidomain lithium niobate single crystals might be used in low frequency, ultra-sensitive, cheap and high-temperature magnetic field sensors for biomedical or space applications.

The study was supported by the Russian Science Foundation, project No. 19-19-00626.

Phase transitions and phase transformations in the phase separation nano-regions in $ErMn_2O_5$

Khannanov B.Kh.[1], Lushnikov S.G.[1], Golovenchits E.I.[1], Sanina V.A.[1]

[1] *Ioffe Institute, 194021, St Petersburg, Russian Federation*

$ErMn_2O_5$ are the type 2 multiferroics, in which the magnetic ordering with T_N= 42 K induces the ferroelectric ordering with T_C = 37 K. It contains the same number of Mn^{3+} and Mn^{4+} ions located in layers perpendicular to the c-axis of the crystal and has Pbam symmetry at room temperature. The finite probability of electron tunneling between Mn^{3+} and Mn^{4+} ions with ferromagnetic spins (double exchange) leads to the appearance of nanoscopic regions of phase separation that occupy a small volume of the crystal. The equilibrium state of the phase separation regions is formed by a balance of strong interactions: double exchange (with energy E≈0.3 eV), the Jahn-Teller effect (E≈0.8 eV), and Coulomb repulsion (E≈1eV), which ensures the existence of phase separation regions up to temperatures above room temperature. These regions are multiferroic, i.e. they have interconnected magnetic and electric polar orderings. At the same time, they are ferromagnetic semiconductor heterostructures, the layers of which contain pairs of Mn^{3+}-Mn^{4+} ions and their recharging electrons in different ratios. The Er^{3+} ions (ground state $^4I_{15/2}$, S=3/2, L=6) have a large magnetic moment (J=9.6 μB), to which the main contribution is made by the orbital moment strongly associated with the lattice and rigidly orienting the moment of Er^{3+} ions along the c axis. The exchange interaction of Er-Mn orients the magnetic moments of Mn^{3+}-Mn^{4+} ion pairs in the layers of the heterostructure along the c axis.

Measurements of the set of ferromagnetic resonances from the layers of the heterostructure, as well as the temperature dependences of magnetization and electric polarization along different axes of the crystal correlate with each other and confirm the presence of semiconductor heterostructures. Measurements of the temperature dependence of the heat capacity reveal anomalies at the temperatures of the magnetic and ferroelectric transitions, as well as at the temperatures of the disappearance of magnetizations and electric polarizations of the phase separation regions along different axes of the crystal. This correlation of the temperatures of the above-mentioned phase transformations, obtained by various methods, confirms the proposed picture of changes in the magnetic and polar properties in the $ErMn_2O_5$ multiferroic.

Coexistence of two ferromagnetic phases in perovskite binary systems of multiferroics (1-*x*)$BiFeO_3$–*x*$RMnO_3$ (R = Y, Sc)

Mikhaylov V.I., Tarasenko T.N., Kravchenko Z.F., Kovalev O.E.,
Golovchan A.V., Valkov V.I.

Public Institution «Donetsk Institute for Physics and Engineering named after A.A. Galkin», 283114, Donetsk, DPR

The effect of co-substitution in of Bi^{3+} ions by rare earth ions (R^{3+}= Y^{3+}, Sc^{3+}) and Fe^{3+} ions - by Mn^{3+} ions on the magnetic properties of the well-known multiferroic $BiFeO_3$ (BFO) has been studied. The Y^{3+} and Sc^{3+} ions with much smaller ionic radii than those of the Bi^{3+} ion strongly destabilize the R3c phase characteristic of "pure" BFO, which reduces the tolerance factor and increases the octahedron tilt angle. When distortions reach the upper limit of the rhombohedral structure and it becomes unstable, a decrease in symmetry causes a transition to the orthorhombic Pbnm phase. A change in crystal symmetry from rhombohedra (s.g. R3c) to orthorhombic (s.g. Pbnm) has been observed with co-substitution in BFO [1,2], wherein R3c and Pbnm phases coexist in the synthesized nanoceramic samples (1-x)$BiFeO_3$–x$YMnO_3$ in the range of substitutions $0.1 \le x \le 0.2$ [2].

It is known that BFO has a G-type antiferromagnetic structure, which is deformed by the Dzyaloshinskii-Moriya (DM) interaction acting in the (111) plane, with the formation of a spiral spin structure with a period of ≈62 nm. Because the DM interaction strongly depends on the rotation angles of oxygen octahedra, the magnetic properties of BFO are closely related to the local structure of the FeO_6 octahedron. The emergence of remanent magnetization with the addition of RMO was detected at room temperature and explained on the basis of the partial destruction of the spiral spin structure of BFO [1].

An increase in the magnetization upon co-substitution at the A- and B-sites is due to distortions of the crystal field symmetry on Fe^{3+} ions, and hence, with a change in the magnetic crystallographic anisotropy constant, as a result of which the existence of the spiral spin structure becomes energetically unfavorable. The suppression of the spiral spin structure leads to an increase in the magnetization, magnetoelectric effect, and an increase in the dielectric constant ε [1].

The magnetic properties of (1-x)BFO–x$RMnO_3$ (RMO) are determined by Fe^{3+} ions and by Mn^{3+} ions. The ionic radii of these B-cations in the ABO_3 perovskite structure are practically equal: $r(Fe^{3+}) = r(Mn^{3+}) = 0.645$. However, the Mn^{3+} ion has one 3d-electron less compared to Fe^{3+}, which performs a perfect perturbation of the FeO_6 local structure [3]. The coexistence of two crystallographic phases (R3c and Pbnm) with different values of the remanent magnetization (Mr(R3c) > Mr(Pbnm)) is observed in the $BiFe_{1-x}Mn_xO_3$ compounds [3]. With an increase in the Mn concentration, a redistribution of the volumes of these phases occurs: V(R3c) decreases, and V(Pbnm) increases. Therefore, the total magnetic moment at a certain concentration of Mn^{3+} reaches a maximum, and with a further increase in x, it begins to decrease.

The ceramic samples with compositions $Bi_{1-x}R_xFe_{1-x}Mn_xO_3$ ($0.1 \le x \le 0.35$) (R = Y, Sc) were synthesized using nitrate technology. The final annealing was carried out at T = 850 ° C for 10 min on air. The crystal structure and phase composition of the obtained samples were

determined by X-ray diffraction on a DRON-1.5 diffractionmeter with Cu Kα radiation. The obtained diffraction patterns indicate the presence of two crystallographic phases. At x=0.1 the structure of the sample slightly differs from R3c, for the x=0.15 besides reflections of the R3c structure, reflections of the Pbnm structure appear. Two peaks of high intensity ((104) and (110)) at 32є in BFO gradually merge into one intense peak, moreover, the superlattice peak (006) at 39є disappears with an increase in the degree of substitution. For the x=0.2 the Pbnm structure already predominates. Thus, the crystal structure changes from R3c to Pbnm through the two-phase region with increasing x(RMO) concentration.

A similar situation was observed in (1-x)BFO-xYMO compounds [2]: the x=0.15 compound contains 61.77% of the R3c phase and 38.23% of the Pbnm phase, and the x=0.2 compound - 52.42% and 47.58%, respectively. Thus, with an increase in x, a redistribution of the volumes V of the coexisting phases occurs: V(R3c) decreases, and V(Pbnm) increases.

The results of the performed studies of the magnetic properties of the (1–x)BFO–xRMO system, where R = Sc or Y ($0.05 \le x \le 0.4$), indicate the presence of ferromagnetic (FM) ordering in these ceramic multiferroics at room temperature, in contrast to "pure" BFO. The asymmetry of the magnetic hysteresis loops with respect to H=0 indicates that, in addition to the FM phase, an antiferromagnetic phase is also present in the (1–*x*)BFO–*x*RMO (R = Y, Sc) systems. An increase in magnetization with an increase in the degree of co-substitution x(RMO) on the concentration dependences M(x) at H = 2.5 kOe was observed (Fig.1).

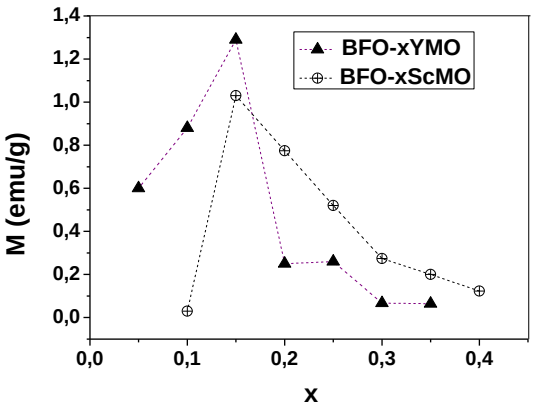

Fig. 1. The concentration dependences M(x) for (1–*x*)BFO–*x*RMO (R = Y, Sc) at H = 2.5 kOe.

The presence of a maximum M(x) for *x*=0.15 for both systems of solid solutions is due to the coexistence of two crystallographic phases R3c и Pbnm with different magnetizations and redistribution of these phases volumes. At a higher percentage substitution (>15% both for Y and for Sc) a decrease in M(x) occurs, the amount of the high M(R3c) phase decreases, and the amount of the low M(Pbnm) phase increases. Thus, the total magnetic moment at a certain concentration of x(RMO) reaches a maximum and then begins to decrease.

Consequently, the substitution of Bi^{3+} ions in BFO for Y^{3+} or Sc^{3+}, as well as Fe^{3+} ions for Mn^{3+} up to a certain value of x(RMO), plays an important role in improving the magnetic and magnetoelectric properties of materials based on bismuth ferrite $BiFeO_3$.

References

[1] R. Pandey, L.K. Pradhan et al., Ceramics Internation. 44 (15), 18609 (2018).
[2] S.N. Tripathy, K.K. Mishra, S. Sen et al., J. Appl. Phys. 114, 144104 (2013).
[3] L. Chen, L. Zheng,Y. He et al., J. Alloys and Comp. 633, 216 (2015).

Fluctuation mechanism of dielectric losses in Bi-doped $Ba_{0.8}Sr_{0.2}TiO_3$ ferroelectric ceramics

Popov I.I., Gridnev S.A.

Voronezh State Technical University, 394026, Voronezh, Russia

Ferroelectric materials are interesting from both fundamental and applied points of view, since they change their properties under an electric field [1]. Barium titanate is a classic example of a perovskite-structured ferroelectric. Materials based on barium titanate are widely used in the electronics industry [2], since they exhibit good dielectric properties, for example, high dielectric permittivity and low dielectric losses at room temperature. The great advantage of this ceramics is the absence of lead in its composition. Therefore, the aim of this work was to study the features of the cubic-tetragonal phase transition in the ferroelectric $Ba_{0.8}Sr_{0.2}TiO_3$ solid solution with the Bi dopant obtained by ceramic technology.

The temperature dependences of the dielectric permittivity ε and the dielectric loss tangent $tg\delta$ were measured in $Ba_{0.8}Sr_{0.2}TiO_3$ ferroelectric ceramics doped with 10 at.% Bi at a frequency of 25 Hz. The $tg\delta$ peak was observed whose temperature is slightly below the temperature of the ε maximum (Fig. 1). This indicates the $tg\delta$ peak belongs to a structural phase transition. Note that the dopant of Bi leads to a decrease in the temperature of the ε maximum and diffusion of the phase transition in comparison with undoped $Ba_{0.8}Sr_{0.2}TiO_3$ [3].

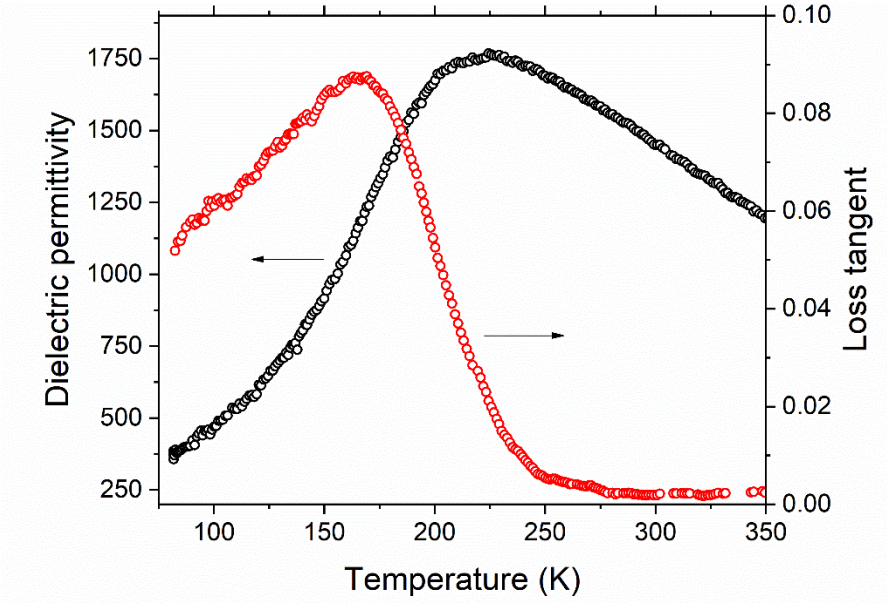

Fig. 1. Temperature dependences of dielectric permittivity and dielectric loss tangent in $Ba_{0.8}Sr_{0.2}TiO_3$ ferroelectric ceramics doped with 10 at.% Bi

The studied ceramics undergoes a first-order phase transition. In the fluctuation model of a new phase nuclei formation of a substance at a first-order phase transition, it is assumed that the transition from one phase to another phase begins due to the thermally activated appearance of critical nuclei of the polar phase and their subsequent growth by means of the movement of the interface through the stoppers system, which leads to losses. In the case of the

fluctuation mechanism of dielectric losses, the $tg\delta$ peak is described by the following expression [4]

$$tg\delta = \frac{(\Delta P_S)^2 \beta \cdot dT/dt}{\varepsilon\varepsilon_0 \omega kT \cdot \Delta T}, \quad (1)$$

where ΔP_S is the jump in spontaneous polarization at the Curie point; β is the volume of critical nucleus; dT/dt is the heating rate; ε is the maximum value of the dielectric permittivity; $\varepsilon_0 = 8.85 \cdot 10^{-12}$ F/m is the electric constant; ω is the circular frequency; ΔT is the half width of the $tg\delta$ peak.

The eq. (1) makes it possible to estimate the volume of a critical nucleus using the data: $\Delta P_S = 25 \cdot 10^{-2}$ C/m^2; $dT/dt \approx 0.017$ K/s; $tg\delta \approx 0.086$; $\varepsilon \approx 1760$; $T \approx 166$ K; $\omega = 50\pi$ rad/s; $\Delta T \approx 100$ K. The value $\beta \approx 10^{-23}$ m^3 was obtained, which is slightly higher than the sizes of the Känzig regions [5], which characterize the size of the nucleus of a new phase at a phase transformation. The deviation of the estimated value of β from the Känzig regions can be caused by the presence of simplifying assumptions, because the influence of the amplitude of the measuring field, the composition fluctuations, and relaxation processes on the formation of a critical nucleus were not taken into account.

This work was supported by the Ministry of Science and Higher Education of the Russian Federation in the framework of the state assignment (project No. FZGM-2020-0007).

References

[1] K.M. Rabe, C.H. Ahn, and J.-M. Triscone, Physics of Ferroelectrics. A Modern Perspective (Springer, Berlin, 2011).

[2] K.A. Vorotilov, V.M. Mukhortov, and A.S. Sigov, Integrated Ferroelectric Devices (Energoatomizdat, Moscow, 2011).

[3] S.A. Gridnev and I.I. Popov, Ferroelectrics 561, 127–134 (2020).

[4] S.A. Gridnev, Ferroelectrics 266, 171–209 (2002).

[5] B.N. Rolov, J. de Phys. 33, 257–258 (1972).

The methods of fine variation of PZT composition in the area of morphotropic phase boundary for MEMS and multiferroic applications

I.P. Pronin[1], E.Yu. Kaptelov[1], S.V. Senkevich[1], M.V. Staritsyn[2], V.P. Pronin[3]

[1]Ioffe Institute, 194021, St. Petersburg, Russia
[2]I.V. Gorynin CRI of Structural Materials Prometey, NRC Kurchatov Institute, 191015, St. Petersburg, Russia
[3]Herzen State Pedagogical University of Russia, 191186, St. Petersburg, Russia

Thin ferroelectric films of solid solutions of lead zirconate titanate $Pb(Zr_{1-x}Ti_x)O_3$ (PZT) are widely used in microelectromechanics, multiferroics, infrared technology, microelectronics, and other fields. The PZT film compositions most in demand correspond to the region of the morphotropic phase boundary (MPB), where the electromechanical characteristics of material reach extremely high values. The optimal electromechanical parameters in composites can be achieved via the thorough stoichiometry variation (element ratio of Zr and Ti atoms) in the MPB area. One possible way to vary stoichiometry in multicomponent thin films is the control of technological parameters during the ion-plasma film deposition.

In the present work, the methods of controlling the technological parameters of RF magnetron sputtering of the ceramic target 1) via changing the working gas pressure (2-8 Pa) at a fixed distance (50 mm) from the substrate to the target, and 2) via changing the distance (30-70 mm) from the substrate to the target at a fixed working gas pressure (8 Pa), were used. The methods were applied for simulating the thermalization and diffusion processes in the ion— plasma sputtering of a PZT ceramic target. The simulation data were compared with experimental results.

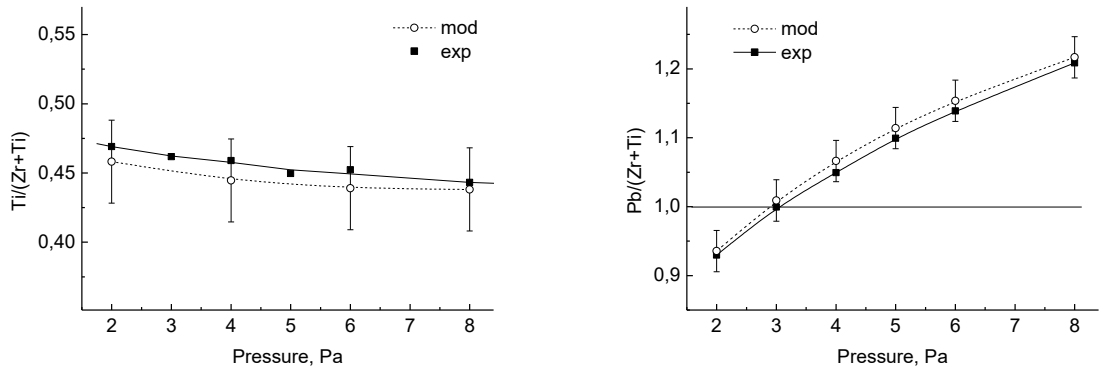

Fig. 1. Comparison of experimental and statistical modeling results for the elemental composition of Ti/(Ti+Zr) (left) Pb/(Zr + Ti) (right) in PZT thin films under gas pressure changing.

The methods have showed the possibility of fine variation in the composition of thin PZT films within Ti/(Ti+Zr) = 1.5 - 2.5% (Fig. 1, left). At the same time, the possibility of a strong variation in the lead content was observed (Fig. 1, right). Comparison of experimental data and simulation results showed good both qualitative and quantitative similarity (Fig .1).

Magnetic structure of Sr-doped bismuth ferrite series

Gervits N.E. [1], Tkachev A.V. [1], Zhurenko S.V. [1], Gunbin A.V. [1],
Pokatilov V.S. [2], Bogach A.V. [1], Gippius A.A. [1,3]

[1]*Lebedev Physical Institute, Russian Academy of Sciences, 119991, Moscow, Russia*
[2]*Moscow Technological University (MIREA), 119454, Moscow, Russia*
[3]*Lomonosov Moscow State University, 119991, Moscow, Russia*

In the initial $BiFeO_3$ composition there is an incommensurate spatial spin-modulated cycloidal structure (SSMS), which prevents the applied use of the multiferroic properties[1,2]. For several decades, various experiments have been carried out to suppress SSMS.

Doping of bismuth ferrite makes it possible to expand the possibilities of its practical application due to its multiferroic properties[3]. Partial substitution of strontium atoms for bismuth atoms leads to a noticeable change in its properties and SSMS modification[4].

Using ^{57}Fe zero-field NMR, we were able to observe the modification of SSMS in the $Bi_{1-x}Sr_xFeO_3$ series for x = {0.035; 0.07; 01; 0.14} at 4.2 K up to its destruction and draw conclusions about the effect of heterovalent substitution of Bi^{3+} with Sr^{2+} on the anharmonicity parameter.

XRD and magnetic measurements were carried out to observe the evolution of magnetic properties and structure of the samples of the series.

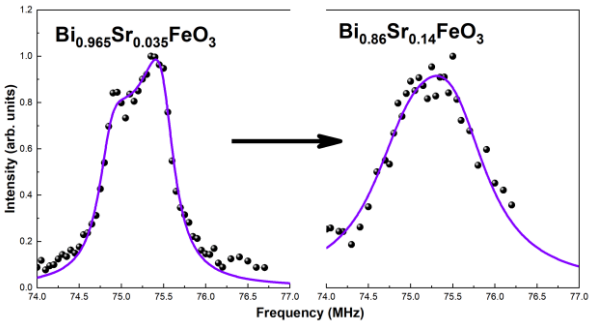

Figure 5. ^{57}Fe ZF-NMR spectra of $Bi_{1-x}Sr_xFeO_3$ for x = {0.035; 0.14} at 4.2 K

This work was supported by grant 21-72-00112 from the Russian Science Foundation.

References

[1] I. Sosnowska, A.K. Zvezdin, J. Magn. Magn. Mater. 140–144 (1995) 167–168.
[2] A. V. Zalessky, A.A. Frolov, T.A. Khimich, A.A. Bush, V.S. Pokatilov, A.K. Zvezdin, Europhys. Lett. 50 (2000) 547–551.
[3] V.S. Pokatilov, A.O. Makarova, A.A. Gippius, A. V. Tkachev, S. V. Zhurenko, A.N. Bagdinova, N.E. Gervits, J. Magn. Magn. Mater. 517 (2021).
[4] A.A. Gippius, A.V. V. Tkachev, N.E.E. Gervits, V.S.S. Pokatilov, A.O.O. Konovalova, A.S.S. Sigov, Solid State Commun. 152 (2012) 552–556.

Planar voltage magnetoelectric transformer

Fetisov L.Y., Chashin D.V., Savelyev D.V. and Fetisov Y.K.

MIREA –Russian Technological University, Pr. Vernadskogo 78, 119454 Moscow, Russia

A planar magnetoelectric voltage transformer based on a layered composite structure containing layers of amorphous ferromagnet and piezoelectric lead zirconate-titanate has been fabricated and investigated [1]. The transformer uses a coilless system (the so-called "magnetic capacitor") to excite the direct magnetoelectric effect at the frequency of the acoustic resonance of the structure, which made it possible to significantly simplify the design.

Schematic view of the planar composite ME resonator with a coilless excitation system is schematically shown in Fig. 1. The main element of the resonator is a plate made of lead zirconate-titanate ceramics. Layers of amorphous FM alloy of the composition FeBSiC are glued on both surfaces of the PZT plate. The resonator was placed inside a «magnetic capacitor», as shown in Fig.1. The magnetic capacitor was made by bending a 16 mm wide and 30 μm thick conducting Cu-strip. The parallel planes of the capacitor were 16 mm × 16 mm in plane and placed at the distance 1050 μm from each other. Thus, one round of a strip with current and a small input active resistance of $R_1 \approx 30$ mΩ is used instead of the volumetric coil with many turns.

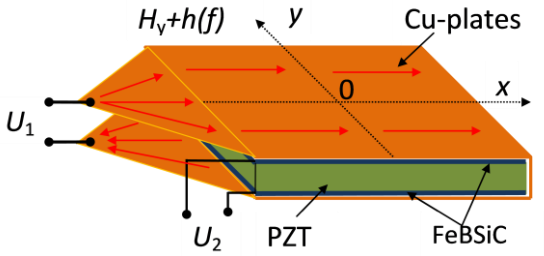

Fig. 1. Schematic view of a composite heterostructure with a coilless system of the «magnetic capacitor» type for excitation of the ME effect. The red arrows indicate current

The voltage transformation ratio of the magnetoelectric transformer, in contrast to the known electromagnetic or piezoelectric transformers, can be tuned by an external magnetic field from zero to 13.2 with an increase in the field from zero to 30 Oe. The operating range of the output voltage of the transformer is 0-400 mV, and the output power reaches 9 μW at optimal load resistance. Such planar transformer can be fabricated using traditional integral technologies, which, in turn, will provide easier implementation of ME transformers in modern electronics.

This work was supported by the Russian Science Foundation [grant 19-79-10128].

References

[1] D.V.Chashin, L.Y.Fetisov, D.V.Saveliev, and Y.K.Fetisov, Sensors and Actuators A: Physical, 328, 112773 (2021).

Parametric noise generation in the piezoelectric-ferromagnet structure

Burdin[1] D.A., Chashin[1] D.V., Ekonomov[1] N.A., Fetisov[1] Y.K., Preobrazhenski[2] V.L.

[1]Russian Technological University – MIREA, 119454, Russia
[2]Prokhorov General Physics Institute RAS, Moscow 119991, Russia

Layered piezoelectric(PE)-ferromagnet(FM) structures exhibit a strong converse magnetoelectric effect when the magnetization of the ferromagnetic layer changes under the influence of an applied electric field. When excited by a high-amplitude alternating electric field, various nonlinear and parametric effects were observed: generation of harmonics of the ME signal, mixing of the frequencies of magnetic and electric fields, parametric generation and parametric amplification [1]. In this work, the effect of stochastic (noise) generation in a two-layer structure of the PZT-Metglas composition was investigated.

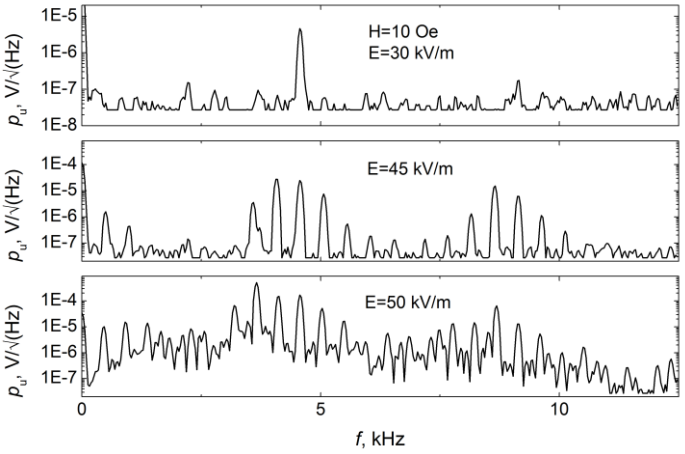

Fig. 1. ME signal spectra at different harmonic excitation levels.

The structure was disk-shaped with a diameter of 16 mm. The thickness of the PE layer was 0.3 mm, and that of the FM layer was 20 μm. Layers of the structure were bonded with glue. A signal u_e was applied to the plates of the PE layer from the output of the Agilent 33210a generator with the frequency of the main mode of bending vibrations of the structure f = 4.5 kHz, which created an alternating exciting electric field E. The voltage u generated by the coil encircling the structure was applied to the input of the SR770 spectrum analyzer. Herewith a constant magnetic field H = 10 Oe was applied along the axis of the read coil.

Figure 1 shows the frequency dependences of the spectral density of the ME voltage ρ (f) taken at three different levels of the exciting electric field. It can be seen that when the field increases from 30 kV / m to 45 kV/m, in addition to the fundamental frequency, multiple components with frequencies both lower and higher than the fundamental appear in the spectrum. An increase in the amplitude E to 50 kV/m leads to the appearance of a continuous noise spectrum in the frequency range from 0.1 to 10 kHz with a density of about 10^{-6}-10^{-5} V/√Hz. Thus, the phenomenon of stochastic generation in the ME composite structure was first discovered and investigated. The results of the study can be used to create new devices for solid-state electronics based on the magnetoelectric effect.

This work was supported by Russian Found of Basic Research, grant 19-07-00594\20.

References

[1] D.A. Burdin, D.V. Chashin, N.A. Ekonomov et al., JMMM, V.358-359, p. 98-104 (2014)

Photoexcited phonon modes in $Ba_{0.8}Sr_{0.2}TiO_3$

Brekhov K.A., Bilyk V.R., Gaponov M.S., Ilyin N.A.

MIREA — Russian Technological University, 119454, Moscow, Russia

In traditional memory devices the recording information speed is determined by the magnetization switching speed. In [1], the possibility of magnetic order parameter switching under the single femtosecond laser pulse action was demonstrated. At present it is the most effective way control the medium at extremely short times. Application of the same technique to ferroelectric materials will allow to build new effective and non-volatile memory devices. However, the problem of ultrafast ferroelectric order parameter switching is not solved yet.

The reason is that ultrafast magnetization switching is determined by the spin-orbital [2] and exchange [3] interactions, but there are no the same mechanisms in ferroelectric materials. One of the first steps towards all-optical magnetic order parameter switching was the photoinduced excitation of spin oscillations at the magnetic resonance frequency near the phase transition [4]. The study of the possibility of phonon soft mode photoinduced excitation in ferroelectric materials is a similar step on the way to all-optical control of the ferroelectric order parameter. Today, there are several works that show the possibility of direct ferroelectrics soft mode excitation by optical or THz pulses [5,6]. However, the polarization switching in these works was not achieved. Later, an approach to ferroelectric polarization switching not through the direct excitation of the soft mode, but indirectly through the excitation of a high-frequency mode, that has a strong nonlinear coupling with the soft one, was proposed. This approach was used in [7]. It was shown that the switched state lasted 200 fs, and then returned to the initial one. Thus, the study of the all-optical ferroelectric polarization switching through excitation of a soft or higher-frequency mode is still an urgent task.

Here we present the possibility of several phonon modes optical excitation in the $Ba_{0.8}Sr_{0.2}TiO_3$ (111) ferroelectric film on MgO substrate. We show that several phonon modes of frequencies 2.1 THz, 2.95 THz and 8.2 THz are excited in the film depending on the optical pump wavelength. Moreover, the frequency of 2.1 THz corresponds to the soft mode in this material. However, we did not observe the oscillation frequency decreasing in the vicinity of Curie temperature T_c that was reported previously. Thus, we cannot unambiguously determine the nature of photoexcited phonon modes.

This work was supported by the Russian Science Foundation (grant № 20-72-10178).

References

[1] K. Vahaplar et al., Phys. Rev. Lett., 103, 117201 (2009).
[2] A. M. Kalashnikova et al., Phys. Rev. Lett., 99, 167205 (2007).
[3] R. R. Subkhangulov et al., Sci. Rep., 4, 4368 (2014).
[4] E. G. Galkina, I. Y. Mikhailov, B. A. Ivanov, JETP Lett., 93, 711 (2011).
[5] K. A. Brekhov et al., JETP Letters, 102,372 (2015).
[6] E.D. Mishina et al., Ferroelectrics, 532, 199 (2018).
[7] R. Mankowsky et al., PRL, 118, 197601 (2017).

Relaxation of the current at constant voltage in the reduced lithium niobate.

Shportenko A. S.[1], Kubasov I. V.[1], Turutin A. V.[1,2], Kislyuk. A. M.[1] Zhukov R. N.[1], Malinovich M. D.[1], Parkhomenko. Yu. N. [1]

[1] National University of Science and Technology MISiS, Moscow, Russia
[2] Department of Physics and I3N, University of Aveiro, 3810-193 Aveiro, Portugal

Lithium niobate (LN) is a material widely used in optics, electronics, and engineering. For several applications it is necessary to control the change of the electrical resistance over a wide range. One of the methods is high-temperature annealing in an oxygen-free environment. This treatment increases the electrical conductivity of the material significantly. However, measuring the electrical conductivity and interpreting the results for both the annealed samples and the original crystals is a difficult task.

When measuring the electrical conductivity in LN crystals, a long-term relaxation of the current with time at a constant voltage is observed. The possible cause of long-term relaxation processes may be due to electrochemical interactions between the electrode material and the dielectric, as in the cases described by the authors of works (1) on triglycine sulfate and (2) on lithium-galium tantalate. According to these studies, similar relaxation processes can be characteristic for all uniaxial polarized ferroelectric crystals.

To test the assumption about the galvanic nature of relaxation processes, the method of dielectric spectroscopy was used. The measurements were carried out on a series of samples reduced in vacuum with a residual gas pressure of no more than 10^{-6} Torr at a temperature of 1050 °C for 2, 20 and 40 minutes with different electrodes. The obtained results were presented in the form of Nyquist-plots. Experimental results were approximated by an equivalent circuit, which is a parallel connection of a resistor and a capacitor. No patterns characteristic of the Warburg element was found on the graphs, which indicates the absence of significant diffusion currents (3).

The study was supported by the Russian Science Foundation, project No. 21-19-00872.

References

[1] N.S. Kozlova, E.V. Zabelina., M.B. Bykova and A.P .Kozlova. Russ Microelectron. A 48(8), 545–52. (2019).

[2] O.A. Buzanov, E.V. Zabelina., N.S. Kozlova and T.B. Sagalova. Crystallogr Reports. A 53(5), 853–7 (2008).

[3] J. R. Macdonald, Impedance spectroscopy: theory, experiment, and applications (John Wiley & Sons, 2018).

Magnetoelectric Effect in PVDF - nanoparticles composite

A. Omelyanchik, V. Antipova, V. Kolesnikova, K. Sobolev, A. Amirov, Ch. Gritsenko, K. Levada, V. Rodionova

[1]*Immanuel Kant Baltic Federal University, 236004, Kaliningrad, Russia*

In this work, we prepared nanocomposites (NCs) based on two types of polymers, poly(vinylidene fluoride) (PVDF) and its copolymers with trifluoroethylene (PVDF-TrFE) [1, 2]. NCs based on PVDF-TrFE demonstrated a higher magnetoelectric performance and thus were chosen for further experiments. New strategies to increase magnetoelectric response were involved: (i) application of magnetic field during crystallization of polymer to align clusters of magnetic NPs and (ii) creation of 3-component composite with ferroelectric $BaTiO_3$ particles [2].

Samples of $CoFe_2O_4$ NPs were prepared by the self-combustion method described in detail elsewhere [2]. $BaTiO_3$ (BTO) particles were prepared by the solid-phase reaction method, followed by sintering using conventional ceramic technology described in detail elsewhere [3]. Nanocomposites of NPs embedded in the piezoelectric polymer matrix were fabricated by the solvent evaporation method assisted by a doctor blade technique [4]. Magnetic properties were studied with a vibrating sample magnetometer in the magnetic field up to 1.1 T at 295 K. The magnetoelectric studies were carried out using a custom-designed setup for measuring the magnetoelectric voltage ΔV with a lock-in amplifier at frequencies of 1 Hz–100 kHz. Piezoresponse force microscopy (PFM) and local polarization switching spectroscopy measurements were carried out with a scanning probe microscope. Magnetic force microscopy (MFM) images were obtained using magnetic probe.

In our study, the magnetoelectric voltage coefficient (α_{ME}) of oriented 3-component PVDF-TrFE/BTO5/CFO composites was about 18.5 mV/cm·Oe that is four times higher than in the randomly oriented 2-component PVDF/CFO composite. A model based on magnetostatic interactions of magnetic nanoparticle clusters with randomly distributed easy axes for the explanation of the ME transformation in 3-component composites has been proposed. Local magnetic and piezoelectric properties have been studied using scanning probe microscopy. Further researches will be aimed to increase the magnetoelectric performance by changing particle (both magnetic and ferroelectric) size, shape, and concentration in such composites.

This work was supported by the Russian Science Foundation No. 21-72-30032.

References

[1] Meng, N., et al. J. Mater. Chem. C 2017, 5, 3296–3305, doi:10.1039/c7tc00162b.
[2] A. Omelyanchik S., et al. Nanomaterials 2021, 11, 1154. https://doi.org/10.3390/nano11051154.
[3] Shilkina, L.A., et al., J. Alloys Compd. 2020, 829, 154589, doi:10.1016/j.jallcom.2020.154589.
[4] Ribeiro, C., et al., Nat. Protoc. 2018, 13, 681–704, doi:10.1038/nprot.2017.157.

Dilatometry technique in a study of the ferroelectric composites

V. Rodionov, D. Borov

Immanuel Kant Baltic Federal University, 236004, Kaliningrad, Russia

Dilatometers are used to measure the changes in linear dimensions of the samples. In this work, we have developed a setup to measure the size changes of the ferroelectric composites caused by an external magnetic field. The experimental setup consists of a primary coil, precision lever system of non-magnetic material (aluminum), mirror, translucent screen and high definition camera. The main distinguishing feature of developed approach is the use of computer vision. The lever system releases a laser beam, which, reflecting from the mirror, falls on a translucent screen, where it is snapping by the camera. When the linear dimensions of the sample change, the laser spot on the screen shifts, so that 1 mm on the screen corresponds to a change in the size of the sample by about 10 nm. A high-resolution camera connected to a computer and used to accurately measure the movement of a laser spot on the screen. A real-time object tracking program was developed in the LabVIEW development environment.

To perform the measurements, the system is calibrated and the initial dimensions of the sample are measured. The incoming video stream is processed by several filters and then the patter matching process is applied. The pattern matching process consists of two stages: learning and matching. During the learning stage, the algorithm extracts gray value and edge gradient information from the template image. The algorithm organizes and stores the information in a manner that facilitates faster searching in the inspection image. The information learned during this stage is stored as part of the template image. Then, the algorithm finds the matches by locating regions in the inspection image where the highest cross-correlation is observed and outputs the coordinates of the center of this region. Together with tracking the object, the program supplies voltage to the magnetic coil and reads data from the Hall sensors. Thus, at the output of the program, we have data on the dependence of the change in the linear dimensions of the sample on the magnitude of the magnetic field. This allows us to draw conclusions about the size changes of the studied sample. In the case of the magnetoelectric composites the size changes goes thought the magnetic materials shiftless in the piezoelectric matrix.

This work was supported by the Russian Science Foundation No. 21-72-30032.

High-Tc ferroelectricity in a new molecular magnetoelectric ytterbium(III) complex

Gorbatova A.V.[1], Ivanov M.S.[1], Avdizhiyan A.Y.[1], Guskov A.A.[1], Long J.[2]

[1]*MIREA - Russian Technological University "RTU MIREA", 119454 Moscow, Russia*
[2] *Institut Charles Gerhardt Montpellier, UMR 5253, Université de Montpellier, ENSCM, CNRS, Place E. Bataillon, 34095 Montpellier Cedex 5, France.*

Magnetoelectrics (MEs) are multifunctional systems that combine magnetic and ferroelectric behavior [1]. With the ability to switch ferroelectric (magnetic) domains by small external fields MEs create the basis for development of low-consumption devices, including high-density data storage, spintronics, and optoelectronics [1]. For these applications, MEs must have strong ME coupling at room temperature, which is rarely observed for classical inorganic MEs such as metal oxides [1,2]. However, there are several studies showing that molecular MEs based on metal-organic complexes can be an alternative to the currently actively studied ME systems [3-5]. Molecular MEs also have a wide functionality due to their flexibility, non-toxicity, and high manufacturability. Earlier, we showed the presence of a strong ME-coupling in a new molecular ZnYb complex, which combines ferroelectric and paramagnetic properties at room temperature [5]. Here we present a study of the ferroelectric phase transition in the ZnYb compound.

Using nonlinear optical microscopy, we investigated anisotropic dependencies of the second harmonic generation (SHG) in the ZnYb single crystal. The ZnYb complex at room temperature is a monoclinic system described by the polar point group 2 [5]. In this case, the electric-dipole term makes the main contribution to the SHG signal. Then we obtained the temperature dependence of the SHG intensity in the range from 293 K to 493 K. To approximate the obtained dependence, we used the classical Landau theory. Found values of T_c and critical exponent β are 473 K and 0.5, respectively. The nonzero SHG signal in the region above T_c is because chiral structures can crystallize only in noncentrosymmetric space groups. Thus, according to Aizu notation [3], we assume that in the paraelectric phase the ZnYb compound is an orthorhombic system described by a point group 222. The phase transition 222→2 characterizes the ZnYb compound as a uniaxial ferroelectric system, which is also consistent with Folk's theory, where the value of the critical exponent β = 0.5 corresponds only to ferroelectrics with uniaxial dipole interaction [6].

This work was supported by the Russian Science Foundation (grant № 20-79-10233).

References

[1] N.A. Spaldin, R. Ramesh, Nat. materials. 18, 203 (2019).
[2] M. Fiebig et al., Nat. Rev. Materials, 1, 1 (2016).
[3] T. Hang, et al., Chem. Soc. Rev. 40, 3577 (2011).
[4] W. Zhang, R. G. Xiong, Chem. Rev. 112, 1163 (2012).
[5] J. Long et al., Science. 367, 671 (2020).
[6] R. Folk, Phase Transitions, 67, 645 (1999).

Section 7
Topological Materials and Materials for Quantum Technologies

Quantum fluctuations in quasi-one-dimensional superconductors

K. Yu. Arutyunov[1,2], J. S. Lehtinen[3], A. Radkevich4, A. G. Semenov [1,4], A. D. Zaikin[4,5]

[1] *National Research University Higher School of Economics, Moscow, Russia.*
[2] *P.L. Kapitza Institute for Physical Problems RAS, Moscow, Russia.*
[3]*VTT Technical Research Centre of Finland Ltd., Centre for Metrology MIKES, Espoo, Finland.*
[4]*I.E. Tamm Department of Theoretical Physics, P.N. Lebedev Physical Institute, Moscow, Russia.*
[5]*Institute for Quantum Materials and Technologies, Karlsruhe Institute of Technology (KIT), Karlsruhe, Germany*

Over more than 100 years since discovery of superconductivity it continues to provide open questions. Among various phenomena, associated with macroscopic size systems, zero resistance and complete diamagnetism (Meissner effect) are considered to be the essential attributes of a superconductor. In addition to these 'integral' properties, observable in objects of finite dimensions, another attribute of superconductivity – the energy gap in excitation spectrum of a (conventional) superconductor – can be measured 'at a point': e.g. using atomically sharp tip of a scanning tunnel microscope .

Later developments have revealed that in low-dimensional superconductors fluctuation phenomena play an essential role. In particular case of a quasi-one-dimensional superconductor, it has been demonstrated that quantum fluctuations of the order parameter may dramatically suppress those 'integral' attributes: zero resistance and persistent currents [1,2]. However, not much has been known about the impact of quantum fluctuations on 'local' properties.

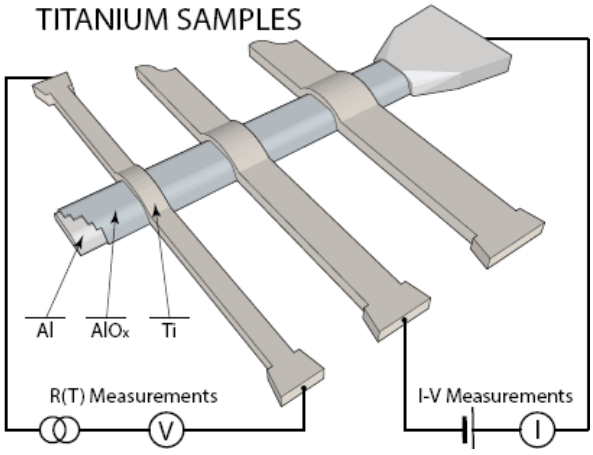

Fig. 1. Schematics of experiment and sample lay-out. Long and thin titanium nanowires having the form of narrow strips overlapping a relatively wide aluminum electrode through a tunnel barrier (aluminum oxide). The structure enables one to carry out both pseudo-four-terminal measurements of the total resistance for all nanowires and local measurements of the current-voltage characteristics for all Al-AlOx-Ti tunnel junctions [4].

To answer the question, in this work multi-terminal nanostructures were fabricated, enabling measurements of the 'integral' property (resistance of a nanowire of finite length) and

the 'local' property (tunnel conductance between the nanowire and another massive superconductor) in one experimental run using the same nanostructure (Fig. 1).

In a full accordance with our earlier work [1], we find that the resistance vs. temperature R(T) dependencies for the thinnest nanowires are very broadened without reaching the zero resistance state even at T→0 (Fig. 2, left). However, the study of tunnel characteristics, reflecting the 'local' property of a superconductor, reveals that the energy spectra of both nanowires look very similar just with the density of states being slightly broadened in the thinnest samples (Fig. 2, right) [3].

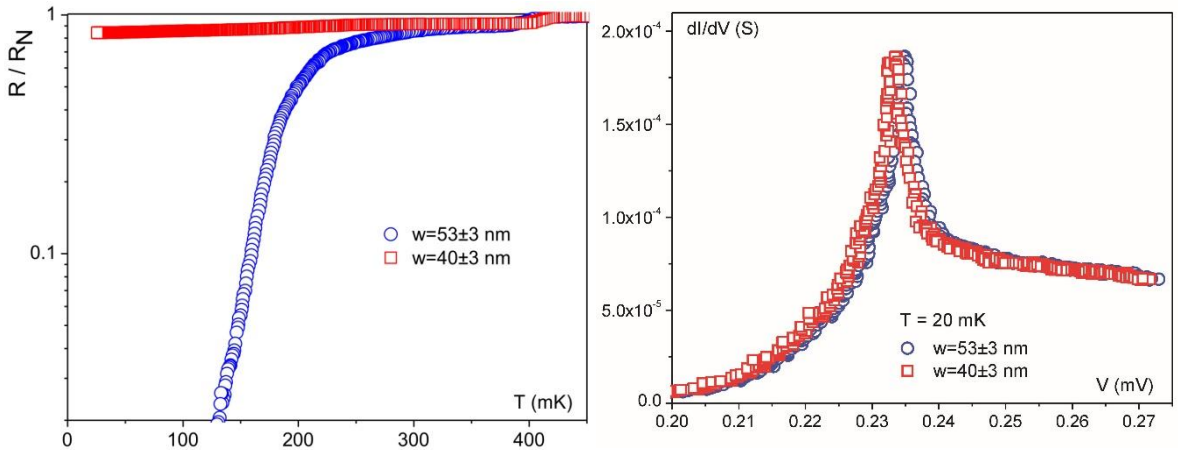

Fig. 2. Integral and local measurements of the same nanowires. (Left) R(T) dependencies of two Ti nanowires of various widths w, but of the same thickness d=35 nm. (Right) Zoom of the tunnel conductance dI/dV(V) close to the gap singularity for the same Ti nanowires overlapping massive Al electrode.

The striking difference between the integral and local properties of a quasi-one-dimensional superconductor originates from a complicated interplay between the rate of individual fluctuation events and the interaction between such fluctuations happening at different time-space points [4]. This fundamental property of nanoscale superconductors needs to be accounted for while designing various nanoelectronic devices with novel functionalities.

References

[1] K. Yu. Arutyunov, D. S. Golubev, A. D. Zaikin, Phys. Rep. 464, 1 (2008).
[2] Arutyunov, K. Y. et al. Sci. Rep.2 , 293 (2012).
[3] K.Yu.Arutyunov, J.S.Lehtinen, A.A.Radkevich, A.G.Semenov, A.D.Zaikin, Journal of Magnetism and Magnetic Materials, 459, 356-358 (2018).
[4] K. Yu. Arutyunov, J. S. Lehtinen, A. Radkevich, A. G. Semenov, A. D. Zaikin, Comm. Phys. (2021). https://doi.org/10.1038/s42005-021-006

The mechanisms of spin polarization in Doped Perforated Bilayer Graphenes

Avramov P.V.

Department of Chemistry, Kyungpook National University, Daegu, 41566, South Korea

The atomic and electronic structure and spin states of undoped and doped AA and AB perforated bigraphenes was studied using Density Functional Theory. It was found that AA folded nanopores possess extremely high curvature of 0.34Å-1. Dramatic structural deformation of perforated bigraphene lattices causes severe changes of electronic and chemical properties of the carbon atoms localized at the nanopores converting the folded edges to local oxidative fragments. It was found that asymmetrical coordination of either Li, Ca, or Al to nanopores is coupled with electron transfer from metal to carbon atoms localized at the edges and breakdown of nanopore local inversion symmetry. Li-, Ca-, and Al-doped perforated AA bigraphene revealed ferromagnetic spin ordering with 0.38, 0.14, and 0.32μB/unit cell, respectively, and spin polarization energy gain equal to 0.037eV for Ca-doped nanoporous superlattice. It was shown that ferromagnetic state contradicts to Nagaoka's theorem for nanoporous bigraphene hexagonal lattice doped by light elements for either strong or weak repulsive potentials and 1-5 doping electrons, which excludes strong electron correlations as a reason of spin polarization. The lift of spin degeneracy in anisotropic low-dimension lattices was interpreted in terms of perturbing intense local electrostatic fields formed by extra electron charges localized at the nanopore edges with extreme curvature coupled with breakdown of space inversion and local translation invariances. It was shown that the energy splitting between the spin channels is proportional to the matrix elements calculated on Bloch states with opposite wavevectors and perturbing electrostatic fields with broken inversion and translation invariances.

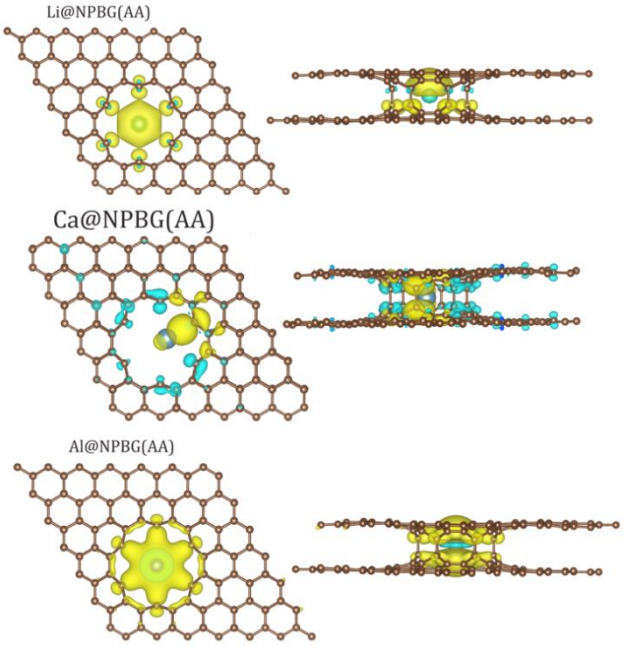

Fig. 1. Spatial spin density distribution of Li@NPBG(AA), Ca@NPBG(AA), and Al@NPBG(AA).

Phase change materials for neuromorphic applications

Ionin V.V., Eliseev N.N., Burtsev A.A., Kiselev A.V., Mikhalevsky V.A., Lotin A.A.

ILIT RAS — Branch of FSRC "Crystallography and Photonics" RAS
140700, Shatura, Russian Federation

Chalcogenide materials such as GeTe, Ge-Sb-Te, Ge-Sb-Se-Te and their derivatives with different stoichiometric ratios are widely used in the field of non-volatile memory modules, high-density optical disks and optoelectronic devices, since their physical properties differ significantly for two stable phase states - crystalline and amorphous [1]. A high optical contrast was demonstrated in the spectral range from 200 to 22000 nm and a large difference in electrical conductivity between the amorphous and crystalline states [2]. In this work, we experimentally demonstrate a multilevel reversible change in the optical properties of thin-film samples associated with phase transitions under the action of pulsed laser radiation. A cell based on thin chalcogenide films can store several states, which correspond to different ratios of the amorphous and crystalline phases [3, 4]. Switching between multiple states was controlled by the radiation of a pulsed laser (532 nm, 20 ns) of various energy densities in the "pump-probe" scheme previously implemented in [5]. A numerical model based on the thermal conductivity equation in a solid and the classical Stefan problem was used to predict the ratio of amorphous and crystalline phase states. This study offers a promising way to create new devices based on thin films of chalcogenides, such as multilevel memory with a phase transition, optical logic elements and their arrays that do not contain electrical connections, biosimilar optoelectronic devices, including synapse-like neuromorphic devices and systems. Cells of multilevel states based on chalcogenide alloys have a number of fundamental properties, such as a pre-threshold energy storage mode, a threshold value of the transition energy, and nonlinear behavior when switching states, which allows us to consider the work as analogs of a biological neuron [6].

This work was carried out with financial support from the Ministry of Science and Higher Education of the Russian Federation grant No. 075-15-2019-1950, State task of the Federal Research Center "Crystallography and Photonics" of the Russian Academy of Sciences No. 075-00486-21-00 and RFBR grant No. 19-29-12024.

References

[1] S. R. Ovshinsky, Phys. Rev. Lett., 21 (1968) 1450.
[2] N.N. Eliseev, A.V. Kiselev, V.V. Ionin, V.A. Mikhalevsky, A.A. Burtsev, M.A. Pankov, D.N. Karimov, A.A. Lotin. Results in Physics, 19 (2020) 10346
[3] N. Papandreou, A. Sebastian, A. Pantazi, M. Breitwisch, C. Lam, H. Pozidis, E. Eleftheriou, International Electron Devices Meeting, 2011 3.5.1-3.5.4.
[4] H.-S. P. Wong, S. Raoux, S. Kim, J. Liang, J. P. Reifenberg, B. Rajendran, M. Asheghi, and K. E. Goodson, Proc. IEEE, 98 (2010) 2201–2227.
[5] V. V. Ionin, A. V. Kiselev, N. N. Eliseev, V. A. Mikhalevsky, M. A. Pankov, A. A. Lotin, Appl. Phys. Lett. 117 (2020) 011901.
[6] S. R. Ovshinsky, Jpn. J. Appl. Phys. Vol. 43, No. 7B, 2004, pp. 4695–4699.

Laser-controlled optical properties' contrast change dynamics of GeTe and $Ge_2Sb_2Te_5$ thin films

Kiselev A.V., Ionin V.V., Burtsev A.A., Eliseev N.N., Mikhalevsky V.A., Lotin A.A.

ILIT RAS — Branch of FSRC "Crystallography and Photonics" RAS
140700, Shatura, Russian Federation

Chalcogenides are materials containing one (or several) elements of group VI of the periodic table, namely S, Se or Te. They are metastable in nature and can undergo transitions between different states, usually by heating. Rapid heating can be carried out by exposing the material to laser radiation of sufficient intensity. The use of optical methods makes it possible to change the phase composition for times lying in the range of 30-800 ns for the direct transition [1,2] from amorphous to crystalline, and about 10 ns for reverse transitions from the crystalline to the initial amorphous state [2,3]. One of the most well-known phase change materials (PCM) is germanium telluride (GeTe) and its $Ge_2Sb_2Te_5$ (GST) alloy. These materials are widely used in high-density optical memory devices, displays, as well as in optical modulators, synapses, and memristors [4]. This work experimentally demonstrates a reversible change in the optical properties of thin-film samples associated with phase transitions under the influence of pulsed laser radiation according to the pump-probe scheme [5]. The samples were exposed by crystallization and amorphization. The spectrometry data demonstrated the contrast of optical properties in a wide range from 200 to 22000 nm [6], and also determined the rates of change in optical properties lying in the range of tens of nanoseconds for both forward and reverse changes associated with laser-initiated phase transitions.

This work was carried out with financial support from the Ministry of Science and Higher Education of the Russian Federation grant No. 075-15-2019-1950, State task of the Federal Research Center "Crystallography and Photonics" of the Russian Academy of Sciences No. 075-00486-21-00 and RFBR grant No. 19-29-12024.

References

[1] S. Raoux, H.-Y. Cheng, M. A. Caldwell, and H.-S. P. Wong. Appl. Phys. Lett. 2009, 95, 071910

[2] P. Guo, A. M. Sarangan and I. Agha. Appl. Sci. 2019, 9, 530

[3] S. Raoux, M. Wuttig (ed.). Phase Change Materials. Science and Applications. Springer Science+Business Media, 2009.

[4] Zhang W., Mazzarello R., Wuttig M., Ma E. Nature Reviews Materials 2019, 4: 150–168.

[5] V. V. Ionin, A. V. Kiselev, N. N. Eliseev, V. A. Mikhalevsky, M. A. Pankov, A. A. Lotin, Appl. Phys. Lett. 117 (2020) 011901.

[6] N.N. Eliseev, A.V. Kiselev, V.V. Ionin, V.A. Mikhalevsky, A.A. Burtsev, M.A. Pankov, D.N. Karimov, A.A. Lotin. Results in Physics, 19 (2020) 10346.

Electronic structure and properties of topological Weyl semimetal $MoTe_2$ and WTe_2 single crystals

Domozhirova A.N.[1], Naumov S.V.[1], Makhnev A.A.[1], Shreder E.I.[1], Lukoyanov A.V.[1], Podgornykh S.M.[1], Marchenkova E.B.[1], Chistyakov V.V.[1], Huang J.C.A.[2], Marchenkov V.V.[1, 3]

[1]*M.N. Mikheev Institute of Metal Physics, UB RAS, 620108, Ekaterinburg, Russia*
[2]*National Cheng Kung University, 70101, Tainan, Taiwan*
[3]*Ural Federal University, 620002, Ekaterinburg, Russia*

Transition metal dichalcogenides (TMDs) attract great attention due to their diverse electronic properties and are considered to be promising materials for optoelectronics, high-speed electronics, and spintronics. Some of them can exhibit superconductivity, charge density wave, and topological behaviour. TMD $MoTe_2$ and WTe_2 are classified as type-II topological Weyl semimetals (TWSs) [1, 2]. TWSs possess unique quasiparticles in their bulk, chiral massless Weyl fermions, which are topologically protected. Non-trivial topology of their electronic band structure cause intriguing electronic properties such as non-saturated extremely large magnetoresistance, ultrahigh current carriers mobility, spin-polarized transport, etc. Therefore, the investigation of such materials is of great interest. The purpose of this work is a comprehensive study of electronic structure and properties of TWS $MoTe_2$ and WTe_2.

$MoTe_2$ and WTe_2 single crystals were grown by the chemical vapour transport method with bromine as a transport agent. As-grown $MoTe_2$ crystals were quenched from 910°C to stabilize the "semimetallic" phase [3]. The electrical resistivity and galvanomagnetic properties were investigated in the temperature range from 2 to 300 K and in magnetic fields of up to 9 T using a PPMS setup. The values of current carrier concentration and their mobility were estimated from Hall Effect data. Optical characteristics were measured using the polarimetric Beattie method with a reflection from the (00*l*) plane of the samples in the spectral range of 0.2–5.0 eV at room temperature. Results of optical studies showed good agreement with electronic transport data and electronic band structure calculations. The revealed features, such as high mobility of charge carriers, along with their relatively low concentration, electron-hole compensation, as well as electronic band structure and optical signatures are apparently the manifestation of the topological nature of these materials.

The research was carried out within the state assignment of Ministry of Science and Higher Education of the Russian Federation (themes "Spin", No. AAAA-A18-118020290104-2 and "Electron", No. AAAA-A18-118020190098-5), supported in part by RFBR (project No. 20-32-90069) and the Government of the Russian Federation (Decree No. 211, Contract No. 02.A03.21.0006).

References

[1] L. Huang et al., Nat. Mater. 15, 1155 (2016).
[2] Y. Wu et al., Phys. Rev. B. 95, 121113(R) (2016).
[3] A.N. Domozhirova et al., AIP Advances 11, 15226 (2021).

Thermodynamic, dynamic and transport properties of quantum spin liquid

V.R. Shaginyan

Petersburg Nuclear Physics Institute of NRC «Kurchatov Institute», vrshag@thd.pnpi.spb.ru

The exotic substances have exotic properties. One class of such substances is geometrically frustrated magnets, where correlated spins reside in the cites of triangular or kagome lattice. In some cases such magnet would not have long-range magnetic order. Rather, its spins tend to form kind of pairs, called valence bonds. At low temperatures these highly entangled quantum objects condense in the form of a liquid, called quantum spin liquid (QSL). The observation of a gapless QSL in actual materials is of fundamental significance both theoretically and technologically, as it could open a path to creation of topologically protected states for quantum information processing and computation. In the present review we consider QSL formed by spinons that are chargeless fermionic quasiparticles with spin 1/2, filling up the

Fermi sphere. The excitations of QSL are spinons, which are chargeless fermionic quasiparticles with spin 1/2. We expose a state of the art in the investigations of physical properties of geometrically frustrated magnets with QSL. As the QSL excitations are fermions, the most appropriate description of observed phenomena should be based on some fermionic formalism rather than on different forms of standard spin-wave approaches. So, one more purpose of our review centers on a theory employed, demonstrating its range of applicability to a novel expression of magnetic behavior. Unique feature of our review is to elucidate the nature of the used QSL in terms of both experimental facts and the theory of fermion condensation (FC). Our analysis, based on FC concept, permits to describe the multitude of experimental results regarding the thermodynamic and transport properties of QSL in geometrically frustrated. Based on the experimental facts and the theory, we show that the considered magnets exhibit the universal scaling behavior resembling that of heavy-fermion metals, including T/B scaling with T being temperature and B magnetic field [1,2]. We also show that QSL as a member of strongly correlated Fermi systems represents a new state of matter. We make predictions, which can help to stabilize gapless QSL in frustrated magnets.

References

[1] V. R. Shaginyan *et al.*, J. Mater. Sci**. 55**, 2257 (2020).

[2] M. Ya. Amusia and V. R. Shaginyan, *Strongly Correlated Fermi Systems: A New State of Matter*, Springer Tracts in Modern Physics, Vol. 283 (2020).

Reentrant superconductivity in proximity to a topological insulator

Karabassov T.[1], Vasenko A.S.[1]

[1]*HSE University, 101000 Moscow, Russia*

Superconducting hybrid structures with topological order and induced magnetization offer a promising way to realize fault-tolerant quantum computation. However, the effect of the interplay between magnetization and the property of the topological insulator surface, otherwise known as spin-momentum locking on the superconducting proximity effect, still remains to be investigated. We relied on the quasiclassical self-consistent approach to consider the superconducting transition temperature in the two-dimensional superconductor/topological insulator (S/TI) junction with an in-plane helical magnetization $\mathbf{h}(y) = h_0(\cos Qy, \sin Qy, 0)$ on the TI surface, where $Q = 2\pi / \lambda$, and λ actually determines the spatial period of the helical magnetization (see [1] for details).

It has emerged that the presence of the helical magnetization leads to the nonmonotonic dependence of the critical temperature on the TI thickness, see Fig. 1 [2]. In this work we also considered the case when the magnetization evolves perpendicular to the S/TI interface [2]. The results obtained can be helpful for designing novel superconducting nanodevices and better understanding the nature of superconductivity in S/TI systems with nonuniform magnetization.

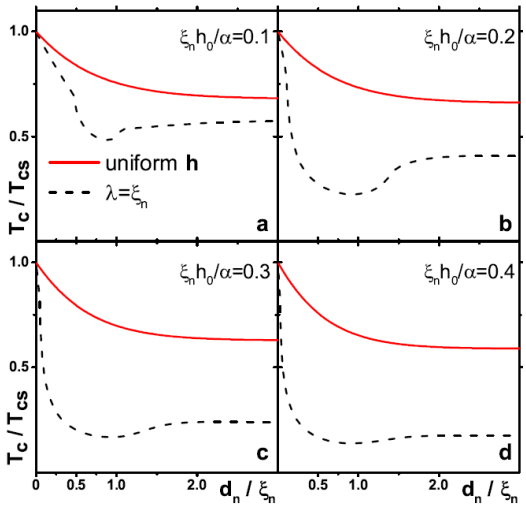

Fig. 1. Comparison of the critical temperature behavior between the S/TI bilayer with uniform magnetization $\mathbf{h}$ and S/TI bilayer with helical magnetization pattern $\mathbf{h}(y)$ [2]. Here α is a Fermi velocity on the surface of the topological insulator.

References

[1] A. Zyuzin, M. Alidoust, and D. Loss, Phys. Rev. B 93, 214502 (2016).

[2] T. Karabassov, A. A. Golubov, V. M. Silkin, V. S. Stolyarov, and A. S. Vasenko, Phys. Rev. B 103, 224508 (2021).

Self-dual criticality in the problem of the complexity emergence: superconducting materials between types I and II

A. A. Shanenko[1], M. A. Sarmento[2], W. Y. Córdoba-Camacho[2], A. Vagov[1,4], V. S. Stolyarov[5]

[1]*HSE University, 101000 Moscow, Russia*
[2]*Universidade Federal de Pernambuco, Recife PE 50740-560, Brazil*
[3]*Institute for Theoretical Physics III, University of Bayreuth, Bayreuth 95440, Germany*
[1] *Moscow Institute of Physics and Technology, 141700 Dolgoprudny, Russia*

The emergence of complexity in nature raises two important questions about how spontaneous self-organized patterns [1] arise and why their inexhaustible variety exists in nature. It is now commonly accepted that spontaneous patterns appear due to competition of different length-scales [1]. For the second question, adaptation is typically mentioned in biology but frustration, resulting from competing interactions, was also suggested as a possible origin [2]. In any case, the key word in this scenario is "competition". Here we report a qualitatively different framework, where modus operandi is, say, "unison". As a prototype we consider the system of coupled scalar and gauge fields with the self-dual critical point. The self-dual state is infinitely degenerate, including a panopticon of patterns exhibiting equal scalar and gauge spatial lengths. Our investigation reveals that in addition to various arrangements of Nielson-Olesen vortices [3], the two entities acting in unison produce also a plethora of bizarre superstructures made of bubbles and stripes of the scalar condensate surrounded by Nielson-Olesen vortices. When degeneration is lifted, self-dual patterns become quasi-degenerate, giving rise to countless arrangements in the phase diagram. An important example of the complexity driven by the self-dual criticality is the superconductivity between types I and II [4].

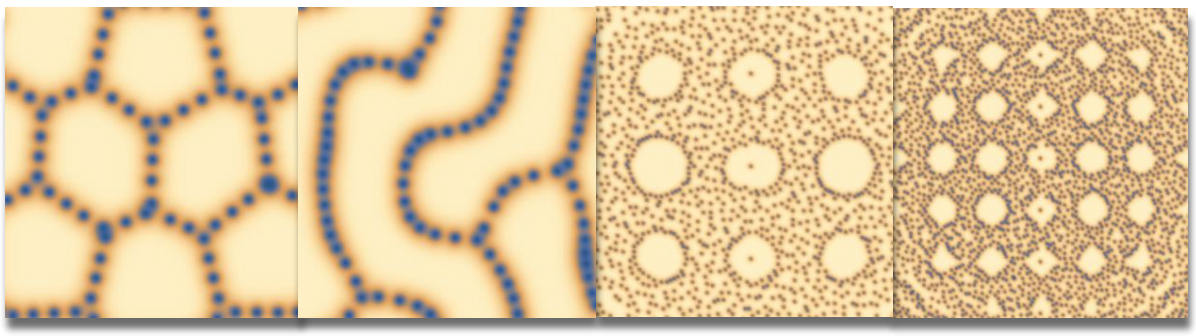

Fig. 1. Examples of the self-dual patterns of the superconducting condensate (yellow color corresponds to the bulk value of the condensate density, points represent vortices). One can see the bubble (islands) and stripe patterns in their complex interplay with the Nielson-Olesen vortices.

References

[1] F. M. Turing, Philos. Trans. R. Soc. Lond. Ser B **237**, 36 (1952); M. C. Cross and P. C. Hohenberg, Rev. Mod. Phys. **65**, 851 (1993); M. Seul and D. Andelman, Science **267**, 476 (1995).
[2] Y. I. Wolf, M. I. Katsnelson, and E. V. Koon, PNAS 115, E8678 (2018).
[3] H. B. Nielsen and P. Olesen (1973). Nucl. Phys. B **61**, 45 (1973).
[4] A. Vagov, S. Wolf, M. D. Croitoru, A. A. Shanenko, Commun. Phys. **3**, 58 (2020); W. Y. Córdoba-Camacho, A. Vagov, A. A. Shanenko, J. Albino Aguiar, A. S. Vasenko, and V. S. Stolyarov, J. Phys. Chem. Lett. **12**, 4172 (2021).

Magnetic properties and structural perfection of $Fe_{1-x}Ga_xBO_3$ single crystals designed for monochromatization of synchrotron radiation

Lyubutina M.V.[1], Snegirev N.I.[1], Lyubutin I.S.[1], Kulikov A.G.[1], Zolotov D.A.[1], Vasiliev A.L.[1], Yagupov S.V.[2], Mogilenec Yu.A.[2], Seleznyova K.A.[2], and Strugatsky M.B.[2]

[1]Shubnikov Institute of Crystallography of FSRC "Crystallography and Photonics" RAS, 119333, Moscow, Russia
[2]Physics and Technology Institute, V.I. Vernadsky Crimean Federal University, 295007, Simferopol, Russia

Iron borate is a unique crystal that allows one to observe the "pure" nuclear diffraction effect of X-ray radiation [1]. This is because the extinction of X-ray reflections from lattice atoms takes place in the FeBO3 crystal (for the family of crystal planes of the (NNN) type, where N is an odd number in rhombohedral system), since the X-ray scattering amplitudes from two Fe ions in the unit cell have different signs [2]. The diffraction of resonant (Mössbauer) radiation, whose polarization depends on the orientation of the magnetic moments of ^{57}Fe nuclei, is allowed because of the antiparallel ordering of two magnetic sublattices in $FeBO_3$ [2].

In our study, a series of $Fe_{1-x}Ga_xBO_3$ single crystals was grown by the flux technique (Fig. 1). The atomic structure of crystals has been investigated by high-resolution electron microscopy. Crystal structure perfection of the crystals with $0 \leq x \leq 1$ was studied by X-ray diffraction and X-ray topography, and structural defects were visualized. Visualization of the atomic structure in the high-resolution transmission scanning microscopy mode, as well as "angular movie" obtained by X-ray topography, make it possible to reveal fine details of the perfection of the crystal structure of iron borate $FeBO_3$ crystals "diluted" with diamagnetic gallium ions. It was found that the partial isomorphic substitution of gallium for iron leads to a certain decrease in the degree of structural perfection of "mixed" crystals in comparison with crystals of "pure" phases $FeBO_3$ and $GaBO_3$. However, in each of the investigated samples, there are regions free of defects and stresses. The advantages due to the reduced value of the Neel point give grounds to make a choice in favor of $Fe_{1-x}Ga_xBO_3$ when carrying out nuclear resonance synchrotron experiments.

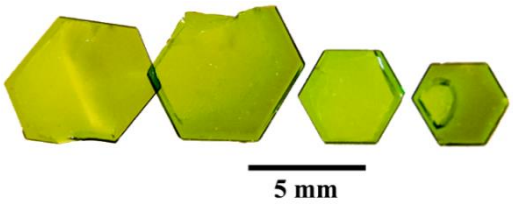

This work demonstrates the possibility of using $Fe_{1-x}Ga_xBO_3$ crystals as X-ray filters in synchrotron experiments based on nuclear resonances. The results obtained are also important for further optimization of the method for growing these crystals.

Acknowledgment: This work is funded by RFBR, project number 19-29-12016\20-mk.

References

[1] G.V.Smirnov, M.V. Zelepukhin, W.van Bürck, J. Exp. Theor. Phys. Lett. **43,** 274 (1986).
[2] G.V. Smirnov, V.V. Sklyarevskii, R.A. Voskanyan, A.N. Artem'ev, J. Exp. Theor. Phys. Lett., **9,** 123 (1969).

Simulation of quantum system using neural networks

Kozacheck V.V.[1], Klevets Ph.N.[1], Yarygina E.A.[1]

[1] *V.I. Vernadsky Crimean Federal University, 295007, Simferopol, Russian Federation*

Numerical simulation of quantum systems is one of the important research methods. Unfortunately, the use of numerical methods in quantum mechanics is quite costly, especially in the context of studying open quantum systems with a large number of degrees of freedom. The complexity of these studies is associated with the fact that the rank of the density matrix grows exponentially with an increase in the size of the system. Of course, the numerical simulation of quantum systems is not as expensive as, for example, the construction of an accelerator, but still significant computing power is required for high-quality simulation of quantum systems.

Different approaches are used to minimize costs, but, recently, neural networks have become one of the most promising. The concept of neural networks was introduced a long time ago, but recently the dawn of this technology has been observed, associated both with the increase in the productivity of computing systems and with the development of fundamentally new computing devices – quantum computers.

In this work, we use the simplest property of a neural network – the ability to train it and respond to external influences in an appropriate way.

The factors described above were a prerequisite for the emergence of the idea of using neural networks in modeling open quantum systems. In the present work, we develop a variational method for simulating the nonequilibrium stationary state of Markov open quantum systems. This method is based on the variational Monte Carlo methods and the representation of the density matrix in the form of a neural network. With the help of neural networks based on variational regeneration (bringing the system to an equilibrium state), it is possible to represent a quantum system in the form of a matrix of weights, which later makes it possible to determine the state of the system based on the input data.

Developed instrument was applied to the well-known Ising system. We compared the results obtained using "classical" numerical solutions with the results obtained using developed neural network. An example of the equilibrium distribution of the spins is shown in Fig. 1 below.

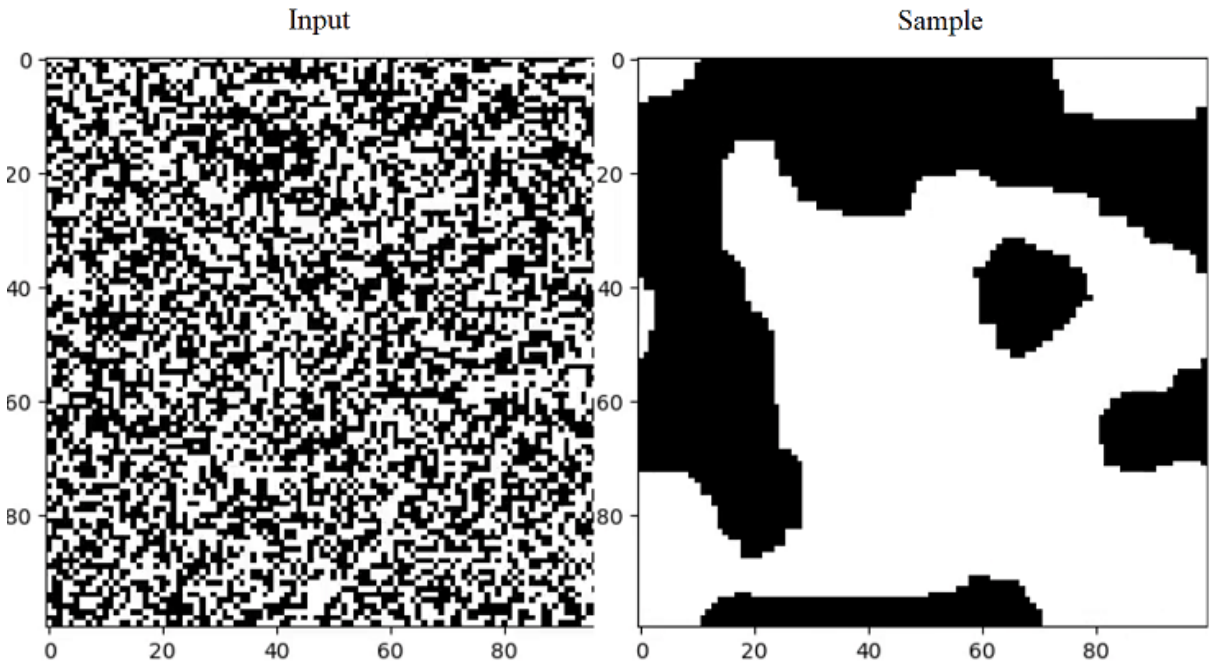

Fig. 1. Initial distribution of the spins for 100x100 Ising model (left) and equilibrium distribution of the spins (right), obtained using our neural network.

The results of neural network coincide with the “classical” numerical analysis, but the speed of calculation exceeds the “classical” approach by several orders.

Acknowledgements

The research was funded by RFBR and Republic of Crimea, project number 20-42-910003, and by RFBR, project number 20-32-90027.

Electrical conductivity kinetics due to the nanosecond laser radiation induced phase changes in GeTe and GST thin films

Eliseev N.N., Ionin V.V., Burtsev A.A., Kiselev A.V., Mikhalevsky V.A., Lotin A.A.

ILIT RAS — Branch of FSRC "Crystallography and Photonics" RAS
140700, Shatura, Russian Federation

Thin films of germanium telluride (GeTe) and its alloy $Ge_2Sb_2Te_5$ (GST) can be used not only in nonvolatile memory devices [1], but also for new generation computing elements that combine the functions of storing and processing information, and can find application in neuromorphic computing framework [2].

These materials can undergo rapid crystallization when illuminated with short nanosecond laser pulses, which is accompanied by a noticeable increase (more than 50%) in the reflectivity of the films in the middle and far IR range, due to the electronic structure, between the amorphous and crystalline states [3, 4]. Due to the cylindrical intensity distribution of the pulsed laser radiation, a complete transition from the amorphous phase to the crystalline and back in thin GeTe and GST films can be realized by single-pulse or multi-pulse (5 and more) modes [5].

The stepwise character of the change in the electrical conductivity by more than two orders of magnitude and a high switching rate for direct phase transitions from the amorphous state to the crystalline state, where the time of the change in the conductivity of thin GeTe films is 20.2 ns and 52 ns during the reverse phase transition (glass transition), for thin for GST films - 32 ns and 62 ns, respectively.

A controlled stepwise change in electrical conductivity, high switching speed, optical contrast, and the presence of several crystalline phases confirmed by X-ray diffraction — all this can provide multi-bit recording and high information processing speed in hybrid optoelectronic devices based on these materials [6].

This work was carried out with financial support from the Ministry of Science and Higher Education of the Russian Federation grant No. 075-15-2019-1950, State task of the Federal Research Center "Crystallography and Photonics" of the Russian Academy of Sciences No. 075-00486-21-00 and RFBR grant No. 19-29-12024.

References

[1] P. Guo, A. M. Sarangan and I. Agha. Appl. Sci. 2019, 9, 530

[2] Zhang W., Mazzarello R., Wuttig M., Ma E. Nature Reviews Materials 2019, 4: 150–168.

[3] N.N. Eliseev, A.V. Kiselev, V.V. Ionin, V.A. Mikhalevsky, A.A. Burtsev, M.A. Pankov, D.N. Karimov, A.A. Lotin. Results in Physics, 19 (2020) 10346

[4] V. Weidenhof, I. Friedrich, S. Ziegler, M. Wuttig. J. Appl. Phys 89, 3168 (2001)

[5] V. V. Ionin, A. V. Kiselev, N. N. Eliseev, V. A. Mikhalevsky, M. A. Pankov, A. A. Lotin, Appl. Phys. Lett. 117 (2020) 011901.

[6] S. R. Ovshinsky, Jpn. J. Appl. Phys. Vol. 43, No. 7B, 2004, pp. 4695–4699.

Quantum size phenomena in thin superconducting films

K. Yu. Arutyunov[1,2], E. A. Sedov [1], V.V. Zavialov [1,2],

G. Konstantinidis [3], A. Stavrinidis [3], G. Stavrinidis [3], I. Vasiliadis[4], T. Kehagias[4], G. Dimitrakopulos[4], Ph. Komninou[4], M. D. Croitoru[5,6], A. A. Shanenko[1]

[1] *National Research University Higher School of Economics, Moscow, 101000, Russia.*
[2] *P. L. Kapitza Institute for Physical Problems RAS, 119334, Moscow, Russia.*
[3] *Institute of Electronic Structure \& Laser (IESL), Foundation for Research & Technology Hellas (FORTH), P.O. BOX 1385, Vassilika Vuton, Heraklion 70013, Greece.*
[4] *Department of physics, Aristotel University Thessaloniki, Thessaloniki, GR-54124, Greece.*
[5] *Institut f\"{u}r Theoretische Physik III, Bayreuth Universit\"{a}t, Bayreuth 95440, Germany*
[6] *Departamento de F\'isica, Centro de Ci\^encias Exatas e da Natureza (CCEN), Universidade Federal de Pernambuco, 50670-901, Recife, Brazil.*

Since the early works on superconductivity, it has been discovered that for thin films the critical temperature of transition T_c to supeconducting state can be considerably different from its value for corresponding bulk material [1]. Remarkably, as the film thickness diminishes, T_c becomes lower in some (e.g., niobium) and higher in other materials (e.g., aluminum). Despite a fairly large body of experimental data on the subject and abundance of theoretical models, to date there is no consensus in the scientific community regarding the nature of this phenomenon. Here we present experimental study of high-quality aluminum films on various substrates. Irrespectively of the substrate material and the method of film formation, all aluminum samples demonstrate the same tendency: the thinner the film, the higher is the critical temperature (Fig. 1). We claim that the observation is the manifestation of the quantum size effect [2].

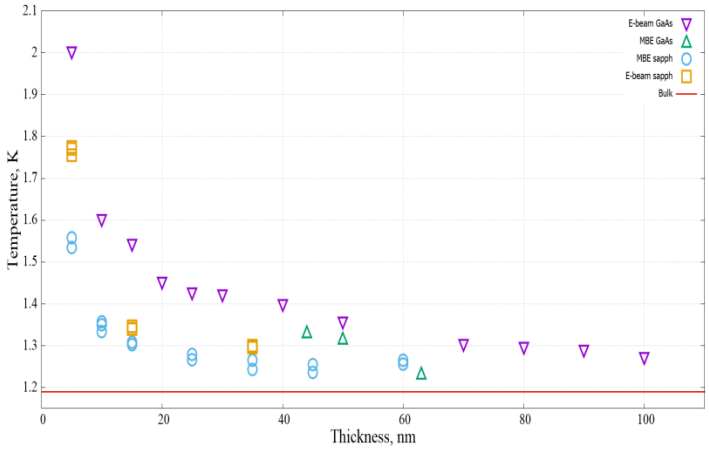

Fig. 1. Variation of the critical temperature T_c vs. thickness for aluminum films fabricated using various methods and on various substrates. Horizontal line corresponds to T_c=1.19 K for bulk aluminum.

References

[1] A. I. Shal'nikov, Nature 9, 142 (1938).
[2] K. Yu. Arutyunov, et. al., Phys. Status Solidi RRL 13, 1800317 (2019).

Electronic structure of atomically thin $Mo_xW_{1-x}S_{2y}Se_{2(1-y)}$ alloys

Pimenov N.Y.[1], Lavrov S.D.[1], Avdizhiyan A.Y.[1]

MIREA - Russian Technological University, 119454, Moscow, Russia

First successful exfoliation of graphene by Novoselov and coworkers in 2004 [1] caused a great surge of interest in the study of its properties. This led to the grow of intrest to new two-dimensional materials with unique physical properties. Transition metal dichalcogenides (TMDs) are one of these materials. TMDs are van der Waals bonded materials with the MX_2 structure, where M is a transition metal (such as W or Mo) and X is a chalcogen (such as S or Se). TMDs have a band gap of 1÷2 eV, in contrast to graphene, which is a metal by its properties. Bulk TMDs have an indirect bandgap, but when the thickness is reduced to one layer, the bandgap becomes direct [2]. Direct bandgap, high mobility of charge carriers and a number of other properties make two-dimensional TMDs excellent materials for creating one-dimensional field-effect transistors, photodetectors, solar cells and other devices of opto- and nanoelectronics [3]. It is possible to create solid alloys due to the similar atomic structure of two-dimensional TMDs (for example, $Mo_xW_{x-1}S_2$ or $Mo_xW_{1-x}S_{2y}Se_{2(1-y)}$, where x, y = 0÷1). The band gap can be changed by changing the composition of solid alloys. According to this properties, optimally parameters of devices based on two-dimensional TMDs could be achived.

Theoretical bandgap dependence of two-dimensional solid alloys $Mo_xW_{1-x}S_{2y}Se_{2(1-y)}$ on their morphological composition was carried out in this work. All calculations were carried out on the basis of the density functional theory using the QUANTUM ESPRESSO software package [4]. Exchange-correlation contributions are treated with Perdew-Burke-Ernzerhof functional. All calculations were carried out with a 2x2 super cells, which includes 4 metal atoms (Mo and/or W) and 8 chalcogen atoms (S and/or Se). It was show that the direct bandgap with the maximum valence and minimum of the conduction band is located at the Kk point of the Brillouin zone. The dependence of the bandgap on the morphological composition was determined.

This work was supported by the Russian science foundation (Grant 19-72-10165).

References

[1] Novoselov K.S. et al. Science (80-.).Vol. 306, № 5696. P. 666–669. (2004).
[2] Yun W.S. et al. Phys. Rev. B - Condens. Matter Mater. Phys. Vol. 85, № 3. (2012).
[3] Choi W. et al. Mater. Today. Vol. 20, № 3. P. 116–130. (2017).
[4] Giannozzi P. et al. J. Phys. Condens. Matter. Vol. 21, № 39. P. 395502.(2009).

Inverse Spin Hall effect in ferrite-garnet/topological insulator heterostructures

Shilina P.V.[1,2], Gogueva D.S.[1], Kapralov P.O.[3], Tereshchenko O.E.[4,5], Zvezdin A.K. [1,2], Belotelov V.I. [3,6].

[1]*National Research University Higher School of Economics, 101000, Moscow, Russia*
[2]*Moscow Institute of Physics and Technology, 141700, Dolgoprudny, Russia*
[3]*Russian Quantum Center, 121205, Moscow, Russia*
[4] *Saint Petersburg State University, 198504, Saint Petersburg, Russia*
[5]*A.V. Rzhanov Institute of Semiconductor Physics, 630090, Novosibirsk, Russia*
[6] *V.I. Vernadsky Crimean Federal University, 295007, Simferopol, Russia*

In this work we investigated the excitation of spin current by laser heating in ferrite-garnet($(YBi)_3(FeAlSc)_5O_{12}$)[4 μm]/topological insulator ($BiSbTeSe_2$) heterostructures. We irradiated structures, deposited in the external magnetic field, with laser diode. Laser beam was modulated by a low frequency. A spin current flowed along the temperature gradient due to the Spin Seebeck effect (SSE) [1] in ferrite-garnet layer. Spin current was injected into the topological insulator (TI) layer and due to the inverse spin Hall effect (ISHE) [2] the charge current flowed perpendicular to the spin current. We measured the voltage of ISHE.

During the experiments with samples with different thicknesses of TI, it was revealed that there is a boundary thickness, above which the voltage of ISHE is suppressed by the Hall effect. The dependence of the optically-induced voltage on the external magnetic field for sufficiently large thicknesses of the topological insulator (more than 200 nm) is linear and corresponds to the Hall effect.

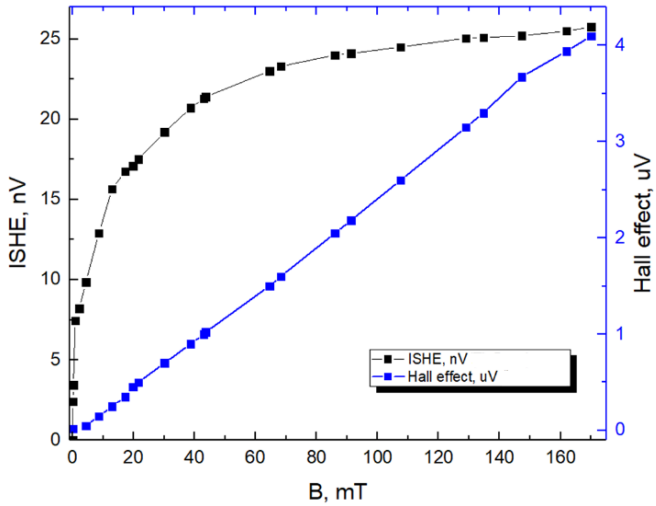

Fig. 1. Dependences of laser induced voltages on the external magnetic field in samples with different thicknesses of TI (ISHE (black curve) - for samples with a thickness of 100 nm, Hall effect

This work was supported by RFBR (project N 18-52-80038).

References

[1] K. Uchida et al. Nature 455.7214 (2008): 778-781.
[2] J. Sinova et al. Rev.Mod.Phys. 87.4 (2015): 1213.

Section 8
Materials for Medical and Ecological Applications. Biosensors

A first MEG-feasible fluxgate magnetometer.

P.M. Vetoshko[1,2], A.N. Kuzmichev[1], M.I. Ostras[1], N. Koshev[3], A. Butorina[3], E. Skidchenko[3], M. Fedorov[3], A. Ossadtchi[4]

[1]*Russian Quantum Center, 121353, Moscow, Russia*
[2]*Institute of Radioengineering and Electronics, Russian Academy of Sciences, 103907, Moscow, Russia*
[3]*Skolkovo Institute of Science and Technology, 121205, Moscow, Russia*
[4]*Higher School of Economics, 101000, Moscow, Russia*

In the current article, we present the first solid-state sensor feasible for magnetoencephalography (MEG) that works at room temperature. The sensor is a fluxgate magnetometer based on yttrium-iron garnet films (YIGM). In this feasibility study, we prove the concept of usage of the YIGM in terms of MEG by registering a simple brain induced field — the human alpha rhythm. All the experiments and results are validated with usage of another kind of high-sensitive magnetometers — optically pumped magnetometer, which currently appears to be well-established in terms of MEG. Magnetoencephalography (MEG) is a unique neuroimaging modality that combines noninvasiveness with high spatial and temporal resolution. These properties place MEG among the most informative neuroimaging tools capable of localizing neuronal activity with distinct temporal structure and suitable for studying complex functional integration processes. The first demonstration of MEG in humans dates back to 1972 when Cohen (1972) used superconducting quantum interference devices (SQUIDs) to register human alpha activity. Since then MEG found numerous applications in both medicine [1-3] and neuroscience [4-7]. Here we present the first solid-state MEG-feasible sensor that operates at room temperature according to the fluxgate principle and uses appropriately shaped yttrium-iron garnet films [8] as the sensitive element. The high-sensitivity fluxgate technology exploited in our sensor may offer a set of serious advantages over OPMs and SQUIDs in the context of MEG application. Our yttrium-iron garnet magnetometer (YIGM) is solid state, has wide dynamic range, operates at room temperature and unlike modern commercially available SERF-based OPMs does not require calibration before each use. The theoretical sensitivity of YIGM is lesser than 1 fT/√Hz, which in combination with its compact dimension and other properties make it a perfect candidate for the multichannel MEG application. In our experiments, we have observed sensitivity of about 35 fT/√Hz which is likely to be improved by the factor of 10 in the nearest future. In what follows below, we will present the initial MEG feasibility study that uses our YIGM sensor for registering human alpha rhythm. We will also describe the basic operational principle and the initial analysis of the sensitivity and intrinsic noise properties relevant to MEG application. In order to validate our measurements, we use the OP-MEG system, which has been chosen due to comparable YIGM scalp – sensor distances.

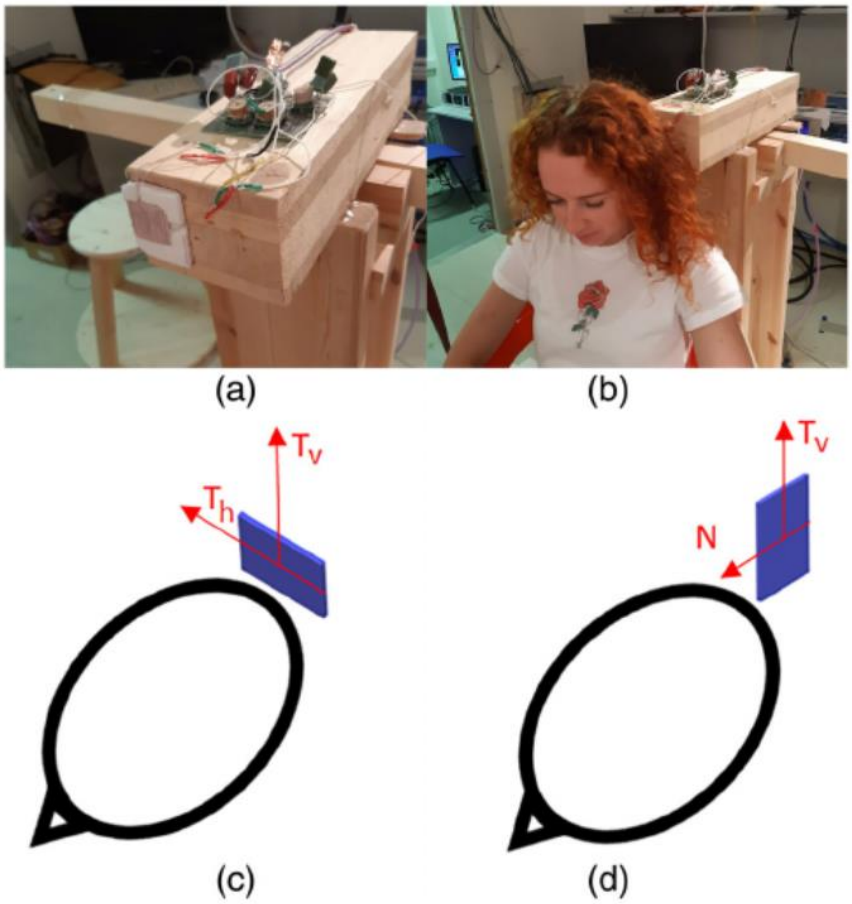

Figure 1: The experimental setup for alpha-rhythm registration using the YIGM: the sensor (a), subject position for alpha-rhythm registration (b); YIGM sensitive axes with respect to mutual head–sensor location: tangential displacement (c); normal displacement (d).YIGM, Yttrium-iron garnet magnetometer.

References

[9] Boon, L. I., Geraedts, V. J., Hillebrand, A., Tannemaat, M. R.,Contarino, M. F., Stam, C. J., & Berendse, H. W, Human Brain Mapping 40(9), 2827–2848 (2019).
[10] Koptelova, A., Bikmullina, R., Medvedovsky, M., Novikova, S.,Golovteev, A., Grinenko, O., et al., Epilepsy Research 140, 162–165 (2018).
[11] Mandal, P. K., Banerjee, A., Tripathi, M., & Sharma, A., Frontiers in Computational Neuroscience 12, 60 (2018).
[12] Baillet, S., Nature Neuroscience 20(3), 327–339 (2017).
[13] da Silva, F. L., Neuron 80(5), 1112–1128 (2013).
[14] Hari, R., & Salmelin, R., NeuroImage 61(2), 386–396 (2012)
[15] Pulvermüller, F., Shtyrov, Y., & Ilmoniemi, R., NeuroImage 20(2), 1020–1025 (2003).
[16] Vetoshko, P., et al., Technical Physics Letters 42(8), 860–864 (2016).

Tantalum oxide nanoparticles for cancer therapy and diagnosis

Koshevaya E.D.[1,2], Morozov V.N.[3], Kolyvanova M.A.[2,3], Krivoshapkina E.F.[4], Krivoshapkin P.V.[4]

[1]*Institute of Chemistry, Komi Science Centre of the Ural Branch of the Russian Academy of Sciences, 167000, Syktyvkar, Russia*

[2]*State Research Center-Burnasyan Federal Medical Biophysical Center of Federal Medical Biological Agency, 123182, Moscow, Russia*

[3]*Emanuel Institute of Biochemical Physics, Russian Academy of Sciences, 117997, Moscow, Russia*

[4]*SCAMT Laboratory, ITMO University, 197101, Saint-Petersburg, Russia*

The present work is aimed to investigate the potential of Ta_2O_5-based nanoparticles (NPs) for multimodal theranostic applications. Theranostics is a novel approach to create pharmaceuticals which combine both therapeutic and diagnostic capabilities. Tantalum oxide NPs are a perspective platform for developing multimodal theranostic agent because they inherently possess biocompatibility, radiosensitising properties (therapeutic capability) and X-ray contrast performance (diagnostic capability). This enables to design a converter for the radical destruction of malignant cells for enhanced radiotherapy, which at the same time could be used for diagnosis. An additional advantage is a high chemical inertness that makes Ta_2O_5 NPs safe for human organism while being non-irradiated.

In this regard, the developing of the synthesis procedure of 30 nm-sized Ta_2O_5 NPs was performed. The structure, morphology, surface properties and thermal behavior of the obtained material were studied by XRD, EDX, TEM, FTIR, TG/DSC, and nitrogen gas adsorption-desorption. A multilateral study on the influence of different parameters (pH, electrolyte concentration) on hydrosol stability of Ta_2O_5 NPs were studied in a wide range of pH (2–9) and background electrolyte concentrations (0.001–0.15 M NaCl) by dynamic light scattering, laser Doppler electrophoresis, potentiometric titration, and photometry. The influence of the time of ultrasonic treatment on the stability of aqueous dispersions was investigated. Based on the obtained results, the preparation protocol of highly stable hydrosols with concentrations 0.2–20 mg/mL and mean hydrodynamic diameter of aggregates <100 nm was developed. *In vitro* Cytotoxicity (MTT-test) and *In vivo* Acute Toxicity studies were performed for the obtained materials. The radiosensitizing effect of Ta_2O_5 NPs was showed on a plasmid DNA model, as well as on human fibroblast cells. The obtained sols provide high contrast in computed tomography (450 HU for a 20 mg NPs/mL) both in theoretical calculations and *in vivo* (rat gastrointestinal tract) [1].

Acknowledgements. This work was supported by Russian Foundation for Basic Research (project No 18-29-11078).

References

[1] Koshevaya E. D., Nazarovskaia D., Simakov M., Belousov A. V., Morozov V. N., Gandalipov E., Krivoshapkina E. F., and Krivoshapkin P. V., Journal of Materials Chemistry B, **8**, 8337-8345 (2020).

Biomimetic layers of acrylic composites based on SiO_2-hydroxyapatite complex for Enhanced Bone Regeneration

Burunkova J.A.[1], Sviazhina D.S.[1], Fisenko A.A.[1],
Mizina D.R.[1], Levshits M.D.[1], Strelnikova I.E.[1], Charnovich I.[2] , Kokenyesi S.[2]

[1]ITMO University, 197101, St. Petersburg, Russian Federation
[2]University of Debrecen, 4028, Debrecen, Hungary

Today, the actual problems of materials for medical applications remain the solution of issues related to increasing biocompatibility with organic tissue and reducing inflammation associated with implantable elements insertion. Despite the fact that titanium implants have proven themselves well in orthopedics and dentistry, the problem of reducing the number of rejections and postoperative complications is relevant.

This work proposes a method for solving the problem of increasing biocompatibility by applying a polymer coating with a bioactive complex to the surface of titanium, which partially resorbs after its insertion into the body and promotes the bone tissue cells proliferation into the material.

The coating material is developed on the basis of partially resorbable synthetic bifunctional monomer and bioactive complex of gelatin and an acrylic monofunctional monomer with silicone hydroxylapatite. The liquid composition is applied to a titanium surface. After photo-curing modified implant is kept in an aqueous medium. As a result of desorption of one of the components in composition, a porous structure is formed in the material. The resulting pore volume was determined by the gravimetric method and is at least 15%, depending on the components set.

Pure acrylic and urethane-acrylic monomers were chosen as synthetic bifunctional monomers. It's advantages include the fact that the composition based on it exhibits a higher decomposition rate, which was determined by keeping the film composites in a physiological environment model. As is known [1], calcium phosphate particles insertion can promote the proliferation of bone tissue cells in materials. Therefore, a technology was developed for obtaining silicone hydroxylapatite submicron particles coated with a shell of gelatin and acrylic monomer. Particle size is determined by the DLS method and is 500-700 nm.

Research of the composites wettability angle indicates that the materials are hydrophilic and have high moisture absorption. The effect of the materials composition on toxicity and biocompatibility with microorganisms by their cultivation on the surface coatings has been studied. Created polymer nanocomposites do not change the human dendritic cells viability and do not inhibit the probiotic lactic acid bacteria proliferation. Zinc oxide nanoparticles insertion suppresses growth of S. aureus and E. coli.

The results indicate that further studies of the obtained compositions for implant coatings are promising.

References

[1] Feng Q. et al., ACS central science. T. 5, №. 3, p. 440-450 (2019)

Study of MXenes as novel therapeutic agents for the liver cancer treatment

Sobolev K.V.[1], Motorzhina A.V.[1], Pschenichnikov S.E.[1], Levada E.V.[1], Pazniak A.I.[2], Rodionova V.V.[1]

[1]*Immanuel Kant Baltic Federal University, 236041, Kaliningrad, Russia*
[2]*University of Duisburg-Essen, 47057, Duisburg, Germany*

MXenes are the class of novel two-dimensional materials with the general structural formula $M_{n+1}X_nT_x$, where M is an early transition metal, X is carbon or nitrogen, and T are surface functional groups (mainly -O, -OH or -F). MXenes are synthesized by selective chemical etching of the MAX-phase precursor that has a layered "nanolamellar" crystal structure. The first published results on MXenes are dated 2011 [21] and, since then, the number of papers is growing annually, which emphasizes the relevance of this topic. The key advantage of MXenes is the colossal variability of properties achieved by changing the chemical composition and type of surface functionalization. This feature makes it possible to use MXenes in a large number of application areas, such as: energy accumulation, flexible electronics, electromagnetic shielding, absorption of microwave radiation, sensorics (for gas and pressure sensing, etc.) or biomedicine [2].

Biomedicine is one of the most relevant topics for MXenes usage nowadays [3]. The main advantage of MXenes for biomedical applications is their high biocompatibility, colloidal stability, the possibility of large-scale and environmentally friendly synthesis, and the relative ease of functionalization. MXenes can be actively exploited as agents for biovisualization, biosensing (hemoglobin, glucose, dopamine, etc.) and cancer therapy [3]. Due to the demonstrated efficiency of conversion of laser radiation into thermal energy MXenes are being considered as materials for the cancer treatment by means of the photothermal therapy [4–6].

Due to their relative novelty, MXenes have not been extensively studied as photothermal therapy agents. The main questions, left unsolved, are: what are the cytotoxic effects of MXenes (except for the oxidative stress mentioned in the literature) and how do MXenes affect living cells in the long term, what cellular responses they elicit, where they accumulate in the cellular compartments and what are the pathways for their metabolic elimination [3]. Also the study of biocompatibility of MXenes on real cancer cell cultures is missing. Finding the answers for these questions is mandatory to qualitatively improve the understanding of the mechanisms of action of MXenes on living cells and organisms, and their further application in practice.

Therapy of cancer diseases is one of the most pressing social problems facing the world community. The overall risk of developing cancer between the ages of 0 and 74 years is 20.2% (22.4% in men and 18.2% in women, respectively) [7]. Liver cancer is the fifth most common malignant neoplasm in the world, with a case-fatality rate of about 1/year, indicating that this type of disease is fatal in most patients within a year. Hepatocellular carcinoma (HCC) accounts for 70–85% of all liver cancer cases. Thus, in the present work we performed the complex study of biocompatibility of MXenes with HepG2 liver cancer cell culture. $Ti_3C_2T_x$ MXenes were synthesized using different experimental approaches: delamination of Ti_3AlC_2 MAX-phase precursor either in hydrofluoric acid (HF) solution or in the mixture of hydrochloric acid (HCl) with lithium fluoride (LiF). This was done to check the effect of surface functional groups,

which are different in these two cases, on the biocompatibility of MXenes. After synthesis the produced MXenes were characterized using X-ray structural analysis, energy dispersive spectroscopy, atomic force microscopy and Raman spectroscopy. After the initial characterization MXenes were exposed to cell cultures in three different concentrations (50, 100 and 250 μg/ml) for three different time spots (12, 24 and 48 hours). This was done to comprehensively examine the time and concentration dependency of MXenes' biocompatibility. Additionally we carried out the same study on Jurkat cell culture of the blood cancer. The obtained results can be considered as the first step towards the use of MXenes as therapeutic agents for the liver cancer treatment (for example, by means of the photothermal therapy) and are of the great importance as they reveal the biocompatible properties of these materials for liver cancer cell line. The complementary study of MXenes with blood cancer cell culture Jurkat lets us compare their biocompatibility with two types of cancer cells and estimate their possible efficiency for cancer treatment in more general terms.

References

[1] M. Naguib, M. Kurtoglu, V. Presser, J. Lu, J. Niu, M. Heon, L. Hultman, Y. Gogotsi, M.W. Barsoum, Adv. Mat., 23, p. 4248−4253 (2011).

[2] Y. Gogotsi and B. Anasori, ACS Nano, 13, p. 8491-8494 (2019).

[3] A. Szuplewska, D. Kulpinska, A. Dybko, M. Chudy, A.M. Jastrzebska, A. Olszyna and Z. Brzozka, Tr. in Biotech., 38(3), p. 264-279 (2020).

[4] J. Xuan, Z. Wang, Y. Chen, D. Liang, L. Cheng, X. Yang, Z. Liu, R. Ma, T. Sasaki, F. Geng, J. of Ger. Chem.Soc.,.55, p. 14569–14574 (2016).

[5] X. Yu, X. Cai, H. Cui, S.W. Lee, X.F. Yu, B. Liu, Nanosc., 9, p. 17859–17864 (2017).

[6] A. Szuplewska, D. Kulpinska, A. Dybko, A.M. Jastrzebska, T. Wojciechowski, A. Rozmyslowska, M. Chudy, I. Grabowska-Jadach, W. Ziemkowska, Z. Brzozka, A. Olszyna, Mat. Sc. and Eng.: C, 98, p. 874–886 (2019).

[7] C. Mattiuzzi, G. Lippi, J. of Epidem. and Gl. Health, 9(4), p. 217-222 (2019).

Hydrogen sensing by a Fabry-Perot resonator fabricated from tungsten trioxide and assembled by optical contacting

A.A. Kasyanov[1], D.P. Kulikova[1, 2], S.L. Efremova[1, 2], K.N. Afanasiev[1, 3], P.N. Tananaev[1], A.V. Baryshev[1]

[1]*Dukhov Automatics Research Institute (VNIIA), 127055, Moscow, Russia*
[2]*Lomonosov Moscow State University, 119991, Moscow, Russia*
[3]*Institute for Theoretical and Applied Electromagnetics of RAS, 125412, Moscow, Russia*

Development of a highly sensitive and miniature selective sensor of the gas environment is an actual challenge. Such sensors are widely used to ensure industrial safety associated with the use of dangerous gases, to monitor flammable gases concentrations during equipment operation [1, 2]. The disadvantages of the sensors available today are their lack of sensitivity and selectivity when detecting a particular gas in a significantly different atmosphere (smoky, humid, etc.). The goal of our work is to develop a gas-sensitive sensor that has a miniature size, high selectivity and sensitivity.

The main structural element of the fabricated optical sensor was the Fabry-Perot resonator, assembled by optical contacting [3, 4]. The operating principle is the use of a resonant standing wave (the Fabry-Perot resonator mode) in gas-sensitive layers between two dielectric multilayer structures (Bragg mirrors) based on oxides with high and low refractive indices. The resonant layer consisted of gas-sensitive oxide-catalytic bilayers pair interacting with the flowing gas atmosphere. We chose a pair of ZrO_2/SiO_2 oxides as the basis of the Bragg mirror and WO_3/Pt as the pair of the gas-sensitive/catalyst layer– sitall/$(ZrO_2/SiO_2)^3$/ZrO_2/WO_3/Pt/air gap/Pt/WO_3/ZrO_2/$(ZrO_2/SiO_2)^3$/sitall. The central wavelength of the resonator was 1100 nm for these reasons: WO_3 has a low absorption in the IR range, its optical constants significantly change after reaction with hydrogen and, also, selection of this working range provides increased the air gap for gas flow.

In the report, we will discuss the fabrication technology of the sensing elements under our study and peculiarities of hydrogen sensing. For oxygen-containing and oxygen-free atmospheres, presence of hydrogen was found to result in substantial changes in transmission spectra of the resonator.

References

[1] S. J. Ippolito, S. Kandasamy, K. Kalantar-zadeh, W. Wlodarski, Sensors and Actuators B: Chemical, V. 108, Issue 1-2, P. 154- 158 (2005).

[2] M. Zhang, J.Guo, F. Xie, J. Wang, S. Zhang, X. Guo, Solid State Ionics, V. 347, 115274 (2020).

[3] Yina Li, Chunliu Zhao, Ben Xu, Dongning Wang, Minghong Yang, Optics Communications, V. 414, P. 166-171 (2018).

[4] V. V. Potelov, Journal of Optical Technology, V. 76, Issue 8, P 482 (2009).

Gold-coated Janus-like Fe-Si magnetic nanoparticles for biomedical applications

Lyaschenko S.A.[1], Yakovlev I.A.[1], Tarasov I.A.[1], Velikanov D.A.[1], Nemtcev I.V.[2], Volochaev M.N.[2], Varnakov S.N.[1], Ovchinnikov S.G. [1,3]

[1] *Kirensky Institute of Physics of SB RAS, Akademgorodok 50 bld. 38, Krasnoyarsk 660036, Russia*
[2] *Federal Research Center KSC Siberian Branch Russian Academy of Sciences, Akademgorodok 50, Krasnoyarsk 660036, Russia*
[3] *Siberian Federal University, 79 Svobodny pr., Krasnoyarsk 660041, Russia*

In last decade, magnetic resonance imaging (MRI), as a safe and common medical diagnosis method, lets the use of superparamagnetic nanoparticles with sizes less than 50 nm as a contrasting agent [1]. Also the optimal solution for magnetomechanical activation of apoptosis and suppression of proliferation of tumor cells is the use of superparamagnetic nanoparticles of non-toxic elements with a size less than 150 nm with a high specific magnetic moment, a bioinert shell and anisotropy of shape [2].

We will show results of the synthesis of the Janus-like magnetic nanoparticles [3] with iron-silicon core, gold and bioinert silicon oxides shell (MNPFSA). MNPFSA are obtained by the method of solid-phase synthesis in ultrahigh vacuum and have both a rounded and an elongated shape depending on the density of the vicinal faces of the single-crystal substrate NaCl. From the transmission electron microscopy data (TEM) the MNPFSA sizes is 10-30 nm (Fig. 1) with shell thickness about 3.6 nm.

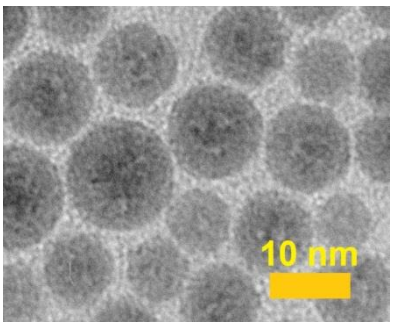

Fig. 1. TEM of MNPFSA

The magnetic moment of the MNPFSA were measured by vibrational magnetometry and it is comparable to that of superparamagnetic magnetite nanoparticles. However, magnetic moment can be increased by varying the stoichiometric composition of the nucleus.

MNPFSA were studied by X-ray photoelectron spectroscopy to determine the chemical composition of the nanoparticle shell. Surface layer of nanoparticles contains iron, 96.7 at. % of which is associated with oxygen and silicon, but only 3.3 at. % has Fe-Fe bonds.

References

[1] M. Shinkai, J. Biosci. Bioeng. 94(2002)606.

[2] I.V. Belyanina, T.N. Zamay, G.S. Zamay et al. Theranostics, 7(2017) 3326.

[3] Y.I. Golovin, S.L. Gribanovsky, D.Y. Golovin et al. Journal of Nanoparticle Research, 19(2017)59.

Magneto-ellipsometry study of MAX-phases: Mn_2GaC thin films

Lyaschenko S.A. [1], Maximova O.A.[1,2], Varnakov S.N.[1], Ovchinnikov S.G.[1,2]

[1] *Kirensky Institute of Physics, Federal Research Center KSC SB RAS, 660036, Krasnoyarsk, Russia*

[2] *Siberian Federal University, 660041, Krasnoyarsk, Russia*

On the one hand, it is well-known magneto-ellipsometry allows to conduct precise non-destructive study of optical and magneto-optical properties of materials [1], on the other hand, MAX phases are highly perspective magnetic media with a wide range of possible applications [2]. That is why, it was decided to study epitaxial Mn_2GaC MAX phase thin films by means of spectral magneto-ellipsometry.

We used magneto-ellipsometry technique in order to find out the dielectric permittivity tensor (ε) elements

$$[\varepsilon] = \begin{bmatrix} (n-ik)^2 & -i(n-ik)^2(Q_1 - iQ_2) & 0 \\ i(n-ik)^2(Q_1 - iQ_2) & (n-ik)^2 & 0 \\ 0 & 0 & (n-ik)^2 \end{bmatrix}, \quad (1)$$

and to analyse the magnetic circular dichroism (MCD) spectrum [3]

$$MCD = -\frac{\pi}{\lambda}\,\mathrm{Im}((n-ik)(Q_1 - iQ_2)), \quad (2)$$

where n is the real refractive index, k is the extinction coefficient, Q_1 is the real part of the magneto-optical parameter, Q_2 is the imaginary part of the magneto-optical parameter, λ is the wavelength of the incident light.

In our report we will present the details of carrying out the magneto-ellipsometry experiment, the procedure of data processing and we will share our findings on the physical properties of the investigated MAX phases in a visible spectrum range. Also we will present a new approach for the analysis of optically-anisotropic structures.

Acknowledgements

The research was carried out with a grant from the Russian Science Foundation № 21-12-00226, https://rscf.ru/project/21-12-00226/ .

References

[1] O. Maximova, N. Kosyrev, I. Yakovlev, D. Shevtsov, S. Lyaschenko, S. Varnakov, S. Ovchinnikov, JMMM 440, 153–156 (2017)

[2] M.W. Barsoum, M. Radovic, Annu. Rev. Mater. Res. 41, 195–227 (2011)

[3] S.A. Lyashchenko, Z.I. Popov, S.N. Varnakov, E.A. Popov, M.S. Molokeev, I. A. Yakovlev, et al., J. Exp. Theor. Phys. 120, 886–893 (2015)

Fe_3O_4-Au nanoparticles as approach for diagnostic of Crohn's Disease

Z. Grigoreva[1], Gritsenko Ch.[1], Efremova M.V.[2], Abakumov M.[2], NevzorovaY. A.[3], Estevez O.[3], Rodionova V. V,[1] Levada E. V.[1]

[1]Immanuel Kant Baltic Federal University, 236041, Kaliningrad, Russia
[2] Department of Chemistry, Lomonosov Moscow State University, Moscow, Russia
3Department of Genetics, Physiology and Microbiology, Faculty of Biology, Complutense University, Madrid, Spain

In recent years, nanotechnology has progressed to a level that makes it feasible to specifically design, manufacture, and characterize nanoparticles suitable for clinical applications, such as diagnostic purposes. Magnetic nanomaterials with a variety of well-controlled properties, as size and surface modification, were used in the study. In this project, we investigated different types of magnetic nanoparticles as the diagnostic agents that can be demonstrated gut leakiness by Chron's disease.

Control and experimental group with induced DSS-colitis of mice were used. To assess gut leakiness, both groups of mice received Janus-like magnetic Fe_3O_4-Au nanoparticles with a DSPE-PEG polymer coating by the oral gavage, and accumulation in regions outside the gut was analyzed. Different sizes (5 nm, 15 nm, and 25 nm) of Fe_3O_4 component of the nanoparticles were used to assess the leakiness in the healthy and inflamed gut. Fe_3O_4-Au nanoparticles were applied by oral gavage in the concentration of 20 mg/kg of a body weight after 5 days of the DSS treatment (2% in drinking water) for experimental and control groups of animals. 24 hours later, mice were sacrificed, blood and organs were collected. Samples were examined for prensence of magnetic moment in dry feces and liver samples.

Magnetic properties of the samples were investigated using vibrating sample magnetometry. Feces samples from control group of mice, showed the diamagnetic behavior typical for biological tissues in the presence of a magnetic field. Nanoparticle magnetic moment of a feces sample mass unit was obtained. For the control group, the highest magnetic moment of nanoparticles with the diameter d (Fe_3O_4) = 5 nm per sample mass unit in feces is observed at 8 hours after their administration, while of nanoparticles with the diameter d(Fe_3O_4)= 15 nm - after 24 hours. For the samples with d (Fe_3O_4)= 25 nm, the highest magnetic moment per sample mass unit is observed after 24 hours. Magnetic moment was also detected in the feces of animals with the induced DSS-colitis. On average, nanoparticle magnetic moment per sample mass unit is 2-5 times higher for the control group compared to the DSS-colitis group, which can confirm the gut leakiness during DSS colitis and can be used as a future approach for diagnostic of the Chron's disease.

Influence of the parameters of an output amplifier on the efficiency of THz radiation detection

Ryabukhin V.E.[1], Mishina E.D.[1]

[1]MIREA – Russian Technological University,
Prosp. Vernadskogo 78, 119454 Moscow, Russia

Modern terahertz antennas have THz response power in microwatts range [1]. This leads to complication of signal processing caused by small signal power. To improve output power ratings of THz antennas Lock-In amplifier is used. In cases of extremely low power ratings an additional amplifier with high gain and low signal-to-noise ratio (SNR) is added to the scheme. The antennas themselves, at the same time, have relatively high SNR [2]. This fact causes a new task associated with need for selective frequency amplification and reduction of external field interference.

We experimentally investigated these characteristics depending on various capacitances in the feedback circuit and the power supply of an amplifier:

- SNR;
- Output signal amplitude.

During the measurement process, an amplifier based on the AD8655ARZ chip with the possibility of varying capacitance in the feedback circuit was used. To exclude the influence of external electromagnetic interference, a shielding housing was used.

Based on the measurements, a spectral analysis of the output signal was performed with variations in the feedback capacitance, power supply, and the method of shielding the amplifier. Added amplifier's noise was measured and compared to other noise sources. The ways to increase SNR by adding amplification stages were tested. According to the obtained dependencies, the rule for the applicability of additional amplifier of the THz antenna signal is formulated: the SNR of the amplified signal must be less than the original one, while gain must be more than 10.

An amplifier was connected to the input of Lock-In amplifier. During the experiment the data was collected serially from a number of antennas. This was done to approximate the results over several measurements and prove their independency from antenna choice.

References

[1] Nomoev SA., Vasil', I. S., Vinichenko, A.N. et al. The Influence of the Annealing Regime on the Properties of Terahertz Antennas Based on Low-Temperature-Grown Gallium Arsenide. Tech. Phys. Lett. 44, 44-46 (2018).

[2] Gorbatova, A.V., Khusyainov, D.I., Yachmenev, A.E. et al. A Photoconductive THz Detector Based on a Superlattice Heterostructure with Plasmonic Amplification. Tech. Phys. Lett.46, 1111–1115 (2020).

Magnetic field induced transformation of NMR transverse relaxation rate for protons in low-concentrated magnetic fluids over time

Gorbovanov A.I., Aleksashkin I.V., Gusev A.N., Dubas V.V, Polulyakh S.N.

V. I. Vernadsky Crimean Federal University, 295007, Simferopol, Russia

Magnetic nanoparticles and functional materials based on them have a wide range of applications. For example, they have utilization as contrast agent in magnetic resonance imaging [1] due to their ability to decrease magnetic relaxation rate for protons in surrounding media [2]. In this regard, it is advisable to study the influence of iron oxide Fe_3O_4 magnetic nanoparticles on the nuclear magnetic relaxation for the environmental protons *in vitro*. To perform NMR experiments we have prepared a series of water-based magnetic fluid samples of the magnetic nanoparticles concentration $c \leq 0.125\ M$. The size of Fe_3O_4 nanoparticles is estimated on average from 60 to 120 nm. To suppress the magnetic adhesion of particles, a surfactant has been introduced in a 1:1 ratio with water at the stage of magnetic fluid synthesis.

To study NMR signals from ^1H nuclei in liquid we have used *Spin Track* NMR relaxometer with permanent magnet which provides magnetic field $B \approx 0{,}564\ T$. The CPMB pulse sequence results in spin-echo decay that is the experimental data source to calculate relaxation rate. As a rule, the exponential approximation of echo decay gives transverse relaxation time T_2 and this method is well applicable for single-exponent decay. The alternate method is the numeric Inverse Laplace Transform [3] which brings the $h(T_2)$ distribution so, that $h(T_2)$ gives the relative part of nuclei having relaxation time T_2.

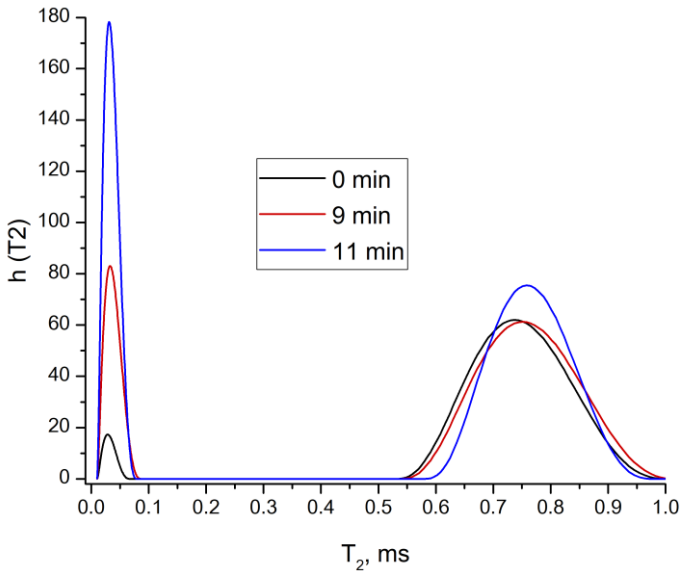

Fig.1. Transformation of relaxation time T_2 distribution for the magnetic fluid of $c = 0.125\ M$ in *dc* magnetic field.

Fig. 1 give an example of relaxation times distribution $h(T_2)$ for the magnetic fluid of $c = 0.125\ M$. There are two types of protons that differ in relaxation times: slow decay of $T_2 = 0.7 \div 0.9\ ms$ and fast decay of $T_2 \approx 0.03\ ms$. We have found out experimentally the evolution of $h(T_2)$ distribution while a sample is located in *dc* magnetic field. The relative part

of protons having fast relaxation increases while the sample is located in *dc* magnetic field. After shaking the sample, the $h(T_2)$ distribution almost returns to the original one. The similar behavior demonstrate all studied samples. However, the third type of protons that differ in relaxation rate appears in dilute fluids (fig. 2). The special experiment for water-surfactant fluid without magnetic particles gives single relaxation time $T_2 \approx 2 \cdot 10^3\ ms$, which is greater than maximal relaxation time for magnetic suspension.

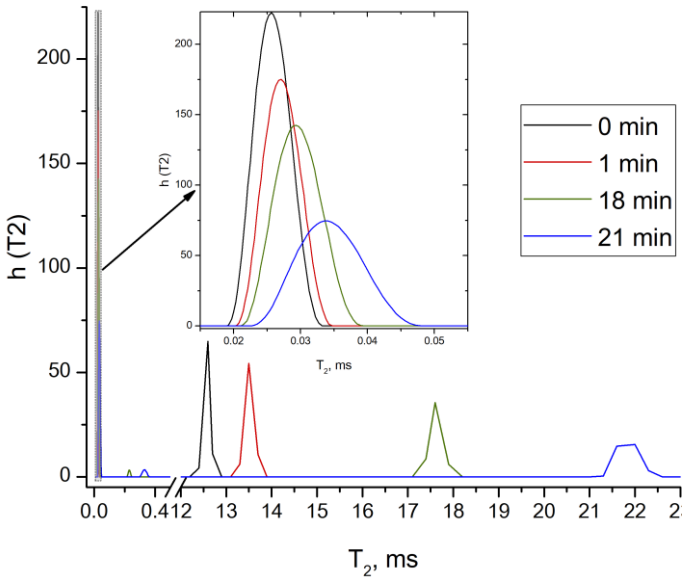

Fig.2. Transformation of relaxation time T_2 distribution for the magnetic fluid of $c = 0.021\ M$ in *dc* magnetic field

Taking into account the experimental results and know data for the magnetic liquids we conclude that the fast nuclear relation demonstrate protons of liquid molecules in the areas near the magnetic nanoparticles conglomerates. The reason for relaxation are the fluctuations of magnetic field on nuclei and these fluctuations are greater in amplitude against field fluctuations for nuclei in the areas out of the magnetic particles conglomerates. The decrease of magnetic particles concentration outside of the conglomerates results in decrease of field fluctuation amplitude and in the correspondent relaxation time increase.

This work was supported in part by the Russian Foundation for Basic Research in the framework of project no. 18-29-02120.

References

[1] X. Yin, S. Russek, G. Zabow et al. Scientific Reports (2018) 8:11863, DOI:10.1038/s41598-018-30264-5

[2] Aleksashkin, I.A., Berzhanskii, V.N., Pershina, E.D. et al. Phys. Lett. 27, 84–85 (2001). DOI:10.1134/1.1345175.

[3] S.W. Provencher. Comput. Phys. Commun. **27**, 229 (1982)

The relaxometry of magnetic nanoparticles with YIG based sensor.

P.M. Vetoshko[1,2], A.N. Kuzmichev[1], M.I. Ostras[1] and V.I. Belotelov[1]

[1]*Russian Quantum Center, 121353, Moscow, Russia*
[2]*Institute of Radioengineering and Electronics, Russian Academy of Sciences, 103907, Moscow, Russia*

This paper presents a new device for magnetorelaxometry. The approach used makes it possible to register specific binding reactions of magnetic nanoparticles, as well as to determine their coordinates. The main advantage and difference of this device from similar ones is the use of a supersensitive solid-state magnetometer based on YIG [1,2]. The crucial property of this magnetometer is that it can operate immediately after switching off the polarization impulse (recovery time is 40 μs). At the same time, it has a noise spectral density of 40 fT/Hz$^{0.5}$ and operates at room temperature. For particles in which the phenomenon of specific binding is observed, the relaxation time increases due to an increase in the hydrodynamic radius, which affects the relaxation mechanism [3]. Thus, the particle size determines the hydrodynamic radius and, therefore, the relaxation time - smaller particles have a shorter relaxation time. Due to the exponential decrease in the relaxation signal, small particles must be measured in a time close to the beginning of the decrease curve in order to maximize the magnitude of the measurement signal. To work inside the human body with minimal harm, such particles must be small (no more than 30 nm) and have low concentrations. The value of the relaxation signal is directly proportional to the local concentration of nanoparticles; therefore, the signal-to-noise ratio of magnetic sensors is a very important parameter. Contrasting MRI does not provide information on the hydrodynamic radius of nanoparticles and does not allow us to distinguish the case of the reaction of specific binding from the simple sedimentation of the nanoparticle. Although the operation of the proposed system may require simple magnetic shielding of external magnetic noise, the system does not require cooling with liquid nitrogen or helium and is cheaper and easier to maintain than both industrial MRI scanners and, even more, Positron Emission Units.

The proposed device for determining the magnetic moments and relaxation times of low concentrations of magnetic nanoparticles in vitro allows registering a minimum concentration of 100 pg/cm^3 (approximately 1 iron oxide particle with a diameter of 30 nm per cm^3) with a relaxation time of 100 μs. Fig. 1 shows the curve of magnetic relaxation of particles measured by the proposed method using a super sensitive magnetometer. Also, the developed device has all the advantages of a conventional solid-state magnetometer, among which are broadband, good spatial resolution, vector nature, the possibility of gradient measurements, low power consumption, compactness, easy handling and low cost.

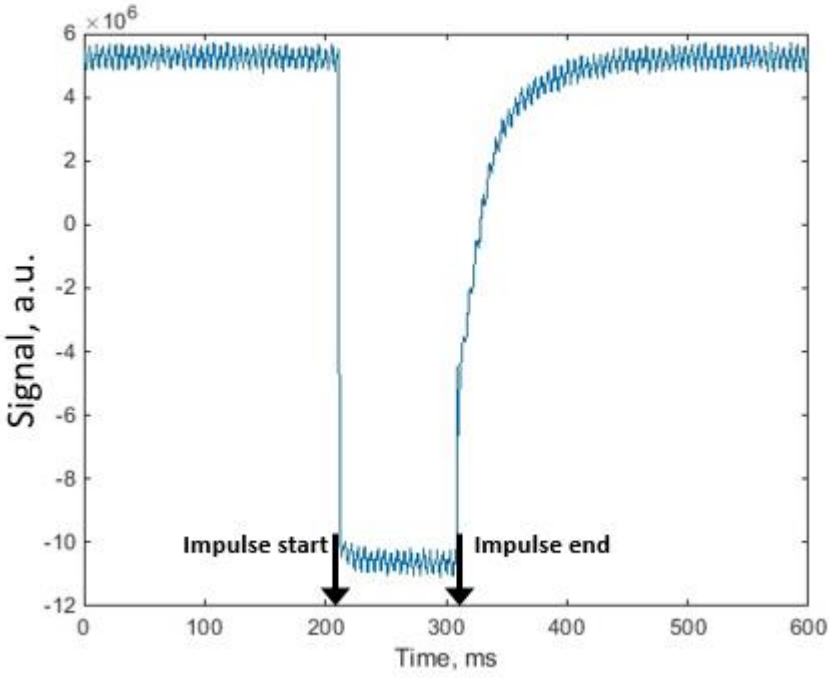

Figure 1: Magnetic relaxation curve of the superparamagnetic nanoparticles. With arrows shown start and end of the polarizing magnetic impulse.

References

[17] Vetoshko, P. M., Zvezdin, A. K., Skidanov, V. A., Syvorotka, I. I., Syvorotka,I. M., & Belotelov, V. I., Technical Physics Letters 41(5), 458-461 (2015)

[18] Koshev, N., Butorina, A., Skidchenko,E., Kuzmichev, A., Ossadtchi, A., Ostras, M., Fedorov, M., &Vetoshko, P, Human Brain Mapping, 1-13 (2021)

[19] De Haro L. P. et al. Biomedical Engineering/Biomedizinische Technik. 60(5), 445-455 (2015)

Microwave heating applied to improve efficiency of metal reduction from EAF dust

Bychkov I.V.[1], Anzulevich A.P.[2], Butko L.N.[2], Kalganov D.A.[3]

[1]*South Ural State University (National Research University), 454080, Chelyabinsk, Russia*
[2]*Chelyabinsk State University, 454001, Chelyabinsk, Russia*
[3]*ITMO University, 197101, Saint Petersburg, Russia*

It is widely known that it is necessary to solve the problems of utilization of the annually accumulated waste of the metallurgical and pulp and paper industries. The production of useful materials from secondary raw materials is possible due to the development of new metallurgical technologies, including the use of microwave energy [1-2].

In this paper, we investigate the interaction of an electromagnetic field with a material consisting of dust from electric arc furnaces and biochar. We considered the chemical processes accompanying the reduction of metals from such a material and built a model based on the Bruggeman – Landauer approximation of the effective medium.

The main chemical processes occurring during the direct reduction of iron and zinc with biochar depend on the initial composition of EAF dust, biochar and binder, but generally correspond to the redox reactions described in [2].

Taking into account the properties of the starting material and intermediate phases, we obtained the following changes in the effective parameters of the material depending on the initial conditions and created a numerical model (Fig. 1).

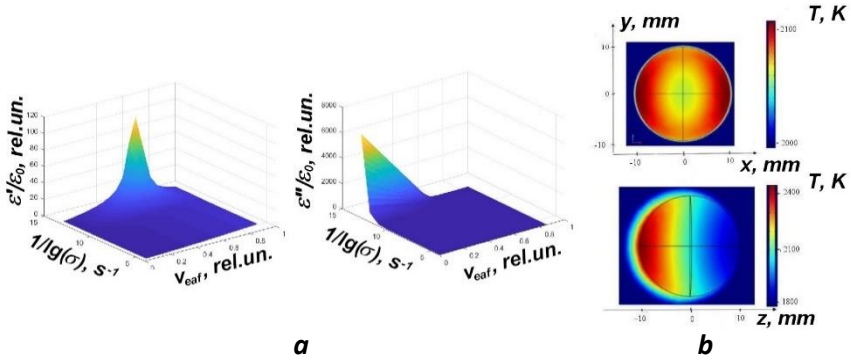

Fig. 1. Changes in the effective parameters of the material, depending on the composition – ***a***, and heating simulation – ***b***.

The reported study was funded by RFBR and NSFC, project number 21-58-53044, and was supported by the National Natural Science Foundation of China under Grant 52111530046.

References

[1] A.P. Anzulevich, D.A. Kalganov, S.N. Anzulevich, I.V. Bychkov and Z. Peng, J. Phys. Conf. Ser. 1461, 012007 (2020).

[2] Q. Ye, G. Li, Zh. Peng, R. Augustine, M.D. Pérez, Y. Liu, M. Liu, M. Rao, Y. Zhang and T. Jiang, Powder Technol. 362, 781–789 (2020).

Obtaining of cylindrical magnetic nanoparticles for modification of polymer microcapsules

Doludenko I.M.[5], Mikheev A.V.[2], Burmistrov I.A.[1], Trushina D.B.[1,3], Borodin T.N.[1,3], Bukreeva T.V.[1,4], Zagorskii D.L.[1]

[1] *FSRC "Crystallography and Photonics" of RAS, 119333, Moscow, Russia*
[2] *Moscow MV Lomonosov State Univ, 119991, Moscow, Russia*
[3] *Sechenov First Moscow State Med Univ, 119991, Moscow, Russia*
[4] *Kurchatov Inst, Natl Res Ctr, 123098, Moscow, Russia*
[5] *HSE University, 101000 , Moscow, Russia*

It is known that magnetic particles are actively used in biology and medicine. So, the actual and actively solved problem at the present time is "targeted delivery of drugs". One of the approaches to solving this problem is the introduction of magnetic particles into a capsule with drugs. These particles can then serve to "attract" the capsule to the desired point of the body, for heating (due to the high-frequency effect of the electromagnetic field - "hyperthermia"), for opening the capsule (due to the possible rotation of the particles in an alternating magnetic field). Often, to solve such problems, a magnetic particle must have certain geometry and parameters.

We have proposed a method for creating nanosized particles having the definite shape and predetermined sizes. The aim of this work was to obtain size-calibrated elongated particles - cylindrical magnetic nanoparticles (CMNP) and to study the possibility of their inclusion in the shell of multilayer polyelectrolyte microcapsules.

To obtain CMNP, the method of matrix synthesis was used. It based on galvanic filling of track etched membranes (TEM). This method is distinguished by the possibility of obtaining nanoparticles with a controlled aspect ratio and high repeatability, which makes them promising as magnetoactive components in medicine. The essence of the method was to create an array of nanowires (NW) from alternating layers of the required magnetic metal and a "sacrificial layers" (Cu). The copper layers was subsequently removed then, dividing each nanowire into separate magnetic segments. This method allows good control of the geometric dimensions of the resulting nanoparticles.

The process of obtaining a suspension of CMNP consisted of several stages. At the first stage, the polymer matrix is prepared for galvanic filling. The choice of the matrix determines the final number of particles on one sample and the diameter of the CMNP. At the stage of preparation, a continuous copper layer was applied to the polymer matrix on one side. At the next stage layer-by-layer deposition of nickel and copper into the pores of the matrix was carried out. The number of layers was determined by the required dimensions of the CSMNP and the thickness of the matrix, which in the work did not exceed 12 μm. The process of obtaining layered nanoparticles implied deposition in a single-bath mode. For electrodeposition an electrolyte of the following composition was used: $NiSO_4 \cdot 7H2O$ - 0.7 M; $CuSO_4 \cdot 5H_2O$ - 0.025 M; H_3BO_3 - 0.51 M, where M is molarity. The alternation of the deposited material was achieved by changing the deposition potential: for nickel it was 1.8 V, for copper - 0.7 V. Potential switching was carried out depending on the flowing charge, which is directly related to the mass of the deposited material. It is needed to control the thickness of the copper and nickel layers with high accuracy, and, as a consequence, to obtain CMNP of a calibrated size.

In this work, the length of the CMNP was 200 or 400 nm (with a diameter of 100 nm, determined by the pore diameter in the growth matrix).

After deposition, the matrix was removed in an alkali solution. Thus, in this work, we obtained NW arrays from magnetic and copper layers on a copper substrate. At the next stage, the samples were placed in an etchant for selective copper removal. After the dissolution of copper (substrate and sacrificial layers) a suspension of CMNP was formed. Then these CMNP were isolated from the etchant with a permanent magnet and placed in an aqueous solution. The geometry and composition of the CMNP were determined by the SEM.

The obtained CMNP were incorporated into the shell of polymer capsules by electrostatic adsorption. To optimize the inclusion of particles in the shells, their zeta potential was investigate. SEM examination of capsules confirmed the presence of CMNP in the capsule shell. The particles are unevenly distributed, which is presumably due to their aggregation. In order to further reduce the aggregation of CMNP and improve the properties of their surface, they were coated with surfactants. Analysis of electron microscopic images of capsule samples formed using modified CMNP showed that modification of their surface somewhat reduces particle agglomeration and does not affect the efficiency of NW inclusion in the polyelectrolyte shell.

Acknowledgements. This work was supported by the Ministry of Science and Higher Education within the framework of the State Assignment of the FRC "Crystallography and Photonics" of the RAS using the equipment of the Center for Collective Use of the FRC "Crystallography and Photonics" of RAS with the support of the Ministry of Education and Science of Russia (project RFMEFI62119X0035) regarding the synthesis of magnetic nanowires and their characterization.

Electronic sensors of relative air humidity based on thin films of polyanilines

Mullagaliev I.N.[1],Salikhov R.B.[1], Zinnatulina A.A[1]

[1]*Bashkir State University. 450076, Ufa, Russia*

In connection with the extreme pollution of the environment and increased environmental problems, the study of new substances with better sensory properties is actualized [1]. Research is being carried out on new materials, polymers, for nanoelectronics, which have good conductivity [2]. The use of PANI in sensors involves the use of physical changes that occur in high molecular weight objects exposed to a variety of chemicals at the level of the molecular and macroscopic structure of polymers [3].

In this work, samples of resistive moisture sensors were obtained and their characteristics were investigated. Sitall was used as a substrate. On top of the sitall, aluminum electrodes were deposited by thermal spraying in a vacuum chamber on a VUP5 unit 400 nm thick. In the region of the gap between the electrodes of 50 μm, a film of polyaniline derivatives was applied by centrifugation from a solution, 500 nm thick. The resulting film was kept in an oven to remove residual solvent. The study of the microstructure of the (co) polymers was carried out using a scanning probe microscope.

The sensory properties of samples of sensors with thin films of polyaniline derivatives for air humidity were investigated. The study of the volt-ampere characteristics of copolymer films of PANI and its derivatives, the effect of the humidity of the current through the resistor at different values of air humidity showed the possibility of their use in a sensor of relative air humidity. The response time of the sensors is no more than 2-3 s, which is a good indicator for electronic hygrometers. The sensors have been found to be reversible and reusable. The relationship between good sensitivity and low inertia and the process of substance synthesis has been revealed.

References

[1] A.N. Andriianova, D.E. Gribko, I.S. Petrov, I.N. Mullagaliev, A.F. Sattarova, R.B. Salikhov, I.B. Abdrakhmanov, and A.G. Mustafin // New Journal of Chemistry V 45, I 14, 6356-6366 (2021).

[2] T.R. Salikhov, Y.M. Yumaguzin, and R.B. Salikhov, 2015 International Siberian Conference on Control and Communications (SIBCON), IEEE Proceedings, 7147207 (2015).

[3] L.R. Latypova, A.N. Andriianova, S.M. Salikhov, R.B. Salikhov, I.N. Mullagaliev, I.B. Abdrakhmanov, and A.G. Mustafin, Polymer International V 69(9), 804–812 (2020)

Thin films of polyanilines for detecting of ammonia vapors concentration

Salikhov R.B., Mullagaliev I.N., Salikhov T.R.

[1]*Bashkir State University, 450076, Ufa, Russia*

The field of chemical sensors has expanded significantly, they are used in various fields, such as medicine, safety at home and at work [1]. Various types of sensors are designed on the basis of polyaniline polymer [2]. Instruments for measuring the concentration of ammonia are in demand in industries where the working environment has an unstable concentration of ammonia. The main direction of research is aimed at finding new substances sensitive to ammonia. [3]

In this work, samples of resistive sensors based on polyaniline derivatives were prepared. As a sitall substrate, aluminum contacts were deposited on it, the gap between the contacts was 50 μm. A film of a polyaniline derivative was applied to the gap region by centrifugation from a solution. To remove residual solvent, the samples were placed in an oven. The thickness of the polyaniline films is 150 nm. Thickness control is done with an atomic force microscope.

To measure the current-voltage characteristics, the samples were placed in a chamber with a controlled concentration of ammonia vapor. The measurements were carried out at room temperature. Using the educational complex of scanning microscopes Nanoeducator II, AFM images of the surface of the studied polymer films were obtained. According to the results of studying the morphology of the surface of the films, a relatively large current flowing through the film with a higher roughness is observed.

The dependences of the current through the sample on the residence time in the medium with ammonia vapors and the dependence of the current on the concentration of ammonia vapors were obtained. Films of polyaniline derivatives react to the presence of ammonia vapors in the environment by decreasing the flowing current. The advantages of the obtained NH3 absorption sensors based on polyaniline films include a small hysteresis. To create sensors with a sensitivity in a wide range of concentration, additional research is needed to improve the characteristics of polymers and their films.

References

[1] R.B. Salikhov, A.N. Lachinov. In: Advances in chemical sensors, edited by Wen Wang. Rijeka, 215-234 (2012).

[2] Y.N. Biglova, R.B. Salikhov, T.R. Salikhov, I.N. Safargalin, A.G. Mustafin, I.B. Abdrakhmanov, Physics of the Solid State, V 59, № 6, 1253-1259 (2017).

[3] R.B. Salikhov, I.N. Mullagaliev, I.N. Safargalin, 2018 XIV International Scientific-Technical Conference on Actual Problems of Electronics Instrument Engineering (APEIE), 20–22 (2018).

Investigation of the spatial structure of bionanoconjugates based on DNA aptamers by synchrotron methods

R.V. Moryachkov[1,2], V.N. Zabluda[1], I.A. Shchugoreva[2,3], P.V. Artyushenko[2,3], A.S. Kichkailo[2,3], V.A. Spiridonova[4], A.N. Berlina[5], A.E. Sokolov[1]

[1]Kirensky Institute of Physics, 660036, Krasnoyarsk, Russia
[2]Federal Research Center "Krasnoyarsk Science Center SB RAS", 660036, Krasnoyarsk, Russia
[3]Krasnoyarsk State Medical University, 660022, Krasnoyarsk, Russia
[4]A.N. Belozersky Institute Of Physico-Chemical Biology, Lomonosov Moscow State University, 119992, Moscow, Russia
[5]A.N. Bach Institute of Biochemistry, Research Center of Biotechnology of the Russian Academy of Sciences, 119071, Moscow, Russia

With the advent of modern research methods, the creation of nanoscale objects and their manipulation, it became possible to develop controllable structures that can be applied for the purposes of medicine and biotechnology. These constructs are conjugates of nanoparticles or various functional materials with biological molecules that are used for drug delivery or as diagnostic tools. Such developments hold great promise in terms of the breadth and variety of practical applications.

Aptamers, short DNA or RNA sequences, the three-dimensional structure of which ensures their specific binding to a molecular target, to which they are selectively selected, can act as biomolecules for drug delivery. For a deeper understanding of how the molecular recognition of the target by an aptamer occurs, what the chemical bonds are responsible for a high affinity to the target, to search for ways to optimize the aptamer molecule, modify it for the formation of conjugates, it is necessary to know their spatial structure.

Not all methods of structural analysis are applicable to the aptamers: they almost do not lend themselves to crystallization and therefore are inaccessible for X-ray diffraction; they have several thousand atoms in their structure, which complicates studies by NMR methods. These are flexible molecules for which the most applicable methods should be those that can be used directly in solution.

The most preferable method for studying aptamer molecules is the small-angle X-ray scattering, which makes it possible to study the structures of biomolecules in solution, track the conformation changes of molecules under varying in environmental conditions, study molecular complexes, and combine the data obtained with other complementary methods.

This work presents the results of a study of biological macromolecules of DNA aptamers using synchrotron and spectral methods, measurement techniques, the main results and conclusions that make it possible to judge the prospects of this direction in the study of the structure and functional properties of aptamers - synthetic oligonucleotides used for personalized medicine.

Copper nanowires as a catalyst for CO oxidation

Panov D.V[1]., Bychkov V.Yu[2]., Tulenin Yu.P[2]., Zagorskiy D.L[1].

[1]*FSRC«Crystallography and Photonics» RAS, 119333, Moscow, Russia*
[2]*FSRC Chemical Physics RAS, 119991, Moscow, Russia*

One-dimensional nanomaterials-nanowires (NWs) are of great interest for catalytic reactions. This is due to the high surface area to volume ratio, electrical conductivity and high surface curvature, which determines the efficiency of the catalyst. [1-3]

This work is devoted to the study of the possibilities of creating structures based on NWs for the catalytic oxidation of CO at the lowest temperature. The oxidation of CO is extremely important - for example, in the aftertreatment of automobile exhaust gases. For this purpose, a commercial Pt-Pd-Rh catalyst is currently used, which converts CO into CO_2 with almost 100% yield at temperatures above 400°C. For practical applications, catalysts that will operate at lower temperatures are important. [4-7]

In the course of this work, NWs were obtained from copper and used as a catalyst in the oxidation of CO. In Fig. 1 shows the values of CO_2 concentration depending on temperature for samples of ordinary copper foil, as well as samples with copper NWs.

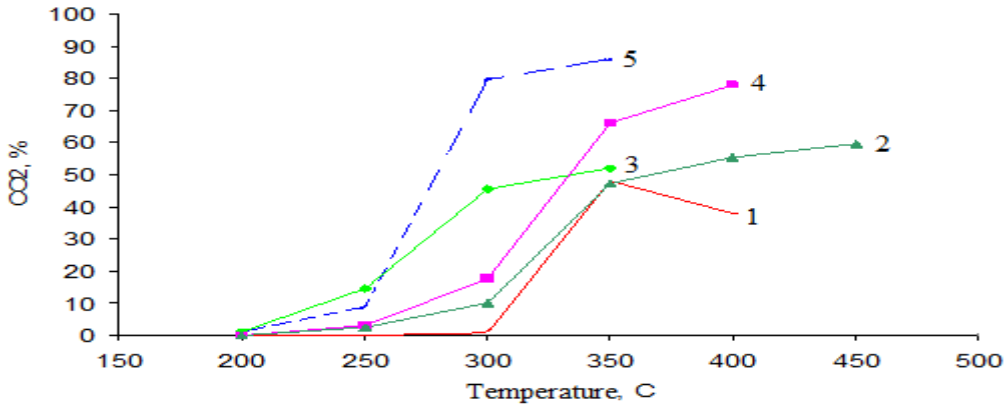

Fig. 1. Formation of CO2 during the interaction of copper samples (16x5 mm) with a flow of a mixture of 2% CO-5% O2 - He (20 ml / min): (1) ordinary copper foil, (2) NW with a diameter of 400 nm and a length of 12 μm, (3) NWs with a diameter of 30 nm and a length of 12 μm, (4) NWs with a diameter of 300 nm and a length of 23 μm, (5) NWs with a diameter of 100 nm and a length of 12 μm.

Analysis of the results shows that for all samples with NW, the CO_2 concentration after catalysis exceeds the values recorded for a simple foil under the same conditions. Comparison of samples 2 and 4 shows that at close values of the NW diameter, the catalytic activity increases with an increase in the NWs length from 12 to 23 μm. Comparison of samples 2, 3, and 5 with the same nanowire length (12 μm) but different diameters (400, 30, and 100 nm, respectively) indicates that the sample with the maximum wire thickness (400 nm) had the lowest catalytic activity. Sample 3 with a wire diameter of 30 nm had the highest activity at a temperature of 250°C, and at temperatures of 300-350°C, sample 5 with a diameter of 100 nm was much more active.

It is shown in this work that the use of surfaces with an array of copper nanowires significantly enhances the catalytic effect in the oxidation of carbon monoxide. It was revealed that during catalysis there is a change in the surface - the formation of copper oxide and hemioxide, as well as the deposition of carbon on the surface of NWs. It was found that the changes after catalysis in the experiments performed are irreversible - the reduction does not lead to the appearance of the original structure.

Acknowledgments. The work on the synthesis of NW from copper was carried out within the framework of the State Assignment of the FSRC "CaP" RAS, and the works on catalysis - the State Assignment of the FRS of Chemphysics.

References

[1] Елисеев А., Лакашин А.//Функциональные наноматериалы.М.: Физматлит. 2010.с456.

[2] Анищик В.М. // Наноматериалы и нанотехнологии. Минск: Изд.БГУ. 2008. 375 с.

[3] Oleinikov V., Zagorski D., Bedin, S., Volosnikov A., // Rad. Meas. 2008. V.43. P. 635.

[4] Lin J.H., Guliants V. // ChemCatChem. 2011. B. 3. S. 1426.

[5] Caldas P. C. P., Gallo J. M. R., Lopez-Castillo A.// ACS Catal. 2017. V. 7. P. 2419.

[6] Wachs I. E., Madix R. J. // J. Catal. 1978 V. 53. P. 208.

[7] Szanyi J., Goodman D. W. // Cat. Lett. 1993. V. 21. P. 165.

Magnetic-plasmonic nanoheterostructures based on gold and magnetic iron oxides

Omelyanchik A.S.[1], Rodionova V.V.[1]

[1] *Immanuel Kant Baltic Federal University, 236008 Kaliningrad, Russia*

Magnetic nanoparticles (NPs) are of interest due to their unique magnetic properties, which have potential applications in biomedicine. However, to date, the use of magnetic NPs in clinics is associated with many difficulties. Thus, their properties should be improved by precise engineering of the structure of the nanoparticle. One of the strategies is to create multifunctional structures consisting of several materials, for instance, core/shell NPs or other types of heterostructures. For example, the combination of magnetic NPs with the plasmonic counterpart in a single heterostructure adds to magnetic properties the optical ones.

The most promising materials which can be used in heterostructures are magnetite (Fe_3O_4) or maghemite (γ-Fe_2O_3) as the magnetic unit and gold (Au) as the plasmonic one. The district surface of the gold counterpart can be functionalized for bioassays and, due to surface plasmon resonance phenomena, these NPs can be used as diagnostic tools or to perform photothermal therapy. Magnetic and plasmonic features can be applied synergistically, for example, simultaneous heating in the alternating magnetic field and optical excitation in magneto-photo-thermal treatment increases the efficiency of therapy preserving multifunctionality.

In this work, we will present several types of iron oxide/gold NPs synthesised via chemical routs in the form of nanoheterostructures [1], dumbbell-like dimers [2] and novel core/shell-like nanostructures. Magnetic, optical and structural properties of synthesised particles were carefully studied with SQUID magnetometer, transmission electron microscopy, X-ray diffractometry, UV-vis spectroscopy and other techniques.

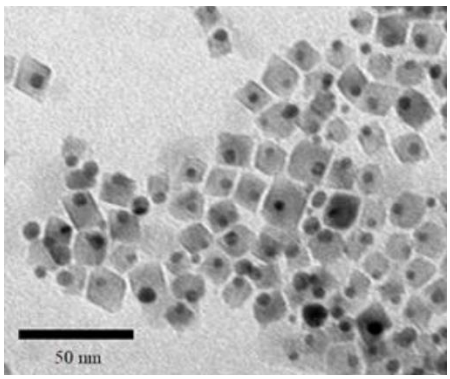

Fig. 1. Transmission electron microscopy image of Fe_3O_4-Au dumbbell-like dimers [2]

This work was supported by the Russian Science Foundation No. 21-72-20158.

References

[1] Omelyanchik, A, et al., Journal of nanoscience and nanotechnology 19.8 (2019): 4987-4993.

[2] Kozenkova, E, et al., Nanomaterials 10.9 (2020): 1646.

Functional materials for magnetomechanical cell surgery

Sokolov A.E.[1,2], Ivanova O.S.[1,2], Svetlitckiy E.S. [2], Zabluda V.N.[1], Borus A.A.[1], C.-R. Lin[3]

[1]*Kirensky Institute of Physics Federal Research Center KSC SB RAS,660036, Krasnoyarsk, Russia*
[2]*Siberian Federal University, 660041 Krasnoyarsk, Russia*
[3]*National Pingtung University, 90003, Pingtung, Taiwan*

Magnetic nanoparticles (NPs) are widely studied and are considered a very promising material for modern technologies such as targeted drug delivery, microsurgery, magnetic separation, catalysis, etc.

The main idea of using magnetic nanoparticles for microsurgery is to immobilize their surface with vector peptides (monoclonal antibodies, aptamers, etc.) and provide mechanical action using an alternating low-frequency magnetic field. Different types of cancer cells require different targeting agents.

Various synthesis methods lead to a wide variety of properties of the obtained NPs. Therefore, the study of particles obtained by a certain method, the determination of their properties and the search for applications remains an urgent task and requires research in each specific case.

The work is a generalization of studies of magnetic Fe3O4 nanoparticles synthesized by the method of thermal decomposition with surface modification with various materials (PEG, SiO2, C and oligonucleotides), depending on the ligands used, the most preferable option for the practical use of nanoparticles is considered.

The crystal structure of the NPs was characterized by X-ray diffraction measurements using a Bruker D8 Advance diffractometer (Cu Kα radiation, 40 kV, 25 mA, λ = 1.5418 Å).

The morphology, microstructure and local elemental composition of the NPs were investigated using transmission electron microscopy (TEM). TEM experiments were performed with a JEM-2100 (JEOL Ltd.) microscope operating at the accelerating voltage of 200 kV. The microscope was equipped with an Oxford Instruments energy dispersive spectrometer (EDS) used to determine the elemental composition of the samples. JEOL JEM-1230 microscope operated at an accelerating voltage of 80 kV was used also in the Precision Instruments Center of NPUST.

Magnetic properties were measured by a vibrating sample magnetometer (Lakeshore 7400 series VSM).

The absorption spectra were recorded with UV/Vis circular dichroism spectrometer SKD-2MUF (OEP ISAN). The quartz cells with optical path length of 5 mm were used.

The reported study was funded by RFBR, project number The reported study was funded by Joint Research Project of Russian Foundation for Basic Research # 19-52-52002 and Ministry of Science and Technology, Taiwan MOST # 109-2112-M-153-003 and # 108-2923-M-153-001-MY3.

Partial measurements were carried out at the Krasnoyarsk Regional Center of Research Equipment of Federal Research Center "Krasnoyarsk Science Center SB RAS"

Author Index

L

M